

REPORT NO. FRA/TTC-82/01

PROCEEDINGS

FAST Facility for
Accelerated
Service Testing
Engineering Conference 1981

**DENVER, COLORADO
NOVEMBER 4 & 5, 1981**

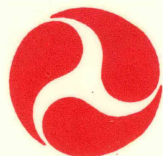
This document is available to the public through
The National Technical Information Service
Springfield, Virginia 22161

AN INTERNATIONAL GOVERNMENT - INDUSTRY RESEARCH PROGRAM

U.S. DEPARTMENT OF TRANSPORTATION
FEDERAL RAILROAD ADMINISTRATION
Washington, D.C. 20590

ASSOCIATION OF AMERICAN RAILROADS
1920 L Street, N.W.
Washington, D.C. 20036

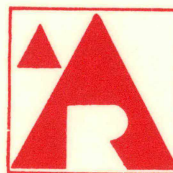
RAILWAY PROGRESS INSTITUTE
801 North Fairfax Street
Alexandria, Virginia 22314



FRA



RPI



AAR

Technical Report Documentation Page

1. Report No. FRA/TTC-82/01	2. Government Accession No.	3. Recipient's Catalog No.	
4. Title and Subtitle FAST Engineering Conference - 1981 Proceedings		5. Report Date January, 1982	
		6. Performing Organization Code	
7. Author(s) Presenters		8. Performing Organization Report No.	
9. Performing Organization Name and Address U.S. Department of Transportation Federal Railroad Administration Transportation Test Center Pueblo, Colorado 81001		10. Work Unit No. (TRIS)	
		11. Contract or Grant No.	
12. Sponsoring Agency Name and Address U.S. Department of Transportation Federal Railroad Administration Office of Research and Development Washington, DC 20590		13. Type of Report and Period Covered Conference Proceedings November 4-5, 1981	
		14. Sponsoring Agency Code DOT/FRA	
15. Supplementary Notes			
16. Abstract <p>This report constitutes the proceedings of the two-day Facility for Accelerated Service Testing (FAST) Engineering Conference held at the Stouffers Inn Convention Center, Denver, Colorado on November 4-5, 1981. Conference papers were presented by representatives of the Federal Railroad Administration, the Association of American Railroads, and Boeing Services International, Inc., current O&M Contractor at the Transportation Test Center, Pueblo, Colorado. The papers cover the development of the FAST Program and results of various experiments conducted at the facility. The topics covered include rail wear and behavior, metallurgy, wheel and truck wear, ballast experiments, concrete and wood tie fastener evaluation and performance.</p> <p>Specific test programs and results of experiments on radial truck curving, fatigue analysis and track degradation are also included.</p> <p>A tour of the FAST facility and associated Transportation Test Center support capabilities was conducted following the conference.</p>			
17. Key Words		18. Distribution Statement This document is available to the public through the National Technical Information Service, 5285 Port Royal Road, Springfield, VA 22161	
19. Security Classif. (of this report) Unclassified	20. Security Classif. (of this page) Unclassified	21. No. of Pages 292	22. Price

ACKNOWLEDGEMENT

The Federal Railroad Administration, Transportation Test Center, wishes to express their appreciation in behalf of all the responsible FAST committees and participants for the efforts expended to make the 1981 FAST Engineering Conference and Proceedings a success.

- o To the authors for their dedication in presenting data and information which will be useful to the Railroad Industry.
- o To Boeing Services International, Inc. for the manpower and efforts in preparing the presentations, organizing the conference, and preparing these proceedings.
- o To the attendees who so intently listened.

TABLE OF CONTENTS

a) Conference Welcome (November 4, 1981) 1
Walter W. Simpson

b) Conference Welcome (November 5, 1981) 5
Peter J. Detmold

c) FAST Overview 7
Gregory P. McIntosh

d) Introduction 11
James R. Lundgren

e) Evolution of Measurement Techniques at FAST 19
Thomas P. Larkin

TRACK

1) Ballast Experiments at FAST 45
Bruce N. Bosserman

Introduction to Tie & Fastener Performance 55

2) Results of Standard Wood Tie and Manufactured Ties Experiments at FAST . . 57
Laurens C. Collister

3) Evaluation of Various Wood Tie Fasteners Under Heavy Freight Railroad
Service Loading 63
Larry Daniels

4) Concrete Tie & Fastener Performance 75
John W. Weber

5) Concrete Tie & Track Systems Engineering Considerations 83
Jack. E. Heiss

6) Tie/Ballast Interaction Comparisons for Wood and Concrete Ties 91
Bruce N. Bosserman

7) Aspects of Concrete Tie Performance on FAST and Revenue Service 97
Howard G. Moody

8) Correlations of FAST and Laboratory Tests with Concrete and Wood Tie
Fastener Results 103
Howard G. Moody

9) Rail: Its Behavior and Relationships to Total System Wear 115
Roger K. Steele, Ph.D.

Note: This paper is composite of 4 papers
presented at Conference:
o Rail Wear and Metal Flow
o Welded Rail End Batter
o Rail Failure Behavior
o Wheel/Rail System Wear

10)	Rail Corrugation Investigations at FAST	165
	Timothy J. Devine	

MECHANICAL

11)	Major Variables that Affect Wheel Wear	175
	Donald E. Gray	
12)	Wear Rates of Freight Car Wheels as a Function of Chemistry	199
	V. E. Kahle	
13)	Radial Truck Wheel Wear	205
	Roy A. Allen	
14)	The Mechanical Aspects of Wheel/Rail Wear	217
	Roy A. Allen	
15)	Fatigue Analysis Tests at FAST	229
	S. K. Punwani	

FUTURES

16)	Track Degradation Experiment	237
	James W. Brent	
17)	Defective Growth Rate Pilot Test	241
	Oscar Orringer	
18)	Radial Truck Curving Performance Evaluation	247
	Roy A. Allen	
	APPENDIX	251

FOREWORD

Since its inception in the United States, the railroad industry has encouraged the development of improved track and equipment. Laboratory testing has screened out potentially unsatisfactory designs. However, final proof of acceptability has always required extensive testing of new track and equipment in revenue service.

In Czechoslovakia and USSR, track loops are in use for the testing of track and equipment in high density or high mileage service before evaluation in revenue service.

Studies made between 1972 and 1975 by the AAR under a jointly funded FRA-AAR contract clearly identified the potential for such loops in the USA. In November, 1975, a series of discussions was held between railroad and FRA personnel. It was decided that it would be highly desirable to begin immediate construction of a Facility for Accelerated Service Testing (FAST). On January 5, 1976, a decision was made to coordinate the planning of such a facility as part of the International Government-Industry Track-Train Dynamics Program.

The Transportation Test Center (TTC) of the Department of Transportation at Pueblo, Colorado, already operating test loops for other purposes, was selected as the obvious site. Railroads, through the Association of American Railroads, and railroads and railroad suppliers, largely through the Railway Progress Institute, agreed to furnish many of the track components, including ballast, rail, rail welding, ties, spikes, turnouts and switches, and related components. Railroads agreed to furnish locomotives and cars. Railroads and suppliers agreed to furnish the necessary car components. The FRA provided some rail and ties and agreed to fund construction and maintenance of the track, operation and maintenance of the train, and collection of the required data.

This massive, cooperative effort has been successful. The track loop was completed about nine months after the initial decision to proceed. Over 100 individuals from government and industry participated in the planning of the track and equipment experiments and hundreds more made their views known on priorities. The FAST loop was completed on August 20, 1976, and operation began on September 22, 1976.

The FAST program is one more outstanding example of the benefits that can arise from effective government-industry cooperation.

The 1981 FAST Engineering Conference was sponsored by the FAST Policy Committee to disseminate major findings from the program. These proceedings are a record of the information provided to the attendees of this two-day conference.

The members of the FAST Policy Committee are:

The FAST Policy Committee is assisted in its technical decision making process by the FAST Technical Advisory Committee. The members of the FAST Technical Advisory Committee are:

FAST POLICY COMMITTEE

CHAIRMAN

Dr. Donald L. Spanton
Office of Rail Safety Research
Federal Railroad Administration
400 7th Street, S. W.
Washington, D.C. 20590
Acting Associate Administrator, R&D

MEMBERS

Mr. Gregory P. McIntosh
Acting Director
Transportation Test Center
Pueblo, CO 81001
FAST Program Manager

Mr. John G. German
Vice President, Engineering
Missouri Pacific Railroad Co.
210 North 13th Street
St. Louis, MO 63103

Mr. Peter J. Detmold
Chairman
Canadian Railway Advisory Committee
Canadian Pacific Ltd.
E301 Windsor Station
Montreal, Quebec H3C 3E4
Canada

Mr. Walter W. Simpson
Vice President, Engineering
Southern Railway System
P.O. Box 1808
Washington, D.C. 20013

Dr. William J. Harris, Jr.
Vice President
Research and Tests
Association of American Railroads
1920 L Street, N. W.
Washington, D.C. 20036

Mr. Paul S. Settle
Vice President
PORTEC, Inc.
5 Brahm's Point Road
Hilton Head Island, SC 29928

FAST TECHNICAL ADVISORY COMMITTEE

CHAIRMAN

Mr. Walter W. Simpson
Vice President, Engineering
Southern Railway System
P.O. Box 1808
Washington, D.C. 20013

MEMBERS

Mr. G. H. Way, Jr.
Asst. Vice President
Research and Tests
Association of American Railroads
1920 L Street, N. W.
Washington, D.C. 20036

Mr. W. E. Thomford
Asst. to Chief Mechanic Officer
Southern Pacific Trans. Co.
One Market Plaza
San Francisco, CA 94105

Mr. R. F. Beck
Chief Engineer
Elgin, Joliet & Eastern Ry. Co.
P.O. Box 880
Joliet, IL 60434

Mr. E. Q. Johnson
Chief Engineer
Chessie System
P.O. Box 1800
Huntington, WV 25718

CONFERENCE WELCOME

NOV. 4, 1981

WALTER W. SIMPSON
VICE PRESIDENT, ENGINEERING
SOUTHERN RAILWAY SYSTEM

CHAIRMAN FAST TECHNICAL COMMITTEE
MEMBER FAST POLICY COMMITTEE

Good morning, ladies and gentlemen. Welcome to Denver and to the first full report of what we have learned at FAST.

I would like this morning, in addition to saying, "I'm glad you're here," to provide you with a brief history of FAST and the reason for its existence--to talk a little bit about its future, and also some of its failures. A clear understanding of past problems of FAST, together with knowledge as to how the problems were overcome can aid in decisions relative to the future value of FAST to the industry.

The Transportation Test Center in Pueblo resulted from an act of Congress--"The High Speed Ground Transportation Act of 1965." The Test Center opened in 1971 and, as you might imagine from the title of the legislation, started researching the movement of people at high ground speeds in unusual looking vehicles.

In the mid 1970's under a program of track research jointly funded by AAR and FRA, we recognized the need for improved facilities to study the interaction of trains and track. This new facility was to be designed to help us learn to run freight trains in a more normal speed range with complete reliability and maximum efficiency.

The FAST track, located at the Transportation Center, was opened on November 8, 1976, and will celebrate its fifth year in existence some four days from now.

Back in 1975, a test track was considered of great potential value to the industry. Basic research in track and equipment areas was badly needed. This new test facility would provide the means to take new developments from testing to practical use ten times faster than could be accomplished in ordinary service. The information available from the accelerated testing mode was particularly important in view of the increasing cost of fuel, rail, cross ties, and rolling stock and the deteriorating financial condition of the railroads. After all, our future success requires that we obtain the maximum return for all of our resources.

The need for FAST, or a similar facility, is probably more important today than it was in 1975. Competition in the deregulated environment is going to become more aggressive, the reliability of our service more important, and control of costs mandatory for our survival.

If we accept the premise that the industry needs such a test facility, what does the future hold? Under the Reagan Administration's budget cutting, the federal funding level is uncertain. In fact, the FRA would prefer private sector operation--and funding--of the Test Center. Because of the budget cutting efforts of the new administration, the Department of Transportation, the Association of American Railroads, the supply industry, and some individual railroads have in recent months examined the value of FAST to the industry and, most particularly, what has been achieved during this five-year period since opening day.

I have been personally involved with FAST for the last two years and other Southern Railway people have worked with the FAST program since its birth. We know the problems FAST has encountered over the years, and the delays that often marked their handling. I'm sure there are some here today who think the reports on the agenda at this Engineering Conference should have been available two or three years ago.

Nevertheless, because of the uncertain future and the need to determine the value of FAST to the industry, I think it desirable that we review some of FAST's failures and consider the corrective actions that were taken. My purpose is to demonstrate that the problems that resulted in delays and sometimes less than satisfactory reports have been addressed. What is coming out of FAST is a quality product.

If you ask some of the statisticians involved in the FAST operation what went wrong, they will say there were too many initial experiments and that they were poorly designed.

If you ask a management expert, he'll tell you that the definition of responsibility between on-site managers, including AAR, FRA, and the contractor, was not properly established.

If you ask a research type, he might say that measurement techniques were not perfected prior to use and maintenance practices interfered with accurate test results.

Finally, if you ask railroad and supply industry engineers, they might say that too much effort went into data gathering and too little effort to analysis and reporting of results.

All of these people would be correct to some extent.

FAST got off to a good start. In September, 1975, the report recommending the proposed facility was submitted; one year later a test was in operation. That accomplishment may have been our first mistake. It produced some hastily designed experiments--along with some good ones--and caused a lack of synchronization that plagued FAST for several years. Considerable data was being gathered very quickly, but there wasn't even a computer at the test site when the test trains started running. This resulted in massive problems in data quality and access. Measurement techniques and instruments commonly used by the railroad industry were adopted on FAST, but many were not accurate enough or required an unusual amount of expertise and time to maintain consistent accuracy.

These measurement tools often had to be modified, and when no tools were available, new instruments were developed. Rail and wheel profilometers as well as tools for hardness tests, longitudinal rail stress measurements and truck wear measurements are just a few examples.

Follow-on experiments were being designed before data from the first experiment in the series could be analyzed or even accessed. Data quality problems, were discovered after the fact. Inventory confusion--what types of wheels were under what cars, and what kind of rail steel was at what location--resulted in delays in data analysis. Far too much effort was required to correct errors and verify operating conditions.

This clogging of the system with massive amounts of incoming data and too little information coming out caused severe communication problems among the three organizations involved in FAST--the FRA, the Contractor, and the AAR. It was months before these data processing problems were resolved and the experiment managers could obtain their data in a reasonably timely fashion. The slow information feedback contributed to delays in the publication of technical reports on findings. And often, as the reports neared completion, new problems developed. There were even problems of report approval, with the approval process itself going through numerous revisions. The objectives--to assure high quality reports and to portray the performance of vendor products fairly and accurately--were admirable, but the delays were discouraging.

Operating problems and unexpectedly high failure and wear rates forced redesign of experiments and resulted in major material and component supply problems. Examples include the high failure rate of wheels in the unlubricated environment and high failure rates of welded rail. Each of these situations had serious repercussions. They forced changes in experiment designs on the fly. Wheels and rail were wearing out so rapidly that the accurate documentation of what was failing and what it was being replaced by caused additional delay.

There were other totally different problems, too. The quality of the design of the experiments, their statistical validity, and their contribution to knowledge varied widely depending on the qualifications of the experiment designer and the availability of data from recently completed experiments. Added to this was substantial variation in the quality of the analysis of various experiments. Again, this was dependent upon the skills and the experience of the analyst.

Looking back over the first few years of FAST operations, I believe our difficulties really stemmed from a confusion of priorities. For a long time the priority was accumulating tonnage, the accelerated service part of FAST. The worst thing that could happen was a train standing idle. But the raw product of FAST was data, not tonnage, and accurate and accessible data was not assigned a top priority until we were well down stream.

What is the situation today? I think it is vastly improved. The problems I have mentioned have been addressed directly and effectively. Organizational problems have been solved by establishing clear lines of authority and clear separation of responsibilities.

Experiments now are carefully designed from the ground up. Ad hoc committees, drawing from the industry those individuals with particular expertise in the area of the experiment, now assist the design process. Statistical validity is assured by making certain that one or more members of the committee is skilled in the field of experiment design.

Data quality has been tackled on a broad front, ranging from improved instrumentation and measurement techniques to a variety of controls to assure high quality data input. Experiment managers can now access the data in a timely fashion. The quality of the analysis of the experiment is steadily improving. Some of the experiments being reported on today and tomorrow, I believe you will agree, are truly at the cutting edge of knowledge in the railroad environment. Each of you, as participants in this engineering conference must in the next two days draw your own conclusions as to the value of FAST to the industry. In its five years of existence it has not been as productive as those of us familiar with the program would have liked. A lot of mistakes have been made, most of them due to the complexity of the problems being dealt with and the organizational problems associated with the cooperative nature of the program. But the past is gone, and we have learned something from it. Today FAST is being managed properly and, as far as I am concerned, has come of age.

As to the future, I would hope that it includes the FAST facility or one somewhat like it, for our industry will need this important range of research activities even more than today.

CONFERENCE WELCOME

NOV. 5, 1981

PETER J. DETMOLD
SPECIAL CONSULTANT
CANADIAN PACIFIC LIMITED

CHAIRMAN FAST POLICY COMMITTEE

HAPPINESS IS JUST A THING CALLED CHANGE*

It is both a pleasure and an honour to welcome you to the second day of the conference on behalf of the Canadian railway community, our public servants as well as our railroaders.

But just before I sit down, my two bits worth will be to tell you why today is going to be so important for all of us.

Railroading is the only sector of the transport industry in which the power, the vehicles and the fixed plant are purchased directly by the operator from more than 350 manufacturers. If you buy a ship or a plane it arrives (all being well) in one piece. Trucks and trailers may be a problem. With railroads, research is made much more complicated by this basic fact of life concerning supply.

In view of its heterogenous nature and the broad variety of operating conditions, although each manufacturer issues a warranty for the successful performance of his product, there is no warranty for the train, no warranty on the track and none, of course, on the train and the track together. Little or no central research effort into the railroad as a system had been made until the advent of programs such as track-train dynamics, and full scale physical experiments such as FAST. There has, therefore, been no assurance that, as technological railroad developments essential to the economies of our two countries took place, new combinations of the component parts of a railroad would be wholly compatible or that the overall operation of the system might not be adversely affected if they were not wholly compatible.

This was probably not too serious a disadvantage during long periods in the past in which technological development was comparatively static and equipment specifications could remain substantially unchanged. But we have entered a new phase in our history in which intensive technical change is not only possible, but in some cases, highly desirable. We have entered a phase in which the cost of capital and energy fluctuate sharply, creating the need to be able to respond rapidly with new technical solutions to problems of an economic as well as of a technical nature.

Many of the large railways in your country and in ours have excellent research departments. But what can any single research department do to ensure that the combinations of track, power, and cars are ideally suited to the specific conditions of their property when maybe more than a quarter of the cars at one time carry someone else's logo--most of them modern cars but just a few with graffiti on the side assuring us that Thomas Dewey will make a very good President.

*A "one-liner" from NEWSWEEK Magazine.

So let me say to FAST, to TTD, to TTC, and to TSC--"we need you!" We need cooperative research in both our countries. We cannot develop further as a thriving modern industry unless we maintain effective means of carrying out the kinds of research we cannot do as individual roads--research that regards railroads as integrated systems, and research that is not too overly respectful of the status quo.

Most of you are well aware that the future of this cooperative research work is currently in some doubt. It would not be my wish to come here from Canada and offer you advice on solutions to the problems of administering programs of this kind. But it is very much my wish to come here and to assure you that the Canadian railway industry will do all we can to cooperate with you in ways that will facilitate the keeping in place of the cooperative research effort that is so essential to us all.

One final thought. To do this research alone is not enough; we also need to apply the conclusions to our operations. Anyone who was here yesterday must already be convinced that a large number of ideas for improving the design of track and vehicles have already emerged and many more will follow. What is the first need in applying research? My goodness, I believe it's cash flow! In our different ways we need to ensure that return on investment in railroading no longer lags behind the average for other industries as it has for so many years in both our countries. Hopefully, the recent tax changes in the U.S. will go some way to improving the situation. In Canada, pious talk about improved safety on the railways, if it is to be effective, must be accompanied by a solution to the Crow grain rate problem. Only then will the cash flow make possible investment on the large scale that will be required. But cash is not the only requirement. We also need to develop a more adventuresome, a more innovative attitude to technical change. We need to increase the pace at which we can alter the nature of our operations. To achieve this, railroaders and manufacturers alike need to regard the component with which they are concerned as a component of an overall system with the implication that it may sometimes be necessary to alter the specification of an individual component to improve safety and efficiency overall.

Conferences such as this one not only indicate directions for change but also challenge the assumption that we should learn to live with problems that are within our collective capability to eradicate.

Thank you.



(Facility for Accelerated Service Testing)

G. McIntosh
FAST Program Manager

To set the stage for the technical papers which are presented in these proceedings, this paper will present an overview of the FAST facility, the operations and the organizations, which are responsible for the administration, implementation and direction of the FAST Program. Mr. McIntosh is the FAST Program Manager and also is Acting Director of the Transportation Test Center.

BACKGROUND

FAST (Facility for Accelerated Service Testing) is a joint industry and government program composed of members from the Federal Railroad Administration (FRA), Association of American Railroads (AAR), and the Railway Progress Institute (RPI). FAST has had international participation from the Canadian and Mexican Railroads as well as a large number of hardware suppliers and manufacturers from various countries throughout the world.

The FAST Program was conceived by a joint industry and Government committee in the spring of 1976. By modifying existing facilities and utilizing a small number of existing staff, the FAST train started operations at the Transportation Test Center, Pueblo, Colorado in September 1976.

The list of participants is found in the appendix of these proceedings.

OBJECTIVE

The primary objective of the FAST Program is to provide a facility and test capability to maintain

and improve the safety and efficiency of the railroad industry. This is achieved by providing the capability to obtain accelerated and closely controlled engineering data. This data base can be utilized by the railroad community to make technical and management decisions relative to track and mechanical components, track structures, mechanical systems and auxiliary equipment, i.e., hot box detectors, grade crossing and fault detection systems.

SCOPE OF CAPABILITY

FAST is a unique Facility. It provides the ability to perform extremely complex experiments, requiring large quantities of highly accurate parametric data under controlled conditions. FAST has the ability to perform experiments of long duration such as wear, life, fatigue, and track degradation. Tests of short duration commonly referred to as "Mini Tests" are also conducted. Examples are; carbody and track accelerations, wheel/rail-loads, instrumented wheels, and angle of attack tests in support of curving performance evaluations.

FAST also provides the capability to develop and improve measurement and instrumentation techniques

and to develop the hardware necessary to obtain repeatable and highly accurate data.

To summarize, FAST provides the capability to conduct the most complex to simple tests under controlled environments and conditions not otherwise available in normal service.

MANAGEMENT

The original management structure was established under the control of the Track-Train Dynamics Program. However, the program was so large and complex that a decision was made to form an independent management organization. The present organization has been in effect since 1979.

As can be seen from the FAST organizational structure, Figure 1, FAST is directed by a Policy Committee chaired by Dr. D L. Spanton. This committee is made up of eight members from AAR, RPI, FRA, Railroads, and Canadian Railroad Advisory Committee. The Policy Committee is further supported by the Technical Advisory committee presently chaired by Mr. W. W. Simpson, Southern Railway Co. This committee is composed of eight members from the railroads and railroad suppliers. The Policy Committee in general provides management and technical policy and is responsible for the selection of experiments and approval of experiment plans and reports. The Technical Advisory Committee advises the FAST Policy Committee on all technical matters including recommendations for new experiments and evaluations of all proposed experiments, and review of experiment results.

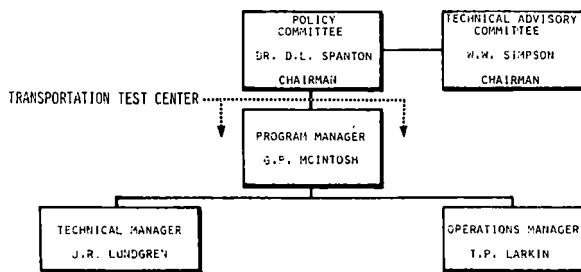


FIGURE 1. FAST ORGANIZATIONAL STRUCTURE.

All FAST Policy Committee directions are implemented through the FAST Organization at the Transportation Test Center in Pueblo, Colorado. This organization is directed by the FAST Program Manager, Mr. Greg McIntosh. Assisting Mr. McIntosh is a Technical Manager, Mr Jim Lundgren and an Operations Manager, Mr. Tom Larkin. Under the direction of the Technical Manager, Mr. Lundgren, are fifteen Experiment Managers. These Managers are responsible for the development of experiment requirements, data analysis, and publication of reports. These Experiment Managers are selected from throughout industry and

the Government according to their expertise and experience. All of the Experiment Managers selected participate on a part-time basis and the majority are not located at the Test Center. To provide continuity between the Experiment Managers and the test operations a staff of ten full time "Experiment Monitors" and Technical Analysts are located at the Test Center. These Monitors report to the Technical Manager and assist the Experiment Managers in all aspects of each experiment - Development, Monitoring, Data Analysis, and Report Preparation. This section of the organization is shown in Figure 2.

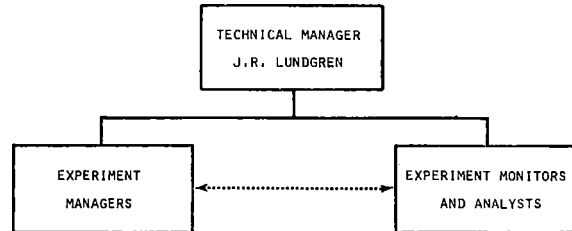


FIGURE 2. RELATIONSHIP OF TEST MANAGERS AND TEST MONITORS UNDER THE TECHNICAL MANAGER.

Experiments can be proposed by anyone; however, all experiments must be reviewed and approved by the FAST Policy Committee prior to their implementation.

FAST TEST SITE LOCATION

The FAST Facility is located at the Federal Railroads Administrations' (FRA), Transportation Test Center, Pueblo, Colorado, Figure 3. It is a 5 x 10 mile site located approximately 150 miles, by road, from Denver. The Test Center has some 58 miles of test track and guideways. The relative layout of these tracks and guideways, including the FAST loop are shown in Figure 4. The FAST Track is a 4.8 mile

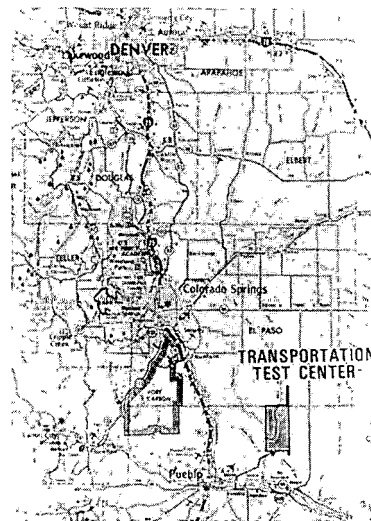


FIGURE 3. FAST FACILITY LOCATION.

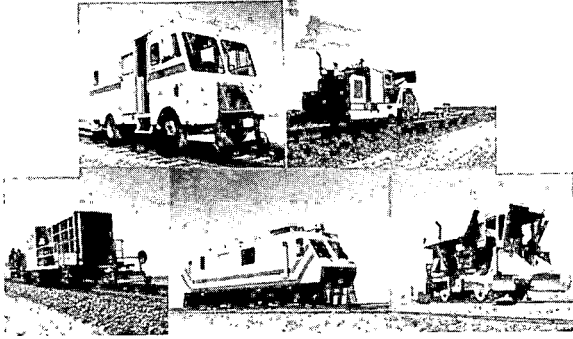


FIGURE 10. SOME OF THE GOVERNMENT FURNISHED MAINTENANCE EQUIPMENT.

Present FAST Status

At present FAST is still in Phase 1, which utilizes 100-ton hopper cars. We have completed 614 MGT and 353,000 miles of operation. Phase 1 will accumulate 818 MGT and 480,000 miles. Currently FAST is not operating due to track rebuild for incorporation of a Track Degradation Experiment and a Concrete/Wood Tie Comparison Experiment. Completion of this activity and restart of Phase 1 is currently scheduled for late November 1981.

Summary

The FAST Program has received contributions and participation from over 160 companies and organizations. It doesn't take an MBA or a Chief Engineer to recognize the potential management and technical problems associated with such a complex program. Because of this we have had our share of problems. However, I feel that we have demonstrated that a joint venture, between Government and Industry of this magnitude and complexity can work.

The future of FAST is viable and worthwhile. However, one must realize that in the present day environment of reduced Government funding, certain impacts will occur. It is expected that the effect will be 1) a reduced rate of mileage and tonnage accumulation and 2) reduced scope or elimination of some experiments.

I would like to take this opportunity as the FAST Program Manager to publicly thank all of those who have contributed, have tried to make it work, and all those who have helped bring us to this point in the FAST Program.

I hope each and everyone of you acquire or learn something useful from the Technical Papers presented herein.

Thank you,

INTRODUCTION TO TECHNICAL SESSIONS

J. R. LUNDGREN
FAST, Technical Manager
Association of American Railroads



On behalf of the FAST Technical Group, I, too, would like to welcome each of you to our FAST Engineering Conference. We appreciate your attendance. We are pleased that all of you have elected to come.

As each of our presenters stands before you today and tomorrow, we recognize that he has been supported by hundreds of individuals and organizations who have enabled us to arrive at the point where we can sponsor this technical conference. FAST is the collective achievement of thousands of people working together toward common goals. These individuals include those who work directly on the program at Pueblo; the Transportation Test Center support staff; Railroad, Railroad Supply, and Government people who have given generously of their time, money, materials, and services; and those who serve on our governing bodies; the FAST Policy Committee and the FAST Technical Advisory Committee. To each of you we express our gratitude.

INTRODUCTORY REMARKS

During the course of the next two days, we have a number of exciting and fascinating technical accomplishments to share with you. We have selected results from many of the FAST experiments to highlight five years of technical progress at FAST.

Although we will be unable to cover all of the topics in depth due to our limited time, we intend to convey the essential features and appropriate conclusions to you. We are confident you will find the two days well spent.

The purpose of my introduction is to set the stage for the experiment results you will hear about in the upcoming 5 technical sessions. This background information will cover those general conditions, the test characteristics, and the common technical elements which define the environment for all of the

experiments. Many of these conditions will be referred to by the presenters as we proceed through the various topics. Let us begin!

Those of us working on the program sincerely believe FAST to be a unique opportunity for the advancement of railroad technology.

FAST

**A UNIQUE OPPORTUNITY
FOR THE ADVANCEMENT OF
RAILROAD TECHNOLOGY**

We are hopeful that the results that you will be given during this conference will substantiate our claim.

OBJECTIVE OF FAST

We have set as our general technical objective the development of improved track and equipment components and subsystems for railroad freight transportation.

TECHNICAL OBJECTIVE

**TO FURTHER THE DEVELOPMENT OF
IMPROVED TRACK AND EQUIPMENT COMPONENTS
AND SUBSYSTEMS
FOR RAILROAD FREIGHT TRANSPORTATION**

As we have all come to know, the "A" in FAST stands for accelerated. The essential features of the accelerated simulated service testing at Pueblo consist of the items in the following list:

ACCELERATED TESTING AT FAST:

- Full scale
- High levels of tonnage accumulation on track
- High rates of mileage accumulation on equipment
- Uniform test environment
- Controlled axle loadings
- Controlled train speed
- Controlled maintenance effort
- Extensive measurement systems available
- Complete data collection and reduction capability
- High inspection frequency
- Secure site, low accident risk

FAST's emphasis is on hardware testing. To that end, our measurements concentrate on the wear, force, and deflection measurements of components under test as shown below:

PRIMARY THRUST OF FAST INVESTIGATIONS:

- Wear and fatigue of track and mechanical components under accelerated life testing
- Force and deflection measurements of test components under simulated revenue service operation
- Comparative evaluations of components and systems

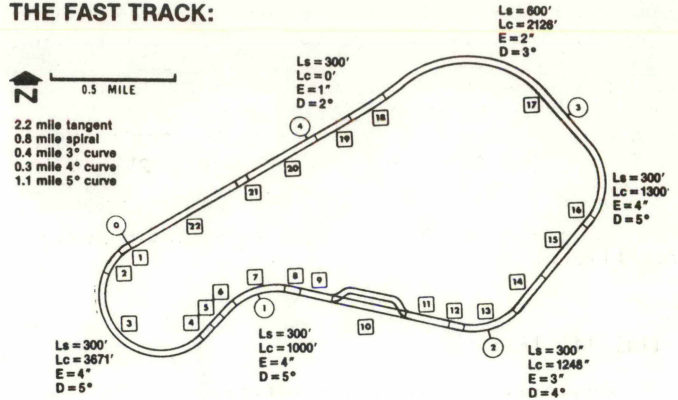
To further reduce the influence of both controlled and uncontrolled factors on test results, FAST has concentrated on using absolute measurements in the comparative evaluation of components and systems.

THE FAST TRACK

The FAST track itself is a 4.8 mile pretzel-shaped

oval of standard gage railroad track built to heavy main-line construction standards.

THE FAST TRACK:

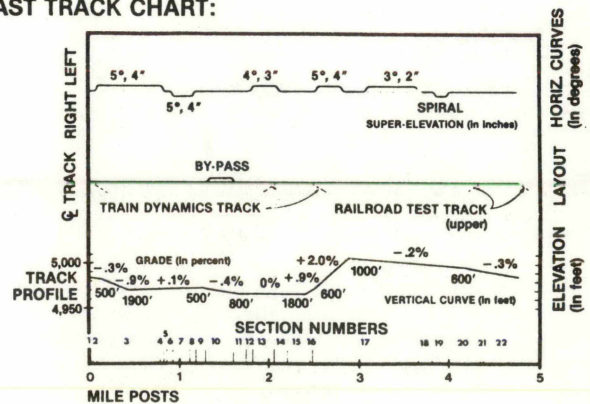


The loop design was chosen to optimize tonnage accumulation over track test sections with a heavy train operating at nominal loaded unit train speeds on curvatures of moderate, but not excessive degree. Twenty-two separate test zones or segments were defined for track component test in accordance with the curvature and gradients available. The characteristics (spiral length, curve length, superelevation, and degree) of each curve are tallied on the diagram above. The length of curve of the various degrees are also compiled. The track in full curvature or spiral accounts for about 54% of the mileage of the loop.

The comparative wear testing of various rail metallurgies was a driving force in the loop configuration design. The 5° curves were felt to provide moderately severe curvature with realistic freight train speeds. Our train operates over most of the loop at an average of 42 miles per hour, about 2 to 3 inches over the balance condition for the curves. Maximum track speed is 45 miles per hour.

The FAST track chart below highlights the significant grade and alignment features and their location relative to the track test sections. We have 5° curves in sections 3, 7, and 17; a 4° curve in section 13; and a 3° curve in section 17. The 5° curve in section 17 is located on a 2% grade. As a matter of note, our operations are carried out at the 5000 foot level of elevation.

FAST TRACK CHART:



THE FAST TRAIN

We now focus our attention on the FAST consist. The FAST train represents traffic similar to that on heavy haul lines. While we do not have a true unit train condition because of some differences in car construction within our fleet, we do apply severe loaded 100-ton car train service to the test components. One important difference is in our practice of running all of our cars in the train fully loaded all of the time. FAST has no empty back-hauls.

The characteristics of the FAST consist are summarized below:

THE FAST TRAIN:

- Motive Power:** Four 4-axle, 2000hp locomotives.
- Car Equipment:** Ninety-nine cars in FAST pool;
Ninety-two 100-ton open-top hopper;
Six 100-ton tank;
One 70-ton TTX.
- Lading:** Hoppers—expanded shale (simulated coal lading);
Tanks—water;
100-ton design cars—loaded to gross weight on rail of 283,000lbs ± 2,000lbs.
- Nominal Consist:** Four units plus 70 cars;
9200 trailing tons;
0.87/hp per trailing ton.

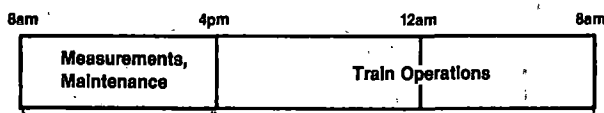
We have restricted ourselves to four-axle power to eliminate the influence of varied motive power characteristics on test results. The expanded shale material used for lading in the hopper cars was chosen for its simulation of the correct center of gravity for loaded coal hoppers and for its non-corrosive properties.

FAST OPERATIONS

The FAST consist operates 5 days per week on a double-shift basis. As shown below, the day shift is devoted to the measurement and maintenance functions which are best performed under daylight conditions. During the night-time operation of the train we set a goal of one million gross tons. To achieve this, roughly 120 laps of the track are required, resulting in approximately 575 train-miles of operation.

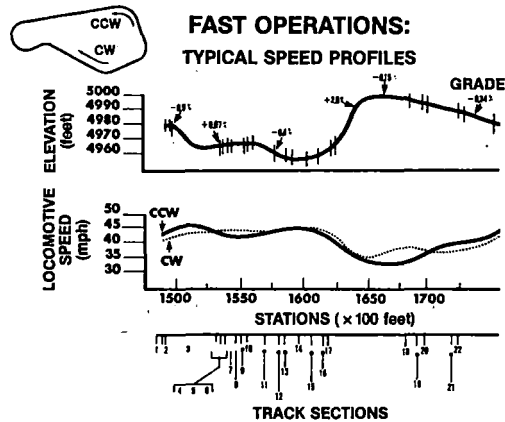
FAST OPERATIONS:

THREE-SHIFT OPERATION, FIVE DAYS PER WEEK



1 MGT }
Nominally 120 laps } per night
575 miles }

During operation of the train, variations in speed occur in response to gradient and curvature restraints. This is shown by the typical speed profiles below:

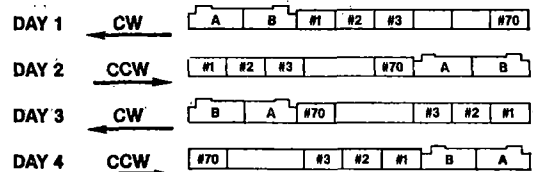


Our maximum speed approaches 46 mph. In the counterclockwise direction, the 2% grade will cause the heavy train to drag down to about 33 mph in Section 17. In the clockwise direction, we crest the hill at about 34 mph to avoid overspeeding in sections 14 and 15. Throttle modulation and dynamic brake are normally used to control train speed. We limit the use of air for the benefit of the wheel wear experiments, attempting to avoid introducing additional braking system variables into wheel wear measurements.

During normal operations, the FAST consist is operated on a four-day cycle to balance the wear exposure on track and mechanical components. In the example shown below the train is operated clockwise the first day, then counterclockwise on day 2 by reversing the power. The entire train consist is wye'd prior to starting operations clockwise on day 3. Reversing the power and running counterclockwise on day 4 completes the cycle. To balance draft exposure on the cars, 10% are moved front to rear daily. To facilitate measurements and maintenance, 4 cars are removed each day and processed through the shop facility for experiment measurements and running maintenance.

FAST OPERATIONS:

ROTATION CYCLE TO BALANCE WEAR ON MECHANICAL & TRACK COMPONENTS




- Four cars removed daily for measurements and maintenance.
- 10% of cars moved front to rear daily to balance draft exposure.
- Train receives daily terminal inspection.

The train receives a thorough terminal inspection each day prior to startup and again during the crew change for the second shift operation.

The 4-day rotation cycle was selected primarily on the basis of equalizing the exposure of the various wheels in the train to the rail in the loop. The effects of the rotation cycle on an individual car are shown below:

FAST OPERATIONS: ROTATION CYCLE TO BALANCE WEAR-EFFECT ON INDIVIDUAL CAR



			Lead Axles	Lead Wheels Outer Rail															
DAY 1	CW	<table border="1"> <tr><td>4</td><td>3</td><td>R</td><td>2</td><td>1</td></tr> <tr><td>A</td><td>#70</td><td>B</td><td></td><td></td></tr> <tr><td>4</td><td>3</td><td>L</td><td>2</td><td>1</td></tr> </table>	4	3	R	2	1	A	#70	B			4	3	L	2	1	4, 2	L4, L2
4	3	R	2	1															
A	#70	B																	
4	3	L	2	1															
DAY 2	CCW	<table border="1"> <tr><td>4</td><td>3</td><td>R</td><td>2</td><td>1</td></tr> <tr><td>A</td><td>#70</td><td>B</td><td></td><td></td></tr> <tr><td>4</td><td>3</td><td>L</td><td>2</td><td>1</td></tr> </table>	4	3	R	2	1	A	#70	B			4	3	L	2	1	1, 3	L1, L3
4	3	R	2	1															
A	#70	B																	
4	3	L	2	1															
DAY 3	CW	<table border="1"> <tr><td>1</td><td>2</td><td>L</td><td>3</td><td>4</td></tr> <tr><td>B</td><td>#70</td><td>A</td><td></td><td></td></tr> <tr><td>1</td><td>2</td><td>R</td><td>3</td><td>4</td></tr> </table>	1	2	L	3	4	B	#70	A			1	2	R	3	4	1, 3	R1, R3
1	2	L	3	4															
B	#70	A																	
1	2	R	3	4															
DAY 4	CCW	<table border="1"> <tr><td>1</td><td>2</td><td>L</td><td>3</td><td>4</td></tr> <tr><td>B</td><td>#70</td><td>A</td><td></td><td></td></tr> <tr><td>1</td><td>2</td><td>R</td><td>3</td><td>4</td></tr> </table>	1	2	L	3	4	B	#70	A			1	2	R	3	4	4, 2	R4, R2
1	2	L	3	4															
B	#70	A																	
1	2	R	3	4															

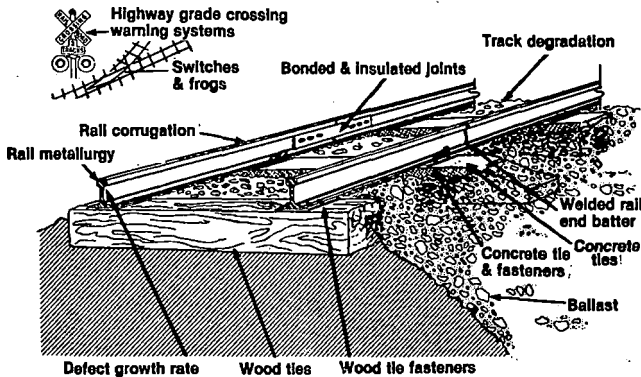
The exposure of each wheel to the lead wheel/high rail condition will balance on a mileage basis over the four-day cycle.

As demonstrated, each wheel's exposure to the lead wheel-high rail condition will balance over the four day cycle. If near equal mileages are run on each successive night, exposure will balance on a mileage basis. In practice, over the life of an experiment, the mileages for each of the four cycles for any given car balance to within a few percentage points.

THE FAST TRACK EXPERIMENTS

The scope of the FAST Track Experiments is best illustrated by the use of the schematic shown below:

FAST TRACK EXPERIMENTS:



We direct our attention to all of the major track components from the ballast on up to the rail surface. In order of effort directed at them the ranking would be:

- rail metallurgy
- concrete tie and fastener system
- wood tie and fastener system
- ballast
- rail corrugation
- track degradation
- welded rail and batter
- defect growth rate

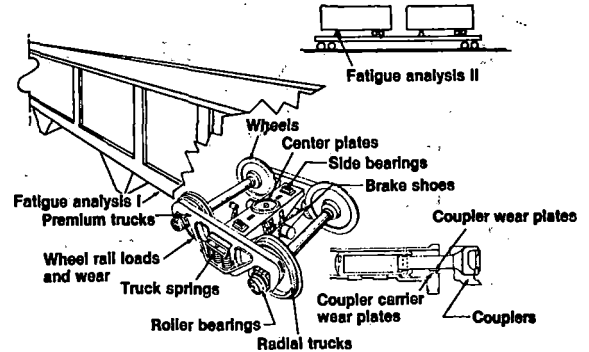
- bonded and insulated joints
- switches and frogs
- highway grade crossing warning systems

Most of these will be covered in our technical presentations during the track sessions.

THE FAST MECHANICAL EXPERIMENTS

In the mechanical area, we have concentrated on running gear and draft system components. Again, the scope of our investigation is readily presented by the schematic below:

FAST MECHANICAL EXPERIMENTS: MAJOR EXPERIMENT COMPONENT AREAS



In addition to a concentration on the running and draft components, we have looked at car structural details and performance in a series of tests designated the fatigue analysis tests. The first of these looked at cracking in the center-sill at the body bolster; the second, at cracking in the members of the TOFC hitch support.

A rough order of ranking by effort placed on the various components is:

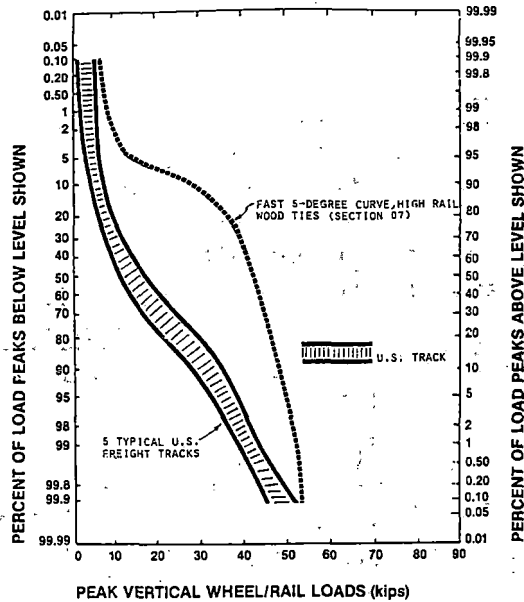
- wheels
- radial trucks
- wheel rail loads and wear
- premium trucks
- roller bearings
- fatigue analysis I
- fatigue analysis II
- couplers; couplers and coupler carrier wear plates
- truck springs
- center plates
- side bearings
- brake shoes

Again, many of these components will receive some attention during the technical sessions on mechanical subjects.

WHEEL RAIL LOADINGS AT FAST

Of particular interest to anyone looking at FAST results is the question of the relevance of the data and conclusions to revenue service. The question is: "How well does FAST represent the real world?"

COMPARISON OF FAST VERTICAL LOAD DISTRIBUTION WITH THAT OF FIVE TYPICAL U. S. TRACKS



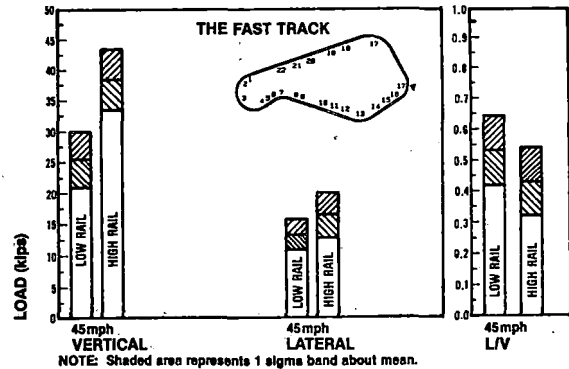
To help us understand how FAST service compares with revenue operations, the above percent exceedance plot is of some assistance. We have plotted peak vertical wheel/rail loads for the 5° curve of section 17 at FAST against the range of peak vertical loads obtained under revenue traffic conditions on the mainlines of 5 Class 1 carriers by Battelle. As one might expect, the operation of 100-ton cars fully loaded all of the time at FAST produces a pronounced shift of the curve to the higher peak vertical loads. For example, roughly 75% of FAST peak loadings are at 40,000 lbs and above, while the revenue service case experiences 2 to 3% at that level. The sharp "knee" in the FAST curve at the 95% exceedance level is a result of the operation of a few empty cars or partial loads in the consist for the benefit of specific tests such as the Wheels III axle load effect experiment. Empties, partial loads and cars of varying nominal capacity are characteristic of the mixed freight service represented by the revenue service band. One significant difference that may arise between FAST peak vertical wheels loads and those found in service is the almost complete absence of impact loads from wheel flats in the FAST train. To date, wheel flats have been closely controlled to maintain consistency for test purposes in applying known load levels to both track and mechanical test components.

The lateral loadings applied to the test components are also of great interest.

The bar chart below shows the maximum wheel/rail loads occurring for one train pass over the 5° curve of section 17. Mean peak verticals on the high rail are 37 kips; on the low, 26 kips. At 45 mph, the mean peak lateral loads on the high and low rails are 17 and 13 kips respectively. An error of one standard deviation is shown about the means to indicate the variability in the load applications. Combining the two mean peaks allows us to show L/V

ratio for both high and low rails. The respective means are about 0.4 and 0.5. While not excessively high, we recall that they represent loaded 100-ton equipment. Consequently the laterals are of significant magnitude.

MAXIMUM WHEEL/RAIL LOADS: PEAK WHEEL LOADS AND L/V RATIO PLOT FOR A 5° CURVE

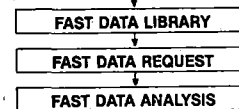


FAST DATA SOURCES

Once we have the track built, the test components installed, and the train operational, a number of data sources are actuated to support the subsequent analyses. Several examples are shown below:

FAST DATA SOURCES:

TRACK		OPERATIONS	MECHANICAL	
Static	Dynamic		Static	Dynamic
<ul style="list-style-type: none"> • Rail profiles • Track geometry car • Track surveys • Maintenance records • Ties • Fasteners • Ballast testing 	<ul style="list-style-type: none"> • Wayside data collection 	<ul style="list-style-type: none"> • Train handling • Train consist • Trailing tonnage • Directional information • Fuel data 	<ul style="list-style-type: none"> • Maintenance records • Wheel profiles • Component wear measurements • Trucks • Couplers • Car body measurements 	<ul style="list-style-type: none"> • Component strains



For convenience, we refer to three categories of data: track, mechanical and operations. Within the track and mechanical categories we classify data as static if collected during non-operating shifts and dynamic if collected while the train is running. Most dynamic data is from strain gage or extensometer techniques. Occasionally, accelerometers and pressure cells are employed.

Much of the data applying to test components is in one of three types: inventory, measurement, or maintenance and repair. A concentrated effort is expended in obtaining accurate operations data on train consist, car weight and operating speeds in order to build completed tonnage and component mileage records.

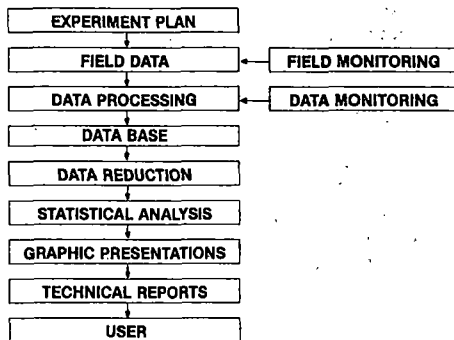
Once collected, the raw data is processed through a multi-tiered edit system prior to being entered into

the computerized data library file records. Once there, the data listings are made available to the experiment managers and others upon request. With the measurement and operations files in hand, data analyses and cross-correlations between data sets may begin.

FAST DATA FLOW

It may be useful to pause for a moment at this point to review the FAST data network. In the chart below we have shown the path taken by the data enroute through the FAST organization.

FAST DATA FLOW:



Measurements are originally specified and methods of collection and accuracy are indicated in the experiment plan document. The execution of the plan leads to the collection of the field data. Quality assurance checks are made on the measurement techniques and instruments as the data is collected. Additional data checking for accuracy and trends is performed as it enters the data processing stream. Once the information is verified it is entered into the FAST data base records where it resides in permanent storage and is readily available for the data reduction efforts. Most of the experiments collect sufficient data to support a thorough statistical analysis. To aid in interpretation and presentation, the data reduction and statistical analyses are converted to graphical output. With suitable interpretive and descriptive support, the graphics can be used in the preparation of formal technical reports on the various experiments. These reports are then available to the railroad community at large for their use in assessing the performance of the various components or techniques evaluated in a given FAST experiment.

CHARACTERISTICS OF TESTING ON FAST

Before moving to the detailed experiment presentations, a summary of the characteristics of FAST may prove useful:

CHARACTERISTICS OF TESTING ON FAST:

- **CLIMATIC**
 - Dry, high desert
 - Low rainfall
- **ROADBED**
 - Excellent subgrade, materials of high stability and modulus
- **CURVATURE**
 - 54% of trackage is in curve or transition spirals
 - High wheel/rail wear per unit of exposure (MGT or miles)
- **OPERATING SPEEDS**
 - Limited to maximum of 45mph (no truck hunting)

CHARACTERISTICS OF TESTING ON FAST:
(continued)

- **LARGE NUMBER OF CONCURRENT TESTS**
 - Interaction between experiments
 - Limitations on some variables
- **TRACK QUALITY**
 - High level of maintenance to preserve test zone uniformity
- **LOW LONGITUDINAL IMPACT LOADS**
 - No yard impacts
 - Limited run-in/run-out severity
- **RELATIVELY SHORT TEST SECTION LENGTHS**
 - Some longitudinal interaction between sections
 - Short transition lengths
 - Limited sample sizes for fatigue studies of some components

As noted in the summary above, FAST is operated in a dry environment on a stable roadbed. There are high rates of exposure of wheels and rail to curve wear. We do not operate at high speeds. The 45 mph maximum speed operated by the FAST train is below any hunting regime for the fully loaded or even for the few empty cars in the consist.

The FAST program includes a large number of concurrent tests in the loop trackage and on the car equipment. Because of this, there are some limitations on the number of variables that a particular experiment may wish to have. In a few instances, there are unavoidable interactions between experiments. One case which comes immediately to mind is the influence between the wheel and rail experiment designs. What is done in one invariably affects the other.

We maintain a relatively high level of track construction and maintenance to preserve uniformity within and between test zones.

There are no significant longitudinal impact loads occurring on the equipment from either yard impacts or in-train forces.

Because of the relatively short loop trackage available for testing, most experiments have limited lengths with short transition sections. There are occurrences of longitudinal interaction between sections. We have a limited ability to introduce large samples of components for fatigue evaluation. In a similar manner, the mechanical tests have a limited number of cars to work with.

Upon reflection, it can be readily seen that the benefits of FAST come directly from the ability to closely control the test conditions. As discussed above, these benefits are gained at a cost of some restrictions and limitations on the scope of individual experiments.

ECONOMIC CONSIDERATIONS

As with any engineering analysis, this introduction would be incomplete without due recognition of the economic implications. The cost-benefit relationship associated with any change in practice is of paramount concern. The successful application of a proposed solution to a problem encountered in revenue service hinges upon a number of factors, many of which are unique to a given operation or location. After considerable thought, the FAST Program has arrived at the following philosophy:

ECONOMIC CONSIDERATIONS OF FAST RESULTS:

FAST PROGRAM PHILOSOPHY

- Provide basic information on comparative performance of hardware and maintenance techniques in terms of engineering units (i.e., wear rates, deflections, manhours, etc.)
- Cost data for the FAST operation is not universally applicable to all revenue service conditions
- Current cost data relevant to individual situations may be readily applied to the FAST comparative results by users

We will provide the quantitative technical information on the comparative performance of items under test. We recognize cost data for the FAST operation is not likely to be representative of any revenue service application. Costs are highly variable and change rapidly over time, reflecting such things as local availability, interest rates, transportation costs, and others. It is our intent to provide comparative engineering results and analyses to which the user may readily apply current cost data relative to his specific application. We are convinced this is the most appropriate way to address the economic aspects of changing practices as a result of FAST recommendations.

FAST HISTORICAL MILESTONES

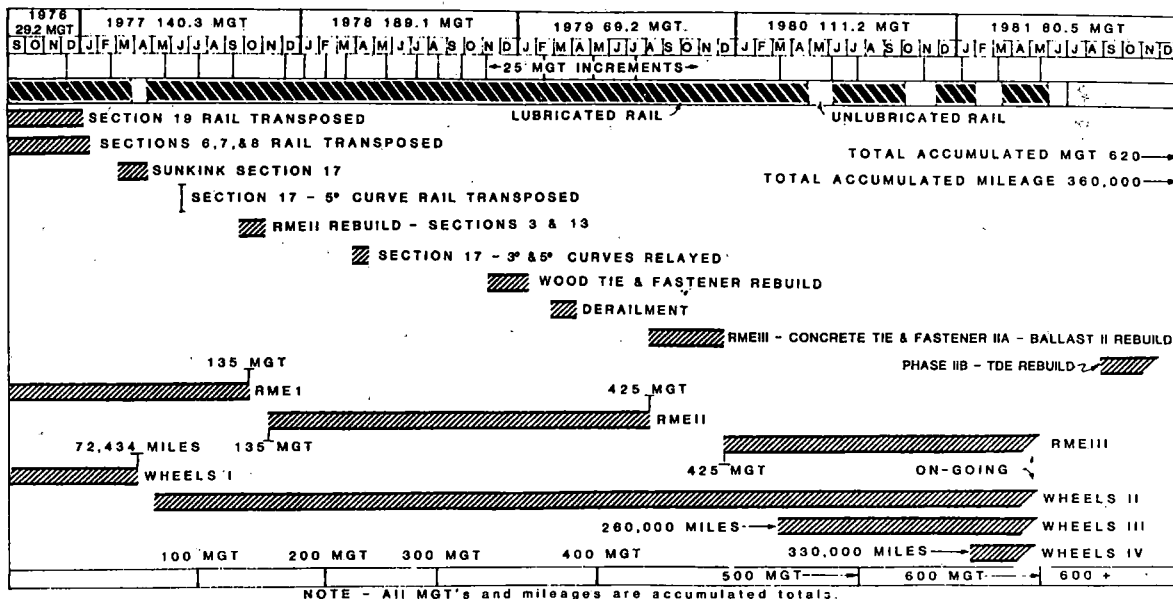
To aid in following the implementation of the various major experiments and the rail lubrication condition at any given time, we have included the following timeline chart for your use.

The horizontal axis is plotted to linear scale on calendar time. To this we have added the MGT accumulation in 25 MGT increments with the 100 MGT milestones denoted on the lower border. Major experiments in the rail and wheel areas are shown by the horizontal bars. The lubrication condition is shown near the top by the heavy diagonal shading.

SUMMARY

With this overview of the technical aspects of FAST testing behind us, we are prepared to move into the detailed experiment reports provided in the technical sessions on Rail, Wheels and Rails, Track, Fatigue and Future FAST Experiments. We will begin with a presentation on rail performance. Before we do, however, a review of the evolution and development of instrumentation techniques at FAST is appropriate.

FAST HISTORICAL MILESTONES



EVOLUTION OF MEASUREMENT TECHNIQUES AT FAST

Thomas P. Larkin
FAST Operations Manager
Federal Railroad Administration

Approximately twenty percent of the total FAST labor budget is expended on the acquisition of data. This equates to 750,000 static measurements and 150 dynamic tapes per year in addition to 205 Train Operations Recording System (TORS) cassettes, and 50 Plasser track geometry tapes. When added to the effort required to process, reduce, analyze and report, it is clearly evident that data acquisition instrumentation occupies a keystone position in establishing the success of the FAST Program. Measurement techniques and instrumentation have evolved as a direct result of increased understanding by experimenters of minimum accuracies and samples required to statistically meet experiment objectives and the necessity to upgrade commercially available measurement devices or design new instruments to meet these requirements. Most of the measurements were developed to satisfy experiment requirements; however, others evolved from efforts to resolve frequent operation problems. Regardless of the source of requirements, instruments and procedures have been developed for which accuracy is well established.

BACKGROUND

FAST proceeded from concept approval to operation in what many regard record time. While the massive efforts by the railroads, railroad supply industries, and the Federal Government resulted in an operational program in less than six months after go ahead, this haste was not without cost. The primary objective of FAST was to expose a track to as much tonnage and consist mileage as possible in the shortest period of time. FAST accomplished this objective. Numerous measurements were defined which were considered secondary to tonnage accumulation and, lacking the necessary time, final use of the measurements to support specific test objectives was not defined; hence, required tolerances and sound sampling densities were lacking.

Approximately one year after start of consist operations, Experiment Managers were selected for the recognized areas of interest. Upon attempts by the Experiment Managers to formulate experiment objectives compatible with data being acquired on FAST, it was immediately apparent that measurements being taken were not necessarily those required to satisfy experiment objectives. Where measurements had been adequately specified, it was found that much data was not usable due to inaccuracy of instruments, errors in recording, or both.

In early 1978, an extensive program to upgrade the quality of FAST data was undertaken, which involved reassessment of all effort from the recording of the data through loading of the data into the data base. Included in this activity was an audit of all existing measurement techniques, both hardware and procedures, in order to define the inherent accuracy that could be expected by using a specific instrument to approved procedures. A policy was estab-

lished which has become standard for implementing new measurements on FAST and which resulted in redesign of many then-existing measurement devices. This standard requires development of a step-by-step procedure for taking the data and rigorous enforcement of the procedure during data collection from a known standard by several different technicians on different days. Finally, the data is reviewed for scatter by the Experiment Manager or Monitor who provides ultimate approval of the instrument and procedure. This approval authority or responsibility has led to early identification of procedure and instrument problems and allowed correction prior to initial use on a test.

Numerous displays of FAST measurement instruments and data collecting hardware and vehicles are presented in Appendix A. These displays are not all-inclusive; however, they do provide an indication of the extensive data collection capabilities of FAST. It is not my intent to discuss each of the instruments or vehicles displayed, but to provide brief examples of measurement developments in the mechanical, track, and operations areas.

MECHANICAL

The mechanical area has probably been more influenced by the efforts to upgrade data quality than the track area due primarily to the number of measurement devices which required redesign and the relatively late attention given to mechanical experiments on FAST. The best example of the progress made in improving measuring techniques in the mechanical area is measurement of wheel wear.

As noted in Figures 1a and 1b, the early years of FAST utilized industry standards in attempting to

obtain wheel measurements. Figure 1b shows the development chronology associated with attempts to improve measurement accuracy ultimately leading to almost exclusive use of the modified Canadian National profilometer and related computer software to accomplish, in a superior manner, data acquisition from previously used measurement devices.

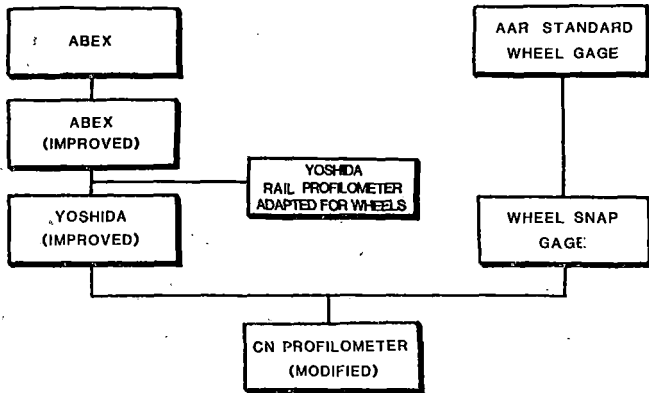


FIGURE 1a. WHEEL WEAR SURFACE MEASUREMENTS.

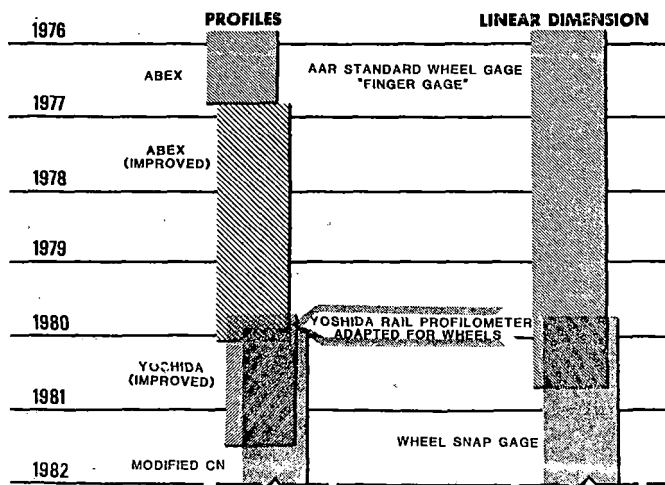


FIGURE 1b. INSTRUMENT MEASUREMENT PROGRESSION.

The original ABEX profilometer (Figure 2) has been and is a railroad standard for wheel profilometry. It was found that this device was unacceptable for experimental data acquisition, primarily due to lack of rigidity and excessive tolerances of many parts. These deficiencies were attacked in 1977 (Figure 3); however, results were less than desirable. Calibration data for the modified and unmodified ABEX profilometers are illustrated in Figure 4. In 1980 an attempt was made to modify a Yoshida Rail Profilometer; however, audit results were unsuccessful and this device was abandoned.

Along the same lines as the ABEX modifications, the Improved Yoshida (Figure 5) incorporated changes to remove excessive tolerances and incorporate a wedge shaped follower to provide more precise measurements on wheel edges and flange areas. The degree of improvement is clearly illustrated by Figure 6; data

taken to the same known standards as earlier illustrated ABEX data.

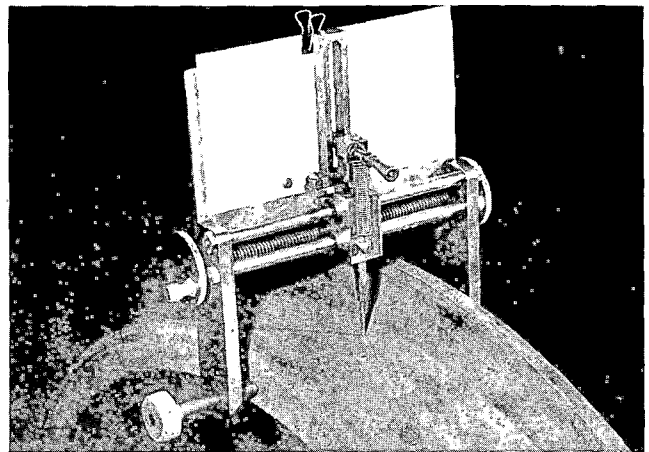


FIGURE 2. UNMODIFIED ABEX PROFILOMETER.

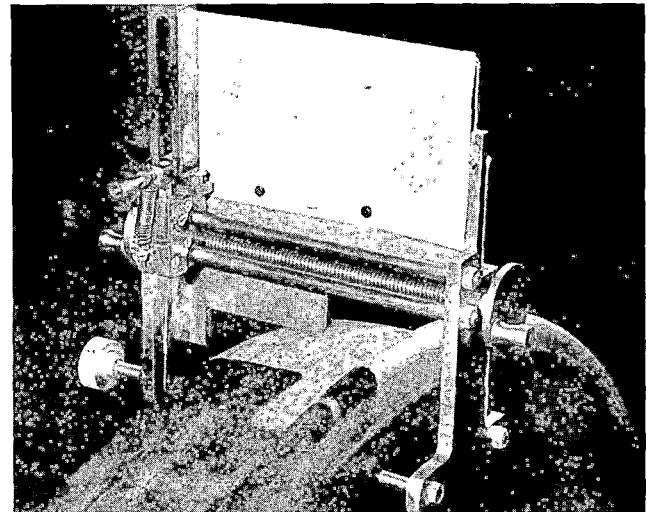


FIGURE 3. MODIFIED ABEX PROFILOMETER.

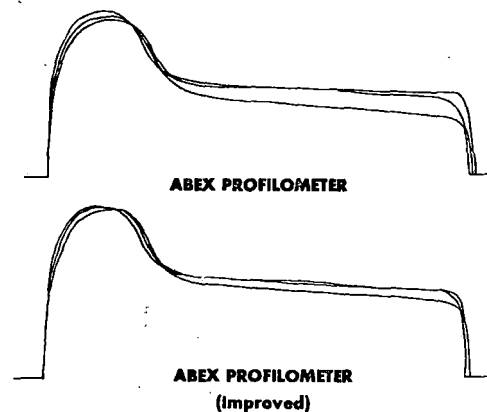


FIGURE 4. ABEX CALIBRATION DATA.

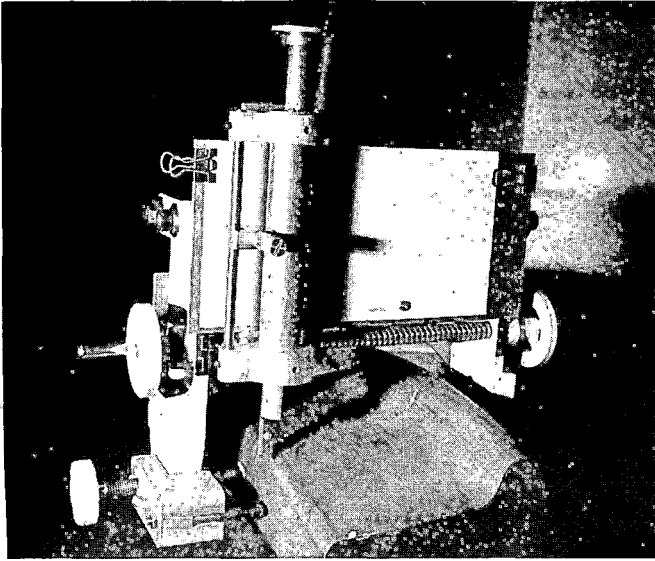


FIGURE 5. IMPROVED YOSHIDA PROFILOMETER.

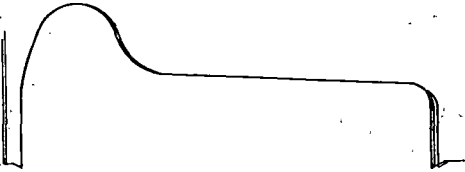


FIGURE 6. MODIFIED YOSHIDA PROFILOMETER CALIBRATION.

Flange thickness and height and rim thickness data were greatly improved when the Wheel Snap Gage was incorporated to replace the Standard Wheel Gage (Finger Gage). The improvement is clearly reflected by Figure 7; however, the need to reduce total measurements and use of different tools to obtain the data still existed resulting in adoption of the Canadian National Profilometer to fulfill all wheel profile/point measurement requirements.

The modified CN Profilometer (Figure 8) provides a digital profile by measuring 80 discrete points on the wheel tread. Outer measurements (on rapidly changing wheel edge and flange profile areas) are at 0.05" increments while flatter tread surfaces are measured at 0.10" increments. The discrete measurement points are determined by indexing the follower crank with each turn providing the dimensions reflected above. The original CN was modified to provide a wider measurement distance, add calibration points on the device to aid in data evaluation, and tighten bearing surfaces to remove unwanted tolerances. In addition, a 3-point fastening system was added to provide positive return to the same measurement points on the wheel at each measurement cycle.

Figure 9 reflects a typical data reduction output for the CN data. Particularly noteworthy is the plot of vertical wear across the tread and area calculations--specifically Flange Area Wear (FAW), Tread Area Wear (TAW), and Total Area Wear (TOT). In addition, Delta Flange Thickness (DTF), Flange Height (DHF), and Tread Height (DTR) are provided.

Of particular interest to the user is the ability of the associated CN software to provide dimensional data previously acquired with the Finger Gage and Snap Gage.

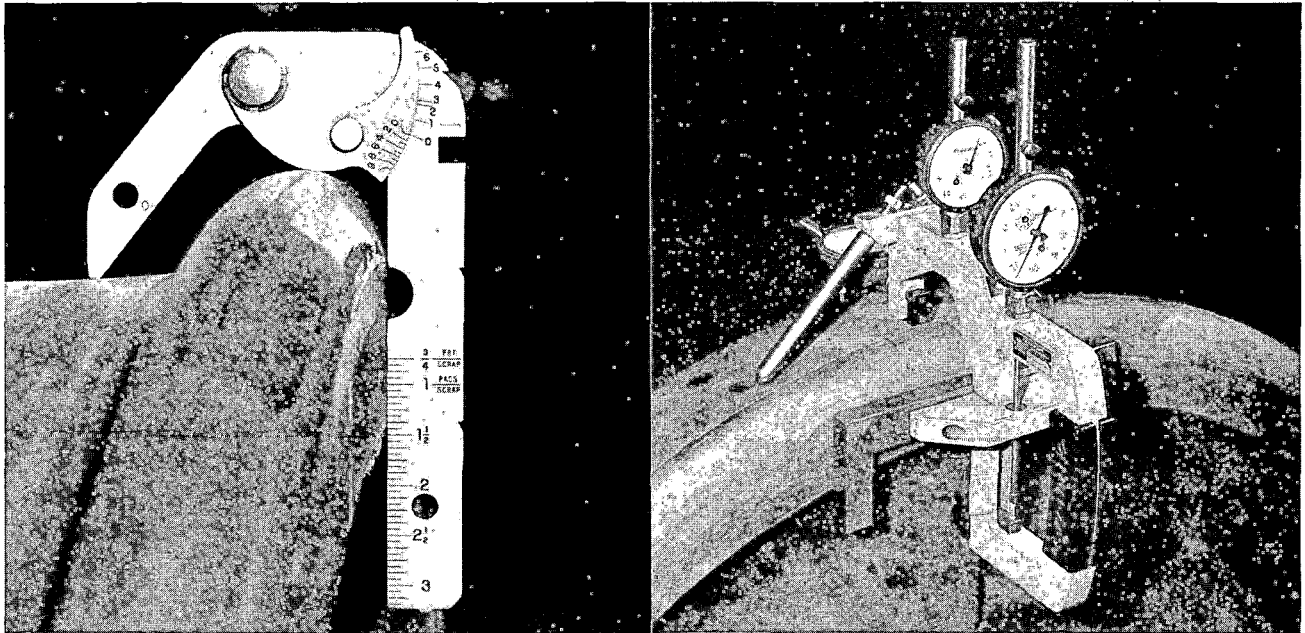


FIGURE 7. WHEEL POINT MEASUREMENTS.

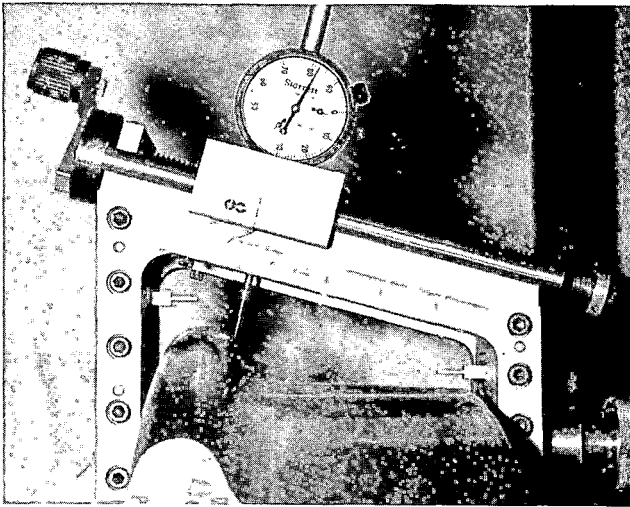


FIGURE 8. MODIFIED CN WHEEL PROFILOMETER.

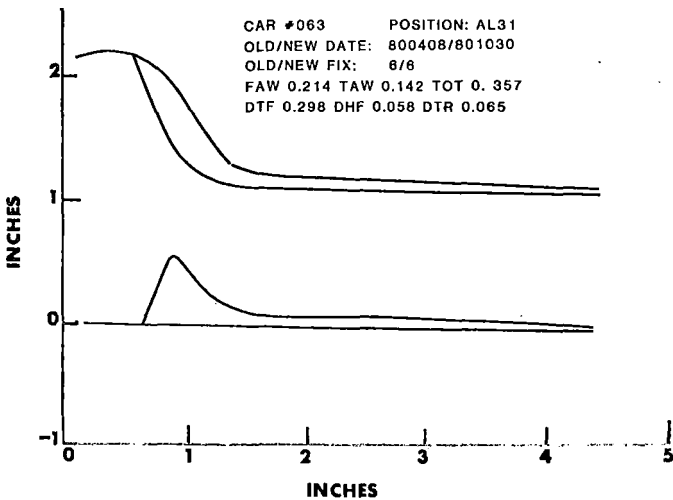


FIGURE 9. CN DATA (TYPICAL WHEEL PROFILE).

As noted in Figure 10, the data accuracies obtained with the CN for point measurements are comparable to the improved Snap Gage data and far exceed accuracy of the applicable Finger Gage measurements.

	STANDARD DEVIATION	
	NEW PROFILE	WORN PROFILE
Flange Thickness	.005	.008
Flange Height	.001	.002
Rim Thickness	.001	.002
Flange Area Loss	.004	.006
Tread Area Loss	.009	.008
Total Area Loss	.012	.009

FIGURE 10. CN PROFILOMETER POINT MEASUREMENT DATA.

The dimensional location in the start of flange and end of tread is accomplished by computer software and is defined as that point on the tread where an imaginary tangent of the profile is 20° from the horizontal. The "X" value of that point is the transition for all subsequent profiles.

TRACK

Since FAST began as primarily a track test bed, relatively heavy attention was given to track measurements early in the program; however, efforts have continued by experiment technical personnel to improve on accuracy of the specific dimensions required for the experiment objectives. An example of this is the extensive use of rail profiles during initial FAST experiments and the resultant unreliability introduced by human error during digitizing. New measurements have been introduced which will lessen the dependence on profilometry and improve quality of dimensional data of interest.

Figure 11 is intended to illustrate the subordinate measurements of interest from the profiles taken at the beginning of the program by use of the Yoshida Rail Profilometer (Figure 12). Since these dimensions (Figure 13) are typically obtained from digitized profiles, the resultant accuracies were questionable. In order to reduce dependence on profiles and to improve data quality, three instruments were developed: The Head Height Loss, Low Rail Metal Flow, and Gage Point Wear Gages.

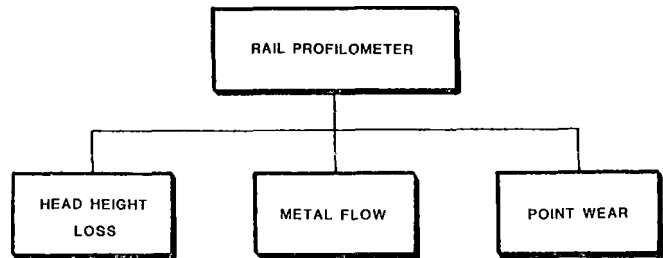


FIGURE 11. RAIL WEAR SURFACE MEASUREMENTS.

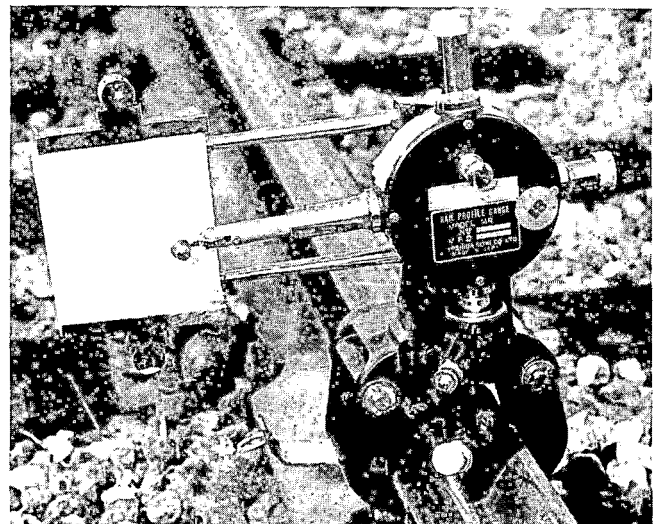
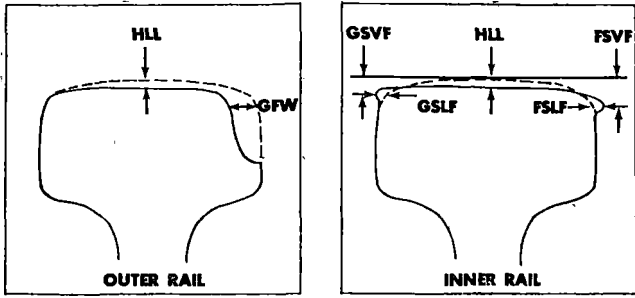


FIGURE 12. YOSHIDA RAIL PROFILOMETER.



HLL : Head height loss
 GFW : Gage face wear

HLL : Head height loss
 GSVF : Gage side vertical flow
 GSLF : Gage side lateral flow
 FSVF : Field side vertical flow
 FSLF : Field side lateral flow

FIGURE 13. RAIL PROFILE DIMENSIONAL REQUIREMENT.

Figures 14a, 14b, and 14c show these gages now in use at FAST, which have, to a large degree reduced the value of rail profiles to illustrative purposes only. Figure 15 provides relative accuracy indications of the various dimensions of interest when obtained through profilometry as compared with the new gages.



FIGURE 14b. LOW RAIL METAL FLOW GAGE.

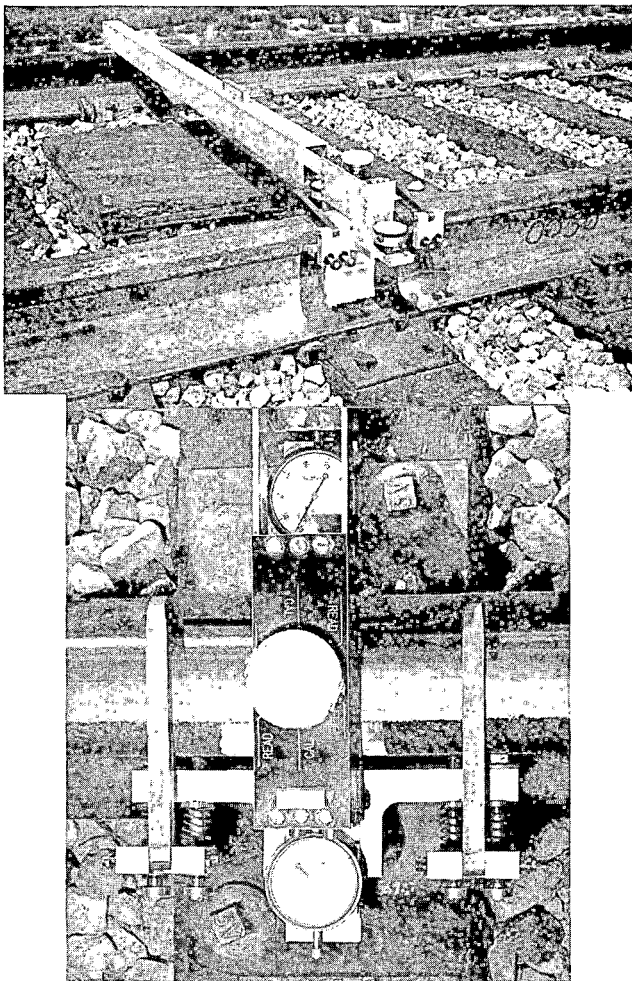


FIGURE 14a. GAGE POINT WEAR GAGE.

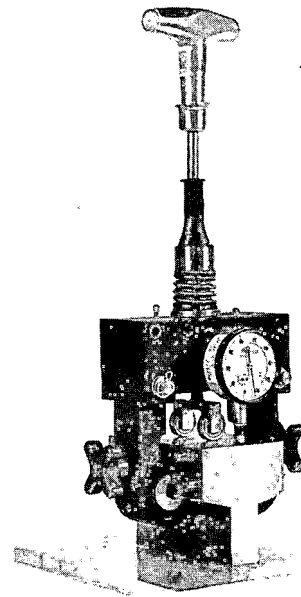


FIGURE 14c. HEAD HEIGHT LOSS GAGE.

	STANDARD DEVIATION (inches)	
	RAIL PROFILOMETER	SNAP GAGE
Head Height Loss	0.026	0.002
Gage Face Wear	0.025	0.001
Low Rail Metal Flow	0.027	0.001

FIGURE 15. RAIL PROFILOMETER/SNAP GAGE COMPARISON.

OPERATIONS

Undesired Emergency Airbrake applications on the FAST consist have been a source of operations delays since early in the program. Initially, attempts were made to locate the defective systems through trial and error. This proved to be time consuming and not especially effective, particularly when more than one defective air brake system was involved and all related airbrake applications were intermittent.

A concept provided by Southern Pacific Railroad was further developed by FAST and has become a routine installation on FAST when Undesired Emergencies become a problem. The principle of operation of the UEL Detector is the ability to measure accurately the time difference between contact closures of two transducers located in the exhaust vents in the emergency portion of the control valve assembly on standard type airbrake equipment. One transducer is installed in the emergency exhaust vent on the locomotive, and another installed in the emergency exhaust vent on the last car in the consist. Circuit logic is illustrated by the block diagram in Figure 16.

It has been found that, with proper temperature compensation, the UEL Detector is accurate to within 15 feet and the specific car affected is generally identified with the first application.

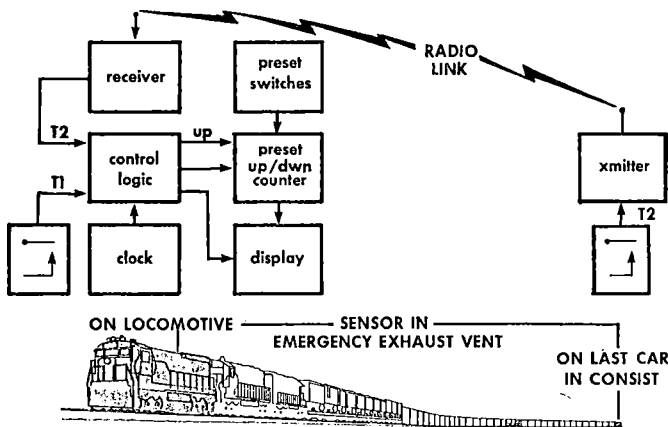


FIGURE 16. UNDESIRED EMERGENCY LOCATOR (UEL).

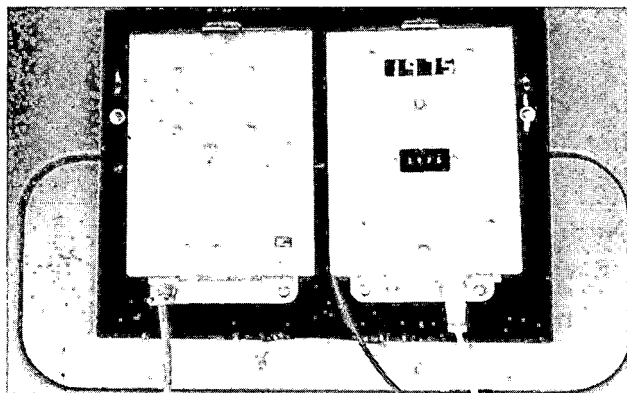


FIGURE 17a. UEL RECEIVER/LOGIC.

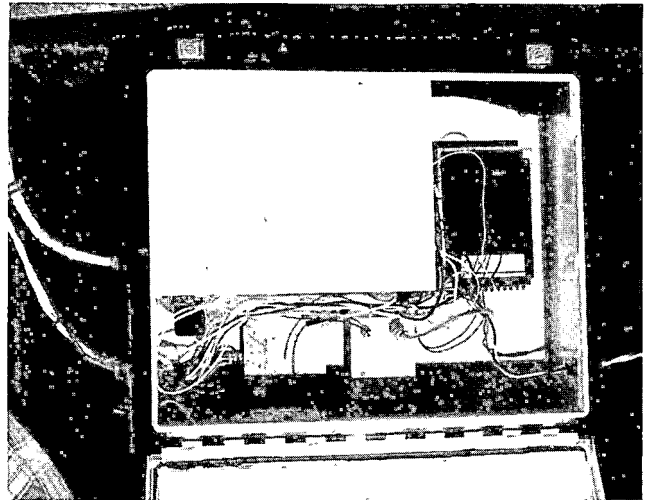


FIGURE 17b. UEL TRANSMITTER/DETECTOR.

Actual hardware installations are shown in Figures 17a and 17b. Since listing consist physical makeup is a routine requirement for all FAST operations the actual car involved in the emergency is easily pinpointed (See Figure 18).

POSITION IN CONSIST	CAR NUMBER	LENGTH IN FEET
1	146 B	0.0
2	147 B	59.2
3	142 A	118.4
4	143 A	177.6
	137 A	233.8
	138 A	288.5
	134 B	343.2
		397.9
70		
71	119 A	
72	19 A	
73	118 A	
74	148 A	3810.9
75	51 B	3854.1
76	36 A	3902.5
77	46 B	3950.2
TOTAL LENGTH		3950.2
HALF CONSIST LENGTH		1975.1

FIGURE 18. FAST TRAIN CONSIST DATA.

SUMMARY

QUESTIONS AND ANSWERS

A combination of efforts of several FAST organizations has been responsible for the increase in quality of data available for analysis. It is felt, however, that success of this effort must be attributed to two specific activities. First, rigorous enforcement of procedures has increased consistency and, second, the on-site availability of experiment personnel has assured that errors, regardless of source, are identified and corrected prior to causing irreparable damage to an experiment. The total effort for data improvement, including the upgrading of measurement devices, has resulted in accurate data being available for the user in a fraction of its previous time. FAST Static Data is generally available in the data base in less than five working days and dynamic data generally within two to three weeks.

Question 1

Is the improved CN wheel profilometer available on a commercial basis? If not, is sufficient information available on how to buy standard CN profilometer and adapt for improvements made at FAST?

Answer

The "improved" profilometer is not available on a commercial basis; however, drawings of the modifications are available from the Transportation Test Center and will be furnished by this office upon request. Information on the availability of the basic profilometer should be obtained from Canadian National. It is suggested that Mr. Nelson Caldwell of CN, (514) 343-5422 be contacted for further information.

In addition to the profilometer, software will be required for data reduction and this subject should also be explored with Mr. Caldwell if obtaining a profilometer is to be pursued.

Question 2

Since FAST wear data is destined to be incorporated into a computer data base, why hasn't an attempt been made to provide digitized data in machine readable form directly from the instrument.

Answer

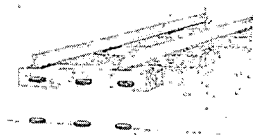
This has been recognized as a desirable goal for several years. FAST is a particularly adaptable environment for this activity and effort was undertaken in 1981 to incorporate a direct output into the CN wheel profilometer. This effort, as well as most new developments, has been abandoned due to successive reductions in FAST budgets. At this time, reinitiation of the effort in the foreseeable future does not appear likely.

APPENDIX A

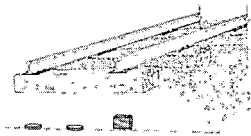
The illustrations of this Appendix are of displays provided at the FAST Engineering Conference and, as previously noted, are not all-inclusive but are representative of the overall measurement capability developed by the program.

Each illustration is self-explanatory and is intended to show hardware involved in the measurement(s), format of data recorded and typical data printed from the storage files. Sizing of the illustrations affects clarity of some of the information furnished. In general, no attempt has been made to illustrate reduced data or analysis outputs.

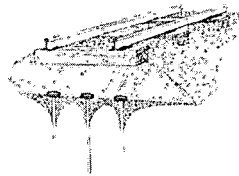
FAST TRACK DYNAMIC MEASUREMENTS



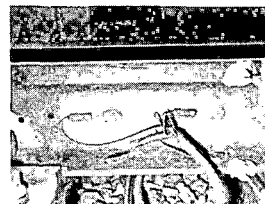
Ballast Strain



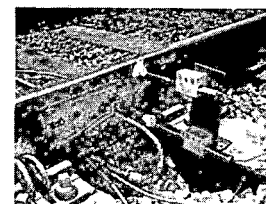
Ballast Load



Subgrade Deflection



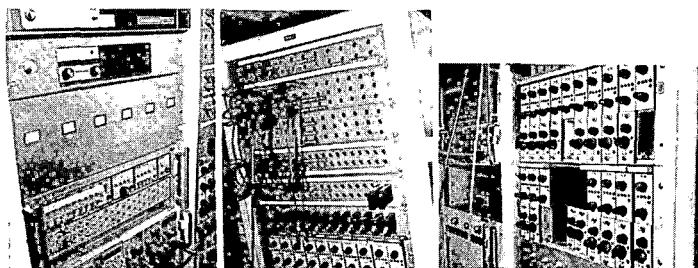
Track Vertical and Lateral Loads



Rail Head and Base Deflection



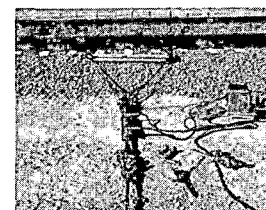
Tie/Rail Acceleration



Digital Data Acquisition System Hardware



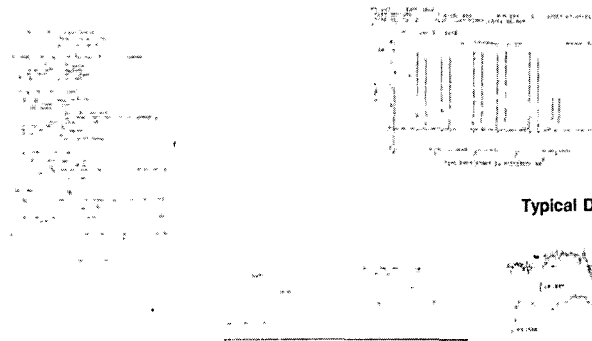
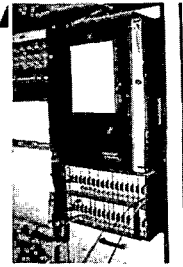
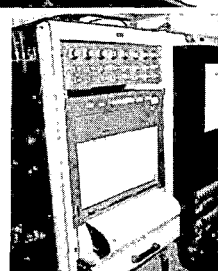
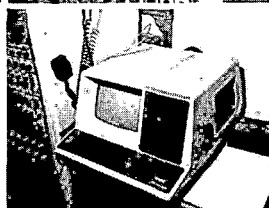
FAST Digital Data Acquisition System Van



Horizontal Track Stiffness

OTHER TRACK DYNAMIC MEASUREMENTS

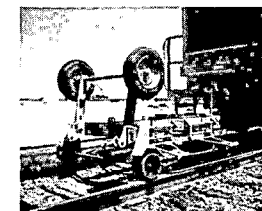
- Rail Flaw Detection
- Track Geometry
- Weather
- Concrete Tie Strain
- Lateral Tie Push
- Rail Vertical Displacement
- Joint Vertical Displacement
- Plate Load Test



Typical Dynamic Data Output

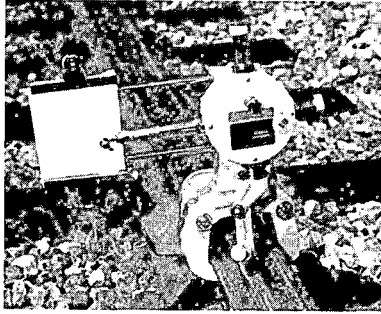


Typical Corrugation Analyzer Output

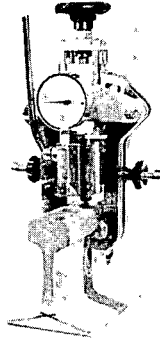


Rail Corrugation Analyzer

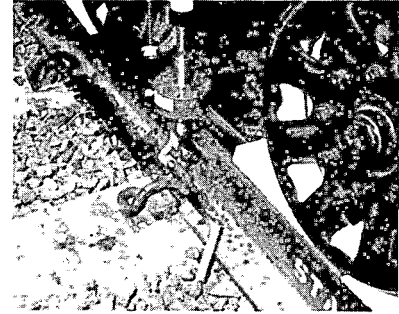
FAST TRACK STATIC MEASUREMENTS



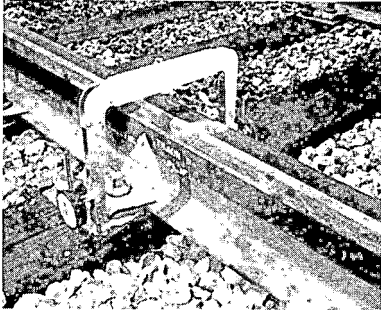
Transverse Rail Profile



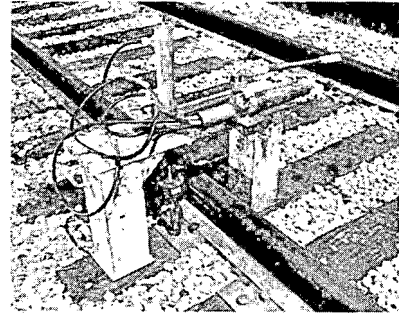
Rail Hardness
(Modified King Brinell)



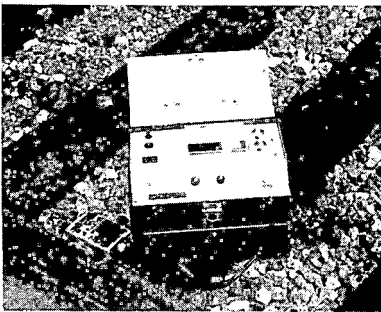
Fastener Toe Load



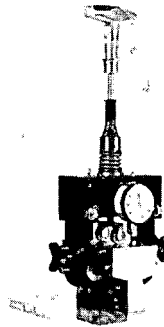
Tie Plate Cutting



Spike Pullout Force



Rail Hardness (Eseyay)

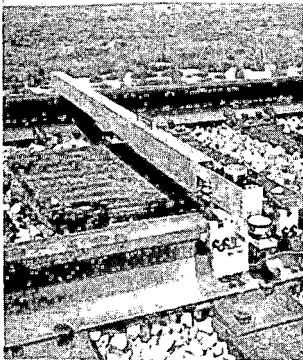
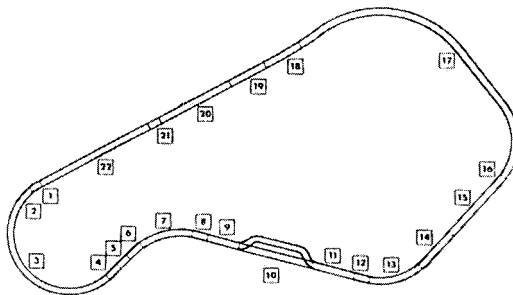
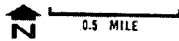


Head Height Loss

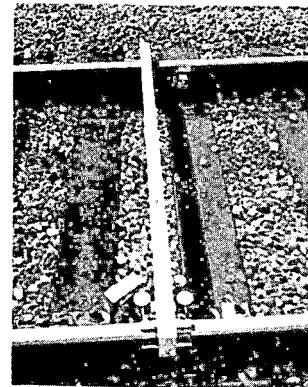
OTHER TRACK STATIC MEASUREMENTS

- | | |
|---------------------------|-------------------------------------|
| Longitudinal Rail Profile | Ballast Density |
| Dynamic Gage Spreading | Ballast Sampling |
| Track Gage | Ballast Shoulder Width |
| Track Modulus | Tie Density |
| Track Settlement | Tie Insulator/Fastener/Pad Movement |
| Survey to Benchmark | Pad Performance |
| Rail Creep | Tie Abrasion |
| Tie Displacement | Tie Face and Top Inspection |
| Ballast Crib Inspection | |

THE FAST TRACK



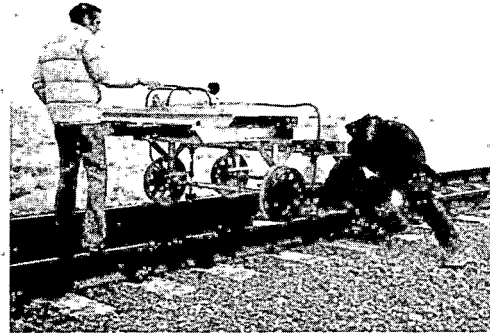
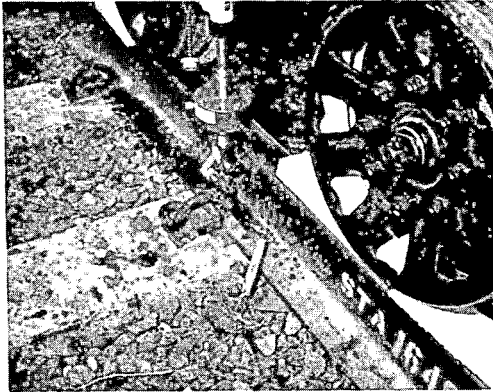
Low Rail Metal Flow



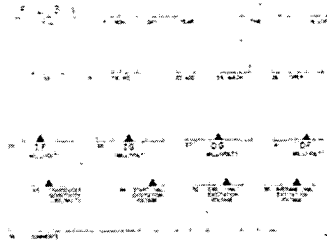
Gage Point Wear

FAST TRACK STATIC MEASUREMENT

Fastener Toe Load

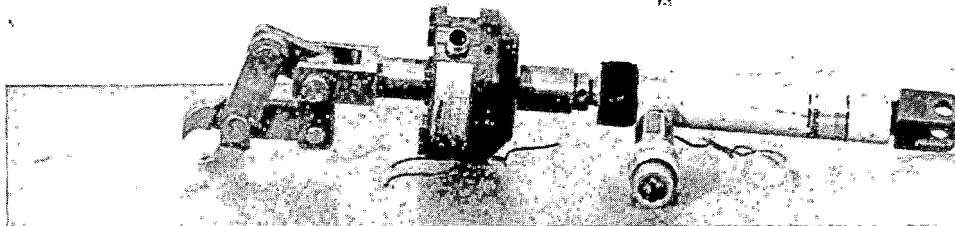
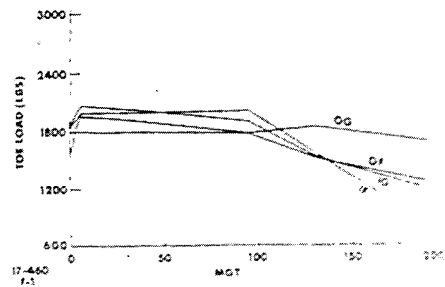


TRANSPORTATION TEST CENTER
FASTENER TOE LOAD



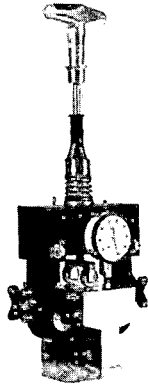
TOE LOAD MEASUREMENT POINTS

TOE LOADS



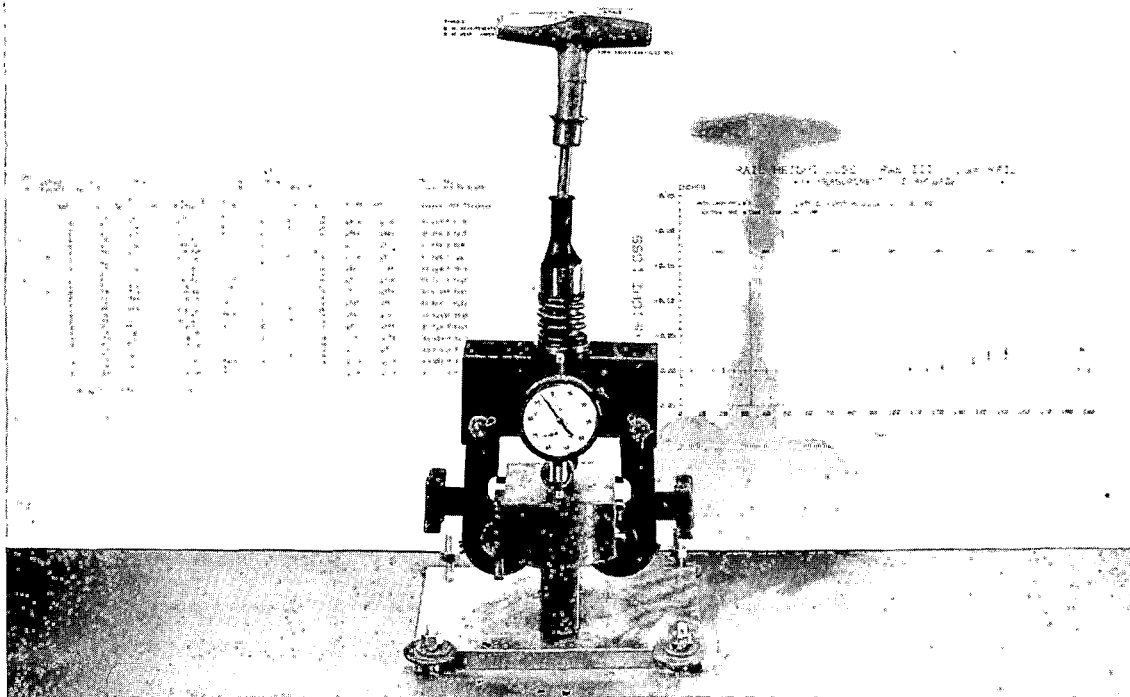
FAST TRACK STATIC MEASUREMENT

Head Height Loss



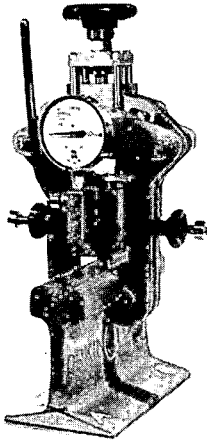
TRANSPORTATION TEST CENTER
HEAD HEIGHT LOSS

1. The head height loss measurement tool is used to measure the head height loss of the rail head. The tool is placed on the rail head and the dial is read. The dial is graduated in 0.01 inch increments. The head height loss is the difference between the dial reading and the nominal head height of the rail head.

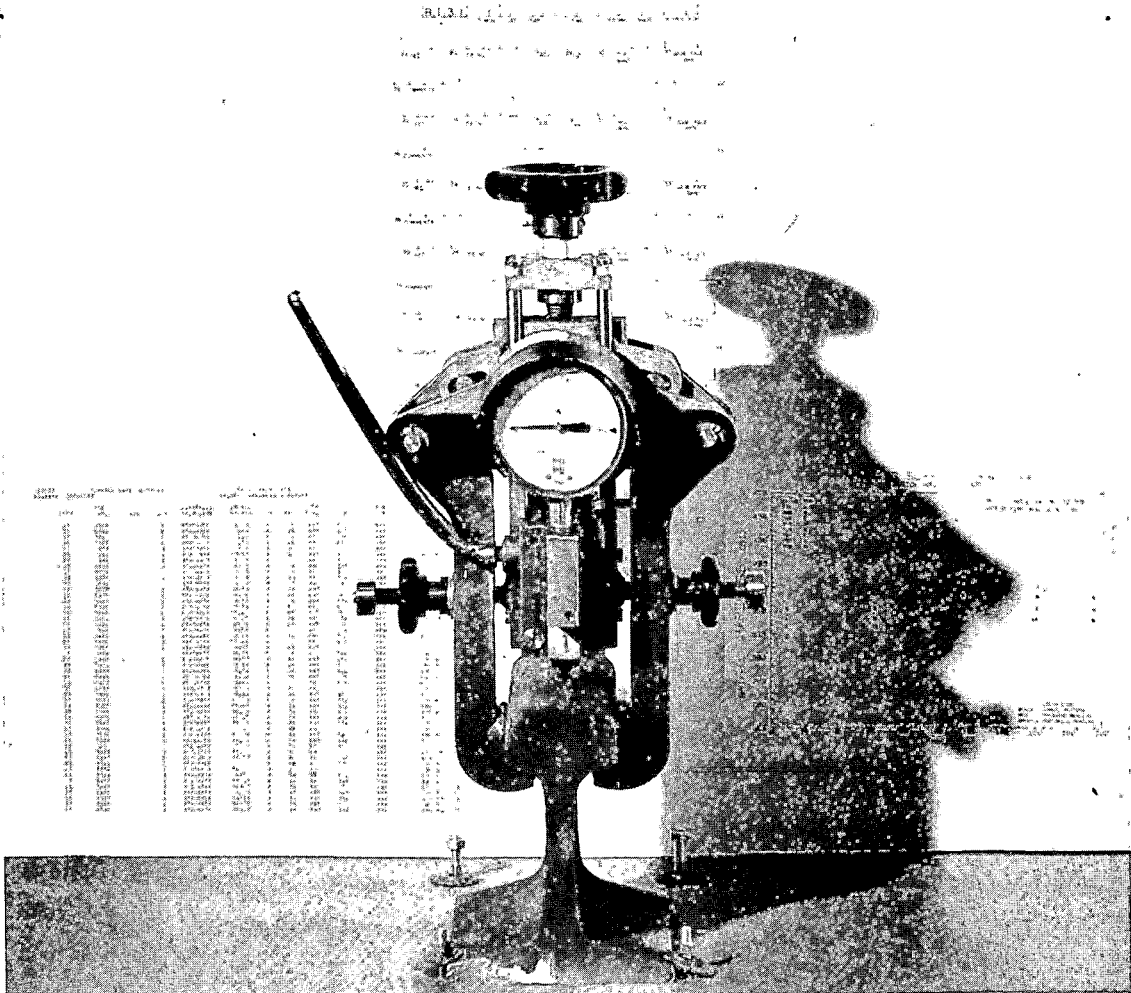


FAST TRACK STATIC MEASUREMENTS

Rail Hardness

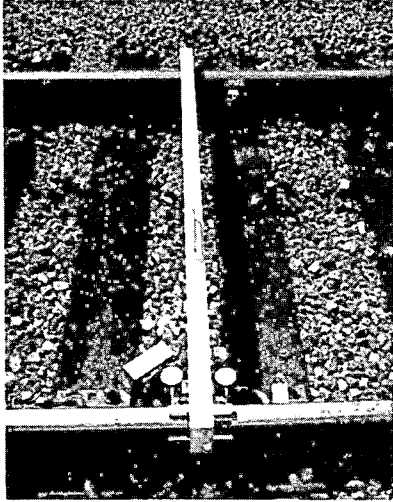


TRANSPORTATION TEST CENTER
BRINELL HARDNESS I



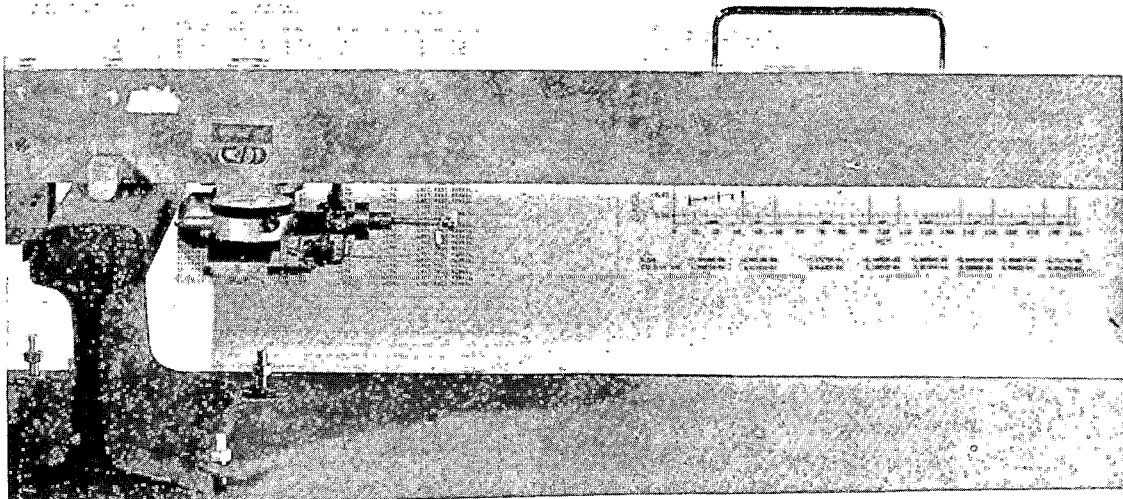
FAST TRACK STATIC MEASUREMENT

Gage Point Wear

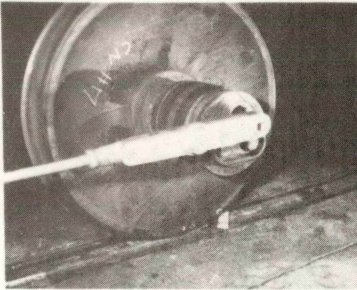


TRANSPORT ON FEET CENTER
GAGE POINT WEAR

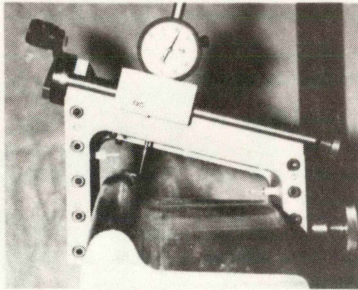
Station	Left	Right
100	0.00	0.00
101	0.01	0.01
102	0.02	0.02
103	0.03	0.03
104	0.04	0.04
105	0.05	0.05
106	0.06	0.06
107	0.07	0.07
108	0.08	0.08
109	0.09	0.09
110	0.10	0.10
111	0.11	0.11
112	0.12	0.12
113	0.13	0.13
114	0.14	0.14
115	0.15	0.15
116	0.16	0.16
117	0.17	0.17
118	0.18	0.18
119	0.19	0.19
120	0.20	0.20
121	0.21	0.21
122	0.22	0.22
123	0.23	0.23
124	0.24	0.24
125	0.25	0.25
126	0.26	0.26
127	0.27	0.27
128	0.28	0.28
129	0.29	0.29
130	0.30	0.30
131	0.31	0.31
132	0.32	0.32
133	0.33	0.33
134	0.34	0.34
135	0.35	0.35
136	0.36	0.36
137	0.37	0.37
138	0.38	0.38
139	0.39	0.39
140	0.40	0.40
141	0.41	0.41
142	0.42	0.42
143	0.43	0.43
144	0.44	0.44
145	0.45	0.45
146	0.46	0.46
147	0.47	0.47
148	0.48	0.48
149	0.49	0.49
150	0.50	0.50



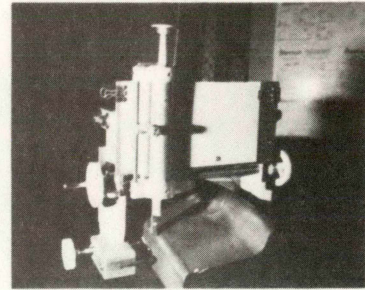
WHEEL MEASUREMENTS



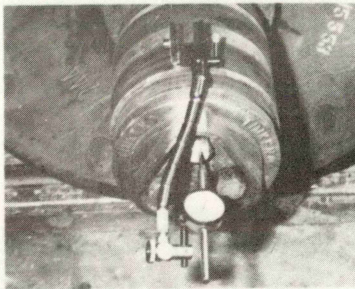
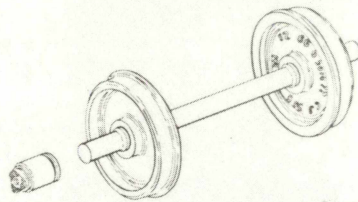
Roller Bearing End Cap
Bolt Torque



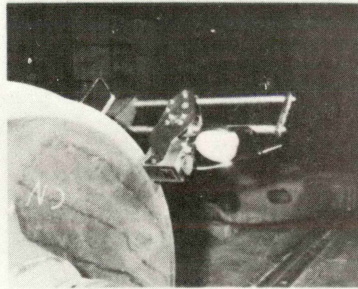
Wheel Profile (Modified
Canadian National)



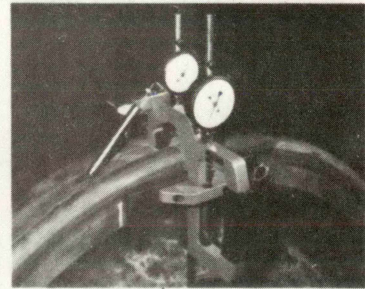
Wheel Profile
(Modified Yoshida)



Roller Bearing
Lateral Movement



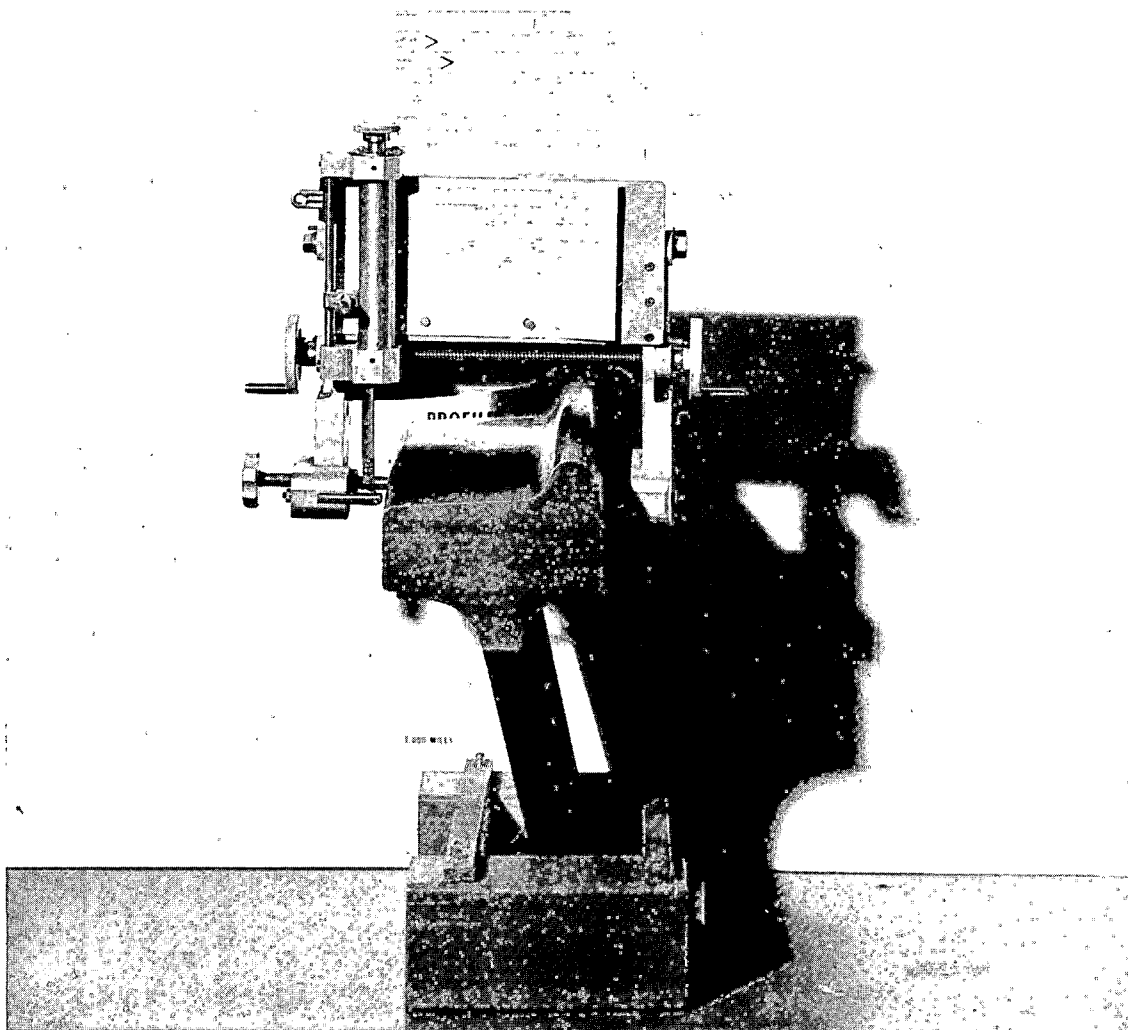
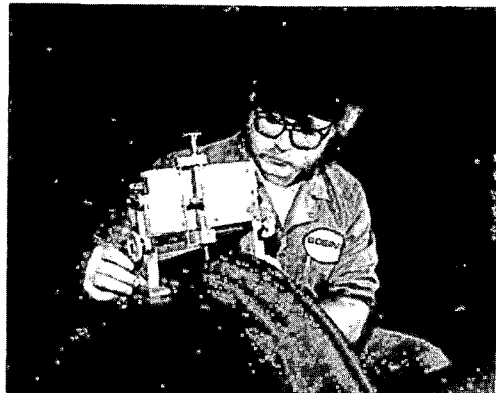
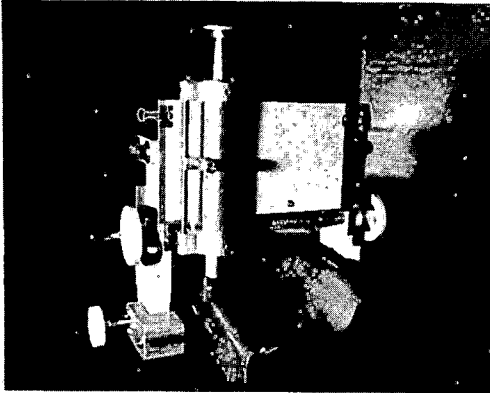
Wheel Hardness



Wheel Wear Snap Gage

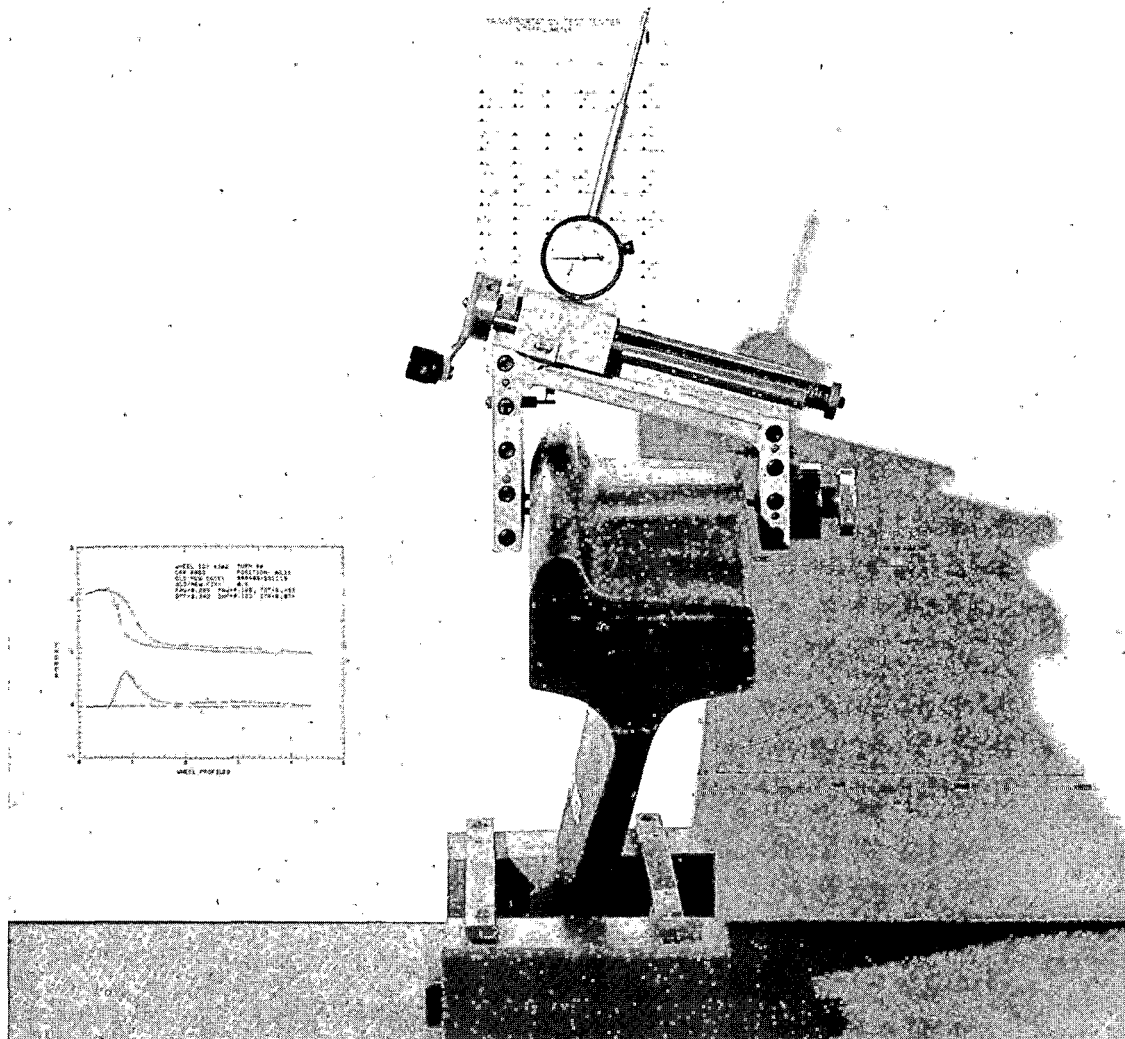
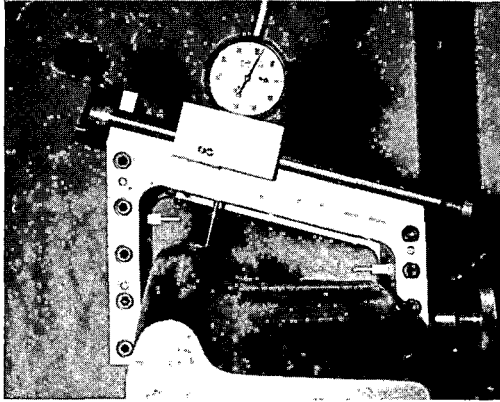
FAST MECHANICAL MEASUREMENT

Wheel Profile — Modified Yoshida

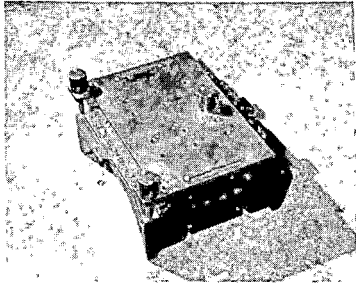


FAST MECHANICAL MEASUREMENT

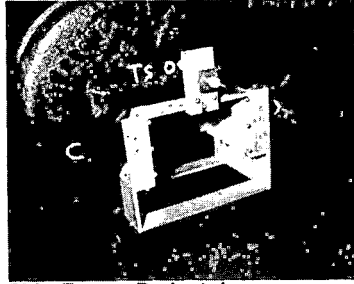
Wheel Profile — Modified Canadian National



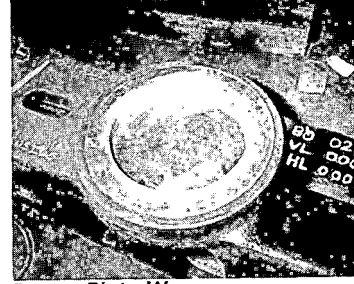
TRUCK MEASUREMENTS



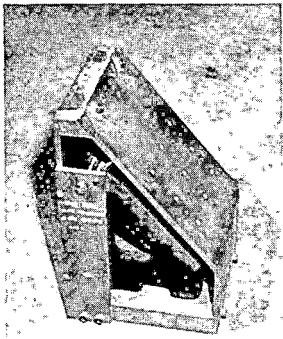
Bearing Adapter Wear



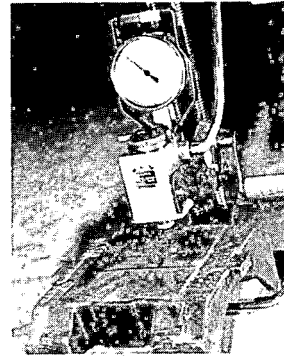
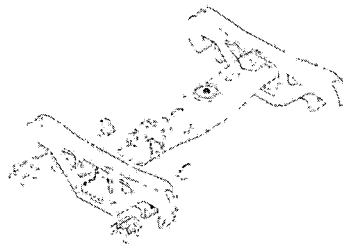
Side Frame Pedestal Wear



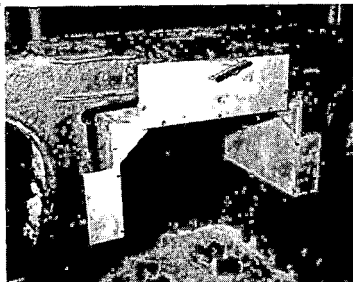
Center Plate Wear



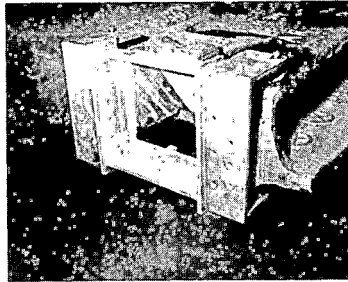
Friction Casting Wear



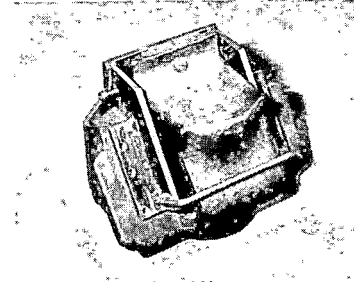
Bearing Adapter Hardness



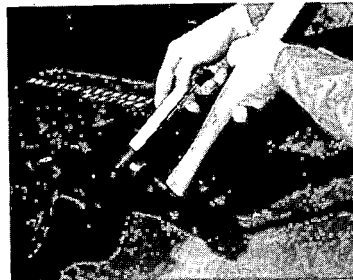
Side Frame Column Wear



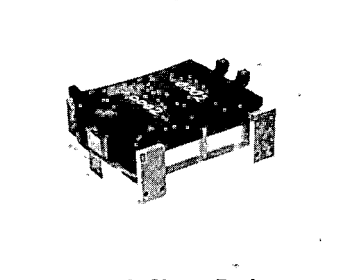
Bolster at Friction Casting Wear



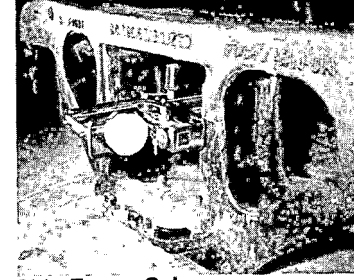
Friction Casting Wear (Wing Type)



Bolster at Friction Casting Hardness



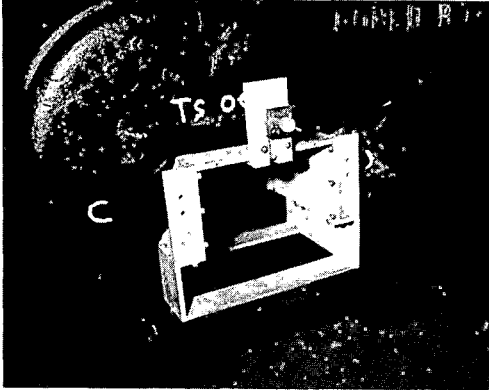
Radial Truck Shear Pad Deformation



Side Frame Column Hardness

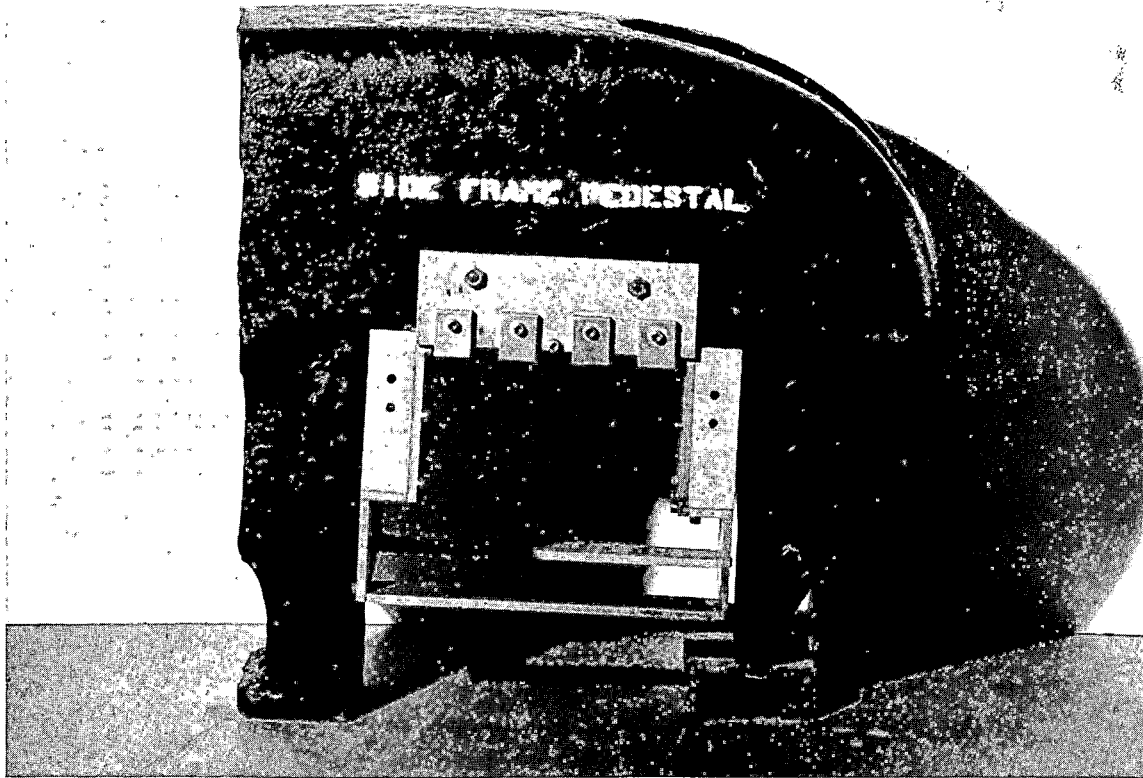
FAST MECHANICAL MEASUREMENT

Side Frame Pedestal Wear



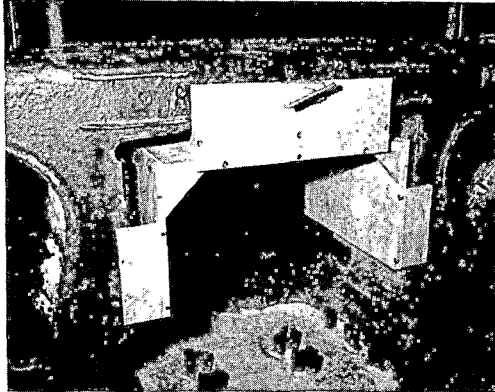
TRANSPORTATION TEST CENTER
SIDE FRAME PEDESTAL MEASUREMENT SYSTEM

ITEM	DESCRIPTION	QTY
1
2
3
4
5
6
7
8
9
10
11
12
13
14
15
16
17
18
19
20
21
22
23
24
25
26
27
28
29
30
31
32
33
34
35
36
37
38
39
40
41
42
43
44
45
46
47
48
49
50



FAST MECHANICAL MEASUREMENT

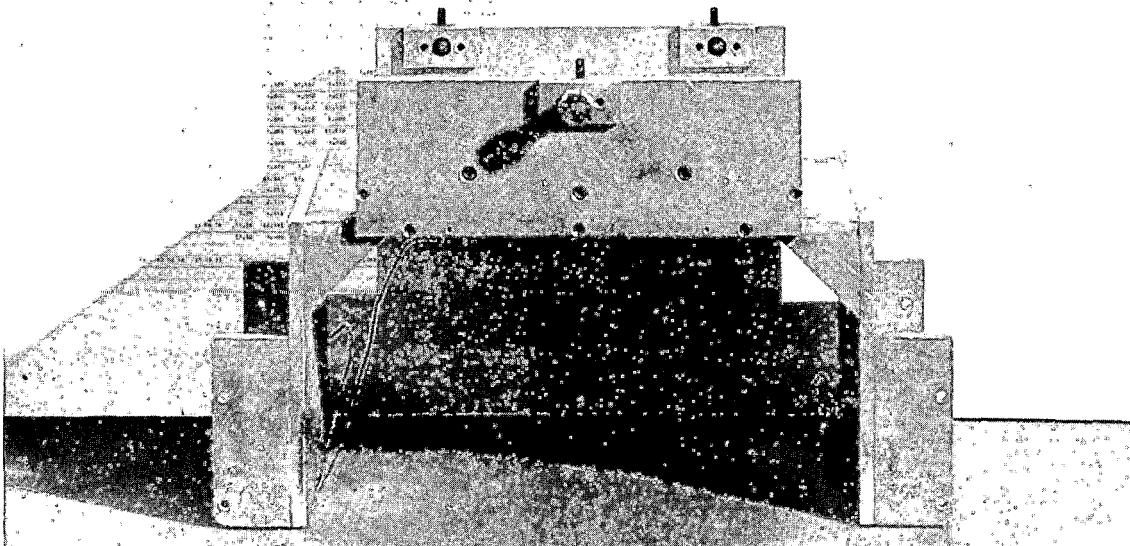
Side Frame Column Wear



TRANSPORTATION TEST CENTER
SIDE FRAME MEASUREMENT II
GALLERY GUIDE

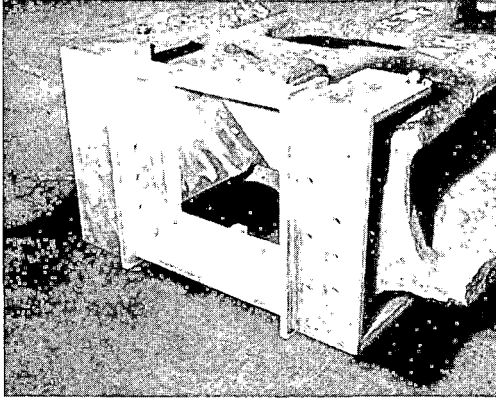
LEFT SIDE FRAME
RIGHT SIDE FRAME

POINT	LEFT	RIGHT
1	2	3
4	5	6
7	8	9
10	11	12
13	14	15
16	17	18
19	20	21
22	23	24
25	26	27
28	29	30
31	32	33
34	35	36
37	38	39
40	41	42
43	44	45
46	47	48
49	50	51
52	53	54
55	56	57
58	59	60
61	62	63
64	65	66
67	68	69
70	71	72
73	74	75
76	77	78
79	80	81
82	83	84
85	86	87
88	89	90
91	92	93
94	95	96
97	98	99
100	101	102



FAST MECHANICAL MEASUREMENT

Bolster at Friction Casting Wear



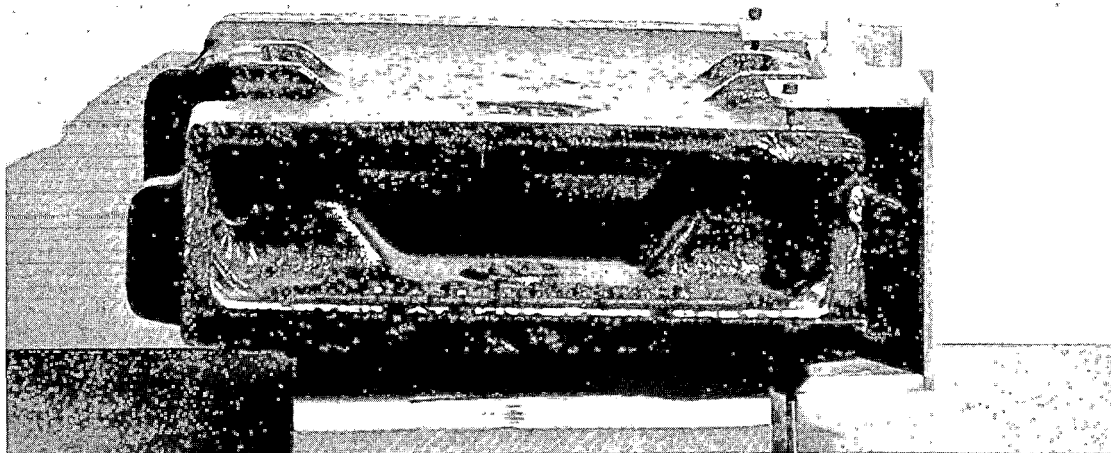
TRANSPORTATION TEST CENTER
 DEPARTMENT OF TRANSPORTATION & ENGINEERING CENTER
 1982-83

Fig. 1-1
 BOLSTER FOR THICKNESS

View	A	B	C	D
Front	▲	▲	▲	▲
Top	▲	▲	▲	▲
Left Side	▲	▲	▲	▲
Right Side	▲	▲	▲	▲
Bottom	▲	▲	▲	▲

Fig. 1-2
 BOLSTER FOR THICKNESS

View	A	B	C	D
Front	▲	▲	▲	▲
Top	▲	▲	▲	▲
Left Side	▲	▲	▲	▲
Right Side	▲	▲	▲	▲
Bottom	▲	▲	▲	▲



TRACK

1981 FAST ENGINEERING CONFERENCE

KEY TOPICS

RAIL METALLURGY

CONCRETE TIES

WOOD TIES

BALLAST

RAIL CORRUGATIONS

BALLAST EXPERIMENTS AT FAST

Bruce N. Bosserman
Experiment Manager, Ballast
Federal Railroad Administration

The major objective of the FAST Ballast Experiments is to investigate and quantify wherever possible, the effect of ballast material type, depth, and shoulder width on track performance. Secondary objectives include evaluation of geotextile performance and investigation of tie/ballast/subgrade interactions for wood and concrete ties (this area will be covered in the tie and fastener session).

This presentation provides a brief summary of the results obtained from the FAST Ballast Experiments. Figure 1 depicts the track layout and ballast experiment test sections. When FAST operations began in September 1976, the ballast tests included ballast shoulder width (Section 15), ballast depth (Sections 18 and 20), and ballast type (Section 18 and 20). These tests were concluded in the fall of 1979 (425 MGT), due to problems with alignment, tie skewing, and ballast fouling, for which the granite (technically hornfels) ballast received most of the blame. Section 17 was rebuilt from the subgrade level with new ballast materials. Section 3 was also rebuilt with some of the same ballast so that concrete ties could be installed there at a later date to compare its 0% grade to the 2% grade in Section 17. Although these are basically rail, tie and fastener test sections, ballast performance is carefully monitored to detect differences which may exist between the ballast types. Section 22 was rebuilt as a direct comparison test of wood versus concrete ties using Northeast Corridor (NEC) ballast, ties, and fasteners. Various ballast of loading differences between wood and concrete ties. While Section 17 was being rebuilt, several types of geotextiles (filter fabrics) were installed in a portion of the section to determine their effectiveness in preventing migration of fines between the ballast and subgrade.

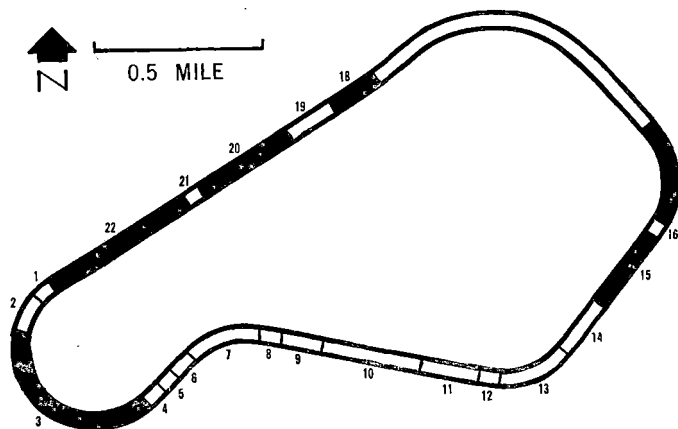


FIGURE 1. FAST TEST SECTIONS

It should be noted the Pueblo area receives very little rainfall (approximately 11" per year). This condition is not typical of a large portion of American railroad track. This should be considered when relating FAST results to areas with different rainfall and resulting drainage conditions.

BALLAST SHOULDER WIDTH TEST

Section 15 contains two 550-ft subsections, labeled A and B, with 6" and 18" ballast shoulder widths (BSW), respectively, as the principal section variables. There are no other known differences between the subsections which could affect their performance. Standard 136 lb/yd jointed rail, on 7" x 9" x 8.5' wood ties on 19.5" centers, are the common track components throughout Section 15. The ballast is an American Railway Engineering Association (AREA) No. 4 gradation blast furnace slag from a local source. Turnouts bound either end of the test section.

The data from the whole of each subsection were not used because of influence from the turnouts. It was evident from the maintenance data that the turnouts had a very great effect extending well into each test section. For that reason, data from 125 ft of test section adjoining each turnout were ignored. Similarly, data were ignored in a 50-ft transition zone between the subsections.

The ballast shoulder is, for purposes of this experiment, defined as the distance along the horizontal surface of ballast, measured from the tie end to the point where the surface breaks into an obvious slope. Measuring the BSW is, therefore, not a precise procedure and requires a great deal of subjective judgment, especially when rounding of the shoulder occurs, as was quite often the case at FAST.

Mean and standard deviations of shoulder width for the duration of the experiment were calculated and are shown below:

Track Subsection	15A	15B
BSW: Mean	9.4"	16.9"
Standard Deviation	3.3"	5.0"

From the student's T test for statistical significance, the shoulder width difference is significant at the 99.9% level. However, the large variation in measured shoulder width as indicated by the standard deviations means that two subsections can be recognized as having different shoulder widths; the magnitude of the difference cannot be precisely defined.

The track parameter believed to be most affected by ballast shoulder width is the horizontal, or lateral, track stiffness. Accordingly, horizontal track stiffness (HTS) measurements were used to characterize the lateral resistance of Section 15 for comparison with available data. However, several procedural inconsistencies and sources of uncertainty were found in the FAST HTS measurement,¹ so the following HTS data are provided only as general information, not as a source for future comparisons.

The HTS measurements consisted of a horizontal load applied through a yoke to two points on the rail. The rail displacement was measured at the centerline and on five ties on either side of the load application points.

The data are quite variable and show little or no effect of BSW, quite contrary to previous experiments that have indicated a pronounced increase in HTS as the BSW increases from 6" to about 12".^{2 3}

Mean load values at two rail displacements from the FAST tests are:

Track Subsection	15A	15B
0.05" rail displacement	6.3 kips	6.0 kips
0.20" rail displacement	13.2 kips	14.3 kips

It has been theorized that the real effect of ballast shoulder width would show up at higher displacements (up to 1"). However, this cannot be verified since at FAST the test was performed to a maximum of only slightly greater than 0.2".

Section maintenance is one of the most important measures of section performance used in this experiment. Maintenance hour expenditures in Subsections A and B were recorded and plotted versus MGT. Figure 2 shows the cumulative maintenance labor calculated per track mile. The figure shows that nearly 40% more hours were expended in Subsection A, with the 6" BSW, than in Subsection B, with the 18" BSW. The paired T test shows the maintenance hour differences not to be statistically significant. This is due to the fact that maintenance occurred at irregular intervals creating a large standard deviation.

Track geometry car data between 50 and 438 MGT were analyzed to determine the effect of shoulder width on the rate of track geometry deterioration; no data

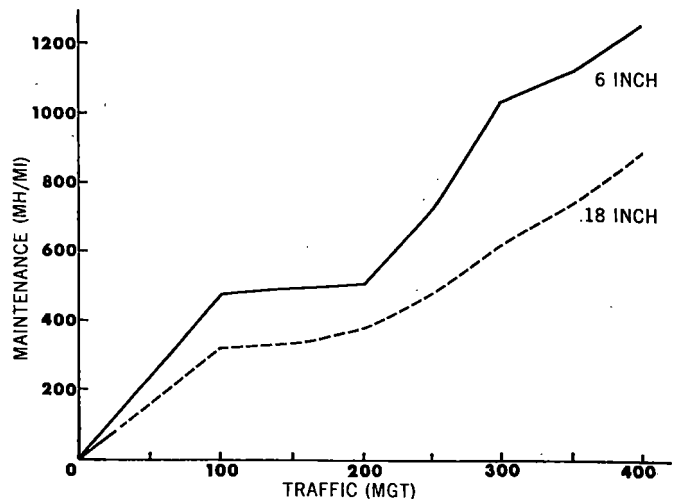


FIGURE 2. CUMULATIVE MAINTENANCE

were available prior to 50 MGT. Geometry parameters measured were profile (left and right), alignment (left and right), twist, gage, and superelevation. FAST Class 6 limits were used to maximize the amount of data available for comparison of the two subsections, since the FAST limits are more stringent than FRA Class 6 and yield a higher number of exceptions. At 25 MGT intervals, the percent of each subsection exceeding the Class 6 track geometry limit was calculated for each parameter. The profile parameter shows the largest amount of deviation from the limits, and Figure 3 records the average percentage of track containing profile exceptions. Up to approximately 175 MGT, both subsections exhibited roughly equivalent surface deterioration. However, after tamping performed at 175 MGT, the 18" BSW section retained a generally constant profile exception level, while the 6" section level increased significantly. Out-of-face surfacing was performed at approximately 430 MGT, and brought the exception level in each section to nearly zero. Alignment and twist exceptions were also generally higher for the 6" section, as also shown in Figure 3. The paired T test shows the exception-differences for each parameter to be statistically significant at the 99% level.

As demonstrated by the above data, an increase in ballast shoulder width can result in a reduction in track maintenance effort and reduce the rate of track geometry deterioration.

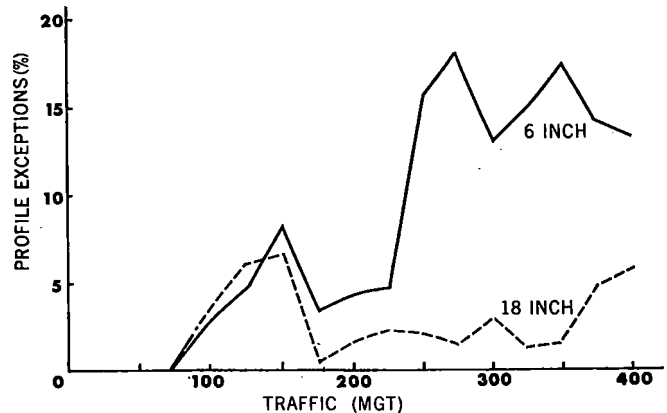


FIGURE 3. TRACK GEOMETRY PROFILE EXCEPTIONS

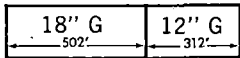
BALLAST TYPE AND DEPTH TESTS

Section 18 consists of two subsections of granite ballast with nominal 12" and 18" ballast depths beneath the ties. Section 20 is made up of nine subsections, one of 6" deep granite and the others of 12" and 18" depths of each of the following: traprock, slag, and limestone from two different sources. Petrographic analysis has shown the latter materials to be primarily dolomite while the other is dolomite limestone. Sections 18 and 20 are both tangent track, with jointed rail on wood ties. The section layouts are shown in Figure 4.

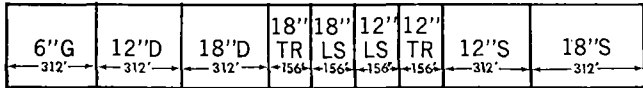
Following are the initial AREA classifications for each ballast type:

Wyoming	Granite	-	AREA 5
Illinois	Dolomite	-	AREA 4
Pennsylvania	Traprock	-	AREA 3-4 (falls between limits)
Indiana	Limestone	-	AREA 4
Colorado	Slag	-	AREA 4

SECTION 18



SECTION 20



LEGEND:
 G WYOMING GRANITE
 D ILLINOIS DOLOMITE
 TR PENNSYLVANIA TRAPROCK
 LS INDIANA LIMESTONE
 S COLORADO SLAG

FIGURE 4. BALLAST TYPE AND DEPTH TEST SECTIONS.

As for the shoulder width experiment, track geometry data were analyzed to provide a comparison of the track geometry degradation rates for Sections 18 and 20. Figure 5a shows a plot of average profile exceptions versus traffic for the five ballast materials. The drop at 175 MGT occurred as a result of surfacing and lining; the sudden jump at 225 MGT has yet to be explained. Figure 5b is a similar plot of alignment exceptions versus traffic. Track maintenance-hour expenditures were recorded and calculated on a manhours per mile basis. Figure 6 shows the results for all subsections of each ballast type. The most obvious conclusion drawn from the two plots is that the limestone shows more track geometry exceptions and higher maintenance-hour expenditures. The ballast showing the best performance based on track geometry and maintenance was the slag.

The principal subsections for the ballast depth test are the 18", 12" (both in Section 18) and 6" (Section 20) depths of granite. Figure 7 shows the variation in profile and alignment exception percentages with traffic for the three subsections. As

(MEAN 0-425 MGT)

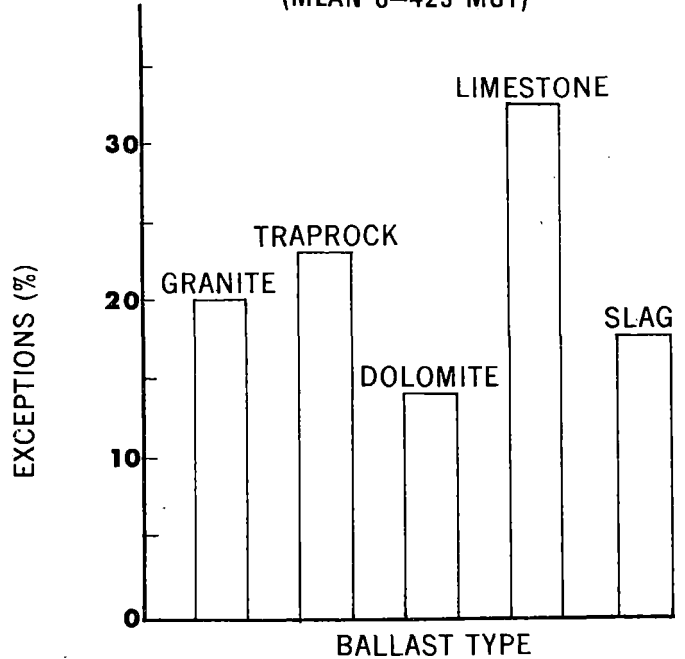


FIGURE 5a. TRACK GEOMETRY PROFILE.

(MEAN 0-425 MGT)

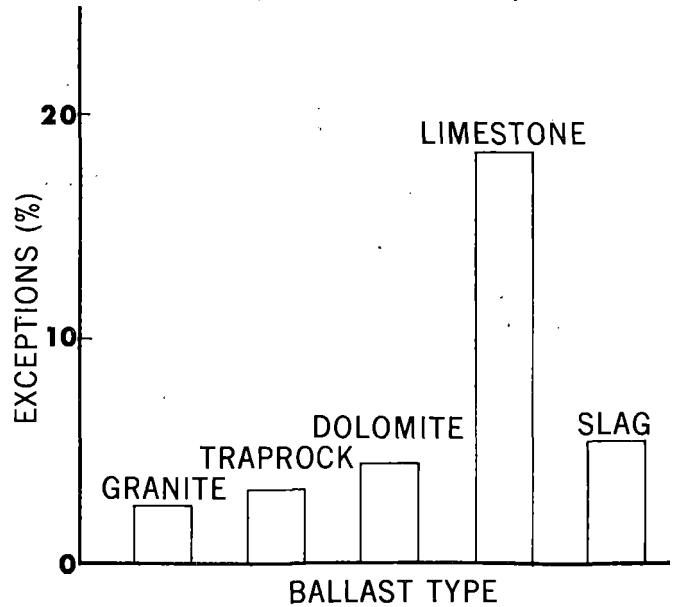


FIGURE 5b. TRACK GEOMETRY ALIGNMENT.

can be seen in both plots, the 12" ballast depth exhibited by far the least amount of track geometry deterioration.

The results of the ballast depth test show that deeper is not always better. A minimum ballast depth is required to reduce the stress applied to the subgrade to an allowable level which is dependent upon the type of soil making up the subgrade. However, increasing the ballast depth above this minimum may increase the rate of track geometry deterioration and thus increase the track maintenance expenditures.

(0-425 MGT)

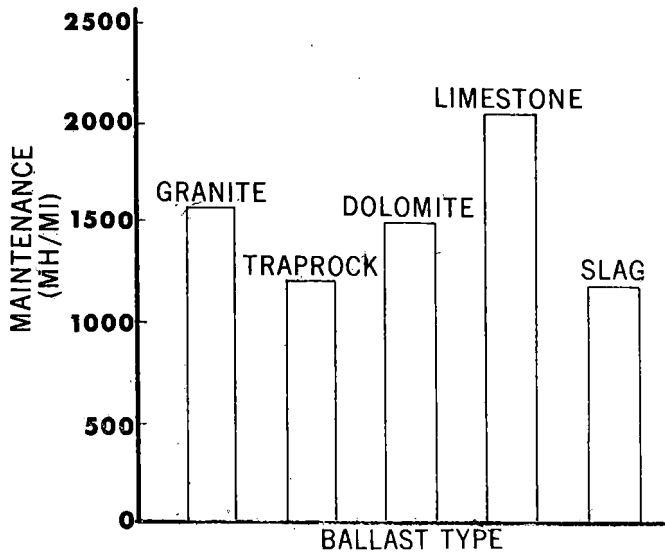


FIGURE 6. TOTAL MAINTENANCE EXPENDITURES.

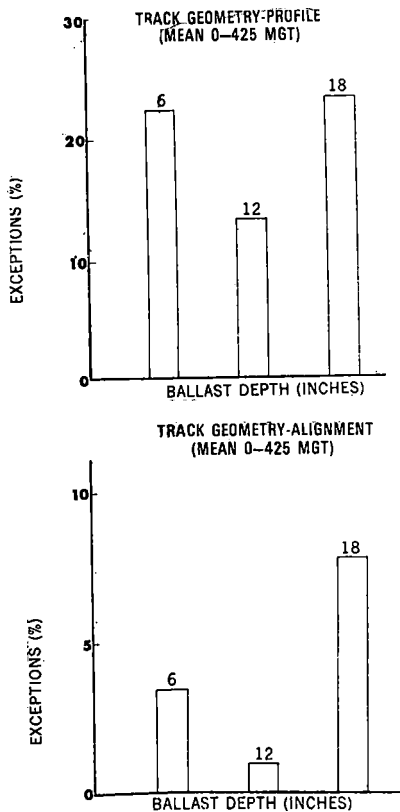


FIGURE 7. BALLAST DEPTH TEST.

Numerous other tests were conducted on the various ballast subsections. These included physical state tests (ballast density, lateral tie push, and plate load);⁴ static measurement of long-term ballast, subballast, and subgrade deformation; and dynamic measurement of deformations and stress applied to the subgrade.⁵ Considerable data were collected concerning the effects of track maintenance on ballast physical state, and the dynamic response of the track substructure due to train loading. There were no significant differences in these test parameters comparing the various ballast types and depths.

REBUILD OF FAST SECTIONS 03 and 17

Section 17 has been a test section for concrete ties since FAST began. Throughout the first 425 MGT, the 5° curve, 2% grade portion of Section 17 experienced numerous instances of fastener fallout and breakage, tie skewing, and some difficulty in maintaining surface and line. Poor ballast support was believed to be a major contributor to those occurrences. The ballast exhibited substantial degradation and intrusion of subballast and subgrade fines. Petrographic analysis revealed that the material is mineralogically and texturally classed as hornfels, a typically hard and brittle rock that is incapable of withstanding great shock effects.⁶ Yet, no significant ballast problems were experienced in Section 17, outside of the 5° curve, 2% grade portion, or in Sections 18 and 20, all of which contained this same ballast material.

In 1979 (at 425 MGT), the 5° curve of Section 17 was completely rebuilt from the subgrade level to provide better ballast support for the concrete tie test. Section 03 (wood ties, 5° curve 0% grade) was also rebuilt to provide two sections with uniform support conditions so that concrete ties could be installed at a later date to compare the effects of 0% versus 2% grade. Since the quantity of ballast required for the rebuild required donations from more than one source, a total of seven ballast types were used. Table 1 contains a geologic description and initial AREA grain size classifications.

Figures 8 and 9 show the section layouts.

Five of the ballasts are nominally called "granite" and labeled Type I through Type V. The word "granite" is used here as a generic term and not as an accurate indication of mineralogical content. A portion of the original hornfels was screened and replaced as a control subsection in Section 17; this is referred to as "CEB"--cleaned existing ballast. The traprock (NEC) in Section 17 is identical to that used in Section 22.

TABLE 1. SECTIONS 3 AND 17.

BALLAST	AREA CLASS
NORTH CAROLINA GRANITE	3-4
MINNESOTA GRANITE	3-4
GEORGIA GRANITE	24
ARKANSAS GRANITE	3-4
WISCONSIN QUARTZITE	24-3
NEW YORK TRAPROCK	3

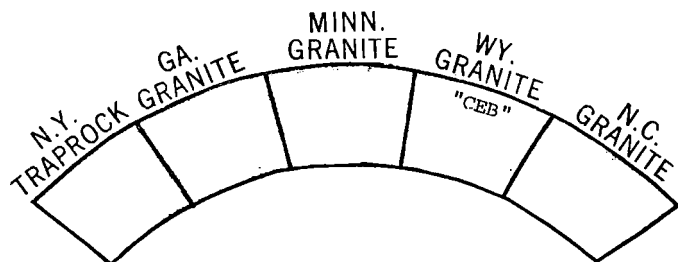


FIGURE 8. REBUILT PORTION OF SECTION 17 (CONCRETE TIES).

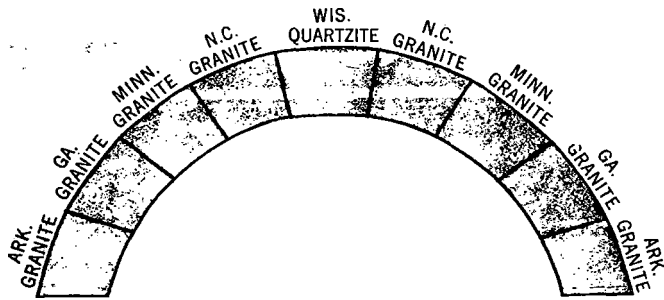


FIGURE 9. SECTION 3 (WOOD TIES).

Due to the number of ballasts used, a large number of measurements are being taken to determine whether uniform support conditions exist within Sections 03 and 17. Brief descriptions of the measurements and summaries of the findings to date follow.

Approximately 10 to 15 ballast samples were collected in each ballast subsection during reconstruction and after 100 MGT of additional traffic (525 MGT). The initial samples were collected at random, while the later samples were taken from under the tie beneath the rail seat. The samples, which weighed 75 to 80 lbs each, were sieved to determine grain size distributions. Georgia granite ballast showed the least amount of degradation; Figures 10 and 11 show its change in grain size distribution for Sections 17 and 03, respectively. Minnesota granite exhibited more degradation, as seen in Figures 12 and 13. Curiously, the Los Angeles abrasion loss values were higher for the Georgia Granite ballast (25%) than for Minnesota Granite (17%). This indicates that the Los Angeles abrasion test is not always a good predictor of ballast degradation. Another interesting finding from the degradation measurements is that through 200 MGT, the much maligned hornfels (CEB) is performing better with respect to degradation than all the Georgia Granite ballast in Section 17.

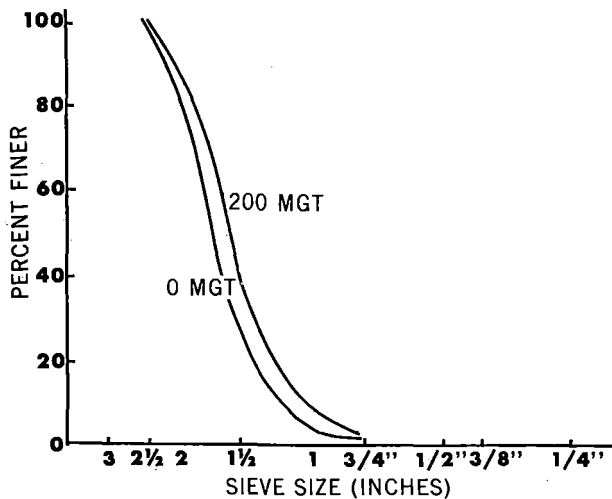


FIGURE 10. CHANGE IN GRAIN SIZE DISTRIBUTION GEORGIA GRANITE BALLAST - SECTION 3 (WOOD TIES).

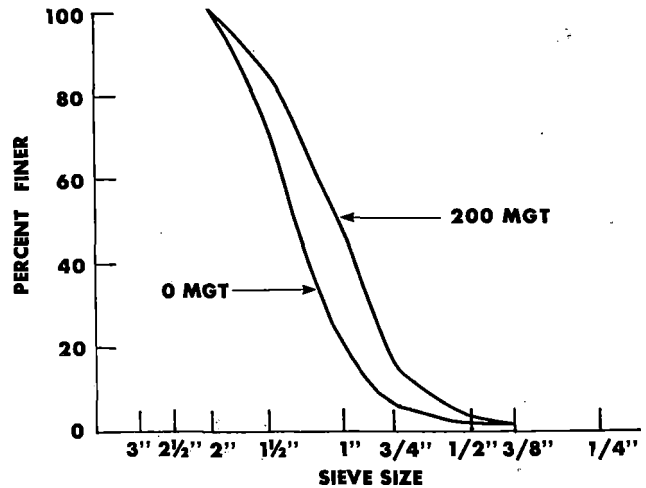


FIGURE 11. CHANGE IN GRAIN SIZE DISTRIBUTION MINNESOTA GRANITE BALLAST SECTION 3 (WOOD TIES).

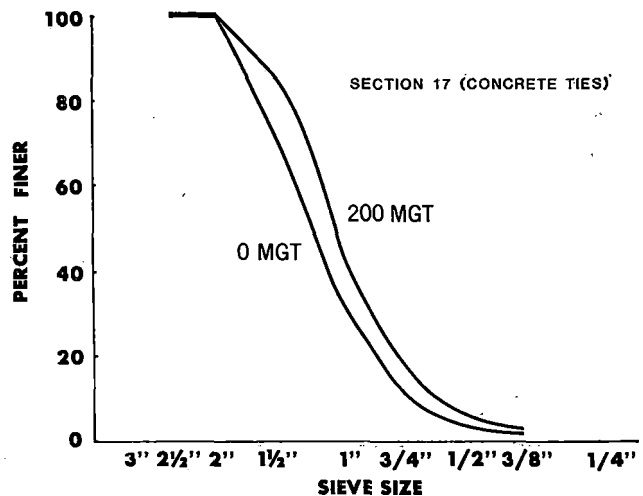


FIGURE 12. CHANGE IN GRAIN SIZE DISTRIBUTION MINNESOTA GRANITE BALLAST.

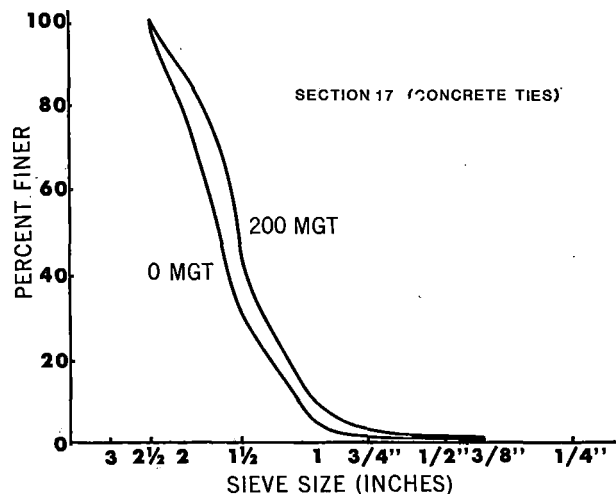


FIGURE 13. CHANGE IN GRAIN SIZE DISTRIBUTION GEORGIA GRANITE BALLAST - SECTION 17 (CONCRETE TIES).

Track settlement is calculated by measuring top of rail elevation to an accuracy of approximately 0.01 ft at 20-ft intervals throughout each test section. Plotting average settlement versus traffic (MGT) yields curves such as those shown in Figure 14. A large percentage of the total settlement is in the first 5-10 MGT of traffic. Settlement continues with additional traffic but at a much slower rate. Analysis of settlement data has shown no correlation between track settlement and ballast type. However, in Section 03, the settlement appears to vary with position in curve. As shown in Figure 14, the mean settlement is highest in the beginning of the section (ties 0-654) and lowest at the end ties (ties 1399-2303). Analysis of track geometry superelevation data also shows a position-in-curve effect for superelevation loss. These observations may not be important in themselves, but could have an impact on the results of other experiments, particularly the rail metallurgy and rail corrugation experiments.

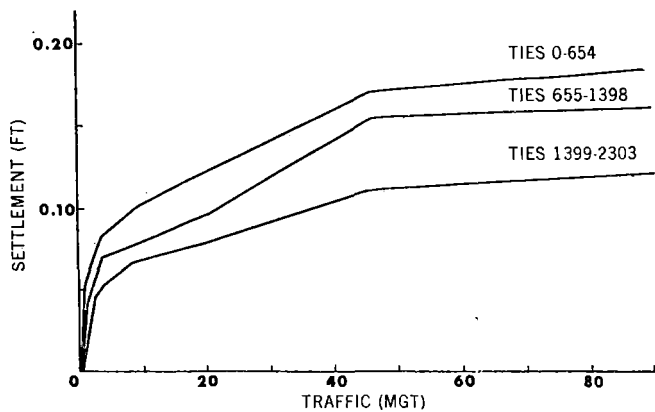


FIGURE 14. TRACK SETTLEMENT, SECTION 3.

Track modulus is determined by measuring vertical rail deflection under a known static wheel load and performing the appropriate calculations based on beam-on-an-elastic-foundation theory.⁷ Measurements were made at three locations, both on the inside and outside rail, in each ballast subsection. Table 2 presents the overall mean modulus values for each ballast type in Sections 03 and 17. Analysis of variance shows the difference between ballast types to be significant at the 99.9% level in both sections. An interesting trend is shown in Figures 15 and 16. Mean modulus for each ballast type in Section 03 (Figure 15) and Section 17 (Figure 16) are plotted versus mean particle diameter (D_{50}). D_{50} is determined from gradation data and is the particle size at which the gradation curve intersects the 50 percentile line. Both figures show a general increase in particle size with D_{50} . The reason for this is unclear and deserves further investigation.

Lateral tie push tests were conducted on each ballast type section 03. These tests were performed, following the procedure described by Selig,⁸ after approximately 90 MGT of traffic and again after an out-of-face surfacing and lining of Section 03. Figure 17 shows the average load-deflection plots for each ballast type before maintenance (after 90 MGT of traffic), and Figure 18 gives the same plots after surfacing and lining. Two trends are evident from these figures. The maintenance operation reduced peak lateral resistance by roughly 50%.

TABLE 2. AVERAGE TRACK MODULUS FOR BALLAST TYPES IN SECTIONS 03 AND 17 (0-90 MGT).

<u>Section 03 - Wood Ties</u>	
<u>Ballast</u>	<u>Modulus (lb/in/in)</u>
Type I North Carolina Granite	2,700
Type II Minnesota Granite	3,000
Type III Georgia Granite	3,500
Type IV Arkansas Granite	2,300
Type V Wisconsin Quartzite	3,400
Average	3,000

<u>Section 17 - Concrete Ties</u>	
<u>Ballast</u>	<u>Modulus (lb/in/in)</u>
Type I North Carolina Granite	6,700
CEB	6,500
Type II Minnesota Granite	5,900
Type III Georgia Granite	9,000
NEC (N.Y. Traprock)	9,300
Average	7,500

Also, there is considerable variability in peak lateral resistance of various ballast types; for the pre-maintenance condition, the difference is pronounced. Analysis of variance shows the differences in lateral resistance between ballast for both pre and post-maintenance not to be statistically significant. However, for all ballast types, the differences between pre- and post-maintenance are significant at the 99% level.

GEOTEXTILES AT FAST

During the rebuild of the 5° curve 2% grade of Section 17, a 300-ft test zone of geotextiles was installed. Fabrics from three manufacturers, labeled Types I, II, and III, each with two different weights, were installed in 50-ft segments between ties 70-220. Type I is a nonwoven, polyester, continuous filament, needle punched fabric with weights of 4 oz/yd² and 6 oz/yd². Type II is nonwoven, polypropylene, continuous filament, also with 4 oz/yd² and 6 oz/yd² weights. Type III is nonwoven, polypropylene, staple filament, needle punched with 5 oz/yd² and 8 oz/yd² weights. The objective of the test is to explore the ability of geotextiles to prevent subgrade intrusion into the ballast and to provide added track strength. Lack of precipitation at Pueblo rules out investigation of drainage improvement capabilities. The original test layout called for 200 ft of two fabric types and 100 ft of track with no fabric to act as a control, all to be located within the 300 ft ballast Type I subsection. Just prior to installation, a third manufacturer was granted permission to place his fabric into the test, which eliminated this 100 ft of control in the subsection.

Plate load tests⁹ were conducted at six points on the ballast under tie locations (with the ties removed) in each fabric type and weight. Table 3 presents the plate load bearing pressures at deformations of 0.1" and 0.2" and shows the modulus as

SECTION 3 - WOOD TIES

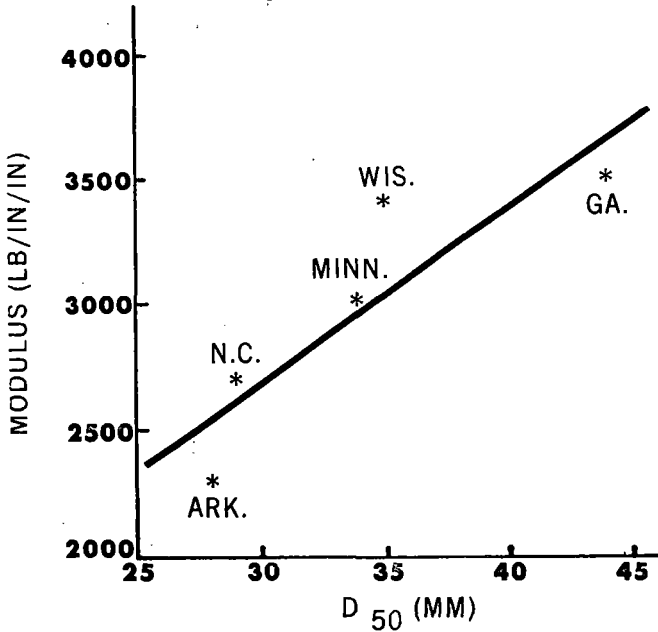


FIGURE 15. VARIATION OF TRACK MODULUS WITH PARTICLE SIZE.

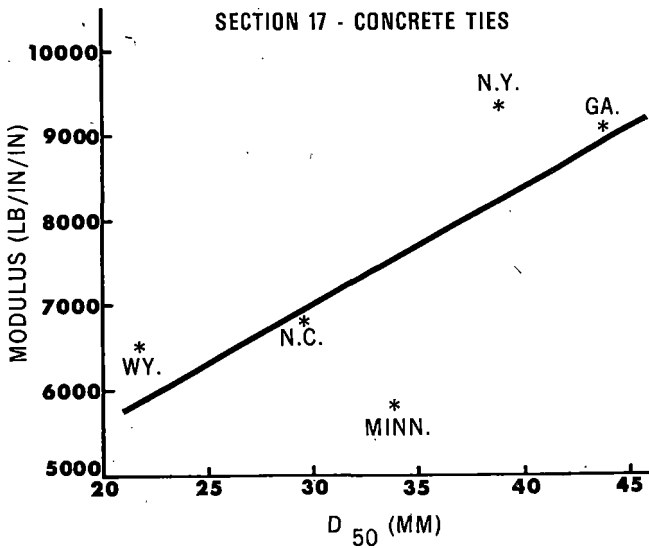


FIGURE 16. VARIATION OF TRACK MODULUS WITH PARTICLE SIZE.

measured from ASTM D-1195 procedure. Also given are the same parameters from Section 03, ballast Type I, which has no fabric; these are included only for comparison. Subgrade conditions vary somewhat between Sections 03, and 17,¹⁰ and due to the tie-type difference, ballast stiffnesses are subject to variation.

Small sample sizes prohibit demonstration of statistical significance. However, the following trends are evident. Except for the case at 0.1" deformation for fabric Type III, bearing pressures were higher for the heavier fabric weight for each type. All of the fabric sections, other than Type I, 4 oz/yd² at 0.1" deformations, exhibited higher pressures than in Section 03. Comparing fabric types, II appears to be the stiffest followed by I and then III. The higher stiffness in the Type II fabric coincides

SECTION 3 PRE-MAINTENANCE (WOOD TIES)

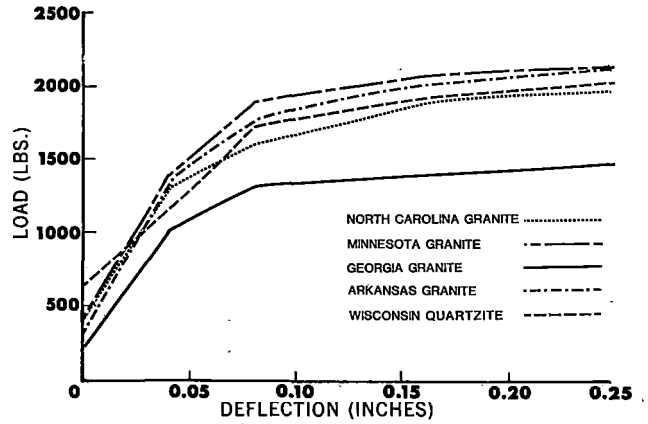


FIGURE 17. LATERAL TIE RESISTANCE.

SECTION 3 POST-MAINTENANCE (WOOD TIES)

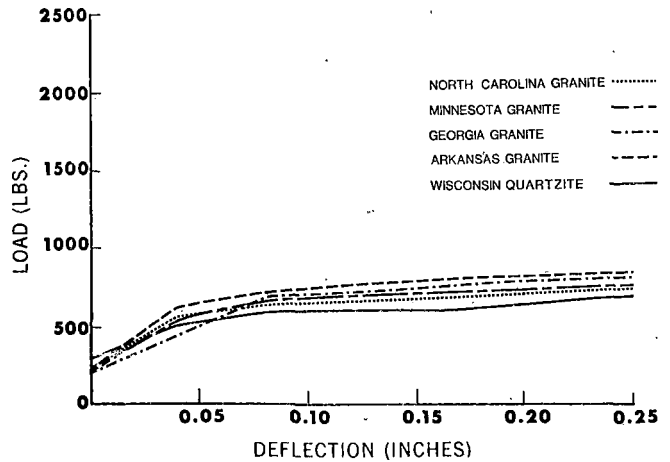


FIGURE 18. LATERAL TIE RESISTANCE.

TABLE 3. GEOTEXTILE TEST

Plate Bearing Pressure (lb/in²)

Deformation	Fabric Type-Weight (Section 17)						No Fabric Section 03
	I-6 oz/yd ²	I-4 oz/yd ²	II-6 oz/yd ²	II-4 oz/yd ²	III-8 oz/yd ²	III-5 oz/yd ²	
0.1 in	230	140	230	190	160	160	140
0.2 in	260	210	360	250	240	200	190

with its much higher modulus. It is surprising that these stiffness differences show up, when one considers the plate load tests were conducted on top of an 18" ballast layer covering the fabrics and the fact that FAST has a very strong subgrade. Further study is necessary to determine whether the fabrics and variations in modulus truly cause an increase in stiffness and if so, the magnitude of that increase.

Track modulus tests were also conducted at each fabric installation. Table 4 presents the average modulus from five tests at each installation. No relationship is evident between modulus and fabric type and weight.

TABLE 4. AVERAGE TRACK MODULUS FOR VARIOUS TYPE FABRIC INSTALLATIONS

Track Modulus (lb/in/in)					
Fabric Type-Weight (Section 17)					
I-6 oz/yd ²	I-4 oz/yd ²	II-6 oz/yd ²	II-4 oz/yd ²	III-8 oz/yd ²	III-5 oz/yd ²
6,800	6,400	7,300	6,700	6,600	7,000

In October 1981 (approximately 190 MGT after installation), the ballast was excavated at one tie location in each fabric type and weight to expose the surface of the fabric for inspection, and a piece of each fabric was removed and photographed. The inspections revealed that both weights of the Type I fabric contained numerous holes caused by penetration of the ballast particles as shown in Figure 19. The Type II fabric had also been penetrated, but to a lesser degree. Few holes were visible in the Type III fabric (see Figure 20). There was no visual

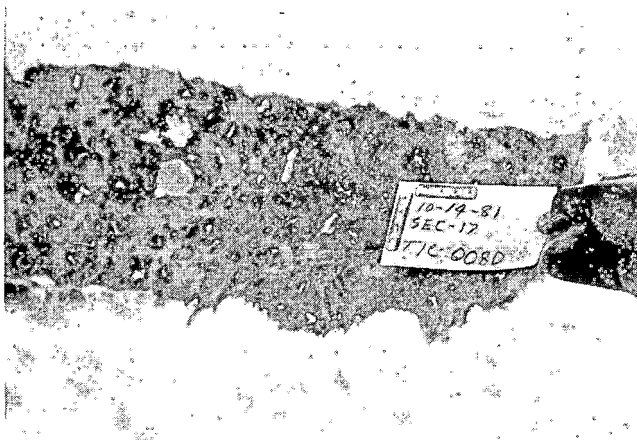


FIGURE 19. BALLAST PENETRATION OF TYPE I FABRIC.



FIGURE 20. BALLAST PENETRATION OF TYPE II FABRIC.

evidence of any intrusion of the subgrade into the ballast in any of the fabrics.

It is the opinion of the author that the fabric weights used in this FAST test are, in general, too light for most railroad applications. Weights of 15 oz/yd² and higher are more suitable.

REFERENCES

- 1 Dean, F. E. and Kish, A. Evaluation of Lateral Track Strength Measurements at FAST, FAST/TTC/ TN-08/05, Transportation Test Center, Pueblo, CO, March 31, 1979.
- 2 Hofman and Pfarrer Influence of Various Measures on the Lateral Displacement Resistance of the Unloaded Track, DT 44/D117/D, Research and Testing Laboratory of the International Railroad Association (ORE), Utrecht, May 1976.
- 3 Investigation of the Lateral Resistance of Concrete Tie Track, Interim Report No. 2, Project Agreement No. 4a, Task 1, Polish National Rail Research Institute, Warsaw, April 1979.
- 4 Selig, E. T. and Sluz, A. Ballast and Subgrade Response to Train Loads, presented at the Transportation Research Board, January 1978.
- 5 Selig, E. T., et al. Ballast Experiments Intermediate (175 MGT) Substructure Stress and Strain, FAST Test Memorandum in preparation, Transportation Test Center.
- 6 Smith, R. K. Composition Analysis Report, University of Southern Colorado, Pueblo, CO, 1978.
- 7 Zarembski, A. M. and Choros, J. On the Measurement and Calculation of Vertical Track Modulus, Association of American Railroads, Report No. R-392, Chicago, IL, 1979.
- 8 Selig, E. T., Yoo, T. S., and Panuccio, C. M. Mechanics of Ballast Compaction - Volume I. Field Methods for Ballast Physical State Measurements, State University of New York at Buffalo, prepared for the Transportation Systems Center, Cambridge, MA, 1977.
- 9 Panuccio, C. M., Dowart, B., and Selig, E. T. Apparatus and Procedures for a Railroad Ballast Plate Index Test, Geotechnical Testing Journal, December 1978.
- 10 Rixner, J. J. and Johnson, K. E. Summary of the Subsurface Exploration Program Performed Prior to the 1979 FAST Rebuild of Sections 03, 17, and 22, FAST Technical Note in preparation, Transportation Test Center, Pueblo, CO.

QUESTIONS AND ANSWERS

Question 1

Will there be future test at FAST on heavier fabrics, i.e., 14-18 oz. and if so when?

Answer

There are currently no plans for future testing due to limitations described in the presentation.

Question 2

All the ballast material types supplied for the project are of high quality and used by a variety of railroads. Isn't it fair to say that all of these can do a suitable job and that a potential user should take the economics of a particular material into consideration when looking for a ballast source?

Answer

Only performance comparisons were provided. FAST does not attempt to provide these economic data. The user certainly must trade off performance and economic considerations when choosing a ballast material.

Question 3

Was a ballast compactor used after tamping to determine the effect this would have on lateral stability?

Answer

No.

Question 4

What is your opinion of the ability of the wet attrition test (developed by British Railways) to predict ballast performance?

Answer

I have seen no data comparing predictions to performance. A test program doing this is beneficial.

Question 5

There are wide differences in the properties of

Limestones in strength, L.A. Abrasion test results and other physical properties. Only one Limestone has been tested. Will different Limestones with different properties be tested in the future? Why was Limestone eliminated when Sections 17 and 03 were rebuilt?

Answer

- 1) There are currently no plans testing of limestone in the future.
- 2) It was the conscientious opinion of the planners of the rebuild that granite/granite like materials would be used to create as nearly uniform performance as possible so as not to adversely affect the tie/fastener and metallurgy tests.

Question 6

Slide shows installation of geotextile looks like textile is being spread out over the track. Where is the textile actually placed, and how is it placed?

Answer

Geotextile was not spread over the track. Fabric was placed on the subgrade surface. Approximately 6" of ballast was hand placed on top before placement of ties to avoid damaging fabric while placing ties.

Question 7

Have you considered a section containing a simulated situation involving poor drainage in which ballast could be evaluated in respect to mud seepage up over the ties (or the avoidance of such seepage) accompanied by moderate to severe tie pumping?

Answer

It has been considered but never implemented due mostly to cost factors and logistics of moving the water.

Question 8

In soil mechanics, molding in foundries and ceramics manufacturing average grain size is not sufficient for evaluations and grain size distribution is used. Have you looked into this for ballast evaluation?

Answer

The only time average grain size was used in

correlating track modulus to ballast properties. Correlation with grain size was much better than with grain size distribution.

Question 9

Would you please explain why the deflection of subgrade still increases significantly after 200 MGT traffic loading? How to define the good subgrade what are the major parameters and characteristics?

Answer

1) Subgrade deflection still increases after 200 MGT but much slower than at the initial rate. I would guess that in the next 200 MGT the deflection rate will be reduced to near zero. This is consistent with previous data.

2) A good subgrade has sufficient shear strength to support loads supplied by the ballast, has minimum compressibility and is not affected by variations in moisture content temperature, etc.

TIE AND FASTENER PERFORMANCE

Howard G. Moody
Experiment Manager, Ties & Fasteners
Federal Railroad Administration

INTRODUCTION

Since the 1960's, and in some cases before, the deterioration of wood ties due to increasing loadings has led railroad researchers to investigate the use of an alternative to the standard wood tie and cut spike fastener system. The component deterioration of ties due to decay, splitting, crushing, or spike killing of the tie was in part blamed on the use of the cut spike fastener and on the increasing vertical and lateral loadings from the use of 100-ton cars and rigid roller bearing trucks.

Two experiments at FAST, the concrete tie and fastener experiment and the wood tie fastener experiment were designed to determine if alternative components would be efficient substitutes for the wood tie and cut spike fastener systems. A third experiment, wood ties, addresses the relative performance of fir and oak ties and manufactured ties. This was in response to a potential wood tie shortage in the future and to disposal problems with old ties. One of the manufactured ties could potentially use chipped, used ties as raw material. To date there have been three wood tie fastener tests, two concrete tie and fastener tests with a third about to begin, and two wood tie tests which will be discussed in the following papers.

The uniqueness of FAST, in providing an alternative to long term tie and fastener tests in revenue service, will be addressed in one paper. The relationship of fastener performance to laboratory testing will also be reported.

When using FAST results in either comparing with or interpreting for use in revenue service, the following conditions should be taken into account:

- o lack of flat wheels in the FAST consist;
- o uniformly high axle loads (few empties);
- o the short test duration and relatively mild, dry climate at FAST which tends to reduce environmental effects; and
- o the configuration of the track to which comparisons are being made.

SUMMARY

FAST, with some caveats, has proven to be an effective test of tie and fastener components.

Wood tie performance has shown that:

- o There is little difference in performance up to 610 MGT between hardwood (oak) ties and softwood (fir) ties in a 300 foot spiral to a 3° curve. There have been no component failures to date. Tie plate cutting has occurred, although only about 1/8" maximum, on both tie types. There was a small amount of gage widening although there was no difference between the tie types.

- o Cedrite ties up to 610 MGT in a tangent track test have shown a tendency to delaminate and plate cut except where rubber pads were used under the tie plate. There apparently was some variability in ties from the manufacturing process. This results in a large amount of tie plate cutting on a few specific ties and almost none on the other ties. A new test of Cedrite ties in a 5° curve should provide a better test and provide a comparison to standard sawn ties.
- o Two-piece laminated ties showed no signs of deterioration after 610 MGT. However, the use of B punch tie plates on this tie is not recommended. The crossgrain laminated ties have, in a few instances, delaminated at the glue line. This has not been serious enough, as yet, to remove the ties. These ties have been in track for about 250 MGT.
- o The injection-molded polyethylene tie plates have failed to perform adequately at FAST in a 5° curve and have been removed from testing. The compression-molded plates are still in the track after 190 MGT. The adzed area in the tie for these tie plates should be 5/8" to 3/4" deep to avoid premature failures.

Wood Tie Fastener performance to date has shown that:

- o Elastic fasteners (Double Elastic Spike, DE system, FORTAX Compression Clips, and Hixson) performed well at FAST in gage holding capacity. Where the coefficient of friction of steel on wood (.33) is not exceeded the lateral translation of different fastener types is the same. Above .33 the Intma Double Elastic Spike, the DE system and the FORTAX Compression Clip have lower dynamic deflections than cut spikes. Elastic fasteners provide greater rotational resistance than cut spikes for all load levels.
- o The elastic fasteners did not have any tie plate cutting. There was a minimal amount of tie plate cutting on cut spikes due to abrasion. Tie crushing or tie decay is not an issue at FAST.
- o Only elastic spikes required less long term maintenance than the cut spike fasteners. The other systems required as much or more maintenance. There are requirements for special tools and maintenance techniques with some of the elastic clips. These requirements need to be met when using these systems. For instance, the FORTAX clip requires a torque-limiting wrench for proper installation.

Concrete Tie and Fastener performance to date has shown that:

- o No concrete ties have been removed from track for service related failure. However, clips, soft pads, and insulators have had fractures, or failed in FAST, particularly in the 5° curve, 2 percent grade.
- o The use of concrete ties requires certain design considerations. CWR is a must since joints in concrete tie track cause fastener deterioration. A quality ballast with large particle size and good shape factor is needed to control tie skewing. The tie and fastener components should have tight dimensional tolerances to alleviate track construction and maintenance problems.
- o Concrete tie track is stiffer, both laterally and vertically than conventional wood tie track under similar ballast and subgrade conditions. Consequently, concrete tie track settles faster than wood tie track after tamping but the concrete tie track will resist buckling better than wood tie track.

Results of Laboratory and Field Correlation are:

- o FAST fastener performance can easily be represented in laboratory tests. Results of laboratory tests in both concrete and wood tie fastening systems were similar to those from the FAST tests.
- o Concrete tie performance is affected by impact loading from irregular wheels in revenue service. This performance is different than the FAST performance because of the lack of irregular wheels (i.e., slide flats) at FAST. However, these high impact loads can be attenuated somewhat by using a resilient tie pad.

RESULTS OF STANDARD WOOD TIE AND MANUFACTURED TIE EXPERIMENTS AT FAST

Lauress C. Collister
Experiment Manager, Wood Ties and Fasteners
Association of American Railroads (AAR)

Wood ties have been in use for over 100 years and have changed little in that period of time. They are bigger than the original ties and in the 1920's creosote treatment of the ties was introduced to increase resistance to decay. Wood ties are susceptible to splitting, fastener related damage (spike killing and plate cutting), decay, and, to a limited extent breakage and decay. In addition to the physical deterioration, there is a concern that the cost of wood ties, because of a reduction in the quantity of large trees and competition from other uses such as palleting, will escalate in the future to the point where alternative ties will be cost competitive.

The intent of the wood tie tests is to determine the ability of various tie types to resist mechanical wear and physical deterioration due to the action of the track under heavy wheel loads at FAST. Because the tests are conducted over a short period of time, and since the climate is very dry at Pueblo, it is unlikely that the environmental effects are significant.

The wood tie tests in FAST are conducted in Sections 2, 3, 4, 9, and 19.

The tests in 9 and 19 have been in track since the start of FAST. The majority of the tests in Sections 2, 3, and 4 began at 359.21 MGT in January 1979. However, tests of two components in Sections 2, 3, and 4 were begun at 419 MGT in December 1980.

Table 1 shows the layout of the current wood tie experiment and the tonnage to date in each segment. The test in Section 19 is a comparison of oak (hardwood) and fir (softwood) ties on two 300 ft spirals. The test in Section 9 compares various reconstituted and laminated ties on tangent track. Both sections are on 136 lb RE rail.

In the wood ties tests in Sections 2, 3, and 4, the test is divided into two 300 ft spiral segments and two 5 degree curve segments.

In nearly all of the tests the standard control segment is 7" x 9" x 8'6" ties on 19 1/2" centers with 1:40 7 3/4" x 14", "A" punch tie plates and 5/8" x 6" cut spikes. An exception to this is in Section 9 where there is no direct comparison to a control segment. Also in Section 9 there are "B" punch tie plates on the dowel laminated ties. In Sections 2, 3, 4, and 19 the ballast is either quartzite or granite. In Section 9 the ballast is blast furnace slag.

The tests in the spirals of Sections 2 and 4 are not

intended to be comparative because of changes in load environment as the spiral superelevation changes. The reason for the test is to demonstrate performances of components that are being tested in the curve under a less severe environment. This will allow the experimenter to evaluate performance over a broader range of conditions.

The experiment design is intended to limit the number of controlled variables affecting tie performance. Ties were selected from the same treatment or manufacturing lot. Ballast is constant in the wood tie test sections and the support conditions are uniform. A high degree of track maintenance is performed so that track geometry anomalies will not affect tie performance. The ties are the main variable except in the segments in Sections 2, 3, and 4 where polyethylene tie plates (which are 8" long) and 7 3/4' x 18" tie plates are being evaluated.

Properties affecting the test are the ability of the tie to resist mechanical wear which leads to tie plate cutting, and the ability to hold cut spikes to prevent subsequent spike killing and loss of gage.

The results to date have shown that in Section 19 there is little difference in performance between hardwood (oak) and softwood (fir) ties. As shown in Figure 1 the amount of vertical tie plate cutting in Section 19 is minimal through 610 MGT. The difference between softwood and hardwood ties in plate cutting is indistinguishable, as are the differences in the amount of maintenance, as shown in Figure 2. The amount of maintenance reflects only that maintenance directly related to tie and fastener performance such as spike replacement and redriving and repositioning rail anchors.

In Figure 3, the amount of track gage widening is shown versus MGT. Again no statistical difference is shown between hardwood and softwood ties. These

TABLE 1. CURRENT WOOD TIE TEST COMPONENTS.

<u>LOCATION</u>	<u>COMPONENT</u>	<u>MGT</u>
Section 9 Tangent	56 Fir Ties, AREA #12 Plates	610
Section 9 Tangent	84 Reconstituted Ties, AREA #12 Plates, 4 Cut Spikes	610
Section 9 Tangent	95 Dowel Laminated, AREA #12 Plates, 4 Cut Spikes	610
Section 9 Tangent	4 Plywood Laminated, AREA #12 Plates, 4 Cut Spikes	610
Section 19 300' Spiral	186 Fir Ties, AREA #12, 4 Cut Spikes	610
Section 19 300' Spiral	186 Oak Ties, AREA #12, 4 Cut Spikes	610
Section 2 300' Spiral	62 Reconstituted Ties, AREA #12 Plates, 5 Cut Spikes	250
Section 3 5° Curve	62 Reconstituted Ties, AREA #12 Plates, 5 Cut Spikes	250
Section 2 300' Spiral	31 Fir Ties, Polyethylene Tie Plates, 4 Cut Spikes	190
Section 3 5° Curve	31 Fir Ties, Polyethylene Tie Plates, 4 Cut Spikes	190
Section 2 300' Spiral	31 Oak Ties, Polyethylene Tie Plates, 4 Cut Spikes	190
Section 3 5° Curve	31 Oak Ties, Polyethylene Tie Plates, 4 Cut Spikes	190
Section 2 300' Spiral	62 Fir Ties, AREA #12 Tie Plates, 5 Cut Spikes	250
Section 3 5° Curve	62 Fir Ties, AREA #12 Tie Plates, 5 Cut Spikes	250
Section 3 5° Curve	62 Fir Ties, 18" AREA Tie Plates, 5 Cut Spikes	250
Section 4 300' Spiral	62 Fir Ties, 18" AREA Tie Plates, 5 Cut Spikes	250
Section 3 5° Curve	62 Fir Ties, AREA #12 Tie Plates, 5 Cut Spikes	250
Section 4 300' Spiral	62 Fir Ties, AREA #12 Tie Plates, 5 Cut Spikes	250
Section 3 5° Curve	62 Cross-Grain Laminated Fir Ties, 5 Cut Spikes, AREA #12 Tie Plates	250
Section 4 300' Spiral	62 Cross Grain Laminated Fir Ties, 5 Cut Spikes, AREA #12 Tie Plates	250

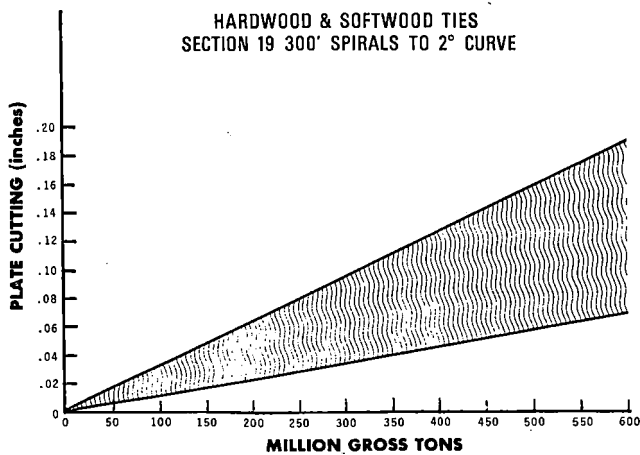


FIGURE 1. VERTICAL TIE PLATE CUTTING.

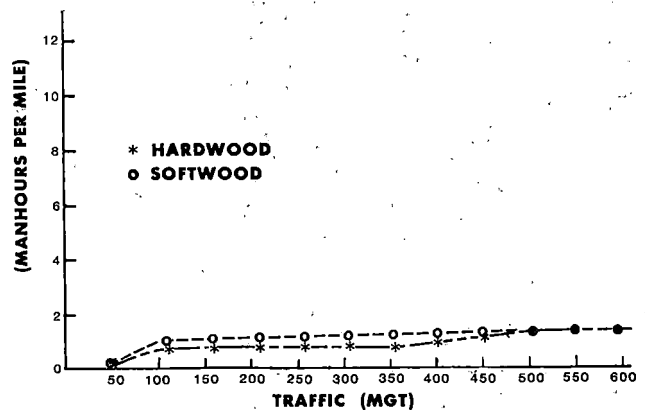


FIGURE 2. TIE MAINTENANCE (HARD AND SOFT WOOD).

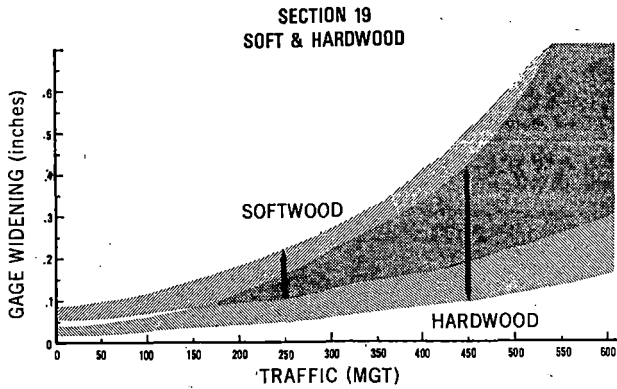


FIGURE 3. TRACK GEOMETRY GAGE WIDENING.

data were obtained from the track geometry car which imparts a 600 lb measurement load on the rail. With train operation producing lateral loads with a mean of about 3.5 kips, very little additional deflection would result. For this section track geometry car gage is an effective means of measuring actual gage widening performance.

In Section 9, nine Cedrite reconstituted ties have been removed in 610 MGT because of delaminations and breaking of the tie under the rail seat. A typical failure is shown in Figure 4. These ties, with the exception of the ties with 1/4" soft rubber tie plate pads under the rail seat, have also plate cut, seven of them severely. Figure 5 shows a plate cut tie without a tie pad and Figure 6 a tie with a tie pad. Even though these pads have protected the cedrite ties from being plate cut, early tie pad tests in Section 2, a 300' spiral into a 5° curve resulted in pad extrusion and failure after 359 MGT. An example of this type of failure is shown in Figure 7.



FIGURE 4. CEDRITE TIE DELAMINATIONS T-A-6.



FIGURE 5. PLATE CUT CEDRITE TIE WITHOUT A TIE PAD.

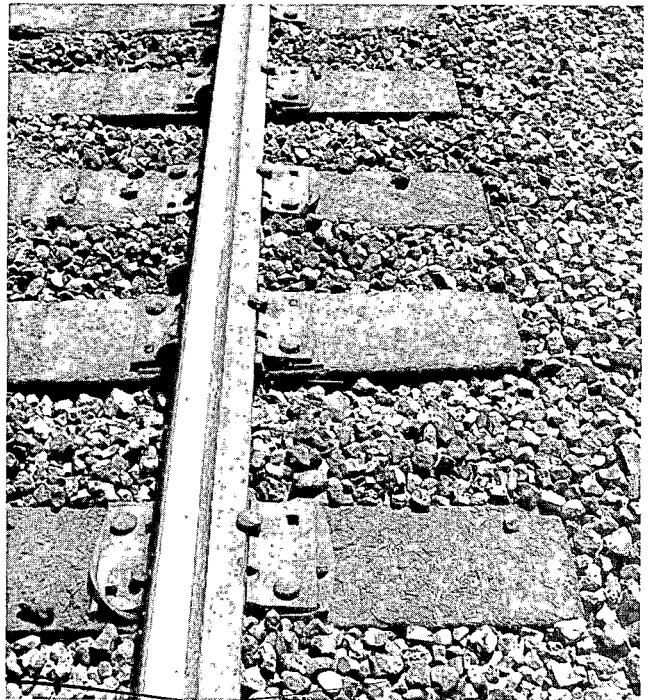


FIGURE 6. CEDRITE TIES WITH RUBBER TIE PADS.



FIGURE 7. TIE PAD EXTRUSION SECTION 2 AT 359 MGT.

In revenue service, Cedrite ties have performed well on one railroad. The ties were installed in 1974 on a 8 1/2 degree curve, 2 percent grade with 50 million gross tons of traffic a year. To date there have been six derailments on these ties and equivalent segments of solid sawn ties. A total of 3% of the cedrite ties have been replaced while over 70% of the solid sawn ties have been removed.

In addition to the Cedrite ties, Section 9 contains 100 dowel laminated ties. These ties are made from two solid sawn pieces 4 1/2" x 7" x 8'6" joined together with 5 four-fluted steel dowels. The ties have performed well to date. However, when originally installed, "B" punch AREA tie plates were used rather than "A" punch (see Figure 8 for configuration differences). As shown in Figure 9, the hold down spike in the "B" punch plate could easily split the tie and in effect make the hold down spike useless. The use of "B" punch plates is, in general, not recommended with solid sawn ties because of the nature of tie shrinkage, as shown in Figure 10. With the tie split most often occurring near the center of each face of the tie, it is relatively easy to aggravate the splitting and make the hold down spike ineffectual by using a "B" punch plate.

Four press laminated ties are in Section 9 as well. This tie is made from 5/8" veneer (plywood veneer) pressed and glued in layers to make a 7" x 9" x 8'6" tie. The four ties, while a very small sample, have performed well and show no signs of physical deterioration after 610 MGT. A test of similarly constructed laminated ties was started on the Pennsylvania Railroad in curved track near Altoona, Pennsylvania in 1954. These ties were visually inspected in the fall of 1980 and were "looking good". 96 of the original 100 ties are still in track.

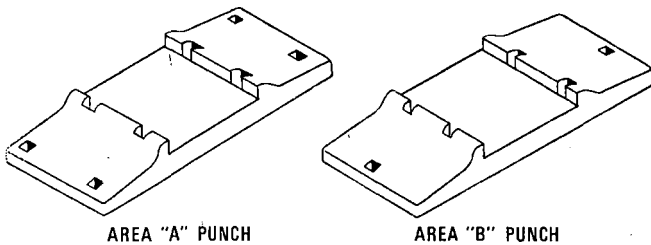


FIGURE 8. "A" AND "B" PUNCH PLATE CONFIGURATION.

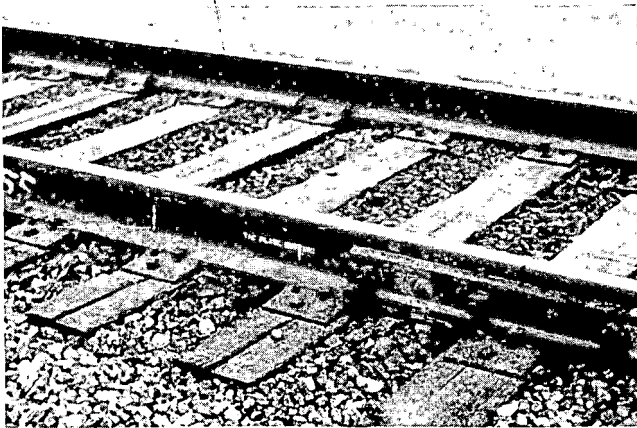


FIGURE 9. DOWEL LAMINATED TIES.

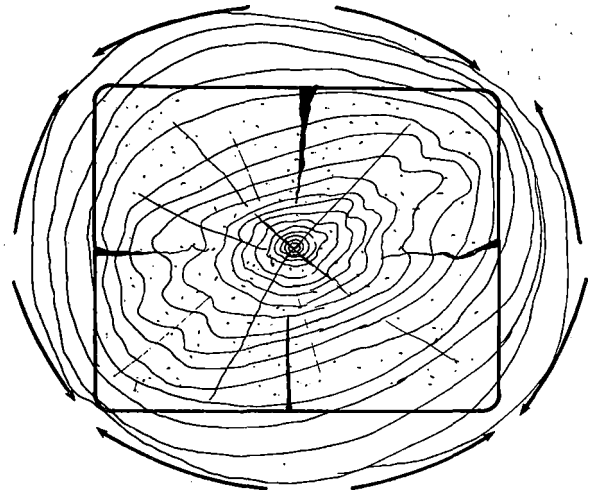


FIGURE 10. CONCEPTUAL VIEW OF TIE SHRINKAGE.

A more recent test of laminated ties has been conducted in Sections 3 and 4 of the FAST loop. These ties are cross grain laminated ties from Koppers Co. Referring to Figure 11 the laminae 1, 3, 5, and 7 of the tie are solid 1 3/8" x 7" x 8'-6". Laminae 2, 4, and 6, the three alternate laminae are made of 1 3/8" x 6" x 7" edge glued together to make a 1 3/8" x 7" x 8'-6" board. These seven pieces are then glued together to make a 7" x 9" x 8'-6" tie, having the 2nd, 4th, and 6th laminae, as mentioned above, made of vertical or end grain pieces. The 1st, 3rd, 5th, and 7th laminae are solid sawn with either tangential or edge grain boards. The end grain pieces are designed to improve the compressive strength of the face of the tie. With the exception of two ties which have partially delaminated as shown in Figure 12, these laminated ties have performed well for 253 MGT.

In addition, as a part of this test, 18" tie plates and 8" polyethylene tie plates are being tested. All are being compared to standard 14" AREA #12 plates on 7" x 9" x 8'6" fir ties. The polyethylene tie plate performance will be evaluated later in this report. Use of 18" plates over 14" plates is not justified from FAST data (188 MGT of experience).

As mentioned previously, a test of soft neoprene rubber tie pads was conducted for the first 359 MGT of traffic in Section 2, a 300 ft. spiral leading to a five degree curve. Damage to the tie pads was estimated from visual observations. The pads were grouped as having extruded a small, moderate, or extreme amount. It was established that 75% of the pads were in the small group, 15% in the moderate group, and 10% in the extreme group. No tie plate cutting was observed in the section protected by pads but there was also little evidence (<1/16") of tie plate cutting in comparable, unprotected ties to 359 MGT.

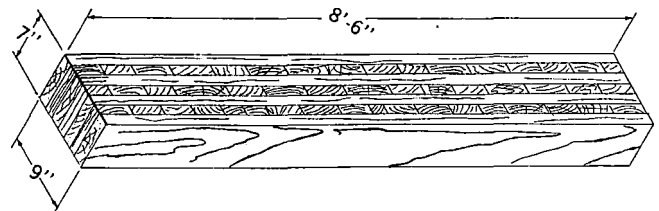


FIGURE 11. SCHEMATIC OF CROSS GRAIN LAMINATED TIE.

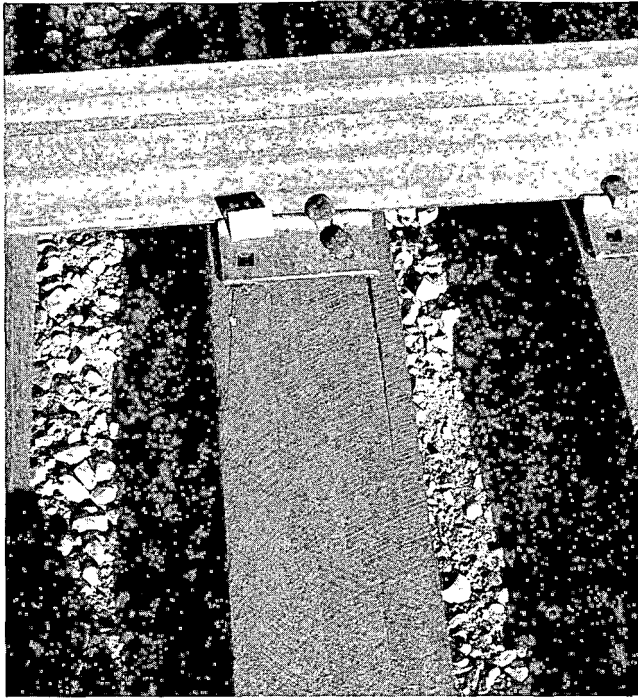


FIGURE 12. CROSS GRAIN LAMINATED TIE DELAMINATION.

Several years ago, after an extensive study of causes of failure of ties on a large railroad, several tests of many types of pads were installed. The life of pads was determined to be 5-15 years. This coupled with the fact that at that time only 25% of ties were removed for plate cutting, indicated that pads could only be specified in special locations, and not for universal use.

Spike pullout data is shown in Table 2 for oak, fir and reconstituted ties at FAST and from some laboratory tests conducted by the AAR. There are differences in the spike retention capacity among the different tie types after 600 MGT. The increase in spike pullout resistance after 100 MGT is attributed to the creosote acting less as a lubricant when the tie was used than when it was new.

TABLE 2. SPIKE PULLOUT FOR OAK, FIR AND RECONSTITUTED TIES.

TIE TYPE	AVERAGE SPIKE PULLOUT FORCE (LB)		
	NEW	AFTER 100 MGT	AFTER 600+MGT
Hardwood:			
FAST (mixed hardwood)	2780	3030	3850
Red Oak	5130*	4688*	
White Oak	5712*	4552*	
Softwood:			
FAST (softwood)	1300	3800	2250
Pine	1481*	2796*	
Reconstituted:	4094*	4575*	878

*Lab Simulation: 2.5 million load cycles, 20,000 lb vertical load, 7,500 lb lateral load

In the early 1950's the American Railway Engineering Association in conjunction with the National Lumber Manufacturing Association made a study of tie failure using the laboratory facilities of the Timber Engineering Company (TECO). Dr. Farber and Dr. Shasha of TECO discovered the reaction of the ferric oxide (spikes and plates) with the acetic acid of oak ties produces a chemical deterioration in the wood, especially around the spikes, causing a tie failure we call spike killed. This type of wear when added to the mechanical wear on the spike and tie plate causes gage widening. Several products have been developed to combat this. The two worth mentioning are: (a) a mixture of iron filings in a sal ammoniac solution; this dry mixture, about 3 oz., is poured into the empty spike hole, and 4 drops of water added. The spike is then redriven and the reaction of rusting sets up; and (b) an asphalt filled sand; this material is poured into the spike hole, about 3 oz., and the spike redriven. The heat of friction of the spike being driven into the mixture caused a thermal reaction. Using either of these solutions should increase the expected tie life. Various estimates of this increase have been indicated with a range of 4-8 years being the most reliable.

The test of the polyethylene tie plates in Sections 2 and 3 has gone through two phases to date. In the first test the plates were removed after 34 MGT due to excessive damage to 100 of 248 plates in service. This damage consisted of field side shoulders sheared off level with the rail seat, longitudinal cracks or break along the field side shoulder fillet and transverse cracks starting at the field side shoulder. An example of the shear cracks is shown in Figure 13 and a transverse break in Figure 14.

As a result of these failures and a subsequent dynamic wide gage of about 3/8" above static gage, the plates were removed and replaced with new ties and plates. The principal cause of the shear failures was a shallow 1/4" dap in the tie which was increased to 5/8" in subsequent tests.

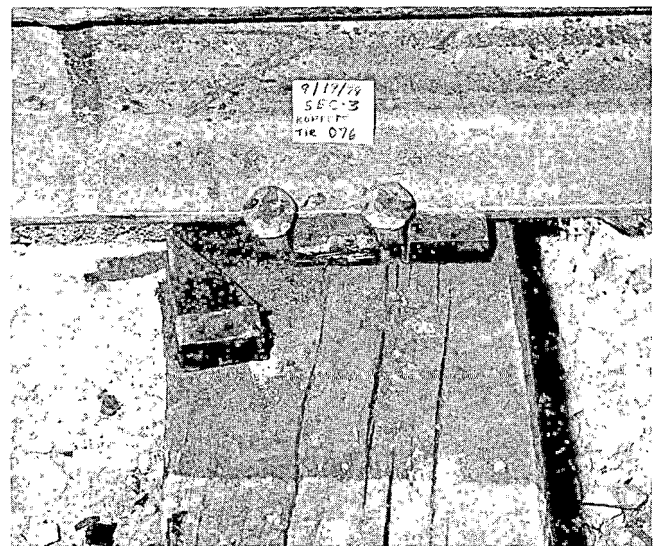


FIGURE 13. KOPPERS POLYETHYLENE TIE PLATE SHEAR FAILURE.

QUESTIONS AND ANSWERS

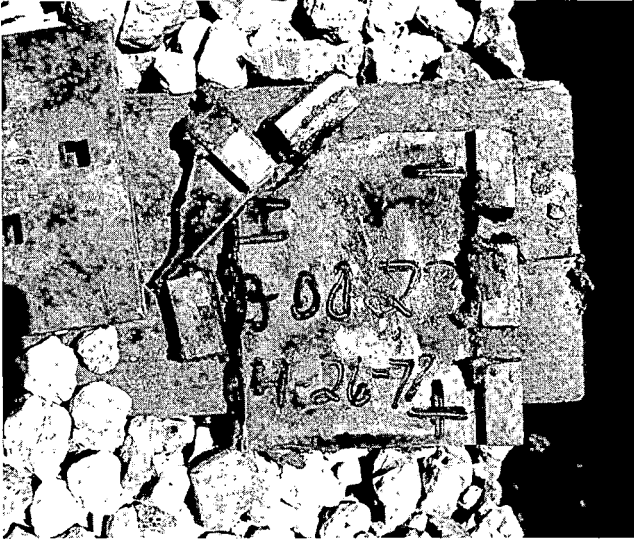


FIGURE 14. KOPPERS POLYETHYLENE TIE PLATE TRANSVERSE FAILURE.

The new tie plates for the second test were in track for 137 MGT. Failures of the field side shoulder similar to those that occurred in the first test, except with fewer shear failures, had allowed rail lateral movement to the point where excess low rail head metal flow had occurred. This flow which did not occur on standard AREA plates, resulted in the removal of the rail and the polyethylene tie plates. During the investigation, it was noticed that the majority of the failed plates were injection molded plates rather than compression molded plates. These two types of plates were installed in the curve in equal quantities. The injection molded plates were also removed from the test in Section 2, leaving only the compression molded plates in test at FAST.

REFERENCES

1. Loomis, A. V. and Anyos, T. - Refurbishment of Railroad Cross Ties, FRA Report, FRA/ORD 77/76, SRI December 1977 PB 283447.
2. Tie Plate Pad Performance, Section 02 TN 79-19, July 1979.
3. Failure of Polyethylene Tie Plates, Sections 02 and 03, TN-16, May 1980.

Question 1

With regard to the Laminated Tie Experiment, were any of the ties inserted with the lamination horizontal (versus vertical to reduce splitting and moisture penetration)?

Answer

No, not at FAST; however, on the Pennsylvania Railroad at Altoona, Pennsylvania a test section of 100 horizontal laminated ties was installed in 1954. In 1980, 96 of these ties were still in track.

Question 2

Are the 7-ply laminated ties being produced? If so, what is the relative cost compared to the standard sawn tie?

Answer

No, they are not commercially available, as yet. At the time the test ties were produced, the manufacturer indicated the ties could be produced for approximately \$50 each.

Question 3

The FAST test is conducted in a dry environment. What do you think would be the effect of wet conditions on the wood ties, particularly the reconstituted and laminated ties?

Answer

With regard to laminated ties, I believe this was answered in Question 1 (Mr. M. D. Kenyon's question). For reconstituted ties, a test section of 600 reconstituted ties was installed on the Union Pacific Railroad at Multnomah, Oregon in 1974. There is an annual rainfall of 100 inches there. To my knowledge, there have been no reported problems with these ties.

EVALUATION OF VARIOUS WOOD TIE FASTENERS UNDER FREIGHT RAILROAD SERVICE TESTING

Larry Daniels
Experiment Monitor, Wood Tie Fasteners
Boeing Services International, Inc.

Howard G. Moody
Experiment Manager, Ties & Fasteners
Federal Railroad Administration

Various alternative wood tie fastener systems have been evaluated at the FAST track to determine the performance of these systems in comparison with the cut spike system. There have been three fastener tests to date. The first two tests provided little information on the performance of the alternative fastening systems. In addition, there were a considerable number of component failures and maintenance problems, including spike killed ties. These tests were terminated prematurely. The third fastener test, however, has been comprehensive enough to allow a thorough evaluation. Descriptions of the test configuration, measurements, and load environment from this third test are presented, followed by an evaluation of component failures, maintenance, plate cutting, and gage widening performance for each system.

DESCRIPTION

The wood tie fastener tests have been exclusively located in a 5° curve on 1½ grade as shown in Figure 1. The train speed through this section is between 40-45 MPH in both directions.

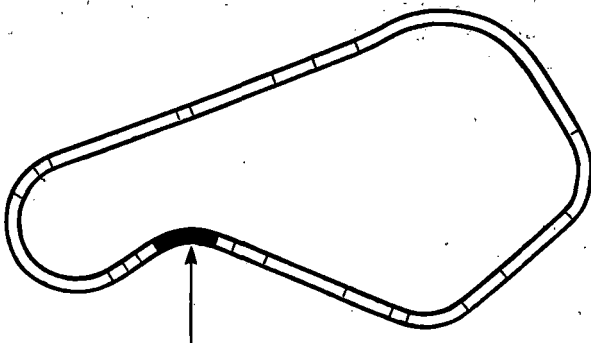


FIGURE 1. WOOD TIE FASTENER TEST LOCATION ON FAST LOOP.

Figure 2 shows a schematic of the test components in their relative position in the test. Each component test section is 100 feet long. All components shown were new at the start of test, January 1979, except the ballast and the rail, which was transposed at the beginning of this test. These components have been in track for 257 million gross tons (MGT) of traffic or about 7.8 million axle cycles.

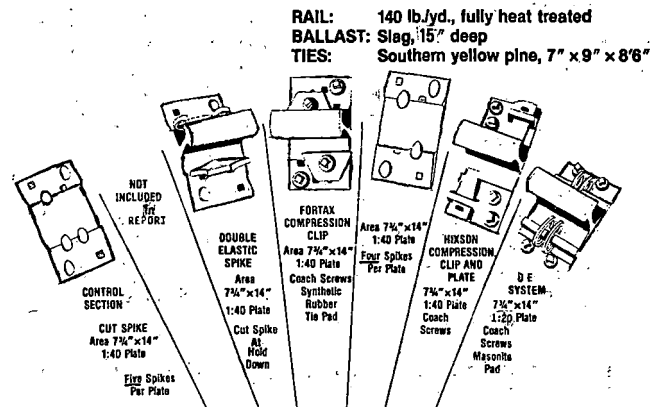


FIGURE 2. WOOD TIE FASTENER EXPERIMENT, SECTION 7.

The Double Elastic Spike is the only alternative fastener that fits standard AREA tie plates without modification. The FORTAX Compression Clip uses a standard AREA plate but requires four additional (non-conventional) holes per plate. All elastic fastener spring rates are between 4500-5000 lb/in when fully applied.

The second component test section from the left in Figure 2 contained the Pandrol Fastener System. The plate used in this system experienced failures at the field side shoulder in sufficient number to justify test termination (Figure 3). These same plates were also included in two previous FAST

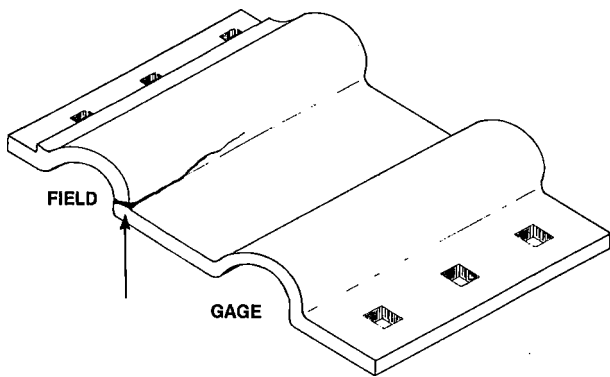


FIGURE 3. PANDROL PLATE TYPICAL FAILURE.

tests. In the first test only one plate out of a total of 496 plates failed after 135 million gross tons or 4.3 million cycles. However, in the second test, 65 plates out of a population of 752 failed in 141 million gross tons of traffic or about 4.5 million load cycles. This pattern of failure continued in the third test with the result that the test of these plates with the fastener in four different test segments was terminated. By that time, approximately 75% of the plates had failed after 465 total MGT of traffic.

Service tests of this plate on the Santa Fe Railroad are beginning to experience the same type of failure observed at FAST. The Bessemer and Lake Erie Railroad, however, has not experienced these failures, but that test has only accumulated approximately 60 MGT.

These Pandrol tie plates may be suitable for branch line service or where track loadings are less severe than FAST. It is not recommended that the plates be used in heavy tonnage lines where the wheel/rail loads approximate those at FAST.

Because of the constant need to replace the tie plates and their premature removal from test, there were incomplete data on this fastener system. No comparative results will be presented. The manufacturer has since redesigned the tie plate to incorporate a heavier cross section in the fracture area of the plates. These new plates have not been tested at FAST.

MEASUREMENTS

There are two distinct types of measurements incorporated into this test. The first type identifies the fastener wear and damage performance. These measurements include component failures, track maintenance requirements, static track gage, rail wear, and track geometry car gage. The second group of measurements are used to characterize the dynamic performance. These measurements include wheel/rail vertical and lateral loads, rail/tie deflection, and track modulus. These measurements were instituted at 75 MGT after the start of the test. The other measurements of component performance began at the start of the test.

The load and deflection measurements are taken at one location in the center of each component test

section on the high rail only. The dynamic loads and deflections are taken during one train pass approximately every 50 MGT. Loads are measured by rail mounted strain gages; deflections are measured relative to the tie by linear displacement transducers (Figure 4).

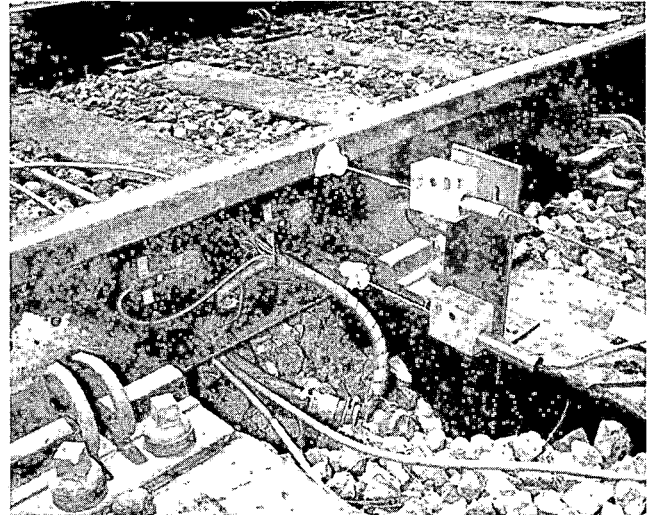


FIGURE 4. STRAIN GAGES AND LINEAR DISPLACEMENT TRANSDUCERS.

The vertical and lateral loads, rail head, and base deflections are recorded simultaneously at each location during a train pass so that load/deflection characteristics can be easily determined.

TEST ENVIRONMENT AND COMPONENT MAINTENANCE

The test environment at FAST consists of the train loads, the track configuration (previously discussed), and the track maintenance.

The FAST wheel/rail load environment is the principal governing characteristic which affects performance. These loads in the vertical and lateral plane are usually unique for each section at FAST, which is the principal reason for restricting a comparative fastener test to one curve segment. The wheel/rail loads are kept as uniform as possible by maintaining uniform track geometry and consist length, tonnage, and speed.

The wheel/rail loads in Section 7 are shown in Figure 5 as a joint probability of lateral and vertical loads at any level. For a perspective of revenue service loading, the same information is shown for a 10° curve taken on the Western Pacific Railroad at 25 MPH. Figure 5 shows a substantial difference in the vertical loadings between the mixed traffic loading of the Western Pacific and the FAST loadings, which are, by design, nearly equivalent to unit train loadings. However, the lateral loadings from the two sets of data show that FAST loading is nearly identical to service loading.

Other revenue service data were also examined to determine if the Western Pacific data were representative of the spectrum of wheel/rail loads. These

LOAD ENVIRONMENT

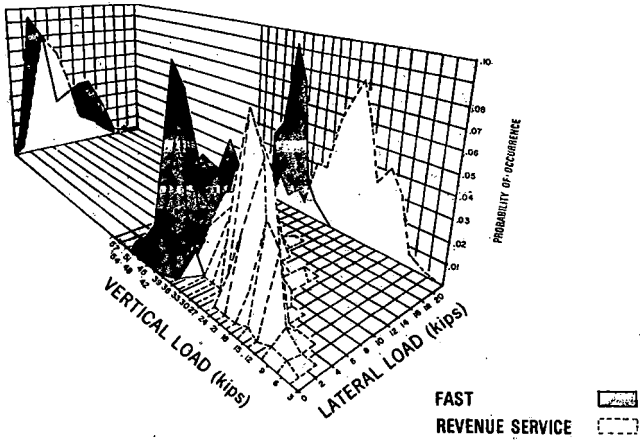


FIGURE 5. WHEEL/RAIL LOADS.

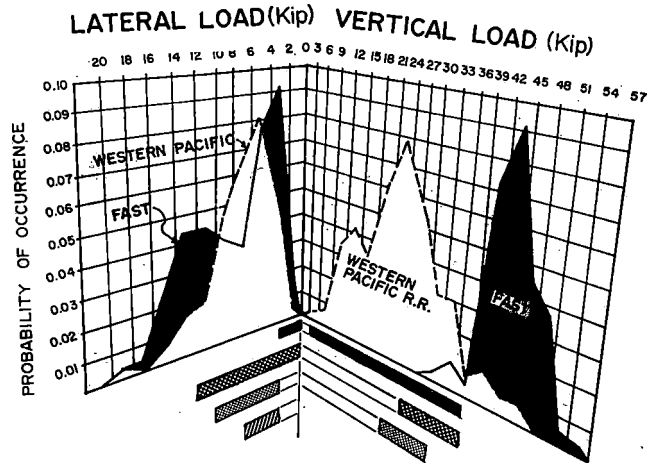
data, as shown in Figure 6, demonstrate that the Western Pacific data are an all encompassing representation of these other service sites. The broad spectrum of speeds and degree of curvature indicates that there is little variation due to speed and degree of curvature within the load spectrum.

With FAST's higher vertical loading but identical lateral loading compared to revenue service, the FAST lateral/vertical load ratio (L/V) is equal to or lower than revenue service L/V loading (Figure 7).

Therefore, the perception that FAST is a severe load environment applies to vertical loading but not to the L/V parameter, which is the essential load variable for evaluating fastener gage widening performance.

The FAST track Section 7 is maintained to achieve uniform test conditions for the components. In general, this conforms to FRA Class 5 at any given time; exceptions are allowed to Class 4 Standards.

Fastener maintenance reflects the effects of fastener failures. Table 1 shows the number of component failures and the percentage of the components that have survived after 257 MGT of traffic. Survival rates are high for all systems. A fatigue limit has not been observed in any system.



- | | | | | |
|------|-----------------------|----------------|-----------|--|
| ref. | FAST | 5° Curve | 40-45 MPH | |
| 1 | WPRR | 10° Curve | 25 MPH | |
| 2 | CHESSIE | 3° Curve | 25 MPH | |
| 3 | STARR, OHIO | 5° Curve | 20 MPH | |
| 4 | CANADIAN NAT'L | 5° & 12° Curve | | |
| 5 | UPRR | 6° Curve | 35 MPH | |

FIGURE 6. FAST VS. REVENUE SERVICE LOADING.

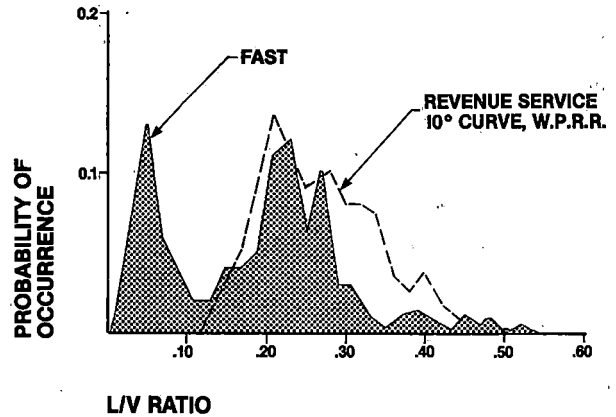


FIGURE 7. PLOT OF L/V RATIO VS. PERCENT OCCURRENCE.

TABLE 1. TOTAL FASTENER FAILURES (250 MGT OF SERVICE, 7.8 LOAD CYCLES)

FASTENER SYSTEM	FAILURES*	% SURVIVING
Double Elastic Spike	None	100
Cut Spike (4 spikes per plate)	None	100
Cut Spike (5 spikes per plate)	1 Plate	99
DE Clip and Plate	1 Clip	Clips 99 Plates 100
FORTAX Compression Clip	15 Clips	94
Hixson Clip and Plate	16 Clips 3 Plates	Clips 93 Plates 98

* Component Failure: Complete loss of component function - either from breakage or from slipping free from its mounting.

A failure is defined as complete loss of component function, either from breakage or working free of its mounting. This definition covers elastic clips falling from the assembly as well as normal breakage.* Normal maintenance items such as high spikes and tightening screw spikes are not included in the reported counts.

In Figure 8, photographs of the various types of component failures are shown. Each photograph is representative of the largest type of failure for each component.



FIGURE 8a. FORTAX CLIPS

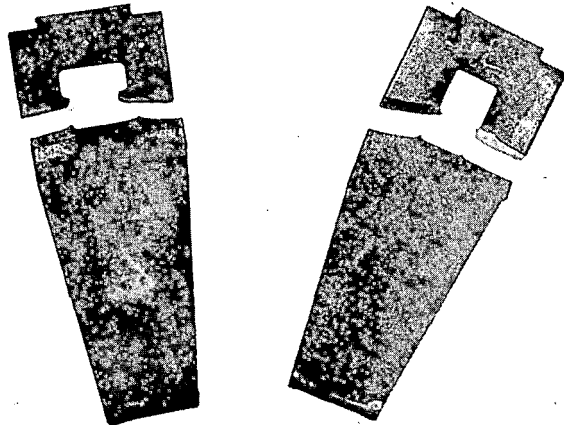


FIGURE 8b. HIXSON WEDGE

* The failures reported on the FORTAX Compression Clips consisted of cracks and these clips were removed, although they could have continued to restrain the rail. Therefore, the stated definition of failure (i.e., complete loss of function) does not apply to the FORTAX clips.



FIGURE 8c. STANDARD TIE PLATE

FIGURE 8. PHOTOS OF COMPONENT FAILURES.

Before discussing fastener maintenance, a caution concerning FAST maintenance is in order. FAST maintenance manhours are not directly relatable to other service environments because maintenance policies and practices differ between railroads and FAST. However, the relative degree of maintenance as represented in FAST manhours can be used as a measure of comparative performance of each fastening system.

Figure 9 shows fastener maintenance manhours for each system. Figure 9a presents the manhours for each system for an out of face rail change at 257 MGT of the test; Figure 9b shows the total manhours expended on fastener maintenance up to, but not including, the rail relay at 257 MGT.

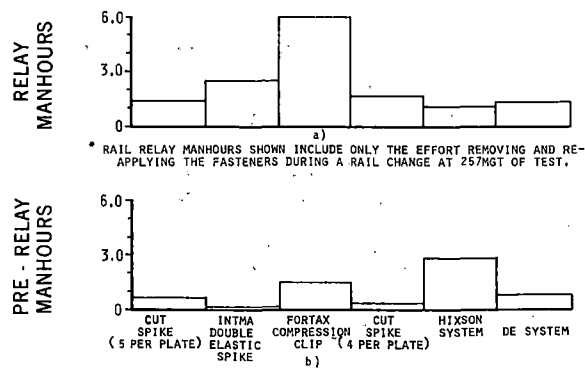


FIGURE 9. FASTENER MAINTENANCE - PRE-RELAY MAINTENANCE MANHOURS AND RAIL RELAY MANHOURS.

During the rail relay, the FORTAX Compression Clip required substantially more effort than any other system because the manufacturer recommends 150 ft/lb installation torque for the clip hold down screw.

This specification was followed during the FAST test using a hand torque wrench. This manhour differential may be minimized by using a torque limiter on a power drive.

The total fastener maintenance manhours for the first 257 MGT of test are shown in Figure 9b. The manhours do not include fastener installation at the beginning of the test, because the installation procedure for test purposes is necessarily different from production oriented railroad installation procedures. The reported manhours also do not include fastener maintenance required to change rail failures.

In Figure 9b, the Hixson system and FORTAX Compression Clip accumulated more long-term manhours than the other systems, reflecting the increased number of component failures in these systems. The Double Elastic Spike System had the least maintenance prior to the rail relay.

Fastener maintenance manhours, as stated earlier, reflect fastener failures and ease of use. To assess the ease (or difficulty) of maintenance of each system, the track crew was surveyed (Table 2). The crew identified the DE Clip as the most difficult to use, but the extra difficulty is not reflected in the DE Clip's rail relay manhours (Figure 9a). Double Elastic Spikes were judged to be difficult to install, which is only slightly reflected in the rail relay effort (Figure 9a).

RAIL FAILURES

While rail failures are not intended as a measure of fastener effects on the rail, it is noted that all failures during this test (8 failed shop welds, one transverse defect and one horizontal split head) occurred within 10 ties of the transition point between different fastener systems. Based on this occurrence, we recommend that the transition between fastener types be placed outside the body and spiral of a curve.

FASTENER PERFORMANCE

Plate cutting is one index of fastener performance. Plate cutting results are shown in Figures 10 and 11. Figure 10 shows average vertical cutting, as shown on the upper left portion of the figure. Only the cut spike systems show any significant amount of cutting, and the amount of tie plate cutting is quite small (0.080"). The other systems had no discernible cutting at all. Similarly, cant plate cutting, as shown in Figure 11, is only significant for one of the two cut spike systems, and the amount of cutting is very small.

Plate cutting potentially occurs because of tie crushing, abrasive damage, or decay. Each of these causes will be discussed in turn.

Tie crushing should not be expected because the maximum load produced at FAST is less than any wood strength (from AREA's list of recommended woods⁶ for ties) perpendicular to the grain. Figure 11 is a plot of tie strength and incident loadings using various tie plates.

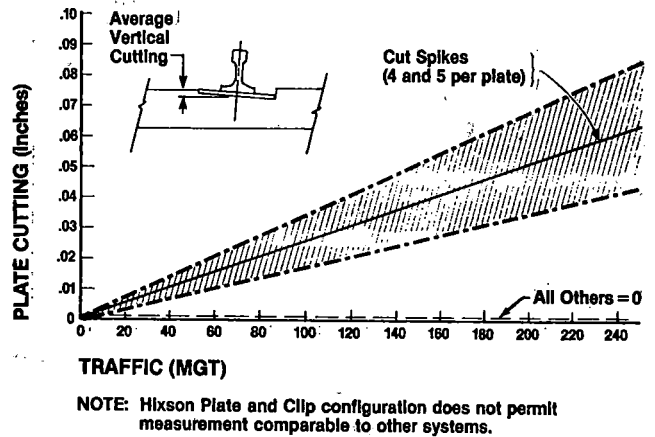


FIGURE 10. VERTICAL PLATE CUTTING.

TABLE 2. EASE OF MAINTENANCE (BASED ON TRACK CREW SURVEY).

EASIEST TO MAINTAIN = 1

Cut Spikes	1
Hixson Clip & Plate	1
FORTAX Compression Clip	1
Elastic Spike	2
DE Clip	3

Track Crew Comments

Hixson Clip & Plate. Easy to install; difficult to remove clips.

FORTAX Compression Clip. Torque wrench or torque limiter needed to meet manufacturers recommendations during clip hold-down screw installation.

Double Elastic Spike. Initially difficult to work with on installation but low maintenance once installed. After initial installation, about same difficulty as conventional spike.

DE Clip. Most difficult to work with. Clip tends to release very quickly on removal.

(HIGH RAIL - NO SIGNIFICANT PLATE CUTTING ON THE LOW RAIL FOR ANY FASTENER)

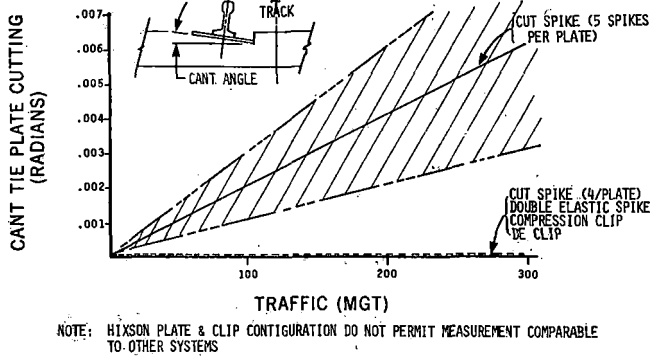


FIGURE 11. CANT TIE PLATE CUTTING.

It is noted that impact loads produced by wheel flats may raise the load at the rail seat by as much as 100% above that shown in Figure 12, which would alter this conclusion. However, such occurrences would not provide sufficient stress to produce tie crushing on hardwood ties (see Appendix A for tie loading calculations).

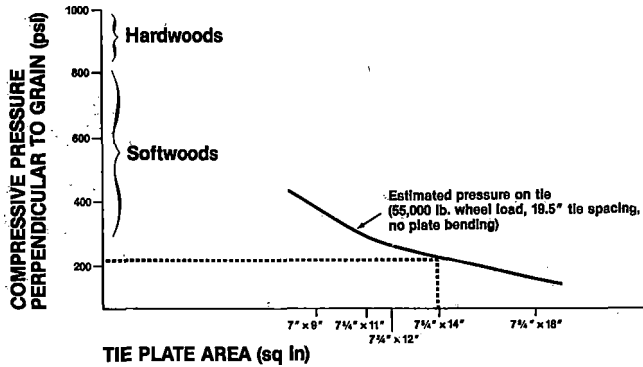


FIGURE 12. COMPARISON OF TIE LOADING AND TIE COMPRESSIVE STRENGTH PERPENDICULAR TO GRAIN.

Plate cutting from abrasion is observed in extreme environments of blowing sand. While the test environment includes some blowing sand, the level is not enough to seriously affect plate cutting.

Also, environmental factors governing tie decay may be a significant cause of plate cutting. Wood decay generally brings to mind the rot caused by fungus infestation. However, wood metal sickness also must be considered as a decay mechanism.

Briefly, wood metal sickness is the interaction of wood acid with corrosion products from spikes and plates. The resultant chemistry destroys wood cellulose. The necessary ingredients are water to create corrosion and acetic acid present in most hardwoods.⁷

The irony is that those woods most resistant to fungus decay are the most susceptible to wood metal sickness. For example, oak has the highest acid content of all AREA recommended woods. Wood metal sickness or rot is not observed at FAST because the incident moisture is very low.

It is evident that the tie plate cutting at FAST is due to abrasive damage from mechanical wearing of the tie plate/tie interface. This mechanical wear, although limited to a relatively small number of occurrences at FAST, does cause a small amount of tie plate cutting. Discussion of the movement of the tie plate relative to the tie will be presented later.

Another performance index is gage widening. This index is measured by three methods--static gage or gage bar with no load, track geometry car gage with a 600 lb lateral load, and dynamic gage under train loading conditions.

Static gage results are shown in Figure 13. The trends in static gage widening are linear with MGT; however, as shown in Table 3, the statistical differences between fastener gage widening rates are insignificant.

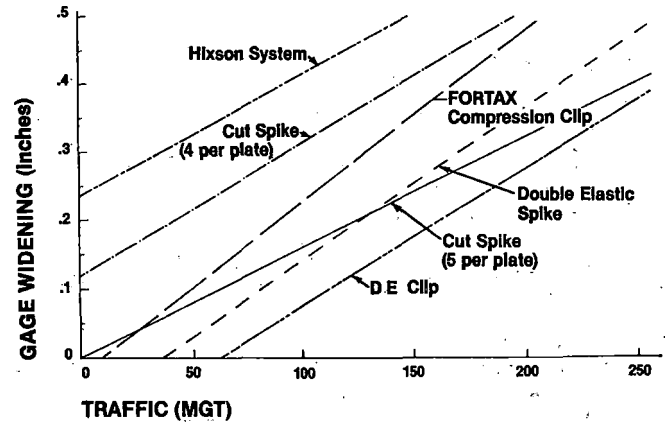


FIGURE 13. GAGE WIDENING (STATIC GAGE, NO APPLIED LOAD).

TABLE 3. LINEAR PLOT VALUES.

Fastener	Gage = a(MGT) + b		Ranking Based on a	Ranking Based on 257 MGT
	a (in/MGT)	b (in)		
DE System	.002	-.126	No	1
Double Elastic Spike	.002	-.082	statistical	1
Cut Spike (5 per plate)	.002	-.001	difference	2
FORTAX Compression Clip	.003	-.024		3
Cut Spike (4 per plate)	.002	.1182		3
Hixson System	.002	.2356		3

Table 3 shows the values for the linear plot in Figure 13. The slope of the line, a, shows no statistical difference for any system. A ranking was established based on the amount of gage widening predicted at 257 MGT. This ranking merely reflects the trend in gage widening and does not imply any significant difference. To be consistent with industry measurement practice, gage values have not been adjusted by rail wear.

Track geometry car gage measurements are taken at 1 foot intervals along the track every 10 MGT of service through a gage measurement device on the EM-80 Track Geometry Car. This device removes all the free play on the track by placing a constant 600 lb lateral load on the rail. No adjustment has been made for rail wear in these data. From Table 4, there is no statistical difference based upon the slope of track geometry car gage widening shown in Figure 14.

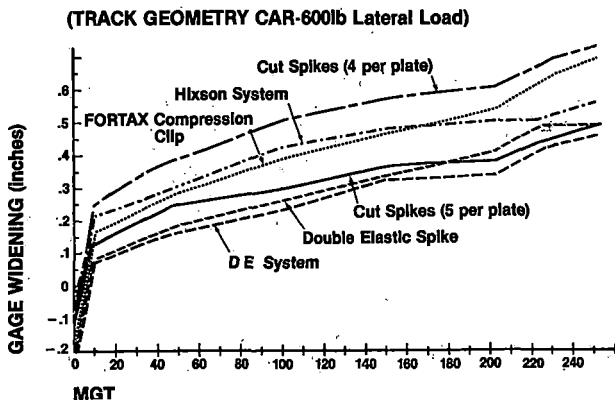


FIGURE 14. GAGE WIDENING.

Track geometry car gage minimizes differences observed using the static gage measurement by removing the lateral slack in the fastener systems. To evaluate the system's dynamic gage widening taken under train loading, dynamic gage widening will be divided into its component parts consisting of lateral rail translation and rail rotation.

Lateral translation of the rail under dynamic loading is measured by the displacements at the rail base. Dynamic rail base deflection is a function of the lateral strength of the rail/fastener system. Lateral strength is characterized by the stiffness

of the system, which is measured under static loading conditions.

Static load/deflection measurements, shown in Figure 15 for the control cut spike system (5 spikes per plate), indicate an expected decrease in strength or stiffness over time. However, the decrease in stiffness is apparent only above the 10,000 lb level.

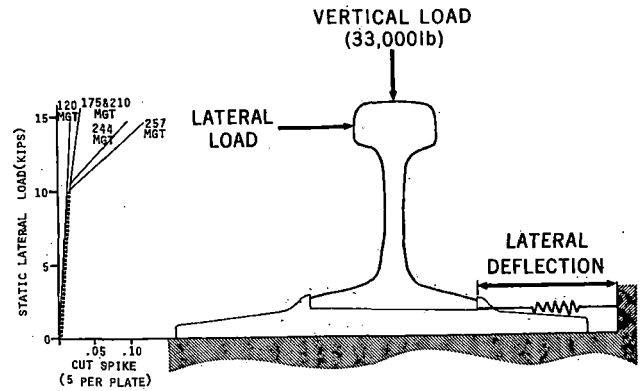


FIGURE 15. LATERAL FASTENER STIFFNESS (@ RAIL BASE)

We observe that the combined loading (33,000 lb vertical; variable lateral load) is resisted not only by the fastener but also the friction generated between the plate and tie by the vertical load. (We previously observed negligible tie plate cutting and therefore can discount any effects a ridge on the tie may produce as a mechanical block to lateral movement.)

The fastener restraint only becomes active once the frictional resistance has been exceeded. Based on Figure 15, friction is overcome when the L/V ratio is 0.33, or coefficient of friction = 0.33

$$\text{Coefficient of friction} = \frac{L}{V} \text{ ratio at slip} = \frac{11,000}{33,000}$$

The value of coefficient of friction observed in this test is low compared to general handbook values for steel on wood:

TABLE 4. TRACK GEOMETRY CAR GAGE WIDENING MEASUREMENTS.

Fastener	Gage = a(MGT) ^b		Ranking Based on a	Ranking Based on b
	a	b		
DE System	.5070829	.0631064	No	No
Double Elastic Spike	.515034	.0851753	statistical difference	statistical difference
Cut Spike (5 per plate)	.595495	.0246576		
Hixson System	.6786868	.0056832		
FORTAX Compression Clip	.604798	.0773014		
Cut Spike (4 per plate)	.689475	.0501821		

"The coefficient of friction depends on the moisture content of the wood and surface roughness. It varies little with species except for those species that contain abundant oily or waxy extractives, such as lignum vitae (tropical American tree types which produce a heavy, durable, resinous wood used for bearing surfaces).

"Coefficients of static friction for wood on unpolished steel have been reported to be approximately 0.70 for dry wood and 0.40 green wood. Corresponding values for lignum vitae on unpolished steel are 0.34 and 0.20."⁸

The value of coefficient of friction observed in this test is low even compared to the green wood value provided by Forest Products Laboratory. (All ties in this test were dried and treated to AREA specifications for wood ties.) We speculate that the coefficient of friction is reduced for railroad service by polishing of the plate and tie seat from small movements between the two surfaces. Also the tie treatment itself may act as a lubricant to reduce friction. Although the value of friction for steel on wood is low by normal standards, the same value has been independently substantiated for railroad track by D. R. Ahlbeck.⁹

Fastener type has no effect on lateral rail deflections at L/V loadings below the coefficient of friction of steel on wood (0.33 in this test). Also, our judgements of lateral fastener stiffness should only be made for L/V values greater than the coefficient of friction.

Figure 16 shows the static load deflection curves for all fastener systems. From these plots we would expect that the two cut spike systems will have the greatest increase in lateral base deflection over time. In truth, no such clear trends could be observed. Returning to our earlier comparison of load environments (Figure 7 repeated as Figure 17), we see that L/V ratios over .33 occur infrequently at FAST. In fact, measurement series late in the test contained no data at L/V ratios over 0.33. Obviously, these are the data points needed to establish increasing trends.

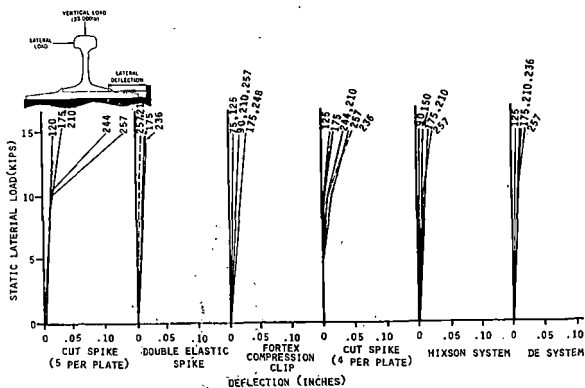


FIGURE 16. LATERAL FASTENER STIFFNESS AT RAIL BASE.

Although trends are not available at this point in the test, we can plot the maximum base deflections over the test life, which will provide some insight

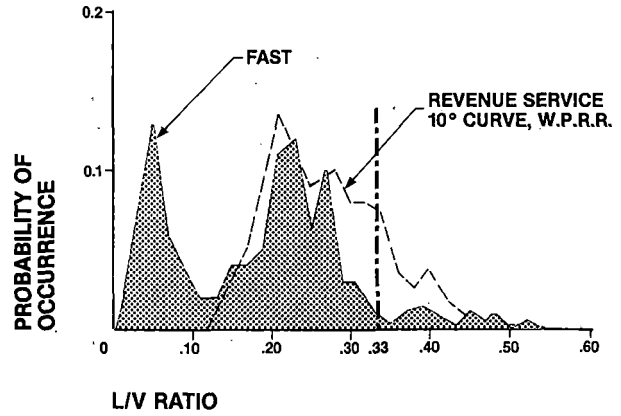


FIGURE 17. L/V RATIO COMPARISON.

into the relative dynamic behavior of each system. The range of maximum dynamic gage widening is plotted in Figure 18.

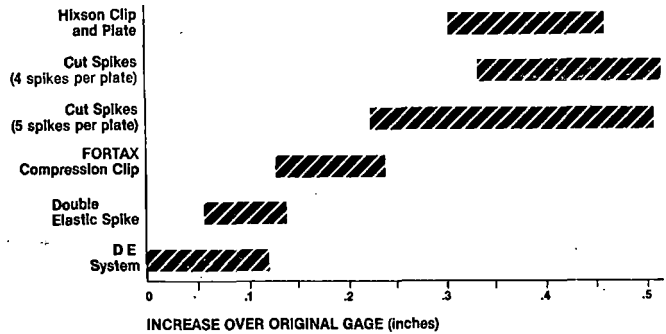


FIGURE 18. MAXIMUM DYNAMIC RAIL BASE GAGE WIDENING.

Figure 18 reflects the range of total lateral displacements including maximum dynamic displacements, relative to the original position of the rail when first laid. These data are based on 5 measured train passes, each at different MGT levels between 75 and 257 MGT. The DE System, Double Elastic Spike and FORTAX Compression Clip are observed to have lower dynamic gage deflections at the rail base than the two cut spike systems and the Hixson System.

Gage widening is the product of both the rail lateral displacement and rail rotation. Rail rotation is a function of both the fastener spring stiffness and the rail torsional stiffness. Rail rotation is defined for the purpose of this paper as the angular rotation of the rail head about the field side base of the rail.

To determine fastener rotational restraint, the rail rotation under static loading is plotted in Figure 19. This is the amount of rail rotation in radians at various MGT levels. We observe that all fastener systems have approximately the same rotational stiffness, and the stiffness does not vary with time.

As with dynamic rail base gage widening, trends in dynamic rail rotation are not apparent. The range

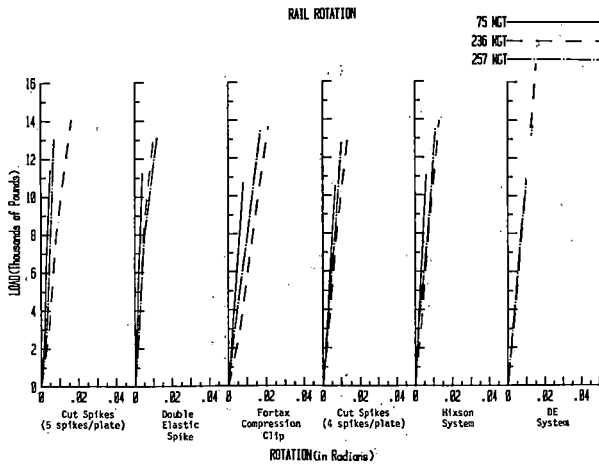


FIGURE 19. RAIL ROTATION.

of maximum values are presented in Figure 20. These values are the maximum values of rail rotation observed for all measurement passes over time. From Figure 20 it is clear that the elastic fasteners provide better rail rotation resistance than the cut spike system, as expected.

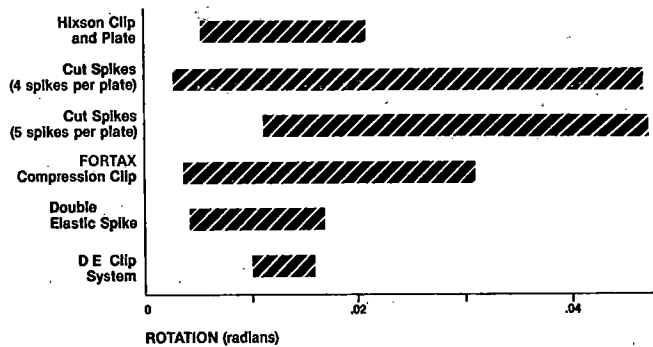


FIGURE 20. MAXIMUM DYNAMIC RAIL ROTATION.

SUMMARY

The results of the wood tie fastener test are presented in Table 5 as a ranking of the various systems according to the previously discussed performance criteria.

The Double Elastic Spike has the best overall performance of the systems tested with the added advantage that the spike fits the standard AREA plate. The DE system performed nearly as well except for a slight increase in long term maintenance. This is attributable to the difficulty in removing and replacing the DE clip. The FORTAX Compression Clip performed nearly as well except for a slightly higher incidence of fastener failure and higher installation manhours associated with torquing requirements on the clip hold-down screw. This could easily be resolved in a production system by using a torque limiter on the application tool.

The durability and simplicity of the cut spike

TABLE 5. FASTENER PERFORMANCE RANKING.

(1 = BEST PERFORMANCE)

FASTENER SYSTEM	RETROFIT TO AREA PLATES	FAILURES	MAINTENANCE		PLATE CUTTING (VERTICAL ONLY)	DYNAMIC GAGE WIDENING (RAIL BASE)	RAIL ROTATION
			RAIL RELAY	LONG TERM			
Double Elastic Spike	Yes	1	1	1	1	1	1
DE System	No	1	1	2	1	1	1
FORTAX Compression Clip	No ¹	2	2	3	1	1	1
Cut Spike (5 per plate)	NA ²	1	1	2	2	2	2
Cut Spike (4 per plate)	NA ²	1	1	2	2	2	2
Hixson System	No	2	1	3	NR ³	2	1

¹FORTAX Clip uses standard AREA plate but requires two non-conventional holes.
²NA = not applicable.
³NR = not rated; no measurement due to plate configuration.

system are distinct assets when comparing the cut spike to the alternative fasteners, but the cut spike allows greater dynamic gage widening than the other systems.

Both the Hixson system and the Pandrol plate did not perform as well as the cut spike system. The Pandrol plate had a large number of fractures and the test has been terminated. The manufacturer now produces a plate with a heavier cross section in the failure region for use in high load environments. The Hixson system did not perform up to par.

Measurements prove that there is no difference between fastener types for lateral rail translation where L/V ratios never exceed the coefficient of friction of steel on wood. For steel tie plate on creosoted wood, the observed coefficient of friction is approximately 0.33.

Because all ten rail failures in this test have occurred within 10 ties of a transition between fasteners, we recommend that no transition between fasteners take place within the body of a curve.

Where tie decay is not present, tie plate cutting due to tie crushing is not expected for 14" AREA tie plate on hardwood ties.

REFERENCES

- 1 Unpublished data, Courtesy of the Western Pacific R.R., C. A. Gerstner, Engineer - Construction.
- 2 Unpublished data, courtesy of Battelle - Columbus Laboratories.
- 3 Ahlbeck, D. R. and Battelle - Columbus Laboratories - Summary Report, Vehicle/Track Interaction Tests - Wayside Test Data Summary, July 27, 1981.
- 4 Telephone Conversation, J. R. Lundgren, AAR, and N. Caldwell, Canadian National R.R.
- 5 Ahlbeck, D. R., Harrison, H. D., Tuten, J. M., and Johnson, Dr. M. R. - Measurements of Wheel/Rail Loads on Class 5 Track, Interim Report under contract to DOT/FRA, June 1979.
- 6 Handbook of Recommended Practice, AREA, Ch. 3.1.1, Specification for Wood Ties.
- 7 Degradation of Wood By Products of Metal Corrosion, Forest Service Research Paper FPL 229, U.S. Department of Agriculture, Forest Products Laboratory, Madison, Wisconsin.
- 8 Wood Handbook: Wood as an Engineering Material, Agriculture Handbook #12, U.S. Department of Agriculture, Forest Products Laboratory, Madison, Wisconsin.
- 9 Ahlbeck, D. R. and Battelle - Columbus Laboratories - "The Effects of Track Modulus on Vehicle-Track Dynamic Interaction," to be published, ASME/IEEE Joint Railroad Conference, April, 1982.
- 10 Timoshenko & Langer - "Stresses in Track," APM-ASME, Applied Mechanics, 1929.

QUESTIONS AND ANSWERS

Question 1

Would the use of the INTMA (Double Elastic Fastener) inhibit rail changing operation?

Answer

Not appreciably. The track crew was surveyed to assess the difficulty of use of each fastener system. The results of that survey are stated in the body of the proceeding paper. The Double Elastic Fastener is said to be roughly equivalent to the standard cut spike in terms of ease of use. However, this spike is difficult to install on first application.

Question 2

Is it reasonable to attempt to draw conclusions (Static or Dynamic) based on geometry deviations limited to approximately $\frac{1}{2}$ those allowable by current FRA Safety Standards and railroad practices?

Answer

FRA Safety Standards and railroad operating limits are not appropriate judgement criteria for performance testing. Such safety limits do not reflect the relationship between MGT, applied load, fastener strength and resulting wear or deterioration.

The trends in deterioration with the appropriate engineering information provides a basis for engineering and economic judgement of performance, irrespective of the safety limits chosen by a railroad.

APPENDIX A
Tie Pressure Under Rail Seat

Train loading at the tie surface is a function of the applied wheel load, the beam strength of the rail, and the structural integrity of the track.

The estimated loading at the rail seat for a static loading condition is given by Timoshenko & Langer¹⁰:

Load delivered to individual tie plate:

$$\text{load} = \beta a P$$

$$\text{where } \beta = \sqrt[4]{\frac{K}{EI}}$$

- K = Track Modulus lb/in/in
- E = Young's Modulus for steel =
= 30×10^6 psi
- I = Moment of inertia of rail
= 96.8 in^4 (140 lb rail)
- a = tie spacing = 19.5 in
- P = applied wheel load.

The relationship offered by Timoshenko is based on the beam-on-elastic-foundation theory which, in this form, is solved only for static loading cases.

However, field measurements (unpublished) by Battelle Institute, under dynamic conditions, indicate that this relationship provides a very reasonable estimate of the load supported by an individual tie.

The maximum FAST load is approximately 55,000 lb. The Track Modulus is measured in this experiment and

averages 1,680 lb/in/in.

No plate bending is included in this estimate. That is, the tie plate load is assumed to be distributed across the full tie plate area (width x length) to the tie.

As a matter for discussion for those interested, the maximum loading at the tie surface should also consider the effects of impact loading, such as that caused by wheel flats or rail joints. The FAST consist contains no significant wheel flats and thus impacts are not pertinent to discussion of why no plate cutting occurs at FAST. However, such impacts do occur in revenue service.

Field measurements of impact loads in revenue service shows that loads at the tie seat are 2 to 5 times greater than the nominal (i.e., static) wheel load.

Theory consideration of structures such as track suggest that a higher rate of loading abbreviates the shape of the wave made by the loaded rail. This decreases the number of ties supporting the load, increasing the load on each tie.

While no field measurements have been made to validate theory, it is intuitively realistic to expect that minimizing the occurrence of wheel flats and rail joints (or battered welds) will also minimize damage to other elements of the track such as the ties.

CONCRETE TIE AND FASTENER PERFORMANCE

John W. Weber
Experiment Manager, Concrete Tie & Fasteners
Association of American Railroads

INTRODUCTION

The use of concrete ties and fasteners is becoming more common on North American Railroads. Large scale installations have been accomplished on the Canadian National, Amtrak (the Northeast Corridor), the Florida East Coast, the Kansas City Southern, the Mexican National Railways, and recently the Atchison, Topeka and Santa Fe. The installations on the CN, Amtrak, and the ATSF have used prestressed mono-block ties and fasteners similar to those tested at FAST.

The FAST test was, in part, installed to prove or disprove the use of concrete ties on Amtrak. The original installation was not expected to last very long but this has not been the case. Most of the original test sections are still in service after 600 MGT.

CONCRETE TIE AND FASTENER PERFORMANCE

The concrete tie and fastener experiment at FAST was originally designed to determine whether or not the current AREA specification tie would perform without massive failures in an extreme service environment. Other than the previously discussed reasons for finding an alternative to the standard wood tie construction, there were two major reasons for the original concrete tie and fastener test and the subsequent second test. They were:

- o A decision regarding the use of concrete ties in the Northeast Corridor Project was imminent and component performance information was an important part of the determination process.
- o Previous use of concrete ties and fasteners on a 2% grade with curved track had resulted in premature system failure and a test of newer ties and fasteners and different ballast types was needed to determine if better performance was possible.

The original concrete tie and fastener test was conducted over a 6125' section referred to as Section 17 in the FAST track. The Section 17 configuration, as shown in Figure 1, consisted of a 5° curve on 2% grade, a short tangent and a 3° curve both on .15% grade. The most demanding environment in Section 17 was the 5° curve 2% grade. The Pandrol 601A was the only fastener located on this curve. The performance of these components in that segment was less satisfactory than elsewhere in Section 17. At 425 MGT the 5° curve 2% grade was rebuilt with some new components installed to further evaluate concrete tie and fastener performance. This rebuild commenced the second test.

The first part of this paper will discuss the performance of the concrete ties and fasteners up to 425 MGT.

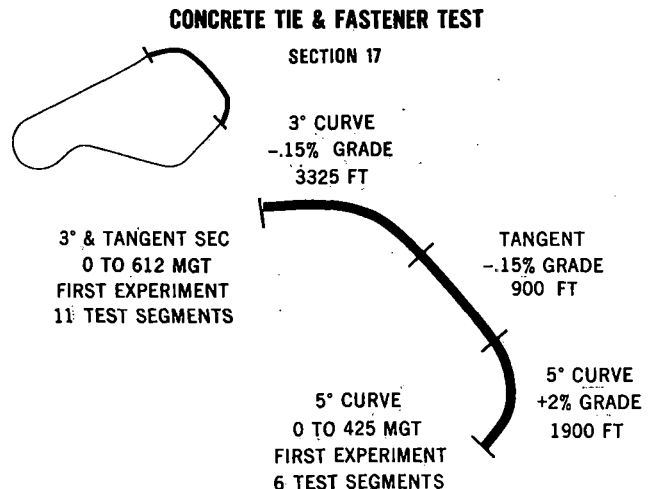


FIGURE 1. CONCRETE TIE AND FASTENER TEST.

The first experiment components were installed in several overlapping segments which are too numerous to identify here. In Table 1 all of the tie, pad, clip fasteners, and insulator components are listed.

At the end of 425 MGT all of the components in Section 17 5° curve were removed and the concrete ties were inspected thoroughly out of the track. Figure 2 shows the various types of tie defects considered during the inspection.

The results of the inspection are as follows:

TABLE 1. FIRST EXPERIMENT COMPONENTS.

TIE:

- o CONFORCE COSTAIN CC244C
- o SANTA FE POMEROY RT-7SS
- o WESTINGHOUSE - BLAKESLEE BW-2
- o SANTA FE POMEROY RT-7
- o DOW - MAC
- o GRINAKE G-23

PADS:

- o POLYETHYLENE
- o CORDED RUBBER
- o FIBER REINFORCED RUBBER
- o POLYURETHANE
- o GROOVED SYNTHETIC RUBBER

FASTENERS:

- o PANDROL 601A USED IN 14 SUB-SECTIONS
- o PANDROL 601A WITHOUT SEPARATE INSULATORS USED IN 1 SUB-SECTION
- o TRUE TEMPER CLIP LOCK USED IN 1 SUB-SECTION
- o PORTEC SIDEWINDER USED IN 1 SUB-SECTION

INSULATORS:

- o INSULATORS, WHERE USED, WERE PANDROL COMPOSITE TYPE

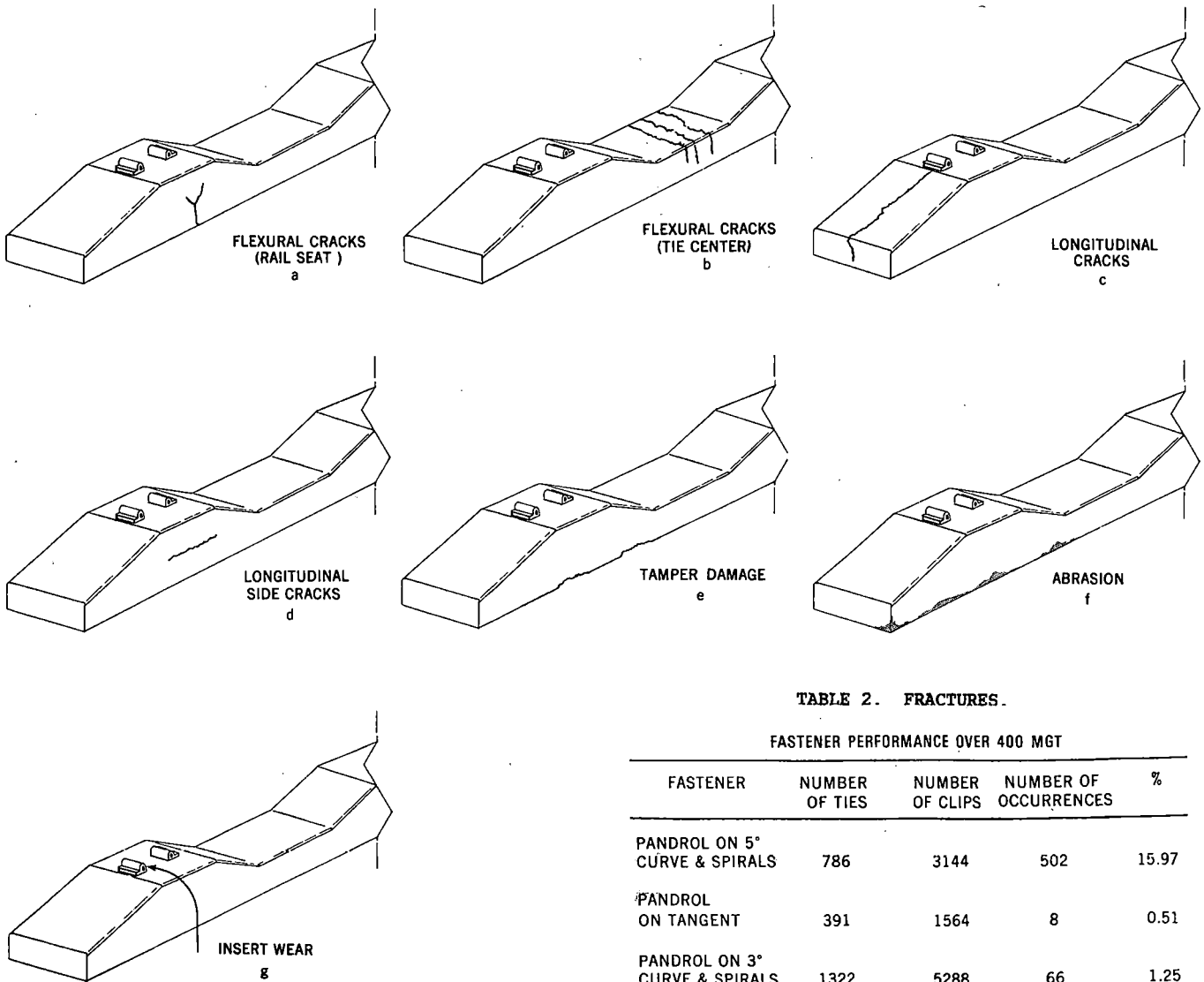


FIGURE 2. CONCRETE TIE DEFECTS.

TABLE 2. FRACTURES.

FASTENER PERFORMANCE OVER 400 MGT				
FASTENER	NUMBER OF TIES	NUMBER OF CLIPS	NUMBER OF OCCURRENCES	%
PANDROL ON 5° CURVE & SPIRALS	786	3144	502	15.97
PANDROL ON TANGENT	391	1564	8	0.51
PANDROL ON 3° CURVE & SPIRALS	1322	5288	66	1.25
CLIP LOCK ON TANGENT	100	400	0	0.0
SIDEWINDER ON SPIRAL	175	700	0	0.0

- o Figure 2a shows flexural cracking under the rail seat. This has traditionally been a very common type of crack in revenue service and has led to tie failure. Unlike the revenue service ties, there were no flexural cracks on the ties at FAST.
- o Figure 2b shows flexural cracking in the tie center. There were a small number (38, 7.4%) of concrete ties at FAST with this type of crack. These cracks were noticed early in the life of the ties and have progressed little since then. It is possible that these cracks were caused by center binding which occurred during the ballasting operation before the track was put in service.
- o Figure 2c shows a longitudinal crack extending from the embedded shoulders. The crack can extend either toward the end of the tie as shown in Figure 2c or inward toward the center. In severe cases, the crack can extend to the end of the tie, down the end face, and along the bottom of the tie eventually leading to splitting of the tie. 78% of the RT7SS ties inspected had these type of cracks, most of which were less than 6" long. Only 4 (1%) of the CC244C ties had this type of crack. The cracks on the CC244C tie were 2" to 3" long. This cracking may be caused by shrinkage of the concrete around the embedded shoulder during curing. Some of these types of cracks have been found in new ties with no service life.
- o Figure 2d shows a longitudinal side crack on the face of the tie at the top prestressed strand. These cracks occurred in 30% of the CC244C ties and 50% of the RT7SS ties. This type of crack could lead to separation of the top surface of the tie.
- o Figure 2e shows typical damage caused by the tamper at FAST. This type of damage, which occurred on all ties, is insignificant to tie performance but can be eliminated by small modifications to the tamping machine.
- o Figure 2f shows typical tie abrasion due to ballast/tie interaction. This damage is also insignificant and generally occurred more on the CC244C ties than the RT7SS ties. Generally the amount of abrasion, which is less than the tolerance of the tie thickness, is very site specific, occurring near battered welds, joints, and engine burns.
- o Figure 2g shows insert wear on the embedded cast iron shoulder which occurred where insulators were not used. Insulation was provided by an epoxy coating on the shank of the insert cast onto the tie. Figure 3 is a photograph of this type of damage. Because of the amount of wear, up to 1/8", this type of installation is not recommended since it could lead to insert failure and wide gage. All of the ties of this type of design showed some of the wear damage to the field shoulders.

The concrete ties in the tangent and the 3° curve have performed well up to 612 MGT. None of the ties have been removed up to that point for a performance failure. In a rebuild initiated in late 1981, a sample of these ties will be inspected for defects after the ties have been removed from the track.



FIGURE 3. WEAR ON CONCRETE TIE EMBEDDED SHOULDER.

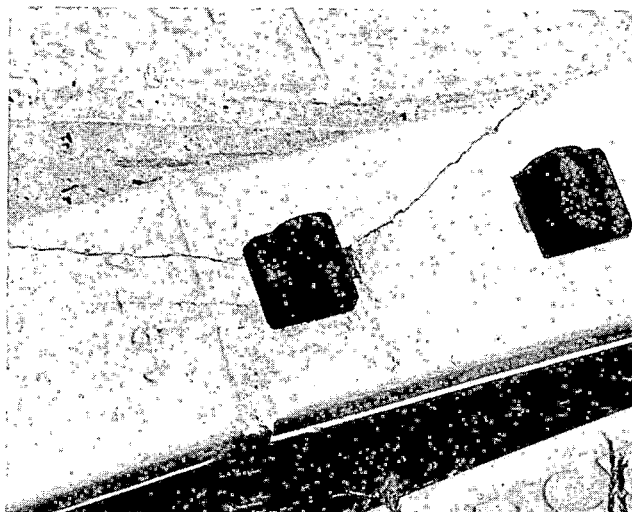


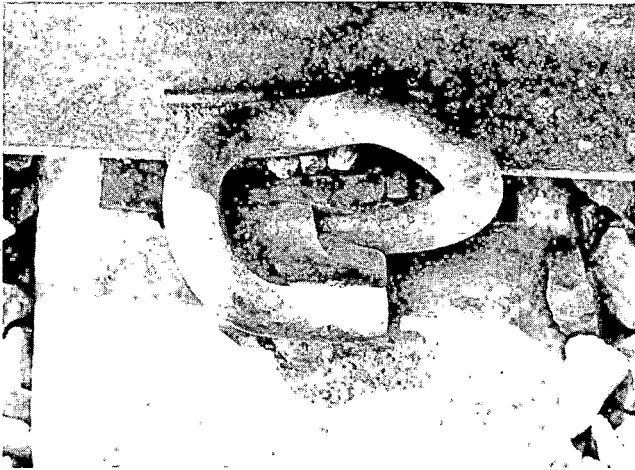
FIGURE 4. TIE DAMAGED BY HAMMER BLOWS TO THE INSERT.

A small number of ties have been removed from the track for damage caused by a sharp hammer blow to the insert (Figure 4) or a broken or cracked insert as shown in Figure 5.

Fastening clips and bolt performance over the first 425 MGT was varied. A considerable number of performance problems were encountered. This included clip fractures, clip fallouts, broken bolts, and insulator failures.

Broken bolts on compression clips occurred on eight ties in Section 17 requiring the removal of all eight ties. These fasteners also required periodic maintenance with a torque wrench to maintain clip toe load.

Table 2 lists the clip fractures by percentage, location, and type over the first 400 MGT. Figure 6 shows a clip fallout. Figure 7 shows a typical clip fracture. Figure 8 is a plot by location of the cumulative clip fractures versus MGT. The majority of these fractures occurred in the 5° curve inside rail gage position.



(a)



(b)

FIGURE 5a & b. INSERT FAILURES ON CONCRETE TIES.



FIGURE 6. CLIP FALLOUT, PANDROL CLIP.

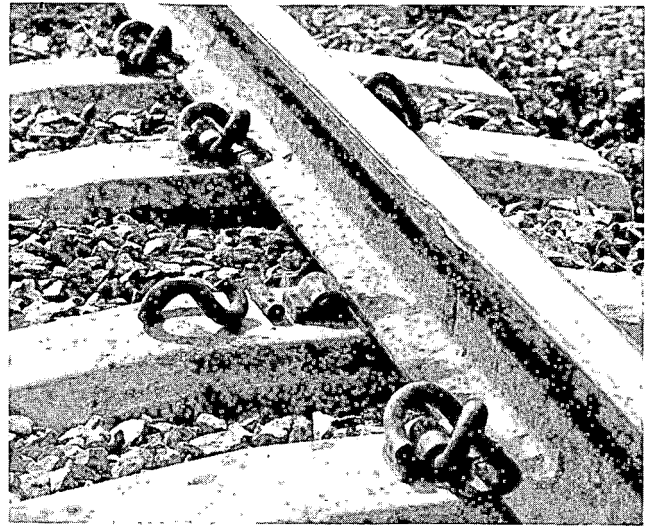


FIGURE 7. CLIP FRACTURE, PANDROL CLIP.

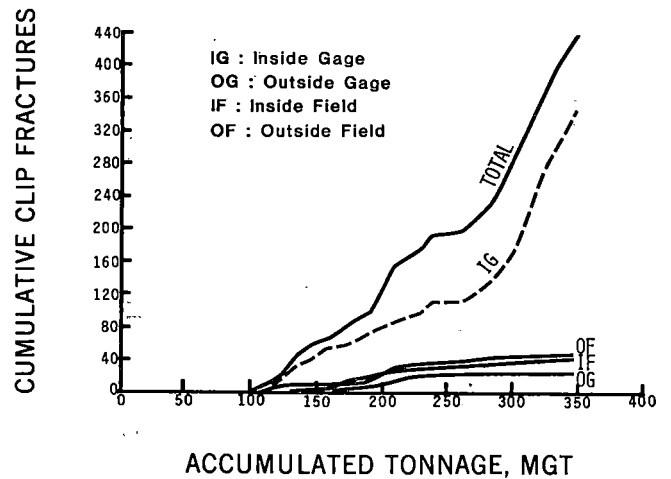


FIGURE 8. CUMULATIVE FASTENER FRACTURES VS. MGT.

Table 3 lists the clip fallouts by percentage, location, and type over the first 400 MGT. Figure 9 is a plot by location of the cumulative clip fallouts versus MGT. Again, as with the clip fractures, the majority of these events were on the inside gage position of the 5° curve.

In both fallouts and fractures, the performance of the Pandrol clip was marginal on the 5° curve. The Pandrol clip and the Sidewinder generally performed well elsewhere. In the 5° curve the Pandrol clips were renewed twice, at 61 MGT and 235.4 MGT, with little effect on the rate of occurrence of fractures and fallouts. Evidently the deflections on the 5° curve, inside gage position exceed the capacity of the fastener to perform over long periods of time. These occurrences were one reason for the complete rebuild of Section 17 5° curve at 425 MGT.

Pandrol insulator performance over the 425 MGT period was also marginal. The composite (two piece) insulator used during this time period was routinely

TABLE 3. FALLOUTS.

FASTENER PERFORMANCE OVER 400 MGT				
FASTENER	NUMBER OF TIES	NUMBER OF CLIPS	NUMBER OF OCCURRENCES	%
PANDROL ON 5° CURVE & SPIRALS	786	3144	688	21.88
PANDROL ON TANGENT	391	1564	17	1.09
PANDROL ON 3° CURVE & SPIRALS	1322	5288	369	6.98
CLIP LOCK ON TANGENT	100	400	8	2.00*
SIDEWINDER ON SPIRAL	175	700	6	0.86

* Broken Bolts

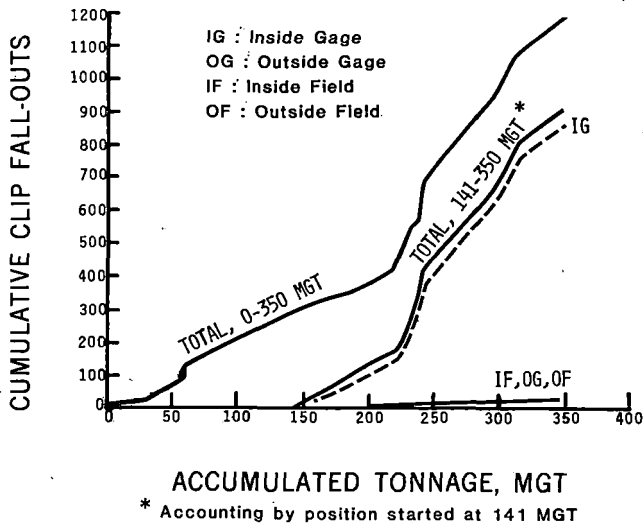


FIGURE 9. CUMULATIVE FASTENER FALLOUTS VS. MGT.

replaced due to wear or damage as shown on Figure 10. Damage readily occurred during installation of the clip as well as during traffic.

Pad performance through 425 MGT at FAST has generally been good depending on material type. Two types of "soft" pads as identified by durometer (see Figure 11) were replaced in the 5° curve 2% grade at 235.4 MGT. These two pad types, the corded rubber pad and the fiber reinforced pad either shredded or wore to the point where there was a considerable loss in thickness. This type of failure is shown in Figure 12.

All of the remaining pads, the grooved synthetic rubber, polyurethane, polyethylene, and nylon polymer pads have performed well. The grooved synthetic and nylon polymer pads have not been tested on the 5° curve 2% grade portion of Section 17 and this may have some bearing on their performance relative to the polyethylene pads. The polyurethane pads were not tested on the 5° curve during the first 235 MGT. However, since that time through 612 MGT, they have performed well.

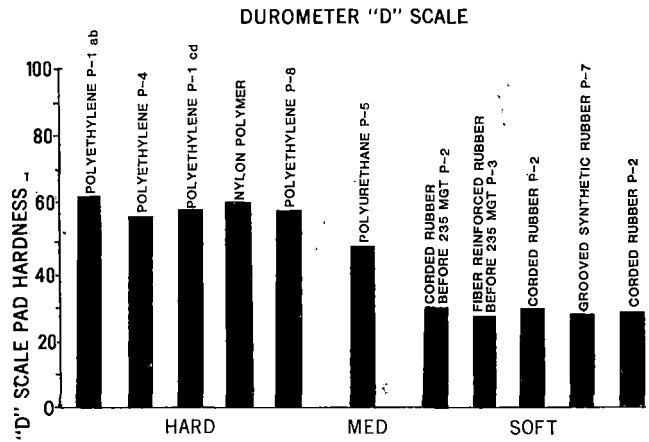


FIGURE 11. PAD HARDNESS IN SECTION 17.

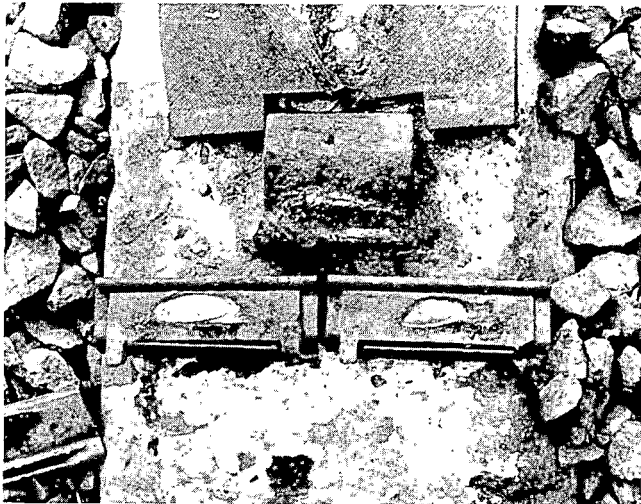


FIGURE 10. BROKEN AND WORN COMPOSITE INSULATORS.



FIGURE 12. FAILED CORDED RUBBER PAD.

At 425 MGT, a track rebuild in Sections 17 and 22 was completed in early 1980. There were several changes made to the components in Section 17 5° curve and concrete ties were installed in Section 22.

Figure 13 shows the layout of Section 17, 5° curve after the rebuild and Figure 14 shows the layout for Section 22. In both cases the existing ballast was removed and replaced with new ballast on a subgrade compacted to uniform stiffness.

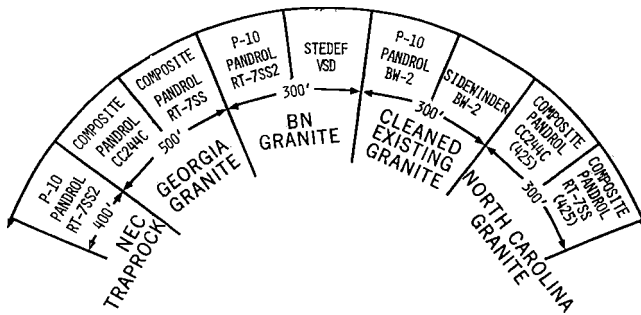


FIGURE 13. LAYOUT OF PHASE IIa 5° CURVE, 2% GRADE, SECTION 17.

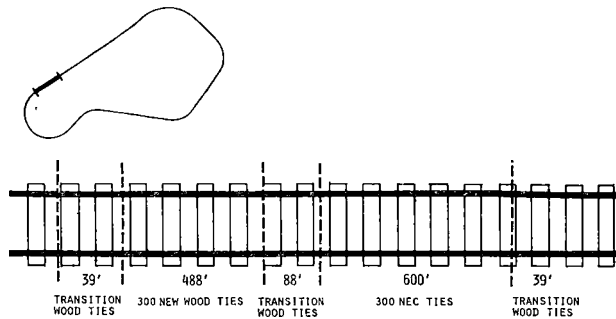


FIGURE 14. LAYOUT, SECTION 22.

There were several reasons for the rebuild. They were:

- o To test another fastener on cleaned existing ballast to determine if a different fastener would perform better on the 5° curve in conditions similar to those in the first 425 MGT.
- o To continue to test a selected group of existing ties in the 5° curve and the spiral leading to the curve, and to determine the life cycle performance of those ties. New North Carolina granite was installed in this segment.
- o To test new ties similar to those on the initial test on new AREA Grade 3 Georgia granite ballast to determine if the ballast was the major contributor to the problem of tie skewing and subsequent loss of alignment and surface. The skewing performance will be discussed in another paper.

- o To evaluate the component performance of North-east Corridor concrete tie track on the curve and spiral on the NEC traprock ballast.
- o To evaluate the differences in performance of concrete tie track with tie pads of radically different pad stiffnesses. The pad stiffness differences are 1.4M lb/in for a 4.5mm grooved synthetic rubber pad and 5M lb/in for a 5.0mm EVA pad.
- o To test the differences in track performance of wood and concrete ties built to NEC specifications in Section 22. This performance will be discussed in the Tie/Ballast Interaction Paper.

Since the rebuild, nearly 187 MGT of traffic has accumulated on the rebuilt track. The performance of the ties was similar to that for the first 425 MGT. No ties have been removed from the track because of a service related failure.

It can be seen in Tables 2, 3, and 4 that the performance of the Pandrol clips with composite insulators has not improved significantly. The performance of the Pandrol clips with P-10 insulators on both new and old ballast did improve significantly over the same clips with the composite insulators. The Stedef VSD system performed exceptionally well over 187 MGT. That system, as shown in Figure 15, does however require more effort to install and remove the clip.

TABLE 4. FASTENER PERFORMANCE OVER 187 MGT.

FASTENER	FALLOUTS AND FRACTURES			
	NO. OF TIES	NO. OF CLIPS	NO. OF OCCURRENCES	%
PANDROL W/COMPOSITE ON OLD TIES	162	648	80	12.35
PANDROL W/COMPOSITE ON NEW TIES	249	996	138	13.86
PANDROL & P-10 ON OLD BALLAST	75	300	11	3.67
IMPROVED SIDEWINDER ON OLD BALLAST	63	252	30	11.90
PANDROL & P-10 ON NEW BALLAST	276	1104	44	3.99
STEDDEF VSD	75	300	1	0.33



FIGURE 15. VSD FASTENER SYSTEM.

Pad performance in the 5° curve since the rebuild has been good. There have been no pad failures to date.

The insulators used on the rebuild have, in general, performed poorly. The P-10, glass filled nylon insulators used with the Pandrol clip, have failed progressively on the field side and were totally replaced once through 187 MGT. The Pandrol composite insulators continued to be replaced at a rate comparable to that on the first experiment. The other insulator that did not perform well was the black polyamide insulator used with the VSD system. These were totally replaced by white delrin insulators which have performed well.

The concrete tie and fastener test in Section 17 has shown that the tie can withstand the traffic induced loads at FAST. There is no reason to not expect this performance to continue. The fasteners have performed well in areas where the lateral loads are moderate such as on the 3° curve and tangent. In the 5° curve only the VSD fastener, with just 187 MGT of traffic, has performed well although the Pandrol with P-10 insulators has shown a significant improvement in performance. Pad performance has been good except for two early pad materials which were probably too soft. Because of severe wear on the cast iron shoulder, it is not recommended that concrete ties be used without an insulator. The use of insulators has been a continuous maintenance problem except for the white delrin insulator used with the VSD clip.

In late 1981, a rebuild of Section 3 5° curve was completed. The intent of this rebuild was to:

- o determine the relative and absolute performance of different fastening systems on concrete ties under similar track conditions and to characterize the deflection environment in order to develop adequate fastener performance specifications.

- o determine the relative and absolute performance of two different types of concrete ties, one made with conventional Portland cement concrete and the other with latex modified concrete.
- o evaluate each of the above systems against a comparable wood tie system.

The layout of Section 3 is shown on Figure 16. Figures 17 through 21 show the various components and Table 5 lists test segment composition.

This test is expected to last for the duration of the 100-ton experiment at FAST.

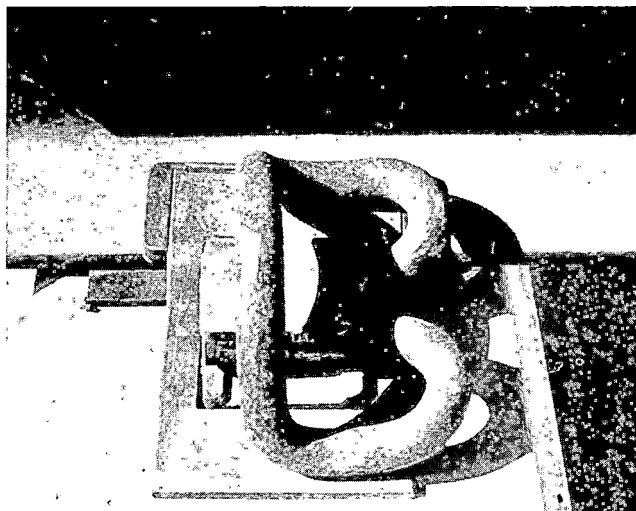


FIGURE 17. SIDEWINDER.

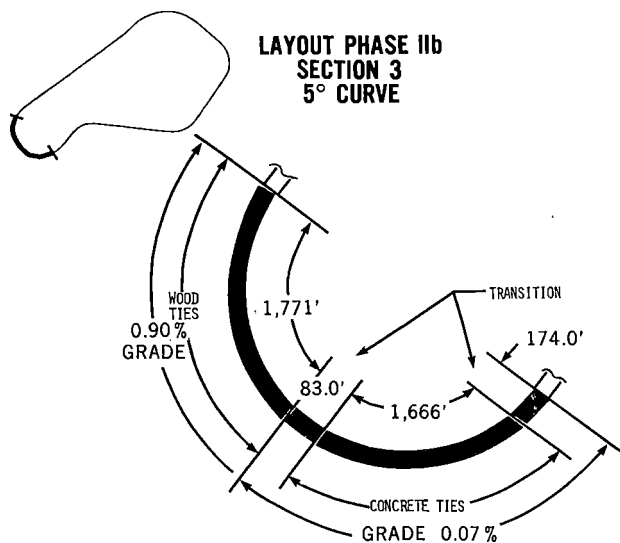


FIGURE 16. LAYOUT PHASE IIb SECTION 3, 5° CURVE.

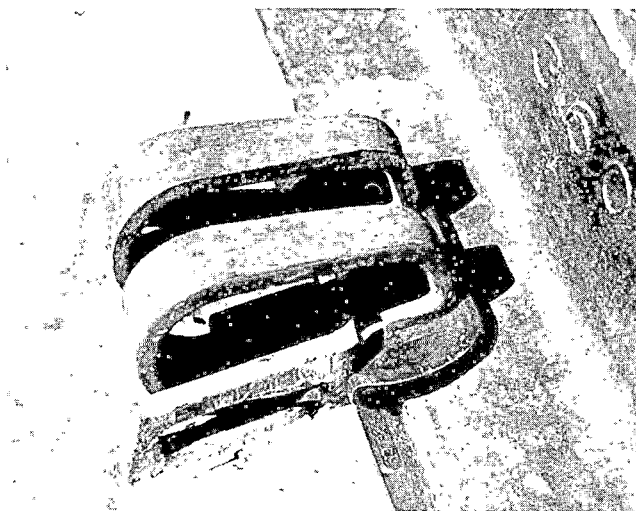


FIGURE 18. MCKAY.

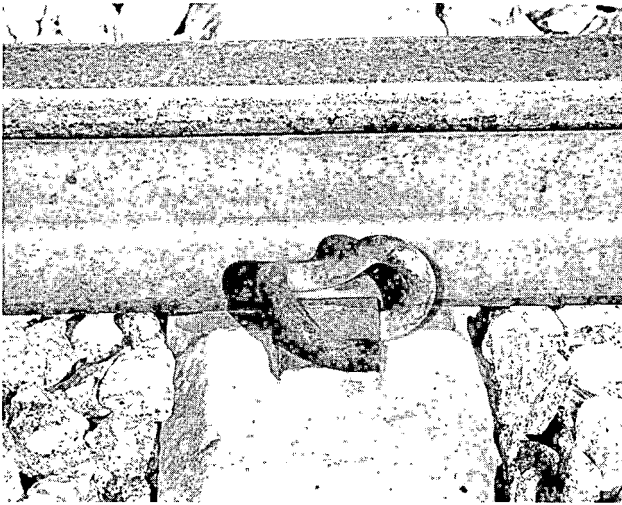


FIGURE 19. PANDROL.

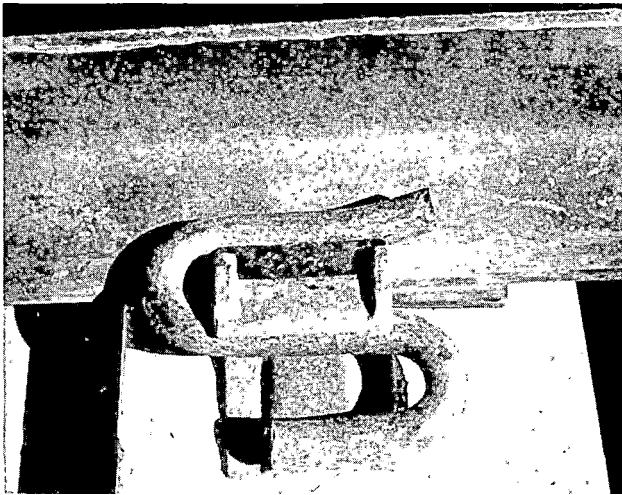


FIGURE 20. LINELOC.

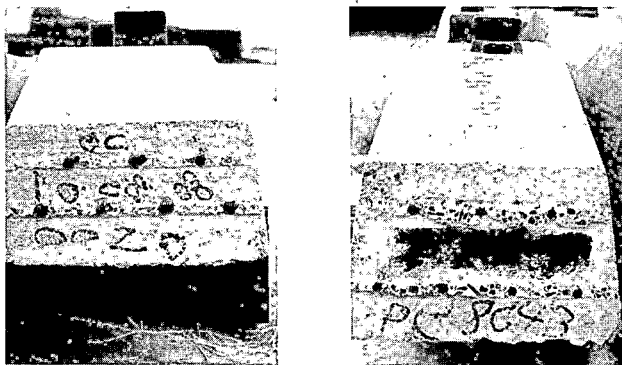


FIGURE 21. LATEX MODIFIED AND STANDARD CONCRETE TIE.

TABLE 5.

SEGMENT	TIE	FASTENER	PAD
1	CC297	Portec Sidewinder	EVA
2	BW3 Latex	Portec Sidewinder	EVA
3	RT7SS-2	Pandrol 601A	EVA
4	BW-2	Portec Sidewinder	EVA
5	RT7SS-2	Pandrol 601A	EVA
6	BW-2	True Temper Lineloc	EVA
7	RT7SS-2	Pandrol 601A	EVA
8	BW3 Latex	Portec Sidewinder	EVA
9	CC297	McKay Safeloc	EVA

QUESTIONS AND ANSWERS

Question 1

If the spring rate increases with increases in frequency, what will happen to pad attenuation of energy at 116 Hz and 300 Hz?

Answer

Each pad has different characteristics over the full range of frequency response. The optimum pad is one that is not responsive at the frequency with which you are concerned. In the case of concrete tie rail seat flexural cracks this is 300 Hz and above. In general, resilient pads transfer less impact from the rail to the tie at the higher (>110 Hz) frequencies than do rigid pads. This appears to be a characteristic of all resilient tie pads and can be determined using the impact test as described in the proceedings.

CONCRETE TIE TRACK SYSTEMS: ENGINEERING CONSIDERATIONS

Jack E. Heiss
Experiment Monitor, Concrete Ties & Fasteners
Boeing Services International, Inc.

As a part of the assessment of the performance of concrete tie track, much analytical work has been done to characterize and evaluate the reasons for component degradation, tie skewing, and track response.

The FAST consist has been characterized as imposing high average axle loads, but absolute peak loads less than those found in revenue service. This situation reduces the probability of catastrophic failures on the FAST loop, but enhances the ability to induce high-cycle fatigue phenomena in the concrete ties.

In the 5° curve 2% grade the lateral and vertical load environment is one of most severe at FAST. The variation in train operating speed causes both over and under balance conditions, depending upon train direction. Braking and draft/buff on the grade adds to the severity of the track loading.

LOAD ENVIRONMENT

In Figure 1, the average and peak vertical load values on the outside (high) rail are plotted versus MGT. The lower pair of lines represent the average of all wheel loads during the measured train pass. These averages are predominately in the 35 to 45 kip range. After an out of face surfacing at 93 MGT, the average loads were reduced to near the static wheel load values of 32.5 kips, but once the track had a significant amount of traffic the average values returned to their former level.

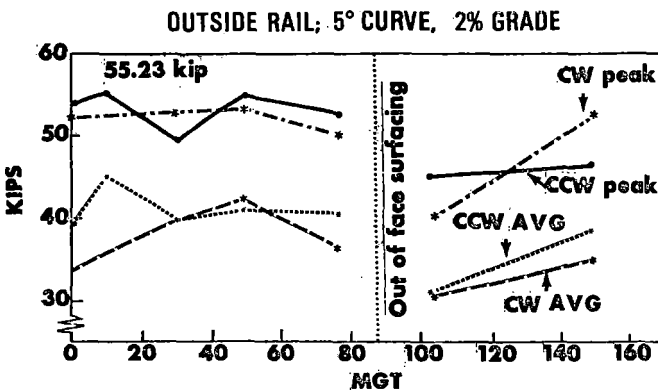


FIGURE 1. VERTICAL LOAD VALUES.

The upper two lines depict the peak load value measured during a train pass on the outside rail. The peak value is 55.23 kips. This is 1.7 times the static wheel load. This multiplier is typical for the concrete ties in the FAST loop and similar

values have been measured on the inside rail of the 5 degree curve and in the tangent track installations.

The average values for the inside rail of the 5 degree curve and tangent track are slightly lower than those for the outside rail.

The one-time peak loading occurrences have special significance for concrete ties. On FAST, where peaks with the 1.7 multiplier have been measured, the flexural cracking of concrete ties at the rail seat has been rare. On revenue service installations, multipliers of static loads are significantly higher in the presence of wheel/rail surface anomalies, and flexural cracking is a common phenomenon.

Figure 2 illustrates the lateral rail loads. Lateral loads in Section 17 are the most severe on the inside (low) rail. The absolute peak measured 23.4 kip, but the bulk of the values fall in the 12 to 15 kip range. On the outside rail, the peak occurred at 19.15 kip, but most values are similar to those on the inside rail. These low rail lateral loads are the result of wheel/rail tread contact and are not from flanging. The clip fractures and fallouts have largely been on the gage side low rail as a result of these forces.

On the tangent track in Section 22, without the benefit of the 5 degree curvature and the 2% grade, lateral loads are approximately half of the curved track values, with most peaks in the 6 to 9 kip range. Clip failures have been rare on tangent track.

In all the track configurations, lateral loadings toward the gage side have been measured. The gage side peaks fall around 5 kips.

INSIDE RAIL; 5° CURVE, 2% GRADE
(FIELD SIDE)

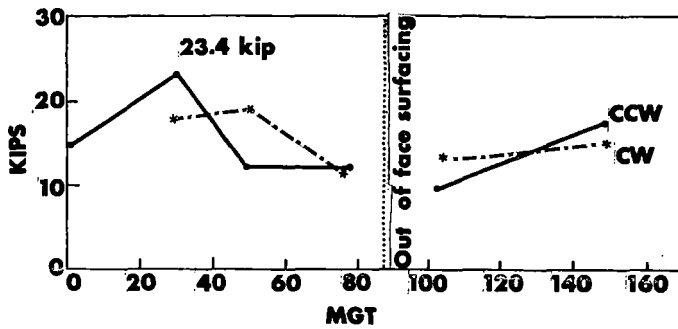


FIGURE 2. LATERAL LOAD VALUES.

TIE BENDING STRESSES

In response to the vertical and lateral loads applied to the track during train operations, the concrete ties are subject to high bending stresses, the highest stresses being at the rail seat and the center of the tie.

Center bending measured at FAST has not been sufficient to produce center cracking. This is expected due to the lack of flat wheels with the resulting extreme impact loads. As shown in Table 1, the maximum center bending in the negative direction measured at FAST has been 194 in-kip in the 5 degree curve and 131 in-kip on the tangent track. This is consistent with the maximum impacts measured. The current AREA specification for negative center bending is 200 in-kip.

TABLE 1. PEAK BENDING MOMENT VALUES.

	FAST Measured Peak Bending Moment in - kip	AREA Design Specification in - kip
Tie Center		
Negative	194	200
Positive	116	140
Rail Seat		
Positive	187	300
Negative	133	160

Positive center bending of 116.3 in-kips has been measured on the FAST loop. The AREA specification calls for a design strength of 140 in-kip.

As tonnage accumulates, a trend of increasing center bending stresses has been seen. This increase is more pronounced in the early MGT's, but stabilizes later on. This phenomenon can be attributed to a long term ballast consolidation, resulting in some degree of center binding. Figure 3 shows this

relationship compared with lateral differential settlement between the tie center and the rail seat. The rate of increase of the tie center bending moment is small after initial consolidation up to 5 MGT. Without large impact loads these values are not expected to exceed the bending capacity of the tie at the center.

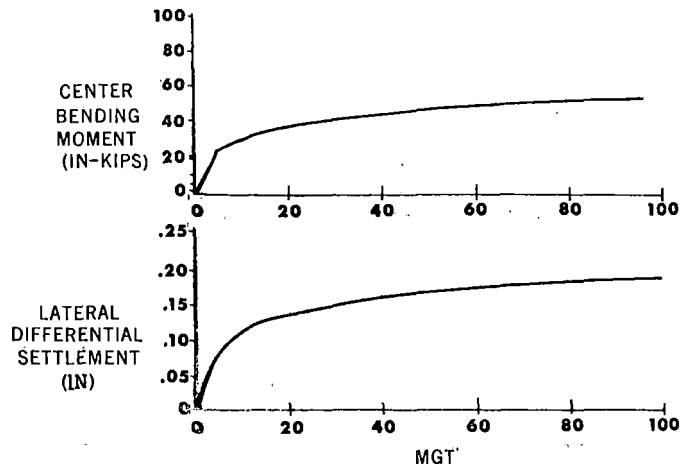


FIGURE 3. AVERAGE CENTER TIE BENDING AND LATERAL DIFFERENTIAL BALLAST SETTLEMENT, SECTION 22.

Bending at the rail seat is predominately in the positive direction. Peak positive bending has been 187 in-kip. The tendency for the average peaks to increase as tonnage accumulates is also seen, but is not as dramatic as with center bending. The AREA specification for positive rail seat bending is 300 in-kip, which has not been exceeded at FAST. Negative bending at the rail seat has also been recorded. The peak occurrence has been 133 in-kip, though this occurrence was an isolated event. A higher concentration of values occurs at 80 in-kip. The AREA specification calls for a negative flexural strength of 160 in-kip before cracking occurs. All measured bending strains or moments at FAST have occurred within the AREA design specification and flexural cracking has not been detected on any ties during the second experiment. However, the measured bending moments do approach the design specification without being subjected to the extreme impacts found in typical revenue service.

Most of the ties in FAST exceed the AREA design capacity in bending by 10-20%. This provides an additional margin of safety for the conditions at FAST. In revenue service the addition of low probability occurrences of high impact loads has resulted in bending moments that exceed the flexural capacity of the ties. This will be discussed in another paper.

RAIL FASTENERS

The rail fastening systems employed on concrete tie track systems have a great effect on the overall performance of the track system. Two main categories of tie to rail fasteners have been tested on the concrete ties at FAST. These are the compression clip fastener and the elastic clip fastener.

Only one type of compression clip fastener had been

installed and it was installed on the tangent track in Section 17, a zone of mild test conditions. The fasteners have performed well under these conditions, requiring minimal maintenance.

The bulk of the experimentation has been conducted on the 5° curve for the second experiment with elastic clip fasteners. Four types of elastic clips have been installed in this section and exposed to the severe conditions inherent on this curve.

The performance of the fasteners is characterized by the rate of fallouts and fractures and by the loss of toe load. The toe load, as shown in Figure 4, is the static force exerted by the fastener on the rail and contributes to restraining the rail laterally and longitudinally. Loss of toe load can indicate impending fastener fracture or fallout and can indicate a general weakening of the track structure resulting in tie skewing.

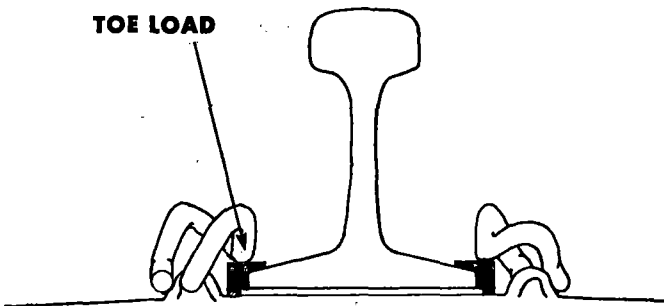


FIGURE 4. DEFINITION OF TOE LOAD.

Three of the four types of elastic clips were measured for toe load during the second experiment. Two of these clips are identical except for slight differences in the steel used to manufacture the clips. A plot of toe load versus MGT is shown in Figure 5 for one sample tie. This plot is representative of the toe load performance of this clip with tonnage at FAST. These clips have an initial toe load in the 1800 to 2100 lb range. This relatively wide range of values is common in track installations.

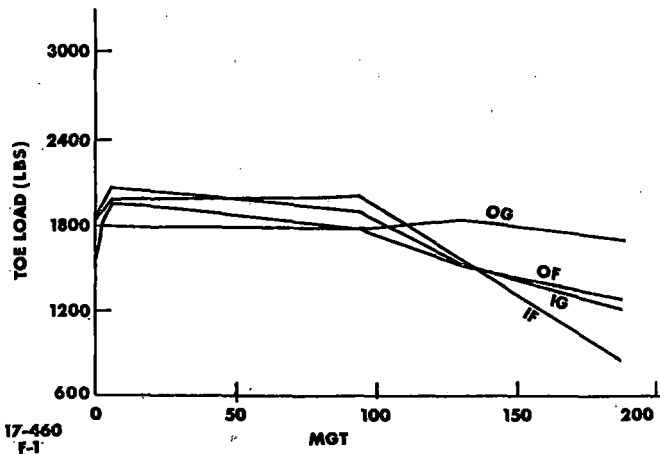


FIGURE 5. TOE LOADS PANDROL CLIP AT TIE #460.

As can be seen in Figure 5, the toe loads decrease substantially during the accumulation of tonnage. A feature of this clip type is the small margin between the pre-stressed load and the yield stress. Measurements on the FAST loop show that these clips regularly are deflected beyond their yield point. We see three manifestations of the excessive strains, loss of toe load, the clip working out of its shoulder, or fracture. Of these two similar types, one fails primarily by fracture, the other by fall-out. However, overall failure rates are equivalent.

Figure 6 shows the toe loads on the third type of clip. These clips have an initial toe load in the 2600 to 3000 lb. range. It is seen once again as a loss of toe load with traffic, and the loss is delayed to higher traffic levels. The feature here is a wider margin between the pre-stress and yield stresses, but only sufficient to postpone, not eliminate, the fatigue effects. Fatigue resistance is based in the margin between the preload stresses and the yield stress on the clip. Some of the newer designs are taking this criteria into account.

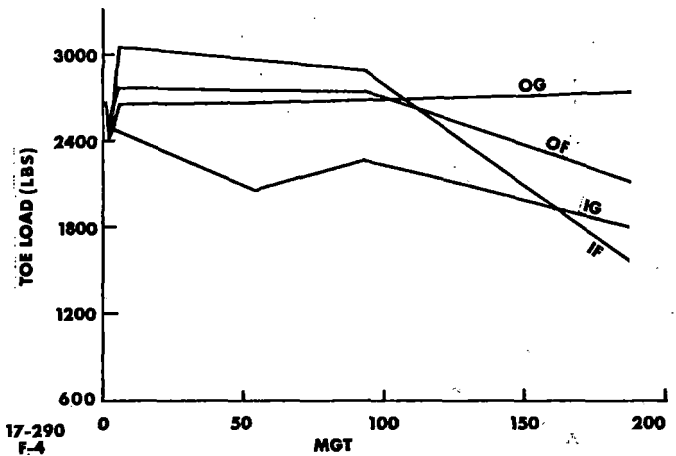


FIGURE 6. TOE LOADS SIDEWINDER CLIP AT TIE #290.

The fourth type of clip has not been measured for toe loads in track, but laboratory tests indicate toe loads between 1600-2000 lbs. The manifestations of fatigue have not been observed in the field with this type of clip.

TIE SKEWING

Longitudinal movement of concrete ties in the ballast and along the rail has shown to be a significant structural and maintenance problem in the 5 degree and in the 3 degree sections of the test. These movements have been termed "tie skewing". An example of tie skewing is shown in Figure 7. Initial visual observation shows a phenomena which appears random in the amount and direction of movement, but to some degree a pattern exists, particularly in the 5 degree curve, 2% grade section. More movement is experienced on the inside rail and the tie generally moves downgrade faster than the rail. Movement also increases in areas where large longitudinal compressive stresses are predicted, such as the bottom of grades and during warm weather.

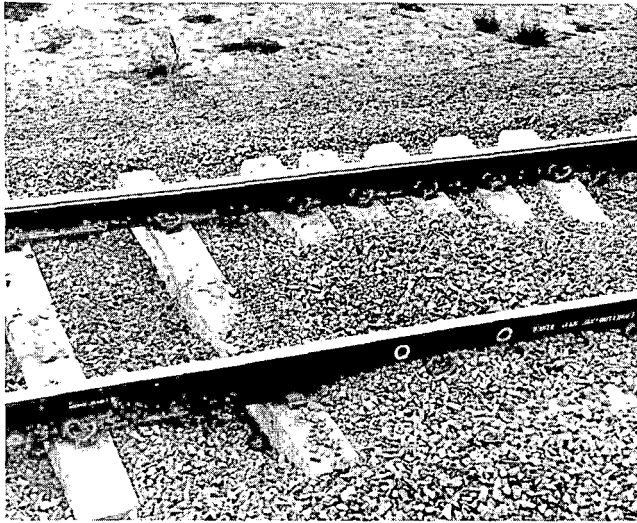


FIGURE 7. TIE SKEWING CONCRETE TIE TRACK.

Another characteristic noted is the rapidity with which the skewing can progress. In one observed instance in an area that had a history of tie skewing, movements of up to $1\frac{1}{4}$ inches relative to the rail in one night's operation, or approximately 1 MGT of traffic occurred. This area of track had not been disturbed for several MGT prior to this event nor had it experienced any unusual movements immediately prior to the occurrence.

Conventional rail anchors have been used to correct the problem but a more direct solution aimed at the cause should be found. Our investigation into the nature and causes of tie skewing has been preliminary and informal. A formal test involving this phenomenon is commencing in February of 1982.

Several factors have been determined as affecting skewing and most can be adjusted to reduce the amount of movement.

One of the most dramatic factors is ballast shape and gradation. Ballasts of smaller size, such as AREA Grade 5, and larger ballasts of Grade 3 with a high percentage of flat particles have displayed poor performance. Large particle size with good shape factors are a must for concrete tie track. Shape factors, though extremely important, are difficult to quantify. Traditional railway engineering judgement is still the best criteria to apply.

It is also important to properly maintain ballast levels in the cribs and to keep the ballast consolidated. Tamping and regulating ballast in concrete tie track is somewhat different than on wood tie track. The tamping tool shank must be longer to allow for the greater tie depth, 7" for a wood tie and about 10" for a concrete tie. Squeeze pressure should be increased slightly to accommodate the greater tie width, 9" versus 11".

Modifications are also required to the squeeze limiter switches to prevent contact between the tool shank and the tie. Caution also needs to be exercised with ballast regulators to prevent striking

fasteners with the plow. Modifications with a cutting torch are usually sufficient to correct this problem.

Rail clips in the higher toe load ranges have also displayed improved skewing performance, but design of the clip system may be such that high longitudinal resistance can be achieved in the lower toe load ranges when incorporated with resilient tie pads.

Ties located towards the bottom of a grade and in higher degree curves show poorer skewing performance. Little can be done to correct this condition outside of line relocation.

The effects of tie pad friction also plays a role in tie skewing. First, the tie pad spring rate must be matched to the clip toe load, to produce a prestress deflection adequate to prevent rail/tie pad separation during vertical deflections but not so high as to restrict dynamic pad performance. Also, a high coefficient of friction is desirable to restrain movement during vertical deflection. To achieve these criteria, resilient pads appear to be desirable. Caution must be exercised in the selection of pad material. Some of the resilient pad materials are extremely temperature sensitive and subject to mechanical wear. Also, some material appearing resilient became quite rigid under dynamic loading. The introduction of a "shape factor", usually in the form of grooves has shown beneficial effects on resilience and material life.

VIBRATIONS

Recently, an investigation into the vibrational behavior of concrete tie track was begun at FAST. Using accelerometry techniques and spectrum analysis, significant advances have been made in understanding the dynamic characteristics of the track structure. Under the guidance of Dr. Robert Baird, FAST staff dynamicist, a close correlation between track vibrations and certain degenerative processes has been found.

In the initial experiments conducted at FAST, four accelerometers are used to measure the vertical movements of the rail and tie. These accelerometers are mounted on the rail base and on the tie at the center, rail seat and the tie end, as shown in Figure 8. The data collected during a train passage is converted into frequency-domain representation using a fast Fourier transformation.

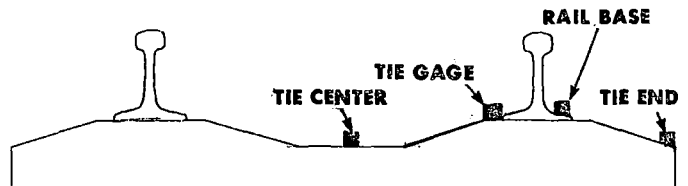


FIGURE 8. CONFIGURATION OF ACCELEROMETERS.

Figure 9 shows the frequency band distribution of energy measured at the tie rail seat. The band of frequencies investigated is from 0 to 200 Hz. Little energy is seen above 200 Hz at FAST. A very predominant spike is seen at 116 Hz. By calculation, the fundamental frequency of a concrete tie is estimated in the 110 to 120 Hz range. We feel confident that the 116 Hz spike is the vibration of the tie.

These vibrations were measured on freshly ground rail with a rigid tie pad installed.

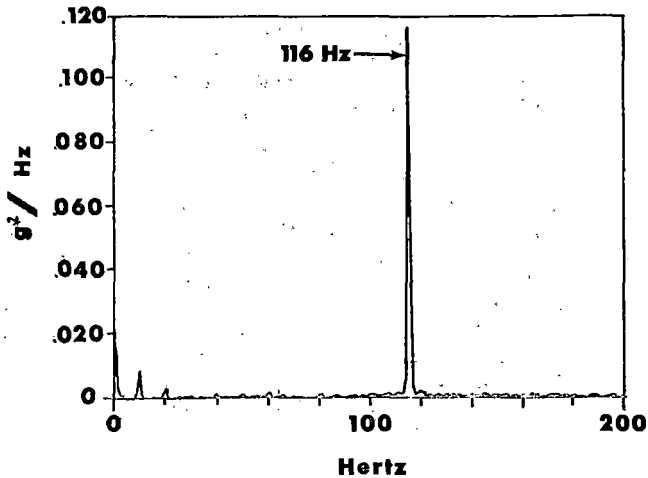


FIGURE 9. AUTO SPECTRUM CONCRETE TIE, NO CORRUGATIONS.

The fundamental of 116 Hz in the tie excites the first symmetrical bending mode, see Figure 10. Higher modes of bending have been reported as significant in the literature, particularly as a result of experiments by British Rail and Battelle - Columbus Labs. These higher modes are seen on high speed trackage but FAST has not seen evidence of excitation other than the first mode under 40 MPH freight traffic. As seen in Figure 10, the first symmetrical mode can exaggerate the center bending stresses in the tie.

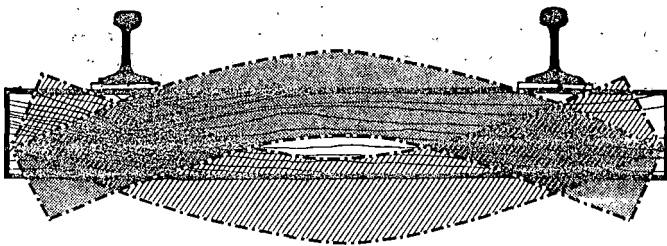


FIGURE 10. 1ST SYMMETRICAL BENDING MODE.

Figure 11 is a spectral analysis of data collected by a Loram Corrugation Analyzer in the vicinity of the previous vibration measurement before grinding of the corrugations at this location. This device operates at a closely regulated 4 MPH and a clear, dominant spike is seen at 11.6 Hz. When converted to the 40 MPH operating speed of the train, the corrugation wavelength yields a frequency of 116 Hz,

the same as the fundamental frequency of the tie! A conclusion to be made is the wavelength of corrugations is defined by the vibrational frequency of the tie. Additional measurements at FAST confirm this conclusion including some preliminary work with wood ties which have a lower frequency and correspondingly longer wavelengths.

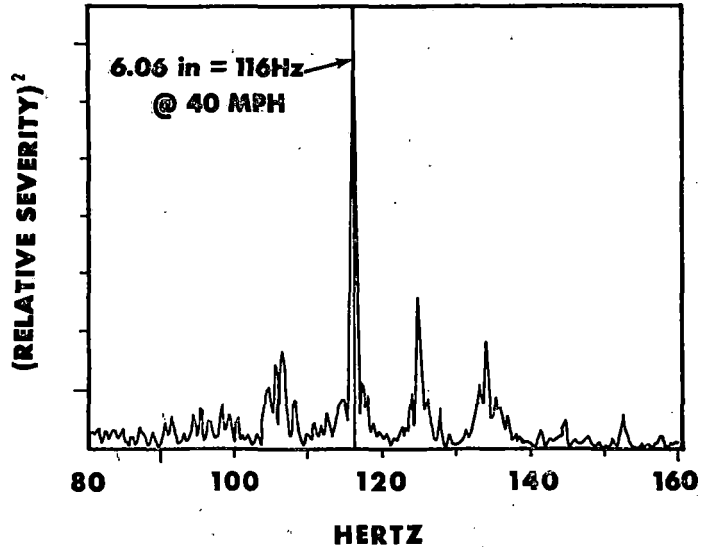


FIGURE 11. CORRUGATION WAVE LENGTH DISTRIBUTION.

Another vibration measurement was made on the base of the rail at the same location before corrugations were ground. In Figure 12 these measurements show a wide band of energy, occupying the band from 100 to 180 Hz. The 116 Hz fundamental is still quite visible. Under this condition, the movement of the rail became very complex as opposed to the simple 116 Hz vibration seen after grinding on smooth rail. This frequency distribution bears some resemblance to the spectrums measured on smooth ground rail with resilient tie pads installed.

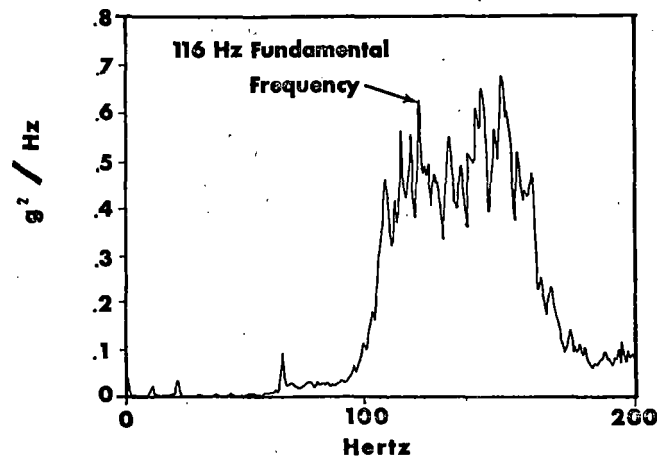


FIGURE 12. AUTO SPECTRUM CONCRETE TIE; HEAVY CORRUGATIONS.

A hypothesis can be drawn that if the rail can be decoupled from the tie at 116 Hz, corrugation growth

could be retarded. Tests of this hypothesis have not been performed though further testing in this area is to be undertaken.

CONCLUSIONS

The decision to use concrete ties in lieu of conventional wood tie construction places many decisions with the track designer not traditionally encountered. Only a portion of those decisions in the selection of components are fully covered by generally accepted specifications.

The most complex decision involves the selection of clip toe load and tie pad spring rate. As experience has been gained with concrete ties on FAST and elsewhere, the individual properties of these two components are seen to act in concert dramatically affecting the overall performance of the concrete tie track system.

In the selection of clips and pads, the designer is faced with the decision of dynamically stiff or resilient track. The thought in North America was to achieve as stiff a track system as possible. This end can be achieved by employing clips with relatively high toe loads and hard tie pads.

The newer fastener systems being made available on this continent generally reflect this philosophy. The basis for this design criteria is that the high toe load clip restricts deflections, hence minimizing fatigue problems. The hard pad is also chosen for the purpose of prolonging service life.

While it has been proven that high toe loads resist tie skewing, FAST testing has not shown that the high toe loads have prevented fatigue in the clip. Hard pad materials have been shown to hold up very well under traffic but tests have now shown that resilient synthetic rubber materials have the ability to withstand heavy traffic.

The designer now has the choice of using resilient tie pads in a concrete tie track system, taking the advantages inherent in resilient pads: resistance to tie skewing independent of high toe loads, attenuation of high transient impact loads and decoupling of the rail from undesirable tie vibrations.

The choice is then left to match clip toe load to the pad. The only resilient tie pad system tested at FAST operated at relatively low toe loads. The system performed extremely well under harsh loading conditions and clip fatigue was not seen to be a problem. Other low toe load systems have shown tendencies to fatigue with rigid tie pads installed. Low toe load clips that withstand large deflections are entirely feasible and such designs exist. Tests have not yet been conducted at FAST of the high toe load clips on resilient pads.

We have reached a point in the testing where by characterizing the loads and deflections of the various component combinations in track and translating these criteria into realistic laboratory tests, a great savings in cost and time can be achieved. Laboratory testing can clarify and quantify these empiric relationships.

RECOMMENDATIONS

CWR rail with field welds is a must as most clip

manufacturers do not recommend the use of clips on rail joints. An additional adverse effect is encountered with the increased dynamic action at mechanical joints. The user should consult with the manufacturer concerning mechanical or insulated joints.

Ballast should have large particle size and good shape factors. AREA Grades 3 and 24 have performed well. Most granites have worked well. If limestone or slag are of interest, the Santa Fe has installed large test sections of these materials in concrete tie track. Results of the Santa Fe experience should be forthcoming.

The questioning of whether concrete ties are adequate for U. S. Mainline Service has past. The elements are almost in place to allow the designer to integrate very successful concrete tie track systems, tuned to the operating conditions which will be encountered.

QUESTIONS AND ANSWERS

Question 1

You mention particle shape is a prime consideration for ballast used under concrete ties. Please define particle shape. Is particle shape a characteristic of individual aggregate formations and crushing methods?

Answer

The definition of ballast particle shape has long been an unquantifiable factor in railway engineering. Many systems have been devised to describe the shapes of the individual particles but none have been accepted into popular use. Terms such as sphericity, flakiness index, and others have appeared but are little understood. The AREA Ballast specifications also say little about shape except that no more than 5% by weight of the ballast shall be flat or elongated particles having a length greater than or equal to 5 times the average thickness.

This leaves the railway engineer with applying qualitative criteria in the evaluation of ballast for concrete tie track. Concrete tie track has shown itself to be very sensitive to ballast with less than ideal particle characteristics.

The criteria which has been traditionally applied by railway engineers to particle quality seem the best to apply from observations of track performance at FAST.

Sharp edges with flat surfaces and relatively cubic dimensions are the parameters which should be rigorously applied. The AREA specification for flat particles should also be considered somewhat liberal for concrete tie ballast.

Another observation at FAST is that ballast that originally has high quality particle shapes but with edges that become rounded with wear will degrade performance. Since ballast will not indent the surface of concrete as it does with wood ties, the interlocking ability of the ballast becomes very important to maintain geometric stability of the track.

Some rock formations naturally fracture into a high percentage of flat particles and would not be suitable for concrete tie tracks.

Question 2

Can you quantify the relative longitudinal resistance of fasteners? Were any tests conducted to measure longitudinal resistance?

Answer

Longitudinal resistance has only been evaluated at FAST by observation of performance in the track. All the fastener systems installed at FAST have passed the AREA acceptance tests, which are static in nature but a wide variation in performance has been observed under traffic.

No correlation between fastener toe load and longitudinal resistance has been found at FAST, however, it appears that tie pad resiliency may be a greater factor in longitudinal resistance under dynamic loads. Because of limited sample size, this result cannot yet be statistically verified.

Dynamic deflection measurements between the rail and tie do show that separation of the tie, tie pad, and rail does occur.

The use of resilient tie pad can reduce these occurrences by increasing pre-load crushing of the pad.

Question 3

In your recommendations for concrete tie systems, it is felt you left out one important consideration--fasteners must be able to fit insulated joints. It is not practical to have special ties for insulated joints and as most main line track has insulated joints, this becomes an important consideration. Further, clips must have adequate restraint to prevent skewing of the ties under insulated joints.

Answer

Insulated joints are one of those necessary evils that must be endured in the track. In dealing with these joints, consult the manufacturer of the clip systems in which you are interested.

The experience of FAST has shown that longitudinal restraint under the increased dynamic action of any mechanical joint is a problem of some significance. Practice developed on the FAST loop is to construct all mechanical joints in a manner that they are suspended and then box anchor both joint ties with conventional rail anchors. Since joints are few and far between, this should not cause any signi-

ficant economic burden. An anchor with deep vertical relief should be selected to contact the concrete tie below the top edge bevel. Adhering to the recommendation for ballast quality and tie pad resiliency will minimize the problems encountered.

TIE/BALLAST INTERACTION

Bruce Bosserman
 Experiment Manager, Ballast
 Federal Railroad Administration

As part of the effort to determine the differences in overall track performance between wood and concrete ties, a related series of ballast and subgrade tests have been conducted. Comparisons have been made in track settlement, track modulus, lateral resistance, ballast degradation, ballast strain, subgrade load, and subgrade deflection between wood and concrete tie track.

As stated in the Ballast Experiment Paper, Section 03 (wood ties) and 17 (concrete ties) contain three common ballast types. Comparison of track settlement rates between common ballast types has shown the amount of settlement in Section 03 to be generally 25 to 50% higher than in Section 17. This is illustrated in Figure 1 for the Georgia granite ballast. The difference in settlement after 93 MGT is shown by the T test to be significant at the 99% level.

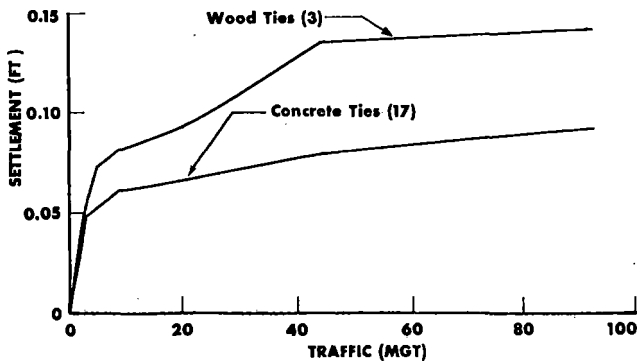


FIGURE 1. TOP OF RAIL SETTLEMENT, GEORGIA GRANITE BALLAST.

The differences in track modulus between the two sections are also highly significant, with the mean for Section 03 being 3000 lb/in/in and that for Section 17, 7500 lb/in/in. Mean variation of track modulus is shown in Figure 2.

For all three common ballasts, the degradation after 200 MGT was approximately equal for wood ties in Section 03 and concrete ties in Section 17, as shown in Figures 3 and 4.

Care must be exercised when considering the above comparisons. There are several parameters (grade,

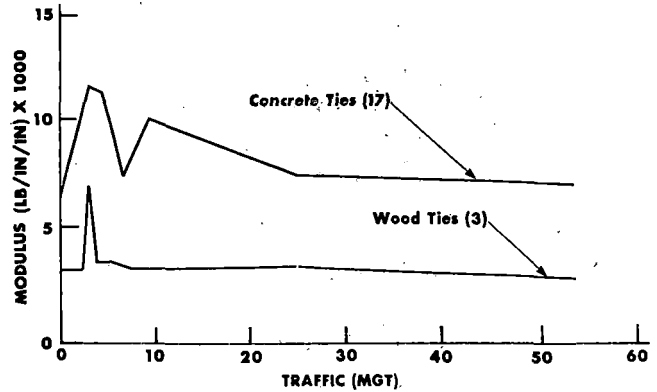


FIGURE 2. VERTICAL TRACK MODULUS, SECTIONS 3 & 17.

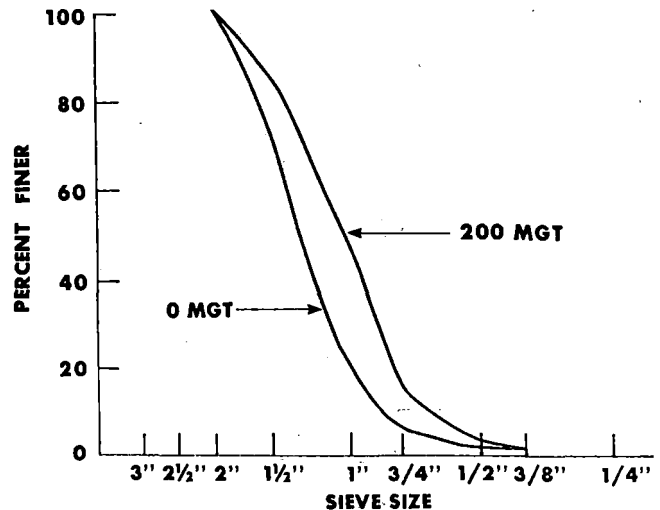


FIGURE 3. CHANGE IN GRAIN SIZE DISTRIBUTION, MINNESOTA GRANITE BALLAST - SECTION 3 (WOOD TIES).

train speed, ballast depth, and subgrade characteristics) which vary between Sections 03 and 17 and may have affected some of the test results. A more valid comparison of wood and concrete ties is provided in Section 22.

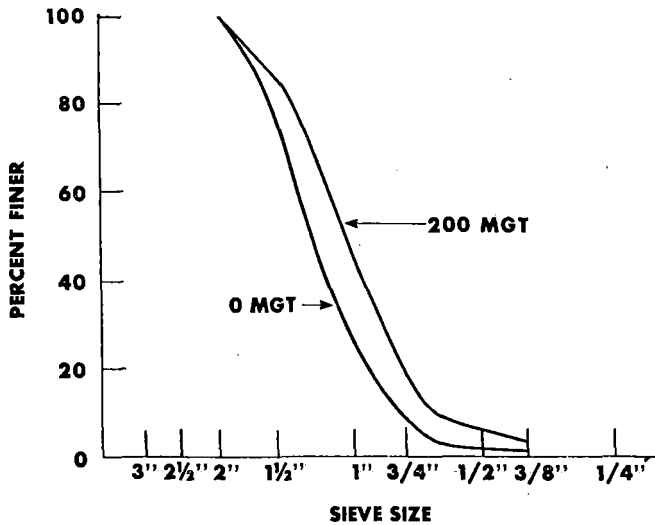


FIGURE 4. CHANGE IN GRAIN SIZE DISTRIBUTION, MINNESOTA GRANITE BALLAST - SECTION 17 (CONCRETE TIES).

At the request of the Office of Intercity Programs (Northeast Corridor Project) of the Federal Railroad Administration, Section 22 was rebuilt at 425 MGT to serve as a test for the Corridor concrete tie design. The test section consists of two subsections, one containing wood ties 7"x9"x8'6" on 19 1/2" centers and standard 7 3/4"x14" 1:40 tie plates with four cut spikes per plate. The other subsection contained prestressed concrete ties approximately 9"x11" (at rail seat) by 8'6" on 24" centers, a rigid tie pad and four Pandrol clips per tie. Each subsection contained 300 ties with 136 lb/yd RE standard carbon rail. The ballast sections under each type of tie were of equivalent thicknesses of AREA #3 traprock similar to that used in the Corridor.

Grain size distribution tests were conducted in Section 22 as in Sections 03 and 17. Table 1 presents the change in gradation for the traprock ballast under both wood and concrete ties between 0 and 200 MGT. There appears to be little difference in

the degradation that occurred under wood and concrete ties.

Top of rail settlement was measured in both subsections. Figure 5 shows the total settlement accumulation with traffic after construction. As can be seen, the settlement after 93 MGT was equal for each subsection. The settlement measurement was repeated after an out-of-face surfacing and lining operation in Section 22. Figure 6 shows that the settlement 100 MGT after tamping was greater for concrete ties than for wood ties. These settlement comparisons will be discussed later.

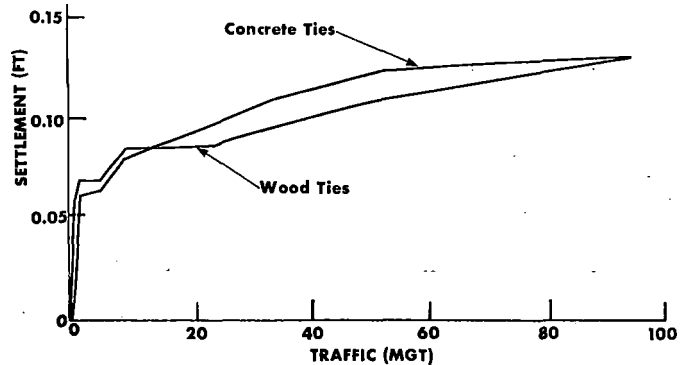


FIGURE 5. TOP OF RAIL SETTLEMENT, SECTION 22 (AFTER CONSTRUCTION).

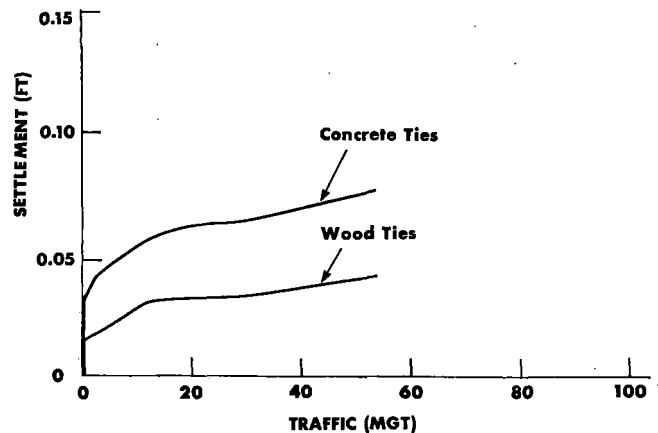


FIGURE 6. TOP OF RAIL SETTLEMENT, SECTION 22 (AFTER TAMPING).

TABLE 1.

NORTHEAST CORRIDOR TRAPROCK SECTION 22 PERCENT PASSING

SIEVE	0 MGT	200 MGT	
		WOOD	CONCRETE
2 1/2	100	100	100
2	97	98	97
1 1/2	49	61	62
3/4	1.3	3	4
1/2	0.4	1.0	1.1
3/8	0.3	.6	.6

Track modulus values were also calculated for Section 22. As in Sections 03 and 17, the concrete ties, on the average, exhibited a much higher average modulus (7,800 lb/in/in) than wood ties (3,700 lb/in/in). The T test shows this difference to be statistically significant at the 99.9% level. Figure 7 shows the variation of track modulus with time. Interesting trends are evident from the figure. Between 2 MGT and 5 MGT, both wood and concrete ties exhibited peaks in track modulus. These peaks correspond to a period of very cold weather preceded by a snowfall that melted into the ballast, thus creating a frozen condition that is believed to have caused the modulus increase.

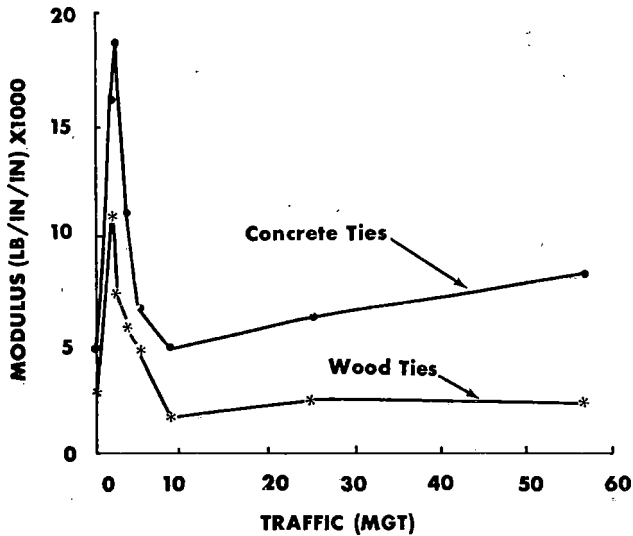


FIGURE 7. VERTICAL TRACK MODULUS, SECTION 22.

Other than the early peak, the concrete ties exhibited a gradual increase in modulus with traffic while that for the wood ties remains essentially constant. Section 03 exhibited a similar trend for wood ties. In Section 17, two of the ballast types showed slight increases in modulus, while for the other three, it remained relatively constant.

A recently designed fixture, developed at the University of Massachusetts, was used to measure lateral resistance of concrete ties for comparison with wood ties in Section 22. As in Sections 03 and 17, lateral resistance was measured both before and after a surfacing and lining operation. Figure 8 shows the load-deflection curves for wood and concrete ties (after 90 MGT of traffic) both pre- and post-maintenance. The reduction in lateral resistance after maintenance is clearly evident for both tie types. Prior to maintenance, the lateral resistance of the concrete ties was 1.6 times that for wood ties. Following maintenance, this factor was reduced to 1.3. It must be remembered that the tie spacing for concrete ties is 24" while spacing for wood ties is 19 1/2". When considering lateral resistance per foot of track, the advantage shown by concrete ties is reduced to 1.3 (pre-maintenance) and 1.1 (post-maintenance). T tests show the differences between tie types to be significant at the 95% level for the pre-maintenance condition, but not for post-maintenance.

Four locations in Section 22, two in each subsection, were instrumented to measure strain in the ballast, stress applied to the subgrade, and subgrade deformation. Ballast strains and subgrade deformations are measured both on a long-term permanent and dynamic (under train loading) basis. Subgrade stresses are measured only dynamically. Figure 9 presents a schematic of the instrumentation installation.

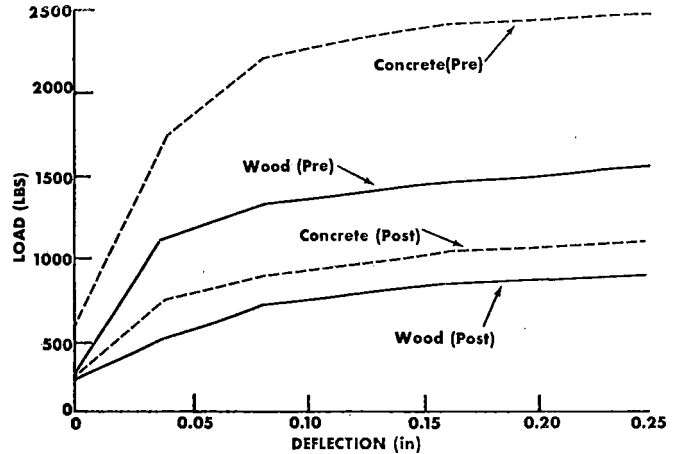


FIGURE 8. LATERAL TIE RESISTANCE, SECTION 22 (PRE AND POST MAINTENANCE).

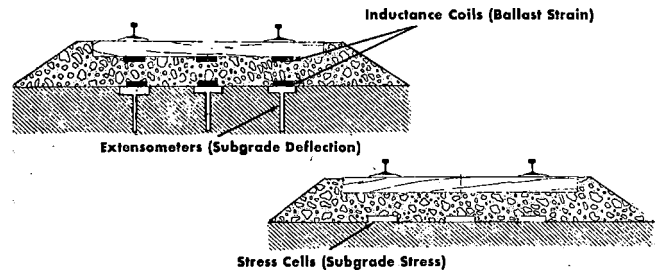


FIGURE 9. BALLAST AND SUBGRADE INSTRUMENTATION, SECTION 22.

Figure 10 presents a plot of long term ballast strain versus traffic after construction. An out-of-face surfacing and lining operation was performed in Section 22 at 93 MGT. Figure 11 shows ballast strain after tamping plotted versus traffic. Both figures show the ballast strains to be significantly higher for concrete ties than for wood ties.

Long term subgrade deflection versus traffic is plotted in Figure 12. Here the trend is opposite from that with ballast strain; subgrade deflection is higher for wood ties than for concrete ties. The observed differences in top of rail settlement can be explained through study of the ballast strains and subgrade deflections. After construction, higher ballast strain in concrete ties was balanced by lower subgrade deflection giving essentially equal total settlement. After tamping, subgrade deflections for both tie types were very small, while ballast strains remained higher for concrete ties. Thus total settlement was higher for concrete ties.

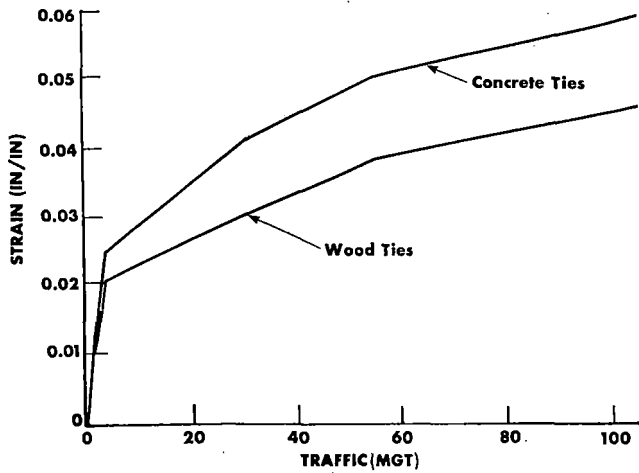


FIGURE 10. LONG TERM BALLAST STRAIN, SECTION 22 (AFTER CONSTRUCTION).

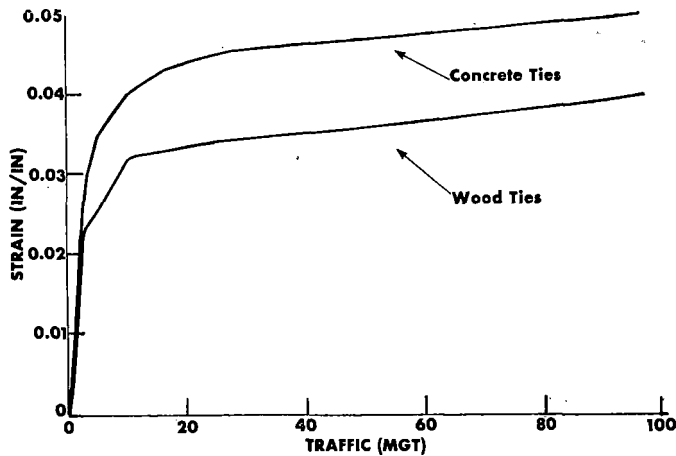


FIGURE 11. LONG TERM BALLAST STRAIN, SECTION 22 (AFTER TAMPING).

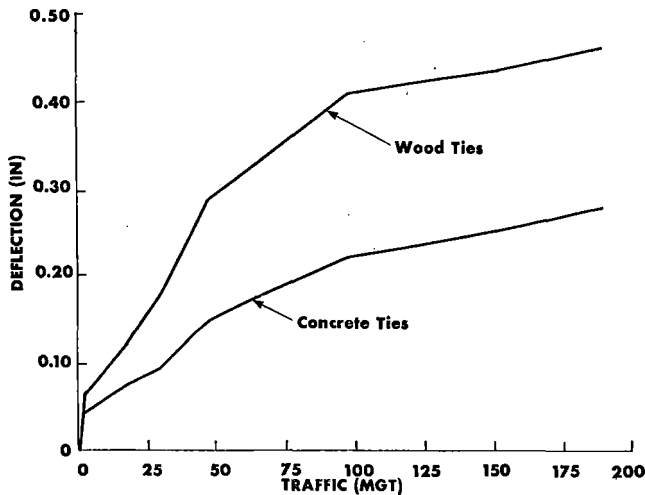


FIGURE 12. SUBGRADE DEFLECTION, SECTION 22.

There was considerable variation in the data for subgrade deflections and the differences between concrete and wood tie track may be a function of this variation and not any real differences between concrete and wood tie track. The higher ballast strains in concrete tie track may be a reflection of the rigidity of the track structure (the higher track modulus). In addition, there may be more vibrational impact into the concrete tie track because of the lack of damping on the tie structure vis-a-vis a wood tie. This latter effect can be negated somewhat by the use of a resilient tie pad.

It may be argued that greater tie spacing for concrete ties counteracts the higher bending stiffness and increases pressures under the rail seat. However, concrete ties are wider than wood ties so that the ratio of width to tie spacing is approximately equal (0.46).

Additional tests at FAST on validating the differences in settlement between concrete tie and wood tie track will improve on this evaluation.

Peak dynamic subgrade stress versus axle load is plotted in Figure 13. For all axle loads, the wood

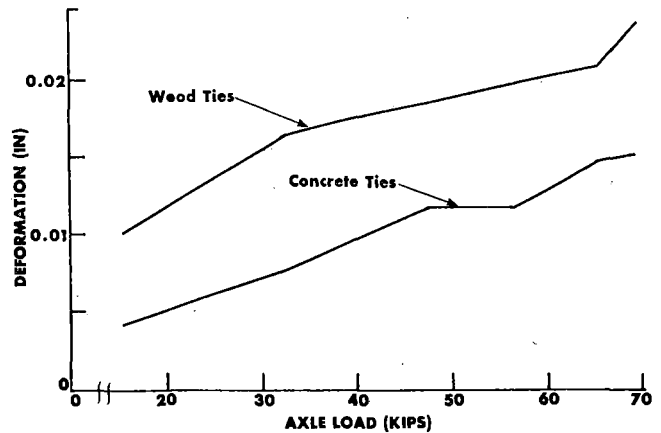


FIGURE 13. VARIATION IN PEAK DYNAMIC SUBGRADE STRESS WITH AXLE LOAD, SECTION 22.

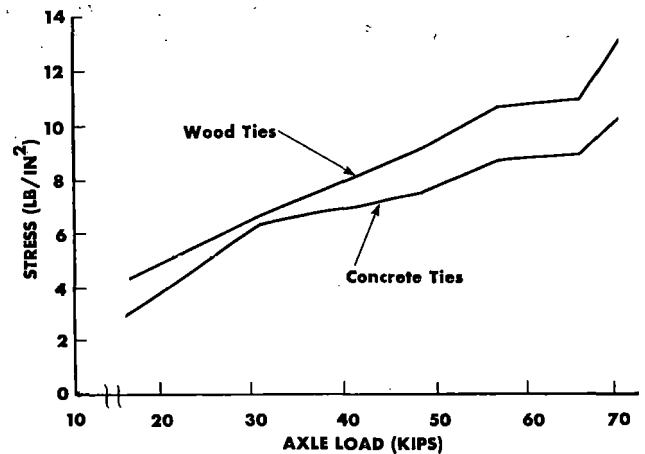


FIGURE 14. VARIATION IN PEAK DYNAMIC SUBGRADE DEFLECTION WITH AXLE LOAD, SECTION 22.

ties stressed the subgrade higher although the difference is not statistically significant due to large variability in the data. Peak dynamic subgrade deflections are similarly plotted in Figure 14. Again, wood ties cause higher deflections in the subgrade. Here, the differences are statistically significant. Dynamic ballast strain data is currently being evaluated.

The results of the comparison of concrete and wood tie track have shown that in Sections 03 and 17 there was more settlement after construction on wood tie track and an approximately equal amount of ballast degradation. The differences in performance in these two sections can probably be attributed more to varying test site conditions than to anything else.

In Section 22, a more valid test where the sections were back to back on the same track configuration, the substantive differences in performance between concrete and wood tie track were higher settlement and greater lateral resistance for concrete tie track. Whether the increased settlement indicates greater differential settlement has not been evaluated. However, it is apparent that there is no detrimental effect on the ballast degradation or subgrade stresses as a result.

QUESTIONS AND ANSWERS

Question 1

You showed relative average settlement under concrete ties and wood ties. Was there any variation in variability of this settlement, for example in standard deviation of settlement.

Answer

Actually it is the differential settlement which controls the maintenance cycle. So far there has been insufficient traffic to show difference in differential settlement.

SOME ASPECTS OF CONCRETE TIE PERFORMANCE IN FAST AND IN REVENUE SERVICE

Howard G. Moody
Experiment Manager, Ties & Fasteners
Federal Railroad Administration

When FAST was originally conceived there was some concern that the test would be truly representative of any revenue service application. Since FAST test results are to determine life cycle performance of various track and mechanical components for use in revenue service, it was reasonable to assume that some relationship should be established. If the relationship of FAST to revenue service is not direct because of some dependent variable not present in FAST, or if FAST is unrepresentative of the load and load frequency distribution in revenue service, corrections to FAST data can be made. In addition the FAST operation could be changed to eliminate or add the appropriate governing factors or variables. This would improve both the quantitative and qualitative results of FAST.

In September 1979 a Federal Railroad Administration contract was awarded to Battelle Columbus Laboratories in Columbus, Ohio to conduct a correlation analysis between FAST and revenue service. The area chosen for study was concrete tie and fasteners because of the existence of four active tests in revenue service to which a correlation could be made.

The objective of the study was to determine whether or not FAST was representative of revenue service and if not, how the results from FAST can be changed to agree with revenue service or how FAST can be changed to conform with revenue service. A summary of each of the four test sites is shown in Table 1. In general the test sites contained prestressed monoblock concrete ties of equivalent length and strength to those being tested at FAST. Bending strength in the rail seat region of the ties exceeded 300,000 in pounds which conforms to the AREA requirements for ties at 30" spacings, even though the ties were placed at 24". There were differences at each test site in traffic density and mix and track construction. This tended, through careful analysis, to reinforce the correlation analysis by providing a broader spectrum of service conditions to compare with FAST.

In three of the four test sites, except the Kumis site on the Norfolk and Western Railway, a complete evaluation was made of concrete tie track performance. This included measurements of wheel rail vertical and lateral loads, tie bending moments, vertical track stiffness, ballast and subgrade

TABLE 1. TEST SITE STATISTICS

Location	Date Installed	Track Configur.	Traffic	Tonnage	Rail	Ties	Fasteners	Ballast
ATSF Leeds, Ill. MP 102	1974	Tangent	Mixed freight to 70mph; AMTRAK to 79mph	20MGT/yr; 140MGT to date	136# RE CWR	8'6" and 9' prestressed concrete at 24"	3 types of elastic clips; 2 types of pads	Area #4 granite
AMTRAK NEC ... Aberdeen, MD MP 68.7	1978	Tangent	Mixed freight to 70mph; AMTRAK to 110mph	20MGT/yr; 70MGT to date	140# RE CWR	8'6" prestressed concrete at 24"	1 type of elastic clip; 1 type of pad	Area #24 trap rock
C&O Lorraine, VA MP 11.6	1974	3° curve	Mixed freight unit coal trains 45mph	30MGT/yr; 220MGT to date	122# CWR	8'6" and 9' prestressed concrete 25"	2 types of elastic clips; 2 types of pads	Area #4 granite (mixed)
N&W Kumis, VA MP 261	1974	Tangent	Unit coal trains 40mph	50-60 MGT/yr; 260MGT to date	136# RE CWR	8'6" prestressed concrete at 24" and 26"	1 type of elastic clips; 2 types of pads	Area #3 granite

properties, track settlement and track geometry. At the Leeds test site a wood tie test section was also evaluated. There was also a wood tie test section at FAST. Due to time constraints a limited assessment of the track performance at Kumis was done. This included the wheel rail loads and tie bending moments.

At every test site location visual inspection of ties, pads, and fasteners was made at frequent intervals to determine component performance. Similar inspections were made at FAST. In early June 1980, while inspecting the concrete tie track on the Northeast Corridor, several transverse rail seat cracks were found in the concrete ties. Subsequent investigations of concrete ties at Kumis and Leeds, added to a previous inspection at Lorraine, revealed that a sizeable population of ties had transverse rail seat cracks of from 1" to 6" in length as shown in Figure 1. None of the cracks had progressed to the point where the tie was no longer functioning but the history of concrete tie performance in this country indicates that these types of cracks will considerably shorten the 50 year life expectancy of the tie. A summary of the tie inspections is shown in Table 2.

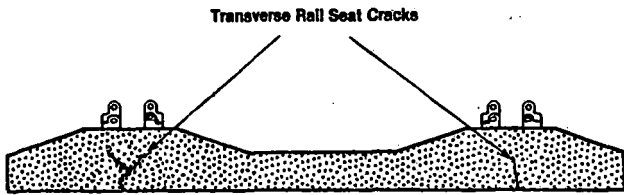


FIGURE 1. CONCRETE TIE TRANSVERSE RAIL SEAT CRACKS

TABLE 2. SUMMARY OF TIE INSPECTIONS

Location	Number Inspected	Number Cracked	Percent Cracked	MGT	Traffic Loads
FAST	600	0	0	425	Heavy; no flats
Streator	80	11	14	125	Medium; moderate flats
Richmond ...	80	44	55	220	Heavy; moderate to severe flats
Aberdeen	60	56	93	70	Light, medium; high speed flats
Roanoke	48	48	100	280	Heavy; severe flats
(N&W)					

In general the greater the percentage of cracked ties, the longer the cracks are. The most severe cracks were found on the ties at the Kumis test site. As stated previously all of these ties meet the AREA standard for concrete tie rail seat bending strength for ties placed at 30". Most of the ties averaged about 20% stronger than the standard or 360,000 in-lbs bending strength.

The periodic inspections of concrete ties in FAST have not revealed any rail seat flexural cracks of the kind found in revenue service. This result indicated that there were differences in loading between FAST and revenue service which needed to be identified. This could, in turn, be used to improve the FAST test environment.

Wheel/rail load and tie bending moments were measured at all revenue service locations and at FAST. The results, as plotted on a log scale in Figures 2

and 3 show that bending moment values that exceeded the strength capability of the tie do occur in all sites except FAST.

FAST & NORTHEAST CORRIDOR DISTRIBUTIONS (1980 DATA)

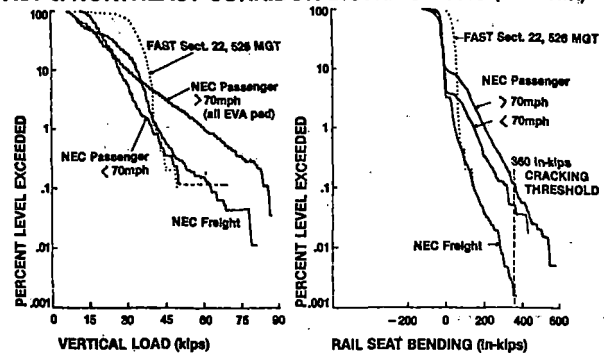


FIGURE 2. LOAD AND BENDING MOMENT DISTRIBUTIONS FOR FAST AND NORTHEAST CORRIDOR.

FREIGHT TRAFFIC DISTRIBUTIONS (1981 DATA)

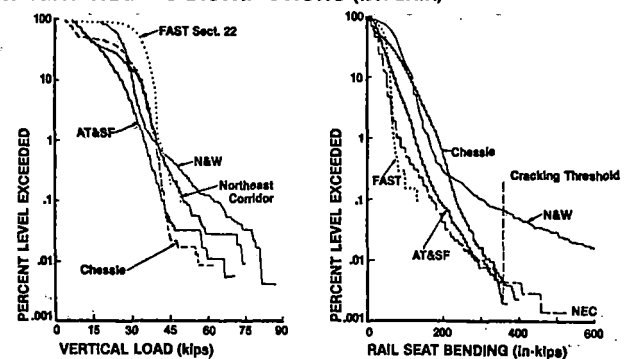


FIGURE 3. LOAD AND BENDING MOMENT DISTRIBUTIONS FOR FAST AND REVENUE SERVICE SITES.

In Figure 2 the data are separated into four groups, FAST, NEC freight, NEC passenger at less than 70 mph and NEC passenger greater than 70 mph. The majority of the bending moments exceeding the 360 in-kip cracking threshold were from the passenger equipment above 70 mph.

For the other sites, the most severe condition was, as predicted by the visual inspections, on the N & W at Kumis. The traffic on that test section is primarily loaded 100 ton hopper cars. The frequency of occurrence of values exceeding the cracking threshold for the N & W and NEC was about .1% or one cracking moment for every 1000 axles. This means for the NEC an event at each tie on the average of one every 1 1/2 days.

The bending moments measured at FAST do not approach the level of severity of any of the revenue service sites. The predominant feature of the FAST loads and bending moments were the higher average values, symptomatic of the 100 ton loaded hopper car consist.

It was evident from these data that the very large loads at the .1% level and above were causing tie cracking. An inspection of the AMTRAK passenger equipment revealed that some of these high loads were caused by long wavelength irregularities on the

wheel tread. On one car an 18" .075" deep irregularity in the wheel tread caused an 80,000 pound wheel/rail vertical load. In two cases there were three of these irregularities varying in depth from .030" to .075" approximately 120° apart on the tread. There were also a considerable number of cars with spalled wheel tread surfaces that in general produced high wheel rail loads and tie cracking moments less severe than the tread irregularities previously mentioned. In all cases these occurred with disc brake equipment and there is evidence that the use of dual brakes (both tread and disc) may help reduce the occurrence of tread irregularities.

The high wheel rail loads producing larger bending moments in freight service were probably wheel flats, although no inspections were done. There were a few very small wheel flats at FAST which explains the lack of high impact loads there which can crack a concrete tie.

Since the occurrence of these cracks was likely to reduce considerably life expectancy of the ties, solutions to the reduction or attenuation of the impact loading on the NEC were sought. There was considerable evidence from experience with concrete ties in Europe that the use of a resilient tie pad would attenuate the impact loads. The pad currently in use on the NEC was very rigid and was not attenuating the impact load.

A proposal was made to and accepted by the Office of Intercity Programs (formerly the Northeast Corridor Project) of FRA to study the use of resilient rail seat pads in lieu of rigid pads to attenuate impact loads.

The first part of this process, performed at Battelle, analyzed the data collected previously to determine the shape of the tie bending moment load pulse, and to analyze the tie reaction to the load pulse.

The time history of the rail seat bending gage strain output was analyzed. This is shown in Figure 4a. The amplitude of the primary impact pulse was accentuated by recording the data at 1200 Hz, which is much higher than normal for track measurements. However, because of the short duration, 1-1½ milliseconds, and the sharp peak of the impact pulse, accurate resolution can only be obtained by recording and analyzing data at the higher frequencies.

To study the effects of the impact loads on the tie a fixture was built, as shown in Figure 5 and schematically in Figure 6 to provide impact loads onto various tie and pad configurations. Internal testing resulted in a bending moment strain gage response, as shown in Figure 4b, identical to that obtained in the field tests. The pulse width was adjusted by placing a resilient shim between the impact hammer and the impact head. By increasing the spring rate of the shim the pulse becomes narrower.

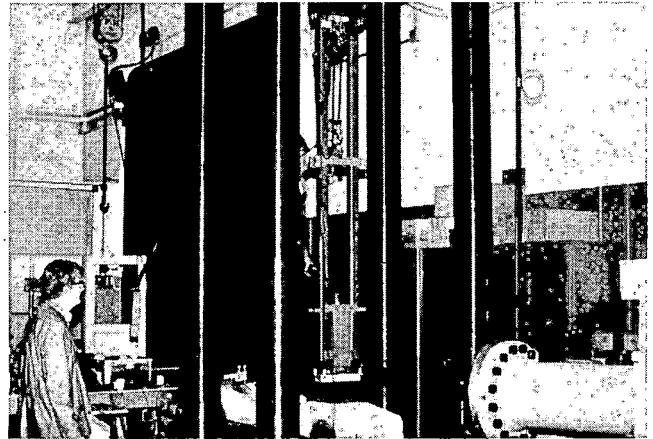


FIGURE 5. IMPACT TEST FIXTURE

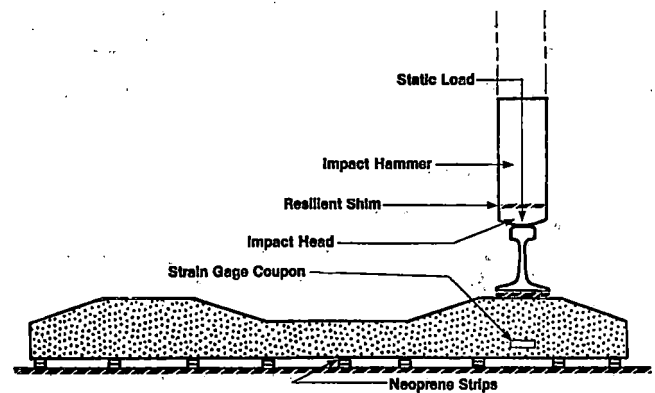


FIGURE 6. IMPACT TEST FIGURE SCHEMATIC

Various test configurations were tried, with different tie support conditions and the use of a vertical preload on the rail. The response of the tie was not very sensitive to either changes in tie support or in the amount of vertical load applied to the fixture. As a result the tie was simply supported on neoprene rubber strips and a 1000 lb vertical preload was applied to hold the drop hammer fixture in place.

The impact tests were begun using a rigid EVA pad and RT7SS-2 concrete tie which is the NEC configuration. At a drop height of 16 inches above the rail head it was possible to crack the tie. An example of the type of crack is shown in Figure 7. Stresscoat, a brittle lacquer was applied to the region where the cracks occur. This accentuates the

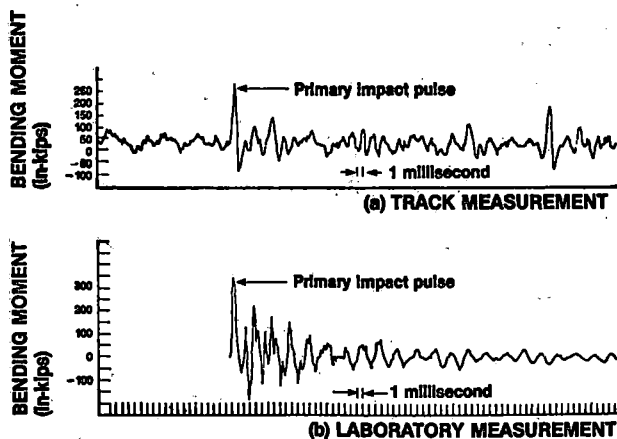


FIGURE 4. TIE BENDING MOMENT TIME HISTORIES

appearance of the crack. Further testing demonstrated that the cracks will continue to propagate with increasing drop height, and that each succeeding growth in the length of the crack requires a larger bending moment. These larger moments are, as shown in Figures 2 and 3 clearly evident in revenue service track particularly on the NEC and the N & W.

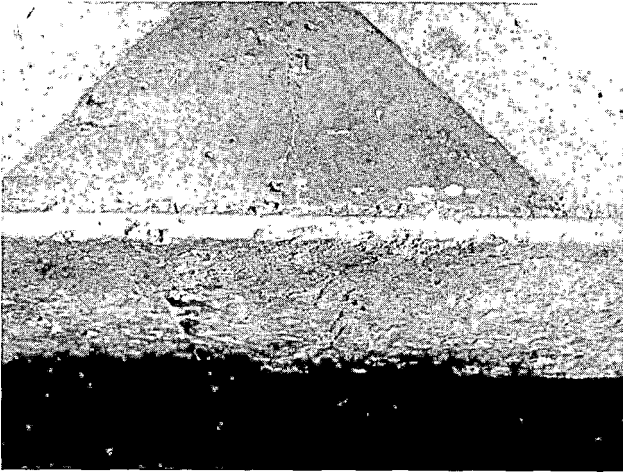


FIGURE 7. TIE CRACK FROM IMPACT TESTS

Using several different types of pads from a large spectrum of spring rates and thickness, it was shown that the pad spring rate has a large effect on attenuation of impact loads.

The pad spring rates were determined by measuring the difference in deflection produced by a range of compressive loads on the pad. A schematic of the fixture used in determining the spring rate is shown in Figure 8. The pad is placed between the rail base and a flat plate of stainless steel. Vertical load is applied through the rail at a rate of one cycle/minute for the static spring rate and 9 Hz for the dynamic spring rate. Deflections are measured by the Direct Coupled Differential Transformer and the results are plotted in real time on an X-Y plotter.

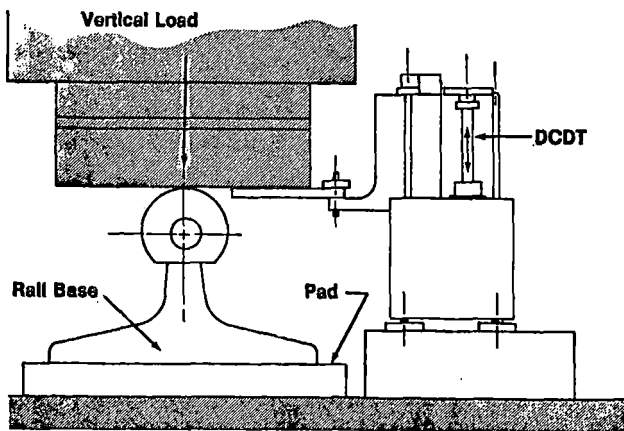


FIGURE 8. LOADING ARRANGEMENT FOR TIE PAD SPRING RATE TESTING.

Sample spring rate plots are shown in Figure 9a and 9b for the EVA pad and the STEDEF grooved synthetic rubber pad. These two pad types are at the opposite ends of the response spectrum. The EVA pad is rigid with a dynamic spring rate of 5.0 M lb/in, essentially infinite stiffness whereas the synthetic rubber pad is resilient with a spring rate of 1.2 M lb/in. It is important to note that the synthetic rubber material is not a "soft" material. The material durometer is 76 in the A scale. The resilience is obtained from the shape factor or grooves in the material. These grooves lower the spring rate while improving durability.

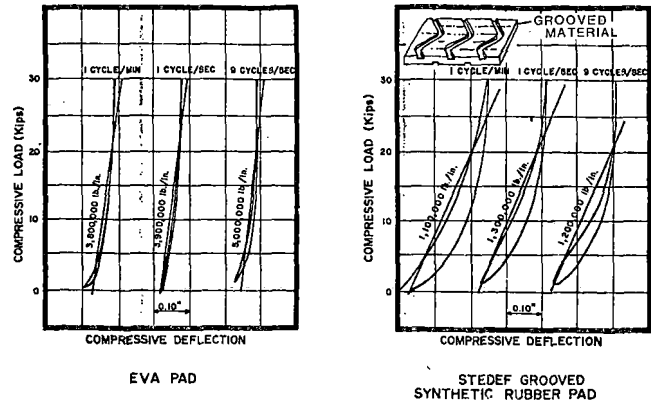


FIGURE 9. VERTICAL LOAD DEFLECTION CURVE

Several resilient pads were tested using the impact load fixture. As shown in Figure 10, all of the resilient test pads reduced the test tie bending moment when compared to the EVA pad. In Figure 10a the pads of conventional 4.5-5.0 mm thickness were compared. To obtain a greater amount of attenuation two pads of thickness greater than 5.0 mm were tested. As shown in Figure 10b these pads provided a significant increase in attenuation by reducing the rail seat bending moment for a given drop hammer height.

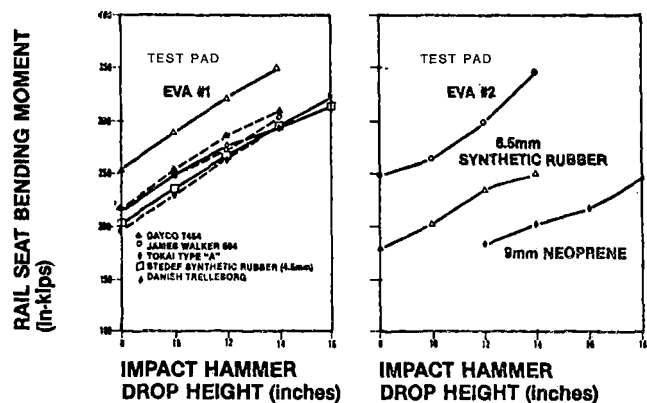


FIGURE 10. IMPACT TEST RESULTS OF VARIOUS TIE PADS

A plot of the relationship between the pad spring rate and the percent attenuation as measured by the impact test is shown in Figure 11. The percent attenuation is measured relative to the EVA pad. The two stiffnesses measures, dynamic at 9 Hz and

static at one cycle/minute are shown for each pad. The results do indicate a relationship between attenuation of impact load and the spring rate. Because the shape factors of the pads were different the relationship is not precise enough to predict the amount of attenuation from the spring rate. To obtain an accurate estimate of the amount of attenuation an impact test compared to a known pad field performance should be done.

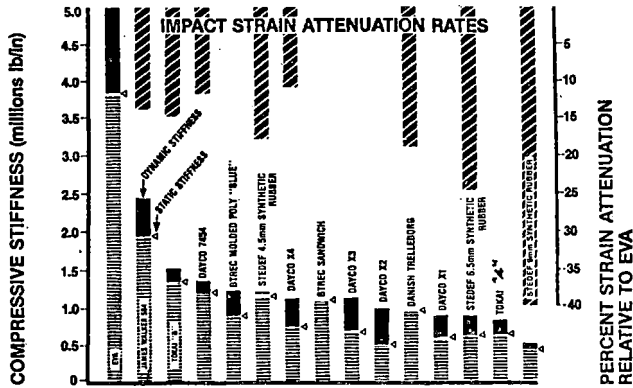


FIGURE 11. TIE PAD PERFORMANCE, TIE STIFFNESS, AND ATTENUATION.

The results from the laboratory impact test were used to select two pads for a test in the NEC track. The laboratory test, even though it was successful in providing relative results, did not provide an absolute value of attenuation. The pads selected were the 4.5 and 6.5 mm STEDEF synthetic rubber pads. They were selected because they provided the largest amount of attenuation for the thickness of pad which could be used in the NEC concrete tie system. Other pads such as the James Walker 584, the Tokai B and the Dayco pads did not provide or were predicted not to provide enough attenuation. The BTREC pads were designed for a unique fastening system not used in the NEC and the 9mm STEDEF pad was considered to be too thick. The Tokai A pad had a radical shape factor which could have caused early pad failure and was not judged to be suitable.

In early July 1981, a field test on the NEC was

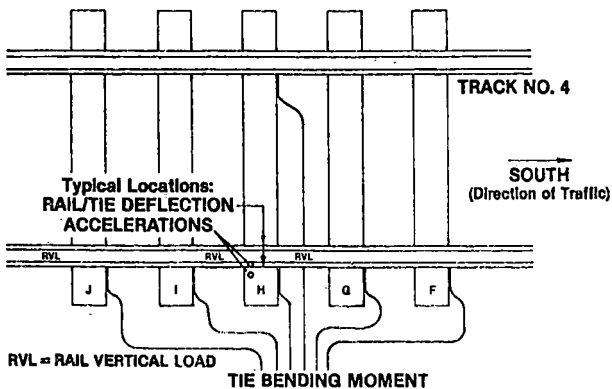


FIGURE 12. LAYOUT OF INSTRUMENTED TEST ZONE

begun using the two STEDEF pads and EVA pad as a control baseline pad. The selected test site had uncracked concrete ties which had been installed six months previously. The instrumentation array, as shown in Figure 12, had five consecutive ties strain gaged for rail seat bending moments in order to measure responses from the entire circumference of each wheel. Other measurements taken were wheel/rail vertical loads, (rail/tye) deflections and rail and tie accelerations.

Data were taken for 5 consecutive days of traffic with at least 2500 passenger axles recorded for each pad type. The pads were installed over a fifty tie test zone to prevent interaction between different pad types. The expected rate of occurrence of bending moments large enough to crack a tie was approximately 1 every 1000 axles for the EVA pad or 2 to 3 per tie for the measurement period. The data were recorded at 2500 Hz to obtain full resolution of the maximum values.

The results as shown in Figure 13 for the vertical wheel rail loads and the tie rail seat bending moments show a distinctly higher rate of occurrence of high rail seat bending moments and a somewhat higher rate occurrence of high vertical wheel rail loads for the rigid pad. The amount of reduction of peak rail seat bending moments, although not precisely calculable, was greater than that predicted by the laboratory tests. This was probably due to the load being spread more on to adjacent ties with the resilient tie pad. This was not the case in the single tie tests in the laboratory.

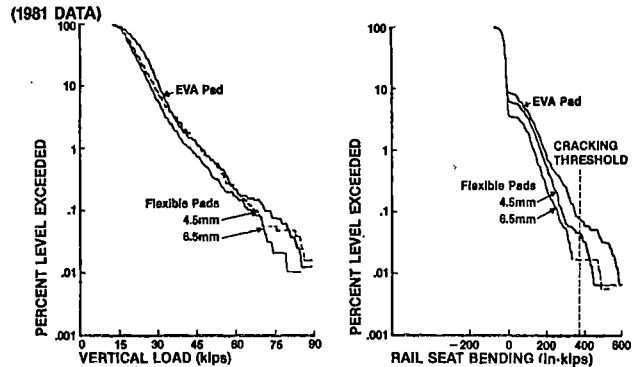


FIGURE 13. LOAD AND BENDING MOMENT DISTRIBUTIONS FOR NORTHEAST CORRIDOR.

It is also apparent from the results that the rate of occurrence and the peak values of the bending moments on the rigid pad were greater than during the June 1980 measurement period which was shown previously in Figure 2. This is an indication of an increase in population of wheels producing the high impacts and an increase in the severity of those high impacts.

Initially, there was some concern about the performance of the Pandrol clip using a more resilient tie pad. Measurement of clip deflections during the field test show no distinct difference in peak to peak clip deflections from one pad to another. The extreme values were on the order of $.020 \pm .002$ inches which is within the range of adequate performance for the Pandrol clip.

There is no doubt that the use of a more resilient tie pad will improve the performance of concrete ties by reducing the incidence of transverse rail seat cracks and preventing the crack from growing to the point where the tie fails.

Even so, when considering the use of resilient pads several pad performance criteria must be considered. The pad spring rate should be relatively uniform over the entire temperature range for the expected track conditions. For the NEC this would be from -20°F to +130°F. Also the spring rate will change over the life time of the pad, depending upon the material, its shape factor, and the environment. The Japanese National Railways found that the Shinkansen pad increased in stiffness by about two thirds over the 10 year life span of the pad. The pad must also be durable enough to withstand the track environment for the expected life. In order to be sure that the durability will be adequate a reasonable life cycle test should be performed.

The results of this part of the concrete tie correlation analysis demonstrate that FAST is not representative of revenue service in one aspect of tie performance. FAST does demonstrate that without high impact loads, concrete ties, in the current AREA design, should last for the expected life of 50 years. To be able to evaluate the degree of impact loading that would affect concrete tie performance and to evaluate the benefits of the use of a resilient tie pad with impact loading, wheel irregularities would need to be introduced into FAST.

With the acceptance and use of a resilient tie pad in concrete tie track in the U.S., there is no reason not to expect concrete ties as presently designed to last, on the average for the full fifty year expected life.

REFERENCES

1. American Railway Engineering Association, Manual For Railway Engineering, Chapter 10, 1980-81.
2. "Description of FAST Track and Mechanical Experiments," February 1979, TN79-02.
3. F. E. Dean - "Measurement and Correlation Analysis Plan for Concrete Tie and Fastener Performance Analysis," to be published, 1982.
4. F. E. Dean - "The Effect of Tie Pad Stiffness on the Attenuation of Impact Strain in Concrete Ties," to be published, 1982.

QUESTIONS AND ANSWERS

Question 1

Was there any evidence that high speed passenger trains caused greater degradation of concrete tie(s) rail seat (cracks) and if so what can be done to allow high speed passenger traffic to operate in mixed traffic concrete ties?

Answer

Yes, there is an abundance of analytical evidence that the passenger equipment was the primary cause of the large impact loads and the subsequent large concrete tie bending moments.

Things can be done with immediate benefits. They are:

- o Use a resilient tie pad. On the Northeast Corridor a pad of spring rate between 800,000 to 1.1 million lbs/in was recommended. Fastener deflections have not proven to be an issue with a resilient pad but pad durability has been. It is expected that the resilient tie pad will last a minimum of 10 years with normal traffic of 20 MGT/year.
- o Use of a wheel detector to determine which axles are producing the high impact loads. This can be done with a rail load or bending moment circuit, a real time data analyzer that can identify each axle and each peak above a specified threshold, and a means of transmitting that data to a location where the car(s) can be inspected.

CORRELATION OF FAST AND LABORATORY TESTS WITH CONCRETE AND WOOD TIE FASTENER RESULTS

Howard G. Moody
Experiment Manager, Ties & Fasteners
Federal Railroad Administration

INTRODUCTION

For any fastener component test at FAST to be successful, the results should be correlated with a laboratory test. This laboratory test could be the precursor to a specification which could serve to screen future test components for FAST or to provide inputs toward revenue service applications.

There have been several wood and concrete tie fastening systems tested at FAST with the primary test sections being Section 7 for wood tie fasteners and Section 17 for concrete tie fasteners. In the concrete tie section, the principal area of interest is the 5° curve, 2% grade. Section 7 is also a 5° curve. Throughout the FAST test programs, there have been fastener component failures. In the concrete tie fasteners section there have been pad failures, clip fractures and fallouts, and insulator fractures and wear. In the wood tie fastener section there have been tie plate failures, hold down fastener failures and fallouts, and line clip fallouts. As a result, there was an increasing amount of spike killed ties in the earlier tests on Section 7 which led to the termination of two test segments in Section 7. Prior to being included in the FAST test, concrete tie fasteners were required to pass the fastener portion of the American Railway Engineering Association (AREA) Concrete Tie Specification. For wood tie fasteners there was no equivalent specification or test requirement to be passed.

To develop a comprehensive link between the current concrete tie specification and FAST track results and to develop preliminary data for the development of a wood tie fastener specification (except for cut spikes where the question of performance is moot), a test program was begun at Battelle-Columbus Laboratories. This program involved measurements of rail to tie deflections and fastener clip strains at FAST and subsequent laboratory tests to duplicate, if possible, the field results.

Following the laboratory tests, the results were analyzed and specific recommendations made for additions and/or modifications to fastener specifications. It is important to remember that the results are indicative of FAST performance and are not designed to indicate how the performance of the fastening systems would be for any particular service application. The systems chosen for the laboratory tests were those for which there was a large amount of FAST performance results.

FIELD TEST

Two test sites were selected for each section. A description of the measurement locations and components in those locations is shown in Table 1. These sites were chosen because in the concrete tie segments, pads of vastly different spring rates were available. In addition, the spring clips in one segment on the concrete ties and one in the wood ties were the same.

The measurements to be taken, as shown schematically in Figure 1, were designed to cover all movements in three planes of rail/tie interaction. These locations are as follows:

- a. Vertical deflection at the "field side left" position,
- b. Vertical deflection at the "field side right" position,
- c. Vertical deflection at the "gage side left" position,
- d. Lateral deflection at the rail head,
- e. Lateral deflection at the rail base, and
- f. Longitudinal deflection at the field side base.

The three vertical deflections combined to determine clip deflections, rail/tie rollover and rail/tie rocking. The difference in rail head lateral and rail base lateral can also define rollover. Rail base lateral defines lateral excursion.

TABLE 1 TEST SITE LOCATIONS AND COMPONENTS

Tie Type	Configuration	Fastener Description
Prestressed Concrete 24-inch centers	5° curve, 2% grade	VSD clip, Delrin insulator, and 4.5mm synthetic rubber pad (1.4 m lb/in spring rate)
Prestressed Concrete 24-inch centers	5° curve, 2% grade	Pandrol clip, nylon insulator, and 5.0mm polyethylene pad (5.0 m lb/in spring rate)
Wood-7" x 9" x 8'6" 19½-inch centers	5° curve, .1% grade	Pandrol clip, spring clip plate and 15/16-inch screw spikes (4)
Wood-7" x 9" x 8'6" 19½-inch centers	5° curve, .1% grade	Double Elastic spike, 7 3/4" x 14" AREA plate and cut spikes (2)

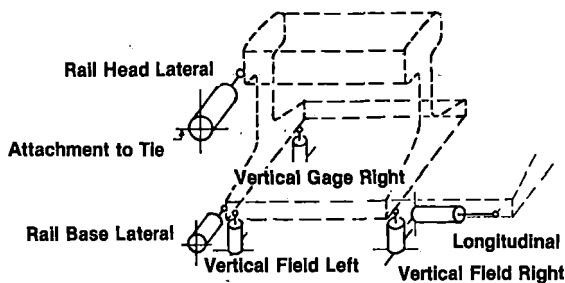


FIGURE 1. POSITION OF DISPLACEMENT TRANSDUCERS.

In addition, the two clips in segments 17-D₂ and 7-3 were strain gaged to provide a correlation with the deflection transducers.

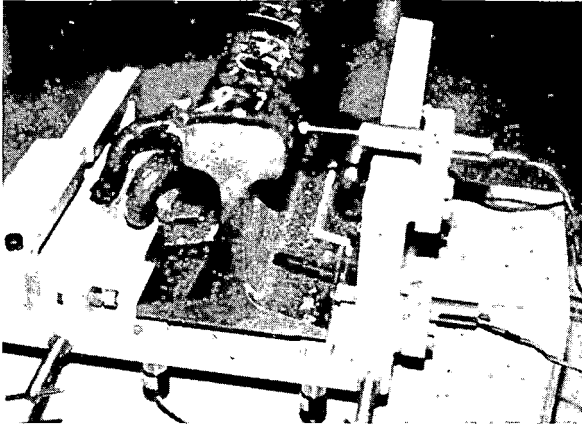
Figure 2 shows the fixture installed in all four fastening systems.

Measurements were taken with a consist composed of 20 100-ton cars and two GP 38 locomotives. Data were taken on both the high and low rail and in most cases in the clockwise and counterclockwise directions. The counterclockwise runs were deleted in the wood tie segments due to time constraints. A minimum of one run was taken at 40-45 mph which is the normal FAST consist operating speed.

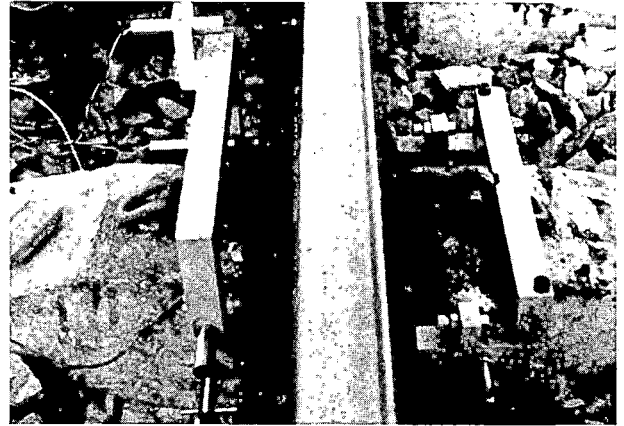
Data from each of the test runs in three locations in each segment were recorded on strip charts. These data provided the following results.

1. The highest clip strain in Section 17 was produced in the gage side clip on the low rail as shown in Figure 3. This location is also the principal location for clip fallout and fracturing.
2. The highest clip deflections and strains occurred in the counterclockwise train operation on the low rail in Section 17. This can be attributed to train action which, as shown in Figure 4, results in the gage and field side deflections being in phase during clockwise operation and out of phase in the counterclockwise operation. Consequently, in one case the deflections cancel each other and in the other they are additive.

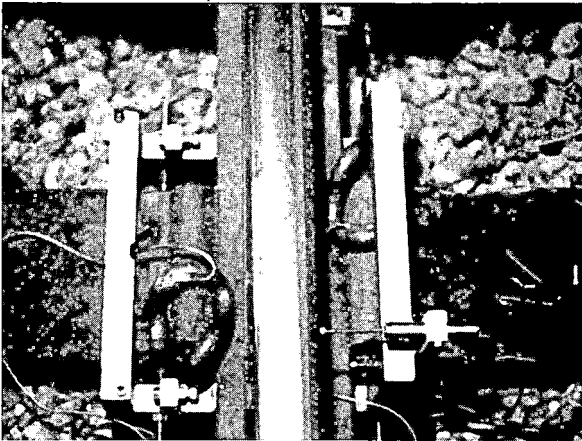
3. Clip deflections and strains were about 30% greater with the rigid pad which had a spring rate of 5 lb/in than with the resilient pad which had a spring rate of 1.4 lb/in. These differences which can be seen in Figure 5 are not significant considering the dissimilarities in the two segments. The location of one of the measurement sites near a weld with the rigid pad may have skewed the results slightly. However, the two deflection ranges could conservatively be considered to be about equal. This is in contrast to the expected result which would have the greatest deflections occurring on the resilient pad.
4. Clip strain was lower by 50% on the wood tie track compared to concrete tie track. This is probably due to tie plate bending on the wood ties. The shoulder on the concrete ties is a rigid cast iron insert which would not be expected to deflect when loaded.
5. There was less tie rocking with resilient pads than with rigid pads in the concrete tie section. The deflections from the two vertical field side transducers are about equal with the resilient pad, and substantially different with the rigid pad. This results in tie rocking, as can be seen in Figure 5.
6. In both the concrete and wood tie track, as can be seen in Figures 3 and 6, there was a distinct difference in the response of the rail on the high and low rails. By looking at the relative amount of motion of the rail head lateral transducer and the rail base lateral transducer, it can be discerned that flanging occurs on the high rail which produces lateral head and base excursions of nearly the same magnitude, and that rail rocking occurs on the low rail due to the change in the point of contact of the vertical load. The length of the consist for the test perhaps limited the size of these lateral loads. However, as a conservative estimate of the load/deflection environment, these results are appropriate.
7. In the wood tie segments there was evidence of considerable plate bending in the spring clip segment when compared to the elastic clip



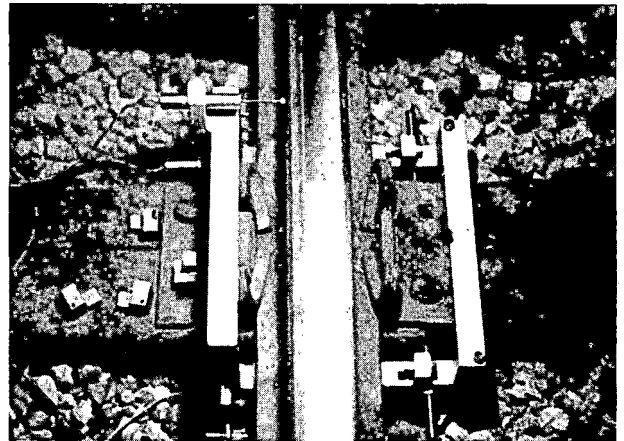
(a) PANDROL CLIP CONCRETE TIES



(b) VSD CLIP CONCRETE TIES



(c) PANDROL CLIP WOOD TIES



(d) INTMA DOUBLE ELASTIC SPIKE WOOD TIES

FIGURE 2. PLACEMENT OF TRANSDUCERS ON THE FOUR TYPES OF FASTENERS.

segment as shown in Figure 7. This is because the Pandrol spring clip reacts against the tie plate and the Elastic spike reacts against the wood tie. Correspondingly, there is more tie rocking as explained previously in the elastic spike segment where the tie plate is more rigid.

There are two current concrete tie specifications in use in the United States. One of these was developed for Amtrak, and the other for the American Railway Engineering Association. There is no comparable wood tie fastener specification. Each of the specifications has several tests which are applicable to fastening systems. These tests as listed below are not mutually exclusive to one specification or the other.

1. Strength of fastener insert in the tie - Fastener insert test, pullout test and torque test.
2. Pad separation load - Fastening uplift test.
3. Insulation capability of tie and fastener - Electrical impedance test.

4. Fastening resistance to fatigue - Fastening repeated load test and Fastening push pull test.
5. Rail restraint capability - Fastener longitudinal restraint test.
6. Gage widening resistance - Lateral load restraint test.
7. Pad resistance to permanent set - Tie pad load/deflection test.
8. Fastener set and yield test - Rail clip load - deflection test and toe load test.

For purposes of this paper only three types of tests will be discussed in detail: the fastener repeated load test, lateral load restraint test, and the fastener longitudinal restraint test.

The initial laboratory tests were set up to repeat the deflection and clip strain data from the field tests. In general, the deflections of the rail head relative to the tie were at a maximum of about .100" for both wood and concrete tie track. Rail tie vertical deflections of the rail clips in the concrete tie sections were nearly .040" peak to peak in uplift and compression.

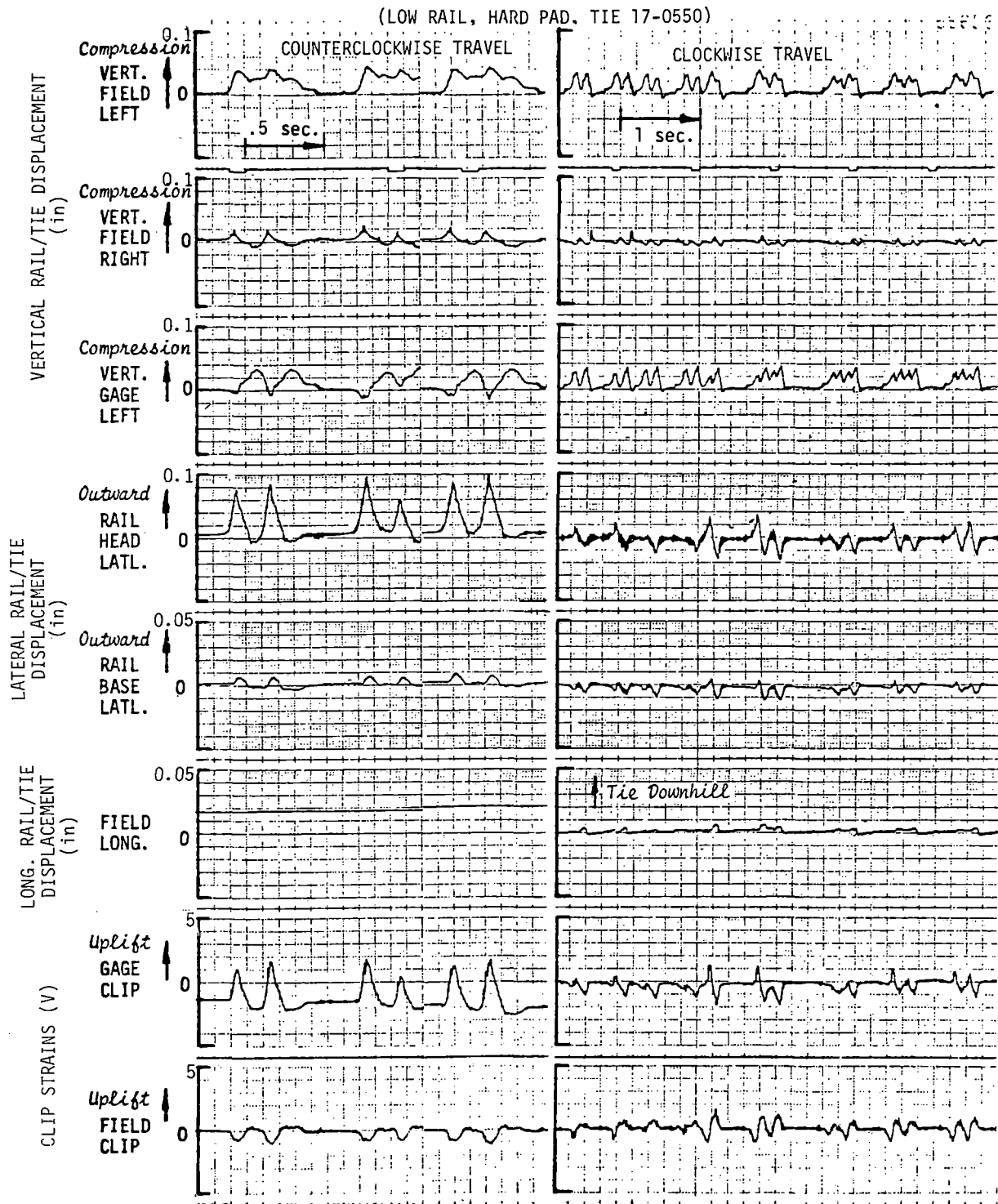


FIGURE 4. EFFECT OF CHANGE IN TRAIN DIRECTION ON MAXIMUM RAIL/TIE DEFLECTIONS FOR CONCRETE TIE TRACK.

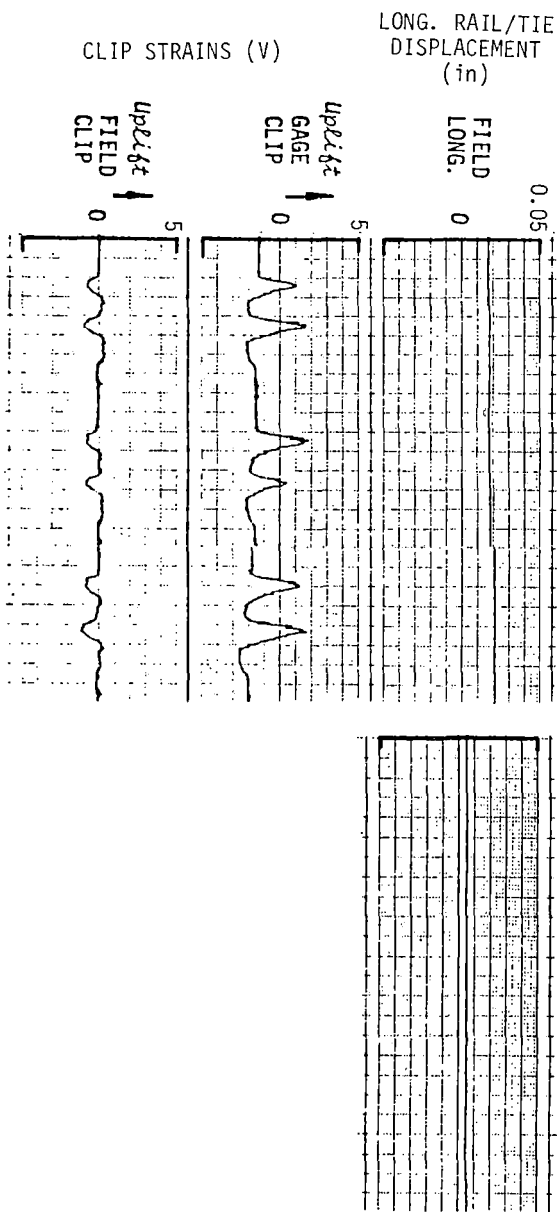
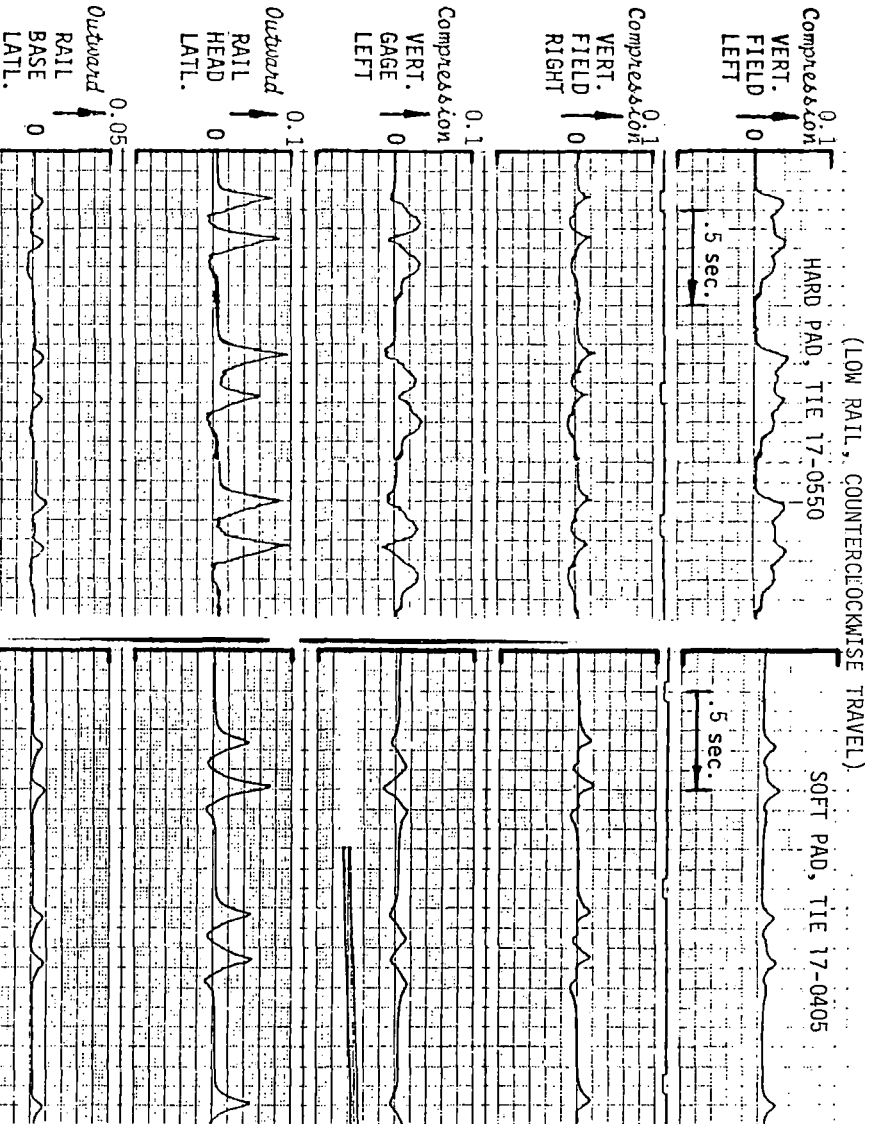


FIGURE 5. MAXIMUM RESULTS FROM HARD AND SOFT PADS ON CONCRETE TIE TRACK (LOW RAIL, COUNTER-CLOCKWISE TRAVEL).

LATERAL RAIL/TIE
DISPLACEMENT
(in)

VERTICAL RAIL/TIE DISPLACEMENT
(in)



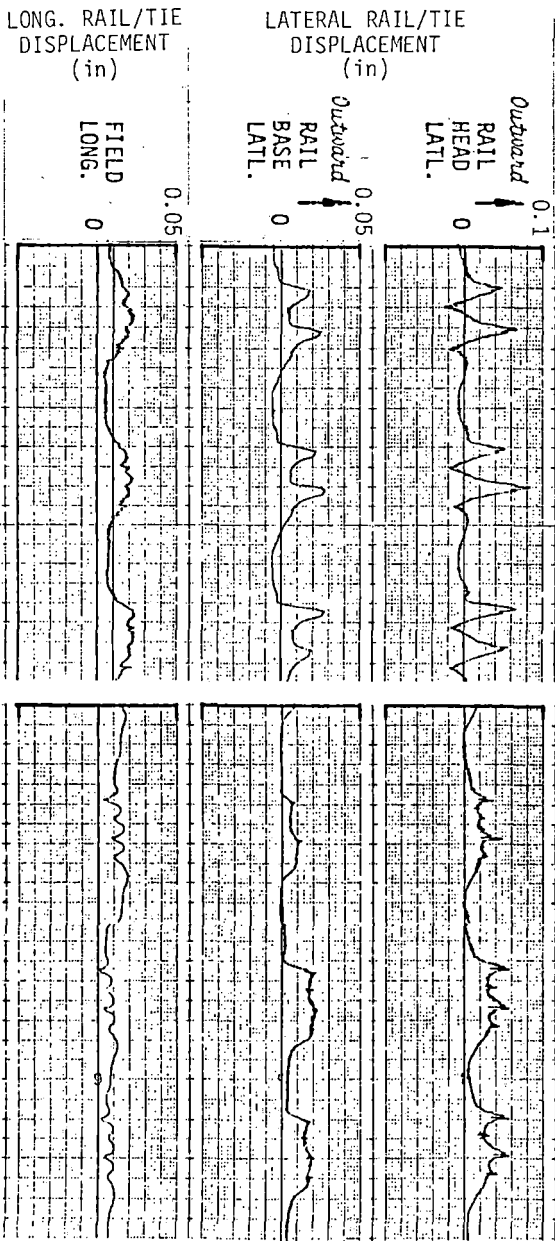
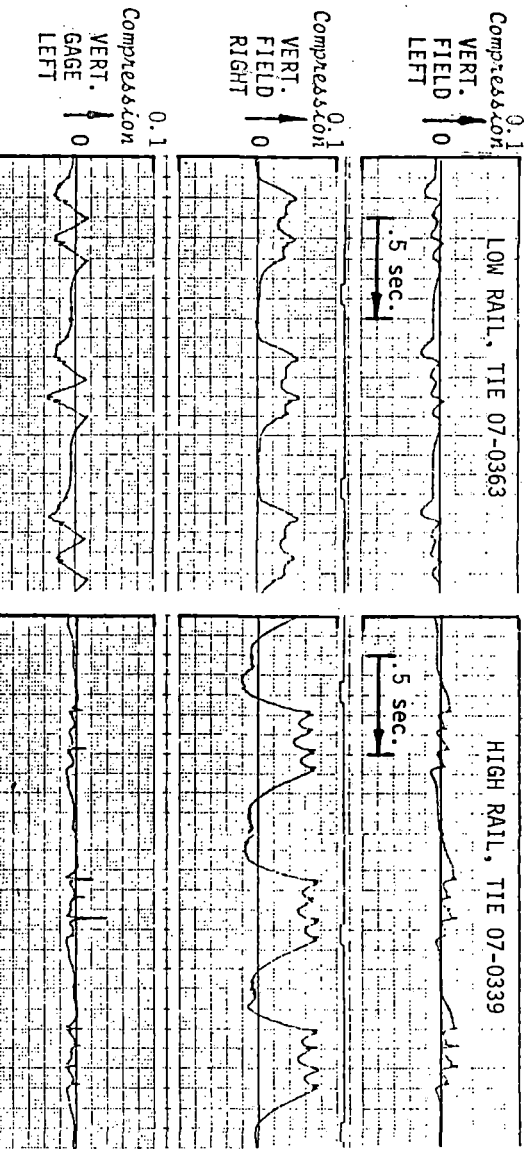


FIGURE 6. MAXIMUM RESULTS FROM MEASUREMENTS ON WOOD TIES WITH DOUBLE-SHANK ELASTIC CLIP-SPIKE (CLOCKWISE TRAVEL ONLY).

VERTICAL RAIL/TIE DISPLACEMENT
(in)



(CLOCKWISE TRAVEL)

ELASTIC SPIKE

ELASTIC CLIP

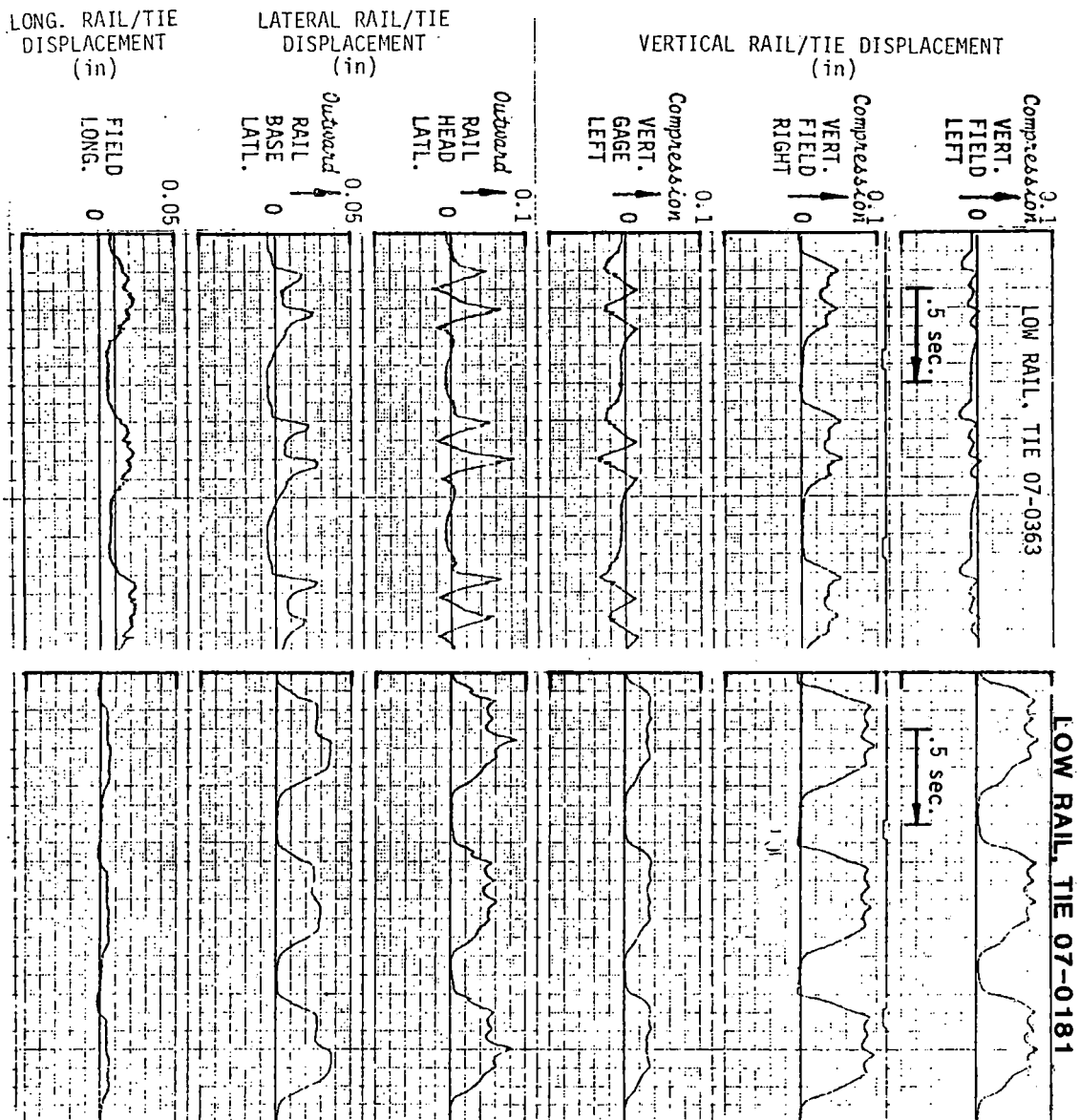


FIGURE 7. MAXIMUM RESULTS FROM WOOD TIES (CLOCKWISE TRAVEL).

The lateral restraint test was conducted at several L/V angles from 20 to 30 degrees to the vertical with several pad types. Figure 8 is a schematic of the fixture used in this test. Clip deflections

LOADING AND MEASUREMENT SCHEMATIC

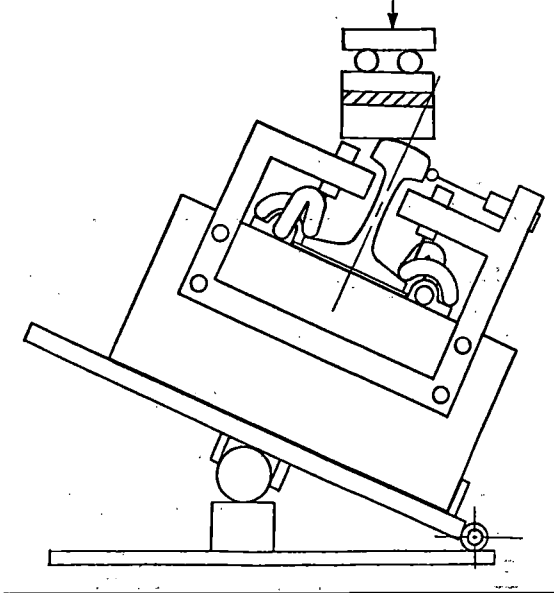


FIGURE 8. LATERAL RESTRAINT.

were measured directly from the clip to correct for inconsistencies in interpreting the vertical deflections from the field test. Also, the rail head lateral deflections were measured. Figure 9 shows

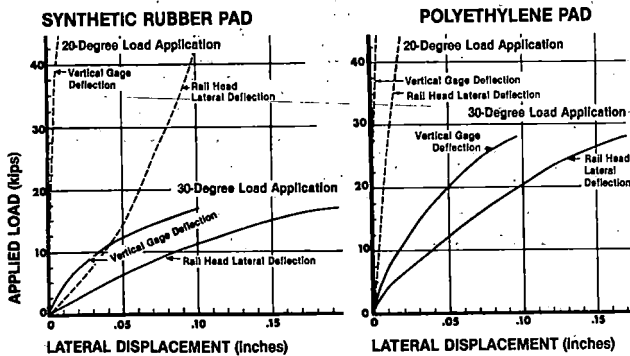


FIGURE 9. LATERAL RESTRAINT TESTS.

the results of load application at 20° and 30° angles for a rigid polyethylene pad (5.0 lb/in spring rate) and a resilient neoprene pad (1.4 lb/in spring rate) which are from the two test segments. Rail lateral displacement and the corresponding clip displacement are both highly dependent upon the angle of application and the pad spring rate. The AREA specification for lateral displacement is conducted at a 20° angle with a 41,000 lb

load at the gage corner and the rail rollover test is conducted at a 30° angle with a 20,500 lb load. The lateral displacement test is designed to determine the shift in the rail base with load. In this case, there was little rail base displacement. Consequently, there was little difference in performance due to pad stiffness. However, there was a substantial difference in the rail rollover test due to pad stiffness. This bias in all probability is not a realistic representation of the actual field test since the effects of load spreading onto adjacent ties is not considered. A more appropriate test might be to calculate the rollover response in the fastener repeated load test.

One of the most significant outputs of this static lateral restraint test was to show the significant differences between load applications at a 20° angle and at a 30° angle. At a 20° angle, there is only .015 inches of lateral deflection produced by a 30,000 lb load. This is not representative of the range of deflection experienced in the field test. These results were of considerable importance when setting up the fastener repeated load test.

The primary effort for these tests was to define a fastener repeated load test, a test to determine the capability of the fastening system to resist component failure. This type of test would be applicable for both concrete wood tie fastening systems.

Historically, even though concrete tie fastening systems passed the AREA and Amtrak repeated load tests, in severe service conditions such as FAST, component fractures and clip fallouts occurred and often in large numbers. In the AREA specification, a compression and an uplift load are applied at a 20° angle. In the Amtrak test, the load is applied at the equivalent of an 18° angle. As was noted previously, these angles of application did not produce the desired rail deflection as reflected in the field test.

A range of L/V angles from 20 to 27 degrees were tried with a final angle of 24 degrees being selected. In order to meet the specified deflection goals of .100" rail head deflection and clip deflection of .040" for the gage corner clip by 10 percent, different loads were required for each pad type. The rigid pad required 20,000 lbs compression and 2,400 lbs uplift load. The resilient pad required a 13-16,000 lbs compression and 1,600-2,000 lbs uplift load. The range of loads for the resilient pad was required to adjust for seating of components and to maintain the required deflections. Figure 10 shows the load schematic for the fastener fatigue test.

At 653,000 cycles of the repeated load test, conducted at 2 Hz, the gage corner clip was noticed to be cracked in two locations. Those locations, as shown in Figure 11, are the same locations where clip fractures had occurred at FAST. However, because the test was being conducted using the maximum deflection values, the failure occurred at a projected tonnage of 22 MGT. There were no fatigue failures at FAST with newly installed clips until 40 MGT in the first experiment. Subsequent experiments at FAST did, however, result in fractures at lower MGT levels.

It was interesting to note that during the 653,000

cycles the clips began to work out and had moved about 1/2" prior to the fractures being noticed.

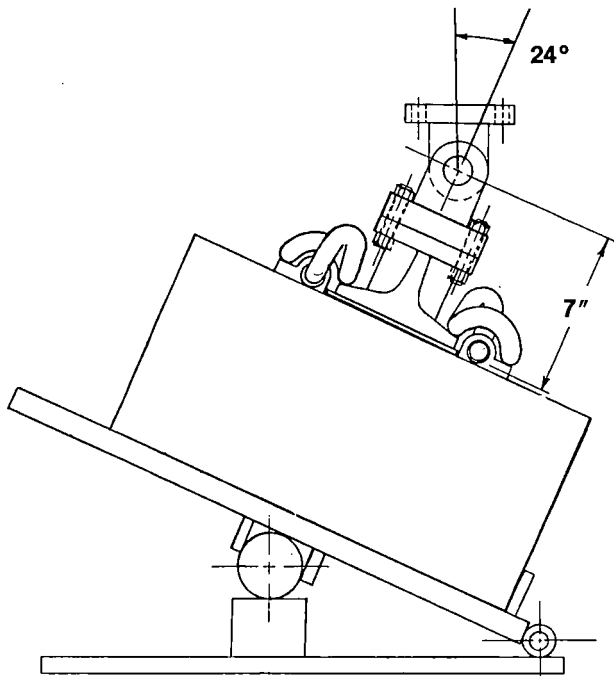


FIGURE 10. LOAD SCHEMATIC FOR CONCRETE TIE FASTENER FATIGUE TEST.

CLIP CRACKS

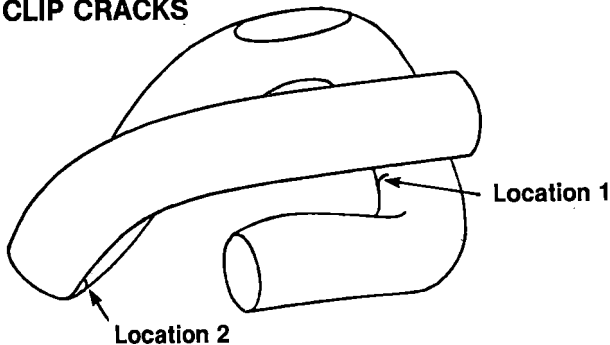


FIGURE 11. CONCRETE TIE FASTENER FATIGUE TEST.

Recent clip deflection measurements taken in tangent track on the Northeast Corridor with both freight and passenger traffic produced maximum deflections of the gage corner clip of .012" in uplift and .008" in compressive deflection for the field and gage side clip. To duplicate this, a considerably smaller value of vertical load at the 24° angle would be required, on the order of 4,000 lbs. There were no laboratory tests conducted with loads in that range but no doubt the performance of the clip would improve.

The wood tie fastener repeated load test, as shown in Figure 12, was conducted using the same fixture and the wood tie fastener components from Section 7, segment 6. At 1,090,000 cycles, the tie plate failed in a fashion similar to those at FAST. This

WOOD TIE FASTENER

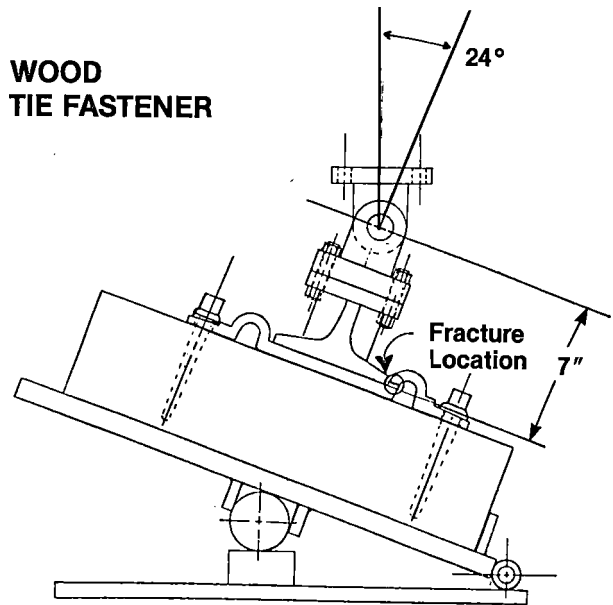


FIGURE 12. LOAD SCHEMATIC FOR WOOD TIE FASTENER FATIGUE TEST.

time the ratio of simulated tonnage in the laboratory to the field was 36/100 MGT. There were two interesting physical problems that needed to be overcome in order to properly conduct the test. The tie plate area needed to be adzed slightly so that the deflections produced in the laboratory would closely match those measured on track. This was a "seating" of the tie plate which occurs in track as a small amount of tie plate cutting. In addition, when conducting the test it was necessary to constantly tighten the screw spikes to prevent them from working out of the tie. This also was a frequent occurrence in the FAST track.

Longitudinal restraint tests were also conducted as a part of the laboratory work. There were considerable difficulties encountered during the initial set up which is shown in Figure 13. The fastener clip did not provide consistent toe loads as a result of installation variations. These variations in toe load resulted in a difference of 15% in longitudinal restraint values.

Consequently, a consistent toe load was provided by applying a known vertical load through the fixture shown in Figure 14. Even with this fixture, it was necessary to constantly change out the pad and insulators to get repeatable results on concrete tie fasteners. These results are shown in Figure 15 which show a large difference in longitudinal restraint, the point at which continuous slip is obtained, with different pad types and with and without insulators. In general, resilient pads have higher coefficient of friction (μ) than rigid pads. This is in part due to the surface texture of the rigid pads being smoother than that of the resilient pad. For wood tie fasteners where there are no pads, slip occurs at a lower load because of the lower friction between the rail steel and the steel tie plate. These results are shown in Figure 16.

These results show that the tie pad has considerable

bearing on the results of the longitudinal restraint tests and should be considered for use with wood tie fasteners if the restraint is insufficient without a pad.

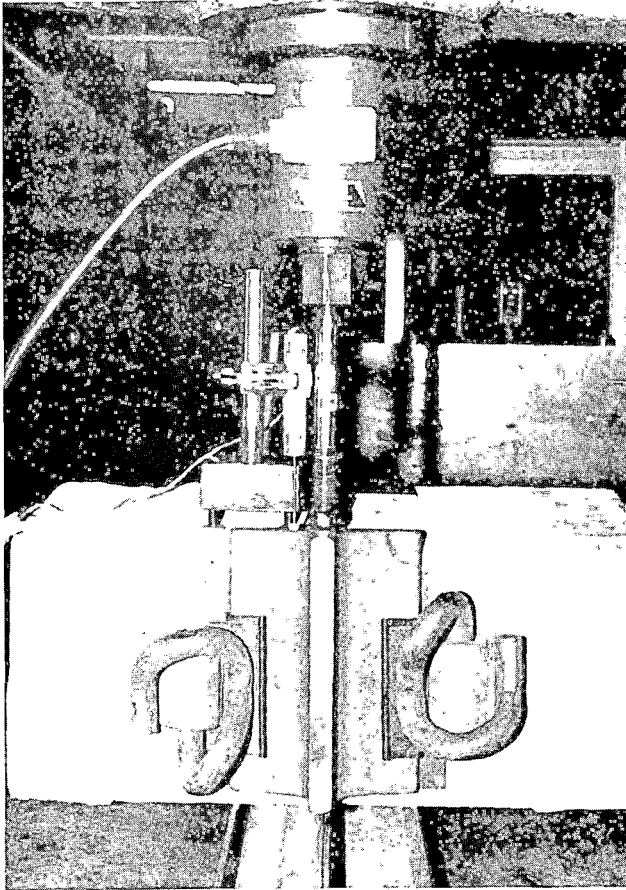


FIGURE 13. LOADING FIXTURES USED FOR LONGITUDINAL RESTRAINT TESTS (TOE LOAD PROVIDED BY CLIP).

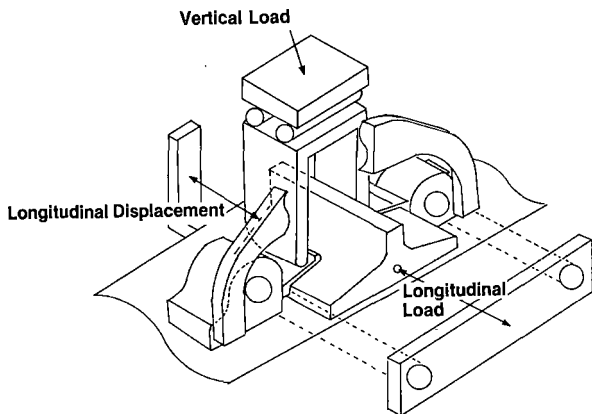


FIGURE 14. MEASUREMENT OF LONGITUDINAL RESTRAINT UNDER CONTROLLED VERTICAL LOAD.

CONCRETE TIE FASTENERS

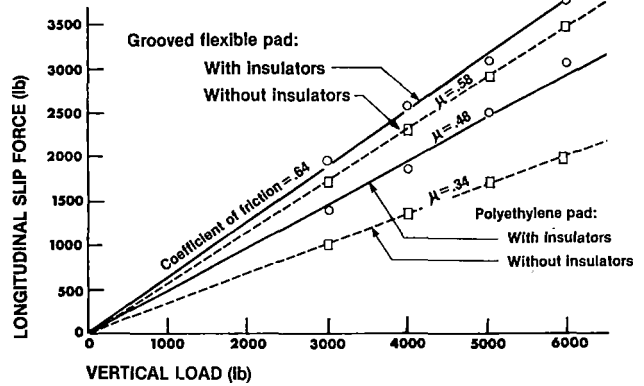


FIGURE 15. LONGITUDINAL RESTRAINT: CONCRETE TIE FASTENERS.

WOOD TIE FASTENER

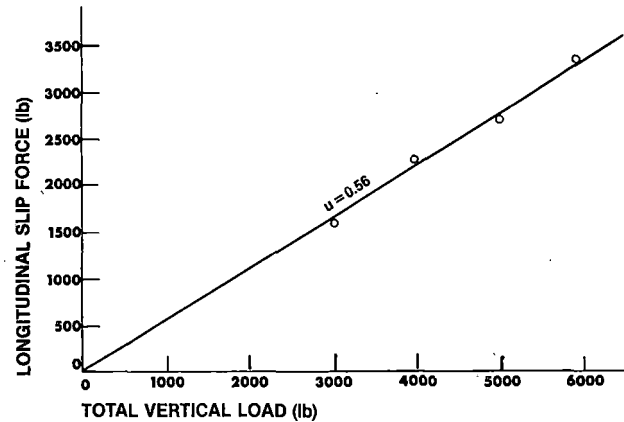


FIGURE 16. LONGITUDINAL RESTRAINT: WOOD TIE FASTENER.

CONCLUSIONS AND RECOMMENDATIONS

The results of the FAST fastener tests coupled with the deflection measurements taken at FAST have been translated into a laboratory test. With that information and the use of current specifications, it would be relatively easy to develop tests which would be appropriate for estimating fastener performance in the field prior to installation. This does not preclude the use of effective field tests but would serve to assist the engineer in anticipating those field test results in analyzing any full scale use of the components.

The following recommendations would be appropriate as a means of improving current concrete tie specifications and for serving as a basis for a wood tie fastener specification.

1. Fastening Repeated Load Test

This test should be conducted with a full fastener assembly which will be used in the service installation. Prior to the test, pad stiffness and fastener critical dimensions such as the toe load height should be measured. The

fastener assembly set up at 24-27° angle to the vertical, apply an uplift load and a compression load large enough to produce a deflection equivalent to the maximum expected lateral rail head deflection in track. For FAST this would mean -.010" to +.100".

This test should be conducted for 3,000,000 cycles at a maximum rate of 2 Hz. Following the test an evaluation of pad stiffness, clip critical dimension and component integrity (i.e., no fracturing of any component) should be made.

2. Fastening Lateral Load Restraint

The existing test as defined in Chapter 10 of the AREA Manual is sufficient but the rollover test should be deleted. The fastening repeated load test can serve as a substitute for that test.

3. Fastening Longitudinal Restraint Test

This test should be conducted under dynamic load conditions of 15,000 lbs vertical compression and 2,000 lbs vertical uplift at 2 Hz using the current static restraint test as outlined in the AREA Specification. The static test should be done on at least four new fastener assemblies, followed by a dynamic test on each assembly. Value of longitudinal force applied should be recorded up to the point of continuous slippage. Acceptance of a fastening system is predicated upon the specific in-track conditions.

REFERENCES

1. F. E. Dean - "Measurements of Rail/Tie Deflections and Fastener Clip Strains at FAST," October 1981, FRA/TTC-81/03.
2. F. E. Dean - Investigation of Rail Fastener Performance Requirements, to be published, 1982.
3. American Railway Engineering Association Manual for Recommended Practices, Volume I, Chapter 10.

RAIL: ITS BEHAVIOR AND RELATIONSHIP TO TOTAL SYSTEM WEAR

Roger K. Steele Ph.D.
Experiment Manager, Rail Metallurgy
Federal Railroad Administration

Richard P. Reiff
Experiment Monitor, Rail Metallurgy
Boeing Services International, Inc.

This paper is divided into three main topic areas:

- o WEAR and METAL FLOW
- o WELDED RAIL END BATTER
- o FATIGUE and FRACTURE

Because the discussion of each topic will sometimes utilize information which is presented elsewhere in this conference proceedings, the reader is urged to refer to these other sections as he proceeds.

The main intent of this paper is to provide a clear and accurate summary of what has been learned about rail in the FAST experiment. However, this information might be of limited or uncertain utility to the reader were it not related to observations made in the real world of railroad operation. In addition, the substantial improvement in understanding the FAST results that can be derived from laboratory examination will be emphasized. The information available for both wheels and rails will be utilized in a unified fashion to provide some insights about total systems (wheel and rail) wear. Illustrations will be given to show how some of the information can be utilized.

INTRODUCTION

At present, the third rail metallurgy experiment (RME III) is in progress. Over the period of time since the beginning in September 1976, the objectives of the experiment have evolved gradually from determining wear and metal flow behavior alone to include the study of welded rail end batter and defect formation and growth in rails and welds as well.

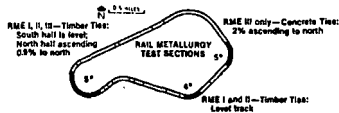
The features of the FAST train are summarized in Table I. The train reverses direction each day. The average train speed is about 41 mph and typically 120 laps of the 4.8 mile loop are made each day imposing approximately 1 MGT of traffic per day on the track. Thus 1 MGT on the track equals approximately 500 miles of vehicle travel.

As shown in Figure 1, the rail metallurgy test sections have been located in Section 3 for all three experiments and in Section 13 for experiments I and II, and Section 17 (5° Curve) for the current (III) experiment. Section 3 is a 5° curve essentially level on its southerly half and ascending to the north with a 0.9% grade on its northern half. Section 13 is a 4° curve on level grade. The 5° curve at Section 17 ascends to the north at a 2% grade.

TABLE I. THE FAST TRAIN.

Motive Power:	Four 4-axle, 2000hp locomotives.
Car Equipment:	Ninety-nine cars in FAST pool; Ninety-two 100-ton open-top hopper; Six 100-ton tank; One 70-ton TTX.
Lading:	Hoppers—expanded shale (simulated coal lading); Tanks—water; 100-ton design cars—loaded to gross weight on rail of 263,000lbs ± 2,000lbs.
Nominal Consist:	Four units plus 70 cars; 9200 tralling tons; 0.87 hp per tralling ton.

In all three experiments the rail in Section 3 has been 132, 136 or 140 lb/yd. The rail in Section 13 has been 115 lb/yd while that currently in Section 17 (5° curve) is all 136 lb/yd. The physical arrangement of the rails in Section 3 in each experiment is also shown in Figure 1. The essential feature of each design is that it provides replication of different metallurgies in different places in the curve to assess the contribution of position-in-curve effect. The designs used previously in Section 13 in the first and second experiments were



FIRST EXPERIMENT												
Segment	A	B	C	D	HH	HSi	FHT	CrMo	Std	F	D	H
Tie Plate Cants	1:40	1:30	1:14	1:14			1:30		1:40	1:40	1:18	1:30

SECOND EXPERIMENT												
Metallurgy	Std	HH	CrMo	FHT	HSi	Std	HH	CrMo	FHT	HSi	Std	HH
Tie Plate Cants	1:40		1:30			1:14		1:40		1:30		1:14

THIRD EXPERIMENT												
Metallurgy	Std	HH	CrMo(A)	CrV	1%Cr	CrMo(C)	HH	Std	FHT	HH	Std	CrMo(A)
Tie Plate Cants	1:40						1:40					1:40

NOTE: CrMo is 1:40 throughout / CrMo(A)=Baldwin / CrMo(C)=Winnable

FIGURE 1. RAIL METALLURGY TEST SECTIONS.

similar to those used in Section 3 except that only four metallurgies (Std, HSi, FHT, and HH) were present instead of the five present in Section 3. In the current experiment standard carbon and head hardened rail are the control (reference) rails and each have been replicated four times in Section 3. The other metallurgies are replicated only twice except for fully heat treated rail which is positioned only at the center of the curve. The originally installed CrMo(A) has been replaced by SiMn (HH) rail; one half of the control head hardened rail has been replaced with new head hardened rail. In Section 17, head hardened rail is the control rail and SiCr(HH), 1 Cr, and CrV are each replicated twice in the curve.

Three tie plate cants, 1:14, 1:30, and 1:40 were utilized in the first and second experiments; however, only the 1:40 cant is utilized in the current experiment.

The essential features of each experiment are summarized in Table II. An important variable in each experiment has been lubrication. Even though two track lubricators had been installed initially, the first 40-45 MGT of the first experiment were char-

TABLE II. EXPERIMENT FEATURES.

Experiment	Dates	Tonnage	Tie Plate Cants	Lubrication Pattern
RME I	8/76 - 8/77	135 MGT	1:14, 1:30, 1:40	Poorly lubricated—first 45 MGT; Well lubricated—remaining 90 MGT
RME II	12/77 - 6/79	290 MGT	1:14, 1:30, 1:40	Well lubricated for entire period except for brief (35 MGT) lubrication experiment
RME III	12/79 - present	190 MGT to date	1:40 only	Alternating well lubricated (~35 MGT) and dry (~15 MGT)

NOTE: In the well lubricated periods, the lubricators were shut down every 2 to 3 MGT for half-MGT intervals to facilitate rail flaw inspection

acterized by ineffective lubrication. Over a period of time, two more lubricators were added and the level of lubrication approached what would be termed most charitably as "generous" after 45 MGT. The lubricators were utilized in the second experiment throughout the 290 MGT period of that experiment, with the exception of a brief period of 22 MGT where only one lubricator was used as part of a lubrication experiment. The level of lubrication throughout the second experiment was sufficiently generous that comparisons between the different metallurgies have not yet been made reliably. In the current experi-

ment, an alternating pattern of lubricated and dry running has been employed (with much improved measurement instrumentation to provide wear information in both lubrication regimes and also as part of an effort to minimize fatigue damage to the rail. Two properly functioning track lubricators have been found more than adequate to generously lubricate the entire loop. An important note to remember is that the lubricated period has not ever represented continuous lubrication; the lubricators are shut down every 2-3 MGT for about ½ MGT to "clean" the rail for inspection.

The average ladle analyses of the test rail in the 1st and 3rd experiments are given in Table III. Several significant details should be pointed out. The FHT rail installed in Section 3 RME I had relatively low carbon and manganese levels compared to those of the other metallurgies; however, the FHT rail in Section 13 had comparable carbon levels to those of the premium rails although its manganese content was lower. In the current experiment, the FHT rail is high in both carbon and manganese relative to the other non-alloy rails.

TABLE III. AVERAGE LADLE ANALYSIS OF RAIL IN THE FAST METALLURGY EXPERIMENTS: RME I & III

Section	Rail Type	WEIGHT PERCENT. (w/o)								
		C	Mn	P	S	Si	Cr	Mo	V	
RME I Section 03 (132 lb/yd)	Std	0.78	0.86	0.027	0.025	0.15	—	—	—	
	HSi	0.76	0.86	0.028	0.027	0.63	—	—		
	FHT	0.69	0.81	0.018	0.032	0.18	—	—		
	CrMo	0.80	0.82	0.026	0.025	0.25	0.78	0.20		
Section 13 (115 lb/yd)	Std	0.73	0.86	0.024	0.020	0.17	—	—		
	HSi	0.77	0.88	0.029	0.024	0.68	—	—		
	FHT	0.77	0.81	0.020	0.041	0.15	—	—		
	HH	0.77	0.88	0.015	0.025	0.18	—	—		
RME III Sections 3 and 17 (5%) (132, 136, & 140 lb/yd)	Std	0.76	0.86	0.022	0.024	0.18	—	—		
	FHT	0.81	0.93	0.018	0.041	0.20	—	—		
	HH	0.77	0.83	0.021	0.030	0.17	—	—		
	NHH	0.76	0.93	0.020	0.020	0.22	—	—		
	SiCr (HH)	0.76	0.82	0.020	0.006	0.82	0.50	—		
	SiMn (HH)	0.76	1.24	0.023	0.009	0.84	—	—		
	1 CR (A)	0.71	0.73	0.014	0.021	0.27	1.16	—		
	1 CR (B)	0.73	1.30	0.023	0.026	0.30	1.25	—		
	1 CR (C)	0.75	0.88	0.030	0.027	0.23	0.95	—		
	CrV (A)	0.67	1.15	0.009	0.013	0.34	1.11	0.11		
	CrV (B)	0.72	1.27	0.014	0.030	0.22	1.04	0.087		
CrMo (A)	0.72	0.79	0.009	0.023	0.25	0.78	0.21			
CrMo (C)	0.79	0.60	0.026	0.016	0.26	0.61	0.17			

In the first and second experiment each different metallurgy was provided in its entirety by a single manufacturer. However, in the current experiment the 1% chromium rail has been provided by three manufacturers and the CrV and CrMo rail by two manufacturers. The two CrMo rails tested in the current experiment have significantly different manganese, chromium, and molybdenum levels. The lower alloy levels in CrMo(C) permit it to be welded without postheat although an additional preheat cycle is recommended. CrMo(A) is much more similar in composition to the CrMo rail tested in the first experiment.

In the case of the 1% Chromium rail the variation in manganese level (0.73 to 1.30 w/o) and chromium level (0.95 to 1.25 w/o) is very significant. The variation in chromium, manganese, and vanadium levels in the CrV rails is less significant. A few words are appropriate for the SiCr(HH) and SiMn(HH) rails. Both of these are alloy rails which are head hardened; their alloy compositions have been adjusted to provide the benefits of increased hard-

enability at the heat affected zones of flash butt welds without the need to resort to postheating.

The average ladle analyses of the AREA standard carbon rail tested in the first and third experiments is very similar. However, significant variations have occurred among ladle analyses for individual standard rail heats. Much more will be said about this in the discussion of equivalent carbon effects.

WEAR AND METAL FLOW

The measures of wear and metal flow are shown in Figure 2. In the first (and second) experiment all the measures were obtained from rail profiles having a long term variability of ±0.020" - 0.030" on any dimension. When wear rates were reduced by lubrication (by as much as a factor of 10 in some cases) as in RME II, the total wear which occurred in a period of observation was comparable with the "noise" characteristic of the profilometer; This is the reason that RME II has not provided a reliable assessment of the effects of different metallurgies and tie plate cants.

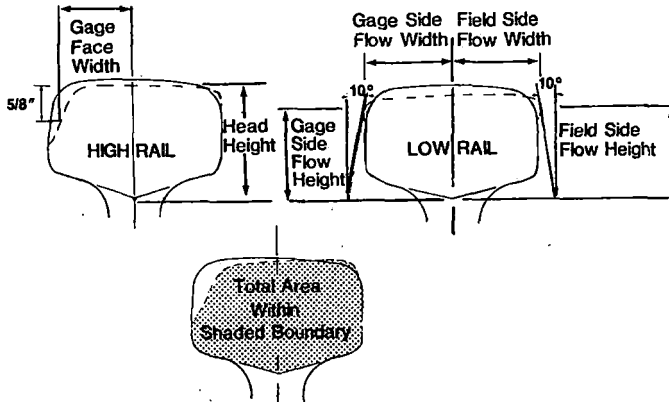


FIGURE 2. DIMENSIONS AND AREA DETERMINATION.

To correct this problem, a series of "snap" gage type instruments has been developed for use in RME III. These instruments accomplish dimensional measurement through the use of dial gauges and have a long term variability of ±0.002" - 0.003". They are used to generate gage face, head height loss, and lateral metal flow information. Cross sectional head area loss still needs to be determined from profilometer traces.

In addition to wear rate information which will be presented in the following paragraphs, reference will be made to the term "figure of merit". The figure of merit (FM) provides a relative assessment of how much better a premium rail is than standard rail. Most simply it is calculated by dividing the average wear rate of standard rail by that of the comparison rail. Because statistically there is some variability in the wear rates of both standard and premium metallurgies, dividing one average wear rate by another is not rigorously correct. Properly, the technique used commonly to calculate the probability distribution function of lateral to vertical wheel loads ratio would be used. The expression for making this calculation is given below.

$$PDF(Z) = \frac{\sigma_x \sigma_y}{\pi (\sigma_y^2 - Z^2 \sigma_x^2)} \exp \left\{ -\frac{1}{2} \left[\left(\frac{\mu_x}{\sigma_x} \right)^2 + \left(\frac{\mu_y}{\sigma_y} \right)^2 \right] \right\}$$

$$+ \left[\frac{\mu_x \sigma_y^2 + Z \mu_y \sigma_x^2}{\sqrt{2\pi (\sigma_y^2 + Z^2 \sigma_x^2)}} \right] \exp \left\{ -\frac{1}{2} \frac{(\mu_y - Z \mu_x)^2}{(\sigma_y^2 + Z^2 \sigma_x^2)} \right\} \operatorname{erf} \left[\frac{\mu_x \sigma_y^2 + Z \mu_y \sigma_x^2}{\sigma_x \sigma_y \sqrt{2 (\sigma_y^2 + Z^2 \sigma_x^2)}} \right]$$

where:

$$Z = \text{Figure of Merit} = \frac{\text{wear rate of Std rail}}{\text{wear rate of comparison rail}}$$

μ_x, μ_y = Wear rate means of comparison and standard rails, respectively

σ_x, σ_y = Variances of wear rates for comparison and standard rails, respectively

The inputs needed are the average wear rates and the variances for each metallurgy. The difference between the simple method and the rigorously correct method will be shown in a subsequent paragraph.

Table IV presents the average gage face wear rates of the different metallurgies tested in Section 3 in RME I. The wear rates given are the averages for all positions-in-curve and all tie plate cants as determined by two independent analyses, one performed by

TABLE IV. AVERAGE GAGE FACE LOSS.

SECTION 3: RME I	Below Lubrication Transition		Above Lubrication Transition	
	Rate, in/MGT	FM	Rate, in/MGT	FM
Std	0.0086	1	0.0012	1
HiSi	0.0061	1.4	0.0012	1
FHT	0.0059	1.5	0.0011	1.1
CrMo	0.0041	2.1	0.0011	1.1
HH	0.0032	2.7	0.0007	1.5

$$FM = \text{Figure of Merit} = \frac{\text{Average Wear Rate of Std Rail}}{\text{Average Wear Rate of Comparison Rail}}$$

the AAR and the other by the Transportation Systems Center. The lubrication transition occurred at 40 - 45 MGT. In the dry (below transition) regime, the CrMo and HH exhibited the least gage face wear with both HiSi and FHT having intermediate wear resistance. The improvement in lubrication that occurred near 40 - 45 MGT greatly reduced gage face wear rates but not uniformly for each metallurgy. While the wear rate of standard rail diminished by a factor of seven, that of each premium rail was reduced by a significantly smaller factor such that improved lubrication reduced the wear rate of HH rail by a factor of only four and one half. This occurrence is termed a metallurgy:lubrication interaction.

This interaction is reflected also in the reduction in the magnitude of the figures of merit of the premium rails upon improvement in lubrication. Thus, premium rails do not offer as great advantage relative to standard rail in the lubricated regime as they do in the dry regime.

The greater uncertainty in establishing the relative benefit of premium rails in the lubricated regime can be seen by comparing the figure of merit probability distribution functions shown in Figure 3. The distributions are relatively narrow in the dry

regime and the FM peak value positions agree well with those calculated from the ratio of average wear rates. However, in the lubricated regime, the distributions are broader and the FM peak values do not agree as well with the ratio of average wear rates. Nevertheless, clearly the distributions tend to superimpose in the lubricated regime whereas they are distinctly separate in the dry regime. This behavior suggests that the metallurgy:lubrication is indeed real.

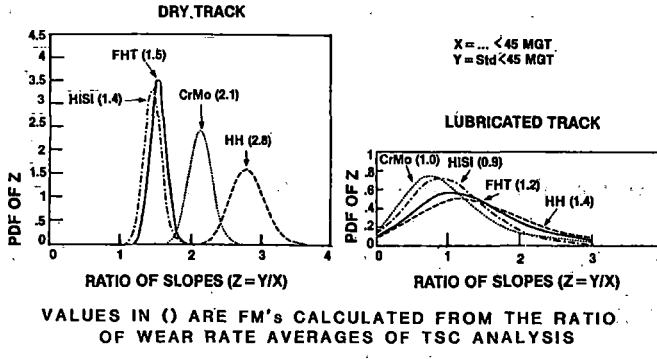


FIGURE 3. PDF OF-SLOPE RATIOS.

In spite of this greater uncertainty in the FM values in the lubricated regime, in the following sections, the simple ratio of average wear rates will be used as a measure of the figure of merit.

One of the potential difficulties with a field type of test is that there may be variations in behavior at different positions in a test curve—a so called position-in-curve effect. If allowances are not made for this possibility in the design of the experiment, there exists the risk that no meaningful information may be derived from the experiment. Indeed, Section 3 does appear to exhibit a position-in-curve effect which is a function of the level of lubrication. As shown in Table V in the dry regime, the south end of Section 3 yielded wear rates about 20% higher, on the average, than those observed in the center and north end of the curve. However, in the lubricated regime, the center of the curve exhibited the highest wear rate, and the relative variation in wear from the south end of the curve to the center was greater than that attributable to different metallurgies, on the average.

TABLE V. POSITION-IN-CURVE EFFECT.

SECTION 3 (ln/MGT): RME I	Position-in-Curve	
	Below Lubrication Transition	Above Lubrication Transition
Section 02 End	0.0052	0.0012
Middle	0.0054	0.0017
Section 04 End	0.0064	0.0006

NOTE: Average of all metallurgies and tie plate cants

The three different tie plate cants used under the high rail of Section 3 also had an effect that appeared to depend upon the level of lubrication; this is shown in Table VI. In the dry regime the 1:14 cant plate caused about 20% higher wear rates than did either 1:30 or 1:40 cant plates on the average. However, there is an important caveat: the wear of standard AREA carbon rail was so rapid on the 1:14 cant plates that the rail shape very quickly conformed to the shape of the average wheel contour and the wear rate of standard rail then became the same as that on the other tie plates. When wear rates dropped due to the presence of "generous" lubrication, the tendency of steeper cant to increase wear rate became more noticeable across all three cants. Because the wear rate of standard carbon rail was much lower, the effect of higher cant persisted longer. The reader must remember, however, that the intent of using high cant is to "unload" the gage corner and thereby delay shell/TD formation—not to reduce wear. In the lubricated regime, where fatigue of rail will become more important, the slightly higher wear rate on 1:14 cant plates might be more than compensated for by greater resistance to shelling and TD formation.

TABLE VI. TIE PLATE CANT EFFECT.

SECTION 3 (ln/MGT): RME I

	Below Lubrication Transition	Above Lubrication Transition
1:40	0.0053	0.0008
1:30	0.0053	0.0011
1:14	0.0062	0.0013

NOTE: Average of all metallurgies and positions in curve

The gage face wear rates in Section 13 (115 lb/yd rail, 4° curvature) are summarized in Table VII. In the dry regime, the wear rates for all metallurgies were only slightly higher at the center of the curve than at the ends. However, this trend was much more pronounced for standard carbon rail. In the lubricated regime, the center of the curve exhibits noticeably less wear than the ends for all metallurgies. This pattern was opposite to that observed

TABLE VII. GAGE FACE WEAR RESULTS FROM SECTION 13.

Metallurgy	Position-in-Curve				Average	Average Figure of Merit
	A	B	C	D		
Below Transition						
HH	0.0021	0.0017	0.0025	0.0021	0.0022	3.5
HISI	0.0052	0.0049	0.0045	0.0043	0.0047	1.6
FHT	0.0038	0.0038	0.0034	0.0037	0.0037	2.1
Std	0.0063	0.0092	0.0094	0.0060	0.0077	1.0
Average	0.0044	0.0049	0.0050	0.0046		
Above Transition						
HH	0.0014	0.0012	0.0003	0.0010	0.0010	1.3
HISI	0.0025	0.0001	0.0006	0.0014	0.0012	1.1
FHT	0.0020	0.0001	0.0010	0.0012	0.0010	1.3
Std	0.0016	0.0010	0.0010	0.0016	0.0013	1.0
Average	0.0019	0.0006	0.0007	0.0013		

A = Section 02 End

B,C = Middle

D = Section 04 End

in Section 3. The figures of merit for those metallurgies common to both Section 3 and 13 are very similar to those in Section 3, i.e.; HH exhibited the best gage face wear resistance while HiSi and FHT fell into an intermediate group. Also the metallurgy: lubrication interaction has been observed again.

To assess the effect of curvature (assuming that the rail section itself does not affect the wear rate), the ratio of wear rates in Section 13 and Section 3 (1:40 cant only) have been calculated and tabulated in Table VIII. On the average, the ratio was 0.8 suggesting a linear relationship between wear rate and degrees of curvature. However, the ratio can vary considerably for each metallurgy and from the dry to the lubricated regime. If the ratios for gage face wear (in the dry regime) are multiplied against head area loss rates from Section 3, a linear relationship of wear rate with curvature is indeed suggested in Figure 4, at least for standard, HiSi, and HH rails. Ratioing the head area loss on the basis of gage face loss is valid for the FAST data because, as will be shown in the next paragraph, the head height loss rate was relatively small compared to gage face wear rates.

TABLE VIII. RELATIVE GAGE FACE WEAR IN SECTION 03: RME I.

RATIO: $\frac{\text{WEAR RATE SECTION 13}}{\text{WEAR RATE SECTION 03}}$

Metallurgy	Below Transition	Above Transition
Std	0.804	0.906
HiSi	0.746	0.671
FHT	0.617	0.809
HH	0.846	0.993
Average	0.753	0.845

OVERALL AVERAGE = 0.789

NOTE: Average of all positions in curves; 1:40 tie plate cant only

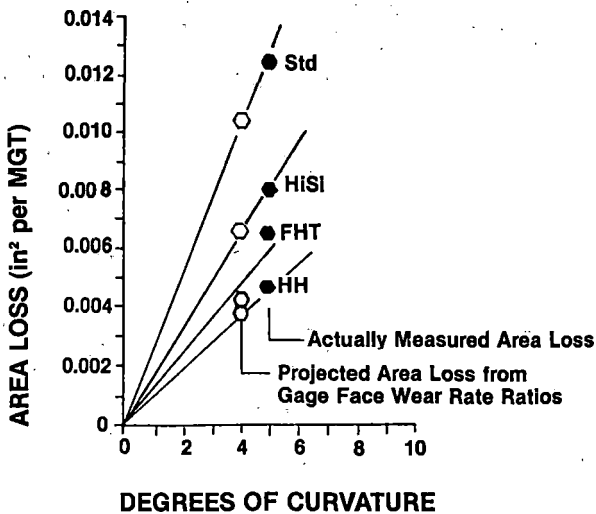


FIGURE 4. EFFECT OF TRACK CURVATURE.

The high rail head height loss rates in Section 3 for each of the metallurgies on each of the three tie plate cants are summarized in Table IX. Overall, the head height loss rates were about one-third the gage face wear rates. There is an important difference, though, in the ranking of the metallurgies, i.e., CrMo and FHT had the highest resistance while HiSi and HH fell into an intermediate category. Also, the 1:30 and 1:14 cant plates tended to produce lower head height loss rates than did the 1:40 cant; the effect became more pronounced for the better performing rails. There was virtually no head height loss in the lubricated regime on any of the premium rails.

TABLE IX. HEAD HEIGHT LOSS RATES.

SECTION 3 (Below Lubrication Transition at 45 MGT): RME I

Cant	1:40		1:30		1:14		Average	
	Rate "/MGT	FM	Rate "/MGT	FM	Rate "/MGT	FM	Rate "/MGT	FM
Std	0.0026	1.0	0.0022	1.0	0.0023	1.0	0.0024	1.0
HiSi	0.0014	1.9	0.0012	1.8	0.0013	1.8	0.0012	2.0
FHT	0.0010	2.6	0.0008	2.8	0.0006	3.8	0.0008	3.0
CrMo	0.0007	3.7	0.0005	4.4	0.0005	4.6	0.0006	4.0
HH	0.0013	2.0	0.0011	2.0	0.0009	2.6	0.0011	2.2

The relationship of gage face wear rate and head height loss rate seems to be a function of both the metallurgy itself along with the cant ratios. This is illustrated in Figure 5 for the ratio of gage face wear rate to head height loss rate. The FHT rail exhibited the greatest sensitivity to cant while standard and HH exhibited the least. It is not clear why different metallurgies should behave so differently but this behavior does suggest that a proper assessment of the wear resistance of a given metallurgy requires both gage face and head height loss measurements.

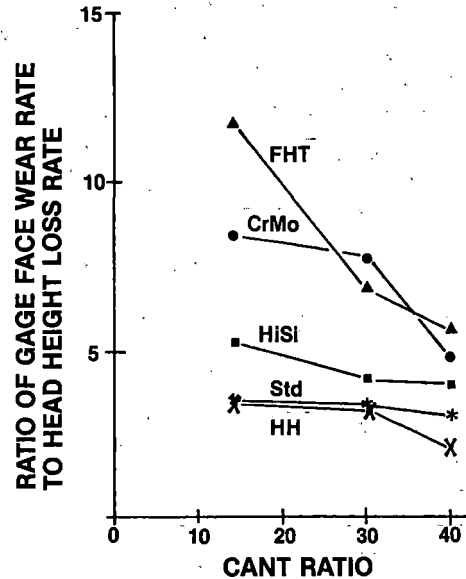


FIGURE 5. RATIO OF GAGE FACE WEAR RATE TO HEAD HEIGHT LOSS RATE.

By having both gage face and head height loss rates, a reliable estimate of relative area loss can be made by creating a composite FM from the dimensional loss rates. The composite FM is

$$\sqrt{\text{FM (gage face)} \times \text{FM (head height)}}$$

The good agreement between the composite FM's and the observed area loss FM's is shown in Figure 6.

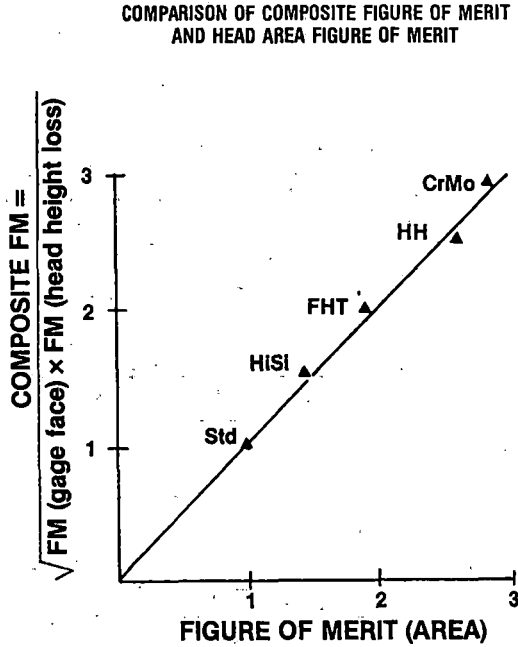


FIGURE 6. FIGURE OF MERIT (AREA).

Turning now to the low rail, the head height loss rates in each of the ten track segments of Section 3 in each lubrication regime are plotted in Figure 7. Virtually no position-in-curve effect was detected in the dry regime but in the lubricated regime the center portion of the curve had substantially higher wear rates than the ends for all metallurgies. The head height loss rates of the different metallurgies were generally less in the lubricated regime. This fact and the occurrence of a position-in-curve effect in the lubricated regime are of some interest because the running surface of the low rail of the curve was not lubricated. Thus, it appears that the head height loss behavior of the low rail was governed by the lubrication level on the high rail.

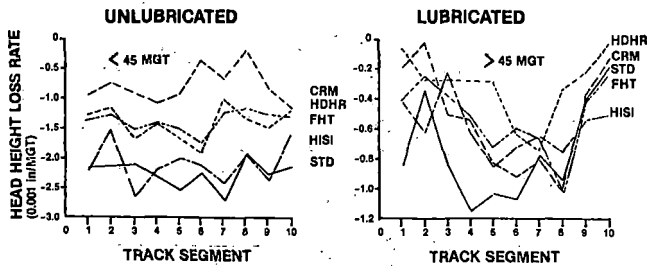


FIGURE 7. HEAD HEIGHT LOSS OF LOW RAIL: RME I.

The metal flow behavior of the low rail is more difficult to describe simply. To do this, both the heights and widths to the point at which a 10° (from the vertical) tangent touches the gage or field side flow lips have been measured. The typical behavior of standard carbon rail in Section 3 is illustrated in Figure 8. The most significant dimensional change was the increase in height to the flow lip on both field and gage sides. This occurred at a rapid rate for the first 35 to 55 MGT as metal crowded into the gage and field corner of the rail. After this period, there is a leveling off of height on the gage side and a gradual reduction in height thereafter on the field side. It is not clear whether the maximum points on the head height curves were associated with the change in lubrication on the outside rails. The width dimensions behaved somewhat differently on gage and field sides. On the gage side, the tangent to the flow lip actually receded for 80 to 90 MGT whereafter it moved more rapidly outward. However, on the field side, there was a gradual increase in width for approximately 100 MGT followed by a leveling off thereafter. The leveling off may be the result of sustained lubrication on the high rail.

LOW RAIL: RME I

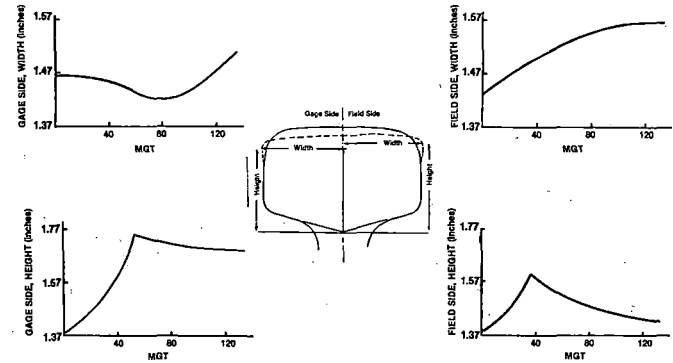


FIGURE 8. METAL FLOW BEHAVIOR OF STANDARD RAIL.

HiSi rail behaved in a fashion similar to standard carbon rail except that field side lateral flow (i.e., width increase) was observed only in the north and south end segments of Section 3 suggesting a very pronounced position-in-curve effect. No statistically significant widening on the gage side was observed at all. None of the other premium metallurgies exhibited any measurable metal flow.

The wear behavior of rail can be related with various degrees of success to its mechanical properties. The most commonly used of these properties is hardness. Figure 9 presents the head area loss figures of merit plotted against gage face hardness ratio which was determined with a 3000 kg indenting force tester at the very end of the RME I experiment (after 45 MGT dry and 90 MGT lubricated). Because the hardness measurements were made only after the active test of the rail had been completed, the behavior observed must not be expected necessarily to be appropriate for a single lubrication regime, dry or lubricated. Nevertheless, the results do suggest that increased hardness achieved in different ways does not necessarily lead to the same improvement in wear resistance. It appeared that increased hardness achieved through heat treatment

alone did not provide as much improved overall wear resistance (gage face and head height) as did alloying. Also, the alloy rail appeared to be more affected by the level of lubrication than did the heat treated rail.

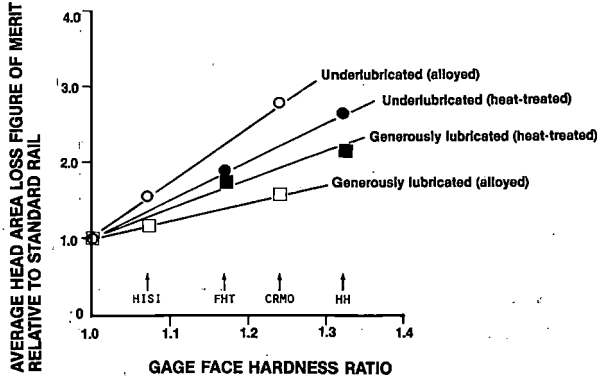


FIGURE 9. EFFECT OF RELATIVE GAGE FACE HARDNESS UPON AREA LOSS FIGURE OF MERIT: RME I SECTION 03.

There appears to be some interest in the industry toward utilizing a mechanical property parameter such as yield strength as a measure of wear resistance. Some recent work by the University of Connecticut¹ suggests that this may be appropriate for resistance to head height loss but may not provide good correlation with gage face wear resistance. Figure 10 plots the figures of merit for head height loss and for gage face wear against the cyclic and static 0.2% offset yield strengths. Perhaps because head height loss may be predominantly a metal flow process, the agreement between head height loss figure of merit and yield strength (both cyclic and static) is good. But the relationship between either yield strength and the gage face figure of merit is much poorer primarily because of the behavior of the FHT rail. As will be discussed later, the mechanism of wear on the gage face may be associated more with shear band cracking than ease of plastic flow, and, therefore, a fundamental correlation of gage face wear with yield strength might not be expected.

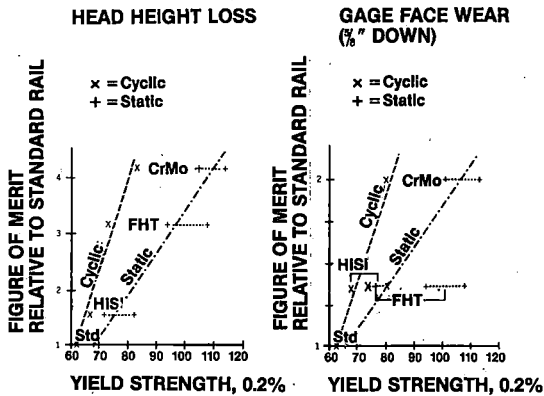


FIGURE 10. RELATIONSHIP OF WEAR BEHAVIOR TO YIELD STRENGTH.

The fact that about ten different heats of standard and HiSi rail each were incorporated into the high rail of Section 3 (RMEI) has permitted an evaluation of the effect of chemistry upon wear resistance. Although there will be differences from one heat to another due to small variations in mill processing, the fact that all rails came from the same mill has made determination of chemistry effects less complicated. The method that has been adopted to illustrate the effect of chemistry has been to convert carbon, manganese, and silicon contents to equivalent carbon in the manner described by Clayton² such that:

$$C_{eq} = \% C + \% Mn/4.75 + \% Si/10$$

Figure 11 is a plot of gage face wear rate in the dry regime versus equivalent carbon calculated from ladle analyses after corrections have been applied for position-in-curve effects. Within the range of chemistry of the standard carbon rails tested, there was an approximate 50% variation in gage face wear rate. Within the range of equivalent carbon calculated from the extremes of C, Mn, and Si, content allowed by the AREA specifications* on rail, there could be as much as a 3:1 variation in wear rate. This behavior suggests that there may be some merit in segregating rails at the high end of the equivalent carbon range for more severe usage (in the fashion of "blue" rails some years ago). Also perhaps a very low cost premium rail could be developed near or just above the upper end of the current allowable AREA range.

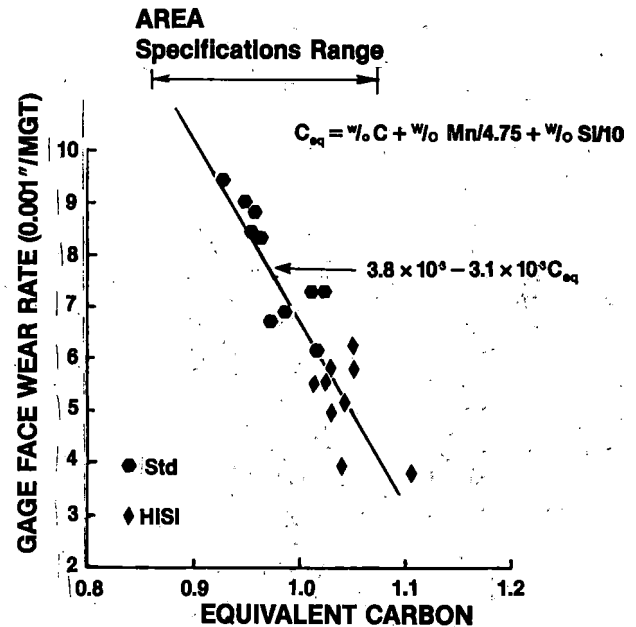


FIGURE 11. EFFECT OF EQUIVALENT CARBON LEVEL ON GAGE FACE WEAR RATE: RME I.

In order to compare the FAST rail wear behavior with that of other types of operations Figures 12a and 12b show the FAST wear data at 5° curvature along with families of curves from other sources. By comparison with the data of Hay, et. al.,³ (Northern Pacific and Burlington Northern), the FAST wear environment is roughly twice as severe. Interestingly, the Hay data show the 132 lb/yd FHT wearing at about the same rate as standard rail. How-

*A lubrication block is one lubricated interval of 30-40 MGT and a dry period of 10-15 MGT.

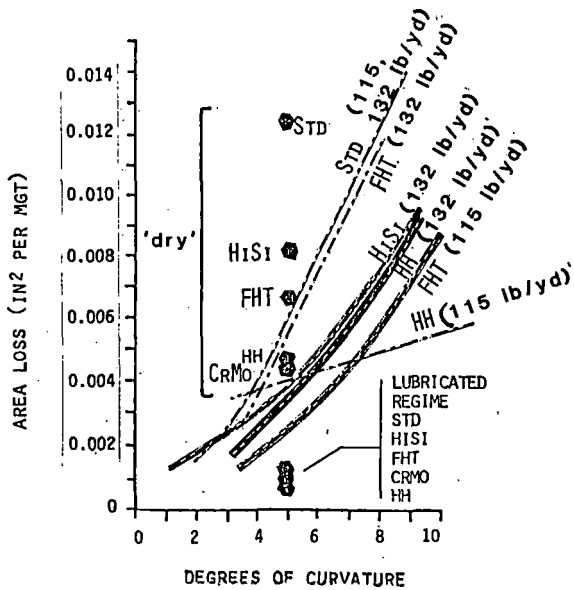


FIGURE 12a. FIELD COMPARED TO FAST DATA (COMPARING HAY et. al).

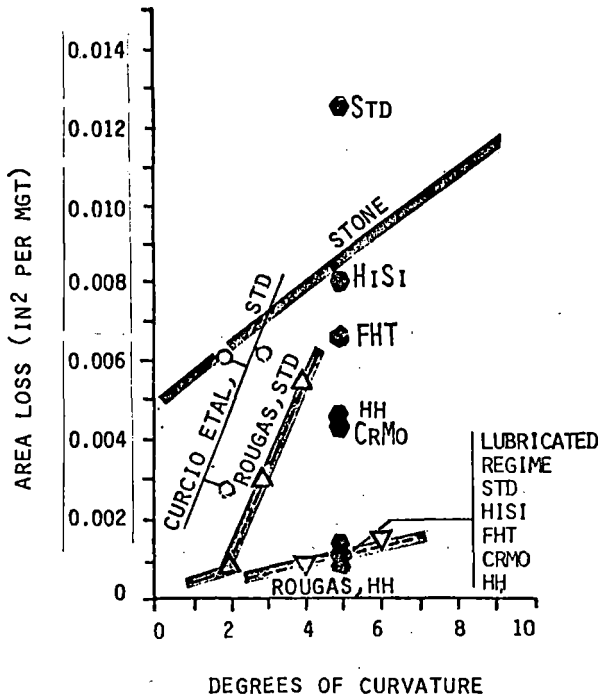


FIGURE 12b. FIELD COMPARED TO FAST DATA (COMPARING STONE, CURCIO, ROUGAS).

ever, the 115 lb/yd FHT performed substantially better. In a similar manner the FAST 115 lb/yd FHT rail performed substantially better on a 4° curve than one would have predicted from linearly interpolating the 132 lb/yd FHT wear rate at 5° back to 4° curvature. Data from Rougas⁴ for 100 ton cars operating on the Bessemer and Lake Erie (Figure 13b) suggest that the FAST environment is roughly twice as severe for standard carbon rail and perhaps four times as severe for HH rail. The FAST wear rate of standard rail seems to be about 50% greater than that reported by Stone⁵ for the Waynesburg Southern

operating at low speeds with 125 ton cars. However the Australian experience with 100 ton cars (albeit reported with lubrication) at low curvatures does extrapolate linearly to wear rates close to those observed at FAST.

Another set of comparisons can be made by taking the linearly interpolated FAST wear rates for standard AREA carbon rail (refer to Figure 4) to calculate lives using 25% head area loss the condemning limit and plotting them upon the data for other railroads as shown in Figure 13. At 5° curvature, the FAST calculated rail life would fall toward the low end of the distribution observed for other railroads. However, as curvature decreases the FAST wear lives calculated from linearly interpolated wear rates fall toward the high side of the distribution—more so as the curvature decreases.

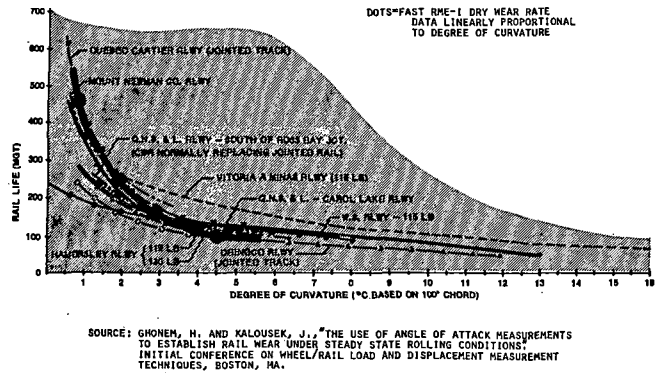


FIGURE 13. COMPARISON OF WEAR RATE DATA DIFFERENT SOURCES WITH THAT FROM RME I.

The distinction of RME III by comparison with RME I is that a greater variety of metallurgies were tested with vastly improved measurement techniques under conditions of planned variation in lubrication level. Attempts were made to provide reasonably close control on the wheel mix of the train. In spite of these controls, there were significant variations in the wear rates of the rails from one lubrication block* to the next. This sort of variation in the dry regime is shown in Table X for the four different standard rail heats tested. The wheel mix and character of the train are given at the top of each column along with the type of mechanical experiment run in that period. The wear rates in the Block II dry regime typically were about 25% higher than those of block I; yet there was virtually no change in the wheel mix or train consist. Then, in Block III, the wear rates dropped, typically by about 40%; the only significant change in the consist was the introduction of some cars of the wheels IV experiment. If B and C wheels were grouped together as 'hard' wheels, the hard wheel content of the train varied from 45% in Block I to 40% in Block II, and then to 53% in Block III; clearly the introduction of hard wheels was not associated with any detectable increase in rail wear rate.

The changes in dry rail wear rate from one lubrication block to another were also associated with a

change in the character of the position-in-curve effect for standard rail. Figures 14a thru 14c illustrate the position-in-curve effect in each lubrication block. From Block I to II, the effect became more pronounced with rail at the south end of the curve exhibiting 25 to 30% greater wear rate than the same heat of rail in the north end. However, in Block III the position-in-curve effect had virtually disappeared.

TABLE X. GAGE FACE WEAR RATES OF STANDARD RAIL: RME III.

(NO LUB REGIME)

Heat #	Segment	BLOCK I		BLOCK II		BLOCK III	
		55% U 42% C 3% B	Valt +RT % Change	60% U 38% C 2% B	Valt +RT +WWI % Change	47% U 43% C 10% B	RT+ WHIV % Change
21178 C _{eq} =0.94	III	0.00578	24	0.00717	-40	0.00430	
	IV	0.00561	37	0.00769			
21180 C _{eq} =0.995	I	0.00502	21	0.00609	-26	0.00448	
	III	0.00654	21	0.00789	-39	0.00483	
	IV	0.00626	35	0.00847	-39	0.00514	
	I	0.00557	21	0.00676	-27	0.00506	
21181 C _{eq} =0.94	II	0.00668	21	0.00812	-39	0.00492	
	IV	0.00765	33	0.01021	-42	0.00590	
21187 C _{eq} =0.97	II	0.00507	14	0.00576	-49	0.00292	

VALT - Variable Axle Load Test
 RT - Radial Truck Test
 WWI - Wheel Wear Index
 WH IV - Wheels IV Experiment

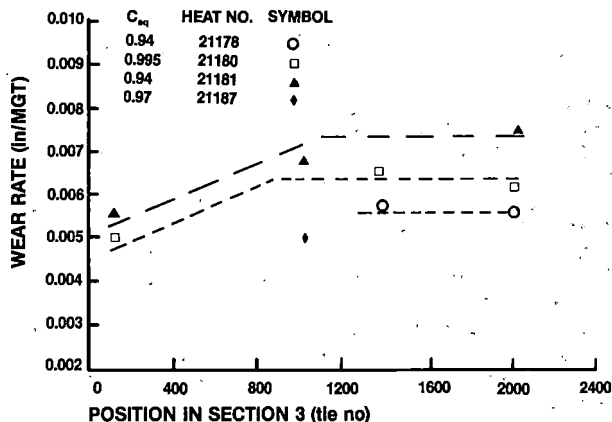


FIGURE 14a. BLOCK I: RME III.

Some variation in super-elevation had occurred throughout this period at tie ranges shown in Figure 15. By the dry period of Block I, the super-elevation had diminished somewhat from its initial construction level. However, just before the beginning of the dry period in Block II, the super-elevation was restored to its initial construction level and it has stayed at that level to the end of operation prior to the summer 1981 installation of concrete ties into Section 3. Thus, the change in super-elevation seems unlikely to be associated with the changes in wear rates and in position-in-curve effect.

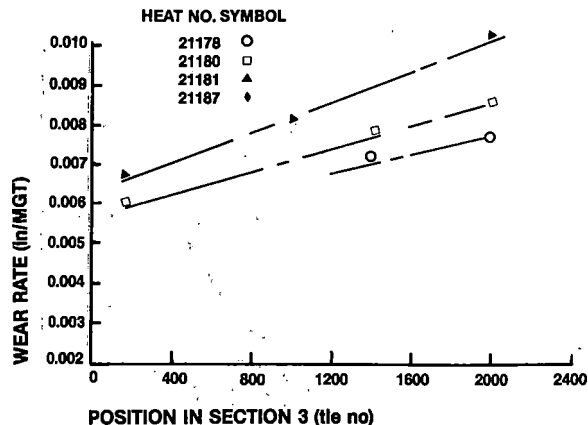


FIGURE 14b. BLOCK II: RME III.

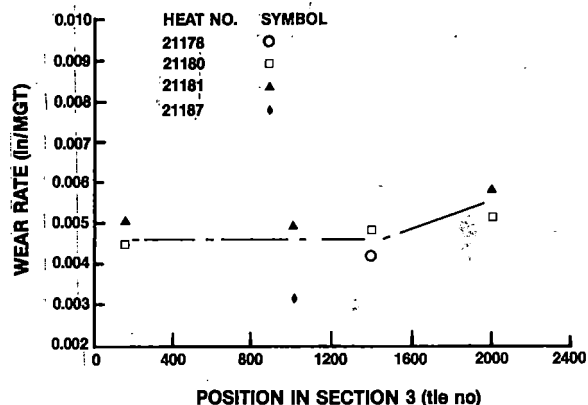


FIGURE 14c. BLOCK III: RME III.

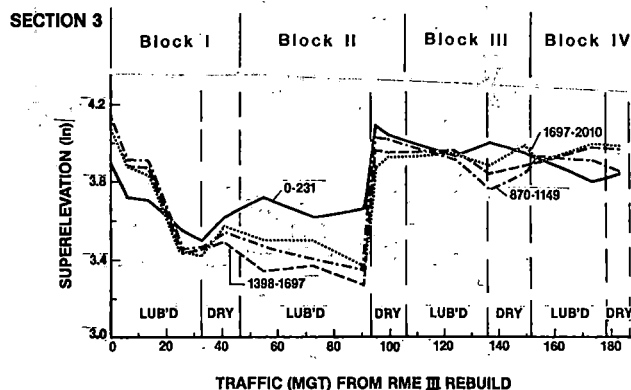


FIGURE 15. VARIATION IN SUPERELEVATION WITH TRAFFIC: RME III.

An overall view of how the wear rates of all test rails in Sections 3 and 17 changed from one lubrication block to the next is given in Figures 16a thru 16d. In the dry periods (Figures 16a and 16b), the premium rails exhibited far less variation in wear rate than did standard rail. Indeed SiCr (HH) exhibited only a mild decrease in wear rate across all four lubrication blocks. FHT rail exhibited a more marked and consistent decrease in wear rate through that period perhaps is indicative of a difference in the gage face resistance of the surface

FIGURE 16a. GAGE FACE WEAR RATES; SECTION 03; DRY.

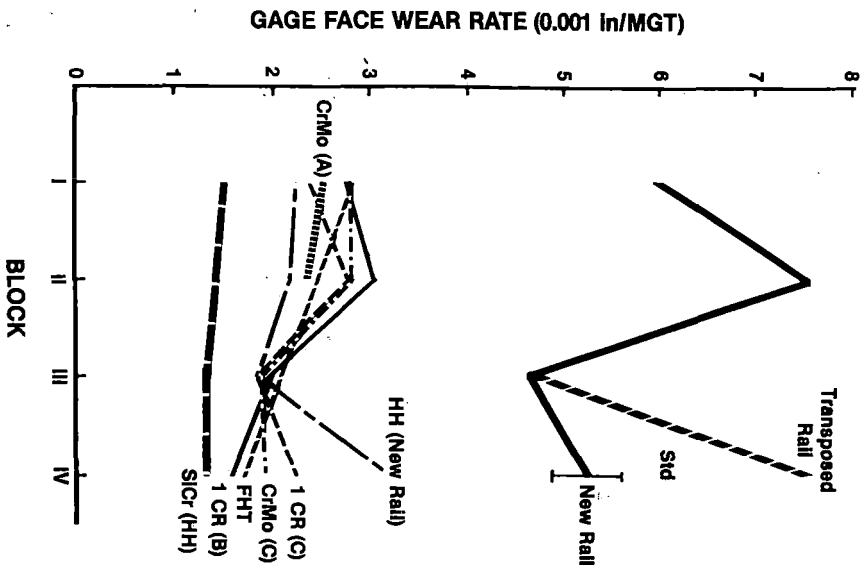
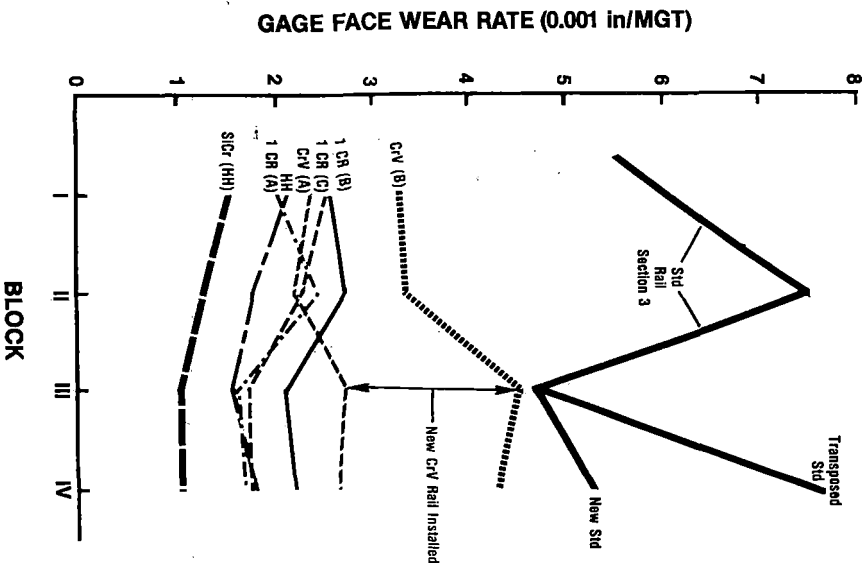


FIGURE 16b. GAGE FACE WEAR RATES; SECTION 17; DRY.



material as opposed to the material further within the rail head. Clearly, though, in the dry periods, SiCr(HH) rail stood by itself as the most resistant rail to gage face wear. All the other metallurgies except for CrV(B) were clustered together, intermediate in performance. The CrV, from two different manufacturers, which was tested only in the 5 curve of Section 17, exhibited differences in performance. While that rail from supplier 'A' behaved about the same as that of the other intermediate group rails, that from supplier 'B' exhibited notably poorer gage face wear resistance.

A similar situation existed for CrMo(A) rail. Within one stretch of rail very large differences in wear rate could occur. The magnitude of this variation is shown in Table XI; at the low wear rate end, the rail performed better than any of the other intermediate group rails, but at the high wear rate end, it performed only slightly better than did standard carbon rail. Notably, it did not exhibit the large change in wear rate observed for standard carbon rail in Blocks I and II.

TABLE XI. CrMo(A) AS A SPECIAL CASE; GAGE POINT WEAR RATES FOR DRY REGIME: RME III.

Segment	Group	Block I	Block II
I	Hi Wear Rate	0.0048"/MGT	0.0048"/MGT
	Lo Wear Rate	0.0018"/MGT	0.0019"/MGT
II	Hi Wear Rate	0.0046"/MGT	0.0049"/MGT
	Lo Wear Rate	0.0032"/MGT	0.0029"/MGT

Invariably when new rail, from the same heats as tested before, was installed in the course of the operation at the beginning of the lub'd period, the wear rate in the subsequent dry period would be greater than that of the same rail just removed from test. This was true for new standard and HH rail (Block IV), and new CrV rail (Block III). In the case of new standard rail introduced in Block IV, the average wear rates were not quite so high as those of the rail originally installed upon construction. Standard carbon rail transposed from the low rail has exhibited an exceptionally high gage face wear rate compared to the same heats of rail installed initially in the high rail.

The behavior of the test rail in the lubricated periods generally has been the same from one block to the next as has the behavior of the rail in the dry periods (Figures 16c and 16d). However, in lubricated periods of Block III, the same factor which led to the general decrease in wear rates observed in the dry periods, lowered wear rates of the premium rails far more relative to that of standard rail than would have been expected.

Only in Block III do the figures of merit of the premium rails in the lubricated periods approach those values observed in the dry period. This can be seen in Table XII. The discrepancy appeared only in the lubricated portion of Block III; in the dry period, the figures of merit of all rail except CrV were generally the same as those observed in the other dry periods. A suitable explanation for the anomalous behavior of the rail in the lubrication portion of Block III is not at hand.

TABLE XII. FIGURES OF MERIT FOR GAGE FACE WEAR: RME III.

	BLOCK I		BLOCK II		BLOCK III		BLOCK IV	
	Sec. 3		Sec. 17*		Sec. 3		Sec. 17*	
	L	NL	L	NL	L	NL	L	NL
Metallurgy	L	NL	L	NL	L	NL	L	NL
Std.....	1.0	1.0	/	/	1.0	1.0	/	/
HH.....	1.6	2.7	/	/	1.7	3.5	/	/
FHT.....	1.4	2.1	—	—	1.7	3.0	—	—
SiCr (HH)	1.7	4.0	1.5	3.7	1.9	5.2	1.7	3.8
A...	—	—	0.8	2.8	—	—	1.1	2.6
1 CR B...	1.9	2.2	1.6	2.3	1.6	2.5	1.4	2.3
C...	1.5	2.5	1.5	2.3	1.6	2.7	1.4	2.7
CrMo A...	1.8	2.4	—	—	1.6	3.2	—	—
C...	1.6	2.2	—	—	1.7	2.7	—	—
CrV A...	—	—	1.0	2.5	—	—	1.2	2.8
B...	—	—	1.2	1.8	—	—	1.0	1.9

* Adjusted against Section 3 by assuming HH in both sections is equivalent

In addition to gage face wear rates some information is available from transverse profile measurements* about head height loss rates of the outside rail. Because of the relatively short lube and no lube periods in each lubrication Block, the results from Blocks I and II have been averaged for presentation in Table XIII. Perhaps because a greater effort was made to keep the running surface free of lubricant, the variation in head height loss rate from lubricated to dry regimes is far less obvious (and less consistent) than it was in the first experiment.

TABLE XIII. HEAD HEIGHT LOSS RATES FOR HIGH RAIL ONLY.

Metallurgy	Section 3		Section 17	
	Lub'd.	Dry	Lub'd.	Dry
Std.....	0.0007	0.0021	—	—
HH.....	0.0004	0.0002	0.0005	0.0004
FHT.....	0.0004	0.0007	—	—
SiCr(HH).....	0.0010	0.0013	0.0003	0.0007
1 CR.....	0.0003	0.0009	—	—
CrMo(A).....	0.0007	0.0005	—	—
(C).....	0.0005	0.0003	—	—
CrV.....	—	—	0.0006	0.0016

Interestingly, the SiCr(HH) rail which exhibited outstanding resistance to gage face wear in the dry periods is grouped with CrV rail in an intermediate category in this regime. All other premium rails exhibited height loss rates less than 0.001"/MGT. In view of the wide scatter inherent in transverse profilometry measurement values, all those metallurgies showing rates less than 0.001"/MGT must be considered to be performing the same.

Metal flow measurements made on the standard carbon low rail with the snap gage type instrument are shown in Figures 17a and 17b. As with the standard carbon (low) rail in the first experiment, the major metal flow was to the field side. However unlike the behavior observed in the first experiment, the lateral flow seemed to have increased rapidly with each succeeding dry period. Because measurements were made only at the end of dry periods, it cannot be established whether most flow occurred in the lubricated or in the dry regimes. But, the fact that flow increased after each dry period in contrast to the levelling off (on the field side)

* Regrettably, the head height loss snap gage did not become available until the beginning of the third lubrication block.

observed in the-lubricated period of the first experiment, does suggest that lubrication of the high rail has a beneficial effect on metal flow on the low rail. There was not sufficient metal flow of any of the premium rails to make a judgement about their relative performance.

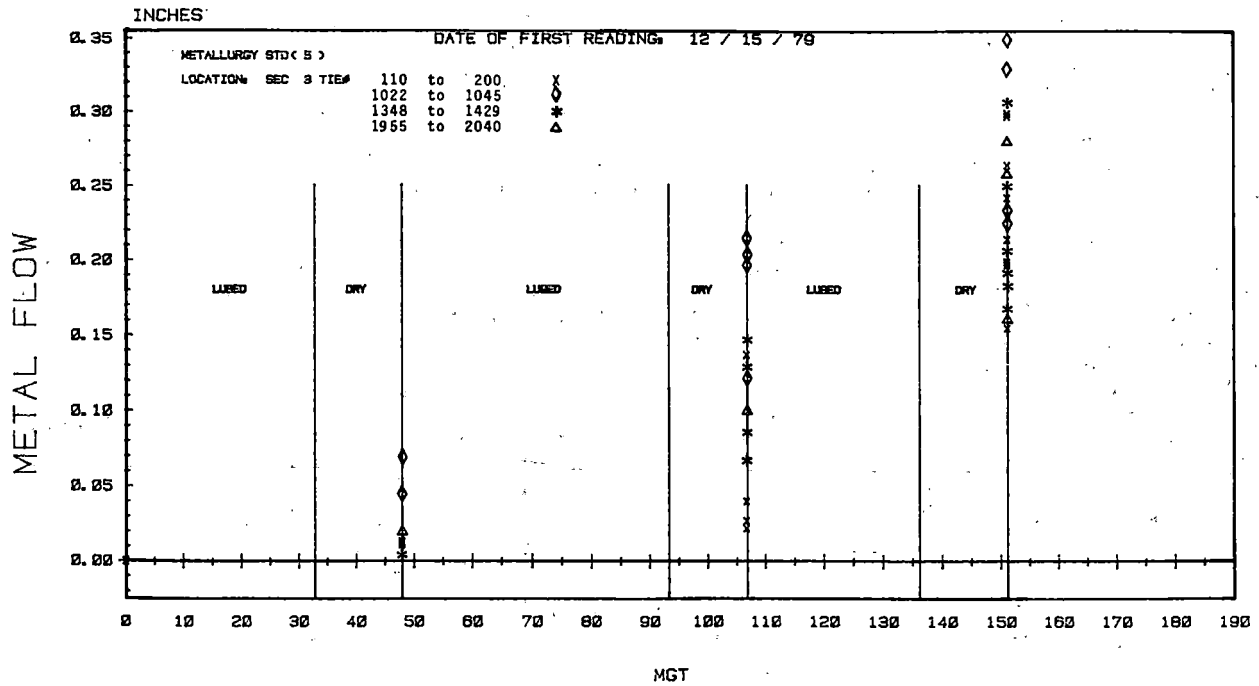


FIGURE 17a. METAL FLOW LOW RAIL FIELD MEASUREMENT
SNAP GAGE: RME III.

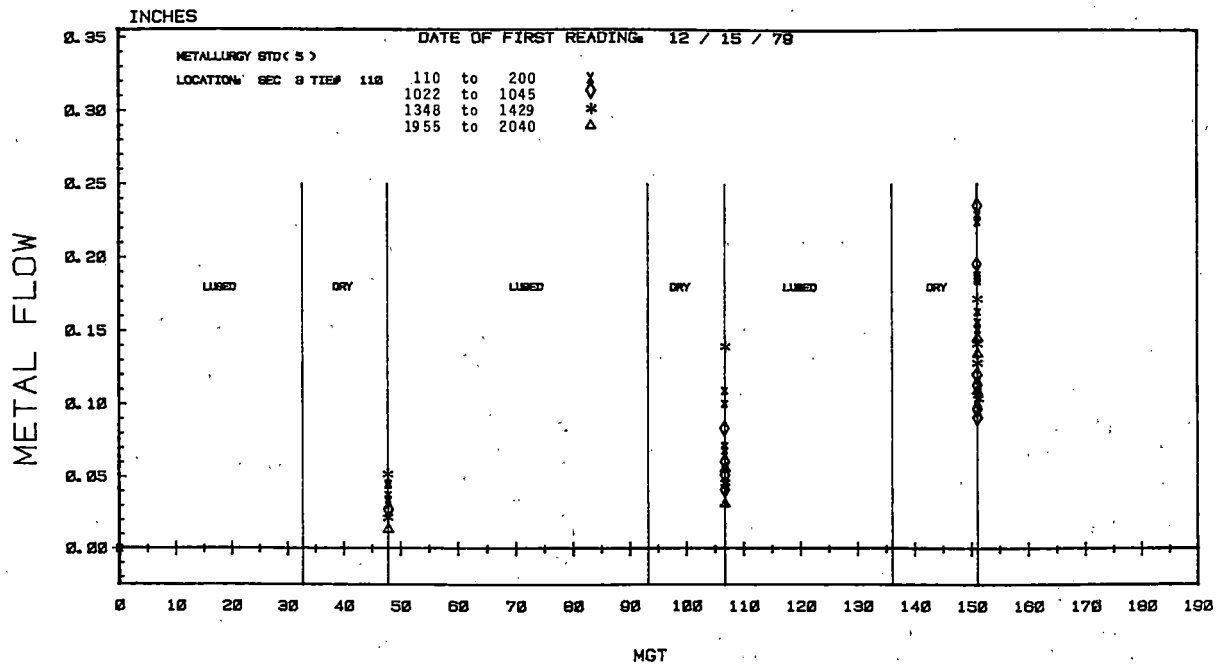


FIGURE 17b. METAL FLOW LOW RAIL GAGE MEASUREMENT
SNAP GAGE: RME III.

Considerably more attention has been paid to hardness of rails in the current experiment than was paid in the first experiment. Both light load (~1 kg Eseway) and high load (3000 kg Brinell) indentation tests have been made at intervals throughout the period of the experiment. Figure 18 presents both types of hardness data for the running surface together at various times during the experiment. As can be seen not all the different metallurgies behaved the same. For instance, SiCr(HH) seems to have exhibited a consistent increase in hardness with exposure to service as determined by both measures of hardness. CrMo(A), on the other hand, seems to have exhibited a continued increase in light load hardness with service but a slight reduction in high load hardness after a maximum was reached following a period of service. 1 Cr exhibited a peak in high load Brinell hardness followed by a slight drop although light load hardnesses appear to have continued to increase with service exposure. Most interestingly standard carbon rail exhibited a peak followed by a decrease in both measures of hardness. The light load is not particularly suitable for making comparisons over long periods of time, but it does provide a reasonable basis for comparison when readings are taken in the same time period. Thus, the indicated continued increase in hardness for SiCr(HH) and the peaking followed by a decrease for standard rail are probably true.

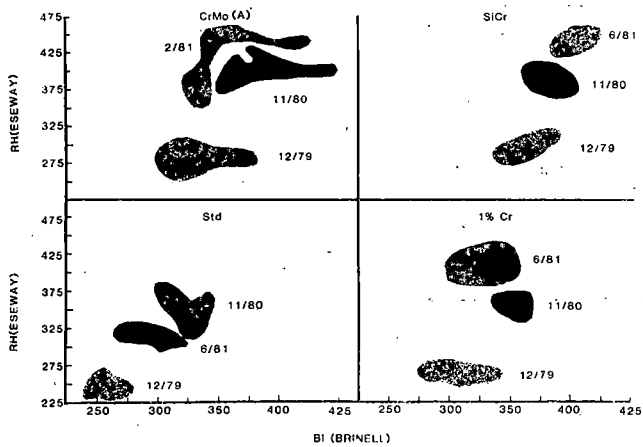


FIGURE 18. HARDNESS POPULATION DISTRIBUTION.

Using the as-worn gage face hardnesses after the second lubrication block along with the average wear rates of each metallurgy, the relationship between wear rate and hardness may be plotted as shown in Figures 19a and 19b for the different lubrication regimes. A semi-logarithmic format has been chosen because a straight line plot of dry regime wear rate against hardness would imply zero rate at 430 BHN - not a very believable situation. The slope of the line in the dry regime is considerably steeper than that in the lubricated regime - a consequence of the behavior observed in the first experiment, the lateral flow seemed to have increased rapidly with each succeeding dry period. Because measurements were made only at the end of dry periods, it cannot be established whether most flow occurred in the lubricated or in the dry regimes. But, the fact that flow increased after each dry period in contrast to the levelling off (on the field side)

metallurgy:lubrication interaction. Most data falls closely along the straight lines; however, both FHT and CrMo(A) are not with that group of data. The CrMo(A) is believed to be at least partially bainitic and therefore may be quite hard but will possess poor wear resistance. The poorer gage face wear performance of FHT rail than would be expected from its hardness is less easy to explain. However, the gradual diminution of its gage face wear rate as metal is removed from the gage face, suggests that there may be a microstructural gradient from the rail surface to the interior. An interesting (but unexplained) observation shown in Figure 19b is that in the first lubricated period the wear rate of rails in Section 17 (5°) was notably less than the same metallurgies (same heats) in Section 3. However, as comparison of Figures 16c and 16d reveals, in the second lubricated period, the wear rates in Section 17 (5°) increased to about same average level as those in Section 3 although the spread of values was substantially greater.

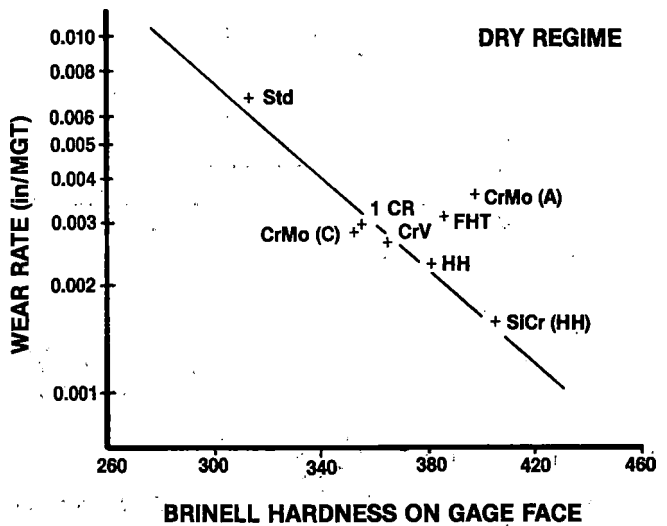


FIGURE 19a. WEAR RATES AS A FUNCTION OF HARDNESS: RME III.

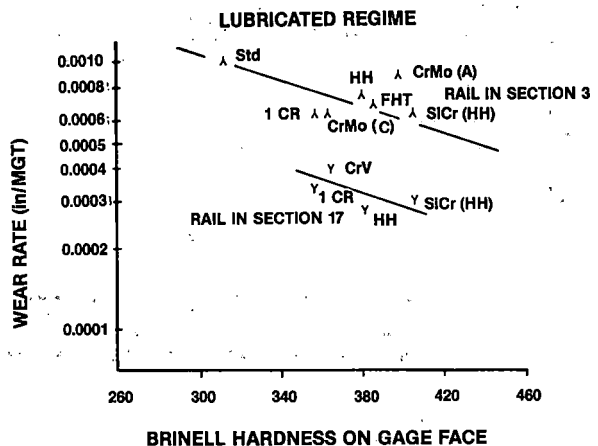


FIGURE 19b. WEAR RATES AS A FUNCTION OF HARDNESS.

One further use may be made of the gage face wear data from the current experiment and that is to extend the formulation for the contribution of equivalent carbon to alloying elements. There has not been enough data available to accomplish this in a rigorously correct statistical fashion, but if the assumption is made that the alloying elements do not interact with each other, (i.e., the effect of X w/o Cr in a Cr alloy would be the same as X w/o Cr in a CrMo or CrV alloy) and that mill processing variables from one manufacturer to another do not dominate over the alloy effects, then one can extend the formulation by first considering the 1 Cr alloy to assess the contribution of Cr and then CrMo and CrV alloys to assess the Mo and V. The basic tenet of this approach is that the slope of the wear rate vs C_{eq} plot is the same, regardless of how the alloy elements contribute equivalent carbon terms. In doing this the 1 Cr(B) and CrV(B) have been excluded from the development of the formulation because they do indeed seem to behave differently from the other alloys of the same nominal composition from different manufacturers. Figure 20 shows that the wear data of the alloy rails (excluding those of manufacturer B) cluster around the dashed line (extrapolated from the standard rail data of the current experiment) parallel to the line observed for Std and HiSi of the first experiment when equivalent carbon is calculated according to the equation:

$$C_{eq} = w/o C + w/o Mn/4.75 + w/o Si/10 + w/o Cr/6.4 + w/o Mo/3.8 - w/o V/4.4$$

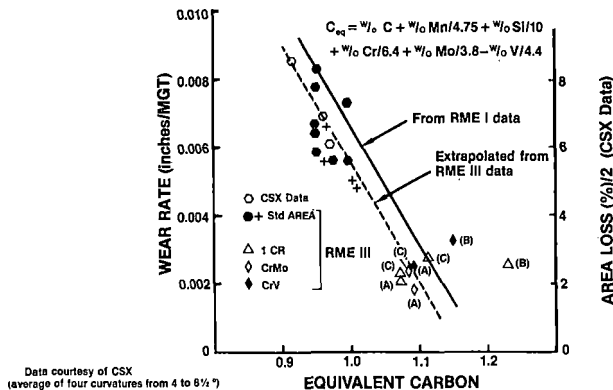


FIGURE 20. EFFECT OF EQUIVALENT CARBON EXPANDED TO INCLUDE ALLOY ADDITIONS: RME III.

This formulation implies that Cr does not have quite as strong an effect on wear as does Mn and that Mo has a slightly stronger influence than does Mn. Vanadium appears to have a negative effect, i.e., its presence may strengthen the alloy but does not improve its wear resistance. Caution is urged in applying this formulation too widely because mill processing variables (as in the case of manufacturer B) clearly can dominate over the alloying contribution. Nevertheless, the results from FAST do raise a serious question of whether vanadium provides the improvement in wear resistance that it is thought to provide.

To summarize now for the topic of wear and metal flow:

- o Typical maximum gage face figures of merit
 - Alloy rail = 3
 - Heat treated std carbon rail = 3
 - heat treated alloy rail = 4
- o The relative benefit of lubrication depends upon the type of rail.
- o Within the full allowable AREA chemistry range a 3:1 variation in gage face wear rate would be expected.
- o Hardness and yield strength are not necessarily good indicators of gage face wear resistance.
- o Metal flow on the low rail does seem to be influenced by lubrication on the high rail.
- o Significant metal flow (low rail) was observed only in standard and HiSi rail.
- o Uncontrolled variations in rail wear and metal flow behavior from one lubrication block to the next substantially weaken comparisons made among blocks; strongest comparisons are made within individual blocks.

WELDED RAIL END BATTER

The introduction of continuous welded rail (cwr) has vastly improved the geometric stability of the track structure. Nevertheless, the localized change in the metallurgical character of the rail that can occur in the vicinity of welds can ultimately lead to a loss of running smoothness which, like corrugations, can promote the development of localized track geometry irregularities, such as the kink shown in Figure 21. Loss of surface, pulverizing and movement of the ballast, release of anchoring action with ensuing movement of ties, and enhanced running of rail are some other annoying problems that seem associated with batter and corrugations.



FIGURE 21. A KINK ASSOCIATED WITH WELDED RAIL END BATTER.

The different metallurgies, types of track, and lubrication levels existing at FAST permit a fairly comprehensive experiment for both flash butt and

thermite welds. At least one plant weld of each metallurgy on the high rail and low rail has been monitored in Section 3 and Section 17 except for FHT where only one site was monitored initially. The primary type of measurement is longitudinal profilometry accomplished with the instrument shown in Figure 22. The instrument produces a paper trace whereon the vertical displacement along the rail is magnified 17 times and the longitudinal dimension is reduced by nearly 4:1. A built-in calibration step permits direct calibration of the instrument on each trace.

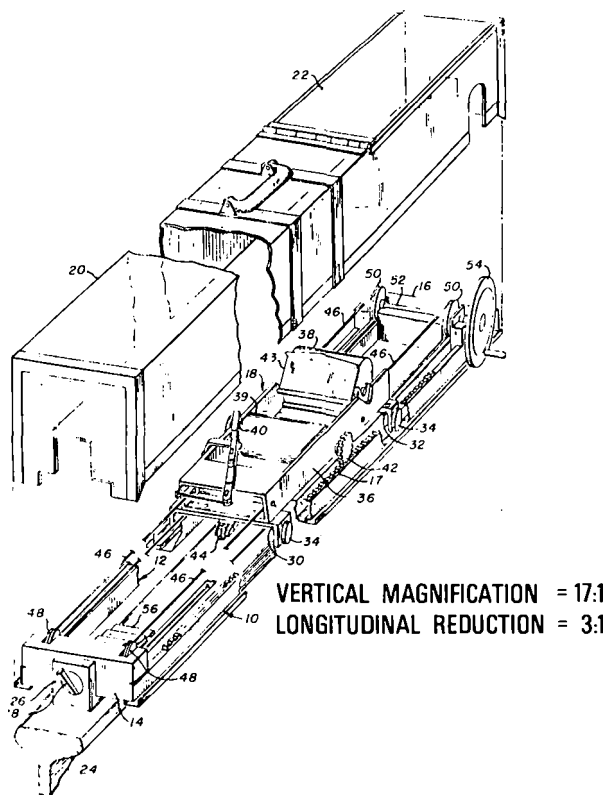


FIGURE 22. LONGITUDINAL RAIL PROFILOMETER.

The weld behavior observed has fallen into the three general categories: single dippers, double dippers, and peaked as shown in Figure 23. The distinction between the double dipper and the peaked configuration is in the position of the valleys and the height of the peak. The valleys of the double dipper occur in the heat affected zones (HAZ) next to the welds whereas in the case of the peaked configuration, the valleys develop outside the HAZ in the base rail. Also, the peak tends to rise above the smooth running surface of the rail.

The heat treated rails exhibited a single dipper behavior, the alloy rail welds were double dippers, and standard carbon rail exhibited the peaked behavior. Some examples of the type of batter found are shown in Figure 24. An unusually bad weld developed 0.05" of batter in 50 MGT whereas a good weld developed only 0.02" of batter in 175 MGT.

Welds of two metallurgies, CrMo(A) and CrV, were tempered at 1000°F for 20 minutes after welding because no post heat that could be applied following

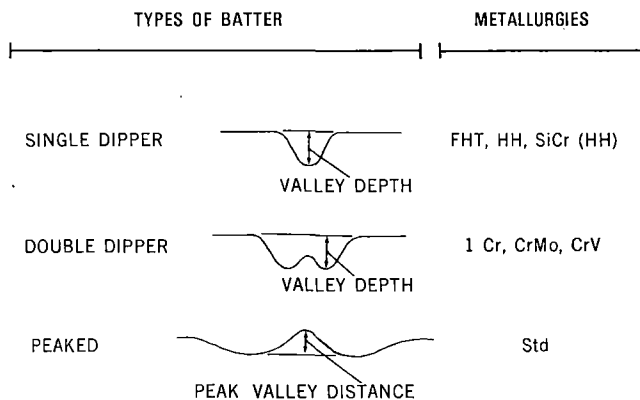


FIGURE 23. CATEGORIES OF WELD BEHAVIOR.

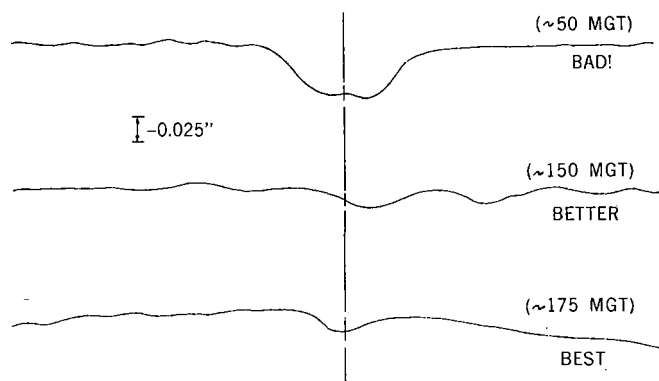


FIGURE 24. EXAMPLES OF WELDED RAIL END BATTER.

weld upset was found to be able to prevent the occurrence of substantial quantities (>30%) of untempered martensite in either the front or back of the base.* Some of these tempered welds performed extremely poor. The behavior of a typical tempered CrMo weldment is compared with the behavior of a weld of weldable grade CrMo that requires no post heat in Figure 25. Although the weldable grade developed about 0.035" batter by the end of the second dry period (106 MGT), the tempered weldment had developed nearly 0.09" of batter at 90 MGT; had not the weld been ground, batter might well have reached 0.150" by 150 MGT. A similar behavior was observed with the CrV rail as shown in Figure 26. For comparison, a 'properly'** postheated weld is shown to exhibit very little batter. It was with these tempered weldments that the aggravating effect of dry running was first noticed.

*The problem appeared to be associated with the development of an uneven heating pattern across the rail base which was especially severe upon post heating.

**The word 'properly' should be interpreted to mean avoidance of untempered martensite; however the postheating practice required seventeen 3 second pulses separated by 27 second intervals.

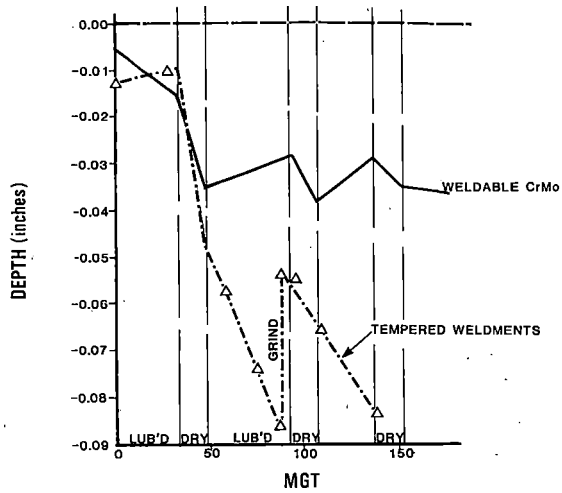


FIGURE 25. CrMo RAIL/VALLEY DEPTH INSIDE/RAIL SECTION 03.

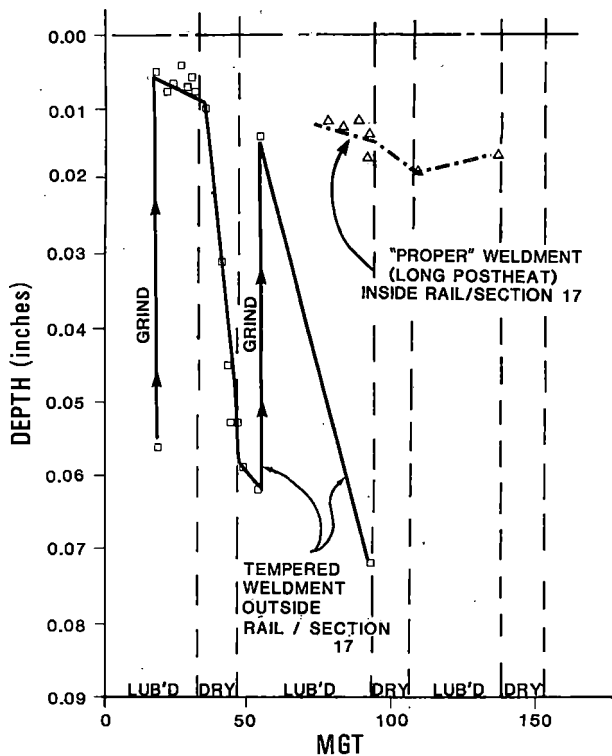


FIGURE 26. CrV RAIL/VALLEY DEPTH.

The behavior of a standard carbon flash butt and a thermite weld in tangent track is shown in Figure 27. Although the initial surface irregularity of the thermite weld was much greater than that of the flash butt weld, the batter development of both types of welds was remarkably similar. After the initial lubricated period, the thermite weld had exhibited some smoothing out of the initial irregularity, even though the width of the HAZ of the thermite weld was much greater than that of the flash butt weld.

By way of comparison, a flash butt weld of standard carbon rail in the 5° curve (Section 3) developed a

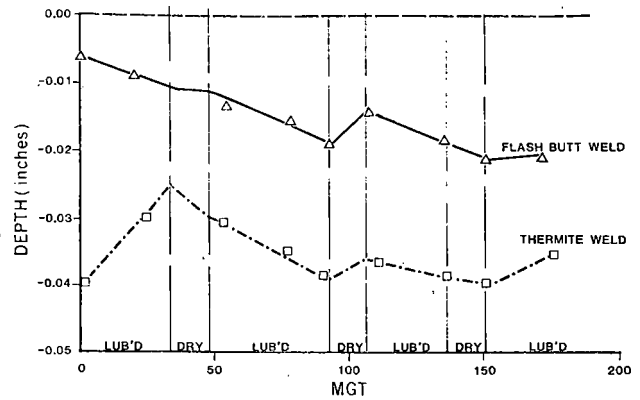


FIGURE 27. AREA STANDARD CARBON RAIL/VALLEY DEPTH FLASH BUTT AND THERMITE/TANGENT WELD.

somewhat different growth pattern (Figure 28). While the valley depth change beneath a smooth surface was not unlike that of a weld in tangent track (except perhaps in the third dry period), a peak had developed above the smooth running surface, probably as a consequence of the smooth running surface receding below the initial running surface while the metal at the weld bond line did not recede. The peak to valley height showed a strong tendency to grow much more rapidly in the dry periods than it did in the lubricated period with the exception of the first lubricated interval. This behavior was somewhat similar to that of the tempered CrMo(A) and CrV and of the CrMo(C) as well.

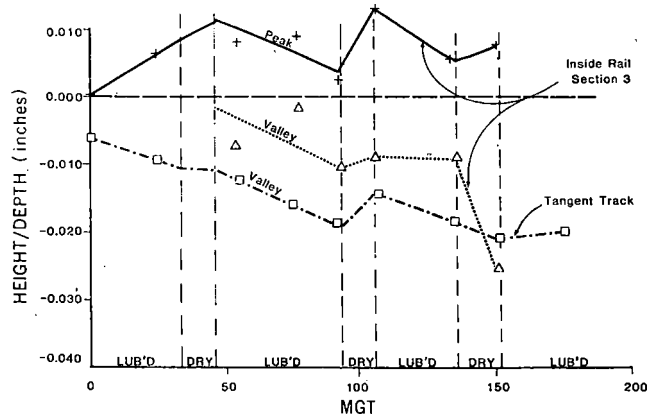


FIGURE 28. AREA STANDARD CARBON RAIL/VALLEY DEPTH AND PEAK HEIGHT.

Figure 29 illustrates the behavior at CrMo(C) on the inside and outside rail. The same general pattern has been observed on both rails, although the effects of dry and lubricated operation seem somewhat more pronounced on the inside rail where batter depth increased by about 0.03" in about 175 MGT. It is important to note again that only the outside rail was lubricated effectively and that the running surface of the inside rail was almost always dry.

However, on weldments which exhibited good resistance to batter, the effect of dry running to accelerate batter was not so certain. As shown in Figures 30 and 31 for 1 Cr and SiCr(HH) respectively,

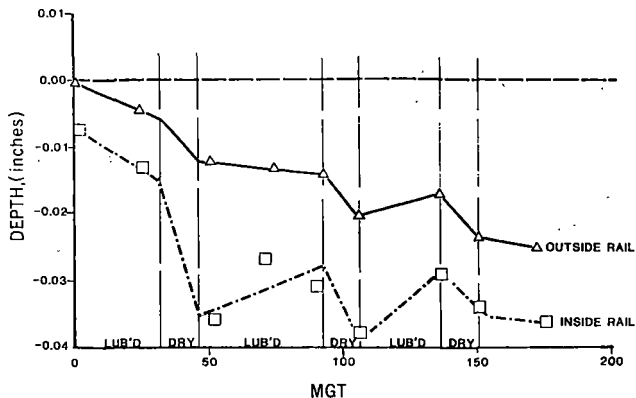


FIGURE 29. CrMo(C)/VALLEY DEPTH.

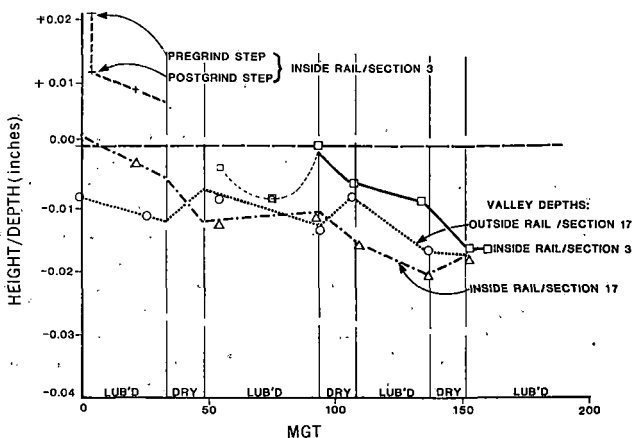


FIGURE 30. 1 Cr/VALLEY DEPTH AND STEP HEIGHT.

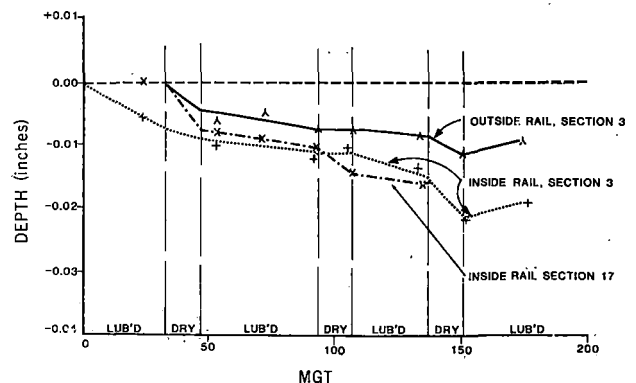


FIGURE 31. SiCr(HH)/VALLEY DEPTH.

there appeared to be some variability in behavior. However, perhaps this lower sensitivity to lubrication is related to the fact that the SiCr alloy has been designed so as to harden upon cooling after welding at the rates (slack quenching) characteristic of the weld and HAZ without post heat. In a similar sense, the 1 Cr welds have been given a very unusual post heat to prevent the formation of untempered martensite which tests had shown would otherwise have occurred on the welder used. For these superior weldments, batter depth would have reached only 0.02" at 150 MGT.

There were some differences in the behavior of heat treated standard carbon rails. Figure 32 shows that an FHT weldment in the outer rail was battering at a rather low rate after the first lubricated period with little or no effect of dry operation. An outside rail HH weldment also was exhibiting minimal batter. However, the inside rail HH weldment which was monitored in the same region, exhibited a rather exceptional batter propensity. The damaging effect of dry operation was particularly noticeable. Grinding at 80 MGT did nothing to slow the deterioration (in a fashion similar to the behavior of the tempered CrMo and CrV). Subsequent checks of other FHT and HH weldments in test Sections 3 (FHT + HH) and 17 (HH only) revealed that other FHT weldments in both inside and outside rail exhibited total batter similar to that of the monitored weldment. However, the HH was behaving in two different fashions--one group of about one-half the weldments had exhibited very little batter while the other half had exhibited total batter similar to that of the inside rail weldment shown in Figure 32. At this time we have no clear explanation for the behavior; with the exception of the SiCr(HH) rail, all rails for which information is presented here were welded on the same (60 kA) welder in the same time frame.

A comparison of inside rail weldments is given in Figure 33. The figure shows that SiCr(HH) and 'properly' post heated 1 Cr and CrV were all about

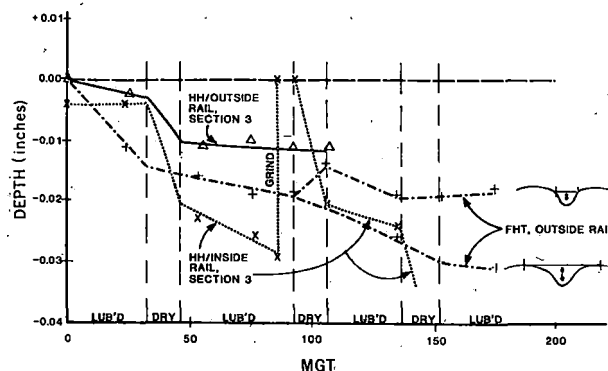


FIGURE 32. HEAT TREATED AREA STANDARD CARBON RAIL/VALLEY DEPTH.

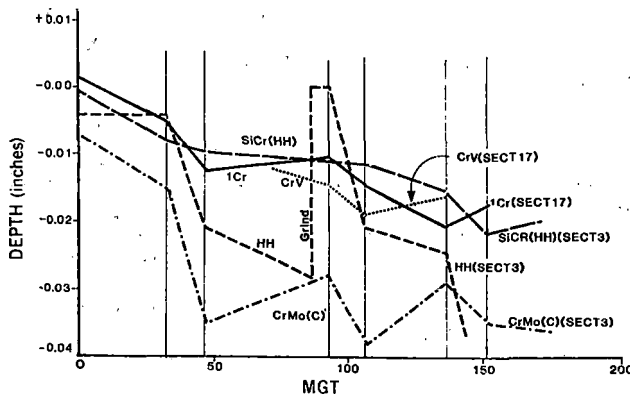


FIGURE 33. COMPARISON OF MAXIMUM VALLEY DEPTHS OF PREMIUM RAIL/INSIDE RAIL.

the same in performance but that weldable grade CrMo(C) had developed somewhat greater batter (mostly in the dry periods). The batter depth increase of the HH weldments in the lubricated periods was not unlike that of SiCr(HH), 1 Cr, and CrV weldment but it appeared to be particularly susceptible to dry operation.

In the alloy rails, the valleys of the 'double dip' occurred in the HAZ on either side of the weld bond line, and, therefore, one might expect a relationship between the depth of batter and the surface hardness. Figures 34a thru 34d plot the hardness profile and the surface profile together and show the correlation, such as it is, between surface hardness and batter. Although the valleys did indeed tend to occur at the places where the hardness, at least initially, was lowest, substantial valley depth occurred without the presence of low surface hardness. Likewise, large dips in hardness occurred without the presence of deep batter at these points. Thus, running surface hardness, at least as measured in the field, would not seem a good indicator of batter resistance.

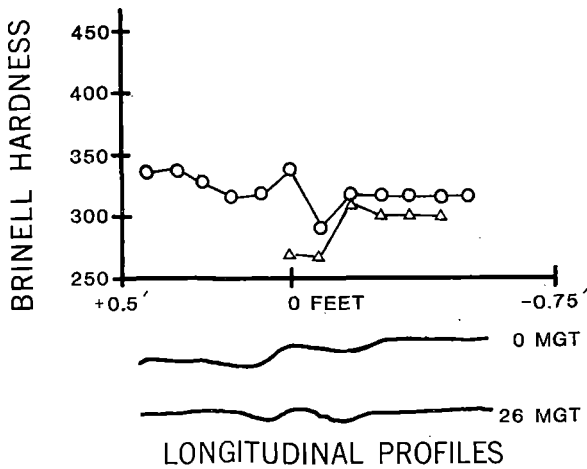


FIGURE 34a. 1 Cr RAIL 1ST LUBRICATION PERIOD.

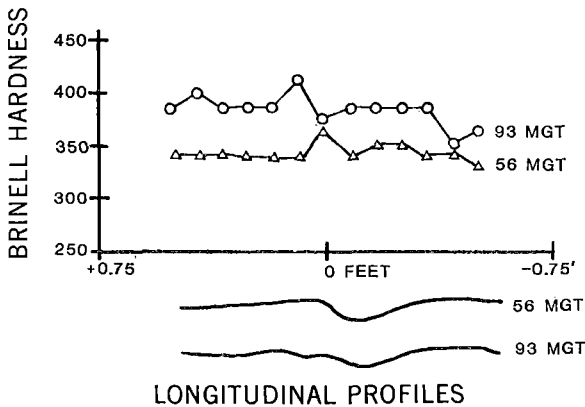


FIGURE 34b. 1 Cr RAIL 2ND LUBRICATION PERIOD.

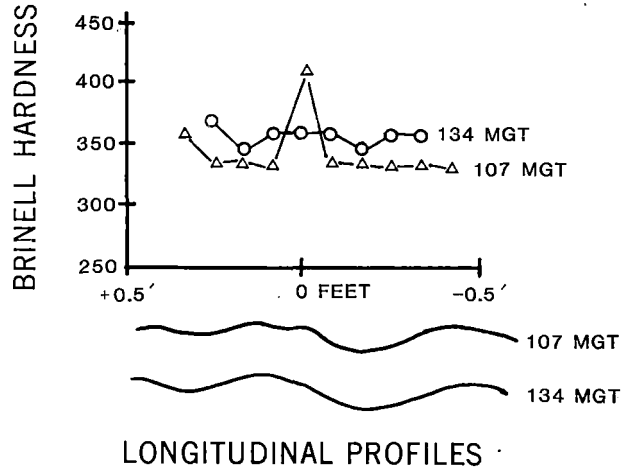


FIGURE 34c. 1 Cr RAIL 3RD LUBRICATION PERIOD.

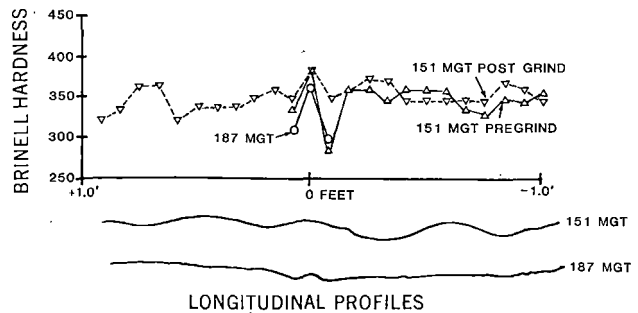


FIGURE 34d. 1 Cr RAIL 4TH LUBRICATION PERIOD.

If the value of hardness in the HAZ does not control batter development, the width of the HAZ may. The superior performance of the 'properly' post heated 1 Cr and CrV weldments as opposed to the performance of the CrMo(C), which does have a wide HAZ, suggests that attention should be paid to the influence of different combinations and types of preheat and post heat for alloy rail.

The width of the HAZ appeared to be a function of the temperature at which the pearlite transformation started in the upset (forged) region of the weld. Post heats fall into two major categories-- the short delay and the long delay. The short delay practice involves holding the weld in the welder for 20-40 seconds after completion of upset and then applying numerous heating pulses (typically of 2-6 second duration) separated by intervals comparable in length to the heating pulses. Thus heat is added to the weldment when it is still hot so that stripping may follow post heating. The long delay practice involves waiting 60 seconds or longer following completion of upset before the post heat cycles are applied. In this delay period, the weld is stripped while it is still hot and, if an external stripper is used, returned to the welder following stripping. After the rail is locked up again in the welder, one or two relatively long pulses (6-10 seconds) are applied to the weldment with a rather long interval (20-30 seconds) between pulses.

In the case of the 'properly' post heated 1 Cr and CrV weldments seventeen 3-second pulses separated by

27-second intervals were applied. The cooling paths each type of practice would follow are shown conceptually on the continuous cooling transformation diagram (Figure 35). The important difference between the two practices is that the long delay practice introduces the additional heat needed to prolong the cooling process at a substantially lower temperature. The interlamellar spacing of the pearlite (S_p) is inversely proportional to the temperature difference below the eutectoid temperature (1333°F) at which the pearlite transformation takes place. Thus, the lower temperature, at which the pearlite reaction occurs for the long delay practice, will result in a more refined microstructure in the weldment.

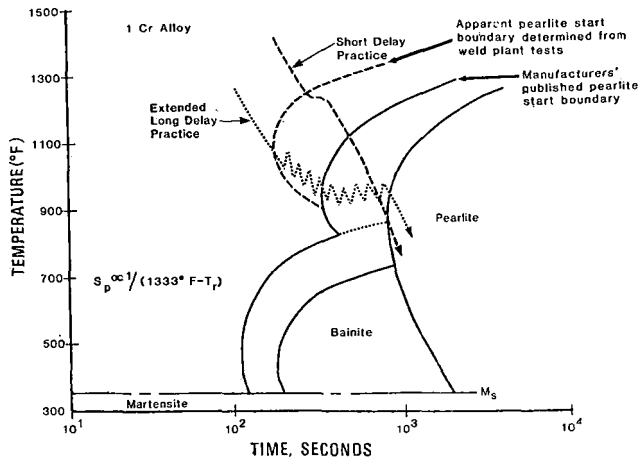


FIGURE 35. COOLING PATHS ON THE CONTINUOUS COOLING TRANSFORMATION DIAGRAM.

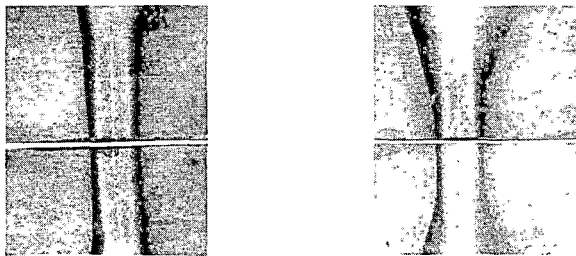


FIGURE 36a. PHOTOGRAPHS OF MACROETCHED PIECES FROM CrMo RAILS.

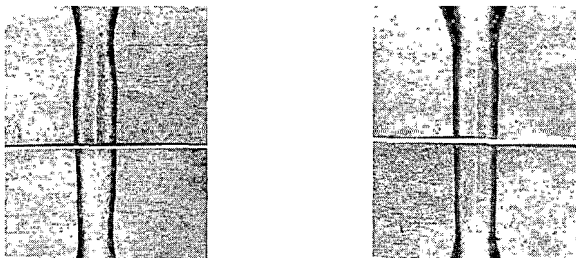


FIGURE 36b. PHOTOGRAPHS OF MACROETCHED PIECES FROM 1 Cr RAILS.

Figure 36a and 36b illustrate the fact that the short delay practice can cause the distance between the HAZ boundaries at the running surface to be about twice as large as that produced by the long delay practice--at least for CrMo(A) weldments on the 60 kA welder. The hardness profile in each of these welds just below the running surface is shown in Figures 37a and 37b.

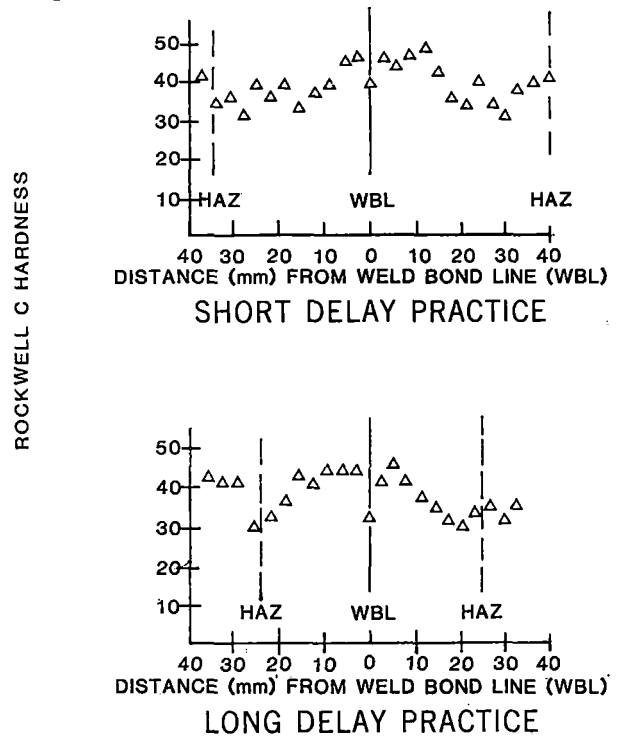


FIGURE 37a. HARDNESS AS A FUNCTION OF DISTANCE FROM WELD BOND LINE CrMo RAIL.

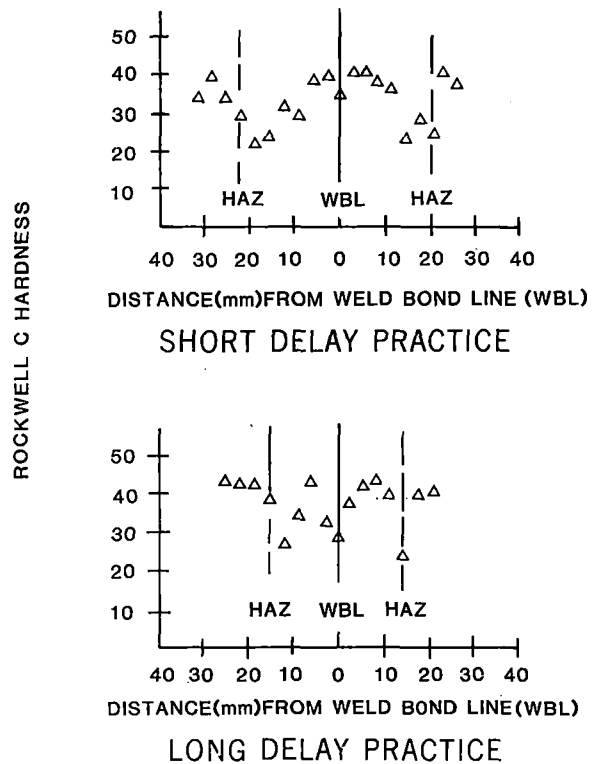
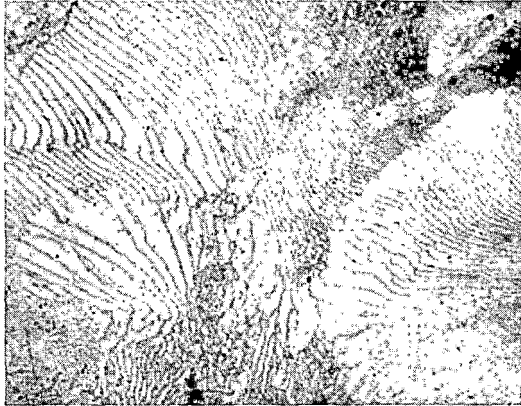


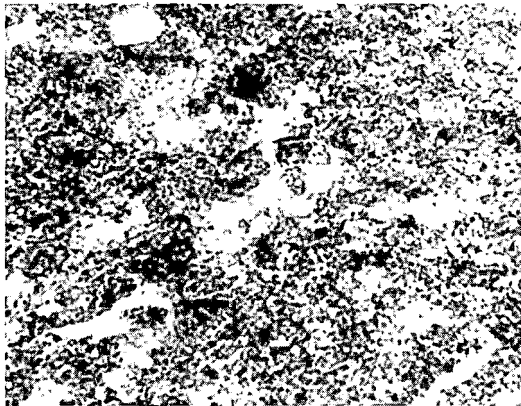
FIGURE 37b. HARDNESS AS A FUNCTION OF DISTANCE FROM WELD BOND LINE 1 Cr RAIL.

The minimum hardness was about the same for either practice, but the extent of the softer region was much greater with the short delay practice for each metallurgy.

The very poor behavior of the tempered CrMo and CrV weldments can be understood in terms of the change in microstructure which the tempering operation induced. Figure 38 illustrates the decomposition of the pearlite structure which had occurred. The decomposition would not have been expected if the temperature of tempering truly were 1000°F; the structure is characteristic of heating to 1250°F or higher.



1600X
A. PROPER PEARLITIC MICROSTRUCTURE



1600X

FIGURE 38. DECOMPOSED PEARLITIC MICROSTRUCTURE IN BATTERED CrV WELD.

Up to this point in the discussion, only depth of batter has been considered. Another important characteristic parameter is the wavelength. One way of treating both amplitude and wavelength (really wave shape) of any continuous curve is the Fourier series. The mathematical representation of this is given as

$$\text{HEIGHT} = A_0 + \sum [A_j \cos(jx) + B_j \sin(jx)]$$

A_0 , A_j , and B_j are empirically determined constants for increasing values of j (as many as needed to provide a suitable description of the curve), and x is the distance along the rail from the weld centerline.

This technique has been used to describe the running surface of a flash butt weldment of standard carbon rail located in Section 3. To simplify the process slightly the wave shape has been made symmetrical about the weld centerline. Separate sets of coefficients for dry and lubricated running have been obtained as a function of MGT by assuming that the change in batter that developed in any one dry or lubricated interval was unaffected by what happened in the immediately-previous period so that the changes in all dry periods and in all the lubricated periods can be summed separately.

For each lubrication regime, seven coefficients and A_0 have been found to provide an adequate description of the batter process in the weld considered. Figure 39 illustrates how these coefficients and constant A_0 changed with tonnage. Clearly the dry periods led to rapid, apparently non-linear, increases in the coefficients after about 30 MGT (dry) of traffic. Lubrication on the other hand tended to lead to a fairly steady value for each of the coefficients. It is also worth noting that coefficients seem to behave in a grouped fashion. For instance, in the dry regime, A_0 and A_1 seemed virtually identical, A_2 was nearly constant near zero, A_3 and A_4 were identical, and A_5 , A_6 , and A_7 were all virtually identical. Thus, in reality the variation of four coefficients and one constant adequately described the batter development.

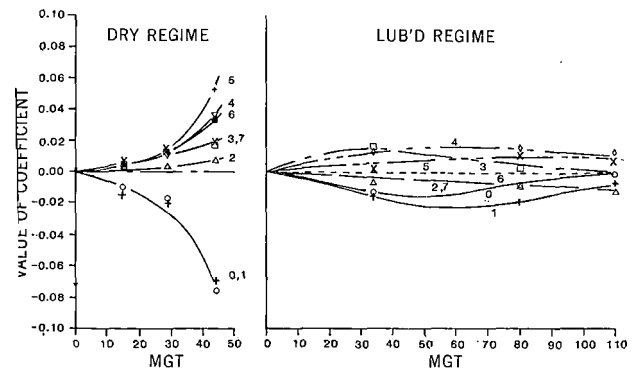


FIGURE 39. VARIATION OF FOURIER SERIES COEFFICIENTS.

The variations in the constant and coefficients have been used to reconstruct the batter profile for a condition of 40 MGT of pure dry operation and for 100 MGT of pure lubricated operation. These curves are shown in Figure 40. In the dry regime, the development of pronounced secondary batter can be seen after 30 MGT. Indeed, small undulations that are close to the weld up to 30 MGT seem to spread rapidly along the rail after 30 MGT has been exceeded. The actual experimentally observed profile after three 15 MGT dry periods plus three lubricated periods totalling 110 MGT is shown as a dashed line on the right hand side of the weld centerline. Clearly secondary batter had developed but the amplitude was far less than would be predicted for purely dry operation, perhaps because of the bene-

facial effect of lubrication in diminishing the amplitude of batter that had developed in the previous dry cycle.

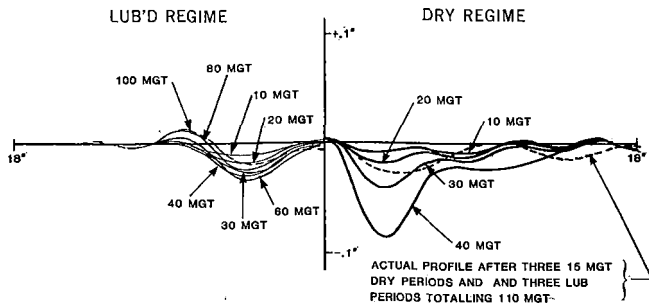


FIGURE 40. BATTER PROFILES FROM CENTERLINE OF FLASH BUTT WELD.

To summarize the welded rail end batter topic:

- o In some cases but not all, dry operation clearly accelerated batter development.
- o The batter rate of standard carbon rail on tangent track was about the same as that on a 5° curve.
- o The batter rate of inside and outside rail weldments on a 5° curve was generally about the same.
- o Standard carbon rail thermite welds battered at about the same rate as did flash-butt welds.
- o There is the hint that long delay post heat practices for alloy rail reduce batter development.
- o The batter rate may be highly dependent on the characteristics of the flash butt welder.
- o A Fourier Series representation of batter appears to provide a suitable description of both amplitude and wavelength (wave shape).

RAIL FATIGUE AND FAILURE BEHAVIOR

The rail metallurgy experiment at FAST has been designed primarily to study wear and metal flow. Yet when the wear rate was reduced massively by lubrication as in the case of the second experiment, rail fatigue became a major concern. The consequences of that fatigue were not inconsiderable as shown in Figure 41. This derailment resulted from three detail fractures that failed one after the other in a very short periods of time under the train. In 177 MGT, the heat of rail from which the failed rail had come had developed seven detail fractures - an extraordinary number.

The rail and weld failure history for the first and second experiment are given in Table XIV. The weld failure problem in the first experiment was magnified by (1) inexperience in making thermite welds to the extent that twice as many field welds failed as were installed initially in Section 3 and (2) the

plant welding of many dissimilar metallurgies together.*

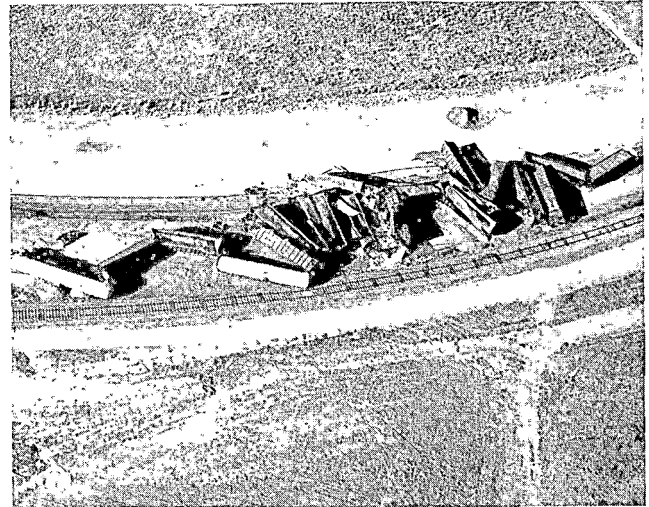


FIGURE 41. -PHOTO OF FAST TRAIN DERAILMENT.

TABLE XIV. RAIL AND WELD FAILURE HISTORY.

	Plant Welds	Field Welds	Head Defects
First Experiment (135 MGT)			
Section 03.....	44 (180)	44 (22)	2
Section 13.....	17 (64)	17 (10)	7
Second Experiment (250 MGT)			
Section 03.....	10 (120)	12 (0)	15 (27/mile)
Section 13.....	4 (48)	8 (0)	7 (10/mile) (30/mile)

*Defect rate adjusted to eliminate failures and rail length associated with "dirty" standard rail.
The number in parentheses () is the number of welds installed upon initial construction

The distressingly large number of weld failures in the first experiment in addition to rapid wear in the dry period necessitated the redesign and reconstruction of the metallurgy test sections at 135 MGT. The second experiment fared substantially better in terms of both plant and field weld failures. However, the prolonged period of operation achieved by improved lubrication allowed a far greater number of transverse fatigue failures to develop in Section 3.

The locations of all plant weld and head type failures in the high rail of Section 3 are shown in Figure 42 by metallurgy and tie plate cant. Without counting those transverse failures of questionable attribution (due to close proximity to a mechanical joint), standard carbon rail developed five failures (44/mile of high rail). HiSi rail developed only two failures (18/mile of high rail). HH rail developed only one valid fatigue failure. FHT had only one head failure, but it was at a segment end. CrMo rail had no head type fatigue failures.

*with care, there is no reason that dissimilar metallurgies cannot be welded together; there may, however, then be a batter problem.

(HIGH RAIL ONLY)

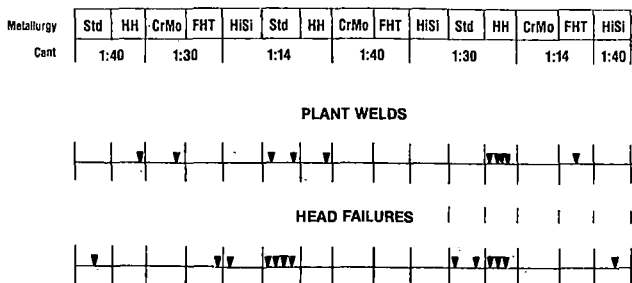


FIGURE 42. FAILURE BY METALLURGY.

HH exhibited the most plant weld failures⁶ in Section 3; in addition, there were others elsewhere in the track. More will be said about the nature of these failures later. Standard carbon rail had two plant weld failures while CrMo and FHT rail had only one plant weld failure each within the metallurgy test section. In Section 13, standard carbon rail had two plant weld failures, while FHT and HiSi had one failure each. It is important to know that except for CrMo, all rail was welded at the same plant in the same time frame.

The 1:14 cant was associated with a total of nine failures, the 1:30 cant with ten failures, and the 1:40 cant with three failures. However, some of these did occur near segment ends (as can be determined from Figure 42) and these must be viewed as suspect. A further consideration is the fact that the experiment design itself placed the Std, HiSi, and HH rails on the 1:14 and 1:30 cants in the mid-region of the curve while these same rails on the 1:40 cant were positioned at the ends of the curve. Thus, what appears as a tie plate cant effect may actually be a position-in-curve effect. The lateral wheel loads as determined from instrumented wheel set measurements at approximately 279 MGT into the second experiment are shown in Figure 43; no exceptional variations at any particular place in the curve were observed on these runs. However, the central one third of Section 3 was observed to have suffered more loss of track alignment than either of the end thirds (Figure 44).

SECTION 3, 45mph (nominal)
LUBRICATED

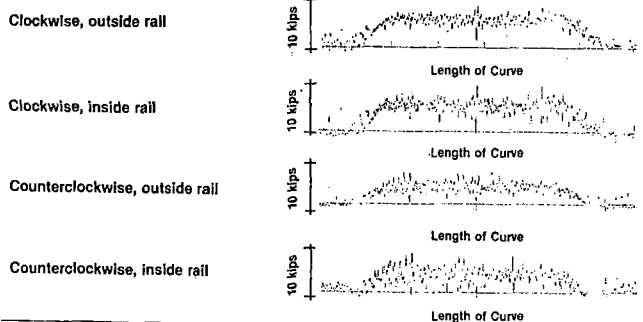


FIGURE 43. LATERAL WHEEL LOADS IN 5° CURVE.

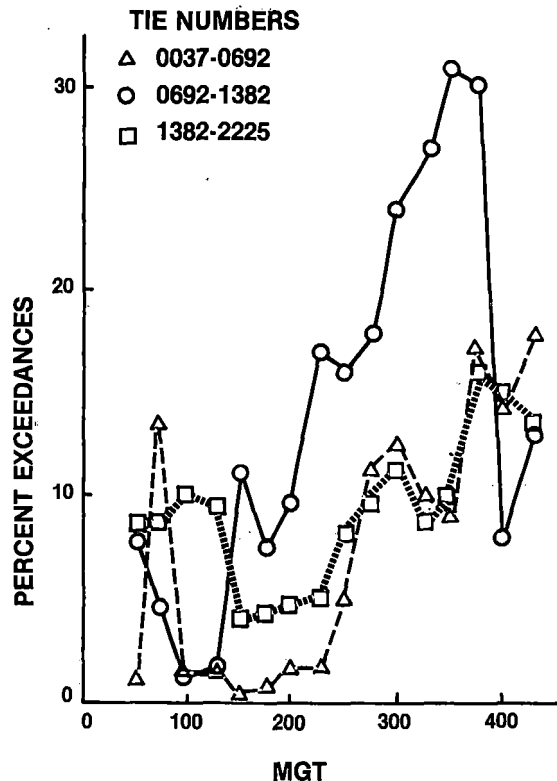


FIGURE 44. LOSS OF ALIGNMENTS BY TIE POSITION.

The relationship between rail failure at FAST and tonnage is shown in the Weibull plot of Figure 45 for standard carbon rail in both the 5° curve (Section 3) and in tangent track. The 'failures' in tangent track were not listed as detail fractures but rather as horizontal separations; they occurred in cwr track remote from welds. The line for the two HiSi failures also is shown. For comparison with rail defect behavior from actual U.S. railroad service, the upper and lower bounds within which the AAR/AREA/AISI survey⁷ data fall are plotted along with the defect occurrence line for the Waynesburg Southern Railroad⁵ upon which 125 ton cars are operated, albeit at lower speeds than those at FAST. The FAST rail failure experience is substantially more severe than that of more conventional U.S. railroad operations where car weights average closer to 75 tons. However, the Waynesburg Southern experience is very similar to that of FAST.

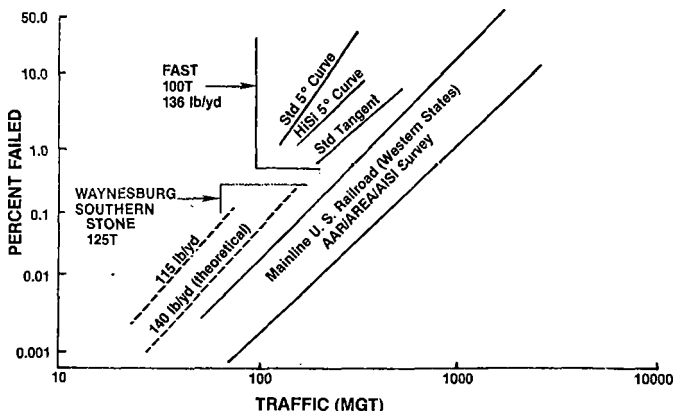


FIGURE 45. AFFECTS OF TOTAL TRAFFIC ON RAIL FAILURES.

The effect of wheel load can be seen by using the FAST rail failure data in conjunction with the defect data of the Waynesburg Southern and two sites (SF1, SF2) of the AAR/AREA/AISI survey where wheel loads are known. The one percentile tonnages have been taken from the Weibull plot (Figure 45) and plotted on a log-log basis (Figure 46). Typically, the slope of the plots was near -1.5. A theoretical prediction by Perlman et. al.,⁷ (estimated at the five percentile life) using an amplified and attenuated Union Pacific load spectra is shown to have a just slightly lower wheel load dependency than that observed for service information. Laboratory tests for contact fatigue performed by British Rail⁹ and Nippon Steel¹⁰ exhibited slopes of -1.5 and -0.7 respectively.

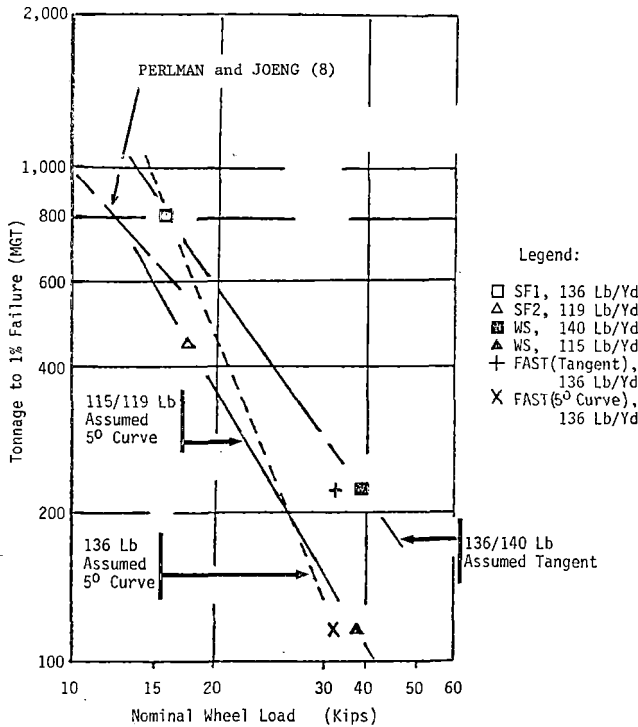


FIGURE 46. WHEEL LOADS VS RAIL FAILURES.

A derailment, such as that shown in Figure 41 resulting from rail failures at multiple undetected rail flaws serves as a substantial stimulus to determine what are the deficiencies of the inspection system used and to correct them. One indication of how well the inspection system is performing is the size distribution of defects found. Figure 47 shows the transverse defect size distributions before and after the derailment along with an estimated distribution for the nation as a whole based upon data from the Sperry Rail Service.* Prior to the derailment, the greatest number of transverse defects found at FAST fell into the range of 10 to 30%--a situation somewhat less conservative than

*The Sperry information has been given in the size categories: small, medium, and large. This author considered 'small' as 5 to 15%, 'medium' as 16 to 30%, and 'large' as >30% of the cross sectional head area.

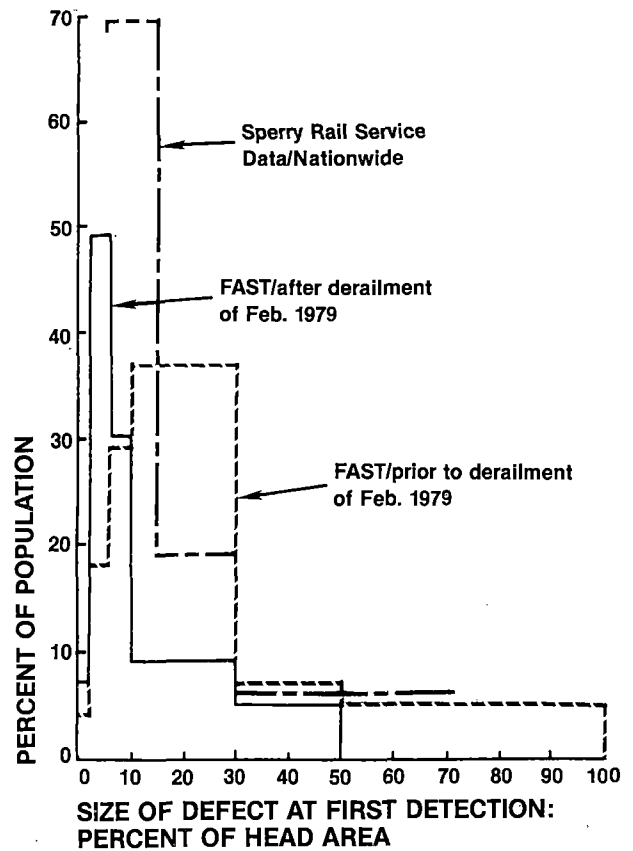


FIGURE 47. TRANSVERSE DEFECT SIZE DISTRIBUTION.

that for the nation as a whole where the estimated peak occurrence was 5-15%. After the derailment, corrections in the inspection procedure and in the system itself caused the peak occurrence to shift to the range of 2 to 5%.

An examination of some of the rail failures that have occurred at FAST will prove informative.

A sideview of a typical HH rail plant weld failure is shown in Figure 48. At first glance, the crack appears to have been a horizontal failure near the mid-web region which turned to run vertically as the crack grew away from the weld. However, upon closer examination, one can see that the horizontal crack actually initiated from a vertical transverse crack which had originated in the head-web fillet region. The appearance of the transverse crack is shown in Figure 49. Each growth ring represents one day of operation (1 MGT) so that the vertical crack would appear to have been growing for well over 20 MGT. The origin of the vertical crack occurred at the edge of the upset region at a location where shear drag was particularly severe as shown in Figure 50. Decarburization also was observed in the vicinity of the origin. As indicated previously, the greatest number of these types of failures occurred in HH weldments even though all other metallurgies except CrMo were welded in the same weld plant in the same time frame.

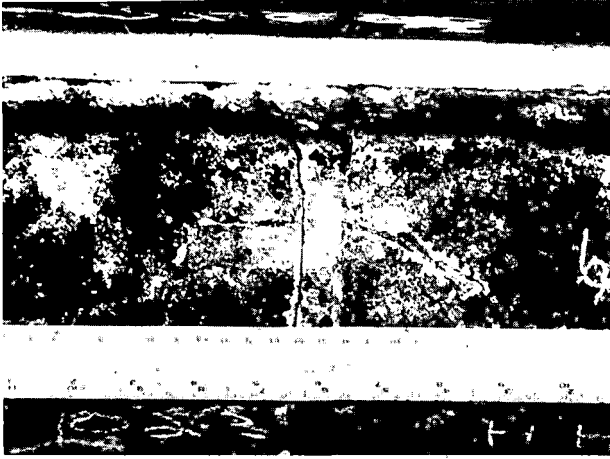


FIGURE 48. TYPICAL RAIL PLANT WELD FAILURE.

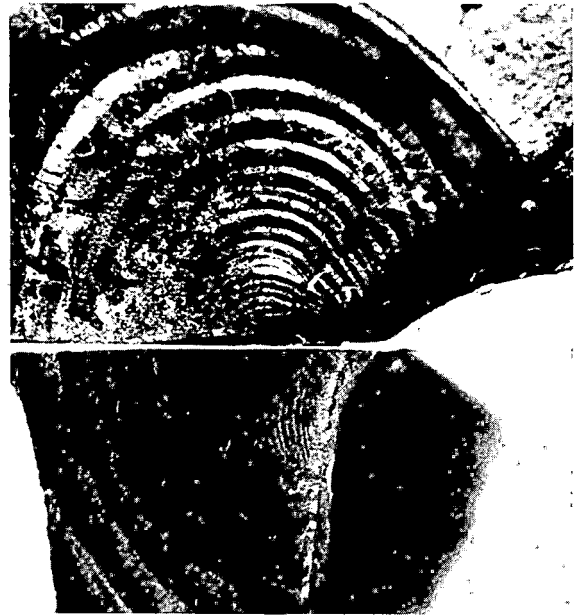


FIGURE 49. PLANT WELD FAILURE TRANSVERSE VIEW.

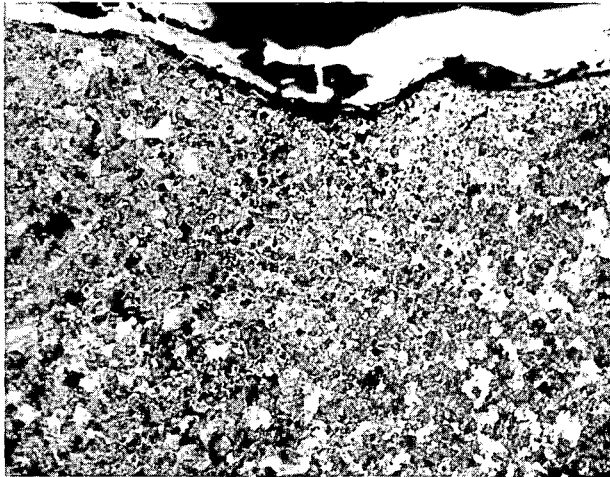


FIGURE 50. ORIGIN OF VERTICAL CRACK.

Figure 51 shows a typical 'long' life failure of a thermite weld. The failure was somewhat unique because a clear cut indication of a fatigue crack can be seen at the edge of the cast region. In addition, a shiny battered region on the opposite side of the weld suggests that the crack traversed this region slowly enough to allow the surfaces to come together and develop the battered pattern. The circular shape of the battered region suggests that the possibility that it may also have been an origin. Many thermite weld failures fall into the 'infant mortality' category. Such a failure is shown in Figure 52. Although the weld was made in accordance with 'proper' procedure, shrinkage cracks developed in the head-web fillet region. Subsequent examination of the cracks revealed finger-like dendrites protruding from what was the liquid-solid interface (Figure 53). The solidification process had been starved of liquid metal. The likely cause was insufficient preheat or insufficient superheat of the liquid metal prior to pouring. Though the procedure may have been 'proper', it clearly was not adequate for the cold, windy day on which the weld was made.



FIGURE 51. THERMITE WELD FAILURE.

Failures of rails or plant welds have been rare in the metallurgy test sections in the approximately 190 MGT accumulated thus far in the third experiment. There have been a few failures though. Figure 54 illustrates the appearance of a transverse failure of a 1 Cr rail. The failure had developed from a longitudinal vertical fatigue crack in the rail base which in turn had initiated from a base

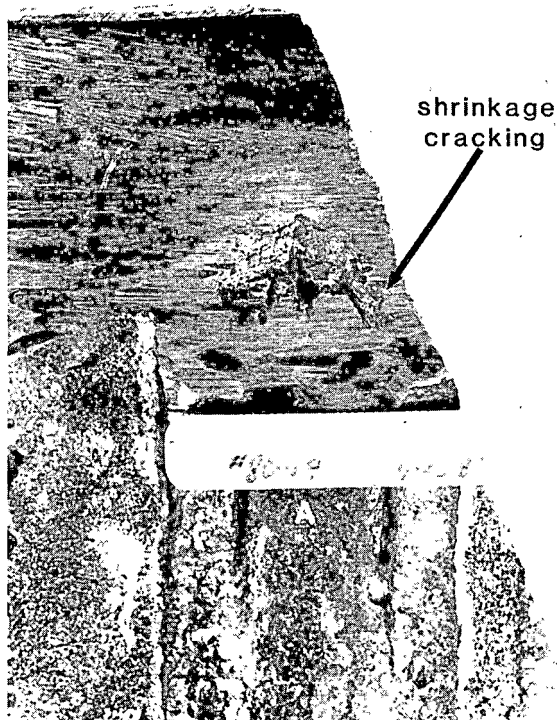


FIGURE 52. WELD FAILURE DUE TO COOLING SHRINKAGE.

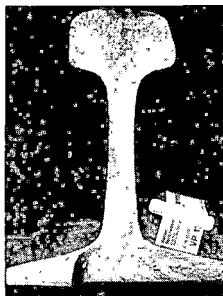
SEM OF DENDRITES
IN WELD METAL 300X

HIGHER MAGNIFICATION
OF DENDRITES 1000X



FIGURE 53. DENDRITE FORMATION IN SHRINKAGE CRACKS.

TRANSVERSE FAILURE IN RAIL
SHOWING POINT OF INITIATION AT
PRE-EXISTING FLANGE CRACK



CRACK IN RAIL FLANGE

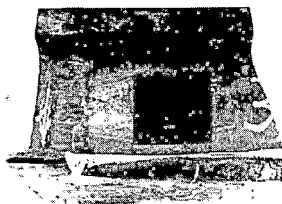


FIGURE 54. TRANSVERSE FAILURE OF ALLOY RAIL.

seam adjacent to a plant weld. The seam itself was approximately 30-40 mm long and 0.7 mm deep (Figure 55). The fact that the rolling practice of this manufacturer at this time left the base slightly concave downward combined with the clamping action of the electrodes at the welding plant is believed to have contributed to initiating a small base crack that subsequently grew under service. Action has been taken by the manufacturer to reduce the number of seams and to prevent concave base occurrence.

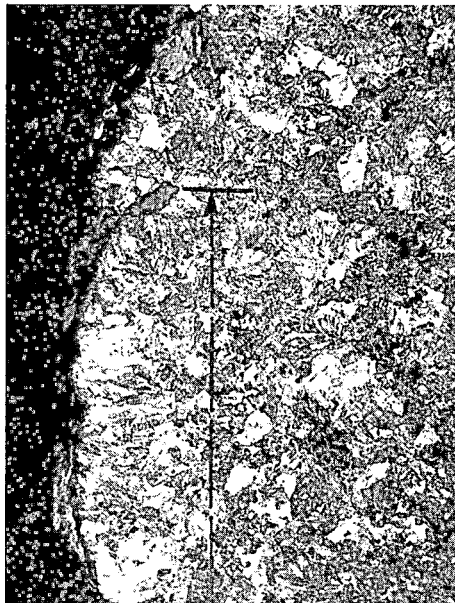


FIGURE 55. MICROGRAPH OF TRANSVERSE SECTION THRU THE LONGITUDINAL CRACK SHOWING THE DEPTH OF THE BASE SEAM.

A base crack and a plant weld failure have occurred in the SiCr(HH) rail. The base crack, shown in Figure 56, originated at the lower edge of the base surface. Metallographic examination revealed that the origin region had been subjected to mechanical action that had produced a 'white' etching layer; in addition, decarburization had occurred in this region; this was not common elsewhere along the rail. These features are shown in Figure 57. Clearly, damage had been done to the rail but gouges or dents from anchors or from an accidental blow of a spike maul were not observed. The weld failure is shown in Figure 58. Unlike other weld failures in HH rail, the crack had no vertical component at the upset region. The origin of this crack was a scratch through a brand mark that was located just on the edge of the upset region. The scratch was probably created upon stripping of the weld. In addition an island of decarburization was found about 0.04" below the surface at the crack origin (Figure 59). It is not clear why the decarburized region occurred below the surface of the rail.

Perhaps the most spectacular rail defect that develops at FAST is the detail fracture-from-shell. The one shown in Figure 60 is one of many that have occurred in the second metallurgy experiment. Each growth ring represents the period in which the train runs in one direction (~1 MGT usually). When the train reverses direction, the crack plane changes orientation slightly. Thus as the crack grows, its plane of growth alternates back and forth, the average growth being roughly perpendicular to the

BASE FAILURE, SiCr (HH) RAIL



CLOSE UP VIEW OF FATIGUE CRACK
SURFACE AT THE END OF BASE

FIGURE 56. OVERALL AND CLOSE-UP VIEWS OF FATIGUE CRACK
SURFACE AT THE END OF BASE.

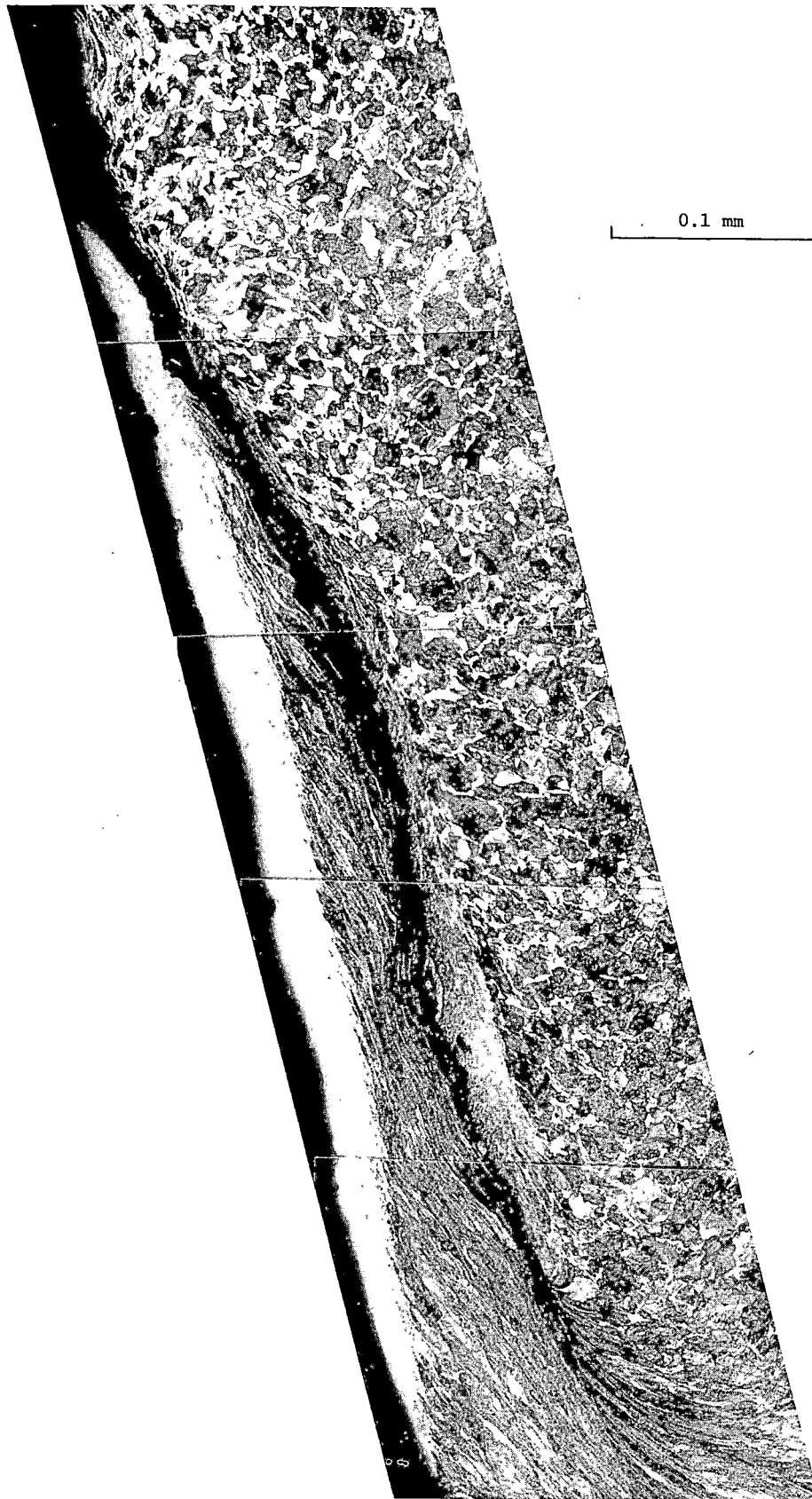
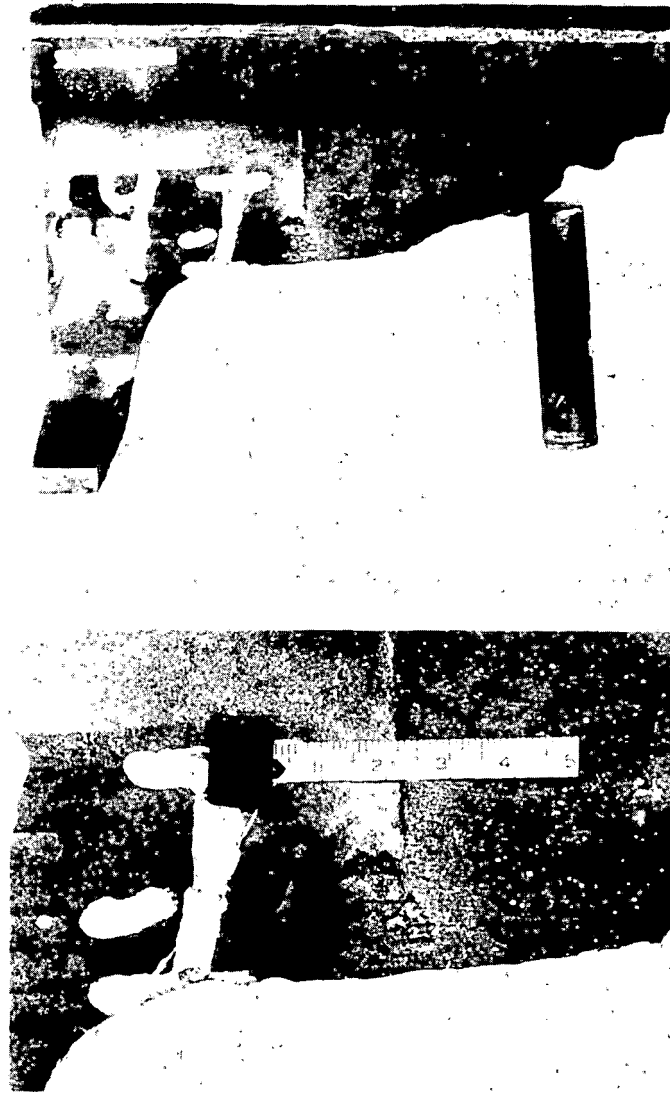


FIGURE 57. MICROGRAPH OF TRANSVERSE SECTION SHOWING
WHITE ETCHING LAYER AND DECARBURIZATION
AT EDGE OF RAIL BASE.

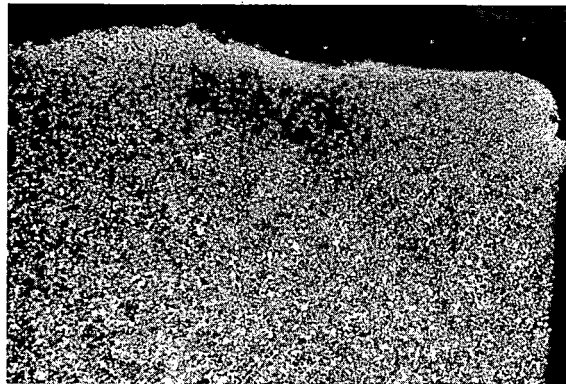
FAILURE AT A PLANT WELD
SiCr (HH) RAIL



CLOSE UP VIEW OF WEB SURFACE
(1 mm/Div)

FIGURE 58. FAILURE AT A PLANT WELD SiCr (HH) RAIL.

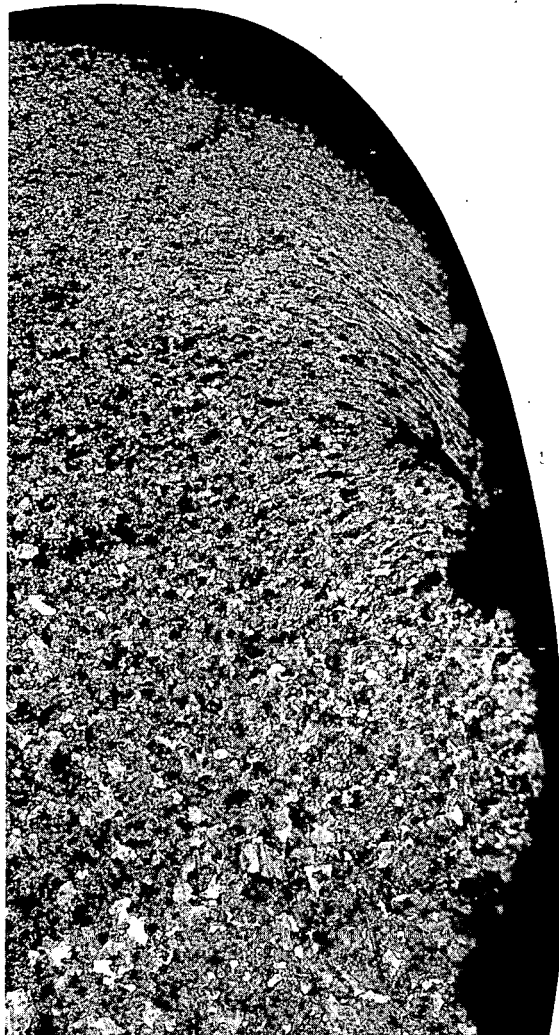
Web surface →



0.5 mm

Fracture
← surface

Web surface →



0.1 mm

Fracture
← surface

FIGURE 59. MICROGRAPH OF LONGITUDINAL TRANSVERSE SECTION THRU THE HORIZONTAL FRACTURE SHOWING A POCKET OF DECARBURIZATION NEAR THE WEB SURFACE.

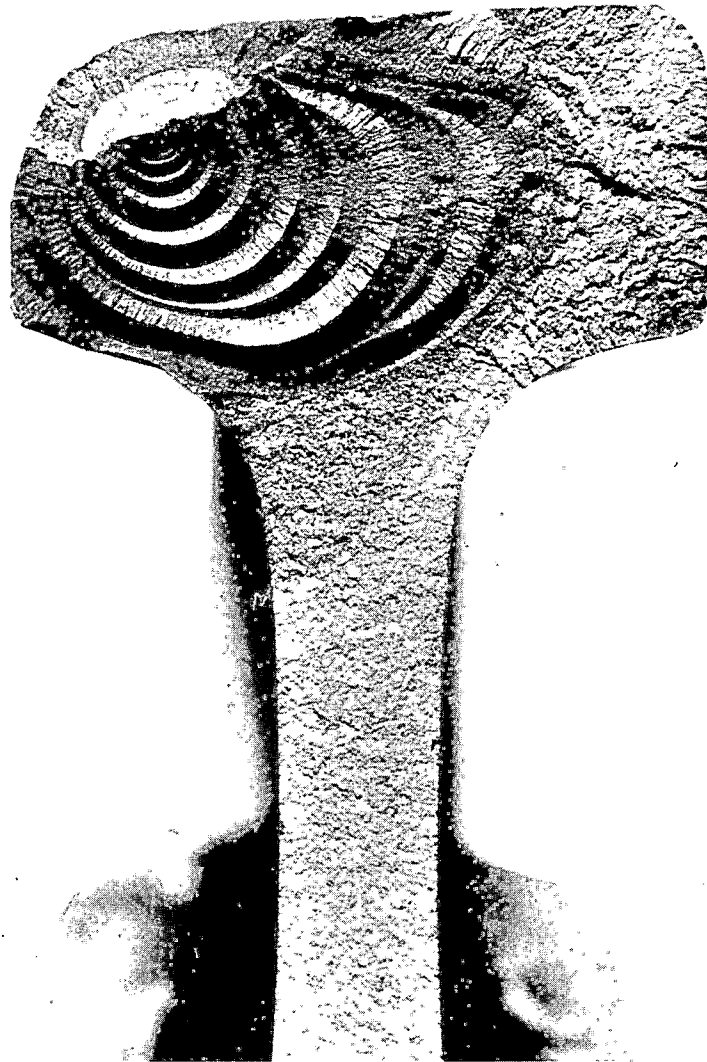


FIGURE 60. DETAIL FRACTURE FROM SHELL.

rail axis. This reversible zig-zag pattern has been very useful for tracking crack growth as will be shown shortly. The pattern also develops on the shell portion of the crack as shown in Figure 61. Here the shell surface has been exposed by sectioning. The origin of the shell is internal beneath the gage corner of the rail. Probably 10 or more MGT had passed before the shell even approached the gage face of the rail. The shell surface gave no indication of grease being present in the crack. Thus, the presence of a fluid (grease) in the shell appears not to be necessary for growth of the crack. After the shell had grown approximately 3/4" from its origin, the detail fracture developed. A vertical longitudinal section taken through the origin of the shell and the origin of the detail fracture is shown in Figure 62. The detail fracture can be seen to be only one of many incipient 'detail fractures' which developed at the valleys of the zig-zag shell surface. There appears to be a critical distance, 1/2" to 1" at FAST (on a curve) for shell growth before bifurcation leads to the dominant detail fracture. The shell proceeded on its zig-zag path

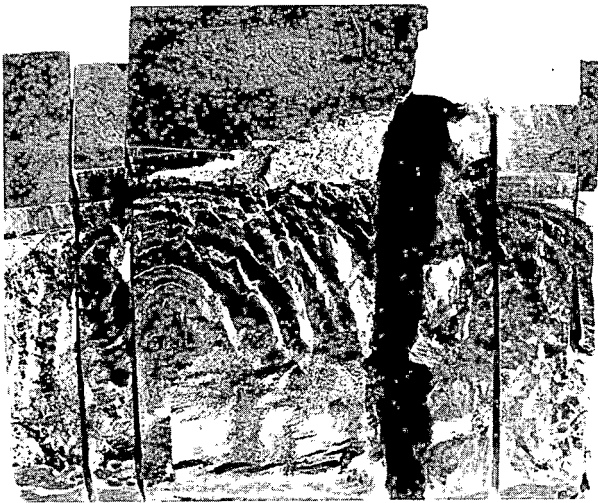


FIGURE 61. VIEW OF SHELL SURFACE.

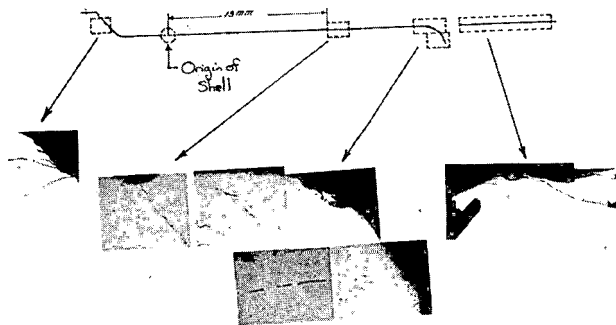


FIGURE 62. RELATIONSHIP OF SHELL ORIGIN TO POSITION OF TD AND DEVELOPMENT OF SECONDARY CRACKS.

even after the detail fracture had started to turn into a vertical plane. No special features such as inclusions seem to be necessary for the detail to develop. However, one would expect inclusions to play a part in the initiation of the shell. Alas, although no inclusions were identified as being associated with shell origin, perhaps they were lost upon sectioning. Microhardness traverses were run across a transverse vertical plane through the rail near the shell (but not actually containing the shell) and a hardness contour map was drawn from the traverses. This is shown in Figure 63. The region in which the shell developed seems to be characterized as an intrusion or lense of somewhat softer metal than much of that around it. This suggests that the shell may form in a region of cyclically softened metal 1/4" to 1/2" below the running surface.

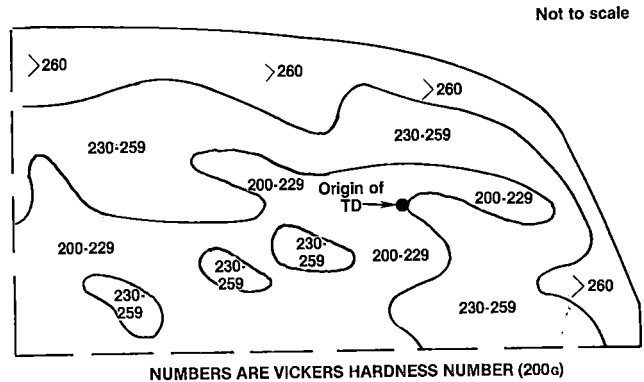


FIGURE 63. HARDNESS MAP OF TD-CONTAINING RAIL.

The zig-zag path of the crack suggests that shear stresses also play a part in the growth of the crack perhaps by causing the residual principle stresses to rotate alternately one way and then the other as the train reverses direction.

The growth rings that are so clearly delineated on the surface of the detail fracture permit some simple calculations to be made which will help define the environment in which the crack grows. There are two dominant stress systems which must govern the growth of the transverse crack--the flexural stress system induced by the passage of the wheel and the steady stress system which is generated by the combined effect of thermal stresses and residual stresses resulting from the cyclic work hardening of the upper part of the head. The rolling action of the wheels may be expected to induce residual compression in the near-surface region but as is the case with shot peening, the region beneath that in residual compression must provide a balance of forces by being in residual tension.

Ignoring the shear stress contribution (since it appears the shear stresses will act only when the crack is under compression and not growing), a rather simple linear elastic fracture mechanics approach can be used to estimate the combinations of flexural and residual stresses which would have caused the observed crack growth. The flexural stresses can be related approximately to an equivalent wheel load (made up of both vertical and lateral components) by beam-on-elastic-foundation methods. Crack growth can be calculated from the integrated form of the Forman expression given below. The general method is described in the reference.¹⁰

$$\Delta K \approx 1.13 \Delta \sigma \sqrt{a}$$

$$da/dN = B \cdot \Delta K^n / [(1-R) K_c - \Delta K]$$

$$[1.13^{2/2}] [B] [\Delta \sigma^n] [\Delta N] =$$

$$[(1-R) K_c / (n-2)] [1/\Delta K^{n-2}]_{\Delta K_c} - [1/(n-3)] [1/\Delta K^{n-3}]_{\Delta K_c}$$

$$\Delta K_{\text{threshold}} = \Delta K_{\text{threshold}}^{R=0} (1-R)^{1/n}$$

The observed growth is shown in Figure 64. The values of B, n, and K_c needed in the Forman expression were derived from specimen crack growth information generated from the failed rail as well as the other sources shown in Figure 65. Because the observed specimen crack growth data of the failed rail was very near the upper bound of the Broek and Feddersen¹² data set, and also near to the behavior observed by Barsom and Imhof,¹³ the following parameter values were selected:

$$B = 3 \times 10^{-9} \text{ in/cycle}$$

$$n = 3.32$$

$$K_c = 50 \text{ ksi} \sqrt{\text{in}}$$

The calculated rail crack growth curves are compared with the observed crack growth of the transverse defect in Figure 66, with the nearest calculated residual stress/wheel load set bracketing the observed curve. For a crack size of 0.4" radius, the combination of wheel load and residual stress needed to make the crack grow in the observed fashion is plotted in Figure 67.

Subsequent to completion of Forman crack growth analysis, Battelle, Columbus Laboratories¹⁴ completed a determination of residual stresses in the failed rail by destructive sectioning methods. The results are given in Figure 68. The residual stress in the region where the crack would have been about 0.4" in radius is near 20 to 30 ksi. Thus, from Figure 67 the equivalent wheel load would be expected to fall between 35 and 45 kips. The actual average vertical wheel load is about 33 kips, suggesting that the effective lateral force augment of the vertical load is between 2 and 12 kips. Typical observed lateral forces in Section 13 (where failure occurred) are near 10 kips. Though the technique does not have great precision in defining the growth environment, it does provide realistic approximate estimates and the success in its use encourages extension to provide some insight into the effects of material and service parameters on rail performance and that, in turn, upon the needs for rail defect inspection.

The key points concerning the FAST rail failure experience to be remembered are:

- o A possible penalty of improved wear life achieved by lubrication is a shift to fatigue as the failure mode.

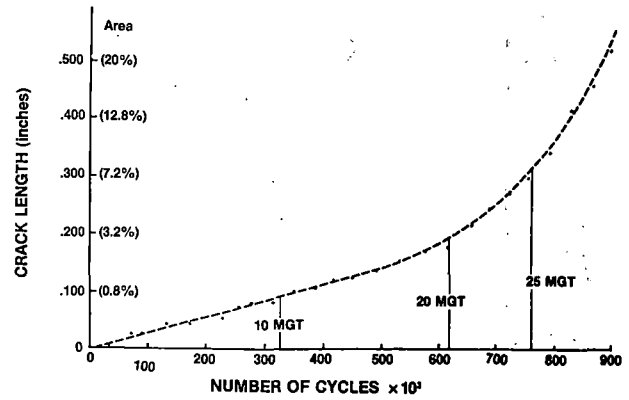


FIGURE 64. OBSERVED CRACK GROWTH.

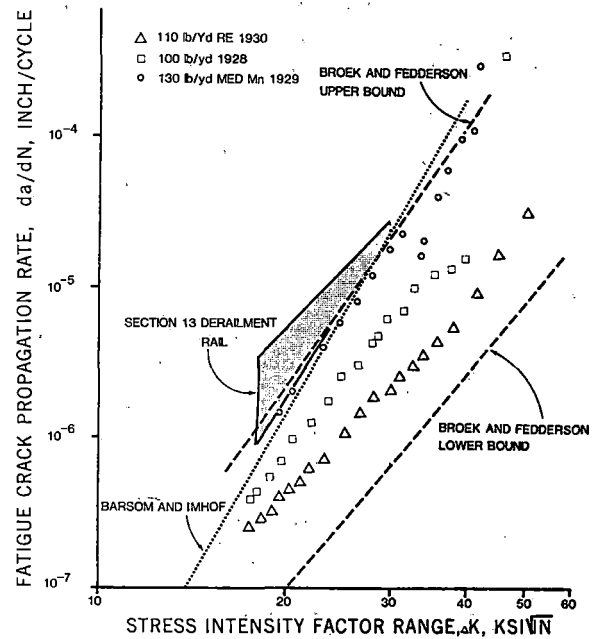


FIGURE 65. VARIABILITY OF FATIGUE CRACK PROPAGATION RATE BEHAVIOR.

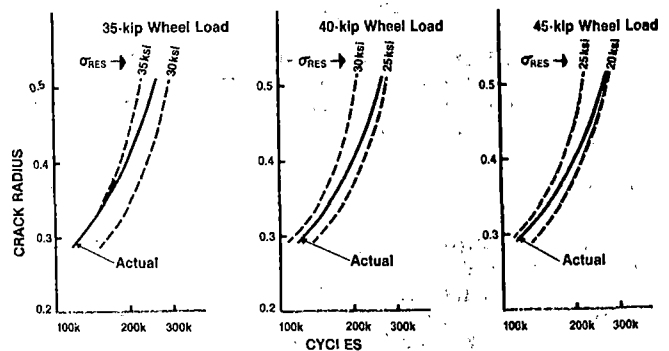


FIGURE 66. COMPARISON OF ACTUAL CRACK GROWTH WITH FAMILIES OF CALCULATED GROWTH CURVES.

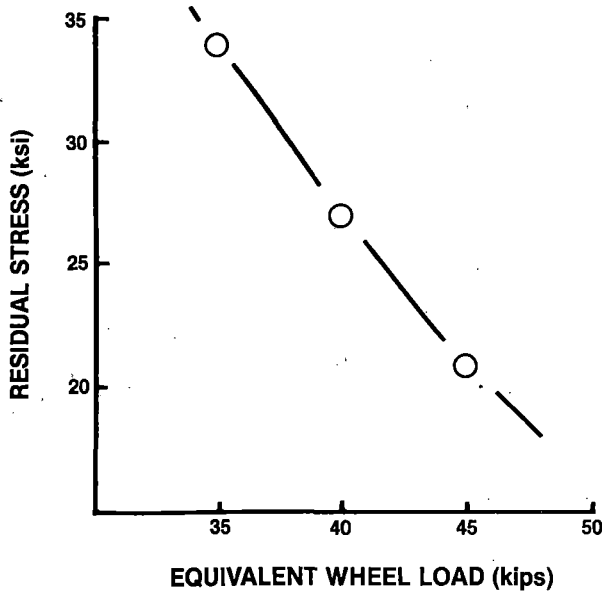


FIGURE 67. WHEEL LOAD/RESIDUAL STRESS COMBINATIONS FOR OBSERVED CRACK GROWTH.

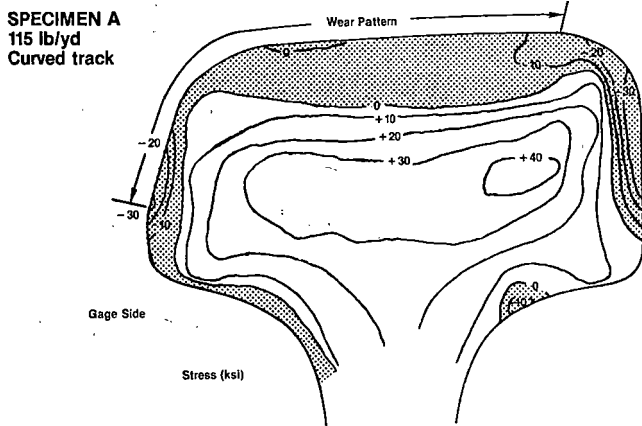


FIGURE 68. AXIAL RESIDUAL STRESS AT 177.7 MGT.

- o From FAST data and from other sources, it would appear that doubling the nominal wheel load reduces the rail life (at a specified percentile) by a factor of two to four.
- o At FAST, the detail fracture is a non-unique bifurcation of the shell crack.
- o Simple linear elastic fracture mechanics predictions of crack growth behavior match observed rail transverse crack behavior reasonably well.

DISCUSSIONS

Much of the information presented in the preceding sections qualifies as "interesting, but...." In the following paragraphs some illustrations will be given to show how this information may be used and how laboratory examinations can help improve our understanding of the processes which are operative.

The metallurgy:lubrication interaction can be understood in terms of variation in surface shear stress with lubrication when adjustments are made for

material characteristics. The importance of surface stress level on the wear progress has been shown by Bolton¹⁵ who observed that in laboratory tests, the logarithm of the wear rate (in the 'mild' wear regime) was a linear function of contact stress. Battelle-Columbus Laboratory studies of Hertzian contact have shown that the amplitude and the location of the maximum octahedral shear stresses change as a function of the friction coefficient at the wheel/rail interface. This variation is illustrated in Figure 69. When the friction coefficient at the surface is zero, the maximum octahedral shear stress is located about 0.1" beneath the surface with an amplitude of 53 ksi for a 19 kip vertical wheel load. However, when the friction coefficient reaches 0.5, the maximum shear stress comes to the surface and increases in magnitude to nearly 80 ksi. In this same range of friction coefficient, the surface shear stresses change from about 25 ksi to nearly 80 ksi. An approximate relationship between the logarithm of shear stress (in ksi), wheel load (kips), and friction coefficient is given in the equation shown below:

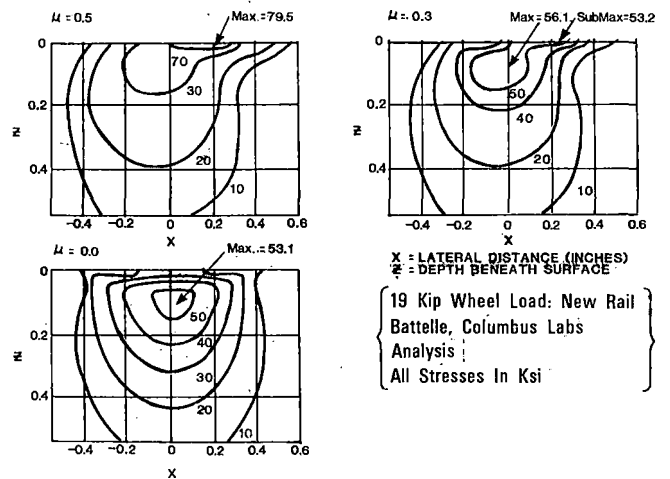


FIGURE 69. SHEAR STRESSES AS A FUNCTION OF FRICTION COEFFICIENTS.

$$\text{SURFACE OCTAHEDRAL SHEAR STRESS} \quad \text{WHEEL LOAD} \quad \text{FRICTION COEFFICIENT}$$

$$\text{Log } T_{\text{OCT}} = \text{Log} \left[10.55 \left[\text{WL} \right]^{0.301} \right] + 0.9976 \left[\mu \right]$$

However, the fact that the metallurgies respond in different degrees to the lubrication level requires that a material sensitive parameter be included in any expression which seeks to relate wear rate to surface stress state. A second equation has been obtained empirically to fit the FAST data when the shear stress is based upon 19 kip wheel load for illustration.

$$\text{WEAR RATE} \quad \text{HARDNESS (A SURROGATE PARAMETER)} \quad \text{COMPOSITE NUMBER FOR A WIDE RANGE OF } \mu$$

$$\text{Log } W = -3.4437 + 27.41 \left[\frac{T_{\text{OCT}}}{H} \right]^{2.5}$$

Brinell hardness has been used as the material sensitive parameter. In reality hardness is a surrogate parameter which we must use because it's the only material parameter which is generally available. However, hardness, as such, is unlikely to have any effect upon the wear process itself. As is shown later, in the dry regime, wear may be more related to a ductility parameter such as the true fracture strain either cyclic or static. In the lubricated regime where little or no asperity contact is likely to occur, the mechanism may be more related to the high cycle endurance strength.¹⁷ In an empirical sense, the difference in the slope of the wear rate vs hardness plots given in Figures 19a and 19b reflects the variation in hardness sensitivity. Thus the exponent 2.5 used is in effect, a weighted composite value for the entire range of friction coefficient from dry to lubricated.

In spite of these approximations, the approach does provide a good prediction of wear rate across a range of lubrication if the dry regime at FAST is assumed to be characterized by a friction coefficient of 0.5 while that of the lubricated regime is taken as 0.1. Figure 70 illustrates that the agreement between the observed and predicted gage face wear rates of the different metallurgies tested in the current experiment was within 0.001"/MGT in the unlubricated regime and 0.0002"/MGT in the lubricated regime. The poorer-than-expected performance of CrMo(A) may be related to its metallurgical structure; it is believed to be at least partially bainitic. Bainitic rail steels have been shown to exhibit much poorer wear resistance than do pearlite rail steels.¹⁸ The behavior of the FHT rail is more difficult to understand. The rail has consistently exhibited poorer gage face wear resistance than its hardness would suggest that it should (even though higher carbon FHT rails were selected intentionally in the current experiment). However, its rapid decrease in wear rate from one lubrication block to the next and the fact that it is processed in the mill by oil quenching followed by tempering admits to the possibility that its surface layers at least may not be entirely pearlitic.

The transition in modes is shown conceptually in Figure 71 as the friction coefficient changes. A variant on the model is a transition to severe wear

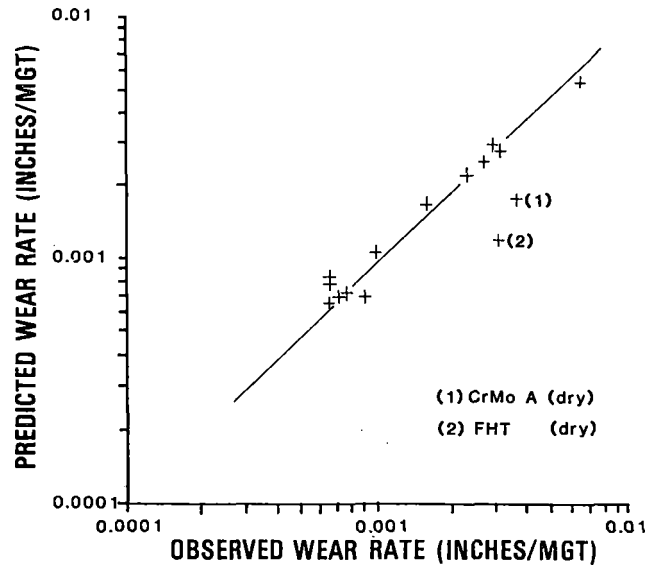


FIGURE 70. PREDICTED VS. OBSERVED GAGE FACE WEAR RATES.

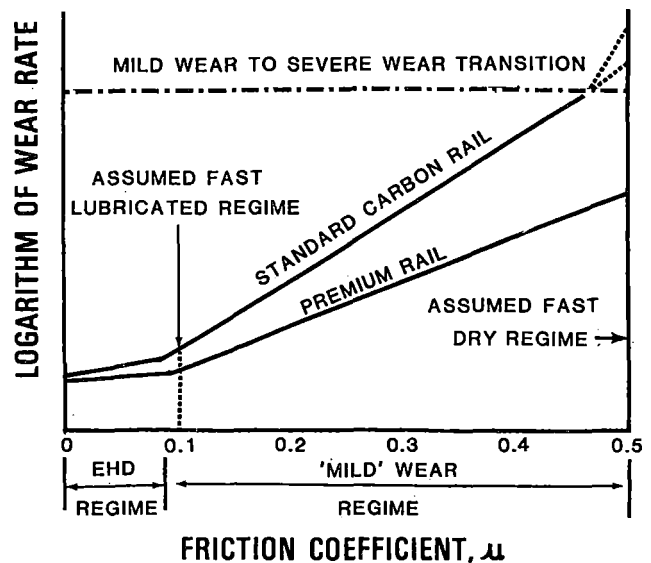


FIGURE 71. CONCEPTUAL VIEW OF CHANGE IN WEAR MECHANISM WITH INCREASING FRICTION COEFFICIENT.

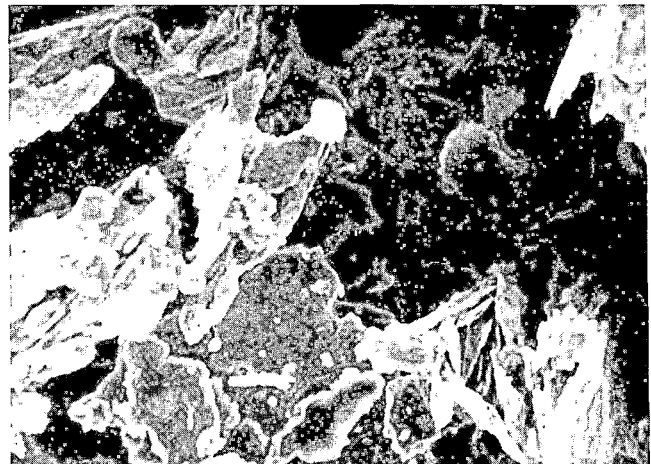
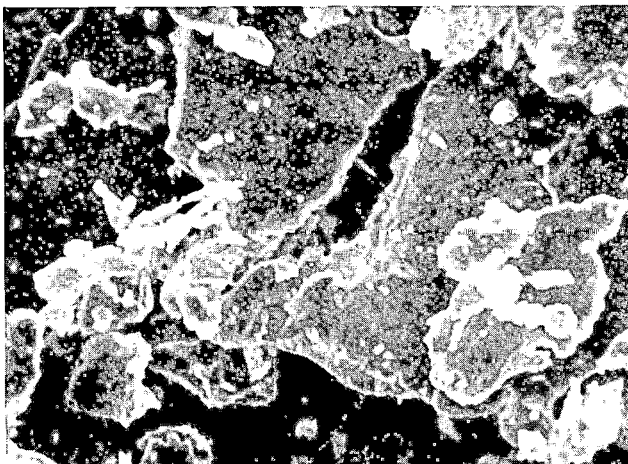


FIGURE 72. WEAR DEBRIS.

for standard rail above a critical wear rate. Wear debris collected at FAST in the previous experiment during a brief dry period was observed¹⁹ to be primarily flakes about 80µm and 140µm long for standard and head hardened rail respectively as shown in Figure 72. Bolton et al, have observed flakes of this size in a mild wear regime suggesting that a wear model based on a mild wear mode may be appropriate to the dry regime of FAST operations.

By combining both wheel and rail wear rate data from FAST in a manner proposed by Rabinowicz²⁰ some predictions can be made about the total rail/wheel system wear. The framework in which this can be done is shown in Figure 73 wherein the logarithm of wear rate is plotted against the logarithm of the ratio of rail to wheel hardness. The underlying presumption is that if the hardness of one component (the wheel) is fixed, the wear rates can be related to the hardness ratios of the two components. In proposing that the diagram shown in Figure 73 can be used to treat total system wear, Rabinowicz noted that there are several assumptions that are appropriate for adhesive wear processes:

- (a) The wear rate of the softer component depends only on the inverse of its hardness (wear rate $\propto 1/\text{Hardness}$).
- (b) The wear rate of the harder component is related to the square of the ratio of lower hardness to greater hardness of the two components of the couple.
- (c) The specific wear rates of the two components of a couple will be equal when hardnesses are equal.

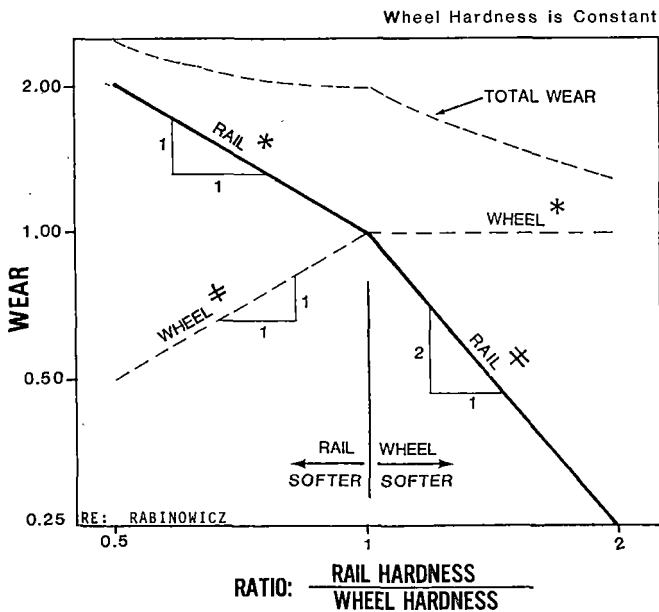


FIGURE 73. COMBINED PRESENTATION OF RAIL/WHEEL WEAR INFORMATION.

Thus, at rail:wheel hardness ratios greater than unity the wheel will be the softer component, and because its hardness is fixed, its wear rate will not change as the rail becomes harder. As the rail

becomes harder, its wear rate will be related to that of the wheel as the inverse of the rail:wheel hardness ratio squared, i.e., $1 \times [2]^{-2} = 1/4$ at a hardness ratio of 2. When the rail:wheel hardness ratio is less than unity, the rail will be the softer component, and because its hardness is changing (decreasing to the left), its wear rate will increase in proportion to the hardness ratio to the -1 power. The wheel which is fixed in hardness will be the harder component to the left of unity hardness ratio, and its wear rate will be governed by assumption (b) such that at a rail:wheel hardness ratio of 0.5 (where the rail wear rate is 2) that of the wheel will be $2 \times [0.5]^2 = 0.5$.

The total system wear is the sum of the wheel and rail wear rates. At a rail:wheel hardness ratio of 0.5, the total wear rate will be 2.5 diminishing nonlinearly to 2.0 at a rail:wheel hardness ratio of unity. At a rail:wheel hardness ratio of 2, the total system wear rate has diminished to only 1.25. Thus, a 4:1 change in hardness of rail relative to that of wheels which, in theory, would reduce the rail wear by a factor of 8, would reduce the total system wear by a factor of only 2.

In order to utilize the FAST rail and wheel wear rate data in the fashion proposed by Rabinowicz, the wear rates of each component must be cast into the same units, and adjustments must be made for the different wear exposures of rails and wheels. To start this process for gage face wear of rail and flange wear of wheels, all of the curves at FAST are converted to equivalent 5° curvature by assuming that:

- (a) rail wear is a linear function of curvature as suggested by Figure 4, and
- (b) that those factors which influence rail gage face wear rate will influence flange wear rate proportionally in the same fashion.

Table XV shows that the total of 9346' at 3°, 4°, and 5° curvature converts to 8246' of equivalent 5° curvature.

TABLE XV. AMOUNT OF EQUIVALENT 5° CURVE.

SECTION	OVERALL LENGTH	EQUIVALENT 5° CURVE
3(5°)	3670'	3670'
7(5°)	1000'	1000'
13(4°)	1250'	1000'
17(5°)	1300'	1300'
17(3°)	2126'	1276'
TOTAL	9346'	8246'

Using the amount of equivalent 5° curvature, the exposure ratio between wheels and rails can be calculated. The approach to do this is summarized as:

- o WHEEL FLANGE EXPOSURE =
8250/9.425 = 875 EXPOSURES/LAP
CIRCUMFERENCE OF 36" DIA. WHEEL
- o BUT EACH WHEEL IS OUTSIDE LEAD WHEEL ONLY
ONCE EVERY FOUR DAYS → 218.8 EXPOSURES/LAP
ON AVERAGE
- o RAIL EXPOSURE = 320 WHEELS/2 = 160
EXPOSURES/LAP
- o EXPOSURE FACTOR = 219/160 = 1.4

A point on the circumference of a 36" diameter wheel flange will strike the gage face of the rail 875 times in traversing the approximately 8250 feet of equivalent 5° curvature. But each wheel is the outside lead wheel only once every fourth day so that on an average, a point on the flange strikes the gage face of the rail only about 219 times per lap of the loop. On the other hand, a point on the gage face of the rail in the curve will be struck by the outside lead wheel 160 times, (one half of the approximately 320 wheels on one side of the train). Thus while a point on the wheel flange will see an average of 219 wear events per lap, a point on the gage face of the rail will see 160 wear events per lap. Therefore, the wheel to rail exposure ratio is about 1.4, i.e., the wheel flange receives about 40% more exposure than does the rail gage face so that 1 MGT is approximately 350 miles of vehicle travel.

Although hardnesses are available for the gage face of each of the different rail metallurgies (see Figure 19a), flange face hardnesses of wheels are not readily obtained with the instrumentation available at FAST. Therefore, to estimate flange face hardness, the microhardness data taken from near the flange surface to a depth of about 5½ mm as shown in Figure 74²⁷ for a FAST U wheel, have been used to determine that the flange metal near the surface is about 20 BHN harder than the base metal. Thus, the estimated flange hardness is taken as the measured rim Brinell hardness plus 20 BHN.

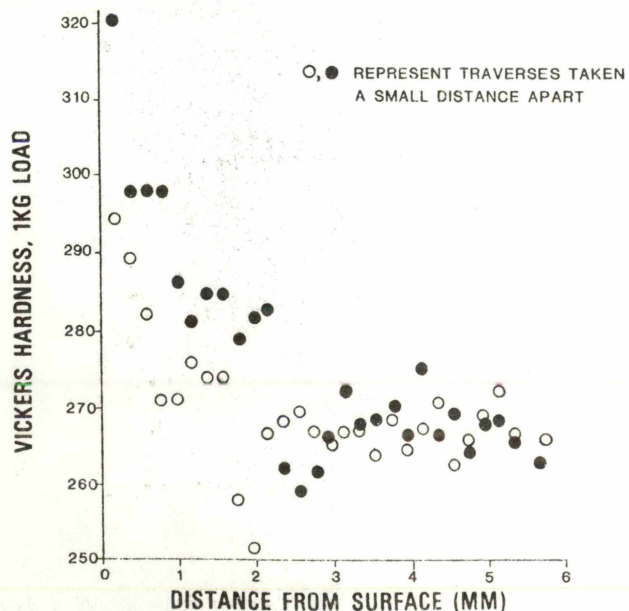


FIGURE 74. HARDNESS PROFILE IN A WHEEL FLANGE.

The dry regime wear rates of rails from both the first and third (current) experiments and wheels (corrected for exposure ratio) from both the Wheels III (VALT) and Wheels IV experiments²² are plotted in Figure 75. The wear rate of rail in the current experiment (1st dry block) appears to be consistently less than that observed in the first experiment although the wear rate dependence on hardness is about the same.

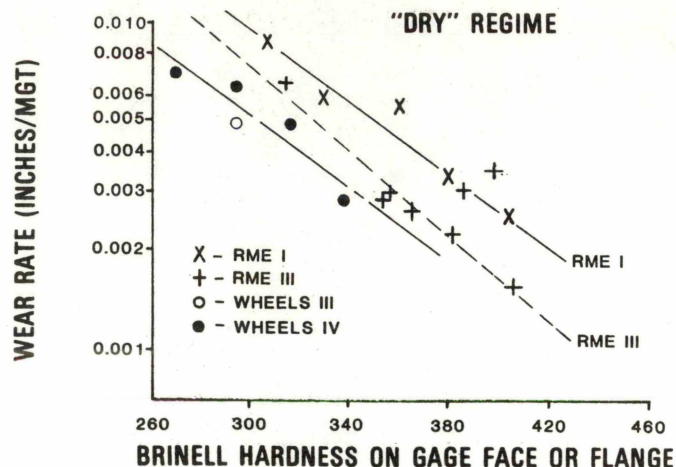


FIGURE 75. WEAR RATES AS A FUNCTION OF HARDNESS.

The rail and wheel (corrected) wear rates are plotted against hardness ratio in Figure 76. The hardness ratios have been calculated as follows for the wheel mix given in Table XVI:

- o Rails: average hardness of a given metallurgy divided by average overall wheel flange hardness
- o Wheels: average overall hardness of the rail curves divided by average hardness of individual wheel types.

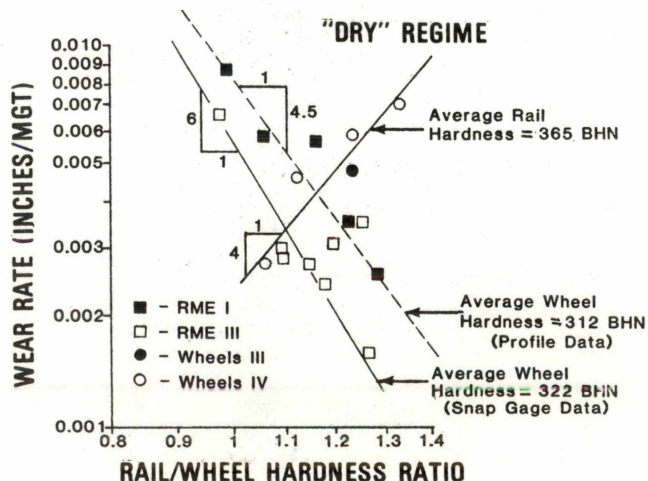


FIGURE 76. WEAR RATES VS. HARDNESS.

The wear rates and hardnesses of rails and wheels are summarized in Tables XVII, XVIII, XIX, and XX. The significant finding is that the slopes of the

TABLE XVI. WHEEL MIX OF TRAIN (RME III/BLOCK I).

DRY REGIME

WHEEL TYPE		
C	B	U
43%	2%	55%

TABLE XVII. RAIL GAGE FACE WEAR RATES.

Metallurgy	Dry	Lub'd	
		Sect 3	Sect 17
Standard (Std)	0.0066	0.0010	--
Fully Heat Treated (FHT)	0.0031	0.0007	--
Heat Hardened (HH)	0.0023	0.00075	0.00028
Silicon Chrome (CrSi(HH))	0.0016	0.00065	0.00030
Chrome Molybdenum (CrMo)	(C)	0.0029	0.00065
	(A)	0.0036	0.00090
Chrome Vanadium (CrV)	0.0027	--	0.00040
1% Chrome (1Cr)	0.0030	0.00065	0.00034

TABLE XVIII. WHEEL FLANGE WEAR RATES (CAST WHEELS/ DRY REGIME ONLY).

Experiment Identification	Flange Wear Rate, Inches/1000 Miles (15.8mm/1000 km)	Normalized Wear Rate, Inches/MGT (28mm/HMPa)	
Wheels III			
U (untreated)	0.014	14000 miles of running (22540 km)	
C (treated)	0.0063*		0.0049
Wheels IV			
Sub U	0.221	7000 miles of running (11270 km)	
U	0.174		0.0070
B	0.135		0.0063
C	0.090		0.0049

*estimated for a C vs U wheel figure of merit of 2.2 based upon a straight line drawn through the Wheels IV data plotted in Figure 4a.

TABLE XIX. RAIL HARDNESS.

Metallurgy	Mean Hardness, BHN	
	Running Surface	Gage Face
Standard (Std)	324	314
Fully Heat Treated (FHT)	366	386
Head Hardened (HH)	355	381
Silicon Chrome (SiCr(HH))	391	405
Chrome Molybdenum, C (CrMoC)	344	353
Chrome Molybdenum, A (CrMoA)	383	398
Chrome Vanadium (CrV)	372	365
1% Chrome (1Cr)	348	353

TABLE XX. WHEEL HARDNESS, SIDE OF RIM (WHEELS IV EXPERIMENT/CAST ONLY).

Class of Wheel	Average Brinell Hardness
Sub U	249
U	273
B	295
C	317

rail lines are near -6 (RME III) and -4.5 (RME I), much steeper than might have been expected for a purely adhesive wear process in the cases where rail is harder than the average wheel hardness. The steep slope of the wheel plot cannot be compared with the horizontal line of Figure 73 because there the wheel hardness was assumed to be constant. Thus, for rails (and wheels also) the steeper slope than that expected for purely adhesive wear suggests that there is some other mechanism of wear that dominates over that of the adhesive component.

By using a somewhat different format, i.e., wear rate ratio* vs hardness ratio, the FAST wheel and rail wear rate data can be compared with that of other investigators. The FAST data for wheels and rails is shown in Figure 77 to be very close to that of Clayton²³ for field observations and Jamison²⁴ for laboratory tests, all three of which have disposition inclined more steeply than that for adhesive wear. Only the information of Marich & Curcio²⁴ approaches a slope of -2. However, before leaving this topic the data of Jamison should be examined more closely. Some specific data has been plotted in Figure 78. It appears that when the relative humidity is low, the slope of the wear rate ratio vs hardness ratio plot becomes quite steep. However, when the relative humidity is high, the disposition of the data is far less steeply inclined. This leads one to wonder if the FAST data would appear differently disposed if it were determined in a more humid area (although the Clayton field data was determined in the UK -- certainly a more humid environment than that of Pueblo, Colorado).

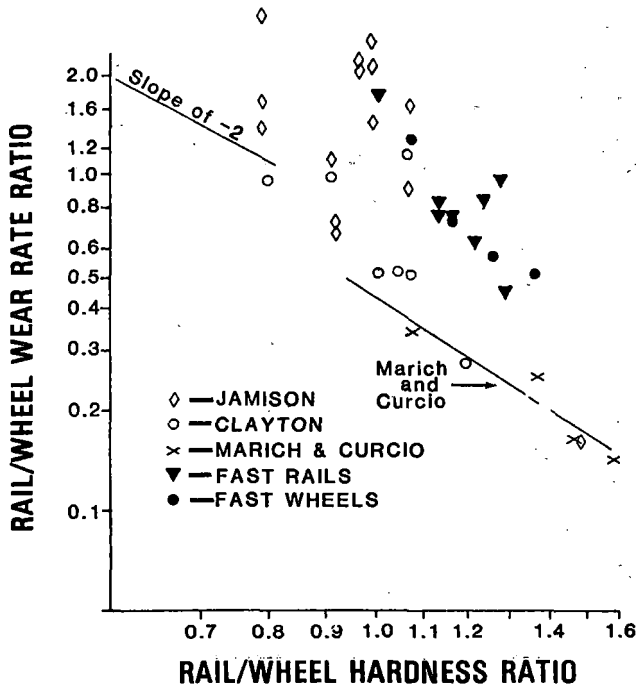


FIGURE 77. RAIL/WHEEL WEAR RATE RATIO AS A FUNCTION OF RAIL/WHEEL HARDNESS RATIO.

*the rail/wheel wear rate ratios have been calculated in the same fashion as the rail/wheel hardness ratios.

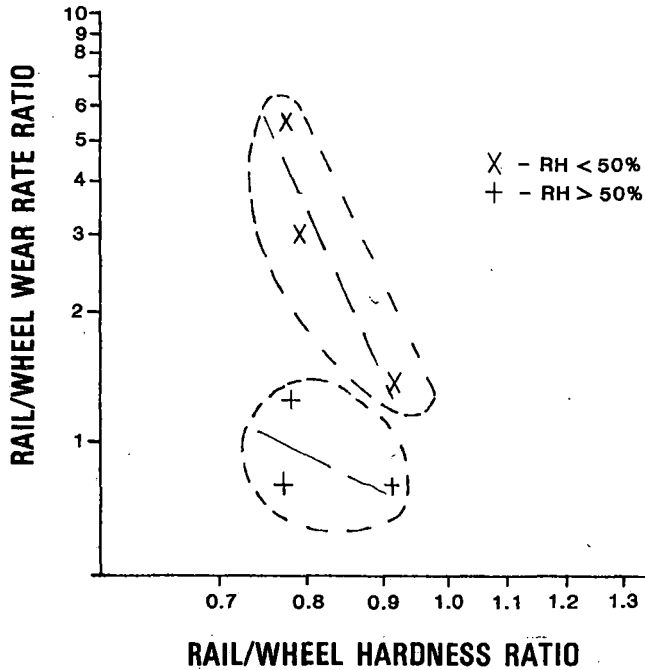


FIGURE 78. JAMISON DATA.

Some additional insight can be gained by plotting the individual wheel and rail specimen wear rates of Marich and Curcio²⁵ and Marich and Mutton²⁶ in the fashion proposed by Rabinowicz. This is done in Figure 79. The wheel data tended to show two different behavior patterns; in one case (upper right) the wheel wear rate decreased as the rail hardness increased while in the other case (lower left) the wheel wear rate increased very slightly as the rail hardness increased over a limited range. Strangely, when 360 BHN rail was substituted for 270 BHN rail the wheel wear rate diminished for a given rail to wheel hardness ratio. The rail behavior in each case (each investigation) behaved somewhat similarly

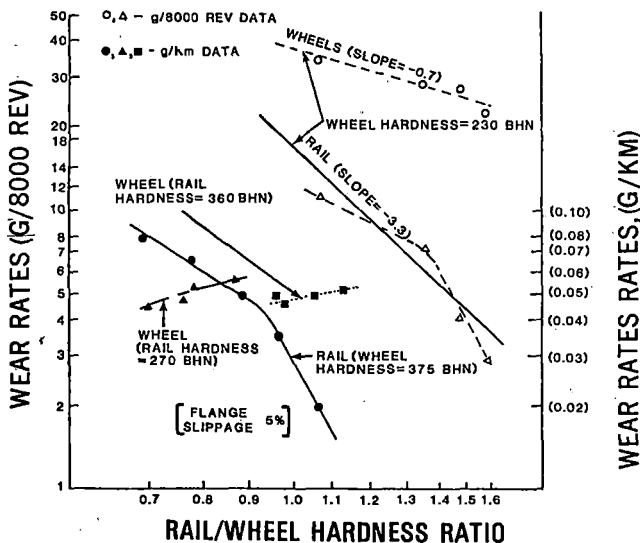


FIGURE 79. LABORATORY RAIL: WHEEL DATA OF 'MARICH AND CURCIO' AND 'MARICH AND MUTTON'.

although the data sets were displaced from each other. In each case there appeared to be a 'knee' in the plot such that at rail to wheel hardness ratios below the 'knee' the slope was much less than it was above the knee--a behavior not unlike that suggested by Rabinowicz.

In Figure 80, the FAST rail data has been plotted to show the effect of varying rail hardness against U wheels of fixed hardness assuming that the assumptions specified previously are appropriate.

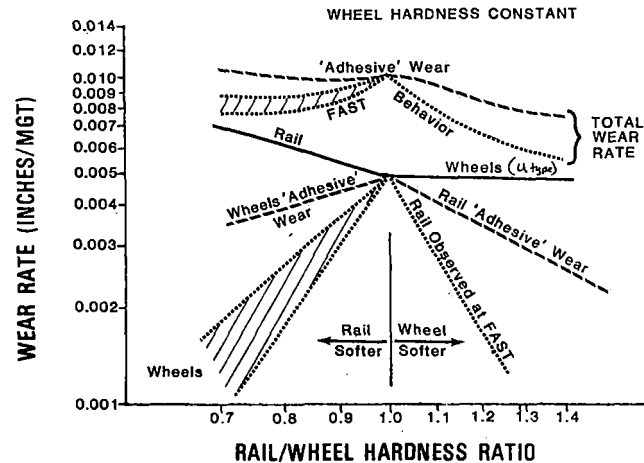


FIGURE 80. CONCEPTUAL ARRANGEMENT OF WEAR RATE FOR ADHESIVE AND FOR FAST DATA.

At fixed wheel hardness and at rail:wheel hardness ratios less than unity the relationship between rail and wheel wear rates would be represented by a rail line sloped upward to the left and a wheel line sloped downward to the left. For 'adhesive' wear the rail slope would be -1 and that for wheels would be +1. However, if the observed (at FAST) slopes for rails and wheels (-6 and +4 respectively) were used, the wheel slope would be between +3 and +5. This presumes that the wear rate of the softer component (the rail) would still be inversely related to the first power of hardness.

The total system wear rate is the sum of the wheel and rail wear rates at each hardness ratio. The wheel and rail lines for adhesive wear are also shown in Figure 80. For essentially adhesive wear, a 2:1 increase in hardness ratio (from 0.7 to 1.4) would be expected to yield only a 27% reduction in total system wear rate. For the actually observed FAST behavior, the maximum system wear rate would be expected to occur at unity hardness ratio with a reduction in system wear rate (~44%) occurring at hardness ratios approaching 1.4.

A somewhat different approach can be used to estimate the effect on rail wear rate of changing the type of wheel. This is shown in Figure 81. The presumption is made that the slope of the rail wear rate vs hardness ratio plot is not influenced by the wheel hardness, and for that matter, that the hardnesses themselves are not functions of the character of the mating materials. For purposes of illustration, the effect on wear rate of head hardened rail of changing from all U wheels to all C wheels is considered for both the 'adhesive' (rail slope of -2) wear and the observed FAST wear (rail slope of -6). If C wheels which wear at about one half the

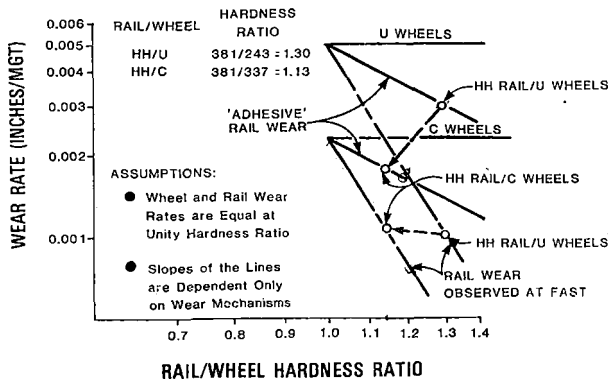


FIGURE 81. ILLUSTRATION OF CHANGES IN WEAR RATES RESULTING FROM CHANGE IN WHEEL TYPE FROM U TO C.

rate of U wheels replaced U wheels in an adhesive wear process, the wear rate of head hardened rail would diminish from about 0.003"/MGT to just under 0.002"/MGT. However, if the process involved were not purely adhesive but were that observed at FAST, the wear rate of head hardened rail would increase very slightly from just below 0.001"/MGT to just over 0.001"/MGT.

Thus, analysis suggests that either improvement or deterioration of wear performance of one component is possible by increasing the hardness of the mating component. Which will occur depends upon the slope of the rail line, (i.e., presumably the slope is a function of the mechanism of wear), the magnitude of the change in hardness and the relative difference in the wear rates of the component (wheels in this illustration) which is changed. The change in hardness and the relative difference wear rate of the component changed are really related to each other. With some simple mathematical manipulation one can show that the point at which a change from one wheel type to another will produce no change in rail wear rate is given by the relationship shown below.

$$\left(\frac{HR_U}{HR_C} \right)^n = FM$$

Rail: Wheel Hardness Ratio

An appropriate question at this point is "What wear mechanism might be associated with the steep rail wear rate vs hardness ratio plots observed at FAST?". Metallographic examination of cross sections taken through the gage faces of high wear rate (low equivalent carbon) and low wear rate (high equivalent carbon) rails (see Figure 82) suggests that the mechanism of wear involves cracking in the shear bands which develop beneath the gage face due to extensive plastic deformation resulting from many wheel passages. The cracks in the shear bands are shown in Figure 83. The depth of the shear band cracking is much greater (0.001" to 0.002") in the case of the high wear rate rail. Subsequent re-

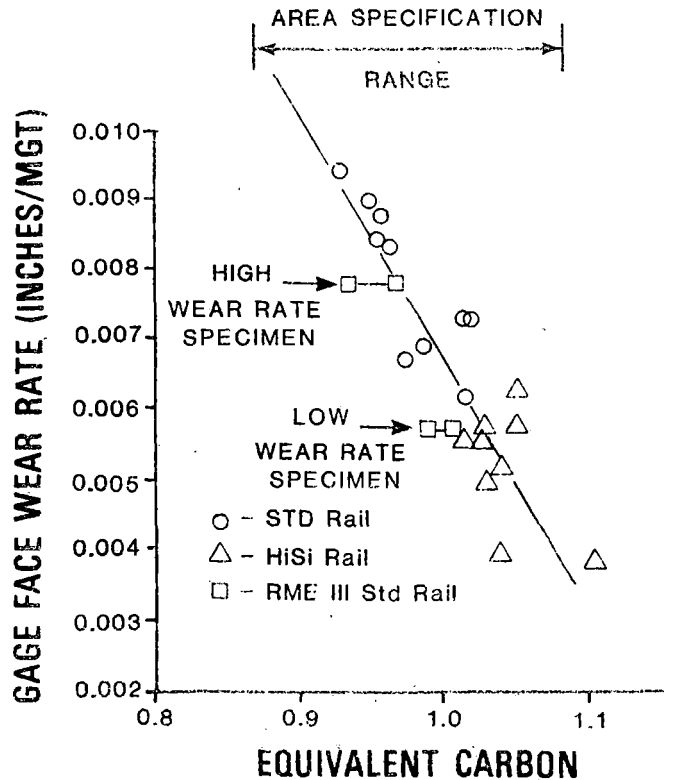


FIGURE 82. EFFECT OF EQUIVALENT CARBON LEVEL ON GAGE FACE WEAR RATE.

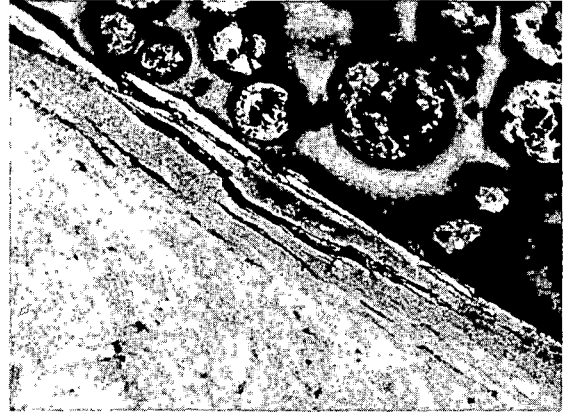
peated polishing and etching examinations have suggested that the cracks initiate beneath the surface and that nonmetallic inclusions may be associated with crack occurrence. Similar behavior has been observed in wheels as shown in Figures 84a, 84b, and 84c. These observations imply that the cleanliness of the steel may influence its wear resistance--a rather unexpected possibility.

Some further insights can be gained by observing the hardness variations beneath the gage face and the flow of metal down the gage face. Figures 85a and 85b illustrate the variations in hardness beneath the gage face surface for both the high wear rate and low wear rate rails. Traverse I (from the running surface just over the gage corner) reveals virtually no difference between rails. However, traverse II (from the gage face just below the gage corner) reveals that the high wear rate was substantially softer at a depth near 1mm, although both rails had about the same surface hardness. In Figure 86, the hardness variation across the region of metal flow at the lower edge of the gage face is shown. Again the high wear rate rail exhibited greater softening beneath the surface. The hardness behavior beneath the surface suggests that metal flow down the gage face may account in part at least for 'loss' of metal from the gage face. The fact that even heavily worked regions may be as soft or softer than the base metal implies that cyclic softening may influence the 'wear' process--at least that part related to metal flow.

Up to this point in the discussion, attention has focused on the use and interpretation of wear information from FAST. Similar exercises may be undertaken with the rail failure information presented previously.

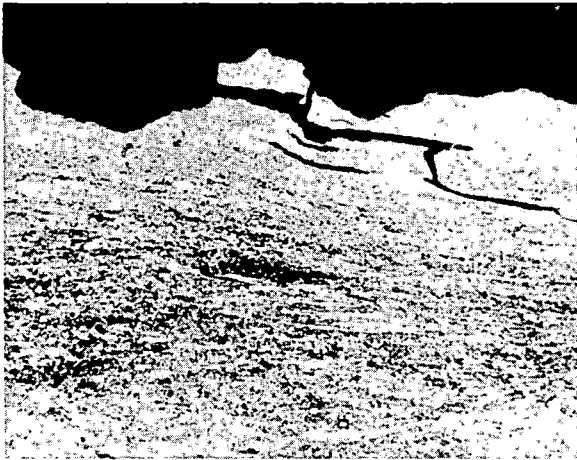


LOW WEAR RATE (200x)

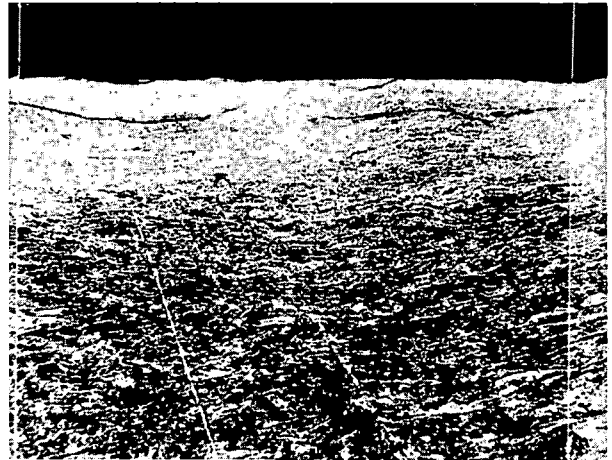


HIGH WEAR RATE (200x)

FIGURE 83. PHOTOMICROGRAPHS OF TRANSVERSE SECTIONS THROUGH GAGE FACE OF HIGH AND LOW WEAR RATE STANDARD CARBON RAILS.



CLASS "U" 800 X
a.



CLASS "C" 400 X
b.



CLASS "C" 400 X
c.

FIGURE 84a, b, & c. PHOTOMICROGRAPHS OF TRANSVERSE SECTIONS THROUGH FLANGE OF U AND C WHEELS.

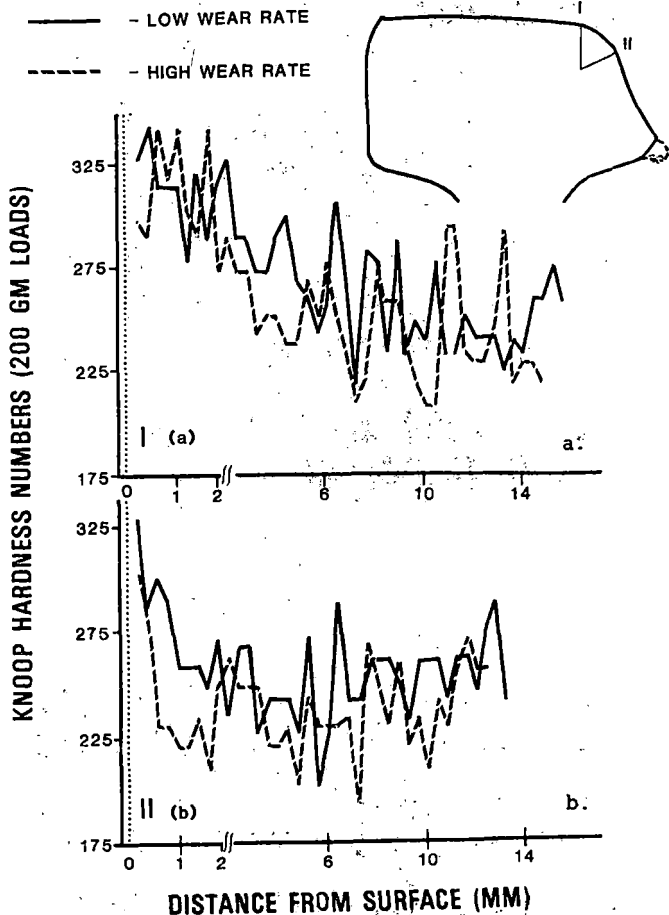


FIGURE 85a & b. HARDNESS VARIATION WITH DEPTH.

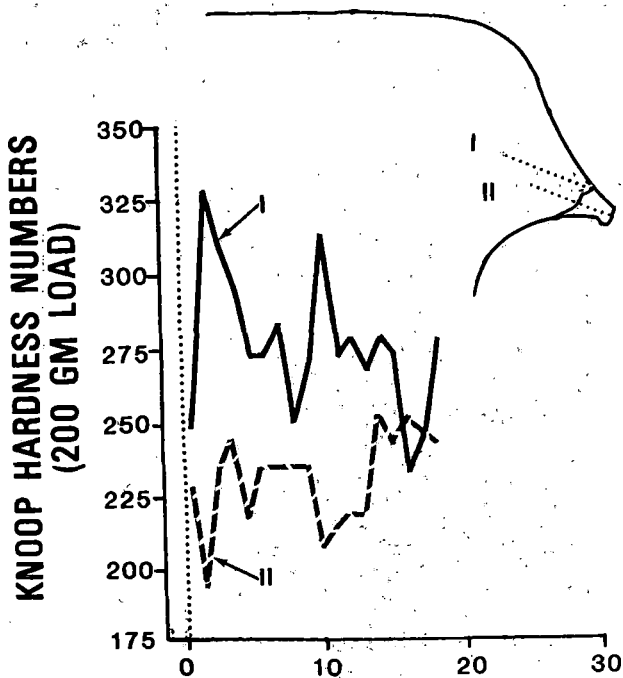


FIGURE 86. HARDNESS VARIATION WITH DEPTH.

The fact that the observed crack growth behavior at FAST seems reasonably in agreement with a prediction made from a rather simple crack growth model indicates that the approach could be applied usefully to more conventional railroad operating conditions to see the influence of a variety of factors upon transverse crack growth and especially upon the capabilities required of rail inspection to assure safety.

Table XXI summarizes a set of base line conditions which would be appropriate for a line in good physical shape carrying a large number of heavy cars (but not entirely loaded unit trains) on a conventional standard carbon rail of recent manufacture having seen enough service to have developed a reasonably high residual tensile stress state within the rail head. Also given in the table is a summary of the formulation and other relationships needed for making the calculations; the method is described in the reference.¹⁰

TABLE XXI. CONDITIONS FOR CALCULATION OF TRANSVERSE CRACK RADII FOR FAILURE IN PERIOD SPECIFIED.

(CENTRAL TRANSVERSE FISSURE/CENTER 0.4" DOWN)

Base Line
 Conditions : RMS Wheel Load = 23.2 kips $K_D = 30 \text{ ksi} \sqrt{\text{in}}$
 $\sigma_{RES} = 30 \text{ ksi}$ $K_F = 50 \text{ ksi} \sqrt{\text{in}}$
 Track Modulus = 1500 psi $B = 3 \times 10^{-6} \text{ in/cycle}$
 Threshold = $\Delta K_{TH}^{R=0} (1-R)$ $n = 3.32$
 $\Delta K_{TH}^{R=0} = 7 \text{ ksi} \sqrt{\text{in}}$

Crack Growth Formulation :

$$\Delta K \approx 1.13 \Delta \sigma \sqrt{a}$$

$\Delta \sigma$ = stress range calculated from beam-on-elastic foundation theory

a = crack radius

$$da/dN = B \cdot \Delta K^n / [(1-R) K_c - \Delta K]$$

$K_c = K_F$ in fatigue situations
 $= K_D$ in impact situations

$$\Delta K_{\text{threshold}} = \Delta K_{\text{threshold}}^{R=0} (1-R)^{\frac{1}{n}}$$

$\frac{1}{n} = 1$ for rail steel
 $R = \sigma_{\text{min}} / \sigma_{\text{max}}$

The results of baseline calculations are given in Table XXII. The defect sizes shown represent the upper limit of inspection sensitivity which would be required to avoid the occurrence of service failures under the baseline conditions at the tonnage rates and in the inspection periods specified. For instance, if a line having the characteristics and traffic specified carried only 1 MGT/yr and inspections were to be made at 2 year intervals, the inspection system would need to be able to find defects no smaller than 21% with 100% reliability to assure freedom from service failures. However, if the line were to carry 50 MGT/yr and inspections were still to be made once every two years. The inspection system would need to be able to find a 0.3% defect with 100% reliability.

Table XXII TONNAGE RATE

Period	1 MGT/yr	10 MGT/yr	20 MGT/yr	50 MGT/yr
1 month	0.68" (29%)	0.63" (25%)	0.59" (22%)	0.50" (16%)
3 months	0.87" (28%)	0.55" (19%)	0.47" (14%)	0.33" (7%)
6 months	0.65" (27%)	0.47" (14%)	0.36" (8%)	0.22" (3%)
1 year	0.62" (24%)	0.38" (8%)	0.25" (4%)	0.13" (1%)
2 years	0.58" (21%)	0.25" (4%)	0.15" (1%)	0.07" (.3%)

10% defect size boundary

Typically, for most inspection systems, the reliability in finding defects drops significantly for defects less than 10% in size. Thus the dotted boundary in the table represents a sort of an upper boundary on inspection interval. For instance, with a 10% sensitivity system and the rail, track, and operation conditions specified, inspections ought to be made, monthly at maximum for 50 MGT/yr, quarterly for 20 MGT/yr line, and twice yearly for a 10 MGT/yr line.

The situation described in the previous paragraph applies to a rail with a relatively high internal residual stress state such as might be achieved after many hundred MGT of service. If for some reason, such as lighter wheel loads, wear, or grinding, a lesser internal residual stress state were achieved, a longer inspection interval would be tolerable. For instance, as shown in Figure 87, at 50 MGT/yr and 20 ksi residual tensile stress, inspections once each year would be adequate; at 15 ksi residual tensile stress, inspections once each year would be adequate. The effect at 1 MGT/yr also is shown in the figure. Although the effect of residual stress on limiting defect size is greatest at 1 MGT, because almost any currently available inspections system would find 10% defects reliably and almost certainly inspections would be made at least once every 2 years, residual stress variations up to and even slightly exceeding 30 ksi would in a practical sense have no effect upon the inspection process.

TRACK STIFFNESS = 1500psi / RAIL TOUGHNESS = 30ksi $\sqrt{\text{in}}$

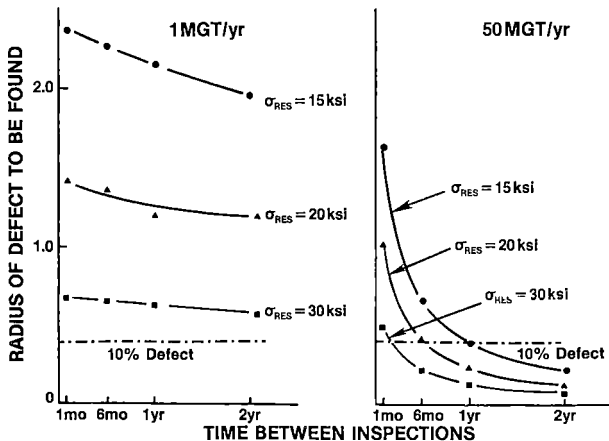


FIGURE 87. EFFECT OF RESIDUAL STRESS LEVEL.

The effects of variations in rail toughness and

track stiffness are shown in Figures 88 and 89. Given that any inspection system generally used would find 10% defects reliably and that inspections would be made at least once every two years, improving the fracture toughness (K_{Ic}) from 30 ksi $\sqrt{\text{in}}$ to 40 ksi $\sqrt{\text{in}}$ would have no real benefit at 1 MGT/yr (unless service conditions changed). However, at 50 MGT/yr improving toughness from 30 ksi $\sqrt{\text{in}}$ to 40 ksi $\sqrt{\text{in}}$ would permit the inspection interval to be lengthened from about 2 months to 3 months. Of course improved toughness is always an advantage because it provides added reserve against rupture particularly under conditions of high impact loading such as flat wheel passages. But the degree to which it provides benefit will depend upon inspection frequency and tonnage rate. The effect of reduced toughness is a bit clearer. For both 1 MGT/yr and 50 MGT/yr, with the 10% defect inspection system, a rail having a toughness of 20 ksi $\sqrt{\text{in}}$ could not be considered safe-by-inspection at any of the periods for which the calculations were made.

RESIDUAL STRESS = 30ksi / TRACK STIFFNESS = 1500psi

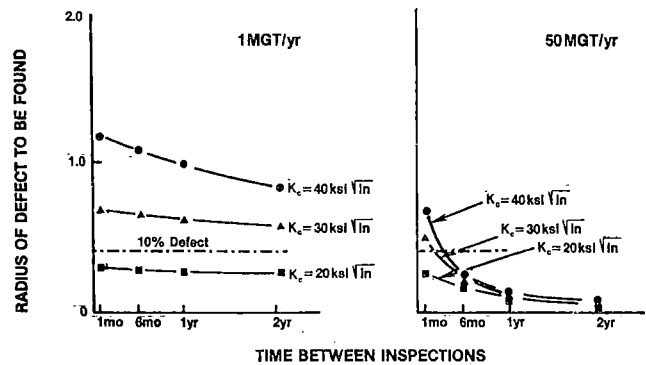


FIGURE 88. EFFECT OF RAIL TOUGHNESS, K_{Ic} .

RESIDUAL STRESS = 30ksi / RAIL TOUGHNESS = 30ksi $\sqrt{\text{in}}$

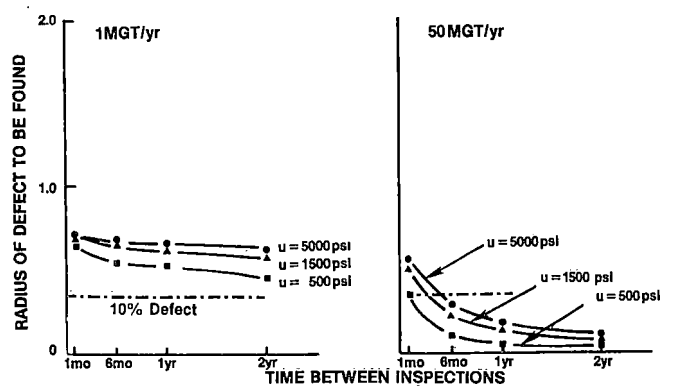


FIGURE 89. EFFECT OF TRACK STIFFNESS, ν .

Increase in track stiffness from 500 psi to 5000 psi would seem to have little real benefit on a 1 MGT/yr line (Figure 89). But at 50 MGT/yr, an increase in track stiffness from 1500 psi to 5000 psi would permit some extension of the inspection interval from approximately 3½ months to 5 months while loss of track stiffness to 500 psi would require shortening of the inspection interval to about one month.

Of course, the numbers discussed here cannot be applied rigorously to actual operation situations

because nobody really knows what the residual stress level is in a given rail at a given time. Nor does one know what the track stiffness or the toughness of the rail really are. The value of this exercise is to alert the reader to the idea that adverse changes that he sees occurring in the track may necessitate increased inspection, the degree of increase depending upon the tonnage carried.

The defect and rail failure information shown in Figure 45 can be utilized in a similar fashion to plan rail inspection on a more rational basis. The FAST data is useful in this respect to help assess the impact of wheel load on defect occurrence. However, to illustrate the utility of this type of data (number of defects as a function of traffic), the mean defect behavior of that found in the AAR/AREA/AISI survey will be employed to study the effects of different types of inspection policy. A central concept of the analysis which follows is that the more rail defects found at a given inspection (at fixed inspection sensitivity and reliability) the greater will be the likelihood that a few of these could have been service failures. This is illustrated conceptually in Figure 90. The rationale for this view is the fact that at FAST many transverse service failures occurred prior to the derailment of February 1979 when the peak defect population occurred in the 10-30% size range, but relatively few transverse type service failures have occurred now that the peak defect population is in the 2-5% size range.

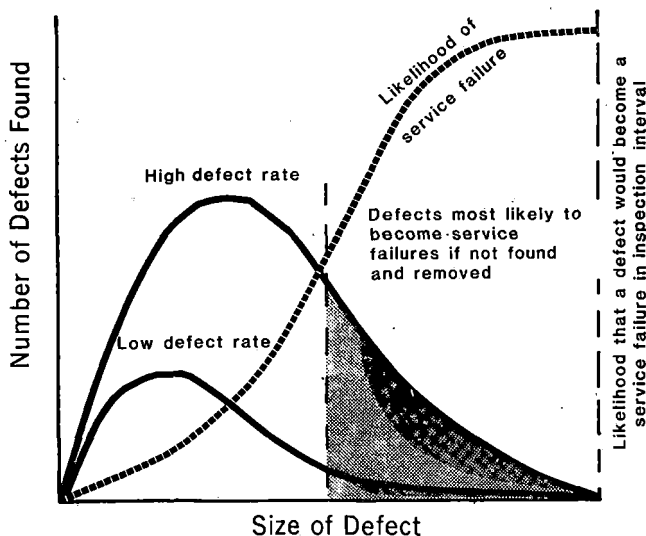


FIGURE 90. SIZE OF DEFECT.

The exercise may be accomplished mathematically starting from the Weibull expression for portion defective, $F(x)$, as a function of tonnage:

$$F(x) = 1 - \exp\left\{-\frac{(x-\gamma)^\beta}{\alpha}\right\}$$

where β , γ , and α are constants which describe the life distribution and x is measured in units of 100 MGT. For the mean survey behavior (and presuming only one defect per rail length), $\gamma = 0$, $\beta = 3.21$ and $\alpha = 16318$. The defect rate, $Z(x)$, the instantaneous slope of the defect vs MGT plot, is given as:

$$Z(x) = \beta(x-\gamma)^{\beta-1} / \alpha$$

For the mean survey behavior, the defect rate curve is shown in Figure 91. There are two obvious main categories of inspection rationale that can be considered:

- (1) Constant inspection rate i.e., fixed intervals of time or tonnage between inspections (basically, the philosophy is that of the current FRA track standards), and
- (2) Variable inspection rate wherein the interval between inspections or the number of inspections per unit of exposure (time or tonnage) is varied in some systematic fashion.

Without becoming burdened with the mathematics of how to do this we may nevertheless benefit from a comparison of the constant rate inspection philosophy with two variable rate inspection philosophies, one adjusting the inspection rate (interval) in proportion to the defect rate and the other adjusting the number of inspections in proportion to the defect rate. To make each approach truly comparable, the variable rate methods have been scoped to find the same total number of defects as does the constant rate approach in 500 MGT of service.

The resulting intervals between inspections for each approach at a tonnage rate of 20 MGT/yr are shown in Figure 92. Note that as the rail sees more service and its defect rate increases (Figure 91), the interval between inspections becomes smaller and smaller while that for the current FRA approach (constant rate inspection) remains fixed. Figures 93 and 94 show that for both of the variable rate philosophies, the number of defects found per unit of track distance per inspection increases and then tends to level off or even drop slightly. The current FRA approach yields a continuing increase in defects found in each inspection as the rail grows older. At fixed inspection sensitivity and reliability, the longer the interval between inspections as the rail accumulates more tonnage, the greater the number of defects present in the inspection interval and the greater the likelihood that some of the population present will either have been service failures before the next inspection or, if not discovered by the next inspection, will be service failures before the following inspection.

A relevant question at this time is whether a variable (increasing) rate inspection philosophy is reasonable in view of the practicalities of rail inspection. Figures 95a through 95d illustrate different approaches currently required (FRA) or proposed (modified FRA and AREA) along with a 'linearized' version of the variable rate approach. When all are superimposed together on one plot (Figure 96) it becomes clear that the variable rate approach (linearized version) is extremely consistent with a combination of both the proposed FRA modification and the AREA recommendation. Common sense has triumphed again.

This type of analysis can be carried one stage further if assumptions are made about the distribution of defects actually generated in the rail and also about the shape of the inspection reliability curve. Figure 97a illustrates what the size distribution of detected defects should look like given

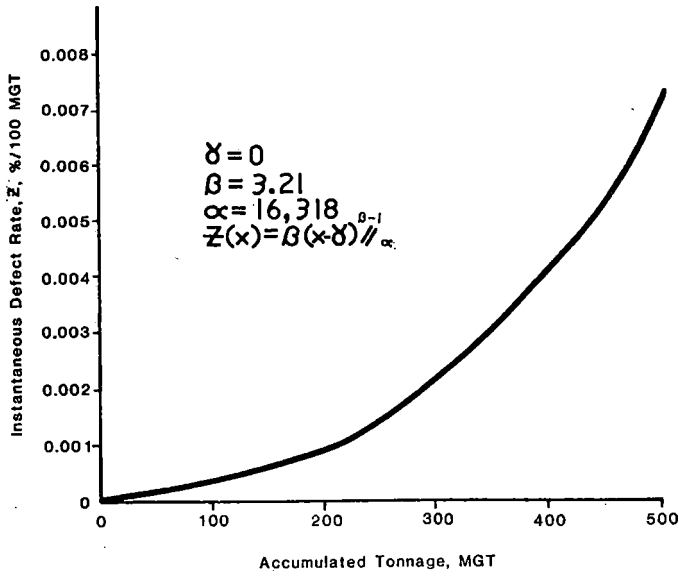


FIGURE 91. INSTANTANEOUS DEFECT RATE AS A FUNCTION OF SERVICE EXPOSURE.

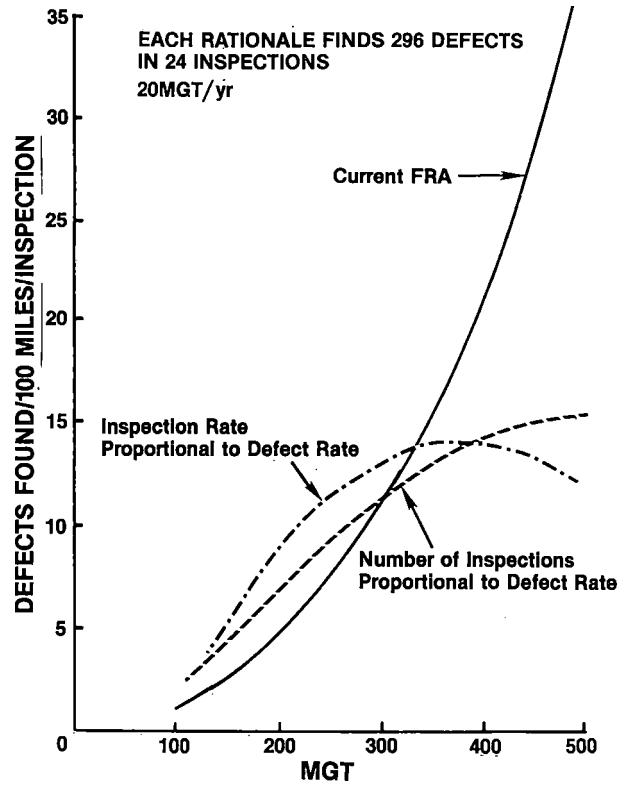


FIGURE 94. DEFECTS FOUND AS A FUNCTION OF TONNAGE.

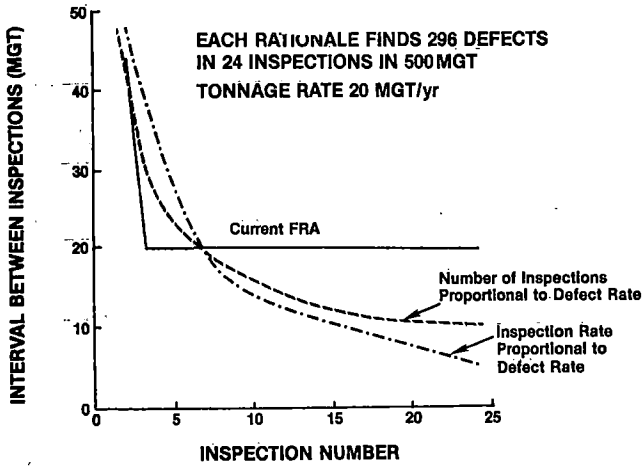


FIGURE 92. VARIATION OF INTERVAL BETWEEN INSPECTIONS.

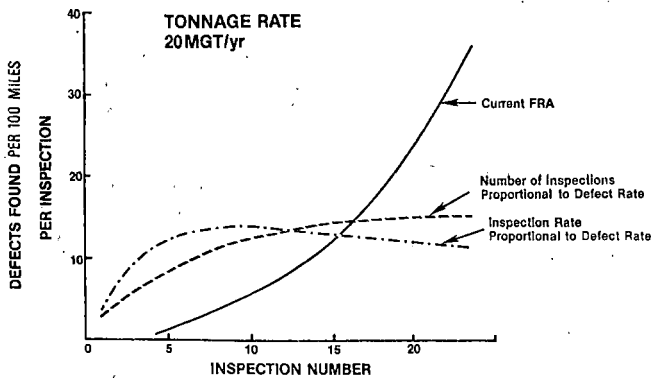


FIGURE 93. DEFECT FOUND AT EACH INSPECTION.

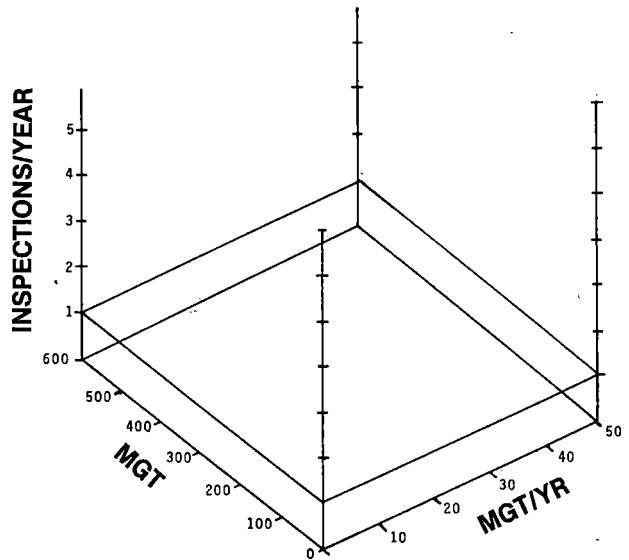


FIGURE 95a. CURRENT FRA INSPECTION REQUIREMENTS.

the assumed total defect size distribution and the assumed inspection reliability function. The detected defect distribution is not unlike those shown in Figure 47. Because no inspection process is absolutely 100% effective there will a high likelihood that some defects will remain undetected as shown in Figure 97b.

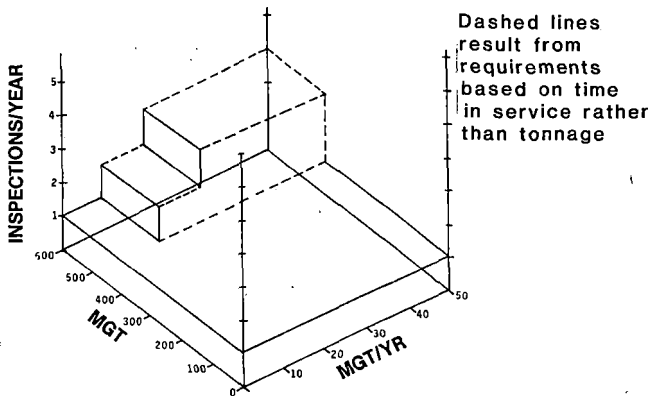


FIGURE 95b. PROPOSED FRA INSPECTION REQUIREMENTS.

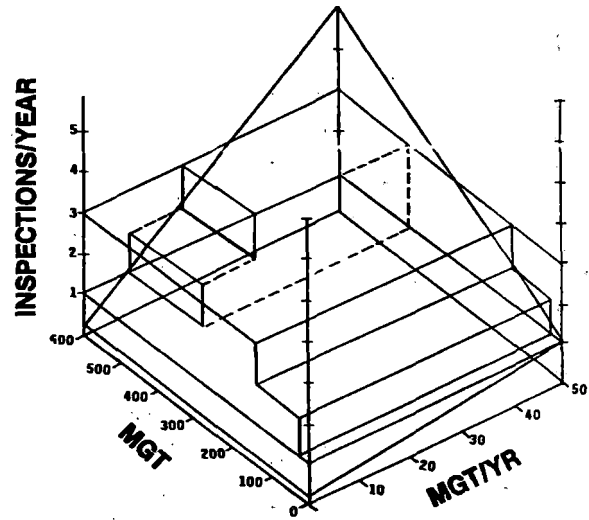


FIGURE 96. COMBINED RECOMMENDATIONS.

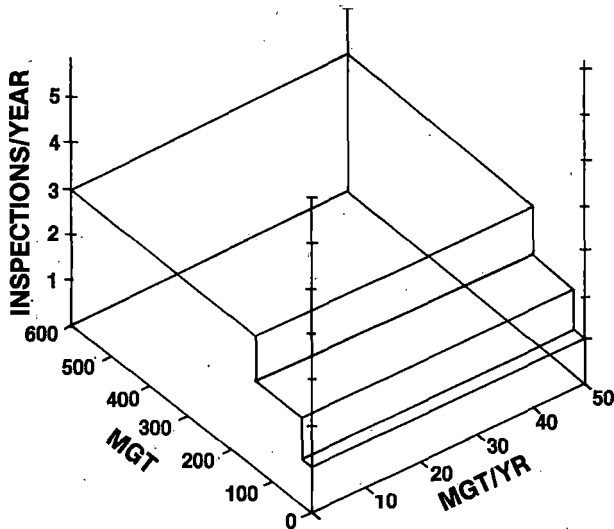


FIGURE 95c. PROPOSED INSPECTION REQUIREMENT BY AREA COMMITTEE 4, SUBCOMMITTEE 9.

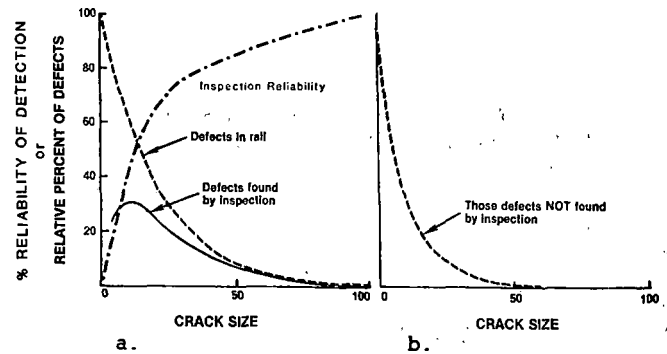


FIGURE 97a & b. ASSUMED DEFECT SIZE DISTRIBUTION.

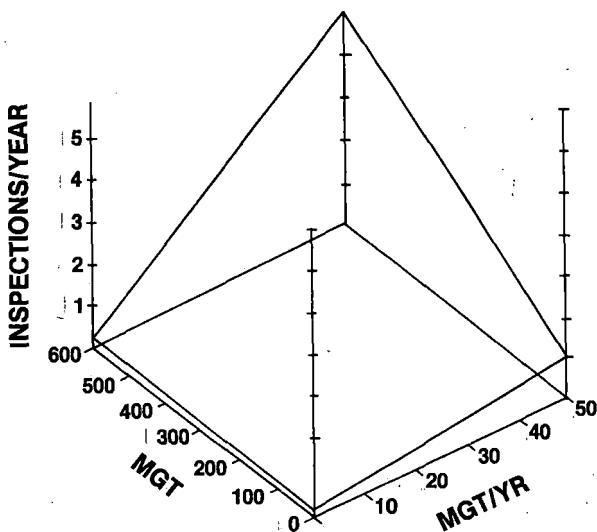


FIGURE 95d. INSPECTIONS PROPORTIONAL TO DEFECT RATE (LINEARIZED VERSION).

Typically transverse defects (detail fracture type) in the size range from 20 to 40% growth can become rapid.²⁷ Thus, some idea of the likelihood of service failure occurrence can be gained by estimating the number of defects likely to reach 30% size or more in less than the inspection interval. This has been done for the current FRA (constant interval) approach (Figure 98a) and a variable rate approach (Figure 98b) wherein both approaches find the same number of defects in 400 MGT and seven inspections. Note that for the variable interval approach the peak occurrence shifts to smaller defect sizes with each subsequent inspection and that the total number of defects found as well as the number greater than 30% in size tends to level off with tonnage. However, the constant interval approach maintains the peak occurrence at about the same size and the total number of defects found as well as the number greater than 30% in size increases non linearly with tonnage.

CONCLUDING REMARKS

The important findings of FAST tests for each topic (wear and metal flow, welded rail end batter, and rail failure) have been summarized at the end of each section and will not be repeated here. What

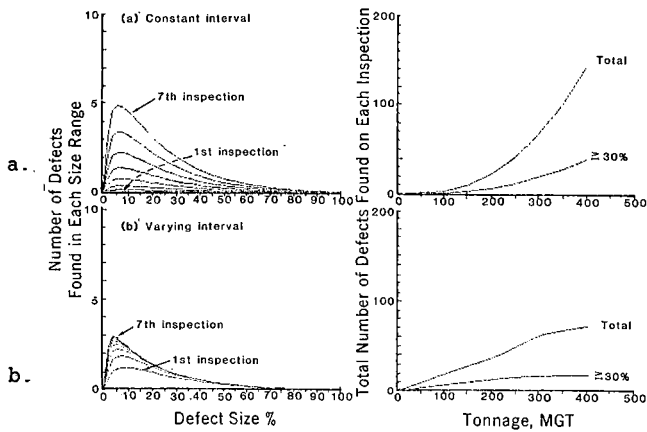


FIGURE 98a & b. DEFECT SIZE DISTRIBUTION AND TOTAL NUMBER OF DEFECTS FOUND.

the 'Discussion' section has sought to show is that there is a great deal that can be done with the information generated at FAST, both in terms of wear and metal flow and also fatigue and failure of rail, and that FAST provides a very suitable test bed upon which to study mechanisms (of wear, for instance) while at the same time generating more practical comparative information which can provide shorter term benefits to the railroad industry. Greater benefit will be derived from the information generated at FAST only if it is related more clearly to real world environments where good measurements and records of service environments are obtained only with much greater difficulty.

Acknowledgements: The information presented here in this chapter on Rail has become available thru the sustained and sometimes painful efforts of a large number of people over the course of several years. We must express our gratitude to the following individuals

- | | |
|---|-------------------------------------|
| Mike Hargrove
Kate Shade | } Association of American Railroads |
| Tim Suazo
Ebby Moin
Glenn Brave
Les Ott
Lahnona Krumanocker | |
| | } Boeing Services International |

and Jesus Prieto, Ferrocarriles Nacionales de Mexico

PHOTO COURTESY OF G. KRAUSS, COLORADO SCHOOL OF MINES. FIGURES 48, 49, & 50.

PHOTO COURTESY OF MANUFACTURER. FIGURES 54, 55, 56, 57, 58, 59, & 84a, b, & c.

REFERENCES

- 1 McEvily, A. J. and Minakawa, K. - "Metallurgical Evaluation of FAST Rail Steels," Final Report, August 1981, U.S. DOT Contract DOT-TSC-1531, University of Connecticut.
- 2 Clayton, P. - "The Relationships Between Wear Behavior and Basic Material Properties for Pearlitic Steels," *Wear of Materials 1979*, American Society of Mechanical Engineers, New York, N.Y., pp 35-44.
- 3 Hay, W. W., Reinschmidt, A. J., Bakas, P. T., and Schuch, P. M. - *Economic Evaluation of Special Metallurgy Rails*, Report No. ENG-76-2002, University of Illinois at Urbana-Champaign, Urbana, IL, January 1976, NITIS #PB 525 024.

- 4 Rougas, M. - 1975 *Technical Proceedings of the 12th Annual Railroad Engineering Conference*, Report No. FRA-OR&D-76-243, October 1975, pp 41-44.
- 5 Stone, D. H. - *Comparison of Rail Behavior with 125-Ton and 100-Ton Cars*, Report No. R-405, Association of American Railroads, Chicago, IL, January 1980.
- 6 Curcio, P., Marich, S., and Nisich, G. - "Performance of High Strength Rails in Track," Paper I.10, *Heavy Haul Railways Conference*, Perth, Western Australia, September 1978.
- 7 Stone, D. H. - *Track Train Dynamics Contributions to Rail Metallurgy*, AREA Bulletin 673, Vol. 80, pp 528-543, June-July 1979.
- 8 Perlman, A. B. and Jeong, D. Y. - "The Effect of Track Load and Structure Characteristics on the Fatigue of Rail," Department of Mechanical Engineering, Tufts University, December 1980.
- 9 Frederick, C. O. and Jones, E. G. - "A Review of Rail Research on British Rail," TRB Meeting, January 1980, Washington, D.C.
- 10 Ichinose, H., Takehara, J., Iwasaki, N., and Ueda, M. - "An Investigation on Contact Fatigue and Wear Resistance Behavior in Rail Steels," Paper I.3, *Heavy Haul Railways Conference*, Perth, Western Australia, September 1978.
- 11 Steele, R. K. - "Fatigue Crack Growth and Fracture Mechanics Considerations for Flaw Inspection of Railroad Rail," *Materials Evaluation*, October 1980, Vol 38, No. 10, pp 33-38.
- 12 Feddersen, C. E. and Broek, D. - "Fatigue Crack Propagation in Rail Steels," *Rail Steels - Developments, Processing, and Use*, STP 644, American Society for Testing and Materials, Philadelphia, PA, 1978, pp 414-429.
- 13 Barsom, J. M. and Imhof, E. J. - "Fatigue and Fracture Behavior of Carbon-Steel Rails," STP 644, American Society for Testing and Materials, Philadelphia, PA, 1978, pp 387-413.
- 14 Groom, J. J. - *Residual Stress Determination*, DOT-TSC-1426, Battelle-Columbus Laboratories, November 26, 1979 (Draft Report).
- 15 Bolton, P. J., Clayton, P., and McEwen, I. J. - "Wear of Rail and Tire Steels Under Rolling/Sliding Condition," ASLE Preprint 80-LC-5B-3.
- 16 Johns, T. G., Davies, K. B., McGuire, P. M., Sampath, S. G., and Rybecki, E. F. - "Engineering Analysis of Stresses in Railroad Rail: Phase I," Battelle-Columbus Lab Report G6266-0101, June 1977, Columbus, Ohio.
- 17 Stone, D. H. and Steele, R. K. - "The Effect of Mechanical Properties Upon the Performance of Railroad Rails," ASTM STP644, 1976, pp 21-48.
- 18 Marich, S. - "Research on Rail Metallurgy," AREA Bulletin, June/July 1977, #633, Vol. 73, page 597.
- 19 "Rail Lubrication Studies at the Facility for Accelerated Service Testing," FAST/TTC/TM-80/08, TTC, US DOT, Pueblo, Colorado.
- 20 Rabinowicz, E. - "Wear Coefficients-Metals," pp 501-502 in *Wear Control Handbook*, ASME 1980.
- 21 Allen, R. - "The Mechanical Aspects of Wheel/Rail Wear," Report No. FRA/TTC-82/01, page 217.
- 22 Marich, S. and Stone, D. H. - "Metallographic Examination of Cracked Wheel Flanges from FAST," paper 5-2, Proceeding of the 6th International Wheelset Congress, Colorado Springs, Colorado, October 1978.
- 23 Clayton, P. - "Lateral Wear of Rails on Curves," *Tribology*, pp 83-90, Illustrated Mechanical Engineer, London, 1978.
- 24 Jamison, W. E. - *Wear of Steel in Combined Rolling and Sliding*, ASLE Report No. 80-LC-5B-1.
- 25 Marich, S. and Curcio, P. - "Development of High-Strength Alloyed Rail Steels Suitable for Heavy Duty Applications," ASTM STP 644, page 188.

²⁶ Marich, S. and Mutton, P. J. - "An Investigation of Severe Wear Under Rolling/Sliding Contact Conditions Existing in Heavy Haul Railways," Seventh International Wheelset Congress, Vienna, October 1981.

²⁷ Rail Defect Manual, Sperry Rail Service, 4th Printing 4/68, page 39.

QUESTIONS AND ANSWERS

Question 1

If hardness and yield strength are not good indicators of gage face wear, what do we strive for to obtain better performance?

Answer

In most cases as-worn surface hardness, and by inference, initial hardness as well, will provide a good correlation with wear resistance. However, some notable exceptions have been pointed out. Likewise, both static and cyclic yield strength seem well related to head height loss rate, but not to gage face wear rate in all cases. Because gage face wear rate (under FAST conditions) appears to involve a shear band cracking process, cyclic ductility (cyclic true fracture strain) may prove to be a better predictor of gage face wear resistance. Work by Paul Clayton at British Rail does suggest that there is a good correlation between wear rate and the total plastic strain at a fixed stress level. Really, though, at this time we don't know enough about the nature of the wear process itself to suggest that any mechanical test parameter will be a truly reliable predictor of wear resistance. However, were I responsible for attempting to find, and control the quality of, a better rail, I'd watch hardness, equivalent carbon level, and microstructure.

Question 2

What, if any, is the effect of lubrication on failures?

Answer

Effective lubrication clearly prolongs the life of rail long enough to allow fatigue to become an important concern. We have not seen any indication that lubricant acts as a hydraulic 'wedge' to propagate a crack. However, the reduction of the friction coefficient at the wheel/rail interface that is achieved by effective lubrication would be expected to move the point at which the maximum shear stresses occur to greater depths beneath the running surface and to reduce the amplitude of these stresses. These changes could well alter the rate and location at which fatigue cracks develop. The FAST results suggest that modest wear may actually serve to prolong rail life by deferring fatigue as a competitive mode of failure.

Question 3

Where are lubricators located?

1. On curve where flange first contacts high rail, or
2. Tangent, if tangent is gage tightened? If so how much?

Answer

In the past, lubricators have been located in tangent track just prior to the entry to the spirals. Most recently lubricators have been located in tangent track, in some cases thousands of feet from the curves which they must lubricate. Track gage has not been tightened in such cases. Perhaps, because FAST is a closed loop and our lubricators in these tangent track installation 'geyser' so much even on the lowest output setting, we are able to get effective lubrication of a high rail (inside loop rail in Section 7) up to two or more miles from the lubricator (in Section 20). FAST does not represent a challenge to achieve a lubricated state but rather to prevent it from overwhelming us.

Question 4

Is there any relationship between change in wear rates vs. work softening and/or work hardening of the rail with traffic?

Is there any evidence of work hardening or work softening behavior at FAST?

Answer

Probably yes. We see that a high wear rate standard carbon rail (low equivalent carbon) does exhibit a layer of what appears to be softened material beneath the surface deformed region and that metal pushed down the gage face is far softer than we'd expect to observe for metal so heavily deformed. Likewise, the region in which a shell has developed in one of our failed rails appears to be softer than much of the metal around it. We suspect that the work softened material may be more prone to fatigue damage. However, the region (0.001-0.002" beneath the gage face) in which wear debris is generated does not seem softer than nearby regions. Thus, at this time we are unable to estimate the effect of work softening on wear itself.

Question 5

Have you (or anyone) looked at these rail samples under transmission electron microscopy? Does this shed any light on the origins of wear in the different rail samples as well as the influence of lubrication?

Answer

No, we have not yet used the transmission electron microscope to examine the character of the metal in the vicinity of the wear inter-

face. To do so would be an extremely useful exercise in that such examination would help define the nature of the deformation processes occurring in the region of debris generation. Thus we could anticipate more accurately what characteristics should be sought for an improved rail--even an improved standard carbon rail. Use of preferred orientation determination techniques (X-ray diffraction) also would provide valuable insights into the processes which occur at the rail/wheel interface.

Question 6

Is the rate of metal flow on rail uniform through age? If not, how does it vary?

Answer

Apparently not! Although data from the first rail metallurgy experiment does show a steady rise and then a levelling off of low rail lateral flow to the field side (in the lubricated regime), information from the third experiment (not available at the time of the Conference presentation) suggests that lateral flow on both field and gage side of the low rail occurs at an increasing rate after each lubrication interval.

Question 7

Have you analyzed the economic cost of different rails based on your data (not including transportation)?

What is the difference between type B, C, & U wheels you showed on graph in Phase III?

Answer

No, but Mike Hargrove at AAR in Washington has been using the FAST rail wear data to calibrate a rail life model prepared by the Canadian Institute of Guided Ground Transport. This model would then be exercised to provide economic cost analysis. Although we've not performed an economic analysis, an improved standard carbon which might have 50% better wear resistance at less than 10% additional cost would appear to be highly attractive and, based upon the FAST rail wear results, would appear to be easily within reach.

With regard to wheel designations, U and C class wheels have the same carbon content, but the C wheel is rim hardened (somewhat akin to head hardened rail). A B class wheel is rim hardened but has a lower carbon content than the C wheel.

Question 8

You infer that there is a substantial improvement in wear due to lubrication, but you did not mention any specific comparison in quantitative terms. What would be the FM (figure of merit) comparing dry standard rail vs lubricated standard rail, dry CrMo, lubed CrMo, dry HH and lubed HH, etc?

Answer

The generous lubrication which we've encountered at FAST improves the wear resistance of standard rail by about a factor of 8 to 10. However, the wear resistance of the better premium rails will improve by a factor of 4 to 5 only. Thus, the figure of merit of premium rails relative to standard rail diminishes significantly as the level of lubrication improves as with SiCr(HH) where the figure of merit exceeds 4 when dry, but is less than 2 when well lubricated. Similar changes occur for the other premium metallurgies.

Question 9

Is gage face wear, head loss, and total wear rate measurement compared to initial no service conditions of each rail metallurgy or compared to a nominal rail section? If the latter comparison, how are the wear rates of different rail sections reconciled?

Answer

The FAST wear measurements have been made by comparing the profiles after service exposure at each measurement site to the initial actual profiles at that site.

Question 10

Is there any information available why a bainitic structure does not fit into the hardness wear characteristic? Why is a bainitic microstructure wearing different than a pearlitic one of approximately the same hardness--test heats with 4.3% Cr, ~400 HBN, structure fully bainitic, done in Germany about six years ago, showed higher wear rate than 1% Cr pearlitic rail steel with ~320 HBN?

Answer

We don't know enough about the mechanism of wear and the relationship of wear to mechanical behavior to explain why bainite and martensite exhibit poorer wear resistance than pearlite of the same hardness. However, it is interesting to note that both bainite and martensite are the products of shear transformations while the pearlite transformation is a two phase nucleation and growth process. As a consequence of the shear transformation, the morphology of the iron carbides in bainite and martensite (tempered) is very different from that of pearlite. Although we can say these differences exist, alas it is not clear why they should imbue bainite and martensite with inferior wear characteristics.

Question 11

You mentioned in your talk that two (or more) types of head hardened rail has been tested and that the second type tested seems to wear somewhat more rapidly than the first.

Do you think this is due to something the manufacturer is doing in the heat treating process, or is it due to chemistry? Is it statistically significant? Are you allowed to name names if it is? Does it have anything to do with rail cleanliness?

This question is asked because we are buying two different types of HH rail at the moment (Nippon and NKK). About 15 years ago we bought some Curvemaster and it failed, mainly with the shell.

Answer

Both conventional standard carbon head hardened and silicon chrome head hardened rail have been tested thoroughly. The silicon chrome rail is an alloy specially designed to benefit from slack quenching (as in the flash butt welding operation). The gage face wear resistance of the silicon chrome head hardened rail is about one-third better than that of conventional head hardened rail when running dry. However, its head height loss resistance (running dry) may not be so good as that of conventional head hardened rail. Both rails are approximately comparable when running in the lubricated state. The difference in chemistry probably is chiefly responsible for the difference in gage face wear resistance.

We try to avoid naming manufacturers. But we do see differences in behavior for rails of nominally the same chemistry which are likely due to differences in processing from one manufacturer to another.

With regard to cleanliness, yes, much to our surprise we think there may be a relationship between gage face wear (not just fatigue failure, i.e., shelling) and the inclusion content of the steel. But this is not yet well established.

Question 12

Does rail design, specifically the slope of gage face side, affect gage face wear? (Slopes of 140 RE and 136 RE rails are different.)

Also, has corrective head grinding affected gage face wear?

Answer

Wear at FAST is rapid enough in the dry regime so that all rails will quickly adopt the same profile after a short period of service. Thus, the original slope of the side of the rail is quickly lost and is replaced by a slope characteristic of the average wheel tread/throat/flange configuration. However, the rate at which this new contour progresses down the side of the rail head may indeed be a function of the head design (as well as of metallurgy). We really don't know. However, once the new contour has extended to the 5/8" gage point, the wear measurements now are all taken at the same representative geometry and the wear rate is governed by the inherent wear resistance of the metallurgy.

We have been able to detect experimentally any effect of corrective head grinding upon gage face wear but this lack of relationship may be attributed to the fact that the experiment has not been designed to study the effect of grinding on gage face wear.

Question 13

You will be interested in the grain refinement being found in hot rolled (not controlled rolled) steel if V&N are present. This observation needs more investigation to be sure. Do you have nitrogen contents of the V rails?

Answer

No, unfortunately, we don't know the nitrogen content of the vanadium containing rails. It would be appropriate for us to find out. We're not sure what structural features other than pearlite interlamellar spacing need be controlled to assure good wear resistance. The relationship between vanadium and nitrogen levels and microstructural refinement is intriguing and this relationship may offer some aid in understanding why chrome vanadium compositions have not done better than we have observed.

Question 14

Has the mechanism of rail wear been investigated from the standpoint of nucleus of origin, i.e., what effects have metallurgical grain size and steel cleanliness been upon wear initiation and progression? If not, is there any plan to investigate these factors?

Answer

We believe the gage face wear process itself is a shear band failure process which may well depend on steel cleanliness. Of course the formation of shells (and TD's) by a fatigue process has long been felt to be related to steel cleanliness. The question at hand is "how much cleanliness is worth paying for?". We have just started to attempt to develop the correlations which might answer that question.

Question 15

Were climatic changes or differences correlated with wear rates, i.e., seasons of high or low humidity which varied from block to block or snow quantities or temperatures?

Answer

We have not been able to detect any relationship between wear rate and the season of the year and the temperature or humidity. Admittedly, we've not gone at this in a rigorous fashion. Though we've not seen a clear correlation (would that we could use this explanation to rationalize our block to block variations), we have an open mind on the subject.

Question 16

Would the introduction of anomalies in the wheel bearing area cause greater metal flow or a more rapid loss of head height?

If so, would there be a difference in rate between dry and lube?

Answer

I interpret this question to mean "will features such as welded rail end batter, engine burns, and corrugations act to accelerate the wear process?". In theory, the higher dynamic forces occurring under such conditions might be expected to accelerate wear. Our measurement techniques have not been sensitive enough yet to shed light on this question.

Question 17

How can my railroad measure the amount of (or effectiveness of) lubricant film on gage face at a specific distance from a lubricator?

Answer

There appears to be no simple, reliable method of measuring the amount of lubricant film in the field. The best approach is to determine the wear rate (preferably with an instrument having a 0.001" measuring sensitivity) in both the dry and lubricated states at the same place in track. If the lubricated wear rate is one-fifth to one-tenth that of the dry state, you are obtaining effective lubrication.

Question 18

Why didn't you use equivalent carbon content of wheels and rail vs. wear rate instead of wheel and rail hardness vs. wear rate as a predictor of overall wear?

Answer

If wear rate were only a function of equivalent carbon, conceivably this would be possible. But heat treatment also influences wear rate at a given equivalent carbon level. Therefore, some parameter such as hardness is used which is responsive both to chemistry and heat treatment. From a practical point of view, hardness is a good parameter because it can be measured so easily.

Question 19

In the derailment of the FAST train traced to detail fracture, why was it not possible to detect the initiation of the fracture or the fracture itself during growth with the detector cars which, it is assumed, are used to greater extent at FAST?

Answer

There were three TD's within one 20' piece of rail. On one inspection, the detection system

picked up two of the three defects but the operator noted neither of the two which appeared on the strip chart record. A few days later on the next inspection, the vehicle had reversed direction and only one of the defects was detected. The defect was detected again on the next inspection (vehicle travelling in the same direction as on the day that the strip chart record indicated two defects); the second defect was not observed. The one which was observed was indicated as a 8% TD--smaller than the size requiring joint bar installation.

This unfortunate series of events resulted from two major causes which have been corrected subsequently. The first of these was that the strip chart record was not examined at the end of the day's run to determine whether defects were found but not entered on the log. The second was the fact that the twelve 70° transducers (six in each rail wheel) were not all functioning at equal sensitivity and that no periodic test of sensitivity of each transducer was required. The fact that three 70° transducers within a group are wired in parallel means that the loss of sensitivity of one or two of these cannot be detected without using a procedure designed to check each transducer individually. Rail inspection at FAST is made every 2-3 MGT which is an appropriate interval. But, inspection at any interval will be ineffective if all parts of the inspection system are not known to be functioning properly.

Question 20

Has there been any consideration of steel metallurgy (for rails) as related to failure rate and impact properties?

Might not the variable hardness zones found in (some) rail fractures be associated with steel solidification dendritic patterns (i.e., higher % C segregation at dendritics)?

Answer

Fracture toughness (both static and dynamic) which can be a function of the type of metallurgy can, as shown in the text, have a large effect on the performance of the rail and upon the inspection sensitivity and intervals required. However, FAST has not been able to provide an effective assessment of how different metallurgies behave because so few premium rails have failed due to fatigue of the rail (as opposed to the weld) itself. Although FAST wheel loads are high, there are virtually no flat wheels which could provide the impact loading needed to increase the rail failure rate. Basically, FAST has not been designed as a fatigue test.

With regard to the second question, the 'softened' zone is only about 3/8" below the running/gage surface and is not found on the field side of the rail. It's hard to imagine that the effects of dendritic segregation would occur only at this depth on the gage side of the rail head while they have been destroyed (by prior hot rolling) on the field side of the head.

Question 21

Has any study been made on flat wheel effect on rail failure or growth of defect?

Answer

FAST has not assessed the effects of flat wheels because philosophically it has focused primarily on wear. From time-to-time proposals have been made to include an assessment of flat wheels not only on rail behavior (primarily rail and weld failure) but also on concrete tie structural behavior and upon track geometry deterioration. Many years ago an AAR study provided some information on the magnitude of loads that flat wheels could induce. More recently British Rail studies have sought to simulate the effects of flat wheels by grinding 'dips' in rail itself. There seems to be no work that actually ties the impact forces generated by flat wheels to flaw growth.

Question 22

Based on population of detail fractures and failed shop welds in certain premium rails, would you change your FM figures given yesterday based on wear?

Answer

The figure of merit, as we have used it, does not consider rail or weld failure behavior. As such, the figure of merit is just one of several factors which must be considered in making a judgement about which rail metallurgy to select for a particular service application. Some factors such as inherent wear resistance, corrugation tendency, and fatigue susceptibility of the rail itself cannot be altered readily once a metallurgy is selected. However, welded rail end batter and susceptibility to weld failure, in many cases, can be modified by changing the welding practice.

Question 23

It would seem, at least superficially, that the mechanism providing rail end batter is somewhat similar to that providing rail corrugation. Would the author care to comment on this? Does it perhaps indicate common dynamic mode(s) of similar frequency(s)?

Answer

Perhaps corrugation and welded rail end batter behaviors are the railroad engineering counterparts of the old question "which came first--the chicken or the egg?". The configuration of the batter may indeed depend on the nature of the dynamic forces acting upon the weldment just as the dynamic forces are themselves likely to be a function of the batter configuration. Part of the experiment, which has not yet been implemented, is a determination of the loads which result from vehicles passing over welds with different degrees of batter.

Question 24

Isn't rail end batter influenced by speed? If so, isn't FAST very limited in batter analysis as it applies to the real world? (Real world defined as Western railroads and their high speed, high efficiency operation.)

Answer

Speed will very likely influence the forces which will develop as a wheel traverses a weld. The rate at which batter develops probably is dependent upon the magnitude of these forces. In this respect, FAST is indeed very limited in scope. However, it seems unlikely that differences in speed, or in other operating parameters for that matter, will cause single dippers to become double dippers and vice versa. Nor does it seem likely that a CrMo weldment performing poorly relative to a CrSi (HH) weldment at FAST would be found to be the better weld if the train speed were very different. Perhaps similarly the strong effect of lubrication seen at FAST would occur in the real world as well. Indeed the FAST experiment is severely limited, not so much because a wide range of speeds are not utilized, but because a wider variety of welding machines and practices have not been encompassed. Insofar as is known to the writer, the welded rail end batter study at FAST, for all its limitation, is the only source of quantitative information available anywhere:

RAIL CORRUGATION INVESTIGATIONS AT FAST: DECEMBER, 1979 THROUGH AUGUST, 1981

Timothy J. Devine
Experiment Manager, Rail Corrugation
Griffin Wheel Co.

Lawrence E. Daniels
Experiment Monitor, Rail Corrugations
Boeing Services International, Inc.

Nancy Blume
Engineer
Boeing Services International, Inc.

In investigating corrugations the concept of a systems approach must be utilized. It isn't merely a rail problem, although that is obviously where the physical effect is evident, but rather a result of wheel/rail interactions caused by track and mechanical vibrations and highly influenced by environmental factors. Because of the complexity of this vibrating system it isn't possible to define one sole mechanism responsible for corrugation formation. We can, therefore, only attempt to identify possible contributing mechanisms. The thrust of this paper will be to report on FAST's experience in monitoring and metallurgically analyzing corrugations. This experience, combined with other static and dynamic test results, will be compared to contributing mechanisms and track features such as geometry and rail metallurgy.



FIGURE 1. LOW RAIL CORRUGATIONS AT SECTION 3, 5°
CURVE, 73 MGT.

CORRUGATIONS AT FAST

Figure 1 shows corrugations as they have appeared at FAST. Throughout the FAST loop these corrugations have developed in wavelengths from 5" to 13". In order to minimize the impact on other experiments they are restricted to a maximum depth of 0.050" before remedial action is required.

Figure 2 is a composite of a series of transverse and longitudinal profiles. By comparing the three longitudinal profiles it is evident that the depth of the valley is greater near the field side than the gage side. Similarly, metal flow which is

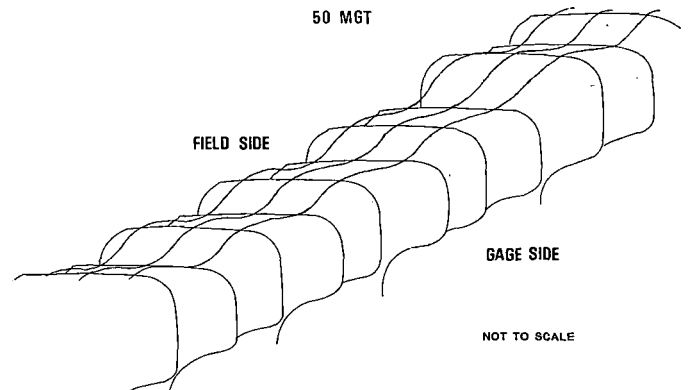


FIGURE 2. COMPOSITE OF TRANSVERSE AND LONGITUDINAL
PROFILES SHOWING TYPICAL CORRUGATED LOW
RAIL NEAR TIE 03-814, 50 MGT.

initially to the field side is later evident also to the gage side, appearing as a ridge in the transverse profiles. By comparing these observations and those of other authors^{1 2 3} we can conclude that the corrugations at FAST are of the "long wavelength" classification found in revenue service.

As expected, corrugations have been somewhat selective in the locations where they've developed. They have initiated, Figure 3, in curves 3° and greater and near track features such as switch points. For the purposes of this test the results presented will be restricted to the two five degree curves in Sections 3 and 17. These sections are also the locations of the rail metallurgy and tie experiments, giving a range of variables to examine.

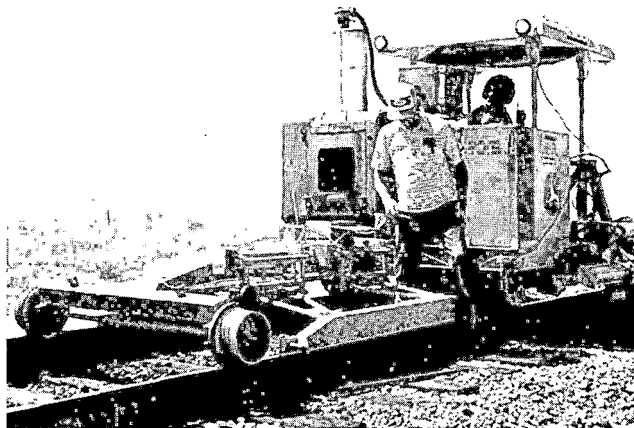


FIGURE 4. PHOTOGRAPH OF EDDY CURRENT SENSING DEVICE AND TOW VEHICLE.

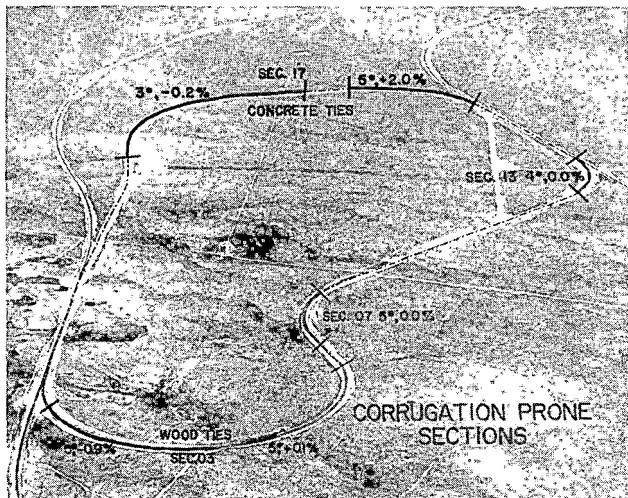


FIGURE 3. AERIAL VIEW OF FAST LOOP HIGHLIGHTING LOCATIONS WHERE CORRUGATIONS HAVE DEVELOPED.

With the controlled operating at FAST, i.e., a nominal speed of 45 mph and 3 inch unbalance, corrugations have initiated almost exclusively on the low rail. It is important to note that these operating conditions imply hard flange contact on the high rail. In heavily corrugated areas, at present only the standard carbon rail in Section 3, they have transferred to the high rail. It is curious that in this instance the 7-8 inch waves on the low rail have resulted in 13-14 inch waves on the high rail.

MEASUREMENT TECHNIQUE

Traditionally corrugations have been measured with a straight edge and taper gage--a reasonable method for spot measurements but not an extremely useful one in a test environment. Because of the large number of controlled variables at FAST, and our inability to predict precisely where corrugations will develop, we made use of the eddy current sensing device shown in Figure 4. This device continuously measures and records the railhead profile. In the center of the six foot ski riding above the rail is an electrical cable. Shown schematically in Figure 5, these leads are connected to an eddy current sensing device. With the six foot ski acting as a planar reference, the sensor magnet-

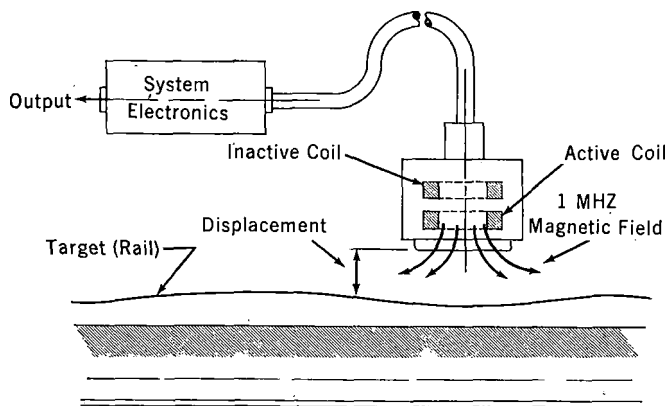


FIGURE 5. SCHEMATIC OF EDDY CURRENT SENSING DEVICE.⁴

ically induces an electrical current in the rail head. The magnitude of the induced current, a function of the distance of the sensor from the rail, is measured by the inactive coil.⁴

While being pulled at 4 mph, the output from the sensor is recorded along with distance and event information in the form shown in Figure 6. This figure contains the low and high rail profiles, distance, and location/event markings. Each major pulse on the distance channel represents 29.5 inches of rail length. Measureable amplitude is between .005 and .100 inch of height. In this output, corrugations are evident on the low rail, these

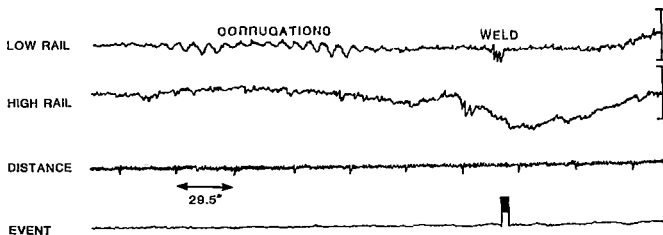


FIGURE 6. SAMPLE OUTPUT FROM EDDY CURRENT SENSING DEVICE.

being about eight inches in wavelength and .020" in depth. Isolating just the low rail, Figure 7, and comparing the profile over MGT, we can see the development of corrugations near tie 814, their removal through grinding, and their subsequent reoccurrence 70 MGT later.

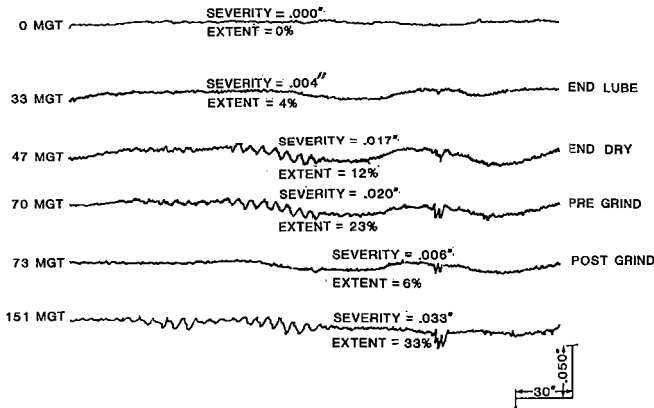


FIGURE 7. LONGITUDINAL RAIL PROFILES OF LOW RAIL NEAR TIE 03-814.

Faced with the large volume of data this technique supplies, we've developed two parameters by which to define corrugations. The first parameter, "extent", is roughly related to an initiation rate. The total length of rail that has discernable corrugations, i.e., are of appropriate wavelength, is compared to the total length of rail in that test section. We define a test section as being any length of track defined uniquely by a set of "corrugating" variables such as tie type, rail metallurgy or geometry. The second defined parameter, "severity", indicates the magnitude of the deepest corrugations within that section. As an example, the extent and severity of corrugations are shown for the area around tie 814 in Figure 7.

Having defined the general appearance of corrugations at FAST and outlined our measurement and analysis techniques we're ready to explore the nature of their formation. The exploration, in the form of metallurgical and dynamic testing, will serve as an introduction to the presentation of

development observations.

METALLURGICAL INVESTIGATION

In an attempt to isolate the type and magnitude of mechanisms present, we looked at a length of corrugated rail in the laboratory.⁵ This rail, shown in Figure 8, was removed from the inside rail in the 5° curve of Section 3 after 170 MGT of traffic. As evident in the photograph, the waves have the typical characteristics of corrugations at FAST--flow towards the gage and field sides and an approximate eight inch wavelength. The corrugation shown had reached a depth of .032".

Figure 9 shows the results of Rockwell hardness measurements taken at three positions along the corrugated wave, the indentations from which are evident in Figure 8. Shown also for comparison are hardness data taken from an adjacent length of uncorrugated rail. As a general statement, there doesn't appear to be a discernable hardness trend from peak to valley. This lack of appreciable hardness difference between peak and valley locations was supported by field Brinell measurements taken at various other locations.

Other researchers⁶ have noted a relationship between a hard white etching layer on the rail head surface and corrugation features. "White etching" indicates a metallurgical transformation induced through high temperatures, high stress, or both. In the rail examined there was indeed a white etching layer associated with the running surface. The location and depth, less than .003", of this layer was not associated particularly with corrugation peaks or valleys. Nonetheless, the presence of this layer does indicate possible high tractive forces during rolling contact.

In order to gain more insight into surface forces, running path samples, Figure 8, were chosen for scanning electron microscope (SEM) examination.

In Figure 10 are SEM photographs which were taken at the 1/2" from field lateral position. The appearance at this location is characterized by a consistent metal flow pattern at all three peak to valley positions. The difference in the peak and valley appearances is therefore one of degree; the valley exhibiting more, but the same type, of metal flow.

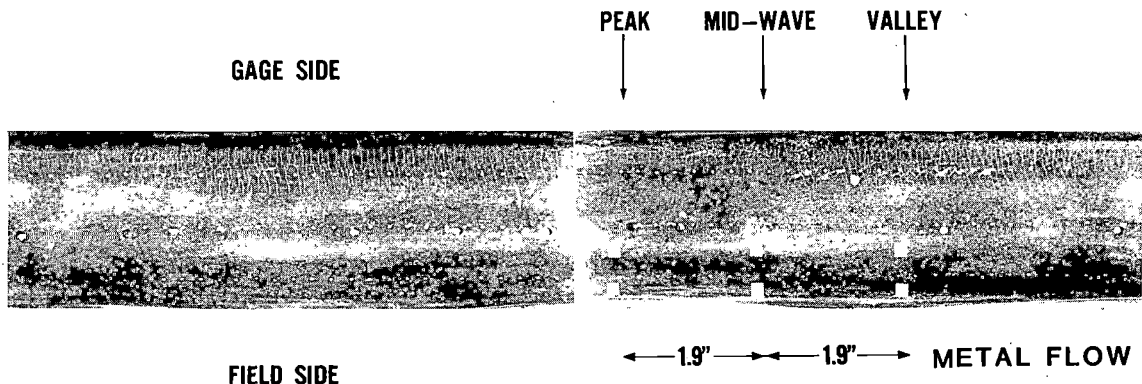


FIGURE 8. RAIL USED IN METALLURGICAL ANALYSIS. WHITE SQUARES INDICATE LOCATION OF SEM SAMPLES.

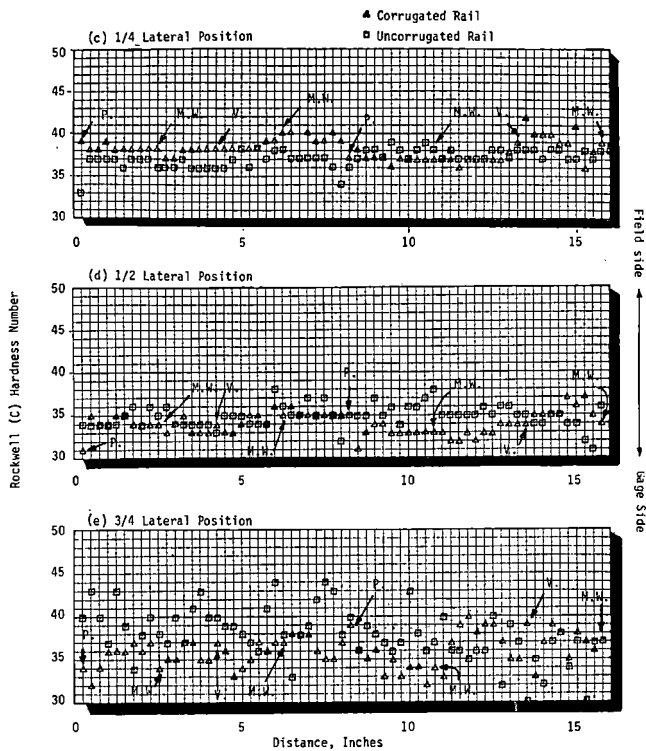


FIGURE 9. ROCKWELL (C) HARDNESS NUMBER VARIATIONS ALONG 16 INCHES OF CORRUGATED AND UNCORRUGATED RAIL.

In no position was there any appreciable evidence of gross sliding, a condition which would result in grooves or abrasions in the SEM analysis.

Looking at the 1" from field lateral position, Figure 11, the SEM gives indications of an entirely different wear mechanism. This type of appearance could be categorized as oxidation-fatigue wear. As the name implies, it is the destruction of the protective oxide layer on the running path through repeated rolling contact cycles. This type of wear is relatively mild as evidenced again by the lack of sliding marks.

It is possible to make inferences as to the nature of the forces causing the above two SEM appearances. First, both the metal flow at the 1/2" from field position and the fatigue at the 1" from field position are a result of rolling contact creepage forces in the absence of gross sliding. It has been well documented⁸ that in this absence of pure sliding the contact area between two elastic bodies will pass through zones of adhesion and microslip in the contact area. Relative changes in the magnitude of either zone will influence the magnitude and direction of the resultant surface stresses. The nature of these creepage forces will in turn affect the type of the surface (wear) appearance. In most cases the pattern of wear that develops will also give indications of the direction of creepage forces operative.

The appearances in Figure 10 are highly influenced by the lack of elastic constraint near the field corner. For this reason, more metal flow is evident and little can be said as to the directionality of creepage forces present. Figure 11, however, does provide some insight into force directionality. Visibly, the photographs give indications of strong longitudinal and lateral creepage forces. Furthermore by observing the "amount" of wear damage, it is evident that these longitudinal and lateral creepage forces increase from peak to valley.

The following is a summary of the metallurgical analysis.

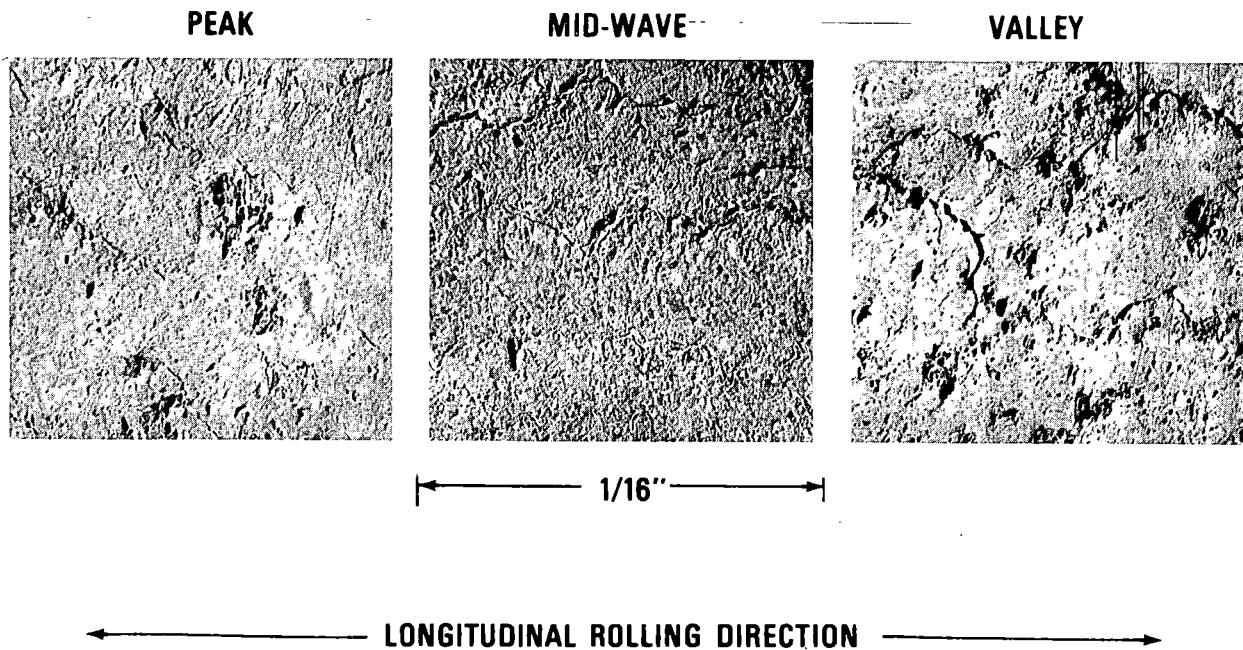


FIGURE 10. RUNNING SURFACE SEM PHOTOMICROGRAPHS 1/2" FROM FIELD, CORRUGATION DEPTH = 0.032", SAMPLE PREPARATION: 34° TILT ANGLE, NO ETCH.

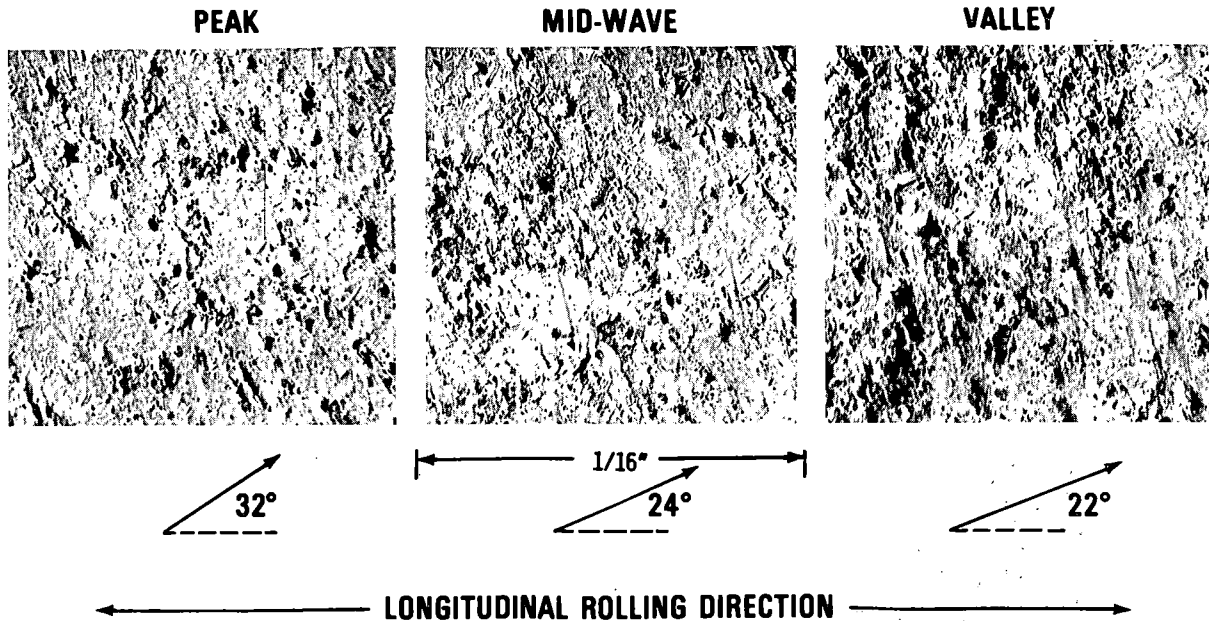


FIGURE 11. RUNNING SURFACE SEM PHOTOMICROGRAPHS 1" FROM FIELD. CORRUGATION DEPTH = 0.032", SAMPLE PREPARATION: 34° TILT ANGLE, NO ETCH.

- Corrugations themselves are a deformation and "mild" wear phenomenon. No signs of more severe wear, as would be the case if gross sliding occurred, were found.
- The wear mechanism, and therefore the force present, is similar from peak to valley. The only variation is the magnitude of the creepage forces present. In contrast, a pure "stick-slip" mechanism for corrugation development implies dramatically changing wear mechanisms from peak to valley.
- The resultant creepage force has significant lateral and longitudinal components which, while being relatively constant in direction, change in magnitude from peak to valley.
- The rolling contact fatigue checks, evident in Figure 8, do not necessarily define corrugation development at FAST where the amount of lubrication on the low rail is minimal.

We've found that longitudinal and lateral creepage forces, by periodically varying in magnitude, cause the corrugations to develop. While this is not an extremely profound statement it is possibly the key to understanding the source of vibrations which cause those changes in force.

SOURCES OF VIBRATIONS AND DYNAMIC TESTING

In this section three sources of vibrations: wheelset torsion, tie bending, and rail roughness, will be examined. As a caveat, by mentioning only three sources it isn't implied that these encompass all significant sources, nor can we make any definite statement as to the most important source.

One source of vibration is the torsional response of the solid wheelset during curve negotiation. The wheelset receives torsional excitation from two

interactions. The first has its origins in the concept of rolling distance differentials in curves, i.e., the outside wheel traveling further than the inside, resulting in increased longitudinal creepage forces.

As the second interaction the "high" wheel experiences a retarding force from flange/gage face contact. Looking at the forces on this wheel, shown schematically in Figure 12,⁷ it is evident that the flange experiences the lateral loads necessary for successful curve negotiation. As a result, a force is generated shown in this figure as $\frac{HL}{\sin \gamma}$. While its significance is apparent from a flange/gage face wear standpoint, it is important to realize the other effect of this force. $\frac{HL}{\sin \gamma}$ acts effectively to retard the rotation of the wheelset as can be inferred from the lateral view in Figure 12. In conjunction with the differences in rolling distances, a torsion is set up in the solid axle which, through winding and unwinding, can cause periodic increases in longitudinal creepage forces at the low wheel/rail interface. This is a feature of corrugation development as seen in the metallurgical analysis. The important elements in this proposal are

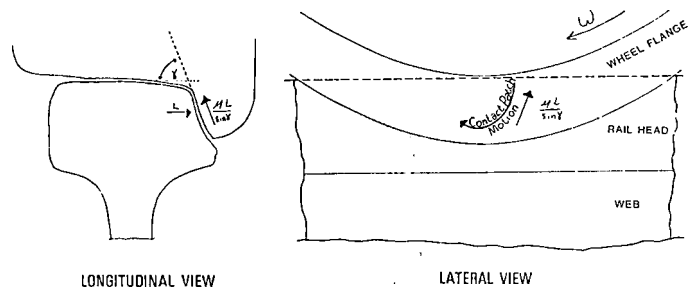


FIGURE 12. SCHEMATIC OF WHEEL ON HIGH RAIL FROM KALOUSEK.⁷

the components of the flange retarding force. First and most obvious, the greater the degree of rail curvature, the greater the likelihood of a larger L factor. Second, the coefficient of friction, μ , between the flange and gage face is affected by the presence of lubricants and the condition of the mating surfaces.

Results from limited dynamic tests support the concept of torsional vibration. Acceleration measurements were conducted to define the movement of both high and low rails in a corrugated region at FAST. Accelerometers mounted on the rail web were aligned so as to discern movement in each of three principal directions--vertical, lateral, and longitudinal. Of particular interest are the measured accelerations in the longitudinal direction. Figure 13(a) contains an auto-spectral density plot of the longitudinal response for both high and low rails. The wheel passings are indicated by high energy, distinct peaks near 10 and 20 Hz. Appreciable vibrations were also noted, however, near 100 Hz. At 45 mph, with corrugations being approximately eight inches in wavelength, the corrugation "passing frequency" is calculated also to be approximately 100 Hz.

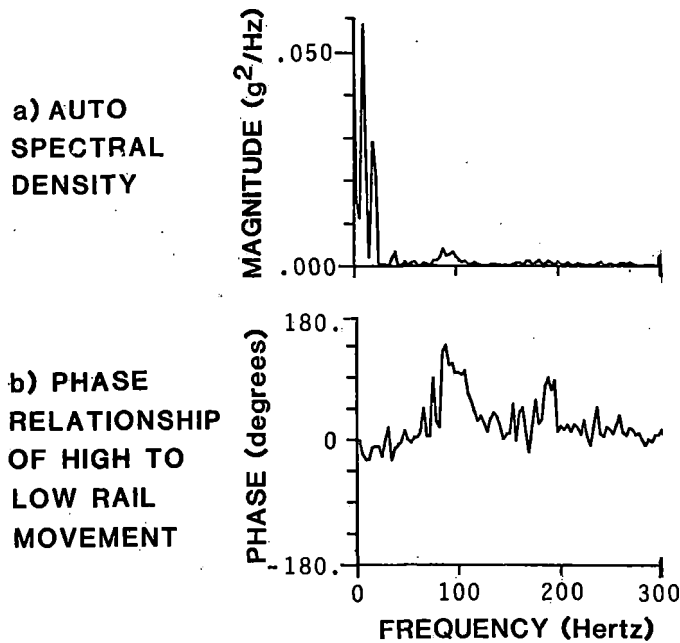


FIGURE 13. RESULTS OF RAIL WEB LONGITUDINAL ACCELERATION MEASUREMENTS, SECTION 3, 5° CURVE, NEAR TIE 825, SPEED = 43 MPH.

Figure 13(b) is an analysis of the acceleration phase relationship between the two rails at any given frequency. As is evident, the high and low rail are moving longitudinally in unison, i.e., zero phase relationship, in response to each wheel passing at 10 and 20 Hz. It is also apparent though, that the rails are moving nearly 180° out of phase longitudinally, i.e., in opposite directions, at the 100 Hertz frequency. It follows then that the wheels themselves should be behaving in a similar, although transposed, manner at this frequency. This out of phase response in the rotation of opposite wheels of the wheelset is an example of a typical torsional response as described in the literature.⁹

The tie itself responds to excitation by vibrating in relation to its natural frequency. It can be conjectured that through vertical, tie-induced rail accelerations, increased loading may occur, contributing to corrugation development. If this is the case, the corrugation wavelength would necessarily be a function of the tie natural frequency and of the vehicle speed.

Tests run using vertical accelerometers mounted on the tie center indicate vibrations in the first fundamental mode which compare reasonably with the corrugation wavelength. On concrete ties in Section 17 results show an acceleration peak at 116 Hz. The rail in this area had been ground to remove residual dynamic effects of corrugations. Results are shown in Figure 14. Shown in Figure 15 are results of calculations of the first symmetrical bending mode, assuming a continuous elastic foundation. By way of comparison, calculations for wood ties and the observed corrugation wavelengths are also shown.

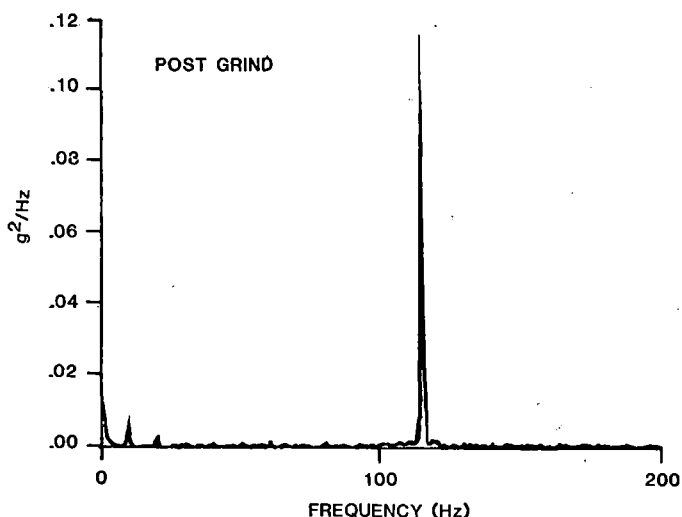


FIGURE 14. AUTO SPECTRUM - SECTION 17, TIE 400-500, AVERAGE CONSIST SPEED = 40 MPH.

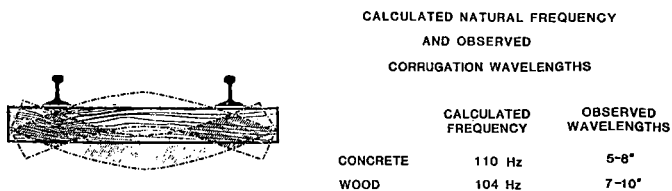


FIGURE 15. TIE VIBRATION FREQUENCIES IN 1ST SYMMETRICAL BENDING MODE.

Rail roughness is initially a function of the rolling and straightening operation at the producing mill. Measurements taken on new rail installed at FAST, Figure 16, give examples of the range of longitudinal profiles put in service. As an initiator of a system vibration, roughness must however be defined by the relevant wavelength range. Long wavelength patterns, up to 30 inches, were observed in most of the installed rail. Superimposed on these long wave patterns was a continuous spectrum of wavelengths to less than 1/2 inch. Australian re-

searchers¹⁰ have reported on the possible relationship between rail roughness and the initiation of corrugations. Because of the dangers of trying to characterize roughness, such as with an R_a value, which tends to obscure the short/long wavelength superposition, we will not quantify initial roughness but rather compare it qualitatively to performance.

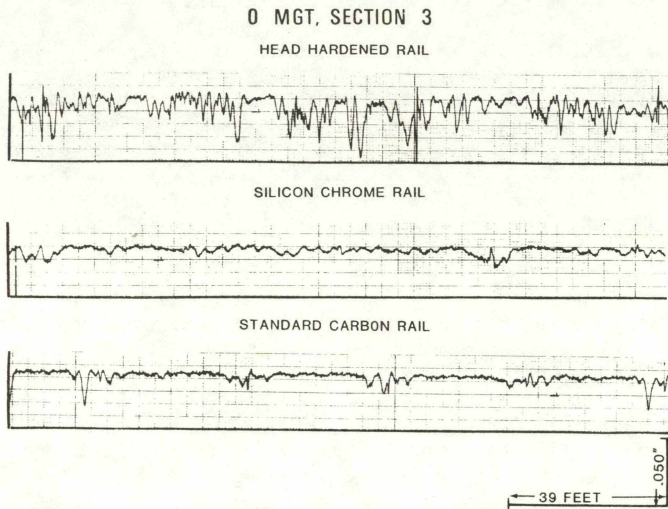


FIGURE 16. EXAMPLE OF LONGITUDINAL RAIL PROFILES AFTER INSTALLATION AND GRINDING FOR SCALE REMOVAL.

RESULTS

Figure 17 shows low rail corrugation development in the 5° curve of Section 3. Data are from three standard carbon subsections, a length of approximately 600 feet. As evident, corrugations have reached depths of .045 inch by 150 MGT. Overall, 55% of the rail in these subsections showed some evidence of corrugations.

Listed above the horizontal axis is the gage face lubrication state of the high rail in the same subsections. Dramatic growth in corrugation depth as well as overall initiation are seen in periods of a "dry" high rail.

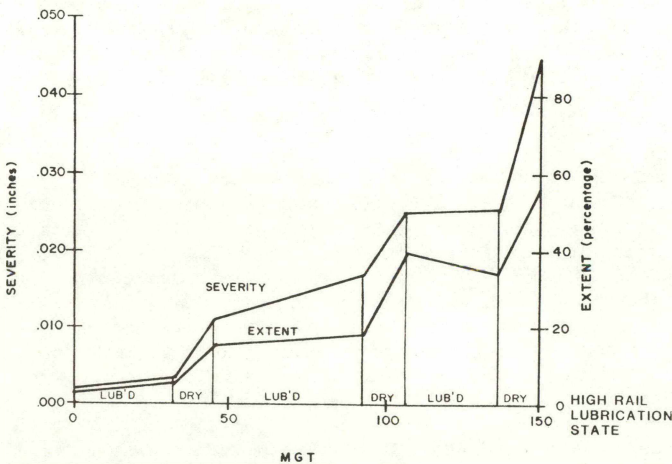


FIGURE 17. LOW RAIL CORRUGATION DEVELOPMENT AND THE EFFECT OF HIGH RAIL LUBRICATION.

Within Section 3, four rail metallurgies are compared in Figures 18 and 19. Figure 18, comparing corrugation severity with MGT reveals a loose relationship between initial hardness and performance.

Again the lubrication effect is evident, influencing the lower hardness materials to a greater degree than the higher hardness rails.

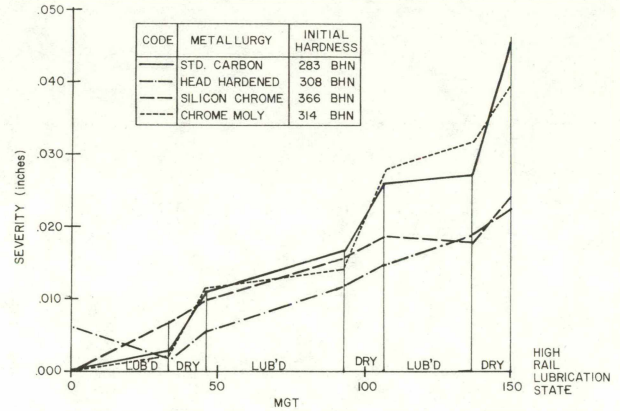


FIGURE 18. SEVERITY OF CORRUGATIONS FOR FOUR METALLURGIES IN SECTION 3, 5° CURVE.

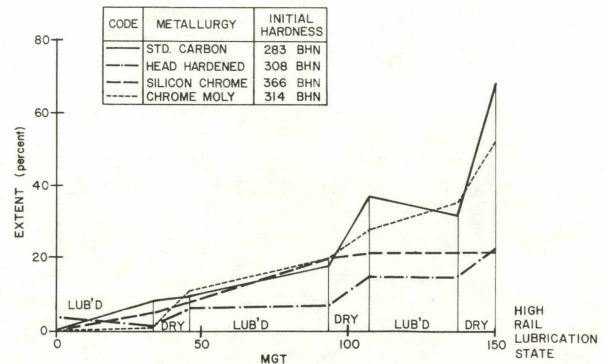


FIGURE 19. EXTENT OF CORRUGATION DEVELOPMENT FOR FOUR METALLURGIES IN SECTION 3, 5° CURVE.

By way of introduction to the effect of geometry on corrugation growth, Figure 20 contains data from the spiral heading into the 5° curve of Section 17. Corrugations appear above 2°, with appreciable growth occurring above 3.2°.

Returning to Section 3, the geometry changes with MGT and corrugation development are shown in Figure 21. With the track system control at FAST and the absence of high dynamic forces, little substantial change is seen in geometry parameters that could affect the phenomenon. Looking at a specific location, Figure 22, localized geometry variations are not enough to account for the observed difference in corrugating tendencies.

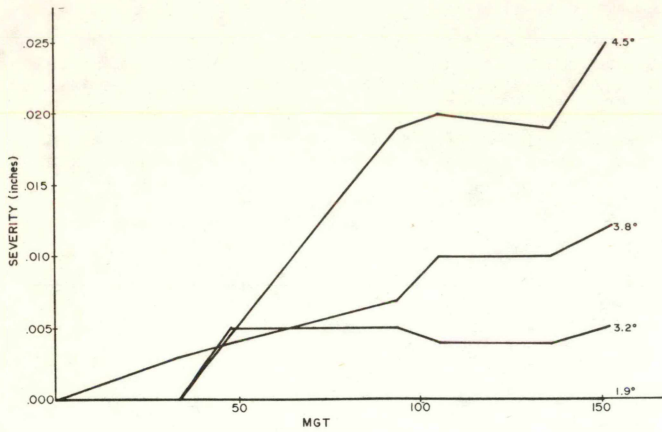


FIGURE 20. CORRUGATION SEVERITY DEVELOPMENT IN SPIRAL ENTERING 5° CURVE OF SECTION 17.

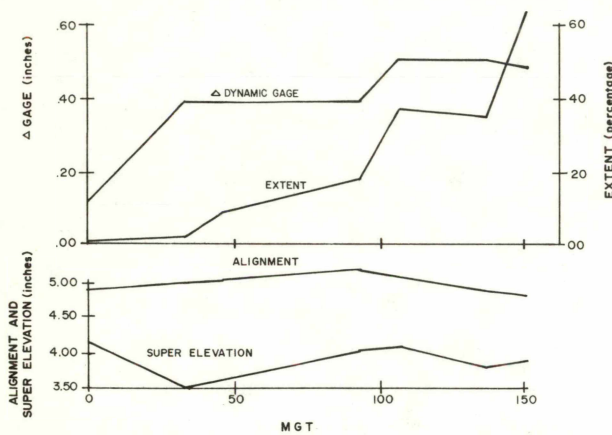


FIGURE 21. CORRUGATION DEVELOPMENT AND GEOMETRY CHANGES WITH MGT, SECTION 3, STANDARD CARBON RAIL.

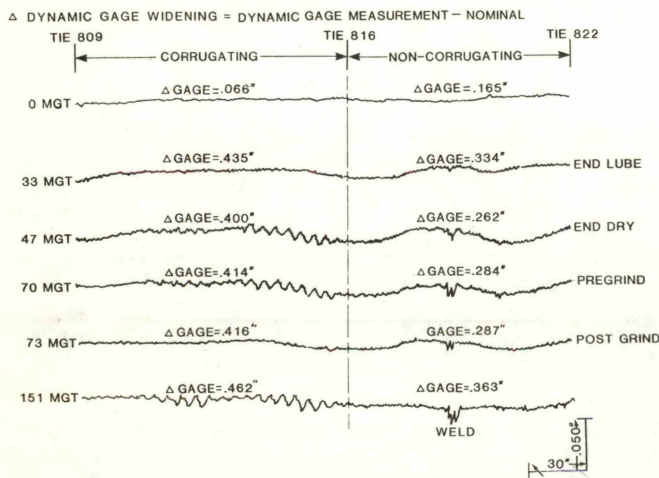


FIGURE 22. DYNAMIC GAGE WIDENING AND CORRUGATION DEVELOPMENT, SECTION 3, CHROME MOLYBDENUM RAIL.

DISCUSSION

Corrugations have been shown to be a deformation and mild wear process induced by high longitudinal and lateral creepage forces. The cause for the cyclic variation in these creepage forces cannot, as of yet, be completely defined. By taking each identified source of vibration and comparing it to the presented data we can make some inferences relative to its effect on "corrugating" forces.

Figures 17, 18, and 19 illustrate the effect of high rail lubrication on low rail corrugation development. Past researchers⁷ have noted that lubrication hydrodynamically promotes the Mode I progression of surface fatigue cracks thereby accelerating the corrugating process on the low rail. Lubrication control at FAST, however, is such that grease is confined for the most part to the high rail. As a conclusion then, if high rail lubrication is to have an effect, this changing condition at the high rail/wheel interface must be translated to the low rail through the solid wheelset. Assuming no changes in the lateral rail head creepage forces, L in Figure 12, a lower μ condition, as in the case of lubrication, diminishes the wheelset's ability to store energy while also decreasing the high rail frictional forces which normally adds to the torsion. This could result in lower longitudinal and lateral creepage forces on the low rail, reducing the likelihood of corrugation development.

The subject of tie accelerations as being the forcing function for corrugation development needs further investigation. The observed wavelengths, Figure 15, while falling in line with calculated bending frequencies were developed in somewhat different environments. The concrete tie observations were made in the 5° curve of Section 17 which includes a 2% grade and associated operational idiosyncrasies. It is for this reason that an overall comparison of corrugation development between wood and concrete ties could not be made in this test. Performance of any subsection within 17 was dependent more on position-in-curve, due to braking or accelerating in response to the grade, than on rail metallurgy or tie type. The FAST track as currently laid out includes a concrete-wood tie comparison in the 5° curve of Section 3, results from which will be reported upon in the future.

Addressing roughness induced vibrations, the head hardened rail which initially has a more visibly rough surface, Figure 23, did not corrugate appreciably worse than the SiCr head hardened rail. This is despite the hardness difference between the two metallurgies.

An effort was made in a corrugation prone 4° curve (Section 13) to initiate corrugations for the purpose of conducting grinding experiments. Starting with an artificial initiator on the low rail, roughness 0.030" deep and six inches wavelength, no corrugations developed to 187 MGT, Figure 24. The combined result of these two observations is that roughness, in the uniform environment at FAST, does not play as large a role in corrugation development as lubrication and, to a degree, hardness.

Rail head hardness is an approximate measure of a rail's ability to withstand deformation and wear. It is not, however, a complete measure of a rail's ability to withstand corrugating mechanisms. Fig-

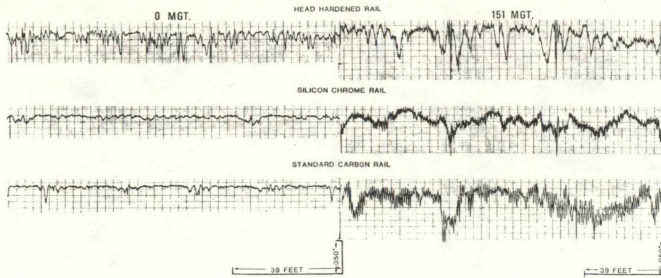


FIGURE 23. LONGITUDINAL RAIL PROFILES OF LOW RAIL.

SECTION 13, 4° CURVE, LOW RAIL

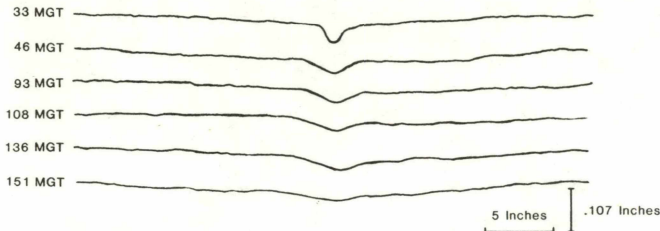


FIGURE 24. ATTEMPT TO INDUCE CORRUGATIONS WITH AN ARTIFICIAL INITIATOR.

ures 17 and 18 indeed show that the standard carbon rail, of lower hardness, does corrugate more rapidly and to greater depths than any of the other alloy or heat treated rails. However, no clear relationship was observed with hardness among the premium rails. This highlights the need for better mechanical behavior definition, taking into account cyclic yield behavior, and also for greater understanding of how individual metallurgies react to the given wear mechanisms. The ability of any one vibrating source to contribute to the cause of corrugations will depend on the magnitude of competing vibration sources as well as on the rail susceptibility, defined presently by hardness, to the phenomenon. Adding to the complexity is the fact that the rail contains a unique source of vibrations in its initial roughness.

CONCLUSIONS

Corrugations are a deformation and wear phenomenon.

High rail lubrication has a definite and dramatic impact on corrugation development and growth.

Initial rail hardness has, to some degree, an impact on corrugation behavior.

Further testing is required to explore the following:

- o Operational impact on corrugation development due to acceleration, braking, and speed variations.
- o The nature and relative impact of various sources of system vibrations.
- o The parameters necessary to better predict corrugation "resistance" for rail metallurgies.
- o The significance of contributing variables such as the effect of altering track strength and response characteristics through the use of different tie and fastener systems.
- o The effect of grinding corrugations of various depths to other depths in an attempt to define optimal practices to inhibit reoccurrence.
- o The impact of wheel hardness and radial design trucks on corrugation development.

REFERENCES

- 1 Mair, R. I., Jupp, R. A., and Groenholt, R. - The Characteristics and Control of Long Pitch Corrugation at Heavy Axle Loads, presented at 1979 Heavy Haul Conference, Session 417, Paper I.8.
- 2 Kalousek, J. - Track Train Dynamics Report #4: Rail Corrugations, Department of Research, Canadian Pacific Limited, Report No. S488-75, February 1975.
- 3 Bruno, A. T., ATB Associates - Rail Corrugations and Rail Grinding.
- 4 RCA Demonstration/Seminar, LORAM Maintenance of Way, Inc.
- 5 Moin, E., Boeing Services International - Metallurgical Examination of Corrugated Rail Section, not yet published.
- 6 Clayton, P., Allery, M. P. B., and British Rail - Metallurgical Aspects of Surface Damage Problems in Rails.
- 7 Kalousek, J., National Research Council of Canada, Bethune, A. E., Canadian Pacific Limited - Rail Wear Under Heavy Traffic Conditions.
- 8 Karamchandani, K. C., Kumar, S., Sciammarella, C., Seth, B., Nailescu, L., and Kalpakjian, S. - Friction, Creep, and Wear Studies of Steel Wheel and Rail, Interim Technical Report No. 2, IIT Trans 75-1, May 1975.
- 9 Timoshenko, S., Young, D. E., and Weaver, Jr., W. - Vibration Problems in Engineering, 4th Edition, J. Wiley & Sons, New York, 1974.
- 10 Mair, R. I. and Jupp, R. A. - Rail Track for Heavy Unit Train Operations, BHP, Melbourne Research Lab, presented at the Annual Engineering Conference, Townsville, May 1976.

Question 1

What recommendations do you make with your current knowledge of when to grind and how much for maximum economy of grinding expense, rail expense, and train delay expense?

Answer

Until recently, the FAST Program has not been able to address the grinding issue as we would have liked. The experiment itself must be careful to avoid impact on other experiments (tie, ballast, etc.). However, we have two programs which will, in the near future, produce results. In the 5° Curve of Section 7, we have alternately ground segments of new standard rail. Results from this test should give us more insight into the grinding of new rail controversy.

Question 2

As stated by the author, the effect is a cyclical dynamic one involving longitudinal creepage (as well as lateral) vertical motion, etc. Since modeling knowledge exists sufficient to simulate wheelset motion in such a regime, has any thought been given to employing these in search of a fuller explanation?

Answer

Part of the original objective of this experiment included only laying the ground work for future testing and the formation mechanisms. Our overall concept was to observe corrugations, trying to isolate where and under what conditions they develop, as well as documenting growth rate and reoccurrence. Using this as a base, we are now in a position to look into formation mechanisms. Our anticipated next phase is just as you suggested. While continuing observational testing, we will address the mechanism issue with coordinated dynamic testing and modelling.

Question 3

I missed magnification, etching, and other particulars for S.E.M. micros. Please supply.

Answer

I hope sufficient documentation is provided in the text of the proceedings. For more references on the use of the technique itself as well as general comments, please contact me directly.

- 1) What causes corrugations to develop?
- 2) What can be done to avoid it? Please give answers in a plain manner - bare facts - which can be easily understood by our everyday track people.

Answer

Corrugations of this type are a direct result of the wheelset negotiating the curve. In doing this, it encounters differences in rolling distances (i.e., the low rail is shorter than the high rail) and also, differences in load because of the forces required to guide a car through a curve. Vibrations are, as a result, initiated within the wheelset itself and, also, within the track and mechanical systems. These vibrations cause periodic, every 8" for example, increases in load which result in increased wear and metal flow.

The method to avoid corrugations can be addressed from two view points. First, is to get rid of the source of vibrations. Disconnecting the wheels from one another or alternating the track design are some suggestions, although neither are very partial. We, therefore, must look at how to reduce the forces present and live for the time being with the vibration. High rail lubrication seems to be an effect at FAST in reducing the forces due to axle response. Also, as documented on the Canadian Pacific, see Reference 2, gage control is important in minimizing contact stresses. High contact stresses can develop and cause metal flow when the wheelset is allowed to run near its front rim face, i.e., areas of excessively wide gage. As a last result, if we don't control the vibrations, and it's not practical to control the forces, it is best to use a type of rail that is able to withstand both. They have found at FAST that harder rails generally resist corrugations better. This is by no means a "hard" and "fast" rule, more work needs to be done to understand why some premium rails perform well and others don't.

MECHANICAL

1981 FAST ENGINEERING CONFERENCE

KEY TOPICS

WHEELS

RADIAL TRUCKS

FATIGUE ANALYSIS

WEAR INDEX TESTING

WHEEL/RAIL LOADS

MAJOR VARIABLES THAT AFFECT WHEEL WEAR

Donald E. Gray
Experiment Manager, Wheels
Federal Railroad Administration

Interest in wheel wear performance has increased in recent years because of the trend toward heavier freight cars with higher axle loads. In addition, wheels continue to be listed as one of the major causes of train accidents under the heading of mechanical and equipment failures; Table 1 provides excerpts from the 1978 and 1979 published accident statistics where wheels are ranked with other mechanical items ranging from brakes to locomotives. It should be noted that the figures in Table 1 concerning wheels are totals due to wear related failures as well as other types of failures. This experiment is designed to address wearing characteristics of wheels. It should be further noted that with several hundred freight car wheels within a given train, wheels may have a higher probability of failure than other items being compared with them.

Wheel wear interest at FAST has led to the initiation of four specific wheel experiments to date as shown in Table 2. The main variables under examination for each experiment are also listed. This paper will address the first three experiments. The last experiment is addressed in a separate paper, "Wear Rates of Freight Car Wheels as a Function of Chemistry," also included in these proceedings.

TABLE 1. ACCIDENT SUMMARY FOR 1978 & 1979 DUE TO MECHANICAL & EQUIPMENT FAILURES.

CAUSES	ACCIDENTS		DAMAGE		INJURIES	
	1978	1979	1978	1979	1978	1979
MECHANICAL & EQUIPMENT FAILURES			(\$ MILLIONS)			
BRAKES	234	206	7.4	4.8	7	8
TOFC/COFC	20	16	0.4	0.5	1	0
BODY	243	186	7.6	6.3	5	7
COUPLER & DRAFT SYSTEM	255	198	7.7	6.7	10	12
TRUCK COMPONENTS	456	401	12.8	13.6	17	17
AXLES & JOURNAL BEARINGS	299	255	13.5	15.7	5	7
WHEELS	415	326	18.5	21.2	69	51
LOCOMOTIVES	199	161	9.8	6.5	47	29
DOORS	21	25	0.4	0.5	0	1
OTHER	27	41	1.0	1.2	1	9
TOTAL	2,169	1,815	79.1	77.0	162	141

TABLE 2. WHEEL EXPERIMENTS INITIATED TO DATE AT FAST

EXPERIMENT	VARIABLES EXAMINED
WHEELS I	TREATMENT CONSTRUCTION DESIGN PROFILE TRUCK SNUBBING CENTER PLATE SIZE
WHEELS II	AS FOR WHEELS I PLUS REPROFILING HARDNESS CHEMISTRY
WHEELS III	AXLE LOADING TRUCK SNUBBING
WHEELS IV	CHEMISTRY

FIRST EXPERIMENT

The initial wheel experiment was set up as a full factorial design with analysis of variance as the intended principal analytic technique. This type of design was selected to best facilitate the detection of interactions between the independent variables if they occurred.

The objective of this experiment was to examine the degree of influence on wheel wear of four wheel variables (treatment, construction, design, and profile) and two conventional truck variables (center plate diameter and snubbing).

Each variable was assigned two values as listed below which therefore yields 2⁶ possible combinations or an experiment matrix consisting of a total of sixty-four cells:

- o Wheel profile (AAR Std., CN)*
- o Wheel treatment (heat-treated, untreated)
- o Wheel construction (cast, wrought)
- o Wheel design (1-wear, 2-wear)
- o Truck center plate diameter (14-inch, 16-inch)
- o Truck type (constant, variable friction snubbing)

Each cell included the four wheels under each truck; thus, the experiment required 32 cars. The actual wheel distribution within the 64 cells is shown in Table 3. The original experiment was designed for a maximum of 256 test wheels, or 128 wheel (axle) sets. However, difficulties encountered with two cars reduced the actual number of wheel sets for analysis to 120.

Periodic wheel measurements included flange thickness and height, rim thickness and wheel profile. Rim hardness and wheel circumference measurements were taken initially and when the wheels were removed, turned or replaced. All measurements, excluding wheel circumference, were taken at two positions diametrically opposite on each test wheel. The AAR finger gage was utilized to obtain flange thickness, flange height and rim thickness values. Profiles were taken with the aid of a profilometer.

All 32 cars used for this experiment were 100-ton open hoppers loaded to a gross weight of approximately 263,000 pounds and were assumed to be sufficiently similar so as not to bias the experiment. In addition, each car was equipped with high-friction composition type brake shoes, roller bearings with non-hardened bearing adapters and double-roller side bearings. The majority of the cars were equipped with standard D-5 suspension springs and all cars were equipped with either truck or body mounted brake systems.

*It should be noted that all wheels were received with AAR standard profiles and therefore, one-half of these had to be turned to the CN profile.

TABLE 3. COMPARISON OF MILEAGE TO FIRST REMOVAL FOR THIN FLANGE IN WHEEL EXPERIMENT.

				14" Center Plate		16" Center Plate	
				Type 1	Type 2	Type 1	Type 2
Treated	1W	Cast	CN	4	2	4	4
			AAR	4	0	4	6
	Wrought	Cast	CN	4	4	6	4
			AAR	4	0	4	4
	2W	Cast	CN	4	4	2	0
			AAR	4	8	4	4
Wrought	Cast	CN	4	4	4	4	
		AAR	4	4	4	4	
Untreated	1W	Cast	CN	0	4	4	4
			AAR	4	4	4	2
	Wrought	Cast	CN	4	4	4	4
			AAR	4	4	4	4
	2W	Cast	CN	8	4	4	8
			AAR	4	0	0	4
Wrought	Cast	CN	4	4	4	4	
		AAR	4	4	0	4	

Since the FAST track is a closed loop containing a large amount of high curvature over a limited length, the test consist was operated in a manner to equalize component wear at all locations on the test cars and involved a four-day cycle. In addition to turning and reversing the train, every other test day two groups of eight cars were shifted from one end of the consist to the other, and each test day four cars were removed from the consist for measurements while four previously measured cars were reinserted. This test procedure ensures that each car is cycled through the consist and receives measurements at least once every twenty-two days. Assuming the test consist completes an average of 104 laps per test day, measurements would be obtained approximately every 11,000 miles.

Rail lubrication was a variable during the first experiment. Both the number and type of rail lubricators were varied during the first 25,000 to 30,000 miles of operation. In addition, the type of lubricating grease was changed at approximately 20,000 miles. And finally, an average of 35% premium rail was used in the curves during this experiment.

Due to excessive flange wear since the beginning of the test, "thin flange" was the predominant reason for wheel removals. Almost 84% of the Class U wheels were removed for this reason. Figure 1 depicts the typical excessive flange wear pattern which resulted. During the first 20,000 miles a wheel/rail wear pattern as represented in Figure 2 developed, primarily due to the use of all new or newly-turned wheels on new rail.

After approximately 40,000 miles, several wheels were removed as a result of flange cracks. Figure 3 presents an actual photograph of a cracked flange section alongside a worn high rail section. A close-up of a representative flange crack is shown in Figure 4. These cracks varied in depth from a few hundredths of an inch near the flange apex to those extending to the tread/flange fillet region and ranged in number from one to more than thirty (30) per wheel. Although they have the physical appearance of thermal cracks, metallographic investigations¹ indicate these cracks are the result of metal fatigue associated with excessive plastic deformation which occurred on the gage face of the flange region during periods of insufficient track lubrication. The effective work-hardening in this

region near the flange surface is shown in Figure 5 in the form of hardness measurements taken along two different paths.

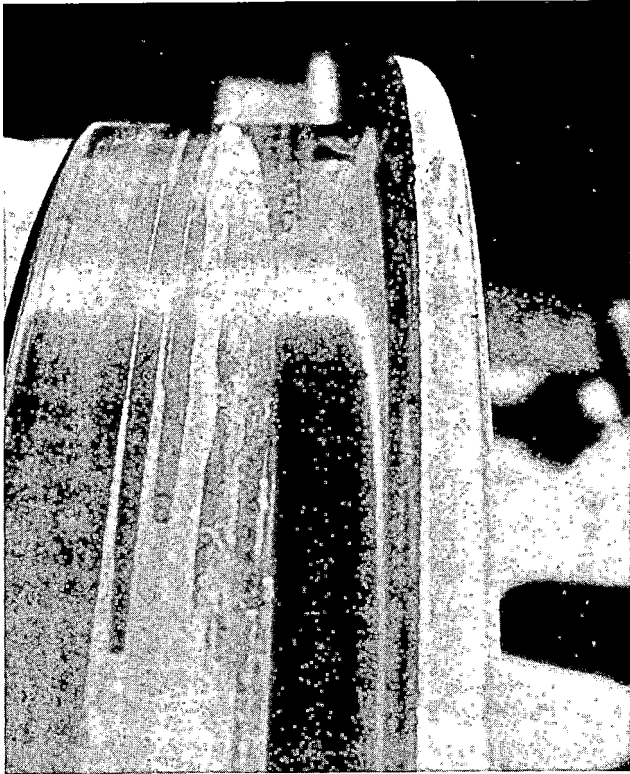


FIGURE 1. TYPICAL WHEEL WEAR PATTERN SHOWING EXCESSIVE FLANGE WEAR.

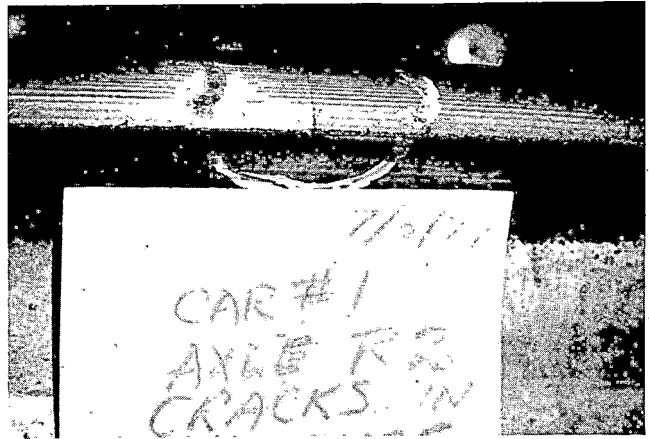


FIGURE 3. SECTION OF CRACKED WHEEL FLANGE

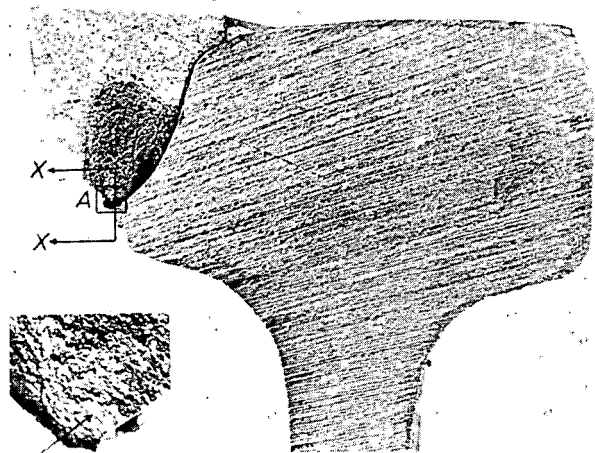


FIGURE 4. CLOSE-UP OF FLANGE CRACK

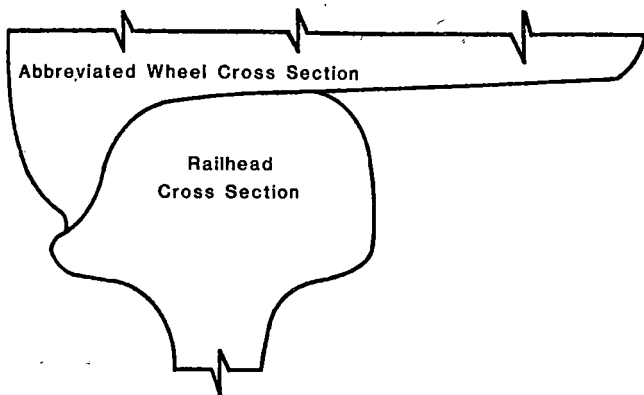


FIGURE 2. RESULTING WHEEL/RAIL WEAR PATTERN WHICH DEVELOPED IN THE FIRST WHEEL EXPERIMENT

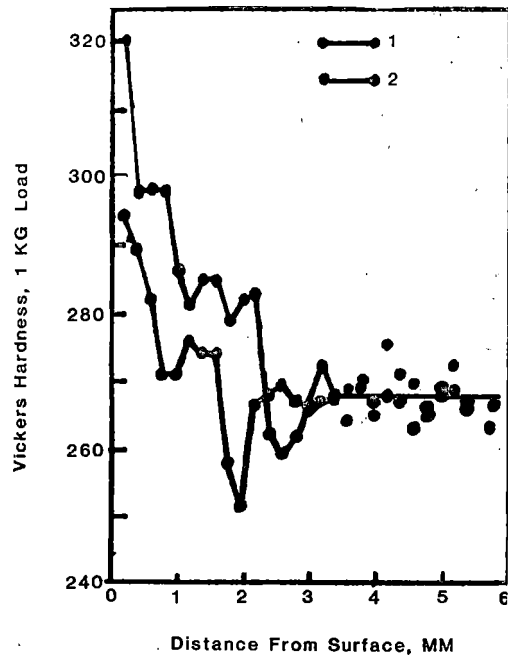


FIGURE 5. FLANGE HARDNESS VERSUS DEPTH BELOW THE SURFACE FOR AN UNTREATED WHEEL

A third reason for wheel removal was the combined development of initial shelling and fine oblique surface cracks in the tread area which were discovered after approximately 45,000 miles. Samples of initial shells and tread cracks are shown in Figures 6 and 7 respectively. Investigations conducted to date² suggest that the oblique tread cracks are mechanically induced. The short transverse cracks may be nucleated by a mechanism that is different from that operating upon the oblique cracks. Approximately 78% of the treated wheels were removed for tread cracks. It should be noted that the degree of tread cracking and/or shelling for most of the wheels removed had not progressed to the stage at which normal railroad practice would have dictated removal; but, not knowing the cause of the flange cracks at this time, they were removed as a precautionary measure. Table 4 provides a summary of wheelsets removed for the above mentioned reasons.

As a result of the combined high wear rates and failure modes experienced, the initial experiment was completed, for all practical purposes, within the first 70,000 miles of testing.

Examination of the finger gage and profilometer data indicated that flange thickness wear was the most prevalent type of wheel wear occurring and that wheel treatment was a major factor affecting flange wear. This is clearly shown by a comparison of Figures 8 and 9. Figure 8 shows the resulting profile wear pattern for a typical heat treated (Class C) wheel after approximately 38,000 miles, and Figure 9 provides the corresponding wear pattern for a typical untreated (Class U) wheel after a similar mileage interval. The slight increase in flange height shown in the worn profiles in both figures is the result of metal flow from the gage-face side. Comparison of these two wear patterns shows the better than two-to-one average flange wear ratio which resulted primarily from heat treatment.

TABLE 4. REASONS FOR FIRST REMOVAL BY WHEELSET IN EXPERIMENT 1

REASON	TREATED WHEELS	UNTREATED WHEELS
Thin Flange	6.7%	83.3%
Flange cracked or broken	5.0%	5.0%
Tread cracks	78.3%	1.7%
Other reasons	10.0%	10.0%

In order to more fully define the relationships between the original six test variables on flange thickness wear, several mathematical models, both linear and nonlinear, were investigated and resulting regression analysis performed. The final resulting model, given below, was utilized to estimate the mileage to first removal for each of the variable combinations. Then ratios were calculated which represented a change in only one variable and the ratios were averaged to obtain an average change.

$$\text{Average Flange Thickness} = 6.056 (\text{Mileage} + 10,000)^B$$

$$\text{where: } B = -0.1649 + 0.0107 X_1 + 0.0007 X_3 + 0.0014 X_4 + 0.001 X_5 + 0.0013 X_6$$

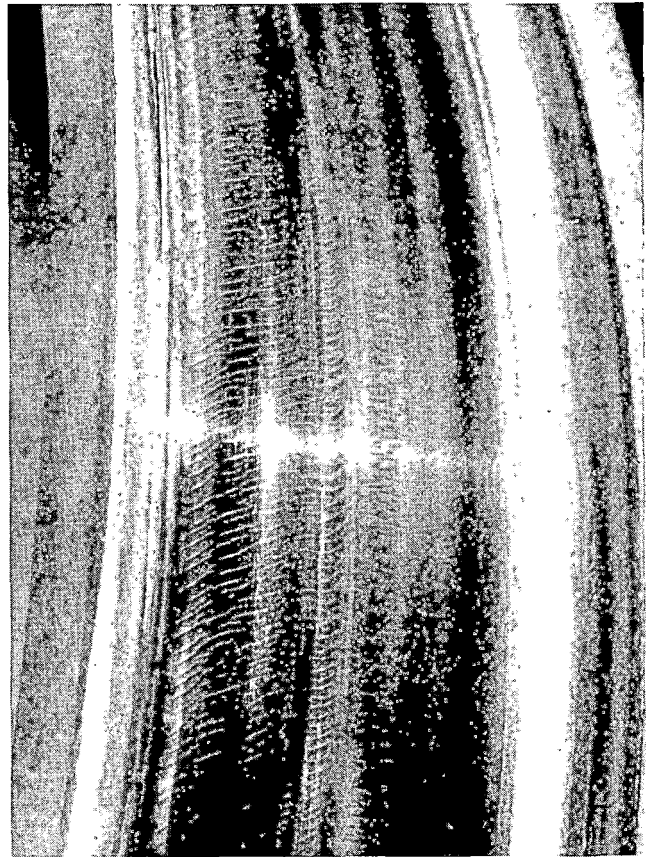


FIGURE 6. OBLIQUE TREAD CRACKS

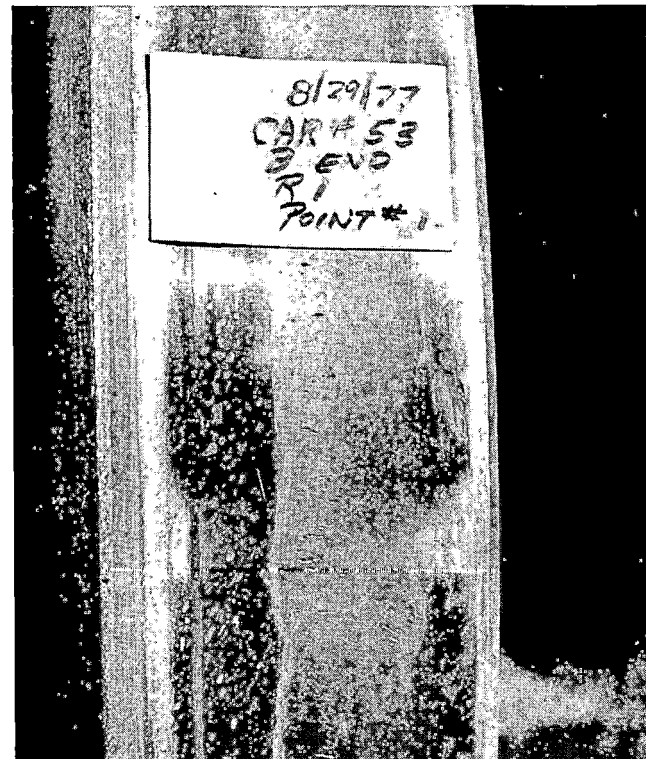


FIGURE 7. INITIAL TREAD SHELLING

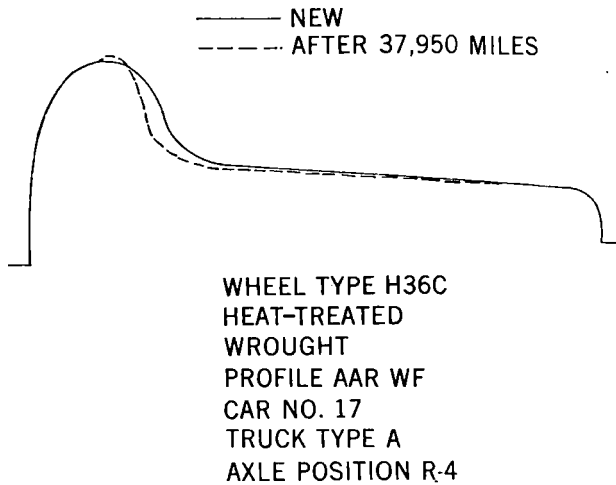


FIGURE 8. REPRESENTATIVE PROFILE WEAR OF CLASS C WHEELS DURING FIRST EXPERIMENT.

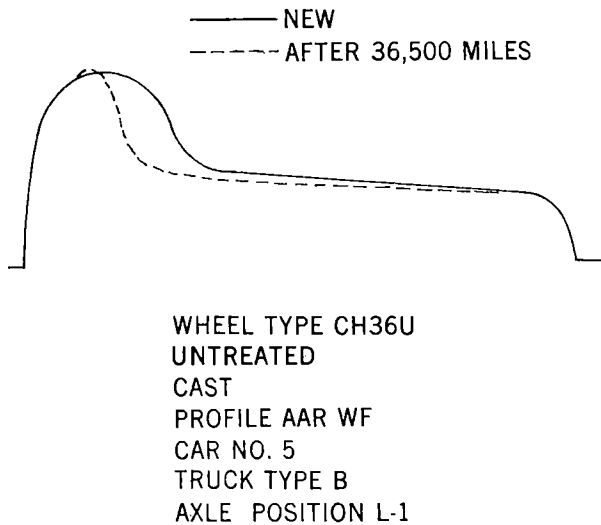


FIGURE 9. REPRESENTATIVE PROFILE WEAR OF CLASS U WHEELS DURING FIRST EXPERIMENT.

where:

$X_1 = 1$ if wheel is heat-treated
 0 if wheel is untreated

$X_3 = 1$ if wheel is cast
 0 if wheel is wrought

$X_4 = 1$ if wheel has CN profile
 0 if wheel has AAR profile

$X_5 = 1$ if truck has 14-inch center plate
 0 if truck has 16-inch center plate

$X_6 = 1$ if truck is Type 1
 0 if truck is Type 2

The results are shown in Table 5. The percentage changes in mileage should be considered only as order of magnitude estimates. The first line indicates that treated wheels last approximately two and one-third times longer than untreated wheels. Essentially, the effects of the next four variables

(construction, profile, center plate size and truck type) can be considered equal based on this data. And finally, it should be noted that wheel design was not statistically significant in affecting flange wear.

TABLE 5. COMPARISON OF MILEAGE TO FIRST REMOVAL FOR THIN FLANGE IN WHEEL EXPERIMENT.

VARIABLE WITH LONGER PREDICTED FLANGE LIFE	VARIABLE WITH SHORTER PREDICTED FLANGE LIFE	ESTIMATED PERCENTAGE INCREASE
Heat-Treated	Untreated	136
Cast	Wrought	6
CN Profile	AAR Profile	13
14 Inch Center Plate	16 Inch Center Plate	9
Type 1 Truck (Constant Column Friction)	Type 2 Truck (Variable Column Friction)	11
1 - Wear	2 - Wear	No Significant Difference

The major conclusions reached from the first experiment are as follows:

- o The predominant wear mode observed was flange wear.
- o Based on flange wear, treated wheels lasted an average of 2-1/3 times longer than untreated wheels.
- o The effects of treatment on flange wear were an order of magnitude larger than the other wheel/truck variables considered.
- o Untreated wheels were removed mostly for flange wear; whereas, treated wheels were removed mostly for cracks.
- o Future testing requires controlled track lubrication.

A full treatment of the analysis of data from Wheels I is contained in Reference ³.

SECOND EXPERIMENT

The second wheel experiment, conducted between August 1977 and July 1979, was designed in part to improve on data from the first experiment and in part to further explore additional wheel wear issues. One major objective of this second experiment was to re-examine the effects of the five variables (treatment, construction, design, truck snubbing and center plate diameter) on wheel wear under controlled track lubrication conditions. A second objective included exploring the effects of different profiles, reprofiling (both new and worn wheels), initial rim hardness and wheel chemistry on wheel wear.

The test conditions for this experiment were, in general, the same as for the first experiment, with certain exceptions. There existed a generous track lubrication environment throughout most of the test period and the amount of premium rail in the curves was increased from 35% to 80%. A key factor in running a successful experiment was providing for the control of track lubricant to maintain sufficient wheel/rail lubrication through the test period. This was achieved through the use of four track lubricators positioned as shown in Figure 10. Three

of the four lubricators were consistently applying lubricant to the rail during the consist's daily run. The specific lubricators utilized varied with running direction as noted in the figure.

The 32 cars for this experiment were sorted into two groups, each having 16 cars and 128 wheels. One group, containing all AAR standard profile wheels, was used to replicate the first experiment by re-examining the five variables which included treatment, construction, design, truck type and center plate diameter.

The actual distribution of test wheels is shown in Table 6. As indicated in this matrix, all 32 test cells were represented with at least four wheels.

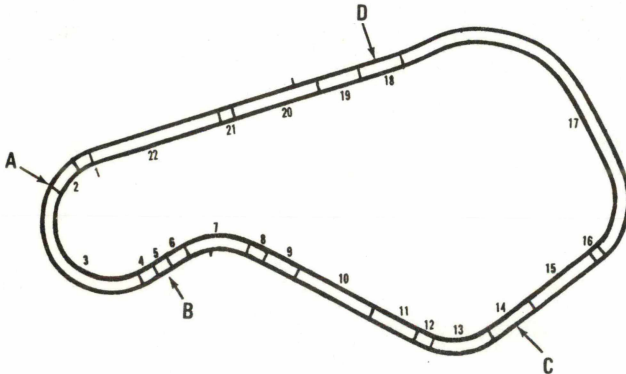


FIGURE 10. TRACK LUBRICATOR LOCATIONS UTILIZED DURING THE SECOND WHEEL EXPERIMENT.

TABLE 6. DISTRIBUTION OF AAR STANDARD PROFILE WHEELS IN EXPERIMENT II.

		UNTREATED				TREATED			
		2-WEAR		1-WEAR		2-WEAR		1-WEAR	
		Wrought	Cast	Wrought	Cast	Wrought	Cast	Wrought	Cast
14" Center Plate	Type 1	6	8	8	10	4	8	8	6
	Type 2	4	8	4	4	6	8	8	4
16" Center Plate	Type 1	6	8	8	8	4	8	8	12
	Type 2	6	8	12	14	6	8	8	6

The collection of data on the three finger gage measurements, (flange thickness, flange height and rim thickness) was used to develop three corresponding wear measures - termed flange wear, flange height growth, and rim wear, that reflected the wear at the various points on the wheel profile. Flange wear is the measure of the loss of metal on the flange as determined by changes in flange thickness. Flange height growth is the apparent measured increase in flange height resulting from the combined effect of tread metal loss (i.e., rim wear) and the flow of metal along the inner face of the flange toward the apex. Rim wear is the measure of the loss of metal on the wheel tread as determined by changes in rim thickness.

An initial objective in the analysis of the second wheel experiment data was to reduce the data to a wear summary form, as well as to undertake a preliminary examination of the summarized data during the course of the reduction process. A combination of graphical analysis and multiple regression techniques was used to accomplish this objective.

To work through the reduction process, it is useful to look at one of the three basic measurements for two sample test wheels of the same type - that is, the same combination of variables. The samples are test wheels, number 1131 and 1142, which were both installed on January 13, 1978, and removed after about 95,000 miles as a result of a February 27, 1979, derailment. The specific variables are cast, 1-wear, nonheat-treated, 14-inch center plate, and type 1 truck.

Figure 11 is a measurement plot showing average flange thickness (in inches) versus mileage for the two sample wheels. The measurement plotted is the average of the two measurements customarily taken during each measurement event. As evidenced by the plot, the measurement events for the two sample wheels occurred at intervals of approximately 10,000 miles. However, because the wheels were mounted under different test cars, their measurement cycles did not coincide.

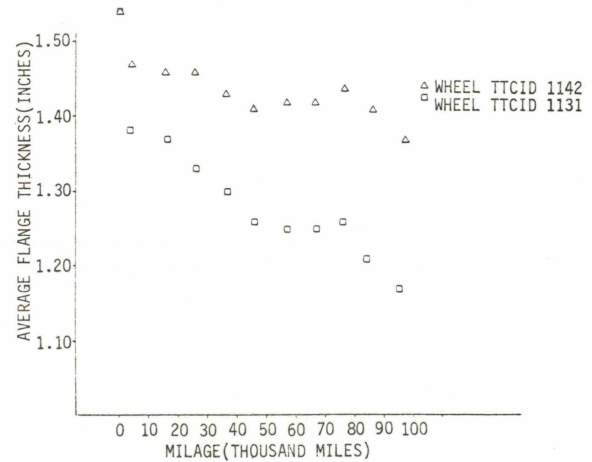


FIGURE 11. FLANGE THICKNESS VERSUS MILEAGE FOR TWO SAMPLE WHEELS OF SAME TYPE.

Figures 12 and 13 are plots for the same wheels showing, respectively, average rim thickness (in inches) versus mileage and average flange height (in inches) versus mileage.

The measurement plots for all wheels within the same wheel type can then be combined to form scatter diagrams for flange thickness, rim thickness, and flange height. Figure 14, for example, is a scatter diagram of flange thickness versus mileage for the ten wheels of the same wheel type-cast, 1-wear, untreated, 14-inch center plate diameter, and type 1 truck. As can be seen, the initial flange thicknesses of the ten wheels, which include the two sample wheels discussed above, range between 1.55 and 1.44 inches.

The differences in initial wheel measurements were eliminated by subtracting the initial measurements from each of the subsequent measurements. Figure 15

shows the plots of the cumulative wear data computed from the same group of flange thickness measurements; it shows the wear pattern for each wheel starting with 0.00 inch of wear at zero mileage and extending over 90,000 miles of service. Similarly, the wear data from rim thickness and flange height measurements can be plotted using the same wear intervals, scaled from 0.00 inch to 0.40 inch, on the (vertical) wear axis. Plotted in this form, the different wear patterns all pass through the origin.

The next step was to systematize the mileage values. As used in Figures 12 through 15, the mileage points between wheels were different but tended to occur at intervals of roughly 10,000 miles. Accordingly, the mileages were blocked in consecutive intervals of 10,000 miles, starting at zero mileage. Thus, initial measurements taken at the zero mileage point were collected under block 1, measurements taken between zero and 10,000 miles were collected under block 2, measurements taken between 10,000 and 20,000 miles were collected under block 3, and so on. In blocking the data in this fashion, it was assumed that all of the measurements were taken at the midpoints of the mileage blocks (see Table 7). Clearly, this assumption introduced some additional error into the data, but in return it permitted a more detailed analysis.

Now the wear measurements for a given mileage block can be directly compared to evaluate whether the difference observed between wheel types are real or whether they are only the result of random error.

In analyzing data, it is important to know both the spread of the data and the central tendency of the data. Instead of using the scatter diagrams of entire data sets, the trends can be shown more easily by plotting the 25th and 75th percentiles (known as quartiles), the extreme data points, and the median and mean values, on a single graph. Such a graph, illustrated for the example flange wear wheel type in Figure 16, summarizes the particular wear measure by mileage block for each of the various selected wheel types.

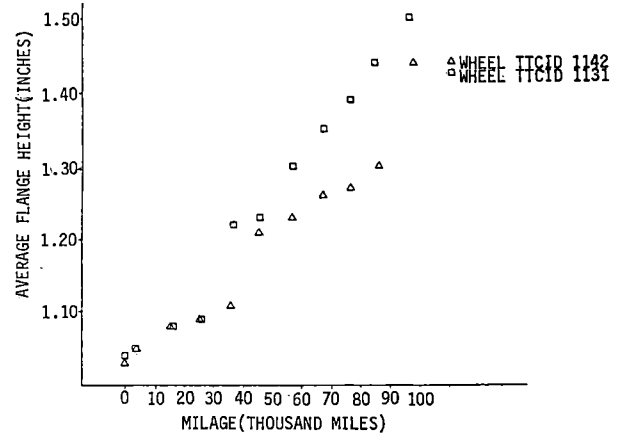


FIGURE 13. FLANGE HEIGHT VERSUS MILEAGE FOR TWO SAMPLE WHEELS OF SAME TYPE.

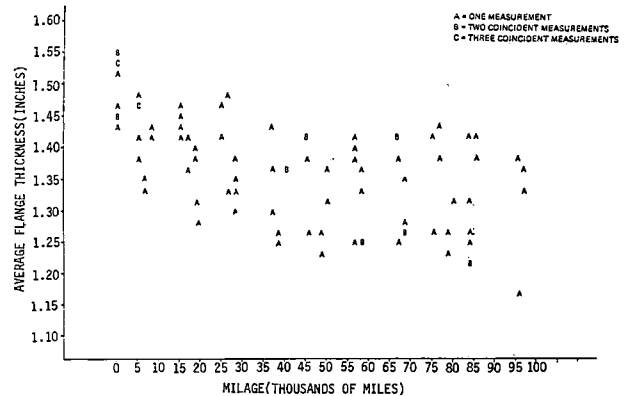


FIGURE 14. FLANGE THICKNESS VERSUS MILEAGE FOR 10 WHEELS OF SAME TYPE.

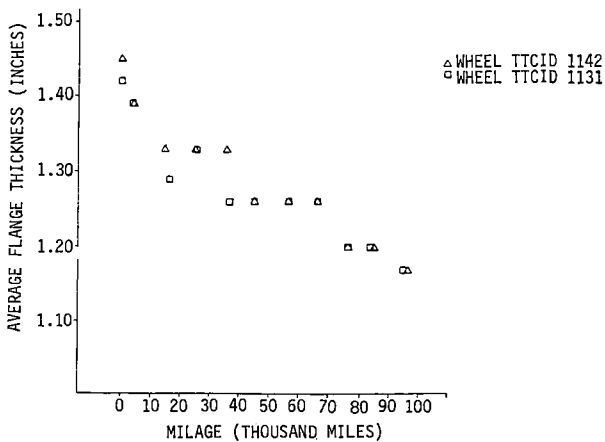


FIGURE 12. FLANGE THICKNESS VERSUS MILEAGE FOR TWO SAMPLE WHEELS OF SAME TYPE.

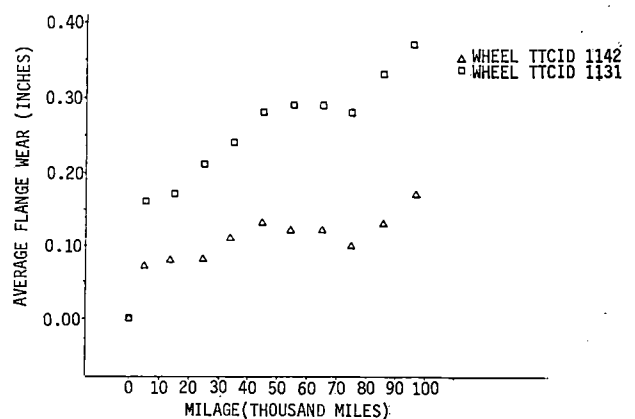


FIGURE 15. FLANGE WEAR VERSUS MILEAGE FOR TWO SAMPLE WHEELS OF SAME TYPE.

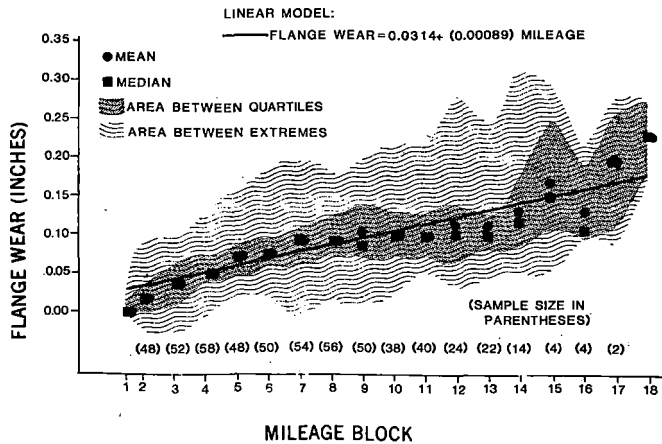


FIGURE 16. EXAMPLE OF FLANGE WEAR DATA IN SUMMARY FORM.

The darker shaded area on the graph represents the data between the quartiles and the lighter shaded area represents the outer 50 percent of the data, between the quartiles and the extremes. A straight line has been drawn across the graph, plotted from the linear regression model equation (also shown), which was developed from an ordinary least squares analysis of the data. Also shown is the number of wheels or samples in each mileage block, given in parentheses just above the horizontal axis.

Instead of using regression analysis to develop prediction models of wheel wear, as was done on the first experiment, regression was used primarily as a screening technique to identify those variables which made a significant contribution towards explaining the variation in the wheel wear data for each of the three wear measures - flange wear, flange height growth, and rim wear. The resulting variables were then used to group the data into wheel types made from the variable combinations for examination.

Several multiple regression techniques were reviewed for use in examining the relationships between the test variables and mileage. Of these techniques, the maximum R^2 improvement technique, developed by James H. Goodnight, is considered the most suitable because in each iterative step all of the test variables are scanned in order to determine the best one-variable model, the best two-variable model, and so on. F-ratios were computed for each variable entry to evaluate the significance of adding the new variable.

The multiple regression techniques were run on the wear data for each wheel wear measure using both a linear and a nonlinear regression formulation. The results of the regressions gave a summary of the data which served to limit the number of variables and determine the effective contribution of each variable (by means of a regression coefficient). Once the number of variables was reduced, graphical techniques were used to quantify and compare the selected variables and their combinations.

The general linear formulation used for the regression analysis was of the form:

$$\begin{array}{l} \text{flange wear} \\ \text{rim wear} \\ \text{flange height growth} \end{array} = A + (B) \text{ mileage}$$

Where A is the intercept at zero mileage and $B = B_0 + b_1 X_1 + b_2 X_2 + b_3 X_3 + b_4 X_4 + b_5 X_5$ X_1 to X_5 are the values of the model's dummy variables which represent the optional states of the actual test variables as follows:

- $X_1 = 1$ if wheel is cast
= 0 if wheel is wrought
- $X_2 = 1$ if wheel is 1 wear
= 0 if wheel is 2 wear
- $X_3 = 1$ if wheel is heat-treated
= 0 if wheel is non-heat-treated
- $X_4 = 1$ if wheel has 14-inch center plate
= 0 if wheel has 16-inch center plate
- $X_5 = 1$ if truck is type 1
= 0 if truck is type 2

Tables 8, 9, and 10 represent the summaries of results using the maximum R^2 improvement technique to acquire linear models for each of the three wear measures. The layout of the tables is designed to show the succession of significant variables as the model expands its number of parameters. In each case, mileage is the dependent response variable, s^2 is the error mean square, R^2 is the square of the multiple correlation coefficient, and F is the ratio of the Type II sum of the squares (SS)* to the standard error of estimate for the last variable entry.

*Type II sum of the squares (SS) is the SS that would be added to the error SS if that one variable were removed from the model.

Also given in each table is the wear model resulting from the regression analysis presented in the general linear form discussed earlier. While the maximum R^2 improvement technique permits every test variable entry into the model, those variables which did not meet a significance level of 0.01 were eliminated from the final model. So, all the variables remaining in the models presented in the Tables are significant to wear based on the F-statistic at the 0.01 level of significance. The elimination from the models of those variables insignificant at the 0.01 level represents the first phase of screening process used to group the wear data.

The model presented in Table 8 for flange wear shows three variables - mileage, treatment (X_3), and construction (X_1) - as having a significant effect on the flange wear data as summarized by the regression. The other variables - design (X_2), truck center plate diameter (X_4), and truck type (X_5) - were insignificant in the model's description of the flange wear data. The nonzero intercept of 0.0314 (inch) is a result of the deviation of the data from a perfect fit with the straight line formula: $y = bx$. Since the wear data had been normalized to zero in its translation from the measurement data, the line of best-fit theoretically should pass through the origin.

TABLE 7. MILEAGE BLOCK STATISTICS

Mileage Block Number	Mileage Range Thousands	Mileage Midpoint	Mean	n	Standard Deviation	Standard Error of Mean
1	0	0	0	234	0	0
2	0 to 10	5	6.2	178	2.65	0.199
3	10 to 20	15	15.0	218	3.24	0.219
4	20 to 30	25	25.1	217	3.00	0.204
5	30 to 40	35	35.2	215	3.00	0.205
6	40 to 50	45	45.2	223	2.93	0.196
7	50 to 60	55	55.4	194	2.86	0.205
8	60 to 70	65	64.9	196	3.06	0.218
9	70 to 80	75	75.2	201	2.90	0.205
10	80 to 90	85	85.1	186	3.06	0.225
11	90 to 100	95	95.0	146	3.25	0.269
12	100 to 110	105	104.7	109	3.15	0.302
13	110 to 120	115	114.3	63	3.24	0.409
14	120 to 130	125	124.5	56	2.55	0.341
15	130 to 140	135	135.8	26	2.01	0.592
16	140 to 150	145	145.8	18	2.93	0.692
17	150 to 160	155	154.5	6	3.25	1.330
18	160 to 170	165	163.0	2	N.A.	N.A.

TABLE 8. FLANGE WEAR LINEAR MODEL - SUMMARY OF RESULTS USING MAXIMUM R² IMPROVEMENT REGRESSION TECHNIQUE ON AAR STANDARD PROFILE WHEELS

Number of Parameters	x1	x2	x3	x4	x5	Mileage	s ²	R ²	F*
1						0	.0035	.3101	1117
2			0			0	.0025	.6132	1037
3	0		0			0	.0026	.6178	24
4	0	0	0			0	.0026	.5184	3
5	0	0	0	0		0	.0025	.5191	4
6	0	0	0	0	0	0	.0025	.5195	2

*F-value of last variable entered into corresponding 'N' variable model as shown. F-values rounded to nearest integer.

MODEL (summarized above):

$$Y = 0.0314 + (0.00182 + 0.00015 X1 - 0.00108 X3) \text{Mileage}$$

Variables in the model are significant at the 0.01 level of significance

KEY: X2: 1 IF WHEEL IS 1-WEAR X4: 1 IF TRUCK HAS 14-INCH PLATE
0 IF WHEEL IS 2-WEAR 0 IF TRUCK HAS 16-INCH PLATE

X1: 1 IF WHEEL IS CAST X3: 1 IF WHEEL IS HEAT-TREATED X5: 1 IF TRUCK IS TYPE 1
0 IF WHEEL IS WROUGHT 0 IF WHEEL IS NONHEAT-TREATED 0 IF TRUCK IS TYPE 2

TABLE 9. RIM WEAR LINEAR MODEL - SUMMARY OF RESULTS USING MAXIMUM R² IMPROVEMENT REGRESSION TECHNIQUE ON AAR STANDARD PROFILE WHEELS.

Number of Parameters	x1	x2	x3	x4	x5	Mileage	s ²	R ²	F*
1						o	.0023	.5498	3035
2			o			o	.0018	.6505	716
3	o		o			o	.0017	.6714	158
4	o	o	o			o	.0016	.6827	88
5	o	o	o		o	o	.0016	.6852	20
6	o	o	o	o	o	o	.0016	.6853	1

*F-value of last variable entered into corresponding 'N' variable model as shown. F-values rounded to nearest integer.

MODEL (summarized above):

$$Y = 0.01303 + (0.00179 + 0.00040 X1 - 0.00026 X2 - 0.00080 X3 - 0.00011 X5) \text{Mileage}$$

Variables in the model are significant at the 0.01 level of significance

KEY: X2: 1 IF WHEEL IS 1-WEAR X4: 1 IF TRUCK HAS 14-INCH PLATE
0 IF WHEEL IS 2-WEAR 0 IF TRUCK HAS 16-INCH PLATE

X1: 1 IF WHEEL IS CAST X3: 1 IF WHEEL IS HEAT-TREATED X5: 1 IF TRUCK IS TYPE 1
0 IF WHEEL IS WROUGHT 0 IF WHEEL IS NONHEAT-TREATED 0 IF TRUCK IS TYPE 2

TABLE 10. FLANGE HEIGHT GROWTH LINEAR MODEL - SUMMARY OF RESULTS USING MAXIMUM R² - IMPROVEMENT REGRESSION TECHNIQUE ON AAR PROFILE WHEEL.

Number of Parameters	x1	x2	x3	x4	x5	Mileage	s ²	R ²	F*
1						o	.0040	.5798	3430
2			o			o	.0021	.7799	2260
3	o		o			o	.0020	.7873	86
4	o	o	o			o	.0019	.7941	83
5	o	o	o		o	o	.0019	.7961	24
6	o	o	o	o	o	o	.0019	.7971	8

*F-value of last variable entered into corresponding 'N' variable model as shown. F-values rounded to nearest integer.

MODEL (summarized above):

$$Y = 0.00298 + (0.00293 + 0.00035 X1 - 0.00028 X2 - 0.00149 X3 - 0.00008 X4 - 0.00013 X5) \text{Mileage}$$

Variables in the model are significant at the 0.01 level of significance

KEY: X2: 1 IF WHEEL IS 1-WEAR X4: 1 IF TRUCK HAS 14-INCH PLATE
0 IF WHEEL IS 2-WEAR 0 IF TRUCK HAS 16-INCH PLATE

X1: 1 IF WHEEL IS CAST X3: 1 IF WHEEL IS HEAT-TREATED X5: 1 IF TRUCK IS TYPE 1
0 IF WHEEL IS WROUGHT 0 IF WHEEL IS NONHEAT-TREATED 0 IF TRUCK IS TYPE 2

The coefficients are analogous to the units of wear in inch(es) per 1,000 miles and the sign of the coefficient indicates which of the dummy variables improves wheel performance based on the regression model. For instance, a negative coefficient of X3 means that whenever X3 = 1, the overall wear rate (expressed by B in the equation: Wear = A + (B) mileage) will be depressed, resulting in less wear. Since X3 = 1 denotes a heat-treated wheel, a negative coefficient for X3 would signify that heat-treated wheels will show less wear than nonheat-treated wheels (i.e. X3 = 0) using the regression model. Of course, if the coefficient has a positive sign, then the reverse is true - that is, the overall wear rate (B) will be increased, resulting in more wear.

The results of the model, displayed in Table 8, show that 31 percent (R^2) of the flange wear is explained solely by the mileage variable, with an increase to 51 percent with the entry of the treatment variable (X3). Further increases in R^2 with the entry of the remaining variables are shown to be minimal. This is reflected in the drop of the F value with the entry of the construction variable (X1). The entries after X1 were found to have an insignificant effect on flange wear at the 0.01 level of significance.

It is important to note that these relationships expressed by the regression model coefficients hold only in the real world to the extent that the model only explains about 52 percent (R^2 is 0.5178) of the variation in wear - that is, 48 percent of the variation in the flange wear measurements is not explained by the model - the coefficients and numbers contained in the model (and the other models, as well) should be interpreted and applied with that qualified caution.

The rim wear model results, presented in Table 9, show that 68 percent of the rim wear is explainable using a four (or five variable model). They show that 55 percent of rim wear is explained solely by the mileage variable, with an increase to 65 percent with the entry of the treatment variable (X3). The additional entry of the construction variable (X1) increases the R^2 to 67 percent, and the entry of the design variable (X2) further increases the R^2 to 68 percent. Although the center plate diameter variable (X4) does have a significant effect at the 0.01 level, the two truck variables produce only minimal increases in R^2 , as reflected in the drop in the F value.

The results summarized in Table 10 indicate that nearly 80 percent of the flange height growth is explainable using a six-variable model. The results show that 58 percent of the flange height growth is explained solely by the mileage variable, with an increase to 78 percent with the entry of the treatment variable (X3). Further increases in R^2 with the entries of the remaining variables are shown to be small, with a further increase of only 0.7 percent with the entry of each of two variables, construction (X1) and design (X2). The remaining variables, center plate diameter (X4) and truck type (X5), while shown to be significant at the 0.01 level, effect a minimal increase in R^2 - 0.2 and 0.1 percent, respectively. This is reflected in the drop of the F value with the entry of these variables.

The three wear measures also were analyzed using a nonlinear or curvilinear model formulation. The basic linear formula was transformed using logarithms into a nonlinear formulation where the variable (X) became a power function of the mileage. This was done by replacing the variables in the linear model with the logarithm of the variables. Thus, the wear became the log (wear) and the mileage became log (mileage + 1). The "1" was added to the mileage to avoid taking the logarithm of "0", (Since mileage is expressed in thousands throughout this analysis, this addition is equivalent to sliding the mileage scale forward by 1,000 miles). The nonlinear formulation, then, used for the regression analysis was of the form:

$$\text{Wear} = A (\text{mileage} + 1)^B$$

Where $B = b_0 + b_1 X_1 + b_2 X_2 + b_3 X_3 + b_4 X_4 + b_5 X_5$ and X_1 to X_5 are dummy variables defined as described earlier.

Regressions also were run using the addition of 10,000 miles i.e., log (mileage + 10), to parallel the formulation used in the first experiment analysis.² In both cases, the nonlinear models did not show a significant improvement over the linear model and thus were not used in this analysis. No further explorations were carried out to try to find other possibly more complex models which might better explain the variation in the data.

To further reduce the number of variables in each of the three wear models, the incremental yields in R^2 improvement were looked at for each variable entry. Those variables which did not increase the overall R^2 by a 0.5 percentage point and showed low regression model coefficients (below 0.00020) were scrutinized for possible elimination. Table 11 dis-

plays for each wear measure (i.e., flange wear, flange growth, and rim wear) the F-value and the incremental improvement in the R^2 for the entry of each new variable selected by the regression technique. A dotted line is drawn on Table 11 above which lie those variables in each model considered to be important for further study.

In the case of the flange wear model, the criteria for selection are based primarily on the improvement of R^2 acknowledging that the F-value associated with the entry of the construction variable is outside the F-ratio criteria for selection. While the construction variable contributes only slightly more than the other nonselected variables, there was interest expressed in a flange wear comparison between cast and wrought wheels which stemmed from remarks published in the first wheel experiment report. Thus, for the flange wear analysis, both treatment and construction were considered the important variables to be used to examine the flange wear data.

In the case of the rim wear model, the important variables were selected by the same criteria - that is, incremental increase in the overall R^2 by a 0.05 percentage point. With regard to the overall R^2 this model as compared to the previous flange wear model shows a better correlation with the data (evidenced by the overall R^2 of .6853), referring to Table 9.

TABLE 11. F - VALUE AND INCREMENTAL IMPROVEMENT OF R²
FOR ENTRY OF EACH NEW VARIABLE SELECTED BY REGRESSION

Number of Parameters	Flange Wear		Flange Growth		Rim Wear	
	Improvement of R ²	F-Value	Improvement of R ²	F-Value	Improvement of R ²	F-Value
2 (X3)	.2031	1038 (X3)	.2001	2260 (X3)	.1007	716
3 (X1)	.0046	24 (X1)	.0074	86 (X1)	.0209	158

4 (X2)	.0006	3 (X2)	.0068	83 (X2)	.0113	88

5 (X4)	.0007	4 (X5)	.0020	24 (X5)	.0025	20
6 (X5)	.0004	2 (X4)	.0010	8 (X4)	.0001	1

Among the five test variables, treatment again shows the most contributive effect. After treatment, construction and then design show statistically significant effects. The relative effects of the other two variables, truck center plate diameter and truck type were much smaller. Thus, for the rim wear data analysis, the variables treatment, construction, and design were considered to be the important variables to study.

The variables selected for flange height growth were similarly determined. Once again, the treatment variable provided the greatest contribution among the test variables, followed by construction, design, truck-type, and truck center plate diameter in order of significance based on the F-statistic. The contribution of truck center plate diameter and truck type were very small. Thus, only the variables treatment, construction, and design were considered important for further study.

Using the mean wear values which are plotted on the summary graphs, variables selected in the regression studies were examined for each wear measure. This was accomplished by holding constant other variable(s) contained in each wheel type and graphically comparing the plotted mean values. As an example, in the examination of the effect of the treatment variable on flange wear, the construction variable was held constant (i.e., wrought wheel and cast wheel flange wear plots were not compared) and for each similar construction type wheel group, the mean flange wear plot of nonheat-treated wheels was compared to the mean flange wear plot of heat-treated wheels. Differences observed between the two means at each mileage block were tested for significance using Student's t-test. The results of significance testing were then presented in tabular form appraising whether or not the differences were within the confidence levels of 95 and 99 percent. This procedure was followed for each of the significant variables for each wear measure.

Further analysis of the effects of the selected variables on the different wear measures examined the initial wear-in, a wear phenomenon which oc-

curred during the initial 5,000 to 15,000 miles of wheel travel at FAST. A nonparametric test procedure was used to examine the significance in initial wear among important wheel types. Differences in initial (new wheel) measurements also were analyzed, examining the combined effects of initial wheel size (i.e., flange thickness, flange height, and rim thickness) and wheel wear for specific wheel types.

Since only a few of the test wheels reached condemning limits in this experiment, estimated mileages were determined for different wheel types using the previously developed prediction models in order to compare the wear from the viewpoint of wheel performance prior to condemnation and removal. The arbitrary wheel dimensions specified for these mileage prediction exercises are defined as follows:

- A. Flange thickness worn to 1.25 inches (regardless of wheel type)
- B. Rim thickness worn to 2.00 inches for 2-wear (design) wheels and worn to 1.50 inches for 1-wear (design) wheels, and
- C. Flange height worn to 1.25 inches (regardless of wheel type).

Using these limits and allowing for differences in values as well as initial wear-in, mileage results obtained represent approximately ¼ inch of wear for each of the above measurements.

In examining the treatment variable, a comparison of nonheat-treated and heat-treated wheels, cast or wrought wheel types, indicates that the rate of flange wear is more favorable with heat-treated wheels. This finding is illustrated in Figures 17 and 18 which represent comparative plots, mean flange wear versus mileage block, of nonheat-treated and heat-treated wheel samples for wrought wheel and cast wheel types, respectively. The t-statistics of the statistical Tables 12 and 13, associated with the two respective figures show that the differences

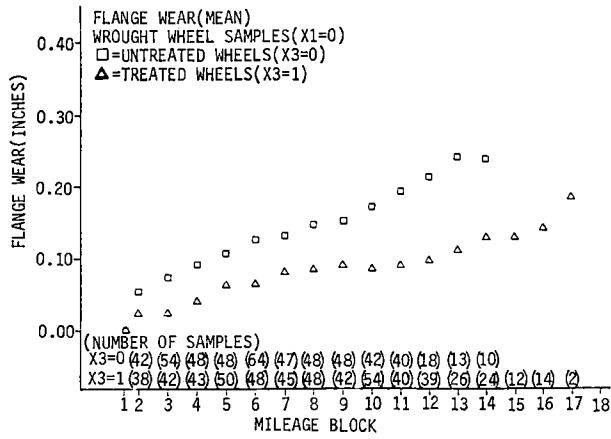


FIGURE 17. MEAN FLANGE WEAR VERSUS MILEAGE BLOCK PLOTS OF NONHEAT-TREATED AND HEAT-TREATED WROUGHT WHEELS (AAR STANDARD PROFILE).

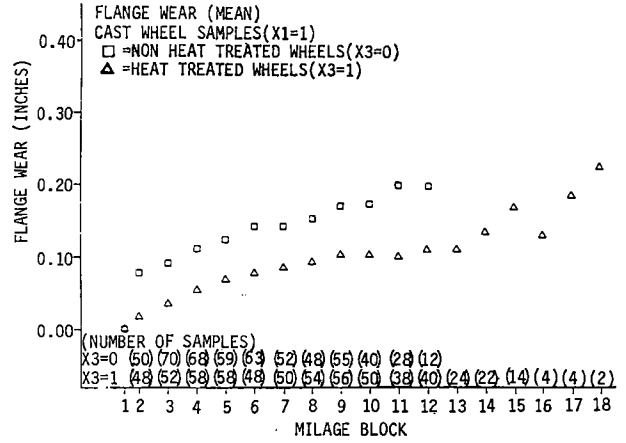


FIGURE 18. MEAN FLANGE WEAR VERSUS MILEAGE BLOCK PLOTS OF NONHEAT-TREATED CAST WHEELS (AAR STANDARD PROFILE).

TABLE 12. RESULTS OF SIGNIFICANCE TESTING ON DIFFERENCES IN MEAN FLANGE WEAR PER BLOCK ON NONHEAT-TREATED VERSUS HEAT-TREATED WROUGHT WHEELS

Mileage Block	Difference in Means ($\bar{x} - \bar{x}$)		t Statistic	Significant at 95% Confidence Level	Significant at 99% Confidence Level
	1	2			
1	0		-	-	-
2	.0285		3.695	Yes	Yes
3	.0504		7.273	Yes	Yes
4	.0502		6.491	Yes	Yes
5	.0444		6.094	Yes	Yes
6	.0605		7.135	Yes	Yes
7	.0488		5.428	Yes	Yes
8	.0621		6.450	Yes	Yes
9	.0646		6.148	Yes	Yes
10	.0837		7.470	Yes	Yes
11	.1027		8.682	Yes	Yes
12	.1178		9.202	Yes	Yes
13	.1315		6.289	Yes	Yes
14	.1082		5.281	Yes	Yes

TABLE 13. RESULTS OF SIGNIFICANCE TESTING ON DIFFERENCES IN MEAN FLANGE WEAR PER BLOCK OF NONHEAT-TREATED VERSUS HEAT-TREATED CAST WHEELS

Mileage Block	Difference in Means (x - x)		t Statistic	Significant at 95% Confidence Level	Significant at 99% Confidence Level
	1	2			
1	0		-	-	-
2	.0607		6.661	Yes	Yes
3	.0553		7.448	Yes	Yes
4	.0570		7.382	Yes	Yes
5	.0562		5.909	Yes	Yes
6	.0649		5.650	Yes	Yes
7	.0556		4.890	Yes	Yes
8	.0604		5.491	Yes	Yes
9	.0679		6.036	Yes	Yes
10	.0699		5.315	Yes	Yes
11	.0957		6.550	Yes	Yes
12	0862		4.275	Yes	Yes

in mean flange wear between nonheat-treated and heat-treated wheel samples are significant throughout, at the 99 percent confidence level (0.01 level of significance).

Treatment had a major effect on flange wear, rim wear, and flange height growth. The effect was that heat-treated wheels showed significantly better performance (i.e., less wear) than nonheat-treated wheels for each of the three wear measures. This finding is evidenced in the results of the regression analysis using the data of each of these three wear measures which showed treatment to be by far the most significant variable relative to the other four--that is, construction, design, plate diameter, and truck type.

The differences in the mean flange wear between the nonheat-treated and heat-treated wheels were significant at the 99 percent confidence level at every mileage block observed. The differences per mileage block for wrought wheel samples tended to show value increases in the differences in mean flange wear, with higher mileage blocks ranging from 0.00285 of an inch at block 2 to 0.1313 of an inch at block 13. The cast wheel samples appeared, however, to have more consistent differences, ranging between 0.0553 and 0.0957 of an inch of flange wear, along mileage blocks 1 to 12.

The differences in mean rim wear between nonheat-treated and heat-treated wheels, although not as great as the differences observed in mean flange wear, also generally showed value increases with higher mileage blocks. The differences per mileage block were shown to be significant at the 99 percent confidence level for all wheel types in the majority

of mileage blocks beyond block 3. The difference between nonheat-treated and heat-treated wheels shown at mileage block 2 (0 to 10,000 miles) was not significant at the 95 percent confidence level for any wheel type, and the wrought 2-wear wheels did not show a significant difference between nonheat-treated and heat-treated wheels at mileage block 3 (10,000 to 20,000 miles).

The mean flange growth differences between nonheat-treated and heat-treated wheels, also showing value increases with higher mileage blocks, were significant at the 99 percent confidence level at most if not all of the mileage blocks for each of the four wheel types. The exceptions are primarily at the initial mileage blocks of the wrought 2-wear wheels which generally showed the mean flange growth differences to be significant only at the 95 percent confidence level. Moreover, neither the wrought nor the the cast 2-wear wheels showed a significant (at 95 percent) difference in mean flange growth at block 2.

While there generally were no significant differences in the mean initial wheel dimensions, that is, flange thickness, rim thickness, and flange height, between nonheat-treated and heat-treated wheels, there were exceptions by wheel type to this generalization regarding initial flange thickness and height. Among wrought 2-wear wheels, the nonheat-treated wheel samples were shown to have a greater mean initial flange thickness than the heat-treated samples by a difference of 0.030 of an inch, which was significant at the 99 percent confidence level. Among the cast 2-wear wheels, heat-treated wheel samples were shown to have a mean initial flange dimension which was 0.014 of an inch thicker than

nonheat-treated wheel samples, a difference which was significant only at the 95 percent level. In terms of initial flange height, the only significant difference between nonheat-treated and heat-treated wheel samples was for the cast 1-wear wheels which showed the heat-treated wheel greater in mean height by 0.015 of an inch, which was significant at the 99 percent level.

In light of these differences in initial wheel measurements, the results of the exercise using the linear regression models of each wear measure to predict the estimated mileages to reach the specified wheel dimension indicate that heat-treated wheels appear to have a greater service life potential than nonheat-treated wheels, regardless of their construction or design. A comparison of the predicted mileages with regard to flange wear, shown in Table 14 gives ratios of nonheat-treated wheel to heat-treated wheel estimates of 2.35 and 2.61. The ratios shown for the nonheat-treated to heat-treated comparisons of the predicted mileages regarding rim thickness are between 1.59 and 2.50, and the ratios shown regarding flange growth are between 1.61 and 1.84. While these ratios were derived from predicted mileages using regression estimates, they do seem to summarize the general results observed earlier in the different wear plot comparisons among the various wheel types - that is, heat-treated wheels appear to experience significantly less wear than nonheat-treated wheels.

Wrought steel wheels and cast steel make up the two options of the construction variable. The construction variable was observed only to have an effect on the rim wear and flange height growth of the non-heat-treated wheel samples. Wrought non-heat-treated wheels generally showed significantly less wear than cast nonheat-treated wheels for rim wear and flange height growth. This finding is illustrated in Figures 19 and 20, which show the differences in mean wear between the two construction options for rim wear and flange height growth. This finding is illustrated in the two construction options for rim wear and flange height growth, respectively.

Although, construction was shown in the regression results to have a significant effect on flange wear at the 99 percent confidence level, the amount of flange wear accountable to construction was practically minimal. In the comparisons of flange wear plots, the differences between wrought and cast wheels were shown to be significant for the non-heat-treated wheel samples only at the mileage blocks (2 through 4). The heat-treated wheel samples generally showed no significant difference in mean flange wear at the 95 percent confidence level.

In examining the differences in the mean rim wear plots between wrought and cast nonheat-treated wheels, it was observed that the values generally

TABLE 14. NON-TREATED TO HEAT-TREATED COMPARISONS OF PREDICTED MILEAGES BY WHEEL TYPE FOR EACH WEAR MEASURE.

Wear Measure	Wheel Type	PREDICTED MILEAGE (thousands)		
		Nonheat-Treated Wheels	Heat-Treated Wheels	Ratio (Heat) (Nonheat)
Flange wear	Wrought	101.429	238.649	2.35
Flange wear	Cast	93.706	244.494	2.61
Rim wear	Wrought 1-wear	108.474	197.957	1.82
Rim wear	Cast 1-wear	80.767	128.414	1.59
Rim wear	Wrought 2-wear	130.181	216.967	1.67
Rim wear	Cast 2-wear	63.796	159.553	2.50
Flange height growth	Wrought 1-wear	65.414	120.337	1.84
Flange height growth	Cast 1-wear	64.882	104.338	1.61
Flange height growth	Wrought 2-wear	73.372	123.826	1.69
Flange height growth	Cast 2-wear	68.917	115.615	1.68

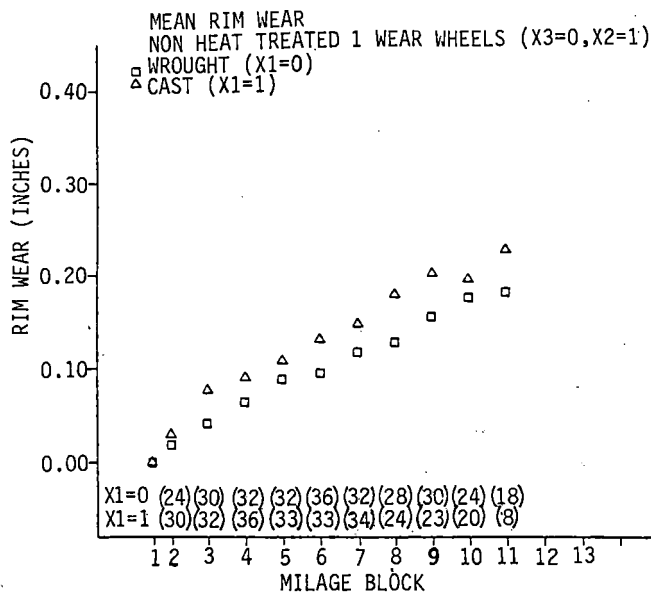


FIGURE 19. MEAN RIM WEAR VERSUS MILEAGE BLOCK PLOTS OF WROUGHT AND CAST NONHEAT-TREATED 1-WEAR WHEELS (AAR STANDARD PROFILE).

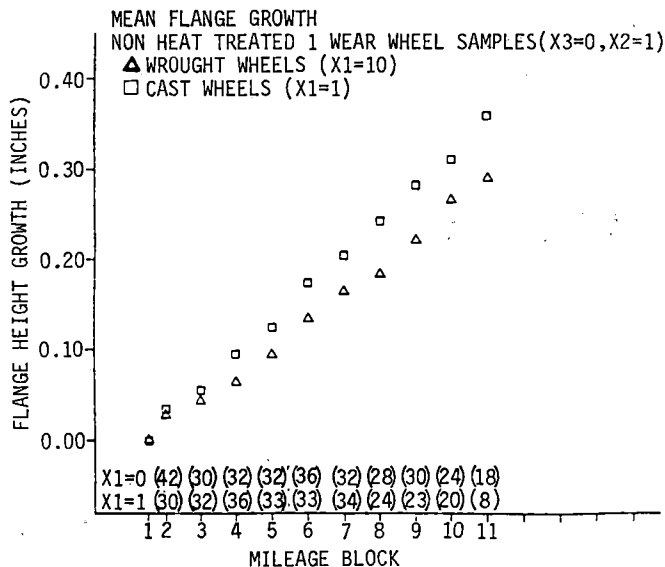


FIGURE 20. MEAN FLANGE HEIGHT GROWTH VERSUS MILEAGE BLOCK PLOTS OF WROUGHT AND CAST NONHEAT-TREATED 1-WEAR WHEELS (AAR STANDARD PROFILE).

appeared to be consistent along the mileage blocks - that is, the tendency of value increases with higher mileage blocks shown earlier between the two treatment options was not apparent in the comparison of the construction options for rim wear.

In the comparison of the mean flange height growth plots, however, the differences of the nonheat-treated 1-wear samples between wrought and cast showed a tendency for value increases with higher mileage blocks. The nonheat-treated 2-wear samples, however, did not exemplify that tendency, showing a

roughly consistent difference between wrought and cast wheels along the mileage blocks.

In terms of initial wheel dimensions, the new cast wheels in general appeared to have a thicker flange than new wrought wheels. Only the heat-treated 2-wear wheel samples showed no significant difference in flange thickness between cast and wrought wheels at the 95 percent confidence level. The other three wheel types all showed differences which were significant at the 99 percent level. For the 1-wear wheel samples, both nonheat-treated and heat-treated, these differences in mean initial flange thickness between cast and wrought wheels were each 0.05 of an inch. For the heat-treated 2-wear wheel type, the difference was 0.03 of an inch.

In addition, new wrought nonheat-treated wheels generally tended to show a higher flange than new cast nonheat-treated wheels. The difference in mean flange height between wrought and cast wheels was significant at the 99 percent level for 1-wear nonheat-treated samples (with a difference of 0.02 of an inch) and 95 percent for 2-wear nonheat-treated samples (with a difference of 0.01 of an inch). The heat-treated wheel samples showed no significant differences in mean initial flange height between wrought and cast wheels at the 95 percent confidence level.

The differences in mean initial rim thickness between cast and wrought wheels generally was not significant at the 95 percent level. The exception by wheel type was that nonheat-treated 2-wear wheels showed a difference in mean of 0.09 of an inch, which was significant to the 99 percent confidence level.

With this information, the results of the prediction exercises using the linear regression models of each wear measure to determine estimated mileage to wheel generally indicates wrought wheels perform better than cast wheels. The ratios derived from the predicted mileage given in Table 15 were greatest for rim wear, particularly among the 2-wear wheel samples, with ratios ranging 1.34 to 2.04. The ratios derived for flange wear and flange height growth, however, were close to 1, ranging from 0.98 to 1.15. To draw conclusions from these ratios is difficult, especially since they were derived using regression estimates. But, the ratios do seem to support at least the observation that wrought wheels perform better (show less wear) than cast wheels with regard to rim wear.

The design in the second wheel experiment consisted of the two wheel design options, 2-wear and 1-wear. This variable appeared only to have a possible effect on flange growth, where 2-wear wheels generally were observed to have less flange height growth than 1-wear wheels. While the design variable was considered important to study with regard to rim wear, the observed differences in mean flange height growth, were not significant (at 95 percent). As previously stated, design was not shown to effect flange wear.

With regard to initial wheel dimensions, aside from the designed difference in rim thickness, initial flange thickness appears to be slightly greater in 1-wear cast wheels than in 2-wear cast wheels but slightly greater in 2-wear wrought wheels than in 1-wear wrought wheels. There was generally no

TABLE 15. WROUGHT TO CAST COMPARISONS OF PREDICTED MILEAGES BY WHEEL TYPE FOR EACH WEAR MEASURE

Wear Measure	Wheel Type	PREDICTED MILEAGE (thousands)		
		Wrought Wheels	Cast Wheels	Ratio: (Wrought) (Cast)
Flange wear	Nonheat-treated	101.429	93.706	1.08
Flange wear	Heat-treated	239.649	244.494	0.98
Rim wear	NonHeat-treated, 1-wear	108.474	80.767	1.34
Rim wear	Heat-treated, 1-wear	197.957	128.414	1.54
Rim wear	Nonheat-treated 2-wear	130.181	63.796	2.04
Rim wear	Heat-treated 2-wear	216.967	159.553	1.36
Flange height growth	Nonheat-treated, 1-wear	65.414	64.882	1.01
Flange height growth	Heat-treated, 1-wear	73.372	68.917	1.06
Flange height growth	Nonheat-treated, 2-wear	120.337	104.338	1.15
Flange height growth	Heat-treated, cast	123.826	115.615	1.07

TABLE 16. 1-WEAR TO 2-WEAR COMPARISONS OF PREDICTED MILEAGES BY WHEEL TYPE FOR EACH WEAR MEASURE.

Wear Measure	Wheel Type	PREDICTED MILEAGE (thousands)		
		1-wear Wheels	2-wear Wheels	(2-wear) (1-wear)
Rim wear	Nonheat-treated, wrought	108.474	130.181	1.20
Rim wear	Nonheat-treated, cast	80.767	63.796	0.79
Rim wear	Heat-treated, wrought	197.957	216.967	1.10
Rim wear	Heat-treated, cast	128.414	159.553	1.24
Flange height growth	Nonheat-treated, wrought	65.414	73.372	1.12
Flange height growth	Nonheat-treated, cast	64.882	68.917	1.06
Flange height growth	Heat-treated, wrought	120.337	123.826	1.03
Flange height growth	Heat-treated, cast	104.338	115.615	1.11

significant difference (at 95 percent) in flange height between 2-wear and 1-wear wheels.

Examining the predicted mileages using the linear regression model of flange height growth and recalling that the predictions were based on different rim thickness measurements which approximated the same amount of wear, the 2-wear wheels overall show slightly higher estimated mileages than 1-wear wheels. However, the ratios derived from these estimates, ranging from 1.03 to 1.12, as shown in Table 16, indicate that the difference in wheel performance between 2-wear and 1-wear wheels is practically minimal with regard to flange height growth. The ratios derived from the predicted mileages using the rim wear linear model are shown to range between 0.79 and 1.24, indicating also that the differences in wheel performance between the two design options is not very great. No predicted mileage comparisons were made for the flange wear measures since the design variable was not identified in the regression analysis of the flange wear data as a significant variable.

Examination of the regression results for each of the three wear measures with reference to 16-inch and 14-inch center plates revealed that the effect of this variable on wheel wear is negligible. In the summary of regression results on the flange wear data, the center plate diameter was not shown to be significant in its effect on flange wear at the 99 percent confidence level. Similar results were shown for rim wear -- that is, plate diameter effects on rim wear were not shown to be significant at the 99 percent confidence level (see Table 9). Finally, while center plate diameter was shown to have a significant effect on flange height growth, its effect was the least was the least significant of the five variables, accounting in the regression model for a minimal amount of flange height growth (0.00008 inch per 1,000 miles) if the plate diameter option was the 14-inch.

Two truck types made up the truck variable in the second wheel experiment. They were defined as type 1 and type 2 trucks. The type 1 truck has a snubbing system with a built-in design for maintaining a constant spring force dampening. The type 2 truck uses a built-in snubbing system that provides variable, or load-sensitive, dampening.

Examination of the regression models of each of the wear measures revealed that the truck type variable is not shown to be significant at the 99 percent confidence level for explaining flange wear, and its effects account for only a minimal amount of rim wear and flange height growth. From the regression results on the rim wear data, the truck type variable is shown to have a significant effect on rim wear at the 99 percent confidence level, but its effect is the least significant of the variables represented in the model, accounting for a rim wear of 0.00011 inch per 1,000 miles if the truck type is type 1. For flange height growth, the regression results indicated that the effects of the truck type when compared with the other variables, although significant at the 99 percent level, are practically minimal with regard to an accountable flange height growth, similar to the amount shown for the rim wear model.

The second group of wheels in the second experiment were used to examine the effects of profile, repro-

filing (new and worn wheels), initial rim hardness and wheel chemistry on wheel wear. Comparisons were made between new AAR and CN profiles, between AAR profiles and reprofiled (after wear) and between CN profiles as received and CN turned profiles to represent the CN wheels used in the first experiment. Additional comparisons included wheels with normal Class C hardness values (321-363 BHN) versus wheels with rim hardness values between 364 and 400 BHN, referred to as B-400 wheels. Also, the effects of carbon content for the available range of 0.65 to 0.78% were examined.

The results of analysis conducted on these additional variables are summarized in the next few paragraphs. In comparing new AAR and CN profiles, no significant difference was observed in the three wear measures among the heat-treated wheels. However, for the untreated wheels, rim wear was found to be significantly lower on wheels with AAR profiles. The resulting difference in rim wear for the untreated AAR and CN profile wheels is shown graphically in Figure 21.

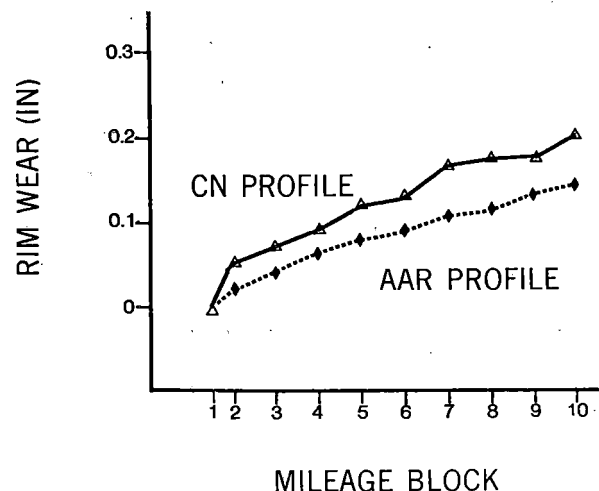


FIGURE 21. EFFECT OF WHEEL PROFILE ON RIM WEAR FOR UNTREATED WROUGHT WHEELS.

The results of reprofiling indicate no significant differences exist in the three wear measures between new and turned (worn wheels) with AAR profiles. However, new CN profile wheels which were turned to represent those used in the first experiment showed significantly lower flange wear than those tested as received.*

The effects of rim hardness indicate no significant difference exist in either flange wear or rim wear between Class C and B-400 wheels. However, flange height growth was found to be greater on the B-400 wheels than on the normal C wheels. And finally, differences in carbon content did not indicate a strong linear relationship with measured wheel wear.

In summary, the analysis of the second wheel experiment data leads to several conclusions regarding the

*A recent review of the initial profile data indicates that there may be some minor differences between the CN profiles turned and those as received in the flange/tread fillet design only. Initial indications are that the as-received profiles were different than specified.

process of wheel wear on the FAST track. The conclusions are as follows:

- A. Heat-treated test wheels consistently showed significantly less measured wear than nonheat-treated test wheels regardless of which other test variable options they possessed (e.g. wrought or cast, 2-wear or 1-wear, etc.).
- B. Wrought test wheels and cast test wheels showed no significant difference in mean measured wear, with this exception: wrought nonheat-treated test wheels showed significantly less measured wear than cast nonheat-treated test wheels with regard to rim thickness and flange height. This difference in rim wear performance may be influenced by a axle position effect.
- C. 2-wear test wheels and 1-wear test wheels showed no significant difference in mean measured wear, with this exception: 2-wear test wheels generally were observed to have less measured wear than 1-wear test wheels with regard to flange height.
- D. Neither truck center plate diameter nor truck type were shown to have a large affect on wheel wear.
- E. "High flange" was the primary reason for the removal of test wheels from service and affected far more nonheat-treated wheels than heat-treated wheels.
- F. Canadian National (CN) profile test wheels and AAR standard profile wheels showed no significant difference in mean measured wear, with this exception: AAR nonheat-treated test wheels generally showed significantly less measured wear than CN nonheat-treated test wheels with regard to rim thickness and flange height.

Figure 22 presents a graphical comparison between the mean flange wear which resulted on the first and second experiments. The two lower curves depict the excessive flange wear rates which occurred during the first experiment for both untreated (U) and treated (C) wheels. The sizeable decrease in wear rate for the Class C wheels at approximately 25,000 miles reflects mainly the change in rail lubricant which occurred at about that point in the test. The upper two curves show the corresponding wear for U and C wheels in the second experiment. The initial

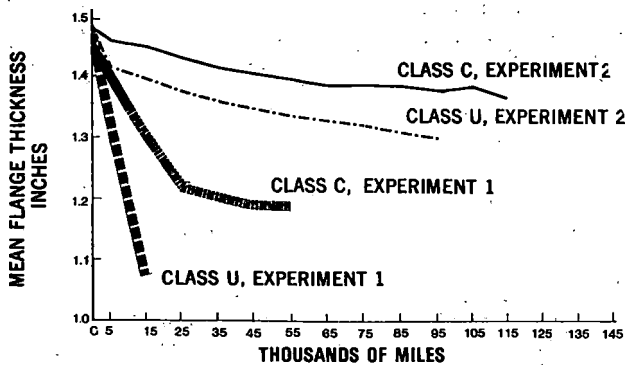


FIGURE 22. COMPARISON OF FLANGE WEAR BETWEEN FIRST AND SECOND EXPERIMENT.

wear-in which occurred during the first 5,000 to 15,000 miles is also visible. And finally, it is of interest to point out that the mean flange wear for C wheels in the lubricated portion of the first experiment (i.e., after 25,000 miles) is in good agreement with that obtained for C wheels in the second experiment.

A FAST report addressing the complete analysis of the second wheel experiment data is in the process of being reviewed for publication and will provide a more in-depth analysis of the data, especially that obtained for the second wheel group.

THIRD EXPERIMENT

The third experiment - still-on-going and - referred to as the variable axle load test (VALT) - was established primarily to examine the relationship between axle loading and wheel wear for both lubricated and unlubricated track conditions. A secondary objective is to examine possible effects of truck snubbing design on wheel wear for loaded (100-Ton) and empty lading conditions. It should be recalled that truck snubbing was statistically significant in the first wheel experiment but was not considered a major factor.

Test conditions for this experiment which are different from the first two experiments include:

- o Using 16 cars of variable loading,
- o Operating on both dry and lubricated track,
- o Using all untreated wheels, and
- o A slightly lower average % of premium rail in curves from that used in Wheels II.

In addition, the measurement interval was reduced from 11,000 miles to 1,000 miles during unlubricated test periods to allow for the expected increase in wear rates.

The experiment design consists of 128 test wheels distributed among six car loadings ranging from empty to 110-tons as shown in Table 17. Sixteen cars are equipped with variable snubbing type trucks - two at 100-tons and two empty.

The wheel measurements include the same six taken for the prior two experiments. The first three measurements were obtained initially using both the finger gage and the new more accurate wheel snap gage, pictured in Figure 23. This instrument, which is described in the proceeding paper "Evolution of Measurement Techniques at FAST", allows us to obtain all three measurements at once and with much improved accuracy over the finger gage. For these reasons, it has replaced the finger gage for this and future wheel experiments at FAST.

The VALT wheels have to-date accumulated a total of approximately 42,000 miles - 14,000 miles unlubricated and 28,000 miles lubricated as shown in Table 18. The remainder of this discussion on the third wheel experiment will address preliminary results obtained to date in the unlubricated "dry track" testing only.

TRUCK	NUMBER OF WHEELS					
	CAR LOADING					
	EMPTY	33 TONS	66 TONS	80 TONS	100 TONS	110 TONS
TYPE II*	16	16	16	16	16	16
TYPE I	16	0	0	0	16	0

TABLE 17. EXPERIMENT DESIGN MATRIX FOR WHEELS III

DATES	APPROXIMATE DURATION	TRACK CONDITION
MAY 1980	7,000 MILES	UNLUBRICATED
NOV/DEC 1980	7,000 MILES	UNLUBRICATED
JAN/FEB 1981	14,000 MILES	LUBRICATED
APR/MAY 1981	14,000 MILES	LUBRICATED

TABLE 18. WHEELS III STATUS



FIGURE 23. WHEEL SNAP GAGE

Figures 24 and 25 show typical flange thickness versus mileage plot obtained during the unlubricated portion of the test. Figure 24 shows the flange wear pattern for four wheels under one truck of an empty car while Figure 25 provides similar data for one truck set of wheels for a car laden to 100-tons. Comparing the two figures, one can easily see the increase in flange wear due to axle loading as evidenced by the steeper slope for the 100-ton car wheels. It should be noted that the wear pattern shown in the first two thousand miles (see Figure 25) resulted from the combination of a very high wear rate and not turning the train frequently enough. After the two thousand mile measurement point, the train was turned after each eight hour shift - or twice as frequently. Only the data from 2,000 miles and on were used in the analysis.

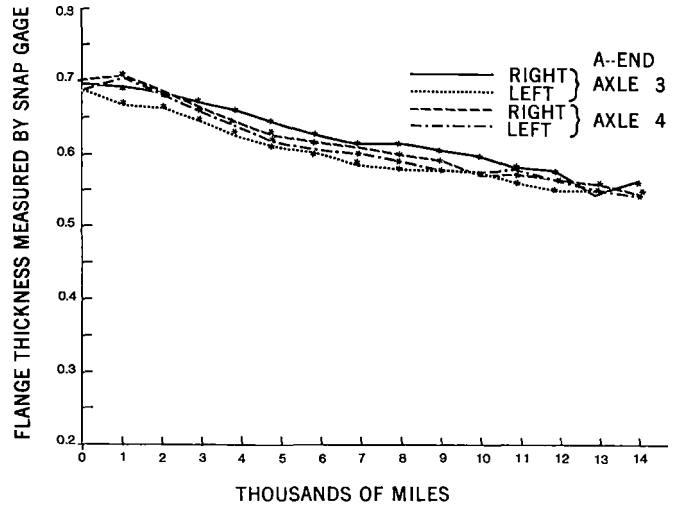


FIGURE 24. AVERAGE FLANGE THICKNESS WEAR PATTERN FOR EMPTY CAR #48.

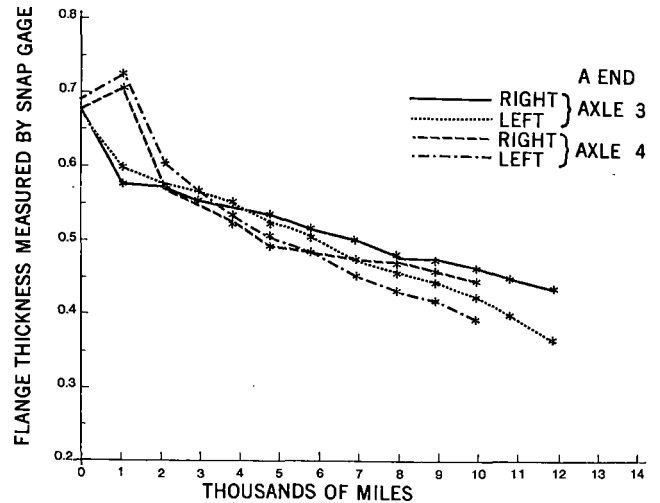


FIGURE 25. AVERAGE FLANGE THICKNESS WEAR PATTERN FOR 100-TON CAR #70.

The resulting relationship between flange wear rate and axle loading is shown in Figure 26 for the unlubricated condition. As indicated, the affect of axle loading on flange wear appears to be insignificant above the 66 or 80 - ton level. Results of tests conducted to identify the statistical difference between the six lading levels are summarized in Figure 27. The dots indicate pairs of lading levels for which there exist a significant difference at the 95% confidence level. These results indicate that the flange wear rates for loadings between 66 and 110-tons are of the same population. A test of wheel hardness distribution among the various car lading values resulted in determining that there is no significant difference in wheel hardness - at the .05 level - among the wheel samples tested as seen in Figure 28 and therefore the wear results obtained are not due to differences in hardness among the wheels.

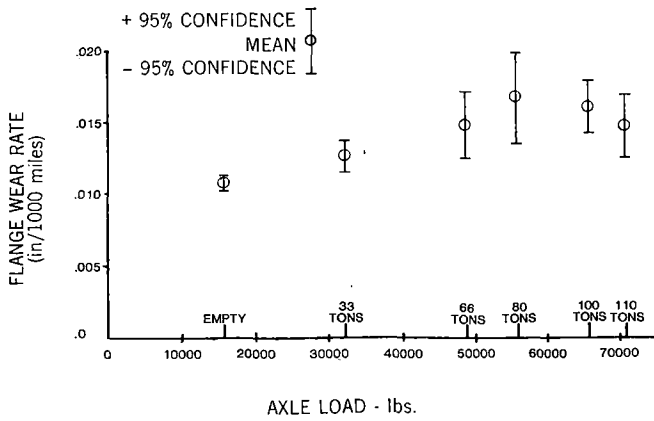


FIGURE 26. FLANGE WEAR RATE VERSUS AXLE LOADING FOR UNLUBRICATED TRACK.

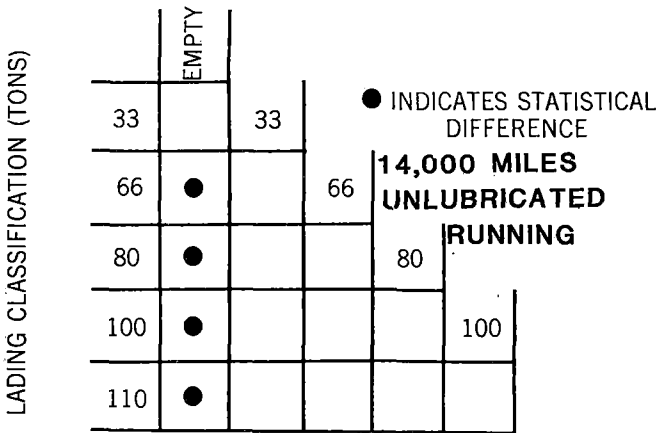


FIGURE 27. STATISTICAL TEST ILLUSTRATING PAIRS OF LADING CLASSIFICATION BETWEEN WHICH THERE IS A DIFFERENCE AT THE .05 LEVEL (14,000 MILES UNLUBRICATED RUNNING).

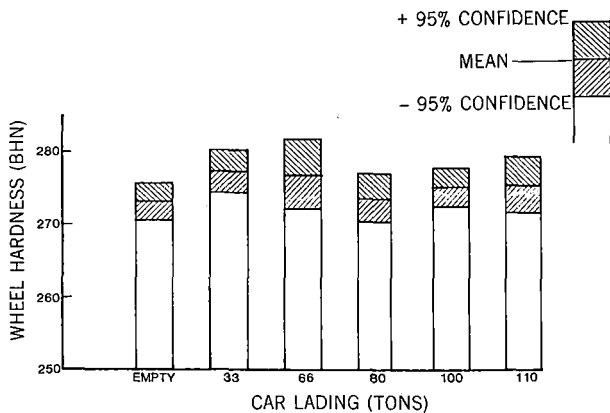


FIGURE 28. VARIABLE AXLE LOAD EXPERIMENT

The resulting characteristic shape of flange wear rate versus axle load obtained from this experiment supports data which is discussed in the proceedings paper "The Mechanical Aspects of Wheel/Rail Wear" concerning the use of wear indices.

Summarizing the results obtained to date on the third wheel experiment:

- A. Only minor differences in flange wear resulted for loadings between 66 and 110 tons on dry track, and
- B. No significant difference was found in wheel wear between constant and variable snubbing trucks at empty and 100 ton lading on dry track.

It is planned to continue the lubricated portion of this experiment through at least 80,000 miles.

ACKNOWLEDGMENT

The author would like to thank the members of the FAST team both at the Transportation Test Center and those originally at the AAR Technical Center for their assistance in conducting the experiments, taking the measurements and collecting the data. The author would also like to give special credit to the following individuals who performed the majority of analyses used in this paper: Messrs. K. Larsen, E. Longstreet, R. Allen, and J. Leary.

REFERENCES

1. "Wheel Flange Crack Evaluation First Experiment", FAST/TTC/TM-81/01, January 1981.
2. Kahle, V. E. - "Wear Mechanisms of Freight Car Wheels", FAST/TTC/TN-DR-89.
3. "Analysis of Data from the First Wheel Experiment at the Facility for Accelerated Service Testing", Report No. FRA-TTC-79-01, July 1979.

QUESTIONS AND ANSWERS

Question 1

What is believed to be the source of flange cracks and tread cracks at FAST?

Answer

The flange cracks observed at FAST appear to be the result of metal fatigue associated with excessive plastic deformation occurring in the gage face region of the wheel flange as a result of insufficient lubrication. The fine oblique tread cracks are believed to be the result of mechanical fatigue of the metal near the tread surface which occurs during periods of operation with track lubrication. The majority of these shallow cracks wear off during periods of "dry" operation.

Question 2

Is there any way to retard or prevent these cracks?

Answer

The addition of sufficient track lubrication appears to reduce significantly the number of flange cracked wheels.

Question 3

When is a crack considered critical?

Answer

According to interchange rules, any crack in the flange area is reason for removal. The flange cracks observed at FAST varied in size from those a few hundredths of an inch at the apex to those extending to the tread/flange fillet region. However, their rate of growth has not been measured.

Question 4

Can you please elaborate further on your basis for comparison of expected mileages to condemning limit for Wheels II experiment.

- Namely flange thickness and flange height worn to 1.25".
- Rim thickness worn to 1.5" (1 wear wheels)
2.0" (2 wear wheels).

The allowable condemning limits should be loss of flange thickness $\approx 9/16$ " for WF wheels increase in flange height $\approx 7/16$ "

loss of rim thickness $\approx 5/8$ " (1 wear)
1 1/8" (2 wear).

Answer

The mileage figures used to compare the relative wear performance of the test wheels in the second wheel experiment are not estimated miles for reaching AAR condemning limits as your question suggests. These figures represent the calculated mileage to reach the wheel dimensions specified for each of the three wheel measurements using the prediction models. The actual wheel dimensions (limits) specified are less than the AAR condemning limits and were selected to obtain approximately 1/4 inch of wear for each measurement.

Question 5

During experiment Wheel I, several flange cracks, in addition to patterns of fine oblique cracks on the tread, were reported. Have these types of defects also been observed during experiments Wheels II and/or III?

Answer

Both types of cracks were observed in wheel experiments II and III. Flange cracks were infrequent in Wheels II, but several developed during the "dry" operational periods of the third experiment. The oblique tread cracks developed during lubricated periods of operation, but appeared to "wear off" after short periods of "dry" running.

Question 6

Is the wheel wear rate going to be related to GTM's and the percentage and degree of curvature experienced during the tests?

Answer

There are no current plans to relate wheel wear rates to Gross-Ton-Miles; however, Dr. Steele has converted some wheel flange wear data to in/lb to compare with rail wear at FAST. He has also adjusted flange wear data at FAST to allow for degree of curvature and exposure in comparing wheel wear with rail wear. Please refer to his paper, "Wheel Rail System Wear", for more details.

Question 7

Did the ratio of flange wear to rim wear for Class U versus Class C versus wrought versus cast stay in the same proportions in experiment 1 and experiment 2?

Answer

Due to the lack of sufficient track lubrication and subsequent low mileage obtained for test wheels in the first experiment, the limited tread data obtained was not suited for regions analysis. Therefore, the ratio of flange-to-tread wear was not determined.

Question 8

Is rim wear significant in the test as compared to the high flange wear rate?

Answer

Significant tread wear did occur in the second wheel experiment and was as significant as "false flanges" in generating "high flange" conditions.

Question 9

Can experiment 1 and experiment 2 be correlated between lubricated versus unlubricated portions as to the effect of flange versus rim wear?

Answer

Since only limited tread wear was determined in experiment 1, and experiment 2 was conducted in mainly a lubricated condition, only flange wear for Class C wheels under lubricated conditions was correlated between the first two wheel experiments.

Question 10

Do the authors think that truck to truck variations (for example in centerplate rotational friction) may help explain further variation from wheel to wheel? Could some such variations be measured and included in regression analyses?

Answer

Truck torsional stiffness variations could very well contribute to wheel to wheel variations unexplained to date; however, it is not clear how one could measure and correct for this without elaborate instrumentation on each truck.

WEAR RATES OF FREIGHT CAR WHEELS AS A FUNCTION OF CHEMISTRY

V. E. Kahle
Experiment Manager, Wheels
Southern Pacific Transportation Co.

This experiment, better known as Wheels IV, was designed and initiated at the request of the Wheels, Axles Bearings and Lubrication (WABL) Committee of the AAR. The committee members, representatives from the railroads, were concerned because of the increased cost of accidents attributed to broken flange and rim, and the dramatic increase in wheel removal because of observed thermal cracking and overheated wheels. The left table in Figure 1 shows a gradual increase in accident incidences from 1976 through 1978 with a substantial reduction in 1979 and 1980. The right table shows that the number of wheels removed because of observed thermal cracks and overheated wheels increased 158% in 1979 and nearly 500% in 1980, partially accounting for the decreased incident of accident in the years 1979 and 1980. Furthermore, the average cost of each accident due to a broken flange or rim is nearly double the average cost of all other incidents. It has been shown in laboratory tests that there is a direct relationship between increase in carbon content of the wheel steel and susceptibility to thermal cracking. Consequently, to reduce thermal cracking it would be desirable to lower the carbon content. However, lowering the carbon content increases the wear rate resulting in increased maintenance costs. As a starting point in the effort to alter the chemical composition of the wheel steels to reduce susceptibility to thermal cracking while maintaining an acceptable wear rate, the Wheels IV experiment was designed to study the wear rates of the various classes of wheels as a function of chemistry.

STATISTICS RELATING TO THERMAL DAMAGE

ACCIDENT INCIDENCE, 1976 - 1980

YEAR	'76	'77	'78	'79	'80
BROKEN FLANGE AND RIM	80	97	92	65	61

AVG. COST - \$75,500/INCIDENT, CONTRASTED TO
\$38,900 AVG. COST
FOR ALL CAUSES

MAINTENANCE OCCURRENCE/10,000

ACTIVE CARS 1976 - 1980

YEAR	'76	'77	'78	'79	'80
THERMAL CRACKS AND OVERHEATED WHEELS	31	57	26	67	398

FIGURE 1. STATISTICS RELATING TO THERMAL DAMAGE.

EXPERIMENT DESIGN

The objective of the experiment is to develop an understanding of the relationship between wheel wear and carbon content in both heat treated and non heat treated wheels. The test conditions of the experiment designed to develop this data are shown in Figure 2. It was decided to control the carbon content of the heats to ± 0.02 percent at the mid-ranges of the AAR specification for Classes B and C and to obtain a Class U with a low carbon and a Class U with a high carbon content both within the AAR specification range. The test matrix of 192 wheels, 128 cast and 64 wrought, is shown in Figure 3. The results presented are only for cast wheels.

- o 100-TON HOPPER CARS
- o CAST AND WROUGHT WHEELS
- o DRY TRACK 7,000 MILES TESTING
- o LUBRICATED TRACK 14,000 MILES TESTING (TO DATE)
- o CARS ROTATED THROUGHOUT CONSIST

FIGURE 2. TEST CONDITIONS

ALL WITH SIMILARLY CONFIGURED CONVENTIONAL TRUCKS
16 INCH CENTER PLATES
TEST WHEELS

	Ulc .82 \pm .02	U .76 \pm .02	B .82 \pm .02	C .72 \pm .02	Total
Cast	32	32	32	32	128
Wrought	16	16	16	16	64
Total	48	48	48	48	192

FIGURE 3. TEST CARS. TWENTY-FOUR FULLY LOADED 100-TON HOPPER CARS.

There were 32 cast and 16 wrought of each class of wheels. To eliminate the effect of manufacturing process, the cast and wrought wheels will be considered separately. All of the wheel sets were mounted on conventional trucks with 16 in. diameter center plates. Installation of the wheelsets followed a strategy which systematically distributed the four classes of wheels throughout all axle positions such that car and axle location effects would not bias any one wheel group. This strategy is depicted in Figure 4. Because the wear measurements were made every 1000 miles during the unlubricated track cycle, the normal four day train operational cycle had to be condensed into a two day cycle, as illustrated in Figure 5. The measurements are listed in Figure 6. The equipment used to determine the levels of the important elements in the wheel steel is also shown in this figure.

AXLE NUMBER	TEST CAR #						ETC....
	1	2	3	4	5	6	
1	B	C	U	ULC	B	C	
2	C	U	ULC	B	C	U	
3	U	ULC	B	C	U	ULC	
4	ULC	B	C	U	ULC	B	

FIGURE 4. WHEEL INSTALLATION STRATEGY.

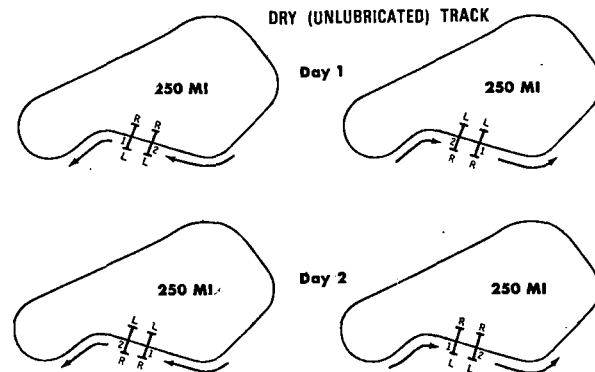


FIGURE 5. TRAIN OPERATIONS DURING THE FIRST 7,000 MILES OF SERVICE.

WHEEL MEASUREMENTS

- FLANGE THICKNESS
- PROFILE
- RIM HARDNESS
- CHEMISTRY
 - CARBON
 - MANGANESE
 - SILICON
 - CHROMIUM

INSTRUMENTATION

- SNAP GAGE
- CANADIAN NATIONAL (CN) PROFILOMETER
- KING BRINELL TESTER
- LECO CARBON DETERMINATOR
- PERKIN-ELMER ATOMIC ABSORPTION SPECTROPHOTOMETER

FIGURE 6. WHEEL MEASUREMENTS AND INSTRUMENTATION.

Figure 7 is a photograph of the "CN" Profilometer, a newly developed instrument which is used to determine the wheel profiles. Figure 8 is an example of a new and worn profile of flange area wear, and tread area wear as measured using this instrument.

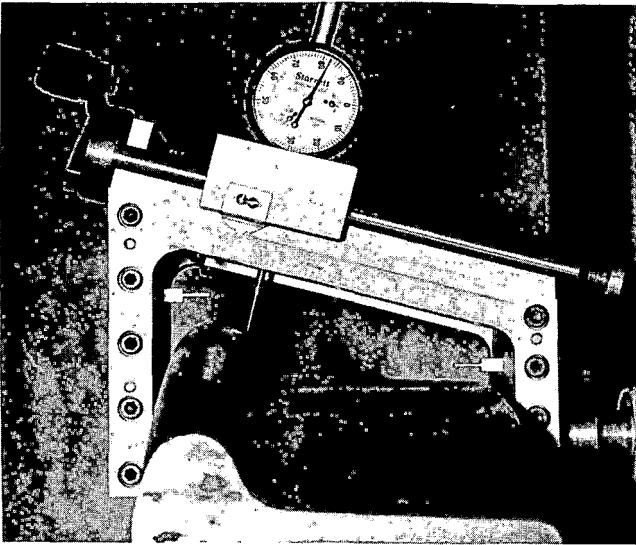


FIGURE 7. PHOTOGRAPH OF PROFILOMETER.

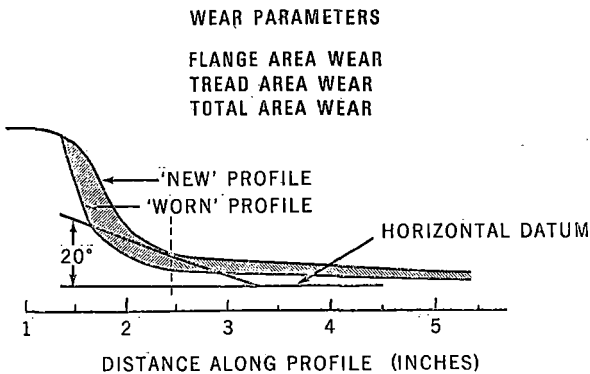


FIGURE 8. TYPICAL WHEEL PROFILES TAKEN WITH CN PROFILOMETER.

The profilometer takes a series of measurements along the tread and flange; these data are then processed by a computer programmed to develop the worn profile illustrated in the figure.

The frequency of measurements and the track environment are shown in Figure 9. The snap gage was used to measure the flange thickness at the beginning of the test and every thousand miles thereafter during the unlubricated cycle. The CN profilometer was used to measure tread and flange profiles at the beginning and end of the unlubricated cycle. In

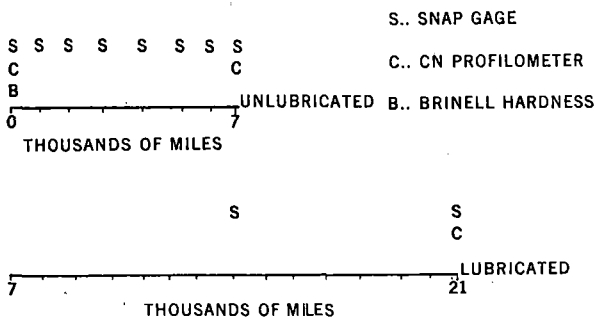


FIGURE 9. FREQUENCY OF MEASUREMENTS AND TRACK ENVIRONMENT.

addition, the Brinell hardness of each wheel rim was measured at the beginning of the experiment. Since the wear rate is drastically reduced during the lubricated cycle, the flange thickness measurement intervals were extended to 7,000 miles and the profile was measured at the end of the lubricated cycle with the CN profilometer.

DISCUSSION OF RESULTS

The results presented in this paper are for Cast Wheels only. An example of the behavior of wheel wear in lubricated and unlubricated environments is shown in Figure 10. The first 2000 miles or so of the unlubricated cycle results in a nonlinear, "break-in" period, after which the wear rate is nearly linear. This break-in period is not included when calculating wear rates. The lubricated cycle wear rate is also linear, but with a much different slope, consequently the two cycles must be statistically analyzed as two populations.

Preliminary analysis of the wear data using ladle carbon analysis showed a wide variation between

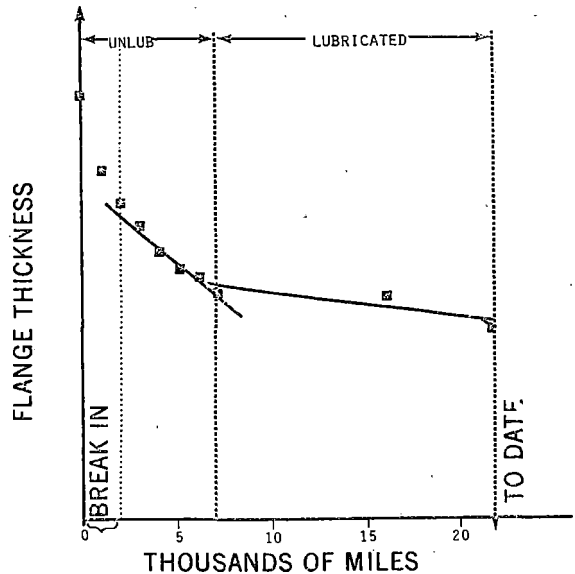


FIGURE 10. EXAMPLE OF WHEEL WEAR IN LUBRICATED AND UNLUBRICATED ENVIRONMENT.

individual wheel wear and ladle carbon analysis. Consequently, it was decided to obtain a chemical analysis for C, Si, Cr and Mn, as well as a Brinell hardness for each wheel to account for the scatter in the data. This not only provides more accurate data but increases the sample size, an important factor in statistical analysis. A histogram of the discrete carbon analysis for each wheel versus the ladle analysis for a heat of wheels is shown in Figure 11. There is a significant shift in the carbon content from that of the ladle analysis to the average of the individual wheels from the heat, which could account for some of the scatter in the wear data.

Scattergrams were prepared to show wear rate of individual heat treated wheels run on unlubricated track as a function of carbon content, wheel hardness and a function called the "carbon equivalent." A regression analysis was run for the elements C, Mn, Cr, and Si versus wear to establish the contribution of each to the wear resistance of the wheels.

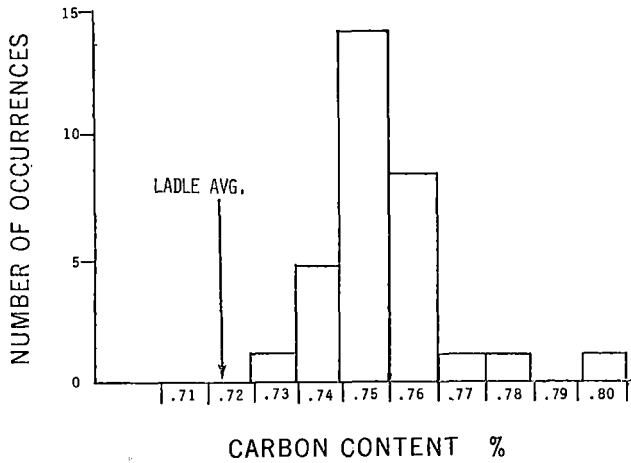


FIGURE 11. HISTOGRAM OF CARBON CONTENT FROM WHEEL CHEMISTRY ANALYSIS.

Cr and Si were present in rather small amounts and did not appear to have a significant effect on wear rates. There was, however, a significant contribution from the presence of manganese. The scattergrams as a whole show a wide scatter between wear rates and the influence of carbon content, wheel hardness and carbon equivalent, see Figures 12 through 14. Despite the scatter in the data a positive correlation between wear rates and carbon content is discernable. Although it is not readily discernable in Figure 14, which shows the individual data points of carbon equivalent for each wheel plotted against flange wear rate, the carbon equivalent obtained by using the carbon-manganese carbon equivalent accounts for about 32% of the scatter in the data.

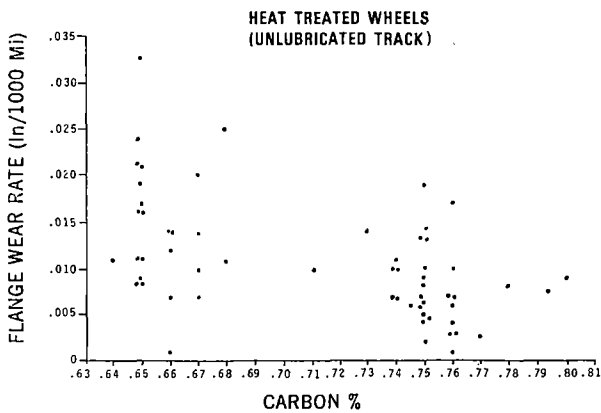


FIGURE 12. WEAR RATE AS A FUNCTION OF CARBON CONTENT.

Figure 15 shows bar graphs of the four wheel classes versus the flange wear rates during the first 7000 miles of unlubricated service. The Class ULC and Class U wear rates are nearly identical. The Class B wear rate is lower than either the Class ULC or Class U; however, it is about 75 percent greater than the Class C wheels. Figure 16 shows the flange area wear rates using the CN profilometer to generate the wear data instead of the snap gage. Although the absolute wear data is different, the trends are identical.

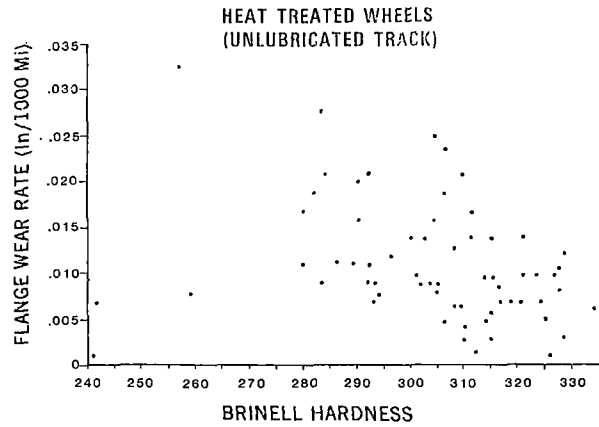


FIGURE 13. WEAR RATE AS A FUNCTION OF WHEEL HARDNESS.

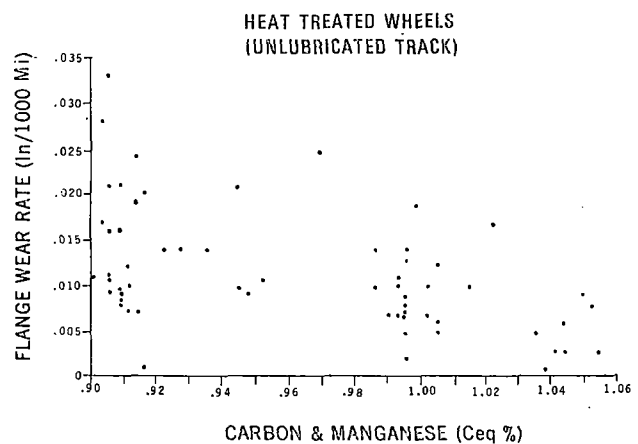


FIGURE 14. WEAR RATE AS A FUNCTION OF CARBON AND MANGANESE.

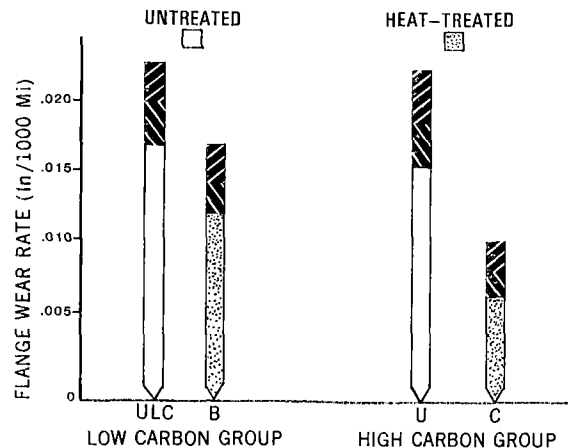


FIGURE 15. WEAR RATE SUMMARY FOR 7,000 MILES OF UNLUBRICATED SERVICE.

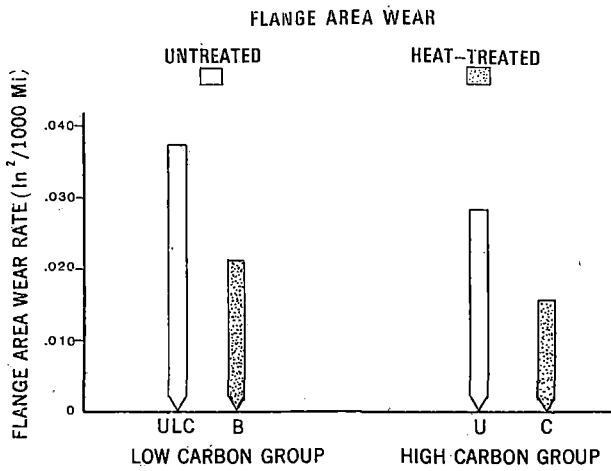


FIGURE 16. SUMMARY OF UNLUBRICATED WEAR USING CN PROFILOMETER.

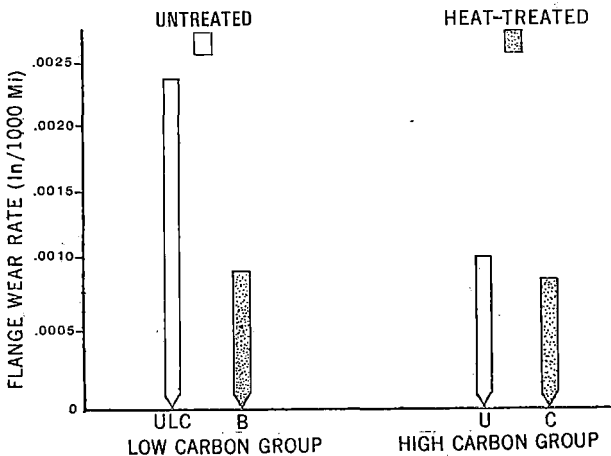


FIGURE 17. PRELIMINARY WEAR RATE SUMMARY FOR 14,000 MILES OF LUBRICATED SERVICE.

Figure 17 shows the wear rates for 14,000 miles of service with rail lubrication. The results in this case are quite different: the Class ULC Wheels had the worst wear rate by a factor of about 2.5 to 3; the wear rates of the Class B, Class U carbon, and Class C wheels were nearly the same. The Class C wheels had the lowest wear rate with the Class B a close second. Since the wear rates in the lubricated regimes are low, this data must be considered very preliminary and any conclusions from it should be made with caution.

(UNLUBRICATED TRACK-7000 MILES)

WHEEL CLASS	ULC	U	B	C
STEADY STATE WEAR RATE (in/1000 Mi WITH 95% CONF INTERVAL)	.020±.003	.018±.003	.014±.002	.008±.002
FLANGE AREA WEAR RATE (in ² /1000 Mi)	.0372	.0284	.0211	.0156

FIGURE 18. SUMMARY OF FLANGE WEAR DATA.

Figure 18 is a numerical summary of the first 7000 miles of the test for cast wheels run on unlubricated track. The first row of data is the steady state wear rate with a 95% confidence interval (also plotted in Figure 15 as bar graphs). The greatest difference in wear rate is between the Class C wheels and the other three classes, the Class B wheels being the nearest competitor with a wear rate about 75% greater. The flange area wear data shown here reflect the same trends.

PRELIMINARY CONCLUSIONS

The following conclusions were drawn from the data obtained from the 7000 mile test on unlubricated track:

1. There is little difference in flange wear between ULC and U class wheels.
2. The wear rate of Class B wheels is about 75% greater than Class C.
3. There is a positive correlation between wear rates and carbon levels in heat treated and untreated wheels.
4. There is a correlation between wear rates and a calculated carbon equivalent (C + Mn) for heat treated wheels.

AREAS FOR FURTHER INVESTIGATION

There are many factors other than chemistry and heat treatment which influence the wear behavior of metals; a few of these factors which could be studied to gain a better understanding of wheel wear are:

1. Work hardening
2. Wheel profile
3. Microstructure
4. Alloying
5. Thermal input

NOTE: The "Carbon Equivalent" relates the combined effects on metal behavior of carbon and alloying elements such as, Manganese, Chromium and Silicon in terms of carbon levels alone

QUESTIONS AND ANSWERS

Question 1

Your data for accidents shows an increase for the number of incidents from 80 to 92 during the period 1976-1978, an increase of 15%. Was the increase truly significant when considering the increase in tonnage or train movements during that period?

The basis for this question is that Santa Fe statistics show a decrease in the accident rate (accidents per billion gross ton miles). For that period primarily this effect is due to efforts to hold the line on the accident frequency while handling increased tonnages over previous years.

Answer

The increase in the number of incidents was insignificant but the increase in cost per incident and the increase in axle set removal to prevent wheel failure due to thermal damage was very significant. The railroads have done a magnificent job of reducing accidents but the reduction was accomplished at a high maintenance cost.

Question 2

In railroad service tests of Class U, B, and C wheels, we have generally found the Class B and U wheels to have similar wear rates and in some cases, the Class U wheels have a better (lower) wear rate than Class B wheels. Would the author care to comment on these differences in service compared to FAST.

Answer

Since the service conditions and carbon and manganese content of the wheels in question are not known to me, it would be difficult to make an intelligent response to the question. It appears that we have much to learn about wear mechanisms of metallic components in unlubricated environments.

RADIAL TRUCK WHEEL WEAR

Roy A. Allen
Experiment Manager, Radial Truck
Association of American Railroads

John F. Leary
Engineer
Boeing Services International, Inc.

In response to manufacturers' making radial trucks available to the Railroad industry, an experiment was implemented at FAST in May 1980 to determine the effectiveness of three designs in reducing wheel wear as compared with conventional trucks on both unlubricated and lubricated track. Only the unlubricated track portion of the experiment has been completed so far, and these results and other results from railroads operating a sizeable number of these trucks, indicate a potential improvement in wheel wear by a factor of approximately $2\frac{1}{2}$ to 3 over conventional trucks. By means of a statistical model, this paper also examines potential causes of asymmetric wheel wear. Differences in tread taper on wheels on the same axle, differences in diameter, and axle misalignment caused wheels to wear at different rates, the effects being more noticeable on some truck designs than on others.

The replacement of wheels and rails due to wear is a high cost item for Railroads. Freight car wheelsets alone are estimated¹ to cost the industry 275 million dollars each year in replacements. The use of harder or more wear resistant wheel and rail steels has been examined for many years and these steels are becoming more prevalent, particularly for rails in sharp curves. The beneficial effect of efficient track lubrication on rail wear is also known, but these units are typically difficult to maintain and can cause other problems such as rail fatigue failures.

In recent years, truck manufacturers have begun to introduce new trucks designed for improved curving performance (as compared with the conventional three-piece trucks) and resulting in decreased wheel and rail wear. These trucks have become known as radial or self-steering trucks, the term "radial" truck being designated because the optimum truck curving performance is achieved when the axles are oriented or "yawed" such that they are perfectly radial to the center of the curve. Although radial trucks rarely achieve the optimum condition, they are designed for improved curving performance by reducing the wheelset angles of attack, i.e., by reducing the angle of each axle with respect to the curve radial line.

The primary objective of the FAST Radial Truck experiment is to determine the effectiveness of three radial truck designs made available by the manufacturers in reducing wheel wear. Wheel wear rates will be determined for all three radial truck designs, and also for two conventional three-piece

truck designs, for both lubricated and unlubricated track conditions. A secondary objective is to compare the wear and failures of various radial truck components with those obtained on the conventional truck designs. At the present time, the phases of testing on unlubricated track have been completed and the wheel wear results are presented. The lubricated track testing phase has only recently begun and thus these results cannot be presented at this time. Similarly, the trucks have completed insufficient mileage to report any truck component wear.

Test Trucks

Fourteen 100-ton open top hopper cars donated by one railroad are assigned to the experiment. Six cars are used as controls, with the two conventional three-piece truck designs installed in them--three cars for each design. Eight cars have radial trucks installed for testing: one radial design is installed in two cars, and the other two radial designs are installed in three cars each.

The two conventional designs consist of a bolster and a pair of sideframes, with suspension springs between the ends of the bolster and the midpoint of each sideframe. The ends of the sideframes rest through adapters on bearings at the ends of the wheelsets. The carbody is supported by a centerplate at the center of the bolster and double roller side bearings are located on either side of the bolster in order to steady the carbody and restrict rolling motion. Friction damping (snubbing) of the suspension is provided by spring loaded shoes be-

tween the bolster and sideframes. The major difference between the two designs is that one has variable friction snubbing, the level of snubbing being dependent upon the car lading, whereas the other design has constant snubbing.

Because of the metal to metal surface between the bearing adapters and the sideframes, a high level of friction has to be overcome before relative movement between the wheelset and sideframes can be achieved. Hence, the wheelsets can be considered as being rigidly fixed with respect to the sideframes and when the truck is moved around a curve it rotates on the centerplate with the trailing axle adopting a near radial position. The truck also takes up a "lozenged" position, i.e., one sideframe moves ahead of the other. As shown in Figure 1, this truck attitude results in a high angle of attack on the lead axle and consequently heavy flange contact occurs on the lead axle outer wheels.

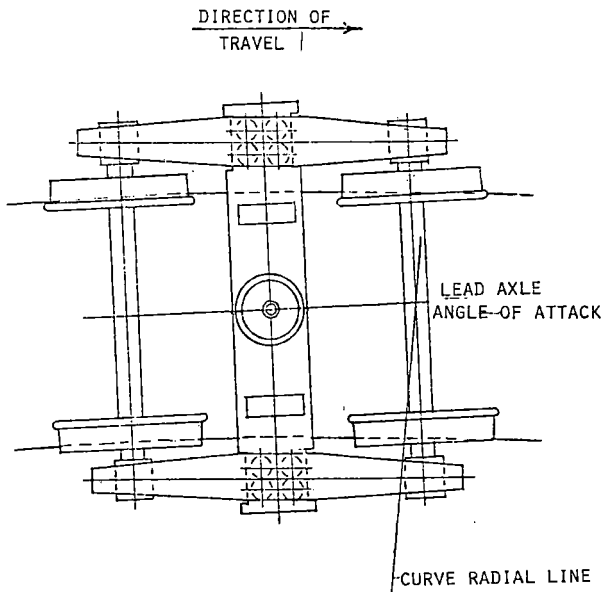


FIGURE 1. THREE-PIECE TRUCK ON CURVE.

On two of the radial truck designs, the manufacturers have attempted to improve this basic problem by introducing springs, in the form of rubber shear pads, between the bearings and sideframes. These shear pads introduce a primary longitudinal stiffness, $\frac{1}{2} K_x$, and primary lateral stiffness, $\frac{1}{2} K_y$, to the otherwise conventional three-piece truck as depicted in Figure 2a. It has been shown by Pollard² that the plan view suspension characteristics of such a truck can be fully described by two parameters, i.e., the axle bending stiffness, K_b , and the axle shear stiffness, K_s , where:

$$K_b = \frac{b^2 K_x}{2} \quad (1)$$

$$K_s = \frac{b^2 K_x K_y}{2b^2 K_x + 2a^2 K_y + \frac{2a^2 K_y b^2 K_x}{K_l}} \quad (2)$$

Thus, by introducing a low value of K_x , the bending stiffness assumes a low value, i.e., the truck has a good ability for the axles to yaw with respect to each other and thus adopt a better radial attitude

in a curve as compared with a conventional truck. However, the low suspension stiffnesses result in a relatively low interaxle shear stiffness and it has been shown previously that this is detrimental to vehicle stability. Thus, although the vehicle shown in Figure 2(a) will have a relatively good curving performance, presuming that K_x is low enough, it will be liable to incur hunting problems.

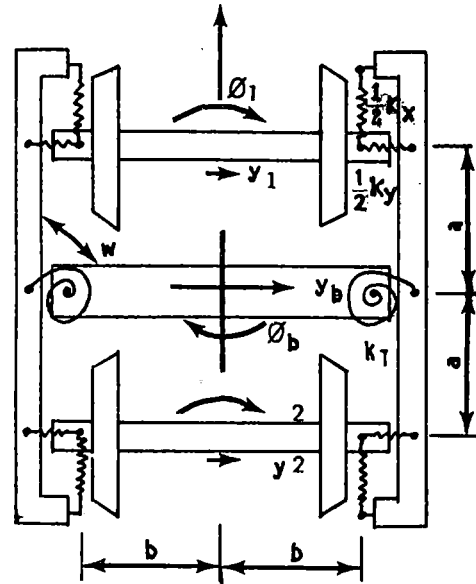


FIGURE 2(a). TRUCK WITH PRIMARY SUSPENSION.

In an attempt to alleviate the hunting problem, the two manufacturers who have followed the philosophy outlined above have attempted to increase the lateral stability by directly inter-connecting the axles (cross-bracing). The technique of cross-bracing, as shown in Figure 2(b), adds shear stiffness directly

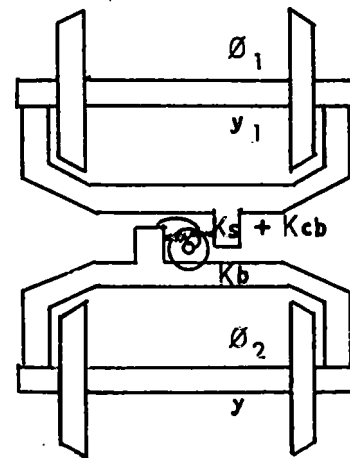


FIGURE 2(b). CROSS-BRACE TRUCK.

to the system while theoretically not affecting the bending stiffness. Thus, after the addition of

cross-bracing, equations (1) and (2) become:

$$K_b = \frac{b^2 K_x}{2} \quad (3)$$

$$K_s = \frac{b^2 K_x K_y}{2b^2 K_x + 2a^2 K_y + \frac{2a^2 K_y b^2 K_x}{K_1}} + K_{cb} \quad (4)$$

Thus, although cross-bracing does not totally eliminate the need for a positive non-zero bending stiffness between the wheelsets, it does provide greater vehicle stability for a given bending stiffness.

Of these two types of radial design employing cross-bracing, there are three carsets of the first design, referred to as the "retrofit" radial truck, in the experiment. The design consists of two C-shaped steering arms that are applied to a conventional three-piece truck to provide the cross-bracing discussed above. The arms are attached at their extremities to specially machined roller bearing adapters, and are universally connected to each other by centerposts through one of the existing holes in the bolster. As shown in Figure 3, elastomeric or "resilient" pads separate the roller bearing adapters and the sideframes.

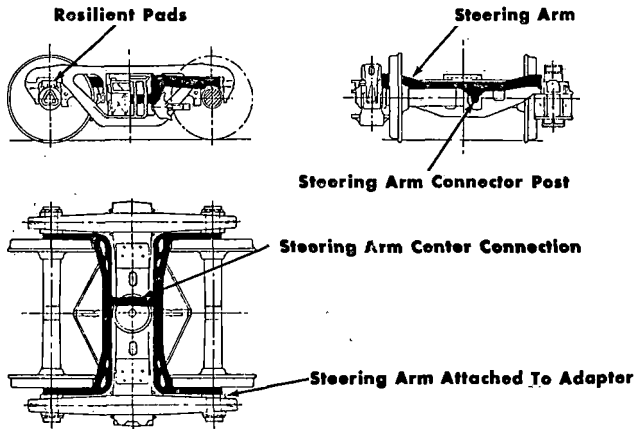


FIGURE 3. ARRANGEMENT OF RETROFIT RADIAL TRUCK.

There are also three carsets of the second radial design referred to as the "diagonal cross-link" radial truck. This is a special three-piece freight truck design with cross anchor struts running diagonally through the truck bolster, connected by pivoting pins at two subframes, see Figure 4. These subframes, one at the end of each sideframe, fit between conventional sideframes and the bearing adapters of each wheelset. The cross anchors provide the high shear stiffness as explained previously and a relatively low bending stiffness is achieved by rubber shear pads between the sideframe and the subframe. The subframes for each wheelset are connected by a lateral strut for additional stability.

The third design, referred to as the "forced steering" radial truck, is fitted to two carsets in the FAST experiment. This truck is a primary suspension type with a fabricated H-frame. The suspension consists of four subframes that are located in pockets at the corners of the H-frame. The four subframes and the carbody are connected by a linkage arrangement so that when the truck swivels under the

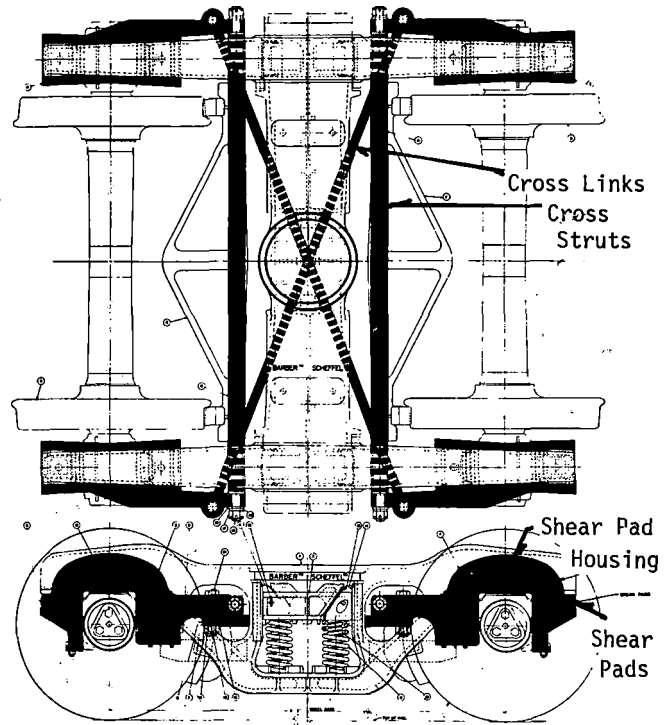


FIGURE 4. DIAGONAL X-LINK RADIAL TRUCK.

carbody on a curve, due to geometric relationship of the wheel tread with the rail (Figure 5), the subframes on the outside of the curve move further apart while the subframes on the inside of the curve move closer together. With this action, the wheelsets are designed to be parallel on straight track and to assume a radial position on curves.

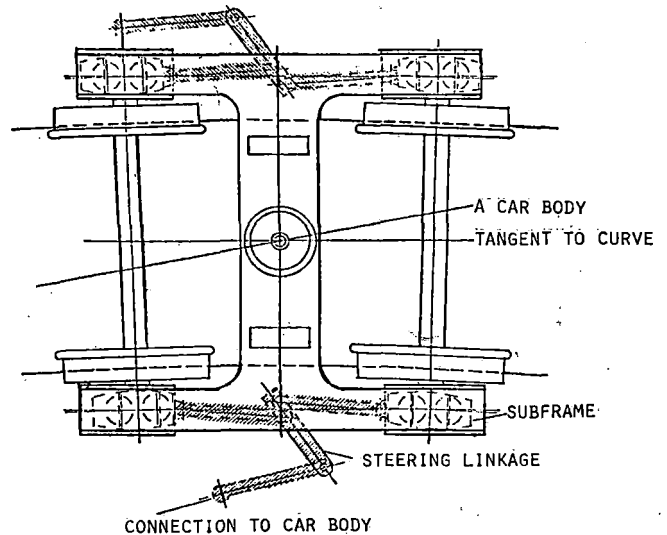


FIGURE 5. FORCED STEERING TRUCK LINKAGE MECHANISM.

Present Status of Experiment

As stated previously, only the unlubricated track portion of the experiment is complete. Four separate phases of the experiment have been completed as outlined in Table 1.

TABLE 1. DURATION OF TEST PHASES.

Phase	Date	Nominal duration (miles)	Track Conditions	Comments
I	May 1980	7,000	Unlubricated	Cone angle problem discovered - decision to restart experiment.
II-a	Nov/Dec 1980	7,000	Unlubricated	New wheelsets fitted, wheel wear test restarted with control on taper and diameters.
II-b	Feb 1981	7,000	Unlubricated	Wheel wear test on dry track is completed.
III-a	Apr 1981	14,000	Lubricated	Begin wheel wear test on lubricated track with reprofiled wheels.

As noted in the Table, a cone angle problem was discovered during Phase I. During this phase, the flanges of the wheels on the two cars with forced steering trucks wore more on one side of the vehicle than on the other as previously reported.³ The problem was investigated by checking several possible causes. Although the uneven flange wear may have been accentuated by other factors (e.g., differences in wheel diameters and axle misalignment), the wear pattern appeared to be related primarily to the phenomenon of having wheels on the same axle with differing tread tapers. For these trucks with the biased wheel wear, all eight wheels with the highest wear were on the right side of the vehicles and all had tread tapers that were flatter than the nominal 1-in-20. Conversely, all the mating wheels on the left side of the vehicles had tapers that were steeper than nominal. The majority of the wheelsets in the experiment had similar differences in tread taper, although not with the same side of vehicle bias, and, as described later, the differences in tread taper did appear to affect the wheel wear on the conventional and retrofit radial trucks, although this effect was not as noticeable as it was with the forced steering trucks.

Because this unanticipated variable had been introduced, the experiment was restarted. New wheels were obtained, and limits were set for the tread taper and wheel diameter, differences between wheels on the same axle. The tread tapers were controlled to relatively tight tolerances (between 1-in-18.2 and 1-in-22.2) by very careful alignment of the profile template on the Hegenscheidt wheel truing lathe (the taper differences in Phase I were primarily due to an initial set-up problem on the lathe) and the tapers were checked using a specially manufactured fixture which is shown in the form of a sketch in Figure 6. The fixture spans both wheels of an axle, is supported by two points on each wheel, and is placed on the wheelset with all four support points in solid contact with the wheels. It is then adjusted laterally until it is positioned centrally over both wheels. The lateral adjustment is checked with a dial indicator gage until the dimensions "a" and "b", shown in Figure 6, are equal.

To measure the tread taper, a dial indicator gage is inserted through each of three holes 1" apart in either end of the fixture, and the distance from the top of the fixture to the wheel tread is measured. By subtracting any two of these measurements and dividing by the hole spacing, the tread taper or

cone angle can be determined for an individual wheel. Obviously, this method is only correct if the wheel tread is a perfect taper, and hence these measurements could not be made on the wheels of the diagonally connected radial trucks because they have special nonconical profiles.

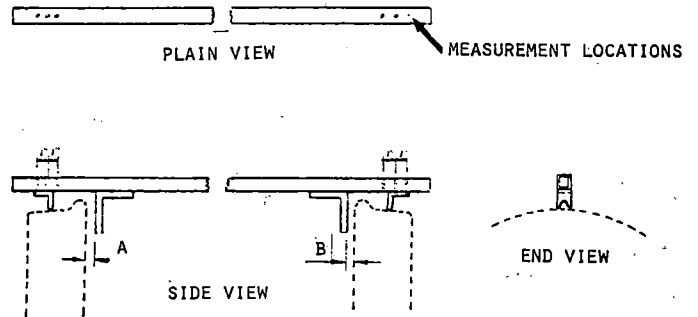


FIGURE 6. CONE ANGLE MEASURING FIXTURE.

Thus, with the tight controls of tread tapers and of wheel diameters (maximum variation allowed was .030" between wheels on the same axle) the experiment was restarted and Phase II-a, which consisted of running approximately 7,000 miles on totally unlubricated track, was completed. The radial truck test vehicles were then withdrawn from the consist while the non-test vehicles in the FAST consist ran with the track well lubricated. These alternating unlubricated-lubricated track conditions are operated primarily as a requirement of the Rail Metallurgy Experiment.⁴ During the next dry track period, the radial truck test vehicles were re-inserted in the consist and completed approximately another 7,000 miles which represents Phase II-b of the experiment as denoted in Table 1. The end of this phase marked the completion of the wheel wear studies on unlubricated track. The same wheels (1-wear, class U) which were used during Phases II-a and II-b, were reprofiled to new profiles and with the wheels returned to the same location in the test vehicles as they were during the dry track test phases, the experiment continued by running on lubricated track (Phase III-a). For most of the remainder of the experiment the test vehicles will run only on lubricated track although it is planned to run another short phase on unlubricated track at the very end of

the experiment in order to gather data of the effects on wheel wear of changing rail metallurgies as a result of the introduction of the Track Degradation Experiment.⁵

It should be noted that in order to leave adequate metal to reprofile the existing wheels for Phase III of the experiment, the wheels were not allowed to incur more than 0.3" of flange wear during Phase II-a and II-b. Some of the test wheels did achieve this limit prior to completion of Phase II-b and were temporarily removed from the experiment. These wheelsets were replaced by non-test wheelsets for the remainder of Phase II testing, but the original test wheels were then reprofiled and reassembled under the test vehicles at the beginning of Phase III-a.

Phases II-a and II-b contain the main bulk of the data which are reported herein from which one of the experiment objectives, i.e., to determine wheel wear rates on totally unlubricated track, was achieved. As noted previously, Phase I data are confounded by the tread taper problem and these data are not used in comparing wheel wear performance of different truck designs. However, as reported later, the Phase I data did enable an analytical study, which was unplanned at the beginning of the experiment, to be carried out to highlight some causes of asymmetric wheel wear.

WHEEL WEAR MEASUREMENT METHODS

At the beginning of the unlubricated test phases, linear measurements of flange thickness, flange height, and rim thickness were taken using both the AAR finger gage and a previously unused fixture called the wheel snap gage. The snap gage, Figure 7, essentially measures the same parameters as the finger gage and does so by means of dial gage indicators as opposed to the graduated scales used on the finger gage. As reported by Larkin,⁶ the accuracy of the snap gage is superior to that of the finger gage and during this experiment the reliability of the fixture was proved. Hence, part way through the experiment, it was decided to cease use of the finger gage and only the snap gage results are discussed.

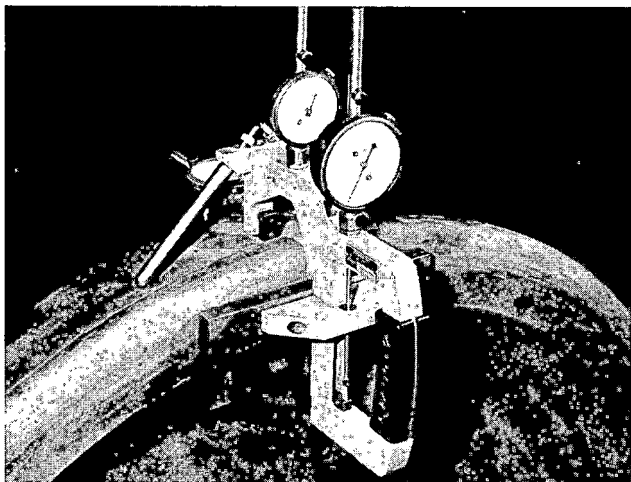


FIGURE 7. WHEEL SNAP GAGE.

Typical snap gage data are presented in Figure 8 which shows the flange thickness readings over a period of 14,000 miles comprising Phase II-a and II-b data. The data represents the flange wear on two wheels (wheels R1 and L1 on car 136) with measurements being taken at two radial positions, 180° apart, on each wheel. As can be seen, the flanges were exposed to initial rapid wear during the first 1,000 - 2,000 miles and thereafter wore at a reasonably linear rate. This phenomena is typical of wheel wear data collected on FAST unlubricated track,^{7 8} and most of the data analysis presented in this paper deals only with data obtained from 2,000 miles onwards.

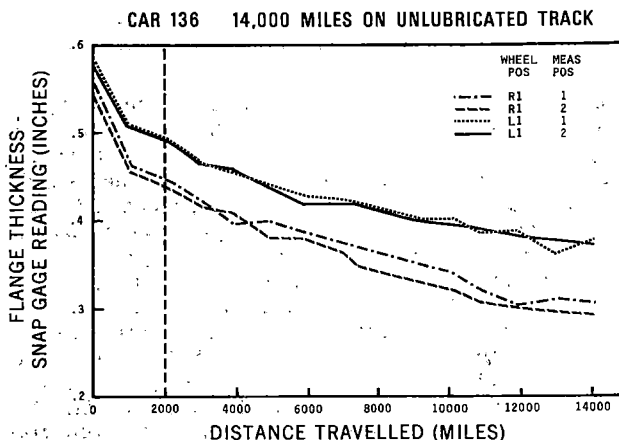


FIGURE 8. RADIAL TRUCK EXPERIMENT SNAP GAGE DATA.

The other wheel wear measurement fixture is the modified CN profilometer which has been described by Larkin⁶ and Kahle.⁸ The profilometer, Figure 9, takes a series of dial indicator readings across the wearing surface of the wheel. These data form the input to a computer program which calculates flange area wear, tread area wear, and total profile area wear by comparing the profile of a worn wheel with the new, original profile of that same wheel.

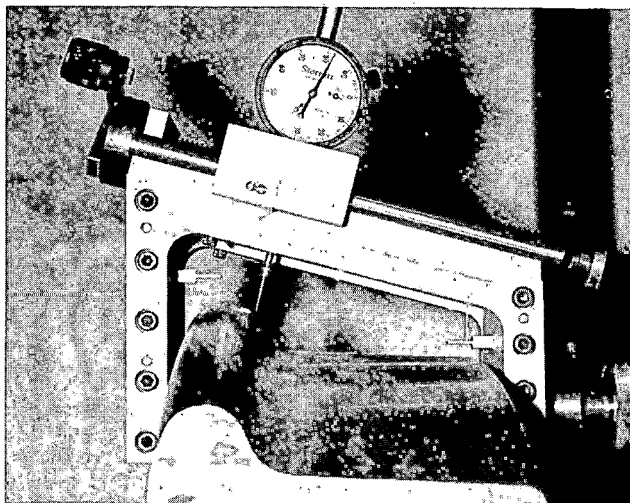


FIGURE 9. MODIFIED CN PROFILOMETER.

Snap gage readings were taken every 1,000 miles (approximately) during the unlubricated track phases with profilometer data taken at the beginning and end of each of the phases outlined in Table 1. Additional measurements taken are as follows:

- wheel hardness, using the King Brinell tester, prior to Phase I and Phase II-a,
- wheel diameter, using the digital read-out on the Hegenscheidt wheel truing lathe, prior to Phase I and Phase II-a,
- tread taper, using the special fixture shown in Figure 6, part-way through Phase I and prior to Phase II-a, and
- axle misalignment, reported previously⁹ and to be discussed later, taken between Phases I and II-a.

WHEEL WEAR RESULTS - TRUCK COMPARISON

In comparing the flange and tread wear of the radial trucks with the conventional trucks, the Phase I data were not used because the differences in tread taper introduced unforeseen noise. This made it difficult to pursue the objective of the experiment. Thus, the data which are reported in this portion of the paper are those obtained from Phases II-a and II-b, i.e., for 14,000 miles of operation on totally unlubricated track.

Before presenting the data, a discussion of the test conditions prevailing during Phases II-a and II-b is necessary in order that the results can be viewed in the correct context. First, the FAST track has a high curve to tangent ratio--approximately 54% of the track is curves or spirals--with all curves being of 3°, 4°, or 5°. In addition to the unlubricated track conditions described above, it should be noted that at FAST the relative humidity is typically very low, and thus high values of the limiting coefficient of friction between wheel and rail are

present. All the test vehicles were fully loaded 100-ton, open top hopper cars supplied by one railroad, and, throughout the experiment, they formed the first fourteen cars at the head end of the consist in order that they always be subjected to the highest drawbar forces. In order to minimize the effects of tread braking on the tread wear data, dynamic braking was used except when slowing the consist to a complete stop, or if, in the opinion of the locomotive engineer, a hazardous situation would have resulted.

As for the wheel chemistry experiment (Wheels IV), reported by Kahle,⁸ the normal FAST end-for-end consist turning operation was modified slightly, such that for each 1,000 mile period of operation during this experiment, each wheel on all trucks received an approximately equal exposure to the high wear condition of running on the lead axle on the high rail. All wheels were untreated class U cast, and all had standard AAR 1-in-20 coned profiles except for those on the diagonal cross-link truck, which had high conicity profiles specially designed based on the work of Scheffel.^{10 11} Because wheels could not be obtained with the special profile, the cast wheels were turned to this profile on the Hegenscheidt wheel truing lathe at the Transportation Test Center. Thus, these wheels could not be tested with the original cast running surface intact and, in order to eliminate a variable which might potentially have affected wheel wear, the remaining wheels in the experiment received a minimal turning cut, typically between .050" and .100" removed from the diameter, on the same lathe.

Finally, as stated before for Phases II-a and II-b, tread tapers and wheel diameters were strictly controlled with tapers being between 1-in-18.2 and 1-in-22.2 and the diameter tolerance allowing a maximum variation of .030" between wheels on the same axle.

The wheel wear results are summarized in Table 2 and 3 for flange and tread wear, respectively.

TABLE 2. FLANGE WEAR IN PHASE II.

Truck type	Flange linear wear rate (in/1000 mi)				Flange area loss after 14,000 mi (in ²)	
	all wheels		worst wheel per axle		all wheels	
	mean	+95% conf	mean	+95% conf	mean	+95% conf
Conventional, variable snubbing	0.0160	0.0023	0.0180	0.0039	.292	.026
Conventional, constant snubbing	0.0147	0.0020	0.0165	0.0032	.247	.020
Radial, retrofit	0.0115	0.0013	0.0134	0.0018	.194	.017
Radial, forced steering	0.0121	0.0029	0.0143	0.0059	.207	.048
Radial, diagonal X-link	0.0067	0.0012	0.0084	0.0013	.117	.011

TABLE 3. TREAD WEAR IN PHASE II.

Truck type	Tread linear wear rate (in/1000 mi)				Tread area loss after 14,000 mi (in ²)	
	all wheels		worst wheel per axle		all wheels	
	mean	+95% conf	mean	+95% conf	mean	+95% conf
Conventional, variable snubbing	0.0061	0.0007	0.0069	0.0008	.110	.017
Conventional, constant snubbing	0.0056	0.0010	0.0063	0.0014	.111	.014
Radial, retrofit	0.0030	0.0010	0.0036	0.0016	.056	.010
Radial, forced steering	0.0013	0.0013	0.0025	0.0015	.052	.016
Radial, diagonal X-link	0.0028	0.0006	0.0034	0.0010	.042	.010

The linear wear rates were obtained by linear regression of the snap gage readings between 2,000 and 14,000 miles. The two columns of data under the linear wear rate heading are calculated using (a) all wheels for each truck type in the regression analysis, and (b) only the highest wearing wheel (worst wheel) on each axle for each truck type. The worst wheel per axle data are presented because, of course, in practice it is the worst wearing wheel which determines when both wheels of that axle are condemned. The third column in each table represents the area of metal lost after 14,000 miles of operation and is simply determined by comparing the wheel profiles at 14,000 miles, as measured by the modified CN profilometer, with the original unworn profiles measured prior to Phase II. It should be noted that some of the wheels, particularly on the conventional trucks, were withdrawn from the consist before the end of Phase II-b because they had reached the artificial condemning limit of 0.3" of flange wear as described previously. In these cases, the area lost at the time of removal was calculated and these values prorated, assuming the wheels wore linearly with mileage, to obtain an estimate of what the wear would have been at 14,000 miles.

Having made this assumption, it is interesting to note that the mean values agree well with the mean linear wear rates obtained from the snap gage data in that all the results indicate that, in general, the wheels on the radial trucks wore less than on the conventional trucks and that all results place the trucks in the same general ranking order. Thus, despite the fact that the profilometer is regarded as a prototype in the respect that FAST has to resolve some operational and computing problems resulting mainly from the fact that the fixture is used on a "mass-production" type basis, the results are very encouraging.

The flange linear wear rate results for all wheels (presented in Table 2) show that the mean wear rates of the conventional trucks are higher than those for all radial trucks and as much as 2½ times higher than the best performing diagonal X-link radial truck. The scatter of the data, as denoted by the values of the ±95% confidence interval values, is large for the forced steering truck and is even larger still when only the worst wheel per axle is used in the regression analysis. The large confidence interval is caused partly by the smaller sample size--two test vehicles as opposed to three for the other truck designs--but is probably due more to axle/truck misalignment. This notion is supported somewhat by data obtained in the FAST wear index experiment¹² where one of the forced steering trucks tested showed a large angle of attack (3 mrad) on tangent track. Large angles of attack on tangent track are indicative of poor axle alignment.¹³ Additionally, the axle alignment results⁹ indicate that one truck (car 141, truck B) was particularly poorly aligned and it is the wheels on this truck which suffered the highest wear, with both wheelsets being withdrawn from the consist, because of the artificial wear limit, after only 6,000 miles. With the exception of one other wheelset, which was withdrawn after 13,000 miles, none of the other wheels on the forced steering trucks had reached the 0.3" flange wear limit after 14,000 miles of operation. Therefore, the large data scatter is primarily attributable to the high wear rates on one truck.

Apart from the large scatter, the worst wheel per axle results in Table 2 are generally in good agreement with those for all wheels except that, naturally, the mean flange wear rates are slightly higher for all truck types.

The tread wear rates in Table 3, although considerably lower than the flange wear rates, show similar general trends with all radial trucks performing better than the conventional trucks, typically by factors of 2 or 2.5 to 1.

Thus, summarizing the results obtained from Phase II--14,000 miles of operation on unlubricated track--the primary conclusion is that the tread wear on all radial trucks and the flange wear on the best performing radial truck were typically approximately 2½ times better than that on conventional trucks. This conclusion is in reasonable agreement with preliminary results obtained by three Railroads operating a reasonable number of radial trucks. For instance, Union Pacific has 100 carsets of radial trucks in iron-ore service and has monitored wheel wear on these trucks and on 150 carsets of conventional trucks operating in the same service. After 145,000 miles of operation, the data indicates that wheel life on the radial trucks will be at least twice (and probably more) than on the conventional trucks.

Southern Railway has a total of 134,100-ton coal cars in service equipped with self-steering, radial trucks; one unit train of 97 cars is completely equipped with self-steering trucks. Preliminary test results after approximately 150,000 miles indicate flange wear life is at least three times greater than conventional trucks in the same service.

Finally, Canadian National has 75 carsets of radial trucks in service of which 15 carsets are being regularly monitored for wheel wear. Seven carsets of conventional trucks in the same service are also monitored for comparison purposes. Many of the trucks have accumulated 160,000 miles of operation and preliminary results indicate that flange wear on the radial trucks, as determined by monitoring both flange area and flange thickness, is on average approximately 1/3 of that on the conventional trucks.

Asymmetric Wheelwear-Parametric Study

Recognizing that the flange on cars fitted with the forced steering design truck wore more on one side of the vehicle than the other during Phase I, a study was carried out to find the source of this anomaly. As previously mentioned, this was thought to be the result of the systematic installation of wheelsets possessing asymmetric wheel tapers. That is, on a given wheelset, one wheel may have had a 1-in-16 taper and its mate a 1-in-23. In fact, a wheelset difference as great as 1-in-14.7 and 1-in-26.3 was discovered.

Consideration was also given to differences in diameter. This difference, which is not solely attributable to taper difference, may also have independently influenced wheel wear since differences in taper were not highly correlated with differences in diameter. Therefore, these two effects were considered separately in this study.

Axle alignment of two radial design trucks was also

measured to see if this was a source of asymmetric wheel wear. This measure was taken on the retrofit and cross-linked radial trucks, as well as the forced steering truck. Time constraints, however, only allowed for the analysis of the first two truck types and thus the effect of alignment on the forced steering truck was not explored.

On conventional trucks the primary longitudinal stiffness consists simply of a metal to metal side-frame-bearing adapter interface with clearances in the longitudinal direction between the adapter and sideframe. Because of the suspension arrangement, determination of one discrete value of alignment is impossible and thus the alignment investigation did not apply to the conventional style truck.

Common to all truck types is natural variation in wheel hardness. This is present even when all wheelsets used came from a single source and were all class U. Recognizing this, hardness was also considered within each model.

Thus, the parametric study of asymmetric wheel wear was carried out on the Phase I and Phase II-a data set. Common to the two sets were the cars and trucks used. Wheelset parameters were unique to the two phases since two separate populations of 112 wheels were tested. Consequently, the cone angle or taper problem actually provided an opportunity to examine some potential sources of asymmetric wheel wear.

Statistical Model

In order to statistically determine the influence of the wheel parameters on flange wear, a general linear model was developed for each of the truck designs. Basically this took the form:

$$\hat{Y} = \beta_0 + \beta_1 X_1 + \beta_2 X_1 X_2 + \beta_3 X_1 X_3 + \beta_4 X_1 X_4 + \beta_5 X_1 X_5$$

where \hat{Y} = estimated flange wear,

- $\beta_0, \beta_2 \dots$ = coefficients
- X_1 = service life (accumulated mileage)
- X_2 = difference in taper (degrees)
- X_3 = difference in diameter (inches)
- X_4 = wheel hardness (Brinell hardness)
- X_5 = axle misalignment (mrads).

Prior to building the wear model, the distributions of wheel-to-wheel taper and diameter difference, Brinell hardness and axle misalignment were checked.

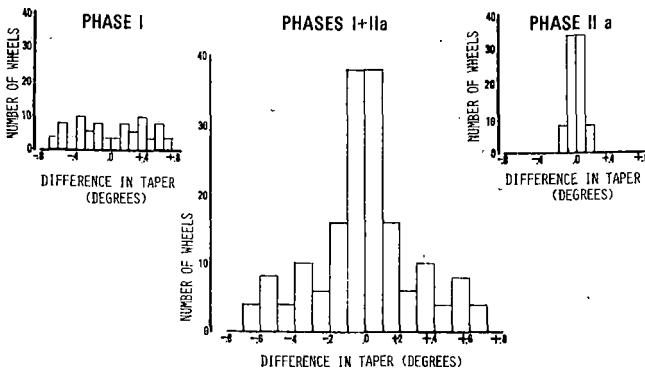


FIGURE 10. DISTRIBUTION OF WHEELS WITH DIFFERENCES IN TAPER.

All of the factors had nearly normal distributions when Phase I and II-a data were combined. The three histograms in Figure 10 illustrate this for wheel-to-wheel taper differences.

As the model for each truck was developed in a stepwise fashion, statistically insignificant factors were eliminated from the equation. Table 4 indicates those factors significant at the .05 level.

TABLE 4.

TRUCK TYPE	VARIABLE				
	X ₁	X ₂	X ₃	X ₄	X ₅
Constant Friction Snubbing*	o	o	o	o	N/A
Variable Friction Snubbing					
Retrofit Radial	o	o	N/S	o	N/S
Forced Steering Radial	o	o	N/S	N/S	N/A
Cross-link Radial	o	N/A	N/A	N/A	o

* indicates both designs combined since there is statistically no difference in wheel wear between them at the .01 level.

o indicates statistically significant variable.

N/S indicates a variable which is not statistically significant at the .05 level.

N/A indicates that this variable was not measured for a particular truck type.

With respect to service life (accumulated mileage), the relative ranking of the four classes of truck is much the same as for the 14,000 mile data from Phases II-a and II-b. Figure 11 illustrates the

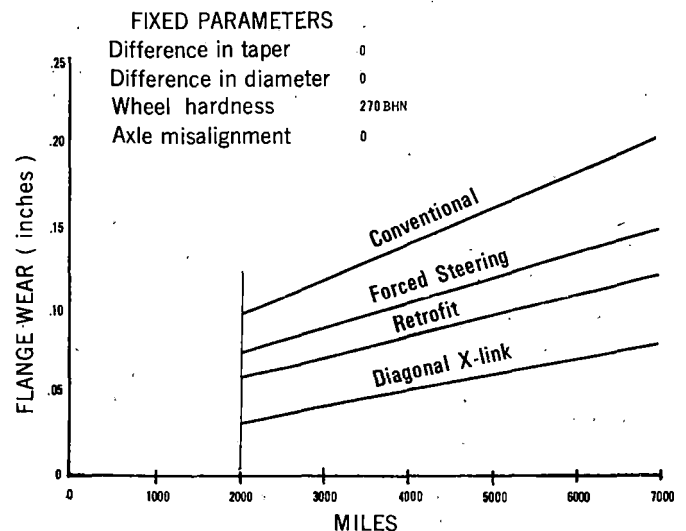


FIGURE 11. STATISTICAL MODEL PREDICTION FOR EFFECT OF MILES.

effect of mileage on flange wear for the four groups. Note, however, that these results are the product of two seven-thousand mile phases of testing. In essence, they represent a 28 car test since the 14 car test group ran twice with both the uncontrolled and controlled profiles.

Having derived separate models for each of the truck designs, an interesting exercise was to control all but one of the statistically significant variables to see the effect on the factor of interest. The first discussed is the taper difference of a wheel in terms of its deviation from the average taper for that wheelset. In Figure 12 the difference in taper effect is presented.

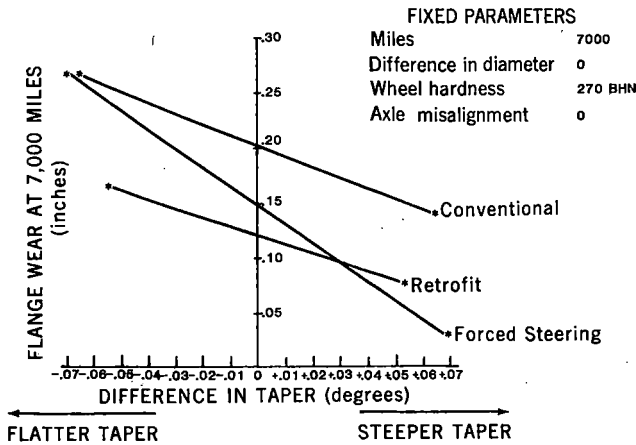


FIGURE 12. STATISTICAL MODEL PREDICTION FOR DIFFERENCE IN TAPER.

The forced steering radial truck was most adversely affected as is shown by the steep curve reflecting estimated flange wear at 7,000 miles. Both the conventional and retrofit radial design are about equally impacted per unit change in taper difference. However, due to improved curving ability, the retrofit truck's magnitude is about 60% that of the conventional. Caution should be exercised when comparing the forced steering with the other designs however. This is because there was an additional effect at work with this truck because all of the more conical wheels were installed on one side of a given car in Phase I. For the other trucks this installation bias did not exist.

From a statistical standpoint, wheel-to-wheel difference in diameter per wheelset was a significant variable in the case of conventional trucks only as shown in Figure 13. Since the experiment was not initially designed to evaluate diameter effects, the sensitivity of the model to detect the impact of diameter asymmetry may have been limited in terms of sample size. As there were six cars equipped with conventional trucks and only three cars each with retrofit and cross-link radial design and two cars installed with forced steering, the conventional group represents a larger sample. Also, the conventional truck causes greater wheel wear making it somewhat easier to dissect statistically the factors which affect this wear.

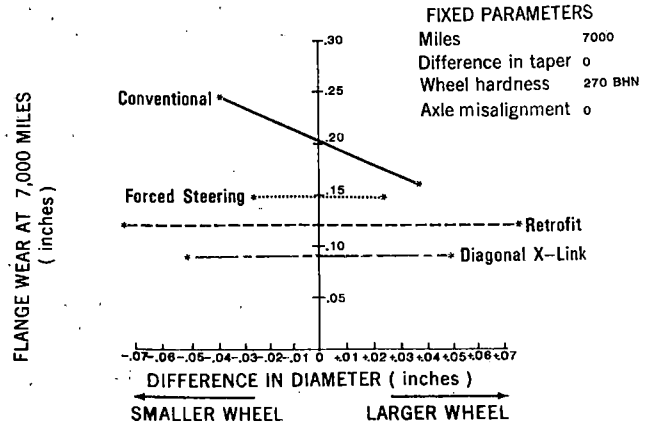
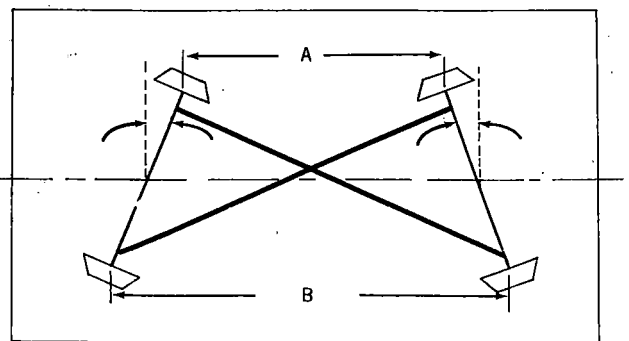


FIGURE 13. STATISTICAL MODEL PREDICTION FOR DIFFERENCE IN DIAMETER.

Lastly, axle misalignment was incorporated into this investigation. The measurement methods and results have been previously reported.⁹ This variable actually is comprised of two components. One is the radial component illustrated in Figure 14 which is the difference in wheel base from one side of the truck to the other. In theory, a truck possessing this misalignment will have a natural tendency to steer well only in one of two directions as shown in Figure 15. This effect should be evidenced by higher wheel wear on the shorter "wheelbase" side of the truck. Its source may reflect the attitude of the wheelsets when installed under the trucks.

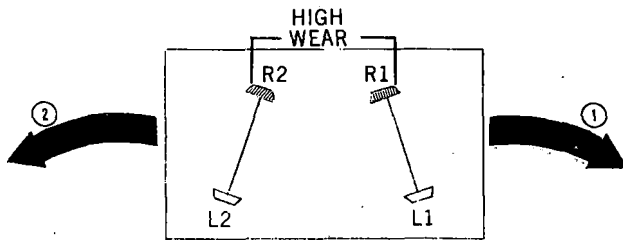
Lateral misalignment is the other component and, as shown in Figure 16, is the result of one axle being displaced laterally with respect to the other. This component can be caused by cross-brace connection distortion or lateral positioning error of the primary suspension.

The direction bias shown in Figure 17 results in higher wheel wear for the shaded wheels. This is because of the high angle of attack which exists between the wheel and rail when these wheels are in the leading outside position.



Misalignment Caused By Difference In Wheelbase, i.e., $B > A$

FIGURE 14. RADIAL MISALIGNMENT.



BOLD ARROWS INDICATE DIRECTION OF TRAVEL CAUSING HIGHEST FLANGE WEAR

FIGURE 15. RADIAL MISALIGNMENT.

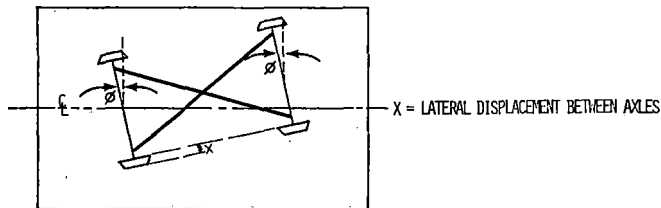
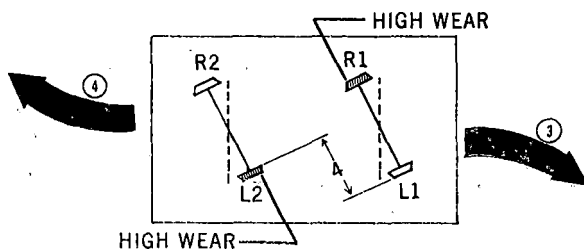


FIGURE 16. LATERAL MISALIGNMENT.



BOLD ARROWS INDICATE DIRECTION OF TRAVEL CAUSING HIGHEST FLANGE WEAR

FIGURE 17. LATERAL MISALIGNMENT.

For the two radial truck designs, the radial component proved insignificant at the .05 level. Presumably, this is a result of the low primary longitudinal stiffness provided by the rubber pads between sideframe and bearing adapter being overcome by the truck's tendency to correctly negotiate a curve. Hence for these trucks the radial component is a 'soft' misalignment which is not a source of concern for the range of misalignments measured in this experiment.

Lateral misalignment, however, did have an affect on wheel wear in the diagonal cross-link truck as is evident in Figure 18. Although the retrofit truck possessed the same range of lateral misalignment, and responds in principal to the same forces that the cross-linked truck does, it was not a statistically significant variable. Possible explanations for this anomaly will be studied in future testing.

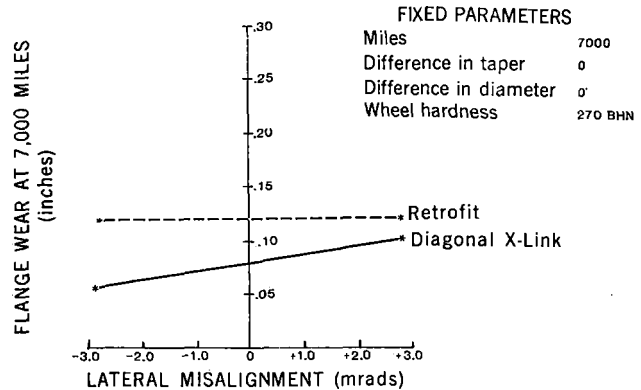


FIGURE 18. STATISTICAL MODEL PREDICTION FOR LATERAL MISALIGNMENT.

CONCLUSIONS OF PARAMETRIC STUDY

The primary findings of the parametric examination of asymmetric wheel wear were:

- substantial difference in taper on the same axle results in asymmetric flange wear for the range of taper differences studied,
- diameter differences may be worthy of further investigation on conventional trucks, and
- lateral misalignment of axles on at least the cross-link radial truck has a detrimental effect on wheel wear.

The first two points are particularly noteworthy since they involve conventional and radial trucks.

In fact, a survey of reprofiled wheels from a major U.S. Railroad revealed variations in taper from 1-in-16.3 to 1-in-57.3. Since the wheels used in this experiment ranged from 1-in-14.7 to 1-in-26.3, it should give an idea of the potential negative effect of taper variation which may be present unrecognized throughout the industry.

The final point regarding lateral misalignment of diagonal cross-link radial trucks may be more of a design consideration unique to radial trucks. In general, however, it brings to light the fact that much more is to be learned about radial trucks before the full potential of this truck design is fully exploited.

Notations

- Kx - primary longitudinal stiffness per axle
Ky - primary lateral stiffness per axle
Kb - interaxle bending stiffness
Ks - interaxle shear stiffness
b - semi sideframe spacing
a - semi truck wheelbase
Kl - anti-lozenging stiffness per bolster end
Kcb - cross-bracing shear stiffness

REFERENCES

- 1 Hengal, M. F. - "Freight Car Wheel Performance," paper presented at the Sixth International Wheelset Congress, Colorado Springs, Colorado, October 1978.
- 2 Pollard, M. G. - "The Development of Cross-braced Freight Bogies," Rail International, September 1979.
- 3 FAST Report FAST/TTC/TN-81/02, "Radial Truck Experiment, Preliminary Observations Prior to Restart," May 6, 1981.
- 4 Steele, R. K. - "Rail Wear and Metal Flow," 1981 FAST Engineering Conference, November 1981.
- 5 Brent, J. W. - "Track Degradation Experiment," 1981 FAST Engineering Conference, November 1981.
- 6 Larkin, T. P. - "Evolution of Measurement Techniques at FAST," 1981 FAST Engineering Conference, November 1981.
- 7 Gray, D. E. - "Major Variables that Affect Wheel Wear," 1981 FAST Engineering Conference, November 1981.
- 8 Kahle, V. E. - "Wear Rates of Freight Car Wheels as a Function of Chemistry," 1981 FAST Engineering Conference, November 1981.
- 9 FAST Report FAST/FRA/TTC/81/04, "Axle Alignment Measurements on Cars in the FAST Radial Truck Experiment," September 1981.
- 10 Scheffel, H. - "Self-steering Wheelsets Will Reduce Wear and Permit Higher Speeds," Railway Gazette International, December 1976.
- 11 Scheffel, H. and Tournay, H. M. - "The Development of an Optimum Wheel Profile for Self-steering Trucks Under Heavy Axle Load Conditions," ASME Winter Annual Meeting, November 1980.
- 12 Allen, R. A. and Jollay, J. P. - "The Mechanical Aspects of Wheel/Rail Wear," 1981 FAST Engineering Conference, November 1981.
- 13 Elkins, J. A. and Allen, R. A. - "Testing a Transit Vehicle for Wheel and Rail Wear," ASME Winter Annual Meeting, November 1981.

QUESTIONS AND ANSWERS

Question 1

Since TDOP showed the retrofit truck had a higher hunting threshold than the cross-braced truck, this would indicate that the cross-braced truck had a lower yaw stiffness which would improve curvability. Wouldn't a simple reduction in the adaptor pad stiffness on the retrofit truck improve wear at FAST?

Answer

The FAST track is not suitable for stability (hunting) tests because of the relatively low maximum operating speed of 45 MPH and the short lengths of tangent track, although such tests could be carried out on other tracks at the TTC. Thus, the Radial Truck Experiment is not designed to evaluate the stability of radial trucks, but I agree with the questioner that I would expect that a reduction in the adapter pad stiffness, i.e., the primary lateral and longitudinal stiffness, would result in a reduction in wear rates. The choice of an optimum primary suspension stiffness often results in a compromise between the requirements to achieve an acceptable critical (hunting) speed and good curving performance.

Question 2

The slides showed the cross-link radial truck to be 2½ times better than conventionals and the retrofit approximately 1½ times better than conventionals at FAST. Industry data shows

CN and Southern (retrofit trucks?)	3 times better
UP (cross-links?)	2 times better

Can you comment on this apparent difference? What about initial profiles on which test trucks were started?

Answer

The data presented in the conference paper deals only with the unlubricated track phase of testing. Remembering that wheel wear data has yet to be collected on lubricated track, the experiment is only part way through completion, and the authors feel that there is insufficient data available with which to draw comparisons between the three radial truck designs. The primary intent of the paper is to show that, in general, the radial trucks show an improvement in flange wear over conventional three-piece trucks by a factor of approximately 2½ to 3 and that the FAST data agrees reasonably well with the preliminary data obtained from three railroads.

Discrepancies between FAST and industry data can probably be accounted for by consideration of the test conditions. The conditions for this experiment have been documented in the paper, although one further consideration is that all components on the test trucks were in a new or nearly-new condition at the beginning of the experiment. Because of the low mileage

accrued during this portion of the experiment, truck component wear was minimal. For a given amount of wheel wear, truck component wear in normal service would be considerably greater than that experienced during this experiment. Thus, the effect of increased truck clearances due to component wear, particularly those components which control truck squaring on conventional trucks, have not been accounted for in this experiment.

The questioner's assumption that CN has retrofit radial trucks in their test consist is correct, but Southern Railway has a mixture of both retrofit and diagonal cross-link radial trucks. The UP data, for diagonal cross-links, indicates an improvement of at least two times, and probably more, over conventional trucks.

As described in the text, the wheels on the diagonal cross-link trucks were turned to a special high conicity profile whereas those on all other test trucks had the standard AAR 1 in 20 profile. These profiles were the result of decisions made by the manufacturers prior to the test, and the effects of wheel profiles on the curving performance of radial trucks is of considerable interest to the industry. A new "mini-test" experiment, described in the paper entitled "Radial Truck Curving Performance Evaluation," will be carried out at FAST in early 1982 which should provide data with which to assess this effect.

THE MECHANICAL ASPECTS OF WHEEL/RAIL WEAR

Roy A. Allen
Experiment Manager, Radial Trucks
Association of American Railroads

James P. Jollay
Engineer
Boeing Services International, Inc.

Wheel/rail lateral load and angle of attack data obtained from two "short-term" experiments on FAST are used to examine their applicability to predict wheel flange wear measured on two long-term wheel wear experiments. The data suggests that the product of lateral load and angle of attack, while not being directly proportional to wheel wear, is a reasonable predictor of the flange wear data examined. The data presented should provide for further detailed examination of wear indices which have been proposed in the past. The data also indicates that neither the presence of rail gage-face lubrication, nor varying axle load, has much effect on the magnitude of the axle angles of attack and only the latter has a definite effect of the magnitude of the lateral loads for conventional three-piece trucks.

INTRODUCTION

The wear of wheels and rails, in particular wheel flange and rail gage face wear, represents a substantial portion of expenditure to railroads, particularly with the fairly recent introduction of unit trains and increases in car capacity and motive power output. On a world-wide basis, many research organizations associated with railroads, their suppliers, and government agencies have sought a better understanding of the wheel/rail interface phenomena, all with common goals to increase railroads' safety and efficiency and to reduce wheel and rail wear.

There are many kinds of wear mechanisms and the interaction and influence of many different factors creates a very complex problem to those researchers studying the phenomenon. The list of factors affecting wheel and rail wear is exhaustive but can be divided into three major categories; i.e., mechanical, metallurgical, and the external environment. Within the mechanical group, such factors as operating conditions (traffic density, speed, braking characteristics, etc.), wheel/rail contact area geometry, creepage, and contact stresses exist. The metallurgical group contains such effects as wheel and rail hardness and chemistry content, heat treatment and microstructure, and within the external environment the effects of track lubrication and relative humidity exist.

Much work has been, and continues to be, carried out in this field although most literature on the subject results from laboratory testing. Relatively little field work has been carried out partly because of the high cost associated with this type of testing but also because of the difficulty in achieving a controlled wear environment in the "real

world". For instance, when studying rail wear in service, the data can be very difficult to analyze because of the wide variety of vehicles, axle loadings, etc. and also because the external environment is rarely constant. Similarly, wheel wear data is confounded by changes in the external environment, varying rail metallurgies and the fact that vehicles typically encounter a wide range of track curvatures. Although it is not perfect for this type of research, FAST provides a more controlled environment than most real world situations and thus lends itself better to this type of investigation. Consequently, the FAST program has begun to investigate the wheel/rail wear phenomenon. Steele¹ has investigated some of the metallurgical and external environment factors, particularly the effects of wheel/rail hardness and track lubrication, and this paper examines some of the mechanical factors.

Thus the metallurgical and external environment factors play an important role in the wheel and rail wear, and the phenomenon is complex. However, it would be extremely important, particularly to truck designers, to be able to relate wheel and rail wear, for a given set of metallurgical and external environment conditions, to the mechanical parameters associated with the wheel/rail interaction. With this in mind, a number of "wear index" formulae have been proposed and, in some cases, used as predictors of wheel and/or rail wear but with little full-size experimental data to determine their validity. This paper describes some data obtained from FAST which can be used to determine the applicability of these wear indices to the prediction of flange wear. Data from two short-term experiments, the Wheel/Rail Loads Test and the Wear Index experiment are compared with flange wear data from the long-term Variable Axle Load and Radial Truck experiments.

WEAR INDICES

Heumann² is believed to be one of the first to suggest a wear index and proposed that

$$W_f \propto \mu_f F_f \theta_w \quad (1)$$

where W_f = flange wear
 μ_f = coefficient of friction in flange contact patch
 F_f = flange force
 θ_w = wheelset angle of attack.

Ghonem and Gonsalves,³ by making certain assumptions, particularly that the creep force of the outer leading wheel is one-half of the flange force of the outer leading wheel, approximated Heumann's index to

$$W_f \propto 2 T_y \theta_w \quad (2)$$

where T_y = total lateral outer wheel force in plane of the rail

Marcotte, Caldwell and List⁴ refined Heumann's index by accounting for the fact that with standard AAR 1 in 20 profiles the rail usually contacts the wheel on both the tread and the flange in curving situations. Thus, they proposed that

$$W_f \propto \mu_f F_f \sqrt{\frac{a^2}{r} + (\theta_w \tan \beta)^2} \quad (3)$$

where a = vertical distance from flange contact point to the tread
 r = wheel radius
 β = flange angle.

The same authors⁴ also proposed another index, albeit an approximation, which has the advantage that the key parameters are measurable with track or wayside instrumentation. This "pseudo" wear index is:

$$W_f \propto \frac{P \theta_w}{809,350} \quad (4)$$

where P is the tie plate force measured in Newtons
and θ_w is measured in degrees.

An approximate analytical model describing the total wear on both high and low rails as a function of the angle of attack has been presented by Ghonem and Kalousek.⁵ Their approximation is:

$$\text{for } \theta_w < 20 \text{ arc-minutes } W_{tr} \propto K_1 \theta_w + K_2 C_{22} \theta_w^2 \quad (5a)$$

$$\text{for } \theta_w > 20 \text{ arc-minutes } W_{tr} \propto K_3 \theta_w \quad (5b)$$

where W_{tr} is the total wear on both high and low rail
 K_1 , K_2 and K_3 are material constants accounting for metallurgical and rheological parameters affecting the worn rail
and C_{22} is the lateral creep coefficient.

Finally, Elkins and Eickhoff⁶ have hypothesized that wheel and rail wear rates should be a function of the work done, which for a wheel moving along a rail is proportional to the summation of the creep forces and creepages. Thus

$$W_w \propto T_1 \gamma_1 + T_2 \gamma_2 \quad (6)$$

where W_w is the total wheel wear (flange and tread)

T_1 and T_2 are the longitudinal and lateral creep forces respectively

and γ_1 and γ_2 are the longitudinal and lateral creepages respectively.

It will be noted that for all these wear indices, the angle of attack and lateral force of one sort or another; i.e., either F_f , T_y , P or T_2 , are the dominant parameters. The effect of the angle of attack in equation 6 may not be readily apparent but $T_2 \gamma_2$ typically is much larger than $T_1 \gamma_1$ for bad curving, high wear situations and of course the angle of attack dominates⁶ the lateral creepage (γ_2) expression. Thus, it appears that careful measurement of lateral forces and angles of attack is a key to understanding which combinations of wheel/rail interaction parameters are liable to provide good predictors of wheel and rail wear.

WHEEL/RAIL LOADS TEST

The wheel/rail load test, carried out at the Transportation Test Center, primarily on the FAST track, in June 1979 has supplied data which can be used to help understand the nature of wheel/rail loads and angles of attack in curving situations. The experiment represented the first attempt to quantify the load environment, both dynamic and quasi-static, at FAST. There were many objectives to the experiment which are too numerous to detail here. Axle, truck, and carbody accelerations were measured as well as axle angles of attack and wheel/rail loads in order to determine the effects of various parameters including train direction and speed, train handling (buff, draft, and drift conditions), different car/truck centerplate and side bearing configurations, car and truck component wear, track lubrication, and axle load. Many of the data have been reported by Allen and Peters,⁷ Johnson,⁸ et.al., and Harrison and Tuten.⁹ The angle of attack data will be reported shortly as a FAST report. From this plethora of information, only the lateral load and angle of attack data pertaining to the effects of track lubrication and axle load are presented here, as these are the primary items of interest for the subject matter being discussed.

INSTRUMENTATION

Data obtained from three items of instrumentation are discussed. Angles of attack were measured using a track mounted (wayside) system developed by and operated by Canadian Pacific Limited personnel⁵. Wheel/rail loads, in both lateral and vertical directions, were measured using wayside instrumentation;¹⁰ i.e., strain gaged rails developed by Battelle-Columbus Laboratory, in Section 7, and by an instrumented wheelset developed and operated by IIT Research Institute staff.¹¹

Angle of attack was measured by a unit which consists of three low power lasers, three photo diode detectors, and the necessary recording systems, Figure 1. The system is setup so that the two lasers (2 and 3) opposite each other intersect in a horizontal plane radially to the rail curve and the beams are 0.25 inches above the rail running surface. The lasers are located on the outside of the

rails and the detectors are located in the center of the track.

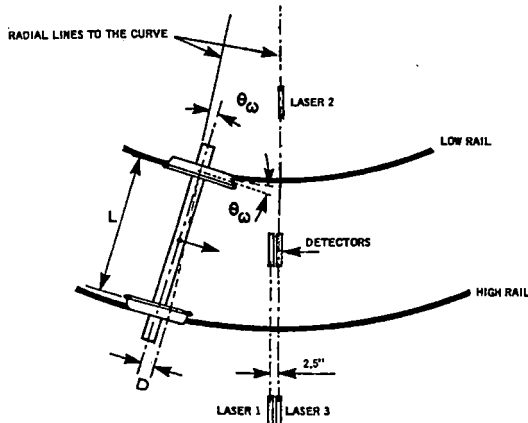


Figure 1 Alignment of Lasers and Detectors

The angle of attack (θ_w in Figure 1) is the inverse tangent of the calculated difference between the wheel centers with respect to the radial position (D) divided by the top of flange to top of flange wheel spacing on an axle (L); i.e., $\tan \theta_w = D/L$. The displacement between the center of the two wheels is obtained by measuring the difference between the time they interrupted and cleared the two oppositely placed laser beams (lasers 2 and 3). To convert the time signals into displacements, the speed of the wheelsets are calculated using lasers 1 and 3 which are placed side by side 2.5 inches apart.

Wayside instrumentation to determine the vertical and lateral loads between the wheels and rail utilized the Battelle Columbus Laboratory Chevron¹⁰ design strain gage bridge circuit. The lateral circuit consists of eight strain gages mounted on the web of rail. The gages are placed on the web of the rail and wired in a bridge to give maximum output for lateral loads and minimum output for vertical loads. The vertical circuit consists of four gages on the rail base. These gages are placed and wired to give maximum output for vertical loads and minimum loads for lateral loads. The data from these two circuits are processed to determine the degree of crosstalk between the circuits so that appropriate adjustment can be made to isolate the vertical and lateral loads.

The wheelsets¹¹ were designed to measure the lateral and vertical forces acting at the wheel/rail interface. This is done by strain gages located on the wheel plate. Six strain gage bridges are used on each wheel. Three bridges respond primarily to vertical load. Data from these are utilized in 60 degree segments of wheel rotation. Two of the bridges respond primarily to lateral forces. These are utilized in 90 degree segments of wheel rotation. The last bridge responds primarily to the lateral position of the line-of-action of the vertical load. The data from all three types of bridges are processed to determine the degree of crosstalk between bridges so that appropriate adjustments can be made in processing the output data to isolate the vertical and lateral loads. For this test, 36 inch diameter wheels setup for 100 ton loads were utilized.

EFFECT OF TRACK LUBRICATION

Because track lubrication has a large effect on wheel and rail wear, let us examine its effect on lateral loads and angles of attack. Table 1 presents instrumented wheelset data for two separate laps of the FAST track, one lap with the gage face of the outside rail well lubricated and the other for completely unlubricated track. The instrumented wheelset was fitted to the lead axle of a conventional three-piece truck running under a fully-laden 100-ton hopper car at the head end of the FAST consist. The nominal speed was 45 MPH and the train was travelling in the counterclockwise direction. The instrumented wheelset measures the lateral loads continuously and the data shown in Table 1 are the mean values as measured by the wheelset throughout each of the curved sections. It can be seen that, as would be expected, the lateral loads on the lead axle outer (high rail) wheel are higher than those on the inner (low rail) wheel on the 4° and 5° curves. More importantly in the context of this paper, with the exception of the 5° curve in section 17 where the uphill grade may have confounded the results, the lateral loads, on both the inner and outer wheels, vary by less than 1,000 lbs. for lubricated and unlubricated track.

Thus, it would appear that track lubrication has little effect on the magnitude of the lateral wheel/rail loads and this conclusion is substantiated by lateral load data as measured by the wayside instrumentation in Section 7 (5° curve). The load exceedance spectrum shown in Figure 2 was generated⁹ from data collected from seven high rail strain gaged sites spread evenly through the curve in Section 7

TABLE 1. MEAN LATERAL LOADS ON LUBRICATED AND UNLUBRICATED TRACK AS MEASURED BY THE INSTRUMENTED WHEELSET.

Track section	Mean lateral loads on lead axle (kips)			
	Lubricated track		Unlubricated track	
	outer wheel	inner wheel	outer wheel	inner wheel
Section 3 - 5° curve	13.7	9.6	13.2	9.5
Section 13 - 4° curve	11.6	7.2	10.6	7.7
Section 17 - 5° curve	11.7	8.2	14.1	10.5
Section 17 - 3° curve	7.4	7.5	8.0	7.5

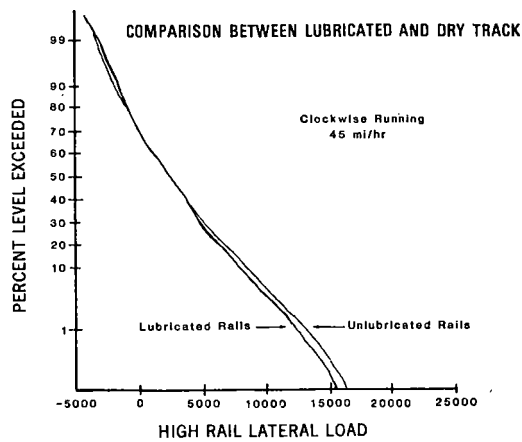


Figure 2 Wheel/Rail Loads Test - Wayside Data

which were monitoring the lateral loads for the complete FAST train, which, for this experiment, consisted primarily of fully laden 100-ton hopper cars with conventional three-piece trucks but also had a few partially laden cars and some fully laden cars with radial trucks. Figure 2 includes loads generated by the trail axles, as well as the lead axles on every car in the consist, which explains why many of the loads recorded are very low, and shows again that only minor differences exist between the lateral loads generated on lubricated and unlubricated track.

Similarly, mean angle of attack values for lubricated and unlubricated track are presented in Table 2. These data were generated by the CP wayside angle of attack system positioned midway through the 5° curve in Section 7.

TABLE 2. MEAN ANGLES OF ATTACK FOR LEAD AXLES OF CONVENTIONAL TRUCKS ON 5° CURVE.

Track condition	Mean angle of attack (m rads)
Lubricated	4.9
Unlubricated	4.3

The values shown are for the lead axles on the conventional three-piece trucks which were part of the consist during the wheel/rail loads test, and are the means for three passes of the consist for each track condition at a nominal speed of 45 MPH. It will be noted that the mean angle of attack on lubricated track (lubrication of the gage face of the high rail) is slightly higher than that on unlubricated track.

Thus, the data from the wheel/rail loads test show that track lubrication has little effect on either the lateral loads or the angles of attack on conventional three-piece trucks and yet, from FAST experiments^{1 12}, we know that effective track lubrication substantially reduces the wear of wheels and rails. If lateral loads and angles of attack, or combinations thereof are in fact good predictors of wear, it is obvious that separate relationships between these parameters and wear rates must exist for the different track conditions.

EFFECT OF AXLE LOAD

An experiment is being carried out on FAST to determine the effect of axle load on wheel wear. In the experiment, named the Variable Axle Load Test (VALT), are 16 hopper cars fitted with conventional three-piece trucks. Two cars are laden at 110-ton, four at 100-ton, two at 80-ton, two at 66-ton, two at 33-ton, and the remaining four cars are empty. Gray¹³ has reported the results from 14,000 miles of operation on unlubricated track which show an unexpectedly low effect of axle load on the flange wear rates with the 100-ton cars showing only approximately 1½ times more wear on average than the empty cars. The results are shown in Figure 3 as the mean flange wear rates, as determined from wheel snap gage¹² data, for each of the six loading configurations, plotted against axle load. The straight line shown in this Figure represents the best characteristic line determined using a least square technique.

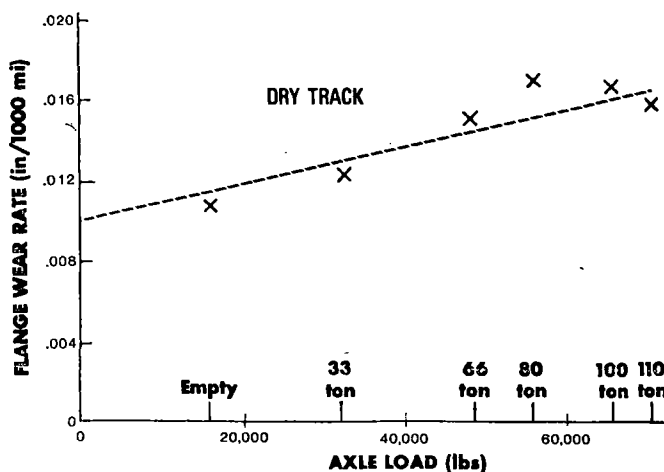


Figure 3 VALT - Flange Wear Rate Data

In order to examine the applicability of wear indices as predictors of wear, and also as an attempt to better understand the VALT data, angle of attack and lateral load data obtained from the wheel/rail loads test for different vehicle loading conditions were examined. For the wheel/rail loads test, only four loading conditions existed, as compared with six for VALT, with three cars each in the empty, 66-ton, and 110-ton conditions. Most of the remainder of the consist was loaded to 100-ton but only three fully laden cars were chosen for this investigation.

The mean angles of attack for the lead axles of the trucks under the vehicles with the four different loading conditions, as measured by the CP angle of attack system in Section 7, are shown in Figure 4. The data indicates that the angles of attack are independent of axle load.

The high lead axle lateral force data measured by the wayside instrumentation in Section 7, is presented in Figure 5 and indicates that the lateral loads are very nearly directly proportional to the axle load.

The product of the mean lateral load and angle of attack is also plotted against axle load in Figure 6. This product has been computed because, as discussed previously, it is the primary parameter

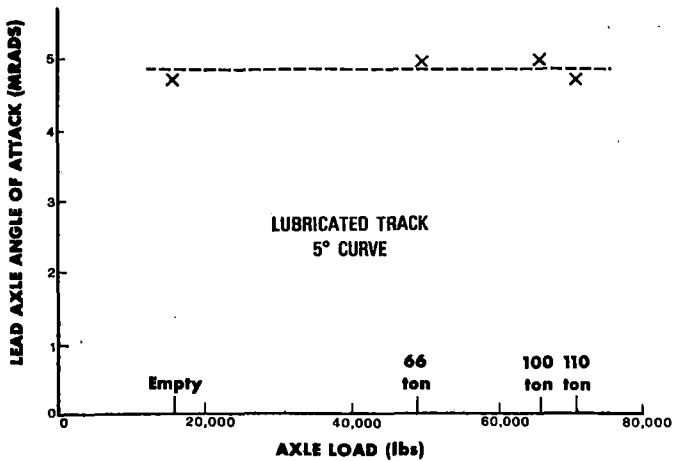


Figure 4 WRL Wayside Angle of Attack Data

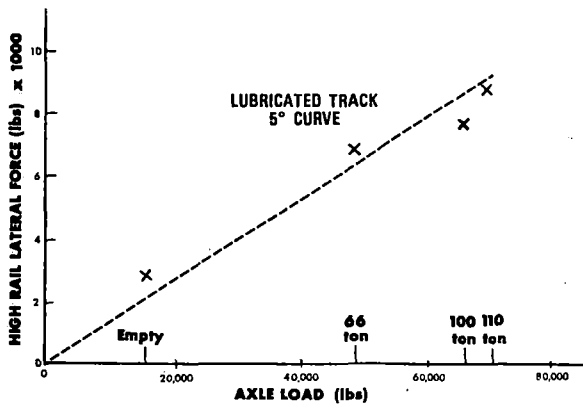


Figure 5 WRL High Rail Lateral Force Data

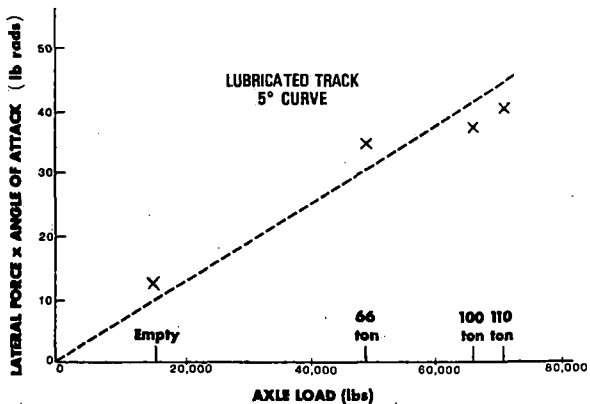


Figure 6 WRL Data Lateral Force x Angle of Attack

which appears in most wear indices. Because of the relationships shown in Figures 4 and 5, the product of lateral load and angle of attack also appears to be directly proportional to axle load.

The lateral load and angle of attack data obtained from the wheel/rail loads test cannot strictly be compared with the VALT flange wear data because the latter data was obtained on unlubricated track whereas the data in Figures 4 and 6 was obtained on lubricated track, although we have noted previously that track lubrication in general has little effect. In addition, the wheel rail loads test data applies only to the 5° curve in Section 7 whereas, of course, the VALT data was obtained from operating on

the complete FAST track which contains 3°, 4°, and 5° curves, although 76% of constant curvature track on FAST is 5°. Despite the above limitations in the data, the differences in the characteristics of the data in Figures 4 thru 6 as compared with the VALT flange wear data in Figure 3 are large enough to speculate that neither angle of attack, nor lateral load, nor the product of these two parameters are directly proportional to flange wear.

WEAR INDEX EXPERIMENT

With the data obtained from the FAST wear index experiment, the investigation of the validity of using wear indices as predictors of wheel and rail wear has taken a step forward. The experiment, the majority of which was carried out in August 1981, was designed with the intention of gathering data which could be used to explore whether relationships exist between a) wheel/rail lateral load, b) axle angle of attack, c) the wear indices described previously, and flange wear data obtained from the Variable Axle Load Test¹² and the Radial Truck experiment.¹³ A second objective was to determine the quasi-static load and angle of attack environment for each subsection of track containing different rail metallurgies. This data will assist the analysis of the results from the FAST Rail Metallurgy Experiment and are not discussed here.

Five trucks were involved in the experiment as outlined in Table 3. The retrofit and forced steering trucks are radial trucks which have been described by Allen and Leary.¹³ Testing was carried out with the normal FAST consist operating and data gathered in both clockwise (CW) and counterclockwise (CCW) directions on lubricated and unlubricated track. Between CW and CCW runs, the whole consist was turned and the same axle on each car became the leading axle in both directions. Because of this, and because the lead axle typically is subjected to a much more severe wear environment than the trail axle, the lead axle for each car during the wear index experiment is noted in Table 3.

In an attempt to reproduce the conditions in which the vehicles operated in the experiments from which the wear data was obtained, in the wear index experiment the vehicles were tested in a position in the consist which was typical of the position that they were most commonly in during either the VALT or Radial Truck experiment. Thus, cars 133, 139, and 140 were tested at the head end of the consist and cars 48 and 63 in a mid-train position. In order to obtain data on the effects of consist position, car 133 was also tested in the mid-train position and at the rear of the consist. All test runs were carried out at the normal FAST operating speed which is a maximum of 45 MPH but varies around the track largely as a result of gradients.

INSTRUMENTATION

Two instrumented wheelsets, both placed on one truck of each vehicle as outlined in Table 3, were used during this experiment. One wheelset was the same one as used for the wheel/rail loads test and the other, again designed and built by IIT Research Institute, was loaned by the Association of American Railroads. The angle of attack measurements were made by truck-borne instrumentation using wheel/rail displacement probes of the type used by British Rail

TABLE 3. WEAR INDEX TEST VEHICLES.

Car #	instrumented truck	lead axle	truck type	car leading	wear experiment
48	A	4	conventional	empty	VALT
133	A	4	conventional	100-ton	Radial Truck
63	A	4	conventional	110-ton	VALT
139	B	1	retrofit	100-ton	Radial Truck
140	A	4	forced steering	100-ton	Radial Truck

on curving tests⁶.

Continuous angle of attack was determined using four wheel to rail displacement probes. The probes were based on a British Rail design and each one consists of a follower wheel and arm, a vertical and a lateral pneumatic cylinder, and a strain gaged bending beam, Figure 7. The follower wheel is designed to contact the rail at an angle which simulates that of the flange on a new profile wheel. The vertical cylinder provides a positive down force on the probe and raises the probe to clear track obstructions. The lateral cylinder provides a positive outward force on the follower wheel and retrack the follower wheel inward before the probe is raised. On the end of the follower wheel arm is a cam arrangement. This cam causes the bending beam to deflect as the follower wheel moves laterally. The lateral deflection of the follower wheel is determined in a calibration procedure in terms of the output of the strain gage bridge on the bending beam. Each probe is calibrated over a range of ± 1.6 inches travel.

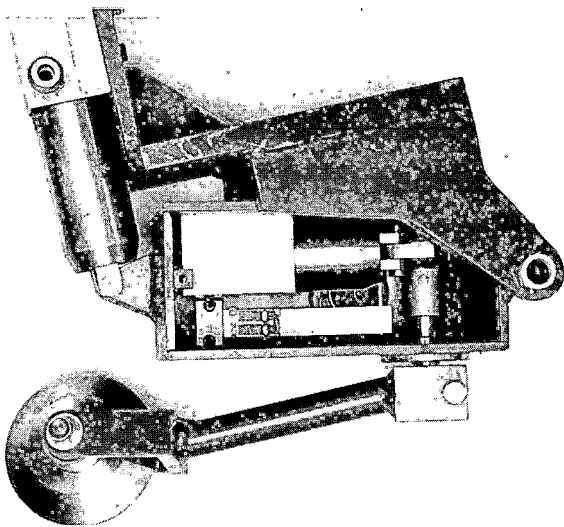


Figure 7 Displacement Probes - British Rail Design

The experiment setup is shown in Figure 8. Two probes were mounted on each side of one wheel per wheelset, Figure 9. The frame used to mount the probes was constructed of aluminum and mounted on the end of the axle. The mount to the axle utilized a spindle that attached using the three bolts for the roller bearing and cap. The frame mounts on the spindle through a bearing which allows free rotation. The probes thus move with respect to the

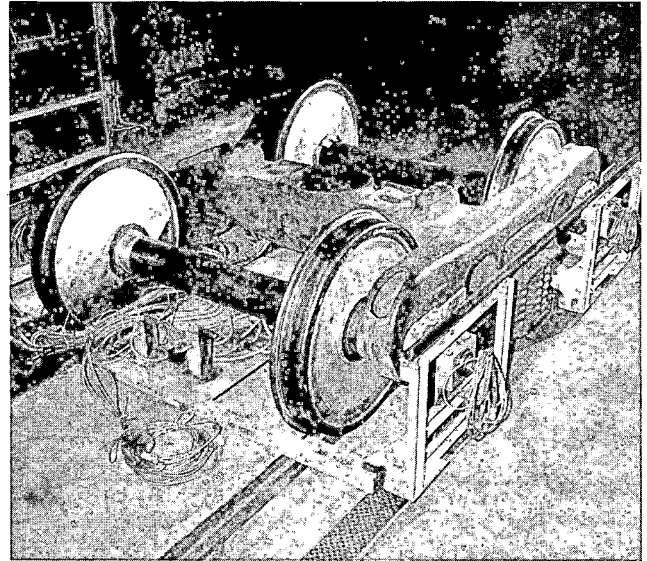


Figure 8 Truck Setup with Probes

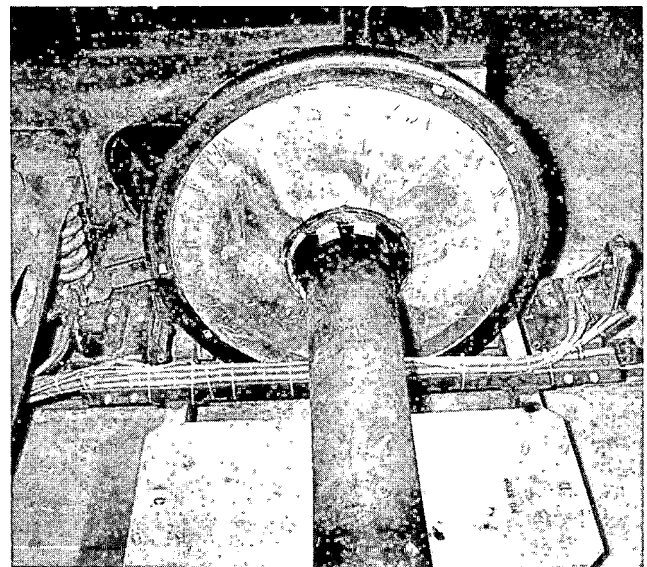


Figure 9 Two Probes Mounted on Track Side of Wheel

center of the axle. The frames on each wheelset are connected together by two pieces angle iron. The angle irons are slotted on one end and metal to metal contact is prevented by using teflon spacers. This connection allows the wheelsets to yaw with respect to each other but prevents the frame from rocking which would adversely affect the measurements.

The displacement of each probe is measured continuously over the test sections, Figure 10. The angle of attack is determined by taking the difference between the two probes on a wheel and dividing by the spacing of the probe follower wheels. The

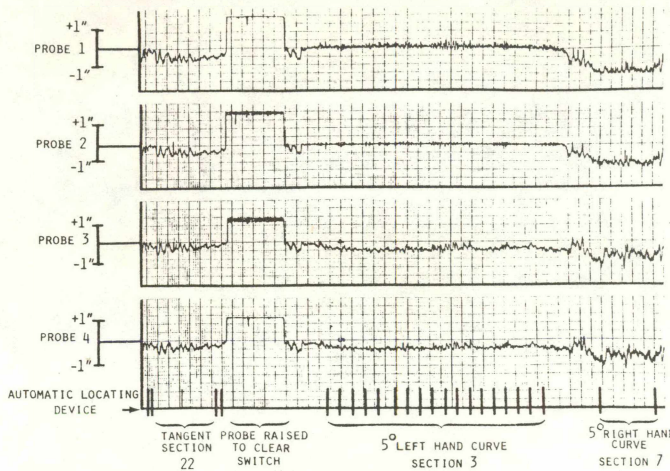


Figure 10 Displacement Analog Data - August 1981

reference zero angle of attack is determined by placing a machined straight edge across the back of a wheel and contacting the two probes at a controlled reference point on the follower wheel. In this position, the probes are set for zero volts output.

ANGLE OF ATTACK AND LATERAL LOAD DATA

Before investigating the relationships between lateral loads, angles of attack, and flange wear, it is interesting to examine the first two parameters as a function of track curvature. Figure 11, for instance, shows the lead axle angles of attack for the 100-ton car with conventional trucks plotted against track curvature of right and left hand curves and with the track both lubricated and unlubricated. The data substantiates one of the wheel/rail loads test conclusions that, for conventional trucks, lead axle angles of attack are slightly higher on lubricated than they are on dry track. As a point of caution, in all of Figures 11 thru 14 a line has been drawn through the data points, straight lines in the case of Figure 11, in order to provide clarity for the reader although the line shown may not properly describe the characteristics. For these graphs, the correct relationships cannot be determined because of the lack of data between 0° (tangent track) and 3° curves. It should also be noted that the data points shown for a track curvature of 5° are the mean values of the data obtained on all three 5° curves on the FAST track.

One other conclusion from the wheel/rail loads test was that axle load had little effect on the angle of attack. Figure 12 presents lead axle angle of attack data for the three vehicles with conventional trucks with different loadings tested at the mid-train position. The angles of attack are similar in magnitude for the 100-ton and empty cars on the right hand curves and for the 100-ton and 110-ton cars on the right hand curves. Although not as convincing as the previous experiment, these data suggest that the wheel/rail loads test conclusion is valid.

The angles of attack for the three truck types tested, all under cars loaded to 100-ton tested at the head end of the consist, are presented in Figures 13a, for right hand curves, and 13b for left hand curves. The rapid increase in angle of attack

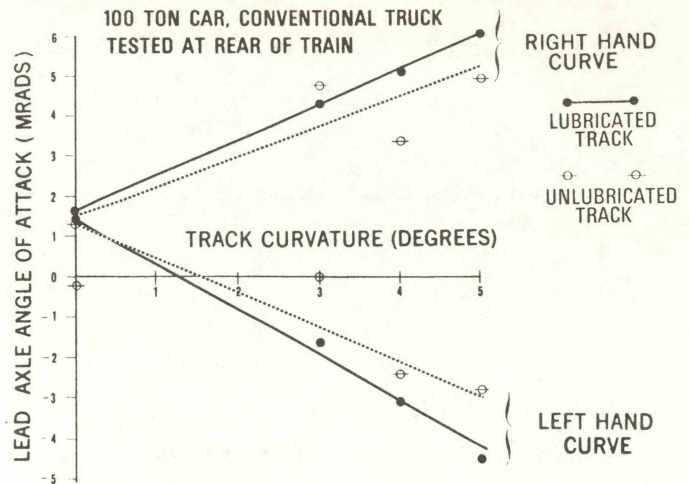


Figure 11 Track Lubrication Comparison - Angle of Attack

ALL CONVENTIONAL TRUCKS

TESTED AT MID-TRAIN POSITION

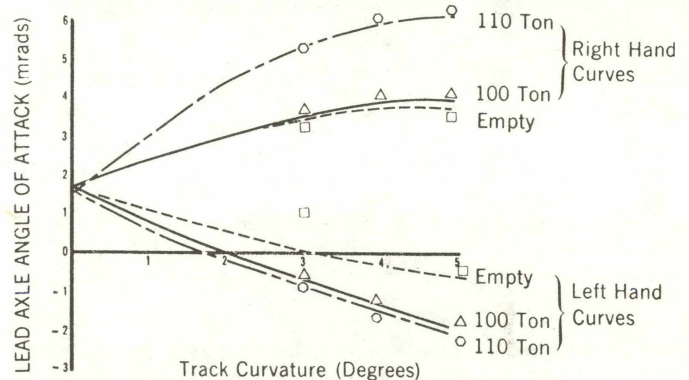


Figure 12 Car Lading Comparison - Angle of Attack

as a function of track curvature for the conventional truck is in contrast to the relatively small changes (less than 1 mrad) measured on both radial trucks. Despite this slow rate of change, the angles of attack, particularly for the forced steering truck on the right hand curves, of the radial trucks tested are of similar magnitude as those on the conventional trucks on the 5° curves. This apparent contradiction is probably due to axle misalignment on these trucks which has the effect of moving the data on a graph of angle of attack plotted against curvature either up or down, depending upon the direction of the angular misalignment, by a magnitude dependent upon the magnitude of the misalignment. Misalignment, which is manifested as an offset on the vertical lead scale in Figure 13 (i.e., it causes a non-zero lead axle angle of attack on tangent track) has previously been acknowledged^{3 6 14} as affecting truck curving performance and has been shown to be a potential cause of asymmetric wear of wheels.¹³ Obviously the angles of attack shown in Figure 13 apply only to the trucks that were tested--other trucks with different values of misalignment would produce different values.

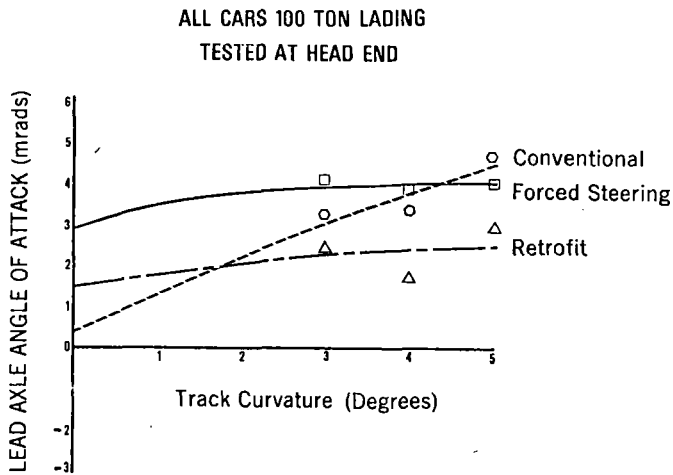


Figure 13a Angle of Attack - Right Hand Curve

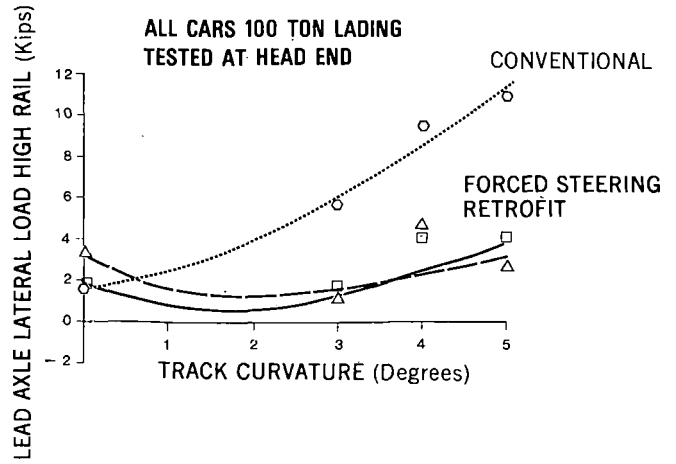


Figure 14a Lateral Load - Right Hand Curve

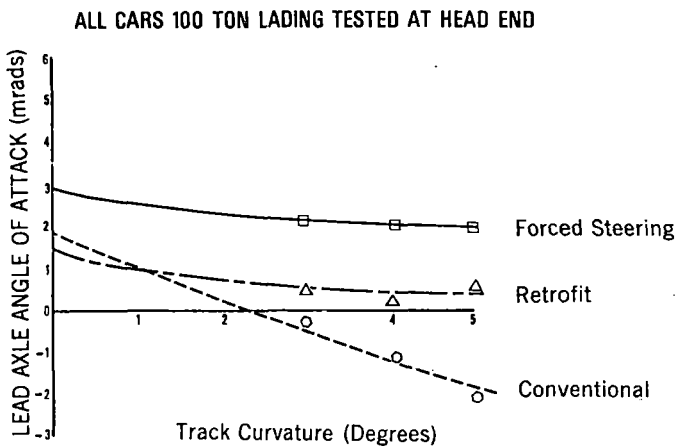


Figure 13b Angle of Attack - Left Hand Curve

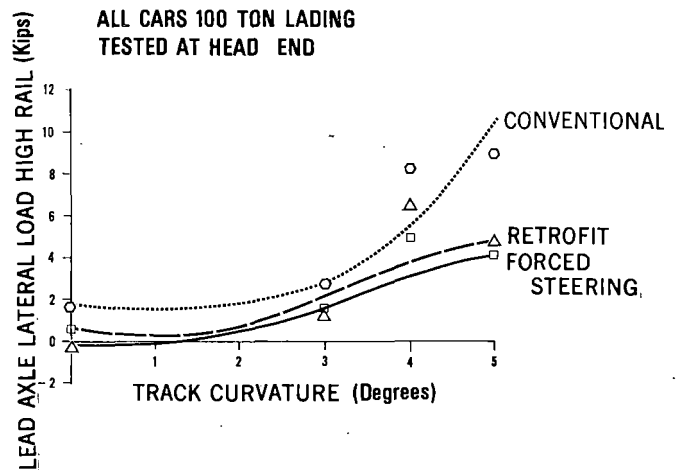


Figure 14b Lateral Load - Left Hand Curve

Finally, mean lead axle outer wheel (high rail) loads are plotted as a function of track curvature in Figures 14a and 14b for the same three trucks examined in Figure 13. The higher lateral loads produced by the conventional truck as compared with the radial trucks are apparent.

COMPARISON WITH FLANGE WEAR DATA

The primary objective of the experiment is to compare flange wear rates with angles of attack, lateral loads, and wear indices. Before examining the comparisons, it is important to understand the methodology involved in making them.

As stated before, there were five trucks instrumented during the wear index experiment. Because angles of attack and lateral loads were measured with the vehicles running in only two directions; i.e., CW and CCW with the same end of the vehicles leading each time, and making the reasonable assumption that only the outer wheel on the lead axle of each truck is subjected to flange wear on any given curve, we have two wheels on each truck with which to make the comparison; thus a total of ten data points comprising five trucks and two wheels on each.

Table 4 presents the basic data, for unlubricated track only, used in the comparison and shows the angle of attack, lateral load, and flange wear rates measured for each of the ten wheels. The angles of attack and lateral loads quoted for each wheel are those that were measured while that particular wheel was the lead outer wheel on each curve; we are again making the assumption that the loads and angles of attack can cause flange wear for any given wheel only when that wheel is in the lead outside position. As an example, let us consider wheel R4 on car 48. During the wear index experiment, data was gathered with axle 4 of this car always as the leading axle and, therefore, wheel R4 was the lead outer wheel when negotiating left hand curves. Sections 3, 13, and 17 are left hand curves when a vehicle is travelling in the CCW direction and, therefore, the angles of attack and lateral loads quoted in Table 4 for this wheel are those measured when testing in the CCW direction. Section 7 is a reverse curve and, therefore, the values quoted for wheel R4 on car 48 for this curve are those measured when testing in the CW direction.

TABLE 4. DATA USED IN LATERAL LOAD/ANGLE OF ATTACK COMPARISON WITH FLANGE WEAR- UNLUBRICATED TRACK.

Car	48	48	63	63	133	133	139	139	140	140	
Wheel	R4	L4	R4	L4	R4	L4	R1	L1	R4	L4	
Curve direction when in outer wheel position during wear index experiment	left hand	right hand	left hand	right hand	left hand	right hand	right hand	left hand	left hand	right hand	
Mean Angle-of-Attack (mrads)	section 3 (5°)	0.0	3.0	-2.4	6.2	-2.1	4.6	0.6	2.8	2.3	4.1
	section 7 (5°)	-1.0	5.1	-1.7	5.7	-3.7	4.8	-0.4	2.6	1.5	3.1
	section 13 (4°)	-1.2	3.5	-1.6	5.9	-1.2	3.3	-0.3	1.7	2.1	3.9
	section 17 (5°)	-1.1	4.2	-1.3	6.6	-2.1	4.7	1.0	3.4	1.9	4.4
	section 17 (3°)	1.0	3.5	-0.9	5.3	-0.1	3.2	0.6	2.4	2.1	4.0
Mean Outer Lateral Load (kips)	section 3 (5°)	1.4	1.5	10.3	11.4	9.2	10.8	3.6	3.2	4.4	3.1
	section 7 (5°)	1.3	1.5	10.0	7.9	10.9	12.0	4.5	1.8	3.0	4.2
	section 13 (4°)	1.3	1.5	9.5	10.4	8.2	9.5	6.2	4.7	4.9	4.0
	section 17 (5°)	1.1	2.0	9.7	12.0	8.9	9.0	4.1	2.5	4.2	3.1
	section 17 (3°)	1.0	0.7	4.7	6.8	2.8	5.7	1.5	1.3	1.3	1.7
Flange wear rate (.001 in/1000 mi)	10.9	10.2	8.7	22.3	13.8	14.8	9.7	10.1	8.7	9.6	

A further point which, although mentioned before, needs reinforcing in that the flange wear rates quoted in Table 4 are those which were determined during the VALT and Radial Truck wheel wear tests,^{12 13} and are for unlubricated track conditions only as the lubricated track portions of these experiments have yet to be completed. During the VALT and Radial Truck experiments, the wheels obviously wore from their initial AAR 1 in 20 profiles during the course of these experiments, whereas the instrumented wheelsets used in the wear index experiment had nearly-new AAR 1 in 20 profiles. Thus, the lateral loads and angles of attack in Table 4 apply to nearly-new profiles, whereas the flangewear data were obtained with wheel profiles which were continually changing. This is a potential source of error in the ensuing analysis.

Finally, the flange wear data was, of course, obtained by operating on the entire FAST track. The angles of attack and lateral loads quoted in Table 4 are for each discrete curve on FAST and "weighted" averages of these parameters require to be determined before comparison with flange wear. The angle of attack was weighted by calculating the summation of the products of the angle of attack in each curve and the distance of that curve and dividing the summation of these products by the total length of curved track on FAST; i.e., the weighted angle of attack is given by (equation 7):

$$W_{\theta} = \frac{(\theta_3 \times S_3) + (\theta_7 \times S_7) + (\theta_{13} \times S_{13}) + (\theta_{17(5^\circ)} \times S_{17(5^\circ)}) + (\theta_{17(3^\circ)} \times S_{17(3^\circ)})}{S_{tcd}} \quad (7)$$

where θ = angle of attack of lead
 S = distance
 tcd = total curved distance
 and the numerical subscripts refer to the FAST_section_numbers.

Figure 15 presents the comparison between flange wear and the weighted angle of attack for the ten test wheels shown in Table 4. The data is extremely scattered and there appears to be no truly definable relationship existing. A line of the form $Y = aX + bX^2$ has been drawn - it is the best fit line of this form - in accordance with the type of relationship suggested by Ghonem and Kalousek⁵ (equation 5a) for angles of attack less than 20 minutes or 5.9 mrads. In fact one data point, for car 63 wheel L4, lies slightly outside the range but despite this fact it is apparent that this equation is not a good predictor of these flange wear rates.

Similarly, the lateral loads, weighted in the same manner as for the angles of attack, and flange wear comparison is made in Figure 16 but again there is no easily definable relationship.

From Figures 15 and 16 it appears that neither angle of attack nor lateral load, on their own, are good predictors of flange wear. However, the weighted product of lateral load and angle of attack, see Figure 17, does appear to be a reasonable predictor of the ten flange wear data points. There is still some data scatter, although markedly less than in Figure 15 and 16, but it was possible to determine the best fit line as shown in Figure 17, yielding a relationship of:

$$W_f = a + b T_y \theta_w \quad (8)$$

where $a = 0.00865$ and $b = 0.0002$
 for the prevailing test conditions and for
 W_f in units of in/1000 mi
 T_y in lbs
 θ_w in radians.

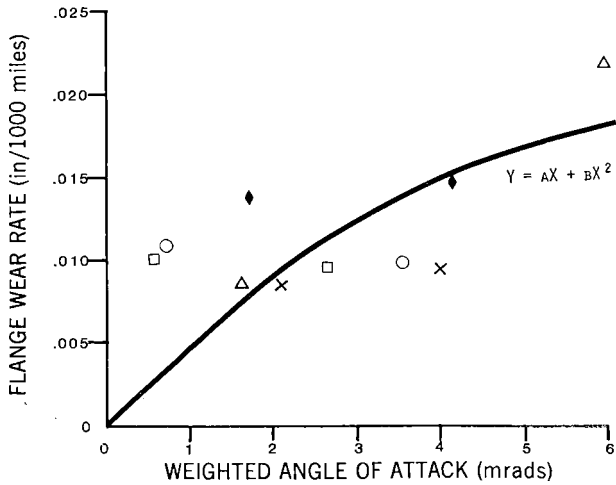


Figure 15 Flange Wear Comparison - Angle of Attack

The magnitude of 'a' in equation 8, and even its existence to a lesser extent, is a little mystifying at first as it suggests that even with zero values of lateral load and/or angle of attack flange wear will still occur. There appears to be three primary areas for investigation.

- A. The weighted products of lateral load and angle of attack were computed from the mean, quasi-static values determined for each of the FAST curves and no attempt has been made to quantify the dynamic effects. It is possible that sizeable wear occurs due to dynamic effects particularly when one considers that even tangent track usually shows cyclic gage face wear, the periodicity of these wear patterns normally being associated with the wheelset kinematic frequency.
- B. The wear indices in equation 1 and 3 use F_f , the flange force, rather than T_y as used in Figure 17. The lateral load, T_y , as measured by the instrumented wheelset, is the difference in the flange force, F_f , acting at the contact point on the wheel flange and the lateral force due primarily to creepage acting at the second contact point on the wheel tread. Thus, the use of the flange force in wear index equations must be examined.
- C. The wear index described by equation 6 accounts for the effects of longitudinal force and creepage (T_1, γ_1) as well as the lateral force and creepage (T_2, γ_2). In poor curving situations, T_2, γ_2 dominates the wear index. However, in better curving situations where the lateral forces and angles of attack are relatively small, the T_1, γ_1 term has a greater effect on the wear index value. To illustrate this point, a recent magazine article¹⁶ quotes data from an analytical model comparing the performance of an existing transit truck design with one modified for improved steering. The results suggest that although the modified truck will reduce the angle of attack from 2.8° to 0.24° (the curve radius was not quoted) and lateral creepage from 4.9% to 0.03% the longitudinal creepage will remain at 2% for both trucks. Furthermore, preliminary laboratory tests¹⁶ indicate that longitudinal creepage does produce measurable wear.

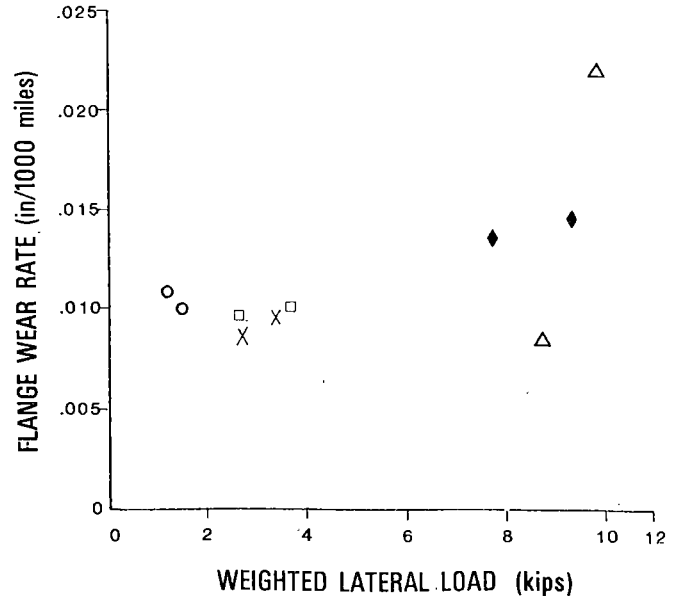


Figure 16 Flange Wear Comparison - Lateral Load

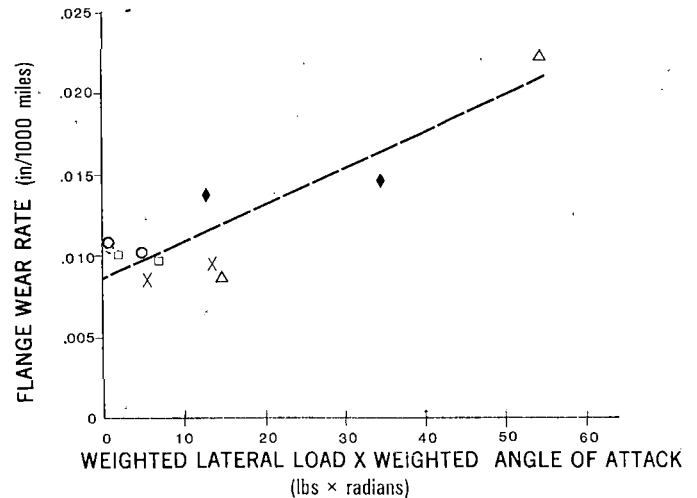


Figure 17 Flange Wear Comparison - Weighted Product

Unfortunately, because the experiment was conducted in August 1981 and the wear index experiment data was processed shortly before this paper was written, the data has not been analyzed in its entirety. However, it is strongly recommended that the above three areas be investigated. Additionally, the wear index data for lubricated track will also be analyzed when the lubricated track flange wear data from VALT and the Radial Truck experiment becomes available.

Despite the need for further work, the $W_f = a + b T_y \Theta_w$ relationship depicted in Figure 17_f provides a useful tool in explaining some apparent inequalities in flange wear data. For instance, the flange wear data obtained from VALT shown in Figure 3 appears to be more reasonable now that it can be compared with Figure 17. The inference is that an increase in lateral load (and/or angle of attack) does not produce a directly proportionate increase in flange-wear and thus, based on flange wear alone, the use of heavier axle loads cannot be precluded.

The apparent fact that decreases in lateral load and/or angle of attack will not produce a directly proportionate decrease in flange wear also helps to explain why lateral loads, angle of attack, and the products thereof have been determined to be as much as six or more times better, in some cases,³ than conventional trucks, whereas data from FAST¹³ and three railroads¹³ indicate improvements in wheel wear by factors of only around 2½ or 3.

It would appear that reductions or increases in lateral load and/or angle of attack are not the "be all and end all" of wheel wear.

CONCLUSIONS

The results of the wear index experiment indicate that the product of wheel/rail lateral load on the lead axle outer wheel and the lead axle angle of attack is a reasonable parameter with which to predict the flange wear on ten wheels tested on unlubricated track in the FAST Variable Axle Load and Radial Truck experiments.

This parameter is not, however, directly proportional to flange wear and the relationship obtained suggests that even with low lateral loads and/or angles of attack significant flange wear will still be present. This relationship helps explain why the Variable Axle Load test data on unlubricated track showed that conventional trucks under empty hopper cars had significant wheel flange wear amounting to approximately 60% of that under similar fully-laden 100-ton hopper cars.

The relationship determined in this experiment cannot be applied universally to predict actual flange wear rates because the relationship will be dependent on other factors, wheel/rail metallurgy and track lubrication for example. In addition, the data was obtained for a relatively narrow range of operating conditions, only 3°, 4°, and 5° curves for example, and more work is required to determine the effects of dynamic activity on wheel wear, and to examine other proposed wear indices in more detail, particularly the effect of longitudinal creep forces and creepages on wear in good curving performance situations where lateral loads and angles of attack are low.

Finally, it has been shown that track lubrication has a large effect on wheel and rail wear but relatively little effect on lateral loads and angle of attack. This suggests that a wear index/wheel wear relationship will be different for lubricated and unlubricated track conditions. At the completion of the Variable Axle Load and Radial Truck experiments, the wheel wear data obtained on lubricated track will be compared with the lateral load and angle of attack data already obtained from the wear index experiment.

REFERENCES

- 1 Steele, R. K. - Rail: Its Behavior and Relationship to Total System Wear, 1981 FAST Engineering Conference, November 1981.
- 2 Heumann, H. - Grundzuge der Fñhrung der Schienenfahrzeuge, R. Oldenburg, Munich, 1954.

- 3 Ghonem, H. and Gonsalves, R. - Comparative Performance of Type II Trucks, Canadian Pacific Ltd. report No. S 576-78, November 1978.
- 4 Marcotte, P., Caldwell, W. M., and List, H. A. - Performance Analysis and Testing of a Conventional Three-Piece Freight Car Truck Retro-fitted to Provide Axle Steering, ASME Winter Annual Meeting, San Francisco, December 1978.
- 5 Ghonem, H. and Kalousek, J. - The Use of Angle of Attack Measurements to Estimate Rail Wear Under Steady State Rolling Conditions, International Conference on Wheel/Rail Load and Displacement Measurement Techniques, Cambridge, MA, January 1981.
- 6 Elkins, J. A. and Eickhoff, B. M. - Advances in Non-Linear Wheel/Rail Force Prediction Methods and their Validation, ASME Winter Annual Meeting, New York, December 1979.
- 7 Allen, R. A. and Peters, A. J. - Wheel/Rail Loads Test, Hopper Car Ride Data, FRA/TTC-80/07, August 1980.
- 8 Johnson, M. R., Joyce, R. P., and Mancillas, C. - Use of an Instrumented Wheelset for Measurement of Wheel/Rail Forces at the Facility for Accelerated Service Testing, Track Train Dynamics Report - 471.
- 9 Tuten, J. M. and Harrison, H. D. - Final Report on FAST Wheel/Rail Loads Wayside Data Reduction, Battelle Columbus Laboratories, Columbus, Ohio, September 1980.
- 10 McIrvin, L. L. and Graff, R. - Evaluation of Weldable Strain Gages for Use on Rails in the FAST Track, FAST/TTC/TN-80/03.
- 11 Johnson, M. R. - Development and Use of an Instrumented Wheelset for the Measurement of Wheel/Rail Interaction Forces, International Conference on Wheel/Rail Load and Displacement Measurement Techniques, Cambridge, MA, January 1981.
- 12 Gray, D. E. - Major Variables that Affect Wheel Wear, 1981 FAST Engineering Conference, Denver, November 1981.
- 13 Allen, R. A. and Leary, J. F. - Radial Truck Wheel Wear, 1981 FAST Engineering Conference, Denver, November 1981.
- 14 Pollard, M. G. - The Development of Cross-Braced Freight Bogies, Rail International, September 1979, pp. 735-758.
- 15 Progressive Railroadng - Radial Truck Designs Come on Strong, October 1981 edition, pp. 58, 60.
- 16 Bolton, P. J., Clayton, P., and McEwan, I. J. - Wear of Rail and Tyre Steels under Rolling/Sliding Conditions, ASME/ASLE Conference, San Francisco, August 1980.

FATIGUE ANALYSIS TEST AT FAST

S. K. (John) Punwani
Experiment Manager, Car Dynamics
Association of American Railroads

Gerald J. Moyer, Ph.D.
Consultant
Association of American Railroads

Many of the cars which make up the FAST consist have been here since the day the train first rolled around the loop. As you can imagine, we have had many wheelsets changed, many brakeshoes changed, and our share of cracks in the freight car bodies and other car components. As a result of some of the cracks that have been observed, we felt that some mini-tests could be conducted that would be beneficial to the railroad car design community in addition to being directly useful to the particular owner/builder of the car on which the failure was observed. Two Fatigue Analysis Tests have been conducted - namely FAT I and FAT II. FAT I was completed and reported on sometime ago. The final report is published and can be found in the list of FAST reports. FAT II was conducted just recently and we will share some data from that test with you.

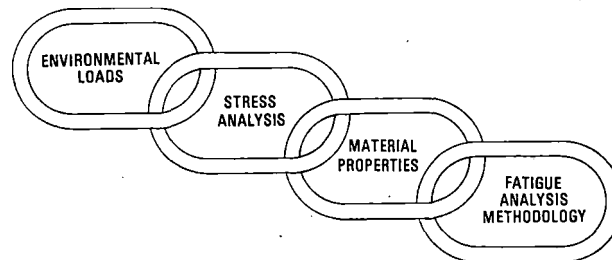


FIGURE 1. FATIGUE ANALYSIS PRACTICE IN CAR DESIGN

FATIGUE ANALYSIS PRACTICE IN CAR DESIGN

The fatigue analysis tests which were conducted must be discussed in the context of the current fatigue design practice.

Many of you know that the FATIGUE GUIDELINES are soon to become a part of the car design specifications. They represent the state-of-the art of railroad fatigue design practice.

There are four essential elements to fatigue design:

- a. Environmental Loads
- b. Stress Analysis
- c. Material Properties
- d. Fatigue Methodology

ENVIRONMENTAL LOADS

Data on environmental loads are being collected to characterize the revenue service environment. This

has come to be known as the FEEST program. This consists of centerplate and side bearing loads. Some of you veterans know that fatigue design practice in the railroad freight car industry has always been centerplate oriented, since the early failures were in the centerplates. Cars operating in parts of Mexico where the track was poor, it was observed, had centerplate failures, whereas cars of like design (sometimes in the same car series) operating on better track did not. This points to the need for environmental load data.

STRESS ANALYSIS

This is an important element in predicting whether fatigue failure will occur. As for FAST, we can directly measure strains to combine the first two elements required in any fatigue analysis.

MATERIAL PROPERTIES

Most freight cars are welded structures. There is a

compendium of Modified Goodman Diagrams which gives the fatigue properties of many welded structures. This compendium has recently been expanded. Any given structural detail can be likened to one of those Modified Goodman Diagrams, perhaps not exactly but close enough for a reasonable analysis.

FATIGUE METHODOLOGY

The Miner's Rule forms the basis of the fatigue methodology. There are other approaches, but we feel the applicability of this approach makes for easier application and for more conservative results.

All of these four elements are essential to fatigue analysis. It must not be forgotten that fatigue analysis is really a "black art," or a queer mixture of empirical design and analytical design practice. Despite this apparently contradictory description, it is widely used and accepted as necessary and useful.

These , then, are the four elements essential to a fatigue analysis.

FAT I BACKGROUND

In December, 1977 interest focused on ten cars of this basic design which had fabricated draft center sills. A crack was found in the center sill web of one of these cars (Figure 2).

Figure 3 illustrates a typical body-bolster/center sill area. The crack in the center sill web runs longitudinally each way from the side-bearing web plate.

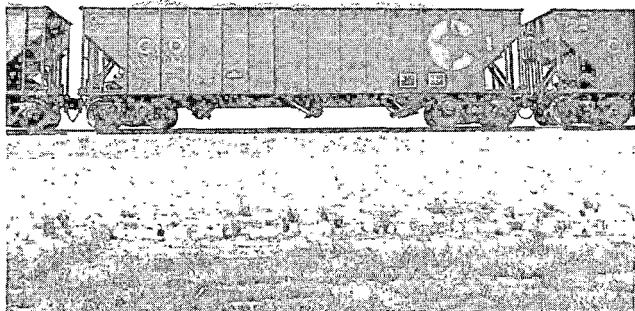


FIGURE 2. PHOTO FAST CAR C&O 159061

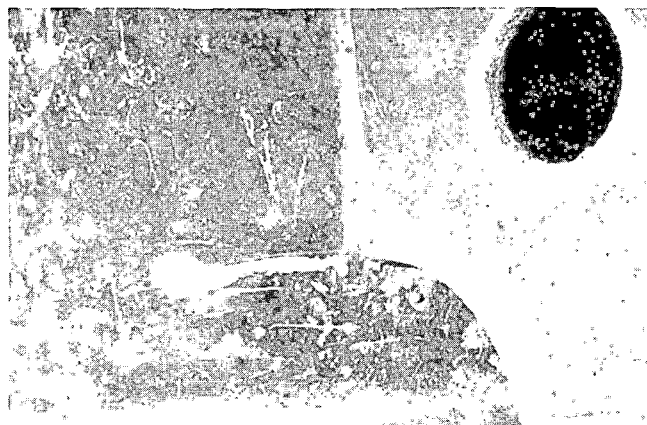


FIGURE 4. PHOTO OF CRACK IN CAR BUILT BY MFR. #1



FIGURE 5. PHOTO OF CRACK IN CAR BUILT BY MFR. #2

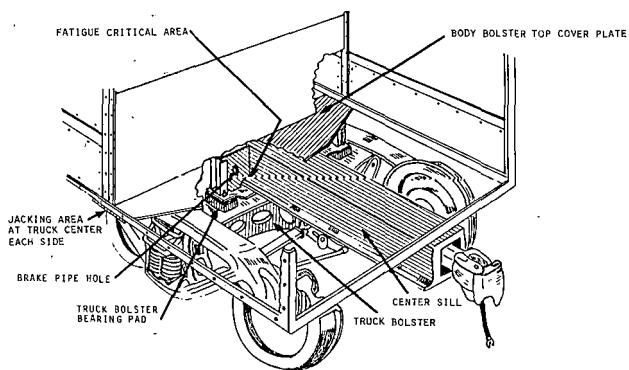


FIGURE 3. TYPICAL VIEW OF FABRICATED CENTER SILL/ LOWER BODY BOLSTER INTERSECTION.

Figure 4 shows the actual crack. This car was built by one manufacturer to its own detail design.

The cracks were not limited to one manufacturer. Figure 5 illustrates a somewhat different design by a second manufacturer. The cracks are not limited to 14 inch or 16 inch centerplate diameters.

In view of the fact that cracks of this type appeared, there was railroad concern that this type of cracking would become a general problem with hopper cars in service. Naturally the railroad was anxious to determine the cause of the cracks. Finally, if it were a problem, could a "fix" be developed both for cars in-service and for future cars to be built?

FAT I OBJECTIVES

Therefore, the objectives of the FAT I test became:

- a. Determine the cause of cracking.
- b. Compare alternate fixes.
- c. Determine if initiation of cracks can be predicted by fatigue guidelines.

FAT I TEST CONFIGURATIONS

In addition, the test configurations consisted of a group of base case cars with both cracked and uncracked center sills without a "fix." A second group of cars included four different center sill fixes. These were:

- a. Doubler Plate
- b. Box Angle
- c. Vertical Bar Redesign
- d. Vertical Bar Support, C-PEP

We won't describe the test program in detail. The idea was to put strain gages and accelerometers (Figures 6-11) and to collect data on the FAST loop so we could determine the cause of the cracking. Some new cars were brought to FAST already equipped with these fixes.

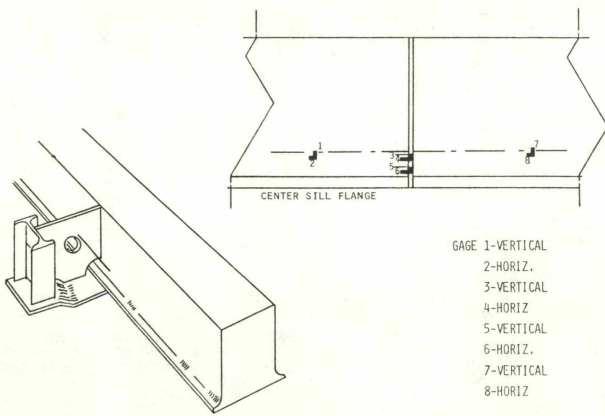


FIGURE 6. CAR 5 WITH CRACK (NO FIX)

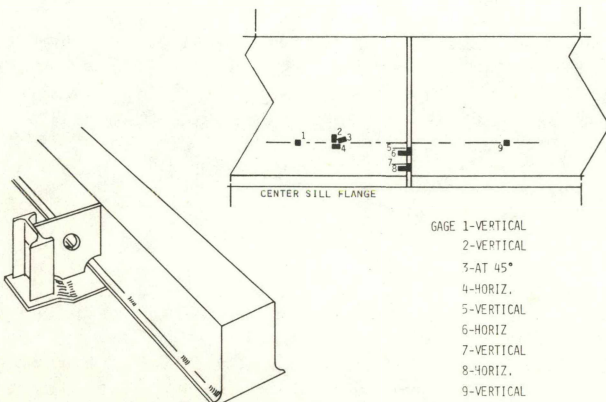


FIGURE 7. CAR 1 NO CRACK (NO FIX)

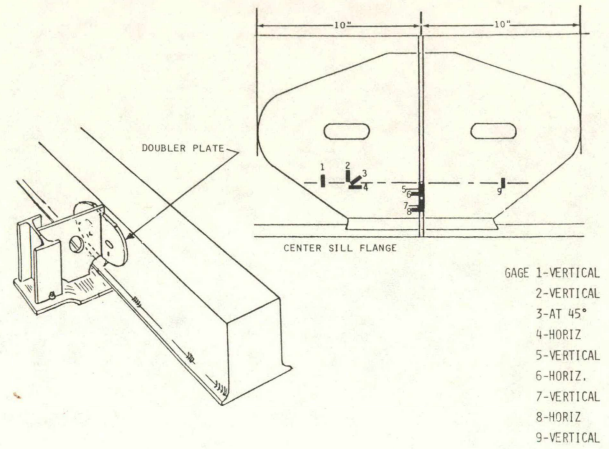


FIGURE 8. CAR 2 NO CRACK (WITH FIX, DOUBLER PLATE)

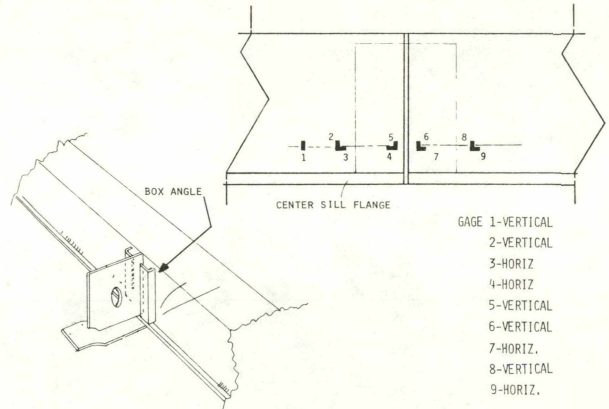


FIGURE 9. CAR 3 NO CRACK (WITH FIX, BOX ANGLE REINFORCEMENT).

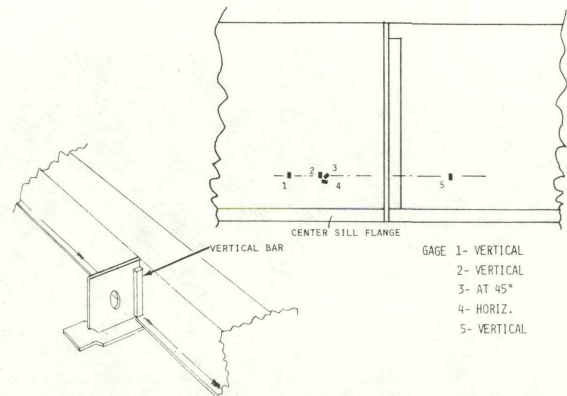


FIGURE 10. CAR 4 NO CRACK (WITH FIX, VERTICAL BAR REDESIGN).

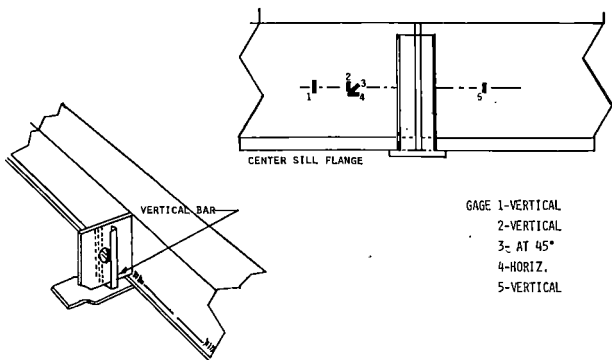


FIGURE 11. CAR 6 NO CRACK (C-PEP PAD, VERTICAL BAR SUPPORT).

A strain gage 4 inches from the web to center sill intersection is common to all the configurations. This was the gage location used for the fatigue analysis made to estimate the relative merits of the fixes. Figure 12 illustrates a typical strain gage installation.

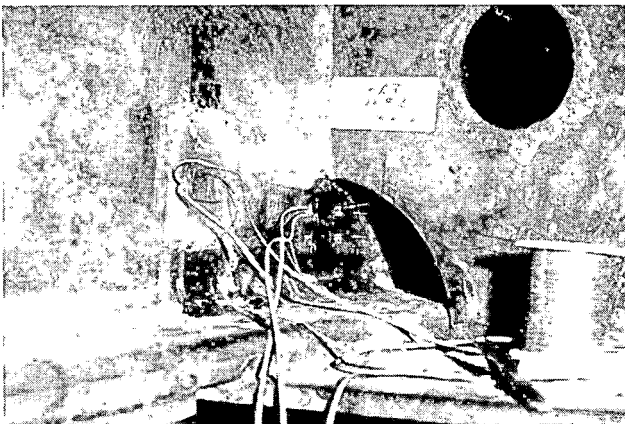


FIGURE 12. PHOTO OF CAR 6

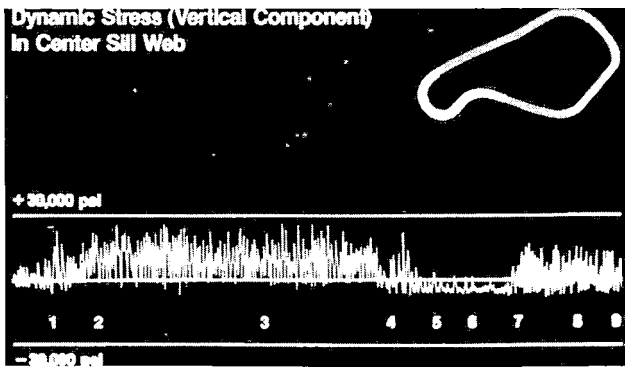


FIGURE 13. PHOTO OF DYNAMIC STRESS (VERTICAL COMPONENT) ON CENTER SILL WEB.

FAT I DATA COLLECTIONS AND ANALYSIS

Each of the test cars was run over the loop and the data recorded on analog tape. It was subsequently digitized and processed. We did the usual thing with it - cycle counting, etc.

A typical time history is shown in Figure 13 over a part of the loop. "History" repeats itself on the FAST loop. High strain values seemed to correlate with opposite side bearing contact. This would indicate more twist and roll activity than vertical bounce. Initial analysis prompted us to do follow-up static tests to establish live load effects and to establish range.

We cannot cover in detail all aspects of the analysis but we would like to convey what we learned from it. For the critical strain gage location, using the strain time history collected at FAST (after doing some cycle counting on it), we estimated a life of 2,400 miles on the FAST loop. Remember that there are many inexact aspects of fatigue analysis. Using a different Modified Goodman Diagram gives somewhat higher predictions. Much the same life is predicted if the measured FAST acceleration time history is used (1,500 miles) instead of the strain time history. For the base car, which was not cracked when received for the FAT I tests, a crack was observed after 23,000 miles in FAST service. Using yet another approach, the stress at the critical location was estimated and compared with others, who have their own stress analysis methods for this location. Then, using the loading environment spectrum (REPOS) provided in the Fatigue Guidelines for revenue service, we estimated a life of 92,000 miles. We will show you a little later how the FAST loading environment is accelerated relative to the revenue service environment. In view of that, the predicted mileage to failure is a reasonable estimate.

TABLE 1. RELATIVE MERITS OF ALTERNATE "FIXES."

TYPE OF FIX	RELATIVE LIFE* (FIGURE OF MERIT)
BASE CAR - NO FIX	1.00
DOUBLER PLATE	3.16
BOX ANGLE	0.65
VERTICAL BAR SUPPORT, C-PEP	0.79
VERTICAL BAR	0.43

*BASED ON FATIGUE ANALYSIS USING MEASURED STRAIN

Using the common gage location as the basis for comparing fixes, we compared their relative merits. See Table 1. The "doubler plate" fix is the most desirable and is currently being considered for incorporation into the car design. Some of the other test cars did, in fact, crack as predicted by the fatigue analysis.

FAT I CONCLUSIONS

It may be concluded that fatigue failures were the cause of the center sill cracking. Also, the relative life (figure of merit) for the base car and alternate fixes are listed in Table 1. The fatigue guideline methods predicted fatigue failure for the base car and for the alternate fix cars, but not for the doubler plate fix.

FAT II BACKGROUND

Figure 14 illustrates one of three TOFC cars which were in the FAST consist. A severely cracked hitch on the 'B' end of one of these TOFC cars was removed on June 1, 1979. This hitch had been inspected 3,000 miles earlier and a pin had been replaced for wear, although no cracks were found.

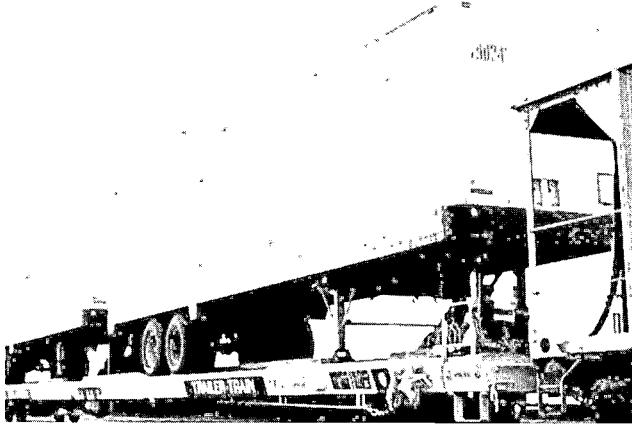


FIGURE 14. PHOTO OF TTX TRAILER

Figure 15 illustrates the hitch assembly. There were three basic areas of cracks:

- a. In the head assembly.
- b. In the strut assembly
- c. Reinforcement member attachment

As we mentioned, the cracking, when discovered, was severe, and so it was hard to say where the cracks started. Did the failure occur at the reinforcement member below the deck, which allowed the floor plate to be more flexible causing the stresses in the hitch to go up? On the other hand, was the stress level on the hitch responsible for the failure of the reinforcement member? These are two structural details of interest. Naturally, the progression of stress levels within the hitch assembly as sub-components failed would be of interest, but they were not part of the test objectives.

Figure 16 is a view of the crack in the web plate joining the two struts. This particular crack started in the plate at the top and progressed 14 inches down. The opposite side was also cracked, with the crack starting in the plate and working its way up towards the top.

FAT II OBJECTIVES

The second mini-test, FAT II, was completed just recently. The objectives were basically similar in nature to the FAT I tests, and are listed below.

- a. To estimate the fatigue life of two structural details in the FAST environment.
- b. To determine the primary cause of cracking.
- c. To provide an example showing implementation of Fatigue Guidelines.

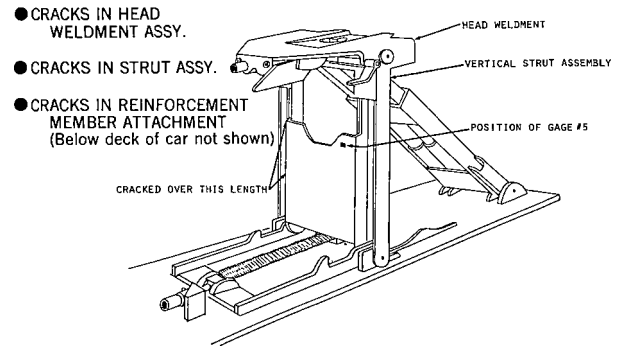


FIGURE 15. CUSHIONED HITCH ASSEMBLY

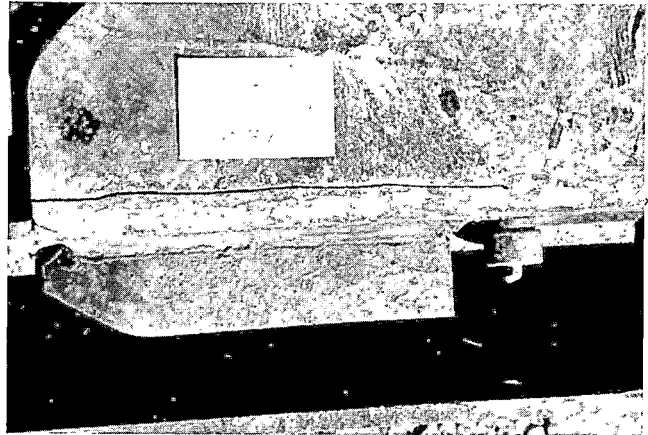


FIGURE 16. PHOTO OF CAR 67

FAT II INSTRUMENTATION AND TESTING

Briefly, we placed several gages on the hitch, some of which were wired to read lateral load. Also, some accelerometers were used and the usual service channels...speed, ALD markers, etc.

The static tests conducted were a lateral pull on hitch, a rock over, and a twist. The dynamic testing took place in two phases. Phase 1 included 1 lap at 5 mph, 2 laps at 25 mph, and 10 laps at 45 mph, clockwise and counterclockwise. Phase 2 of the dynamic testing was the same as Phase 1 except for the removal of the reinforcement channel below the deck. The channel was removed in an effort to determine the primary reason for cracking.

The static tests were done to obtain an idea of the strain range for known applied lateral loads or displacements. The lateral loads were applied with a cable and hydraulic actuator to the hitch with the trailer off-loaded, and to the trailer when loaded. The dynamic data was representative of normal FAST operation, plus some laps at lower speeds.

Gages were placed on the plate that joins the two struts at the top left and top right, both front and back. Also, rosettes were applied to the plate at the bottom left and right and gages on the other face of the plate directly behind. We had gages on the struts, three vertically on each, wired to measure vertical load. We also had gages on the strut to measure lateral load. Take note of Gage 5 (Figure 17).

Ten accelerometers were used as follows:

Four on car deck ... 2 in line with bolster
 ... 2 in line with King pin

Two on car near center plate ... Vert. & lat.

Four on Trailer ... Two at side sill to measure
 vert. in line with king pin
 Vert. & lat. as close to
 trailer center of mass as
 possible

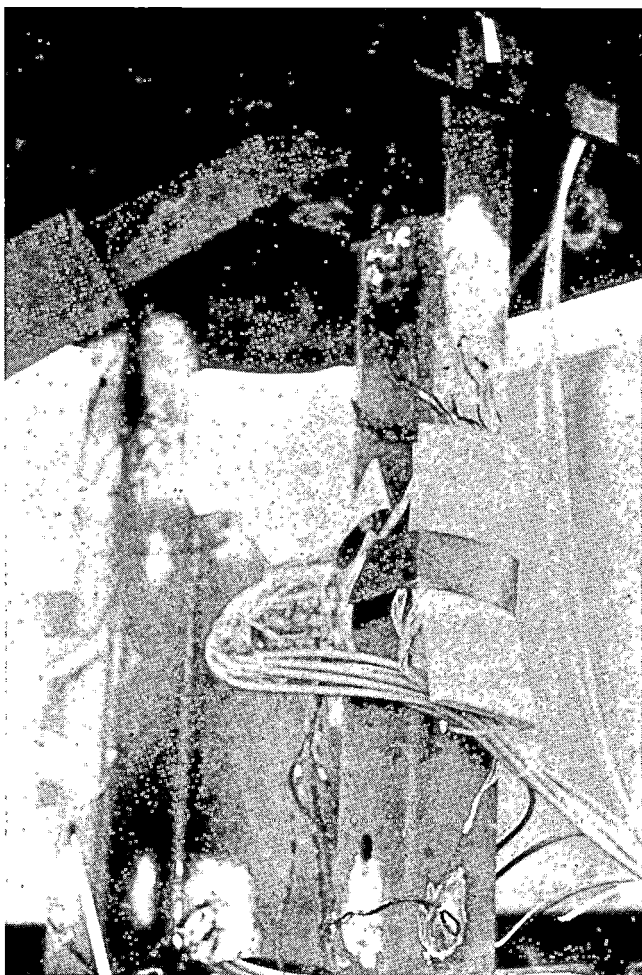
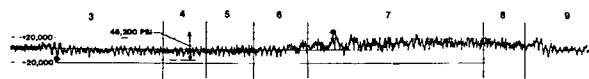
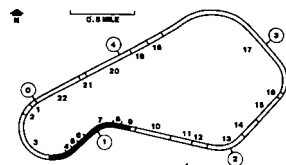


FIGURE 17. PHOTO OF GAGES ON HITCH

FAT II TEST CONSIST

The test consist included the T-8 instrument car, a 100-ton ballast car, and the test car with the instrumented hitch in the leading position. See Figure 18.



MAX. STRESS VARIATION IN TRAILER HITCH (FROM #5)
 BETWEEN SECTION 3 AND 7 FO FOR 46 MPH CCW RUN

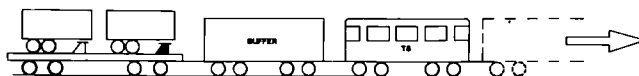


FIGURE 18. MAX. STRESS VARIATION IN TRAILER HITCH

FAT II DATA ANALYSIS

Figure 19 is data for Gage 5, located on the plate joining the two struts where cracks occurred. You can see the equivalent stress in the gage change by 46 ksi as you go through FAST Sections 3 thru 9, so you have at least one cycle per lap with that magnitude. This time history was used for a preliminary fatigue analysis.

(332 STRESS CYCLES PER LAP)

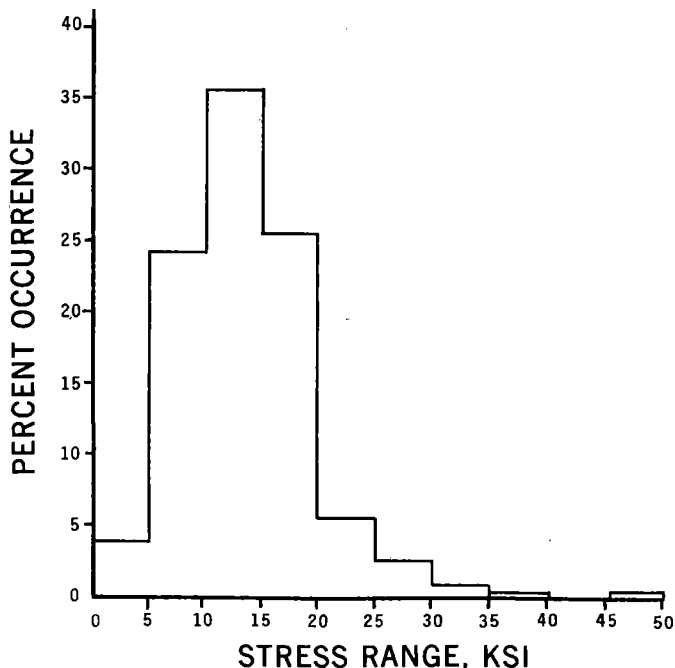


FIGURE 19. STRESS RANGE PERCENT OCCURRENCE HISTOGRAM

We have done a preliminary cycle count on this particular gage. For the stress range values, we note the percent occurrences. We counted 332 cycles, the magnitude and distribution of which are shown, using the rainflow counting program recom-

mended in the AAR Fatigue Guidelines. To be sure, this cycle count did not cover the entire loop, but it did cover the most critical portion.

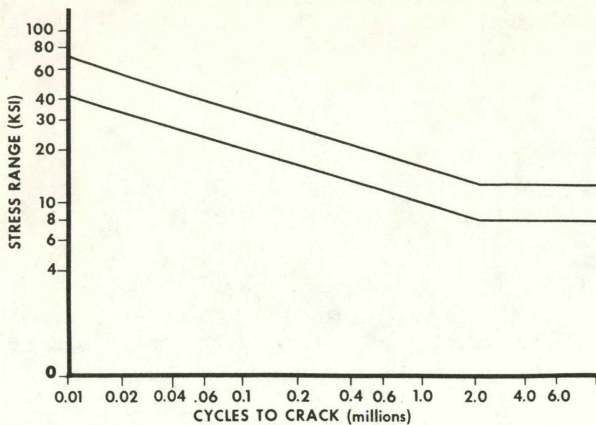


FIGURE 20. TYPICAL SN CURVES

To do a preliminary fatigue analysis we scanned through the fatigue properties for welded structural details provided in the Fatigue Guidelines. While the exact structural detail applicable to the hitch plate is not available, welded structural details with some likeness to our location fall, with some regularity, in the range illustrated here in Figure 20. The fatigue limit for the lower curve is 8 ksi, and 13 ksi for the upper curve. For the stress time history, represented by the REPOS shown in Figure 19, we can estimate the predicted fatigue life, as shown in Figure 21.

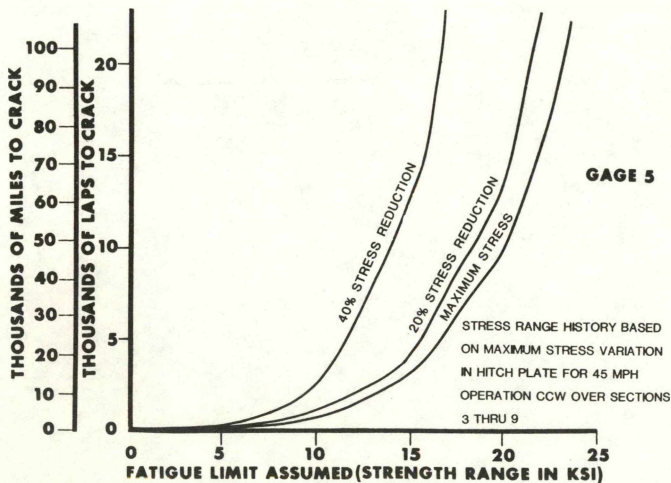


FIGURE 21. FATIGUE LIFE PREDICTION

This fatigue life prediction (Figure 21) is based on the Miner's Rule Methodology recommended by the Fatigue Guidelines. This, for the uninitiated, simply says: The fractional fatigue life used up at

each level of stress range is cumulative, and cracks will occur when this accumulated used up fractional life is Unity.

Using the higher of the two S-N curves with the measured stress, we are predicting a life of 10,000 miles.

These other curves show the sensitivity to change in the stress range as it affects the fatigue life. The predictions are on the conservative side, that is, a shorter life is predicted than would actually occur. A major reduction in stress level is far more effective than improving the material fatigue properties. The stress range observed for this gage location does show that fatigue cracks can be anticipated.

TABLE 2. GREATEST OVERALL MIN-MAX STRESS.

(HITCH PLATE GAGE #5) FOR 45 MPH OPERATION OVER FAST SECTIONS 3 THRU 7

RUN DIRECTION	PHASE I UNMODIFIED CAR		PHASE 2 UNDER DECK WELD REMOVED	
	ANALOG O'GRAPH	DIGITAL 'QUICK LOOK'	ANALOG O'GRAPH	DIGITAL 'QUICK LOOK'
CCW	46.2	49.4	37.9	38.0
CW	28.0	33.3	33.7	34.9

(stress range in KSI)

You will remember that one of the questions was: Did the failure of the reinforcement member (under deck) weld raise the stress level on the hitch structure and therefore cause it to fail?

We see here from the "quick look" data in Table 2 that, in fact, the stress levels for our particular gage, in a fatigue critical location, did not increase when we burned off the weld.

FAT II PRELIMINARY CONCLUSIONS

With the limited look we have had, some preliminary conclusions are apparent:

- a. Strain Range is large enough to cause fatigue cracks.
- b. The load distribution between the two struts can be uneven which may contribute to observed strain range in critical area.
- c. Removal of under deck weld did not increase the stresses on the hitch.

We would, of course, remind you that it is not at all common for a trailer hitch to be loaded to maximum rated capacity and be running around the kind of curves we have at FAST, 100% of the time. This leads us to the last question we would like to address: How bad is the FAST environment relative to yours or mine?

COMPARISON TO REVENUE SERVICE

Figure 22 depicts the 70-ton box car which is currently in the process of visiting railroads around the country. This car is equipped with an instru-

mented truck bolster and load-measuring side bearings. It is the car being used to measure the environmental loads in the FEEST program. It measures total vertical bolster load (centerplate and side bearing) and individual side bearing loads. A recording system stores data in various "boxes," as a count, after rainfall counting. This car recently passed through Pueblo.

Those of you with cars to test can see that various designs can be tested and compared with either mini-tests or in FAST service or both.

We would like to acknowledge the assistance of Mr. Jim Burns, Chessie System, Messrs. Eric Wolf and Frank Stec, Trailer Train, and many others of the Transportation Test Center.

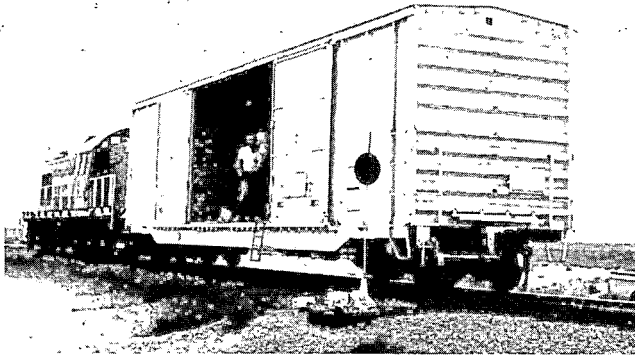


FIGURE 22. PHOTO OF PSX - 96

The car made its way from Chicago to Kansas City and to Pueblo. Its short sojourn in Pueblo included 29 laps around the FAST loop with normal CW and CCW operation. We show the side bearing load counts in Figure 23. The FAST side bearing counts were multiplied approximately by 4 so that a direct comparison can be made with a Kansas City to Pueblo (600 mile) run. Note the big difference in side bearing load strikes. Something you know, intuitively, is that the "curve environment" at FAST is clearly "accelerated" on a per mile basis. Those elements of the car which are loaded or stressed on curves clearly see an accelerated environment. The centerplate load counts, namely the pure bounce environment, are comparable.

QUESTIONS AND ANSWERS

Question 1

What work was performed, if any, to ensure that the defect size distribution of the sill weldments was normal or at least consistent? Could have been faulty manufacture, i.e., an isolated occurrence.

Answer

To my knowledge the welds were not metallurgically examined. However, since more than one manufacturer was involved and quite a few cars did crack, this does not suggest an isolated instance of poor weldments.

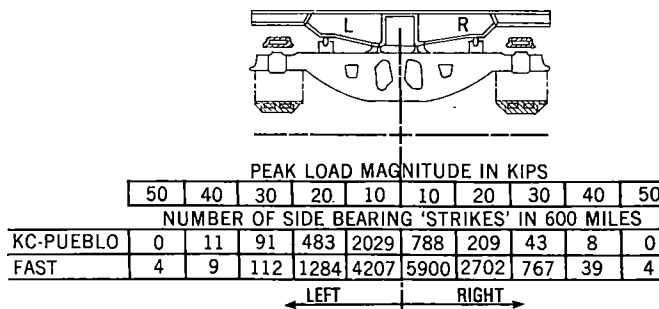


FIGURE 23. FAST VS. REVENUE SERVICE SIDE BEARING LOAD SPECTRUM.

SUMMARY

We have shown you that for cars at FAST, we have an accelerated environment with respect to curving. This is also borne out by the wheel wear results you have seen.

We have shown, with two Fatigue Analysis Tests, how the Fatigue Guidelines can be applied.

FUTURES

1981 FAST ENGINEERING CONFERENCE

TRACK DEGRADATION EXPERIMENT

James W. Brent
Experiment Manager, Track Degradation
Association of American Railroads

The initial program for track-related experiments at FAST included one designated as "The Maintenance of Way Experiment." It was generally described as one aimed at measuring the degradation of the total track structure in relation to the gross-ton miles of operation of a unit train made up of 100-ton cars. In other words, can we determine with any degree of accuracy how many million gross tons (MGT) of operation the track can endure before unacceptable degradation? See Figures 1 and 2. For many reasons, this experiment was never defined and implemented. In October, 1980, the FAST Policy Committee decided that future comparisons of the effect on track structure of different operating modes and vehicle configurations would be severely limited if we did not generate some basic information on degradation of the track structure (specifically geometric degradation) as it related to the operation of the 100-ton car with standard trucks. They appointed an Ad-Hoc Committee to design an experiment to produce the necessary data. This committee developed the experiment now identified as the "Track Degradation Experiment."

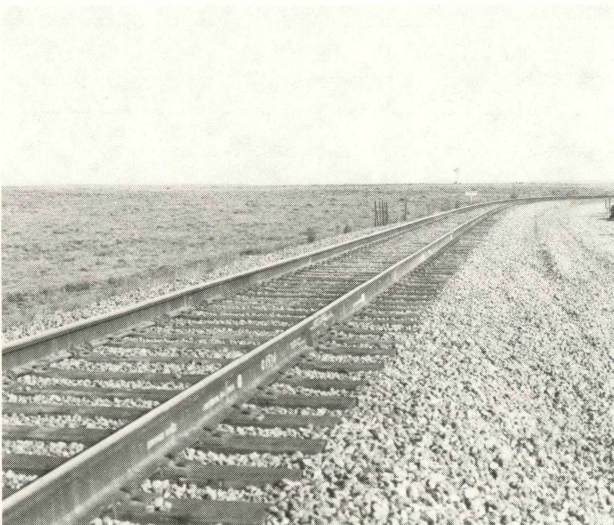


FIGURE 1. WELL MAINTAINED TRACK.



FIGURE 2. THE RESULTS OF INADEQUATE TRACK MAINTENANCE.

The objectives of the experiment were defined as:

- a. Develop a method to quantify track degradation and/or maintenance effort required when operating a controlled consist on track built and maintained to defined standards, which can be utilized when track and/or vehicle parameters are changed.
- b. Using the method developed, measure the track degradation and maintenance effort required as a result of operating the FAST Phase I train consist and other train consists in subsequent phases of the FAST Program.

- c. Determine the feasibility of predicting the rate of degradation of track when subjected to known operating and maintenance practices.

In the development of the experiment, the committee chose to concentrate on the measurement and quantification of the degradation of normally-measured parameters of track geometry. We will gather other pertinent data which may be useful in defining and predicting the degradation rate. We will discuss these in more detail later.

Planning has been to terminate Phase I of the FAST Experiments after the operation of about 800 MGT,

see Figure 3. Therefore, in defining the Degradation Experiment this late in Phase I, a major constraint was recognized at the outset. As you have heard throughout the conference, there are a great many experiments underway relating to specific components or characteristics of the track structure. Many of these have been ongoing for some time and their unique maintenance and data requirements preclude imposition of the Degradation Experiment in the same sections of track.

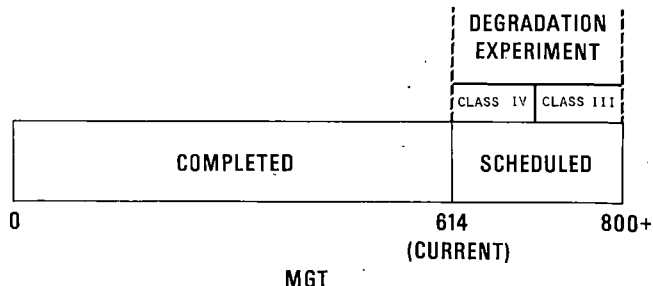


FIGURE 3. PHASE I TESTING.

The only sections of the FAST Loop available to us were Sections 12, 13, 14, parts of 17, and 20.

These sections include a three degree curve with spirals, a four degree curve with spirals, and tangent track, see Figure 4. In order to hold the variables in the track structure to a minimum, it was decided to concentrate the investigation on wood tie track structure, using continuous welded rail and jointed rail with a conventional cut spike tie-plate fastening system. One section of concrete ties on tangent track is included in the experiment to see if we can make any viable comparisons between wood and concrete track structure in a very limited experiment.

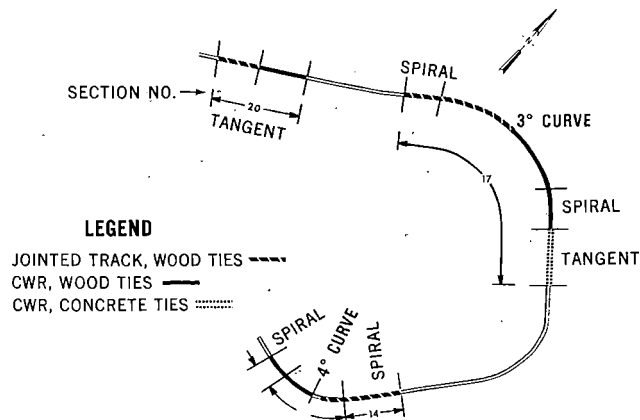


FIGURE 4. TRACK CONFIGURATION.

All of the sections of the loop included in the Degradation Experiment are being rebuilt with new material (Figure 5), surfaced and lined to meet FRA Class 6 Standards. Figure 6 shows the alignment, length and construction of each of the track segments. This experiment, like every other activity at FAST, is a joint Industry-Supplier-Government effort and all the material used in the track reconstruction was donated by a railroad or a supplier. The Government furnished the labor.



FIGURE 5. TRACK REBUILD.

TRACK TYPE	CURVATURE			
	TANGENT	SPIRAL	3°	4°
JOINTED-WOOD TIES	1,100 FT. (#20)	300 FT. (#14) 600 FT. (#17)	1,060 FT. (#17)	670 FT. (#13)
CWR-WOOD TIES	1,100 FT. (#20)	300 FT. (#12) 600 FT. (#17)	1,060 FT. (#17)	660 FT. (#13)
CWR-CONCRETE TIES	900 FT. (#17)			

FIGURE 6. EXPERIMENT TEST MATRIX.

The method chosen to quantify degradation of the track is to measure the deviations in track geometry after the operation of known tonnage over the track structure and then make a series of statistical analyses of the data collected to produce defined relationships between degradation and tonnage, alignment, rail type, etc.

The parameters of track geometry receiving most attention are:

- a. Profile
- b. Alignment
- c. Gage
- d. Super elevation
- e. Twist or Warp

These parameters will be measured and recorded by the Track Geometry Car (Figure 7) after the rebuild is completed and before the train operation begins. The changes in each of these parameters will be recorded and analyzed after each 5 MGT of operation. We will then calculate various statistics relating to each of the parameters, such as the percentage failing to meet FRA Class 5, the percentage failing to meet FRA Class 4, etc.

At 40, 80, 100, 120, 160, and 200 MGT, data will be plotted to produce curves relating the degradation

of each parameter to various other factors such as the tonnage accumulated, curvature, etc.

ing to the track structure, certain other data will be measured and recorded at known intervals throughout the experiment. Various analyses will be made with these data to determine any statistical relationships that may exist between them and the degradation of other parameters and/or the total track structure. Please see Table 1, below.

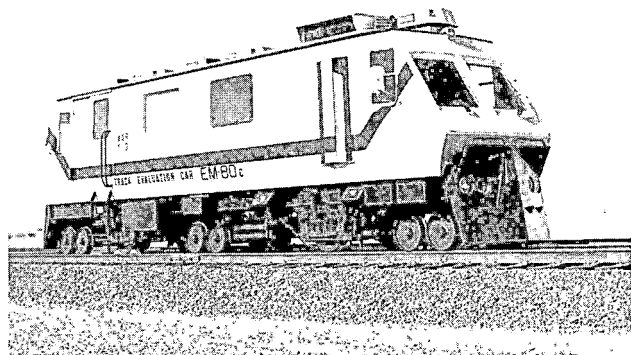


FIGURE 7. TRACK GEOMETRY CAR.

At these same intervals of operation, we will calculate other statistical relationships of degradation on curves vs. tangents, CWR vs. jointed rail, etc. For the first 100 MGT of operation, the track will be allowed to deteriorate from the original FRA Class 6 Standard (Figure 8), to a point that when any parameter degrades to the limit established as a minimum for FRA Class 4 Track, those defects at, or below, the Class 4 Minimum will be corrected and upgraded to meet the average condition of the track adjacent to the defective area--much the same as spot maintenance is performed by the Industry.

After the first 100 MGT of operation, the entire test area will be restored as nearly as possible to the original construction standards, and for the remainder of the experiment (at least another 100 MGT), the track will be allowed to deteriorate to minimum limits of FRA Class 3 Track and then maintained in the same manner as during the first 100 MGT. This will provide better data for relating degradation rates of the measured parameters to increasing tonnage.

During the course of the experiment, we will also be keeping accurate records of the maintenance effort expended on each segment of the track. For the first 100 MGT, the analysis will seek to determine the maintenance effort necessary to prevent the degradation of the track beyond the established limit--FRA Class 4. At the end of the experiment, 200 + MGT, a determination will be made regarding the maintenance effort required to prevent degradation below FRA Class 3 plus the effort required to restore the track to Class 4 after allowing deterioration to Class 3.

The maintenance effort parameters used will be categorized by equipment used, by the type of labor (such as foremen, machine operator, laborer, welder, welder helper), and by the type of materials used.

In order to add to our knowledge of what is happen-

TABLE 1. ADDITIONAL PARAMETERS OF TRACK STRUCTURE TO BE INVESTIGATED.

PARAMETER	EQUIPMENT/ INSTRUMENTATION	REMARKS
LATERAL TRACK STRENGTH	AAR DECAROTOR CAR	CHANGE IN GAGE UNDER LOAD
RAIL WEAR	FAST SNAP GAGE	MEASURED AT LUBE CHANGES
RAIL CORRUGATIONS	LORAM RAIL CORRUGATION ANALYZER	COORDINATE WITH CORRUGATION EXPERIMENT MANAGER
TRACK DISPLACEMENT	TRANSIT	RECORD VERT. LAT'L, AND LONG. MOVEMENT
TRACK MODULUS	STRAIN AND DISPLACEMENT GAGES	COMPARE WOOD TIES WITH CONCRETE TIES
LATERAL AND VERTICAL LOADS	INSTRUMENTED WHEEL SET	RECORD APPLIED LOADS

At the end of the experiment, many other analyses will be carried out, using the track-geometry data and all the other information collected. For degradation of each parameter, we will be calculating several statistics such as Mean, Standard Deviation, and Percentage Failing Specific FRA Classes.

Using these statistical indicators, we will determine the amount of degradation by individual parameter as tonnage increases. We will also develop a "Track Quality Index" to indicate the condition and degradation of the overall track structure. Many railroad-owned geometry cars now produce a Track Quality Index.

We would like to operate several of those cars over the FAST Track after 100 MGT of operation and compare our results with the results obtained by the various operating cars.

We will also identify and quantify the relationship between the rate and amount of degradation and various physical factors such as curvature, type of rail, vertical and lateral loads, etc. In addition, we will evaluate the amount of maintenance required to limit degradation of the track structure under the operation of a 100-ton car unit train. These costs and degradation rates can then be used to compare the effect of other train consists and car designs on the track structure. Figure 8 is a summary of expected results of the Track Degradation Experiment.

- IDENTIFY UNIQUE MEASURES OF TRACK GEOMETRY
- DETERMINE
 - TRACK DEGRADATION (CHANGE IN TRACK GEOMETRY) VS. MGT
 - WHETHER DIFFERENT GEOMETRY CARS MEASURE SAME THING
- RELATIONSHIP (IF ANY) BETWEEN
 - TRACK GEOMETRY AND NET GAGE WIDENING
 - TRACK GEOMETRY AND RAIL CORRUGATION
- EFFECT OF THE FOLLOWING ON TRACK DEGRADATION RATE
 - WELDED VS. JOINTED RAIL
 - CONCRETE VS. WOOD TIES
 - AMOUNT OF CURVATURE
 - AMOUNT OF TRACK MAINTENANCE
 - TRACK MAINTENANCE STRATEGY
- EFFECT OF THE FOLLOWING ON TRACK MAINTENANCE COST
 - CONCRETE VS. WOOD TIES
 - WELDED VS. JOINTED RAIL
 - AMOUNT OF TRACK CURVATURE

FIGURE 8. SUMMARY OF EXPECTED RESULTS.

QUESTIONS AND ANSWERS

Question 1

During this conference - most problems seem to start to occur @ ±200 MGT - will this experiment be long enough to determine the Necessary degradation, including impact loading?

Answer

We are not completely sure. If sufficient degradation has not occurred at 200 MGT we hope the experiment can be extended.

DEFECT GROWTH RATE PILOT TEST

Oscar Orringer
Experiment Manager
DOT Transportation Systems Center

INTRODUCTION

The FAST Defect Growth Rate Pilot Test (DGRPT), scheduled to get underway in early 1982, applies FAST testing to railroad technology improvement in a much more sophisticated way than the usual FAST experiment. The purpose of this paper is to explain how the DGRPT will help to guide railroad technology toward safer operations, why sophistication is necessary, and what is expected from the experiment.

The American Railway Engineering Association Ad Hoc Committee on Track Performance Standards is sponsoring the DGRPT to provide part of the data on which to base a realistic performance specification for controlling populations of rail defects in track. The DOT Transportation Systems Center, under the auspices of the Improved Track Structures Division of the FRA Office of Safety Research, is functioning as experiment design and technical management staff for the DGRPT and related activities. The total effort combines the DGRPT with the post-test metallurgical analysis to establish the tonnage required to grow rail defects in track, and with studies of railroad data to identify rail defect occurrence patterns.

BACKGROUND

Recent studies of rail defect occurrence patterns have indicated that it may be possible to control rail defect populations by adjusting to more frequent inspection as the rate of defect occurrence rises, provided that the inspection method is able to find the defects before breakout is imminent. Defect growth is also an important factor in determining the time available to remove flawed rails prior to breakout. Finally, the ability to modify growth rates by means of an interim remedial action, as permitted under the current Track Safety Standards, Part 213.113, may have an important bearing on the length of time over which a defect can be safely protected in the track.

The Ad Hoc Committee has evaluated the technical and practical feasibility of several alternative approaches to economically improving rail integrity. The Committee has concluded that an approach based on relating inspection frequency to defect occurrence rate offers the most promise, provided that the rate of occurrence of the defect population rather than growth rate of detectable flaws determines the time available for detection. The impact of search time in a performance-based rail integrity specification has a strong influence on railroad operations. Therefore, it is essential that the content of the specification be based on a highly reliable assessment of search time under service conditions.

In order to complete the development of a performance specification based on this approach, two major studies to characterize rail flaw behavior must be completed. These studies are:

- (1) defect population behavior analysis, and

- (2) defect growth rate characterization.


The behavior of the defect population as a function of track usage, and population-size/derailment-incidence correlations is currently being investigated by analysis of the detection histories of four Class 1 railroads. This study will establish the critical population for control of inspection scheduling.

The idea of controlling defect populations by inspection interval adjustment is developed in Figure 1. The studies of railroad defects have indicated that most defects tend to occur in clusters associated with relatively short lengths of track (5 to 10 miles), and that the cluster locations tend to persist for several years. The proposed performance specification would take advantage of this behavior pattern by focusing frequent supplemental inspection on identified clusters, while using continuous search methods less frequently to give early warning about the appearance of new clusters.

A parallel effort is required to quantify defect growth rates to support the approach of control by population level. Both supplemental and continuous search inspections must be performed often enough to avoid the likelihood of defect breakouts between inspections. An appropriate upper limit on inspection interval for this purpose can be defined from the curve of defect size versus tonnage. Figure 2 presents a schematic illustration of the definition for continuous search inspection. Supplemental inspections would probably focus on the larger defect sizes, thus having a larger detectable size and a shorter upper limit on inspection interval.

Despite the potentially critical role of defect growth rates in controlling rail integrity, there

currently exists very little quantitative data on the time required to grow a defect from detectable size to imminent breakout under conditions of actual train loads. Defect growth rates can be evaluated in part by metallurgical analysis of a large number of defects removed from a widely varying spectrum of service conditions on revenue track. This study of revenue service defect growth will provide estimates of the wide range of growth rates expected under



TRACK CHARACTERISTICS	SHORT CLUSTERS WITH HIGH DEFECT RATE	LONG STRETCHES WITH LOW DEFECT RATE
CURRENT SAFETY STANDARD REQUIRES CONTINUOUS SEARCH INSPECTION	ANNUALLY	ANNUALLY
PROPOSED PERFORMANCE SPECIFICATION WOULD REQUIRE CONTINUOUS SEARCH OFTEN ENOUGH TO CONTROL THE LONG STRETCHES AND SPOT NEW CLUSTERS	LESS OFTEN ① ② PLUS SUPPLEMENTAL INSPECTIONS ③	LESS OFTEN ① ②

- ① INSPECTION INTERVAL IS BOUNDED BY TIME AVAILABLE TO DETECT A DEFECT
- ② INSPECTION INTERVALS ARE BASED ON TONNAGE (MGT)
- ③ SUPPLEMENTAL INSPECTION AT SHORT INTERVALS ESTABLISHES CONTROL AT THE PROBLEM SITES

FIGURE 1. RELATION OF PILOT TEST TO PERFORMANCE SPECIFICATION.

actual service conditions. However, it will not be able to provide specific information on train load environment required to develop relationships between defect size, growth rate, and train load environment necessary to fully interpret service growth histories.

Under these circumstances, it is essential to establish such specific relationships by means of a controlled defect growth rate test in a well defined service environment. However, the accurate documentation of defect growth rates as a function of accumulating tonnage in revenue service would substantially interfere with revenue operations, and would require excessively long test time to accumulate the necessary tonnage. Also, the wide variation of revenue consists and track conditions would introduce excessive scatter in the data, making it difficult or impossible to identify trends, to assess the effectiveness of remedial actions, or to translate specific results to service environments different from the test location. On the other hand, the controlled environment and high tonnage accumulation rate make FAST the logical facility at which to conduct this experiment.

TEST OBJECTIVES

The objective of the FAST Defect Growth Rate Pilot Test is to obtain statistically valid direct quantitative measurements of defect size versus accumulated tonnage for two specific defect types subjected to an accelerated test. A sufficient number of defects will be tested to permit the definition of variance as well as average growth rate.

The DGRPT covers defect sizes ranging from detectable size to imminence of breakout. Imminence of breakout is defined, for test purposes, as any defect size that can be expected to result in breakout before the next opportunity to remove the test

rail (i.e., within 1 to 2 MGT of actual breakout, see Figure 2). The intent of the definition is to schedule test rails for removal from FAST prior to breakout in order to permit accurate measurement of breaking load in the laboratory, to prevent damage to the fracture faces which would otherwise impair defect growth rate analysis, and to insure the safety of the FAST consist.

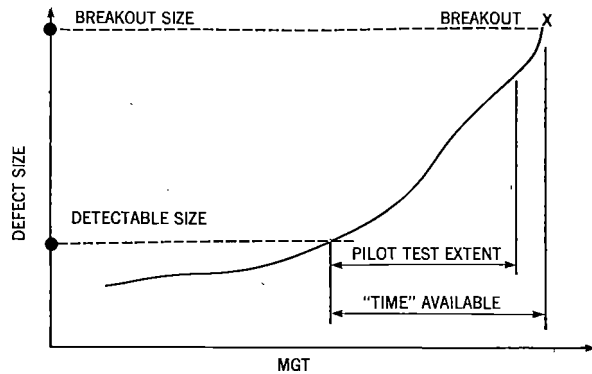


FIGURE 2. TIME AVAILABLE TO DETECT A DEFECT.

Specific test objectives have been established for four test series in tangent track. Each test series will investigate a different defect type, as follows.

Series 1 - Detail fractures in rails of various weights ranging from 132 to 136 lb.

Series 2 - Detail fractures in rails ranging from 132 to 136 lb., with each defect protected by installation of head contact joint bars.

Series 3 - Bolt hole cracks in 132 lb. rail.

Series 4 - Bolt hole cracks in 115 lb. rail.

The four pilot test series are expected to require 16 months in track.

The above choices for testing of defect type and rail weight stem from analysis of accident statistics and from railroad experience. The statistics of defect occurrences and defect-caused accidents are summarized in Tables 1 and 2. These data show that transverse defects in the rail head cause proportionately more accidents than other types and that rail-end defects constitute the largest segment of the defect population. Regarding transverse head defects, railroad experience indicates that detail fractures in 132 to 136 lb/rd rails are the most prevalent type. Regarding rail-end defects, railroad experience indicates that bolt hole cracks have the most serious consequences and also constitute most of the rail-end defect population.

TABLE 1. DEFECT POPULATION

CLASS OF DEFECT	NATIONWIDE	LIMITED MAINLINE(2)		SANTA FE(3) 1977
	SRS(1) 1970-1974	INCLUSIVE 1974-1975	PROFITABLE RR's	
Tranverse Head Defects	20%	27%	55%	22%
Longitudinal Head Defects	18%	29%	8%	25%
Rail End Defects	58%	39%	17%	38%
Total Defects	622,142	2,623	412	6,307
Miles Tested	868,802	1,810	696	---
Defect Rate	0.72 defects/ mile	1.5 defects/ mile	0.6 defects/ mile	---

(1) Sperry Rail Service

(2) Benson, K.D., et al., "Rail Flaw Survey Analysis," August 1977

(3) W. Autrey, Tabulation of Santa Fe Defects, 1/1/77 - 12/31/77

TABLE 2. BROKEN RAIL-CAUSED ACCIDENTS

CLASS OF DEFECT	SRS(1) REVIEW 1970-1974	NATIONWIDE		LIMITED MAINLINE DATA 1974-1975(3)
		FRA(2) DATA 1975	FRA(3) DATA 1970-1974	
Transverse Defects in Head	37%	24%	30%	44%
Longitudinal Defects in Head	26%	18%	13%	8%
Railend Defects	20%	28% max	25% max	29%

(1) Sperry Rail Service

(2) Hitz, J.S., "Analysis of Track Related RR Accident Data," September 1977

(3) Benson, K.D., et al., "Rail Flaw Survey Analysis," August 1977

TECHNICAL APPROACH

FAST Section 10 has been selected for the Defect Growth Rate Pilot Test. Section 10 possesses three key features that make it the logical test location. First, it is equipped with wood ties, and is thus as nearly typical of revenue track conditions as possible. Second, it has adequate length to contain the test section and lead rails. Third, a bypass track is available to continue operations in the event that repairs or defect rail replacement in the test section cannot be completed within one day. Figure 3 summarizes the test zone layout.

Repairs will be necessary if a test defect breaks out during the experiment. Testing to breakout is beyond the experiment objectives, but the possibility of unanticipated breakouts must be recognized and precautions must be taken to maintain operational safety. Three lines of defense have been established for this purpose. First, all test defects will be hand mapped daily to maintain current plots of estimated defect size versus accumulated MGT. In most cases, the defective rail will be removed from the test section immediately when the plot projects imminent breakout before completion of the next operation period. Second, a defect breakout detection system, redundant to the current FAST signal system, will be used to detect fracture of a test rail. This system will then alert the test controller that a defect has broken and trip the FAST signal system to stop and hold the train. Finally, a specially designed protective device will be installed at each defect location. This will provide protection in the event an unexpected breakout does occur, until the locomotive engineer can be signalled and the train stopped or routed to the bypass.

The daily mapping data will also be used to obtain initial estimates of the relationship between defect

size, growth rate and accumulated tonnage. These estimates will be refined in the laboratory by means of strength test and fractography. The strength test will provide an estimate of the wheel load required to break the defect out. Breakage will define the end of the slow growth area on the defect surface. Fractography will then be used to refine the size portion of the size-tonnage relationship.

In addition to daily mapping, records of consist wheel loads will be required periodically to provide data for refining the tonnage portion of the size-tonnage relationship. Strain gaging of the rail near each defect, with leads for wayside readout, will be used for this purpose. Three key factors indicate the necessity of this wayside instrumentation. First, neither dynamic amplification of vertical wheel load nor dynamic lateral wheel load can be computed with certainty from static wheel load. Second, the dynamic loads are subject to random fluctuation from one train passage to another. Third, the load environment is subject to change as a result of consist changes which may occur during the experiment. The need for wayside instrumentation to confirm the load environment has been cited by the FAST Policy Committee based on evaluation of loads data from earlier experiments.

The instrumentation for and technical approach to load characterization will be similar to the wayside portion of the previous load characterization in Section 7 of FAST. However, as indicated in Figure 3, the DGRPT load measurements will include rail bending moment as well as wheel load. Bending moment measurements are necessary because the growth of rail defects has significant dependence on axial bending stress in the rail; the relation between bending moment and wheel load, however, is strongly dependent on local support conditions. The wheel load measurements are being taken as a supplement to allow some correlation with previous measurements of

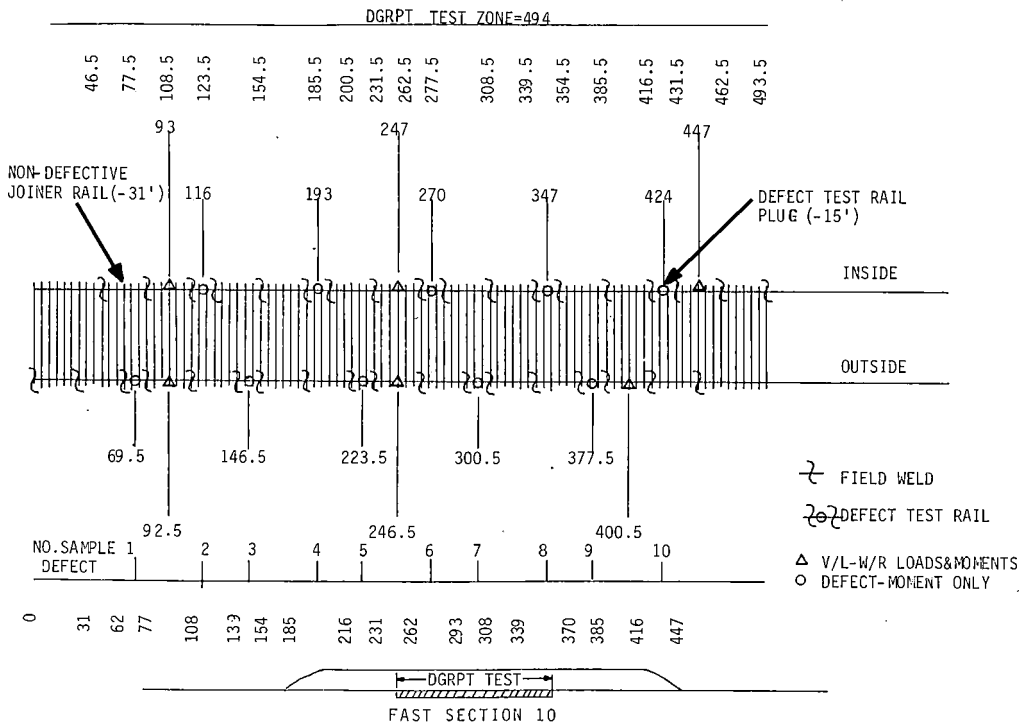


FIGURE 3. DEFECT GROWTH RATE PILOT TEST (DGRPT) ZONE.

revenue service dynamic environment, where only wheel loads were recorded.

Other measurements to be taken during the DGRPT or the post-test phase include track geometry and modulus, static longitudinal stress in the rail, rail residual stress, and lab fatigue performance. The track geometry/modulus data will further assist in the process of correlation between FAST and revenue track. The static longitudinal stress measurements are intended to capture the history of thermal and track adjustment stresses in each test rail during the course of the experiment. In the post-test phase, selected test rails will be destructively sampled to determine the pattern of residual stresses in the rail head. Previous research has shown that plastic flow in the wheel/rail contact zone tends to build up tensile residual stresses inside the rail head, where they may accelerate the growth of detail fractures. Other post-test rails will be subjected to simplified lab-rig fatigue testing in an attempt to determine if a correlation can be established between defect growth rates in the laboratory and in track.

Cooperating railroads have supplied about 75 sample rails containing detail fractures. These samples are currently (November 1981) undergoing receiving inspection, sorting, and instrumentation at the TTC Component Test Laboratory. One partially instrumented sample will be placed in Section 10 during November 1981 - January 1982 for the purpose of shaking down the DGRPT data collection procedures prior to the scheduled February 1982 start of Series 1. DGRPT Series 1 and 2 will consume 20 samples; the remainder will be placed directly in the post-test phase to gather data related to revenue track. The bolt hole crack evaluation associated with Series 3 and 4 will deal with similar numbers of samples.

The interpretation of test results is a complex task because the many factors which affect rail defect growth rates interact with each other and may vary significantly from FAST to revenue track. Detailed history and metallurgy work-ups will, therefore, be prepared for each sample to provide the basis for synthesizing the fundamental characteristics of defect growth rate behavior. These detailed reports will be reviewed by the DGRPT Experiment Technical Assessment Committee, which includes technical specialists from the Transportation Test Center and the Association of American Railroads Technical Center.

EXPECTED RESULTS AND BENEFITS

The FAST Defect Growth Rate Pilot Test and post-test phase are expected to produce curves of defect size versus tonnage for detail fractures and bolt hole cracks in standard control-cooled rail in tangent track, adjusted to account for differences between FAST and revenue track. The curve for bolt hole cracks should be directly applicable to the performance specification for control of rail defects. Detail fractures are sensitive, however, to lateral load effects and will probably require additional testing in a curved section of FAST. Proper adjustment of the FAST results for revenue track may also require limited monitoring of one or two defects in a field test.

Although premium-alloy rails are not a part of the

DGRPT, the performance specification must eventually address this category. Of particular concern in this respect is the use of premium-alloy rail in curves to increase wear life. Such increase may introduce additional head defect occurrences which are not seen on standard-rail curves only because the standard rails are removed from service much earlier. It is hoped, however, that the DGRPT will indirectly support the performance specifications for premium alloy rail by producing a reliable interpretation of laboratory fatigue tests of rail sections, in terms of the performance implied in track. Differences between the lab and track performances with respect to defect growth depend on the mechanics (loads and support conditions) but are independent of the rail material properties. Thus, it may be possible in the light of the DGRPT to cover the premium alloys more quickly and cheaply by means of well calibrated laboratory test procedures.

Finally, it is expected that the DGRPT post-test phase will provide long-term benefits in the form of guidelines for improved mill practice. Recent developments in premium alloy rail have emphasized surface hardness for longer wear life, with little attention paid to the ability of the interior of the rail head to resist the formation and breakout of defects. It is hoped that the post-test metallurgical analysis will provide useful clues to improved processing of rail in the mill for combined long wear life and high resistance to defects.

RADIAL TRUCK CURVING PERFORMANCE EVALUATION

Roy A. Allen
Experiment Manager, Radial Truck
Association of American Railroads

James P. Jollay
Engineer
Boeing Services International, Inc.

A short-term "mini" test is to be carried out at FAST in the near future to evaluate the curving performance of radial trucks over a range of curves varying from $1\frac{1}{2}^\circ$ to $7\frac{1}{2}^\circ$. The experiment should enable the differences in energy consumption between radial and conventional trucks to be quantified and will lead to a better understanding of the mechanics of radial trucks. By combining the experimental results with a computer model, the effects of axle misalignment, yaw stiffness, and wheel profiles will be predicted. The data will form inputs for economic analyses of the benefits of radial trucks and will aid FAST management to decide whether to test a complete consist of vehicles with radial trucks in the next phase of FAST.

INTRODUCTION

The concept of radial, or self-steering, truck designs offers many potential benefits to the railroad industry as a result of lower lateral forces, lower angle of attack, and higher critical hunting speeds as compared with conventional three-piece trucks. Potential benefits certainly include reduced wheel and rail wear and lower fuel costs, and may also include improved track component life. The effect of radial trucks on wheel wear has been, and is being, studied within the industry, including FAST¹ and a few tests have been carried out to ascertain potential fuel savings. Little or no data exists to determine reduction in rail wear, except by using wheel wear results to estimate rail wear and track component life. To this end the FAST program, and the FAST Policy Committee in particular, is considering implementing a new phase of FAST testing which would examine all potential benefits with a complete consist of radial trucks. If adopted, this test would begin after a further 200-250 MGT of traffic has been accumulated with the existing consist of primarily conventional three-piece trucks.

Prior to making a decision, data are required in order to further understand the basic mechanism of radial trucks in curves, to estimate potential fuel savings on FAST, and to determine the effects of such variables as axle misalignment, primary yaw suspension stiffnesses, and wheel profiles. A number of railroads are also interested in determining truck curving performance with the cross-bracing links inoperative, and this variable will also be investigated with a short-term, or "mini", test to be carried out at the Transportation Test Center in the near future (scheduled for January, 1982).

Thus, the radial truck mini-test is designed to

provide a set of base line data on the curving performance and energy consumption of radial trucks. Because it is impractical to test all the variables of interest from a budgetary standpoint, the tests are to be supplemented by the use of a mathematical computer model² which predicts the quasi-static performance of vehicles on curves. The model has been used previously to supplement test data^{3 4} and is used as a truck design tool at British Rail.⁵ After validation with the test data, the model will be used to predict the effect of variables which will not be tested on the track.

Specifically, the objectives of the mini-test are:

- To obtain curving performance data, particularly angles of attack and wheel/rail lateral loads, over curves of $1\frac{1}{2}^\circ$, 3° , 4° , 5° , and $7\frac{1}{2}^\circ$ for five different speeds (one at balance speed and two each above and below balance) on each curve. Three truck designs will be tested: conventional and the retrofit and diagonal cross-link radial designs (see reference 1 for a description of these designs).
- To obtain curving performance data as above on the two radial designs with the cross-bracing members disconnected.
- Using the above curving performance data and truck parameter stiffness data, validate the mathematical curving model and then use the model to predict the effects of other variables.
- To determine the curving resistance of cars equipped with radial trucks when operating on FAST, thus establishing base line data to determine energy consumption differences between conventional and radial trucks.

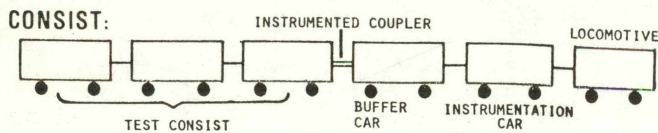
ENERGY CONSUMPTION TEST

Actual locomotive fuel consumption data requires sophisticated instrumentation and is extremely difficult to use in a meaningful way unless the fuel data is gathered over a long period of time in which case statistical techniques can be used to analyze the data. However, in a short-term test such as this, many uncontrolled variables affect the usefulness of the data. Train handling will have a significant impact on such measurements particularly due to the fact that the motive power and train consist may be different on successive test days. Likewise the crew may also be different. Thus, rather than measure fuel usage, this experiment will obtain train resistance data through the use of an instrumented coupler, which will be used to calculate energy consumption.

The tests will be carried out on three test tracks at the TTC - the Transit Test Track (TTT) for the $1\frac{1}{2}^\circ$ curve, FAST for the 3° , 4° , and 5° curves, and the Balloon track for the $7\frac{1}{2}^\circ$ curve. The latter curve is normally used only for turning trains at the TTC but has previously been successfully used for experiments.⁴ Runs will be made on FAST with the track both unlubricated and lubricated. The Balloon and TTT runs will be made on unlubricated track only.

For this portion of the experiment, the instrumentation will include a dynamometer coupler (range: $\pm 30,000$ lb, accuracy ± 30 lb), coupler angularity transducers, and accelerometers measuring carbody longitudinal accelerations to determine grade forces.

The three truck designs will be tested in groups of three cars of each truck design. Each group of three cars will in turn be placed at the rear of a consist containing locomotive power, an instrumentation recording car, and a buffer car. The instrumented coupler will be situated between the buffer car and the three test cars as shown below.



The data will determine the effect of train speed and track curvature on the curving resistance for the conventional and radial trucks. Similar data has previously been obtained on the Truck Design Optimization Program (TDOP)⁶ but was obtained using a single car. The degree of confidence in the data will be increased by use of a three-car test consist in this experiment. It is also proposed to compare curving resistance between the concrete tie section (stiff track) and the equivalent wood tie section on FAST, and the applicability of proposed formulae for calculating rolling resistance will be examined. Two formulae, the traditional Davis formulae representation and the TDOP representation, are shown in Appendix 1. Successful validation of one or the other of these formulae would enable the results of this experiment to be used to estimate the reduction in rolling resistance, and hence potential fuel savings, of radial trucks on other routes.

CURVING PERFORMANCE TESTS

For the curving performance tests, one truck of each of the three designs will be instrumented with two instrumented wheelsets to measure vertical and lateral forces at all four wheels, and four wheel/rail displacement probes to measure lead and trail axle angles of attack as described by Allen and Jollay.⁷ In addition, the primary longitudinal displacements (roller bearing to sideframe) displacements will be measured at each wheel as well as the truck swivel rotation. The latter sets of measurements will enable the mechanism of the expected reduction in angle of attack of the radial trucks, as compared to the conventional truck, to be better understood. The measured data will enable the effects of track curvature and train speed on angles of attack and lateral load to be determined for a wide range of track curvatures. The typical format of the analyzed data will be similar to that shown symbolically in Figure 1.

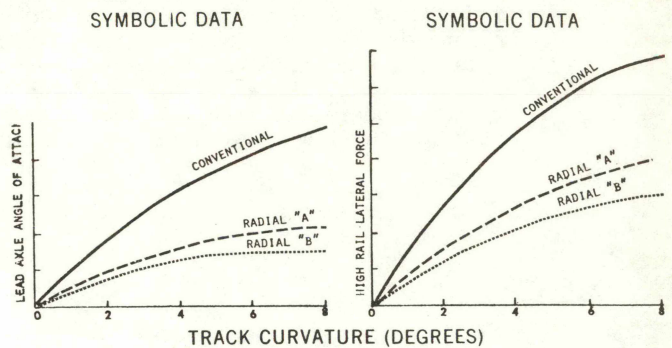


FIGURE 1. SAMPLE DATA FORMAT FOR TRUCK COMPARISON.

There are many variables which affect truck curving performance; e.g., axle misalignment, wheel profile and primary longitudinal stiffness; which, because of the number of variables, cannot be examined directly in this experiment. However, the use of a well-proven mathematical curving model will allow predictions of the effects of these variables to be made with confidence. Before it is used to make predictions, however, it is essential to validate the model using the test data obtained above. The model has shown good agreement with data obtained in a previous experiment⁴ on a transit vehicle carried out at the Transportation Test Center. An example of this is shown in Figure 2 which presents data from this test in the form of graphs of lead axle angle of attack plotted against track curvature. The top two graphs are for a left hand curve, the bottom two for a right hand curve, and the four sets of data represent four different sets of conditions (C1 being the normal suspension, both empty and laden, with AAR 1 in 20 wheel profiles, C2 being with reduced primary longitudinal stiffness and AAR 1 in 20 wheel profiles, and C3 being the softer suspension with CN wheel profiles). The data points represent data obtained experimentally whereas the lines represent the computer model predictions.

In order to obtain this type of empirical/analytical agreement, it is essential to measure certain parameters which are critical to truck curving performance. These data are being used as input data to the model. These parameters include truck rotational

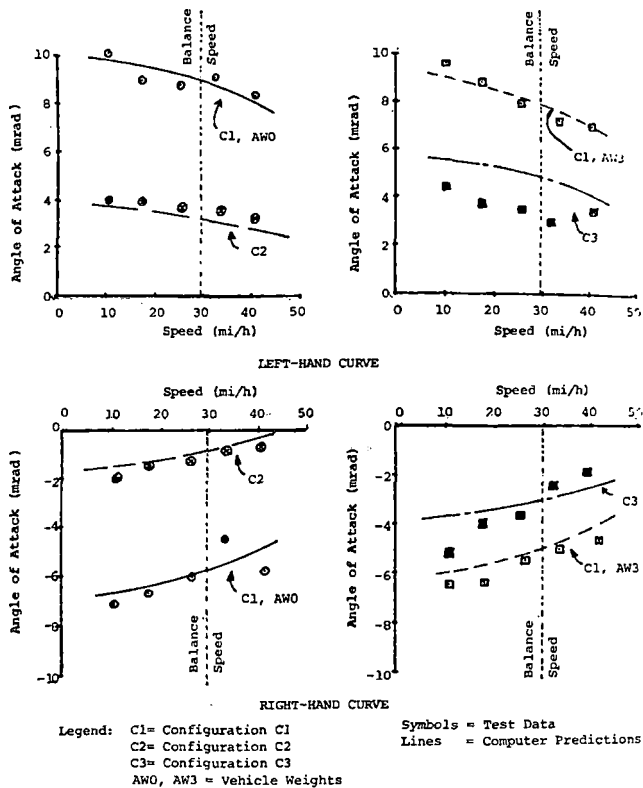


FIGURE 2. LEAD AXLE ANGLE OF ATTACK VS. SPEED (BALLOON LOOP 7.4° CURVE).

stiffness, axle alignment, primary suspension longitudinal, and lateral stiffnesses and the inter-axle shear and bending stiffnesses. These have been shown previously^{1 3} to affect the performance of radial trucks and will be measured at the TTC with the use of air bearings⁸ and other equipment. The wheel and rail profile geometry is an important measurement and typically causes significant non-linearities in the wheel/rail interaction process. Such non-linearities are accounted for in the model and accurate measurement is essential to achieving good correlation between theoretical and empirical results. The TTC has separate machines, designed at British Rail, for measuring wheels and rails (Figures 3 and 4) with the measurement of each wheel or rail made relative to the position of the mate wheel or rail. Each machine consists of a dial gage mounted on a measuring head that is fastened to a frame which rests across the wheelset or track. Dial gage readings are taken in a large number of fixed positions across the profile and these accurately describe the shape of the wheel or rail. Computer analysis then converts these dial gage readings into Y, Z coordinates relative to the track or wheelset centerline. By combining the profiles of a particular pair of wheels and rails, the mutual contacting geometry can be studied. For a series of lateral shifts of the wheelset relative to the track, various parameters⁹--rolling radius difference, contact angles, wheelset roll angles, and contact patch size and slope--are calculated and become another important input to the model.

Assuming that good theoretical/analytical agreement is achieved, the effects of other parameters can then be predicted with confidence. The data would be presented in the type of format shown in Figure 5.

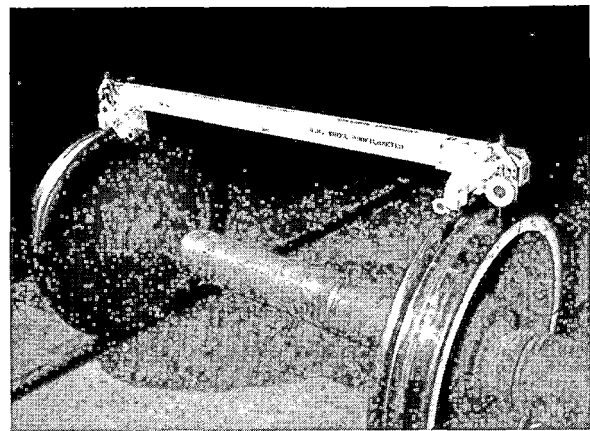


FIGURE 3. TTC WHEEL MEASURING DEVICE.

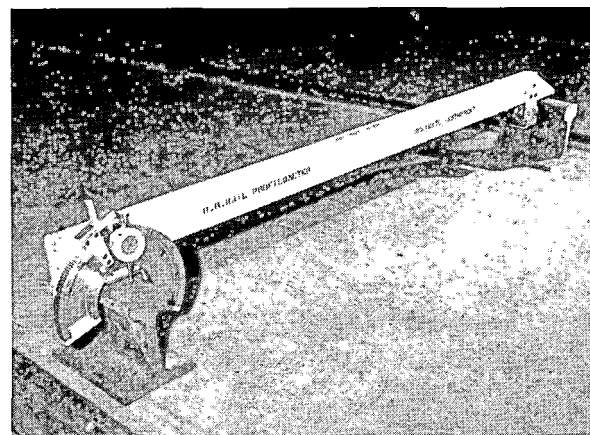


FIGURE 4. TTC RAIL MEASURING DEVICE.

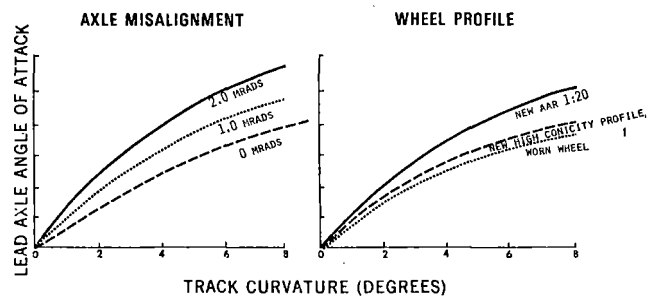


FIGURE 5. COMPUTER PREDICTIONS FOR TRUCK "A".

REFERENCES

- 1 Allen, R. A. and Leary, J. F. - Radial Truck Wheel Wear, 1981 FAST Engineering Conference, Denver, November 1981.
- 2 Elkins, J. A. and Eickhoff, B. M. - Advances in Non-Linear Wheel/Rail Force Prediction Methods and Their Validation, ASME Winter Annual Meeting, New York, December 1970.
- 3 Pollard, M. G. - The Development of Cross-Braced Freight Bogies, Rail International, September 1979, pp. 735, 758.

- 4 Elkins, J. A. and Allen, R. A. - Testing a Transit Vehicle for Wheel and Rail Wear, ASME Winter Annual Meeting, Washington D.C., November 1981.
- 5 Mulcahey, H. W. and Weeks, R. J. - Development of a Cross-Braced Truck, ASME Winter Annual Meeting, Washington D.C., November 1981.
- 6 Wyle Laboratories - Truck Design Optimization Project, Final Report, (to be published, NTIS).
- 7 Allen, R. A. and Jollay, J. P. - The Mechanical Aspects of Wheel/Rail Wear, 1981 FAST Engineering Conference, Denver, November 1981.
- 8 Allen, R. A. - Axle Alignment Measurements: Radial Truck Experiment, Report FAST/TTC/TN-81-04, September 1981.
- 9 Cooperrider, N. K. and Heller, R. - User's Manual for Asymmetric Wheel/Rail Contact Characterization Program, Report FRA/ORD-78/05, December 1977.

APPENDIX 1

Reference 6 is the source document for the material presented in this Appendix.

Davis and TDOP Formulae representation for calculating rolling resistance.

Traditional Representation:

$$RR = 29 + 1.3 W + 0.045 Wv + 0.0006 v^2 + 20 W\theta + (2000 W + 8 W_w) a + 0.8 W\phi$$

Davis Equation Grade Acceleration Curving

TDOP Representation:

$$RR = 29 + 1.3 W + 0.045 Wv + 0.0006 v^2 + 20 W\theta + (2000 W + 8 W_w) a +$$

Davis Equation Grade Acceleration

$$B_1 W\phi + B_2 W\phi^2 + B_3 W \cdot \phi (v^2 - v_b^2) + B_4 W d\phi/dt + B_5 b + B_6 b^2$$

Off Balance Speed Spiral Braking

Curving

Where:

- B_1, \dots, B_6 are the coefficients to be fitted
- W is the car weight (tons)
- W_w is the weight of a single wheel (pounds)
- v is the car speed (mph)
- ϕ is the degree of curvature (degrees)
- θ is the grade (percentage)
- a is the car acceleration (g)
- v_b is the balance speed (mph)
- b is the brake line pressure deficit (psi)
- RR is the rolling resistance (pounds)

***PROCEEDINGS
APPENDIX***

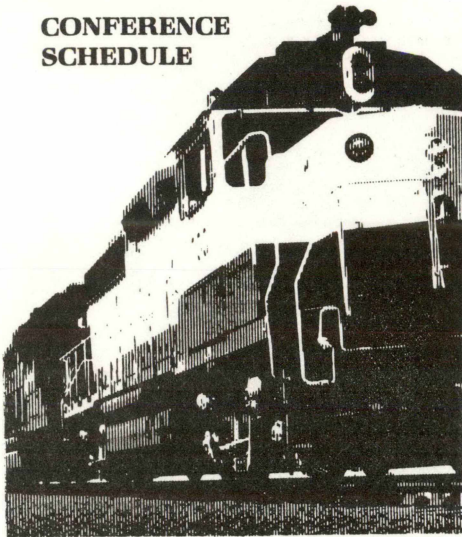
APPENDIX CONTENTS

- o 1981 FAST Engineering Conference Agenda
- o FAST Program Donors
- o FAST Track and Mechanical Experiments
- o FAST Experiment Managers and Monitors
- o FAST Railroad Track and Mechanical Advisors
- o FAST Project Report Index
- o Transportation Test Center Mission Statement and Map
- o Conference Attendees

1981

FAST Engineering Conference

CONFERENCE SCHEDULE



Wheel—RSA Representative
Banquet Chairman: Donald Spanton, FAST Policy Committee Chairman
Keynote Speaker: J. W. Gessner, President and Chief Executive Officer, Missouri Pacific Railroad Co.

Thursday
NOVEMBER 5, 1981
6:45 - 7:45 a.m.
Buffet Breakfast Centennial Square A & B
Breakfast Host: Dresser Industries, Inc.
8:00 a.m.
Introductory Remarks Centennial Square C & D
Paul Settle and Peter Detmold
FAST Policy Committee Members
8:10 a.m.
Session Introduction
James R. Lundgren, FAST Technical Manager

Session 3: TRACK

8:15 a.m.
Ballast Experiments at FAST
Bruce N. Bosserman, Ballast Experiment Manager
9:00 a.m.
Results of Standard Wood Tie and Manufactured Tie Experiments at FAST
Laurens C. Collister, Wood Ties and Fasteners Experiment Manager
9:25 a.m.
Evaluation of Various Wood Tie Fasteners Under Freight Railroad Service Loading
Larry Daniels, Wood Ties and Fasteners Experiment Monitor
9:50 a.m.
Concrete Tie and Fastener Performance
John W. Weber, Concrete Ties and Fasteners Experiment Manager

TUESDAY
NOVEMBER 3, 1981
1:00 - 5:30 p.m.
Registration Stouffers Inn Convention Center Foyer

Wednesday
NOVEMBER 4, 1981
7:00 - 8:00 p.m.
Registration Stouffers Inn Convention Center Foyer
8:00 a.m.
Conference Welcome Centennial Square C & D
Walter W. Simpson
Chairman, FAST Technical Advisory Committee
Member, FAST Policy Committee
8:15 a.m.
FAST Overview
Gregory P. McIntosh, FAST Program Manager
Acting Director, Transportation Test Center
8:30 a.m.
Session Introduction
James R. Lundgren, FAST Technical Manager
Director, AAR Research & Test Operation, Pueblo, CO

Session 1: RAILS

8:45 a.m.
Evolution of Measurement Techniques at FAST
Thomas P. Larkin, FAST Operations Manager
9:15 a.m.
Rail Wear and Metal Flow
Roger K. Steele, Ph.D., Rail Metallurgy Experiment Manager
10:30 a.m.
Rail Corrugation Investigations at FAST: December 1979 through August 1981
Timothy J. Devine, Rail Corrugation Experiment Manager

10:15 a.m.
Concrete Tie Track Systems: Engineering Considerations
Jack E. Heiss, Concrete Ties and Fasteners Experiment Manager
10:40 a.m.
Tie/Ballast Interaction Comparisons for Wood and Concrete Ties
Bruce N. Bosserman, Ballast Experiment Manager
11:05 a.m.
Some Aspects of Concrete Tie Performance on FAST and Revenue Service
Howard G. Moody, Ties and Fasteners Experiment Manager
Correlation of FAST and Laboratory Tests with Concrete and Wood Tie Fastener Results
Howard G. Moody, Ties and Fasteners Experiment Manager
11:30 a.m.
Track Degradation Experiment
James W. Brent, Track Degradation Experiment Manager
11:40 a.m.
Questions and Discussions
James R. Lundgren, FAST Technical Manager
12:00 noon
Luncheon Centennial Square A & B
1:15 p.m.
Session Introduction
James R. Lundgren, FAST Technical Manager

Session 4: FATIGUE

1:30 p.m.
Fatigue Analysis Tests at FAST
S. K. Punwani, Car Dynamics Experiment Manager
2:00 p.m.
Rail Failure Behavior
Roger K. Steele, Ph.D., Rail Metallurgy Experiment Manager

11:00 a.m.
Welded Rail-End Batter
Roger K. Steele, Ph.D., Rail Metallurgy Experiment Manager
11:20 a.m.
Questions and Discussions
James R. Lundgren, FAST Technical Manager
11:45 a.m.
Luncheon Centennial Square A & B

Session 2: WHEELS AND RAIL

1:00 p.m.
Major Variables that Affect Wheel Wear
Donald E. Gray, Wheels Experiment Manager
1:50 p.m.
Wear Rates of Freight Car Wheels as a Function of Chemistry
V. E. Kahle, Wheels Experiment Manager
2:10 p.m. •
Radial Truck Wheel Wear
Roy A. Allen, Radial Truck Experiment Manager
2:40 p.m.
The Mechanical Aspects of Wheel/Rail Wear
Roy A. Allen, Radial Truck Experiment Manager
3:30 p.m.
Wheel/Rail System Wear
Roger K. Steele, Ph.D., Rail Metallurgy Experiment Manager
4:45 p.m.
Questions and Discussions
James R. Lundgren, FAST Technical Manager
5:00 p.m.
Adjourn
7:00 p.m.
FAST Banquet Centennial Square A & B
Banquet Host: The Railway Supply Association
L. D. Gaeth, Senior Marketing Manager, Griffin

Session 5: FUTURES

2:20 p.m.
Defective Growth Rate Pilot Test
Oscar Orringer, DGRPT Experiment Manager
2:30 p.m.
Radial Truck Curving Performance Evaluation
Roy A. Allen, Radial Truck Experiment Manager
2:40 p.m.
Questions and Discussions
James R. Lundgren, FAST Technical Manager
3:00 p.m.
FAST Tour Presentation
Gregory P. McIntosh, FAST Program Manager
Acting Director, Transportation Test Center
3:05 p.m.
Closing Remarks
Walter W. Simpson
Chairman, FAST Technical Advisory Committee
Member, FAST Policy Committee
3:20 p.m.
Adjourn

Friday
NOVEMBER 6, 1981

FAST TOUR

6:00 a.m.
Buses depart Stouffers Denver Inn, front entrance
9:00 a.m.
Arrive Transportation Test Center
Tour of FAST
3:00 p.m.
Return to Denver, Stapleton Airport
3:30 p.m.
Return to Stouffers Denver Inn

FAST PROGRAM DONORS

AAR - Association of American Railroads
 A. Stucki Co.
 Abex Corp.
 ACF Industries (AMCAR Div.) Shippers Carline
 Aeroquip
 Gustin-Bacon Division
 Alaska Railroad
 Algoma Steel
 Allegheny Drop Forge Co.
 AISI (American Iron and Steel Institute)
 American Steel Foundries
 Arthur Railroad Spikelock Corp.
 Atchison, Topeka and Santa Fe Railway Co.
 Automation Industries, Inc.
 Sperry Rail Service Div.
 Belt Railway of Chicago
 Bessemer and Lake Erie Railroad Co.
 Bethlehem Steel Corp.
 Blakeslee Concrete
 Boston & Maine Corp.
 Brenco, Inc.
 British Steel
 Burlington Northern, Inc.
 Camcar
 Canadian National Railways
 Canadian Pacific Ltd.
 Canadian Steel
 CANRON
 Cardwell Westinghouse Co.
 Cedrite Corp.
 Central Vermont Railway (CV Ry.)
 C.F.&I. Steel Corp.
 Chemetron Corp.
 Chessie System Railroads
 Chicago, Milwaukee, St. Paul & Pacific Railroad Co.
 Chicago & Northwestern Transportation Co.
 Chicago & Western Indiana Railway
 Climax Molybdenum Co.
 Cobra Railroad Friction Products Corporation
 Colorado & Southern Railroad Co.
 Colorado & Wyoming Railroad Co.
 Colt Industries (Crucible Spring Div.)
 Conforce Costain Concrete Tie Co.
 Consolidated Rail Corp.
 Creusot-Loire Steel Corp.
 Valdunes Division
 DAYCO
 Dayton Malleable Inc.
 The Denver & Rio Grande Western Railroad Co.
 Devine Manufacturing Co.
 Dixon
 Dow Chemical U.S.A.
 DOW-MAC
 Dresser Industries, Inc.
 Dresser Transportation Equipment Div.
 DU-WEL Steel Products
 Dyer Quarries

 E.I. DuPont DeNemours & Co., Inc.
 Edgewater Steel Co.
 Electronic Flange Lubricator, Inc.
 Elgin, Joilet and Eastern Railway Co.
 Fairmont Railway Motors
 Family Lines Rail System, Inc.
 Ferrocarriles Nacionales de Mexico
 Fountain Sand & Gravel Co.
 Fort Worth and Denver Railway Co.
 General American Transportation Corp.
 General Electric Co.
 Silicon Products Dept.
 Grand Trunk Western Railroad Co.
 Griffin Wheel Co.
 Harmon Industries Inc.
 Hawker Siddeley Canada Ltd.,
 Canadian Steel Wheel Div.
 Henry Miller Spring and Manufacturing Co.
 Holland Company
 Houston Belt & Terminal Railway Co.
 Huck Manufacturing Company
 Illinois Central Gulf Railroad Co.
 Illinois Terminal Railroad Co.
 Indiana Harbor Belt Railroad Co.
 International Track Systems, Inc.,
 Railroad Products Div.
 Intma, Inc.
 Johnson Rubber Co.

 Kansas City Southern Railway Co.
 Kerr-McGee, Inc.
 KMD Enterprises, Inc.
 Koppers Company, Inc.
 L. B. Foster Co. (Weir Kilby Div.)
 LaSalle & Bureau County Railroad
 Lewis Rail Service Co.
 Loctite
 Loram Maintenance of Way
 Louisiana & Arkansas Railway Co.
 Louisville & Nashville Railroad Co.
 Manganese Steel Forge Co.
 McConway and Torley Corp.
 McKay Components, Inc.
 Midland--Ross Corp.
 Midland Steel Products
 Minnesota Mining & Manufacturing Co.
 Missouri-Kansas-Texas Railroad
 Missouri Pacific Railroad Co.
 Monsanto
 Moore & Steele Corp.
 National Crushed Stone Association
 National Lock Washer Co.
 National Railroad Passenger Corp. (AMTRAK)
 NDH Bearing Service
 New Departure Hyatt Bearings
 New York Traprock Corp.
 Newton County Stone Co.
 NHTR--Tomasso
 Nippon Steel Corp.
 Norfolk & Western Railway Co.
 North American Car Corp.
 NVF Company (Railway Products Group)
 Orgotherm Inc.
 Pandrol USA Inc.
 Pennsylvania Power & Light Co.
 Pettibone Corp.
 Pittsburgh & Lake Erie Railroad Co.
 Plasser Corp.
 Portec Inc.
 Prorail
 Pullman-Standard
 Quebec North Shore & Labrador Railway Co.
 Division of IOCC
 Racine Railroad Products, Inc.
 Railroad Friction Products Corp.
 The Rails Company
 Railway Tie Association
 Sacilor
 Safetran Corp.
 Santa Fe - Pomeroy Inc.
 Security Locknut
 St. Louis--San Francisco Railway Co.
 St. Louis Southwestern Railway
 Seaboard Coast Line Railroad Co.
 Servo Corp. of America
 Shell Oil Co.
 Southern Pacific Transportation Co.
 Southern Railway System
 Standard Car Truck Co.
 Stedef, Inc.
 Taylor-Wharton
 Division of HARSCO
 Timken Co.
 Titanium Metals Corp. of America,
 Standard Steel Div.
 Toledo, Peoria, and Western Railroad Co.
 Terminal Railroad Association of St. Louis
 Trailer Train Co.
 Transit Products Company, Inc.
 True Temper Corp.
 Union Pacific Railroad
 Union Spring & Manufacturing Co.
 Union Tank Car Co.
 Unit Rail Anchor Co.
 United States Railway Equipment Co.
 United States Steel Corp.
 U.S. Thermite
 Vanguard Corp.
 Virginia Plastics Co.
 Vulcan Materials Co.
 WABCO--Westinghouse Air Brake Div.
 Warner Co.
 Western Pacific Railroad Co.
 WH Miner
 Woodings--Verona Tool Works

TRACK EXPERIMENTS

MECHANICAL EXPERIMENTS

<u>EXPERIMENT</u>	<u>INITIATED</u>	<u>TERMINATED</u>	<u>CATEGORY</u>	<u>INITIATED</u>	<u>TERMINATED</u>
I <u>BALLAST</u> I II	Sept 1976 Dec 1980	July 1979 In Progress	I <u>CAR STRUCTURES/DRAFT COMPONENTS/BEARINGS</u> Bathtub Gondolas Brake Shoes Centerplates Couplers Coupler & Carrier Wear Plates	Sept 1976 Sept 1976 Sept 1976 Sept 1976	Feb 1976 Nov 1977 July 1979 July 1979
II <u>WOOD TIES</u>	Sept 1976	In Progress	Roller Bearings I Roller Bearings II Roller Bearing Adapters Side Bearings Springs	Sept 1976 Sept 1976 April 1980 Sept 1976 Sept 1976	July 1979 In Progress In Progress July 1979 July 1979
III <u>WOOD TIES/FASTENERS</u> I II III	Sept 1976 Nov 1977 Jan 1979	Sept 1977 Nov 1978 In Progress	II <u>CAR DYNAMICS</u> FAT I FAT II	June 1978 May 1981	Aug 1978 June 1981
IV <u>CONCRETE TIES/FASTENERS</u> I IIA IIB	Sept 1976 Dec 1979 Nov 1981 Start Up	Sept 1981 In Progress	III <u>TRUCKS</u> I II PPLX	Sept 1976 March 1980 Sept 1980	July 1979 In Progress In Progress
V <u>RAIL METALLURGY</u> I II III	Sept 1976 Nov 1977 Dec 1979	Sept 1977 June 1979 In Progress	IV <u>WHEELS</u> I II III IV Wear Index	Sept 1976 April 1977 Mar 1980 Feb 1981 June 1981	April 1977 In Progress In Progress In Progress In Progress
VI <u>RAIL CORRUGATIONS</u> I II	July 1977 Dec 1979	Feb 1979 In Progress	V <u>TTX</u> I II	Sept 1976 Transferred to TTD	July 1979
VII <u>SPECIAL TRACKWORK TURNOUTS</u> I II	Sept 1976 Under Consideration by TTD	July 1979	VI <u>MECHANICAL MAINTENANCE</u> I	Nov 1981	-----
VIII <u>BONDED & INSULATED JOINTS</u> I II	Sept 1976 Feb 1979	Feb 1979 In Progress	VII <u>WHEEL/RAIL LOADS</u>	June 1979	July 1979
IX <u>MAINTENANCE OF WAY</u>	Sept 1976	Sept 1981			
X <u>TRACK DEGRADATION</u>	Nov 1981 Start Up				
XI <u>DEFECTIVE GROWTH RATE PILOT TEST</u>	Mar 1982 Start Up				
XII <u>HIGHWAY GRADE CROSSINGS</u>	Mar 1980	In Progress			

TRACK EXPERIMENT MANAGERS AND MONITORS

<u>Experiment</u>	<u>Manager</u>	<u>Dates</u>	<u>Monitor</u>	<u>Dates</u>
Ballast	A. Sluz, TSC	July 1977 - Mar 1980	B. Bosserman, FRA Vacant J. Heiss, O&M	Sept 1979 - Mar 1980
	B. Bosserman, FRA	Mar 1980 - Present		April 1981 - Present
Wood Ties & Fasteners	L. Collister, AAR	July 1977 - Present	L. Daniels, O&M	Sept 1979 - Present
	H. Moody, FRA	July 1977 - Present		
Concrete Ties & Fasteners	A. Kish, TSC	July 1977 - June 1979	L. Daniels, O&M J. Heiss, O&M	Sept 1979 - Oct 1980
	J. Weber, AAR	July 1977 - Present		Oct 1980 - Present
	J. Putukian, TSC	July 1979 - Dec 1979		
	H. Moody, FRA	Oct 1979 - Present		
Special Trackwork	W. Cruse, AAR	July 1977 - Present	F. S. Mitchell, AAR	Sept 1979 - July 1980
Corrugations	W. Kucera, Griffin	July 1977 - Aug 1979	L. Daniels, O&M	Sept 1979 - Present
	T. Devine, Griffin	Aug 1979 - Present		
Rail Metallurgy	R. Steele, FRA	July 1977 - Present	B. Bosserman, FRA Vacant	Sept 1979 - Mar 1980
Track Degradation	J. Brent, AAR	Feb 1981 - Present	R. Begier, AAR	Feb 1981 - Present
Defective Growth Rate Pilot Test	O. Orringer, TSC	Oct 1980 - Present	R. Brush, FRA	Jan 1981 - Present
Maintenance-of-Way	R. Murphy, TSC	July 1977 - Nov 1979	F. S. Mitchell, AAR	Sept 1979 - July 1980
	W. Cruse, AAR	July 1977 - Nov 1980		
Highway Grade Crossing	W. Cruse, AAR	Nov 1977 - Nov 1978	C. W. Bean, AAR	Aug 1980 - Present
	E. Baicy, FRA	Nov 1978 - July 1981		
	L. Bernardi, Acting	July 1981 - Present		

MECHANICAL EXPERIMENT MANAGERS AND MONITORS

<u>Experiment</u>	<u>Manager</u>	<u>Dates</u>	<u>Monitor</u>	<u>Dates</u>
Car Structure/ Draft Components/ Bearings	J. E. Burns, C&O	July 1977 - Present	R. A. Allen, O&M	Sept 1979 - Sept 1981
			G. Mitchell, AAR	Sept 1979 - Nov 1980
			G. Staeheli, AAR	June 1981 - Present
Car Dynamics	D. E. Gray, FRA S. K. Punwani, AAR	July 1977 - Dec 1978 Jan 1977 - Present	R. A. Allen, O&M	Sept 1979 - Sept 1981
			G. Mitchell, AAR	Sept 1979 - Nov 1980
Mechanical Maint.	W. T. Lehman, CR	Sept 1979 - Present	G. Staeheli, AAR	June 1981 - Present
Trucks	D. H. Propp, BN J. A. Bichsel, BN K. Rownd, BN (Acting) R. A. Allen, AAR	July 1979 - June 1978 July 1978 - May 1979 June 1979 - June 1981 Sept 1981 - Present	R. A. Allen, O&M	Sept 1979 - Sept 1981
			G. Mitchell, AAR	Sept 1979 - Nov 1980
			G. Staeheli, AAR	June 1981 - Present
TTX	E. T. Wolfe, TT	July 1977 - July 1981	R. A. Allen, O&M G. Mitchell, AAR J. Jollay, O&M	Sept 1979 - Sept 1981 Sept 1979 - Nov 1980 July 1980 - July 1981
Wheel Wear Index	S. K. Punwani, AAR R. A. Allen, AAR	July 1980 - Sept 1981 Sept 1981 - Present	R. A. Allen, O&M	July 1980 - Sept 1981
			G. Staeheli, AAR	June 1981 - Present
Wheels	C. Scott, Sou D. E. Gray, FRA V. E. Kahle, SP	July 1977 - Jan 1978 July 1977 - Present June 1978 - Present	R. A. Allen, O&M	Sept 1979 - Sept 1981
			G. Mitchell, AAR	Sept 1979 - Nov 1980
			G. Staeheli, AAR	June 1981 - Present

RAILROAD TRACK ADVISORS

Atchison Topeka and Santa Fe
Keith Pottoroff Jan 1977 - April 1977
Wm. Groh April 1977 - Aug 1978
Stephen P. Heath Sept 1978 - Present

Bessemer & Lake Erie
Bernie Forcier Jan 1977 - July 1981
J. P. Coessens Aug 1981 - Present

Burlington Northern
Joseph Mike Jan 1977 - June 1978
Dale Stevens July 1978 - April 1981
Lloyd Hobbs* May 1981 - Present

Canadian National
William Wood July 1977 - Dec 1978
Eric Summers Jan 1978 - Present
J. Swiderski**

Canadian Pacific
Karl W. Sutherland July 1977 - Present

Chessie
Imre H. Reiner Nov 1979 - Present

Southern
Charlie Scott Sept 1976 - June 1981
Robert W. Blank July 1981 - Present

Southern Pacific
Frank Vanderpool Jan 1977 - Dec 1979
Lee Alcalá Jan 1980 - May 1981

St. Louis & San Francisco Rwy. Co.
Lloyd Hobbs Sept 1977 - (See BN)

Union Pacific
Don Gale Jan 1977 - Dec 1980
Charlie M. Funk Jan 1981 - Present

* Railroads Merged
** Alternate

RAILROAD MECHANICAL ADVISORS

Atchison Topeka and Santa Fe
Larry Hudson Jan 1977 - April 1979
Jerry M. Harris April 1980 - Present

Burlington Northern
Dale Propp Jan 1977 - Aug 1977
Jack Bichsel Aug 1977 - May 1979
Ken Rownd May 1979 - June 1981
Darell Johnson June 1981 - Present

Canadian Pacific
J. P. Normand Jan 1977 - Feb 1978
R. Lapierre* July 1977 - Feb 1978

Chessie
James Burns Jan 1977 - Present
Don Ray* Jan 1977 - July 1979

Conrail
Wm. Lehman Sept 1979 - Present

Missouri Pacific
John Stratton Jan 1977 - May 1980
Lloyd R. Boyar May 1980 - Present

Union Pacific
Joe Car Jan 1977 - Present
Wm. Guess*

* Alternate

BACKGROUND PAPERS, 1 NOVEMBER 1981

Tracking Number Experiment Number	Title, Author
BP-81/001 TE-3-B	Bonded/Insulated Joint Experiment Status Report Daniels
BP-81/002 TE-6	Rail Flaw History, September 1976 through October 1977 Grebenc (Was Dr-07,I)
BP-81/003 TE-6	Rail Flaw History, November 1977 through April 1978 Grebenc (Was Dr-07,II)
BP-81/004 TE-6	Rail Flaw History, May 1978 through November 1978 Grebenc (Was Dr-07,III)
BP-81/005 S	Vertical & Lateral Load Measuring Circuit Evaluation Cheung (Was Appendix A in Dr-110)
BP-81/006 G	Evaluation of Wayside-Wheel/Rail Forces Measurement Methodology Chang (Was Dr-31)
BP-81/007 ME-6	Lateral Force Comparison with 14" and 16" Center Plates Chang (Was Dr-49)
BP-81/008 TE-5	Literature Summary, Rail Corrugation Daniels (Was Dr-137)
BP-81/009 S	Strain Gage Evaluation Graff (Was Dr-110)
BP-81/010	Wheel/Rail Loads Test, Wayside Data Tuten, Harrison (Was Dr-145)
BP-81/011	A Comparison of the Static and Dynamic Deflection Taken on Phase III Wood-Tie Fastener Experiment Baird (Was Dr-151)
BP-81/012	Operational Evaluation of Fastener Toe-Load Devices Heiss (Was Dr-136 Appendix)

Published, 1979

TECHNICAL NOTES

Number	Type	Title
TN 79/01	ME & TR	Description of FAST Operations
TN 79/02	ME & TR	Description of FAST Track and Mechanical Experiments
TN 79/03	TR	Inspection Report of Selected Section 17 Concrete Tie Pads at 175.9 MGT
TN 79/04	TR	Spike Pullout Resistance Status Report
TN 79/05	TR	Screw Spike Performance (Section 07)
TN 79/06	TR	Performance of Laminated and Reconstituted Wood Ties
TN 79/07	TR	Inspection Report of Selected Fastening System Components in Section 17 at 235.4 MGT

TN 79/08	ME & TR	Sample Rail/Wheel Wear Characteristics
TN 79/09	TR	Ballast Physical Properties Tests
TN 79/10	TR	Section 17 Ballast Quality Tests
TN 79/11	TR	Track Component Performance/Replacement Status
TN 79/12	TR	Compression Clip Performance, Section 07
TN 79/13	TR	Longitudinal Rail Stress Measurement Methodology
TN 79/14	ME	Axle Failure - May 10, 1978
TN 79/15	TR	Lateral Track Instability
TN 79/16	TR	Failure of Polyethylene Tie Plates - Sections 02 and 03
TN 79/17	TR	Comparative Performance Evaluation, Wood and Concrete Tie Track (150 MGT)
TN 79/18	TR	Preliminary Evaluation of Locomotive Wheel Flange Lubrication
TN 79/19	TR	Tie Plate Pad Performance, Section 02

TEST MEMORANDA

Number	Type	Title
--------	------	-------

TM 79/01	TR	Ballast Consolidation Test
----------	----	----------------------------

Published, 1980

FORMAL REPORTS

Number	Type	Title
--------	------	-------

IR 80/01	ME	Dynamic Hopper Car Test March 1980 PB 80 187925
----------	----	---

IR 80/02	TR	Concrete and Wood Tie Track Performance through 150 Million Gross Tons March 1980 PB 80 168842
----------	----	--

FR 80/04	ME	Freight Car Fatigue Analysis Test on FAST July 1980
----------	----	--

IR 80/06	TR	Evaluation of Steel Tie Performance at the Facility for Accelerated Service Testing September 1980
----------	----	---

IR 80/07		Wheel/Rail Loads Test, Hopper Car Ride Data August 1980
----------	--	--

TECHNICAL NOTES

Number	Type	Title
--------	------	-------

TN 80/01	TR	Railbreak Detection System, Phase III Microprocessor Development
----------	----	--

TN 80/02	ME	Undesired Emergency Locator System
TN 80/03	TR	Evaluation of Weldable Strain Gages For Use on Rail in the FAST Track
TN 80/04	TR	Evaluation of Rail Wear at the Facility for Accelerated Service Testing
TN 80/05	TR	Evaluation of Lateral Track Strength Measurements at FAST
TN 80/06	ME	Fabricated Truck Evaluation
TN 80/07	TR	Rail Failures, Second Metallurgy Experiment
TN 80/08	TR	Rail Lubrication Studies at the Facility for Accelerated Service Testing

Published, 1980

TEST MEMORANDA

Number	Type	Title
TM 80/01	TR	Tie Insulation Experiment
TM 80/02	TR	Metallurgical Evaluation of Rail Defects in Standard Carbon Steel
TM 80/03	TR	Failure Analysis of Rails from FAST
TM 80/04	TR	Metallurgical Evaluation of Rail Defects in Premium Steel Rail
TM 80/05	TR	Track Geometry vs. Measurement-Axle Loading
TM 80/06	TR	Description of a Failed Rail from FAST
TM 80/07	TR	Fully Heat-Treated 115RE Rail Fracture Adjacent to Flash-Butt Welded Joint
TM 80/08 See TM 81/03	TR	Data Supplement to Ballast Experiments Intermediate (175 MGT) Stress and Strain, Status Report
TM 80/09	TR	Correlation of Plasser Car Data to the Track Walker's Report and Survey-to-Benchmark Test
TM 80/10	ME	Brake Shoe Wear Status
TM 80/11	TR	Ballast and Subgrade Instrumentation, 1979 Rebuild, Section 22

Published, 1981

FORMAL REPORTS

Number	Type	Title
IR 81/03	TR	Measurements of Rail/Tie Deflections and Fastener Clip Strains at FAST
IR 81/04	TR	Wear Behavior of High Rails Tested in 1st Metallurgical Experiment
IR 81/06	TR	Concrete & Wood Tie Track Performance thru 425 MGT at FAST
IR 81/07	TR	A Perspectival Review of Rail Behavior at FAST
IR 81/09	TR	Status Report on Ballast Experiments at FAST

FR 81/10	ME	Hopper vs. Tank Car Truck Loads
IR 81/11	TR	The Effect of Service Loading on the Bending Strength of Concrete Ties

TECHNICAL NOTES

Number	Type	Title
TN 81/01	ME	Description of Selected FAST Truck Measurements, First Truck Experiment
TN 81/02	ME	Radial Truck Experiment - Restart at FAST
TN 81/03	TE	Ballast Shoulder Width Experiment
TN 81/04	ME	Axle Alignment Measurements on Cars in the FAST Radial Truck Experiment
TN 81/05		Alternate Method for Separable Body Center Plate Replacement

Published, 1981

TEST MEMORANDA

Number	Type	Title
TM 81/01	ME	Wheel Flange Cracks Evaluation, First Experiment
TM 81/02	TR	Concrete Tie Instrumentation for the Phase II Tie/Fastener Experiment at FAST
TM 81/03	TR	Ballast Experiments Intermediate (175 MGT) Stress & Strain Status Report
TM 81/04	TR	Summary of the Subsurface Exploration Program Performed Prior to the 1979 FAST Rebuild, Sections 03, 17 and 22
TM 81/05	TR	Operational Evaluation of Fastener Tie Load Devices, October 20, 21, and 22, 1980
TM 81/06	TR	Documentation of Ballast and Subgrade Aspects of 1979 Rebuild of FAST, Sections 03, 17 and 22
TM 81/07	TR	Track Settlement Predictions at FAST

THE TRANSPORTATION TEST CENTER

MISSION

The Transportation Test Center (TTC), is operated and administered by the Federal Railroad Administration, and is charged with the mission of conducting comprehensive testing, evaluation and associated development of ground transportation systems. Such test operations are capable of determining system feasibility, the validity of designs, expected operational cost and environmental impact of new developments. All TTC facilities are available for use by government agencies, private industry, and international projects.

HISTORY

The High Speed Ground Transportation Act of 1965 set the stage for establishing an installation where new developments in ground transportation equipment could be tested. Following a three-year evaluation of potential locations across the nation, 52 square miles of state-owned land near Pueblo, Colorado, was selected as the TTC site in 1969. Construction began the next year and the Test Center was officially opened on May 19, 1971.

CONVENTIONAL RAIL FACILITIES

Today the Transportation Test Center has 37 miles of conventional railroad track, over nine miles of electrified transit track and almost nine miles of high speed advanced systems guideways.

Support facilities include full railroad maintenance and transit maintenance capabilities. Of special note is the Rail Dynamics Laboratory which is a major contributor to improved understanding of wheel/rail interaction and vehicle dynamics.

The Center's longest test track, a 14-mile loop, is intended for high speed testing of locomotives and cars like the 120-mph Amtrak coaches. Electrification of the Railroad Test Track provides information for U.S. electrification projects, including evaluation of equipment soon to be used in rail passenger service from Boston, Mass., to Washington, D.C. Inside this oval is the 4.5-mile Train Dynamics Track where track-induced dynamics, which cause derailments and other train handling problems, are studied on various grades, curves and temporarily misaligned trackage. Linked to this track is a three-quarter-mile straightaway called the Impact Track where instrumented collision tests are conducted in an effort to lead to safer equipment designs.

Also located within the Railroad Test Track is the 4.8-mile Facility for Accelerated Service Testing -- FAST -- Track. The FAST Project began in 1976 as a joint government/industry cooperative effort and is a most promising technical step toward improving the economic operating efficiency of the railroad industry in our country. The wear rates on a wide variety of track structure components and rail car components can be accelerated by a factor of seven-to-ten. The FAST train is made up of three to four locomotives and about 75 100-ton freight cars, donated by the railroads. The train circles the loop 15 hours a day, 5 days a week at an average speed of 41 mph. The loop is divided into 22 sections where a variety of rail, ties, tie plate, ballast, and other tests are performed. The result is the accumulation of data concerning how these components will last under years of normal wear.

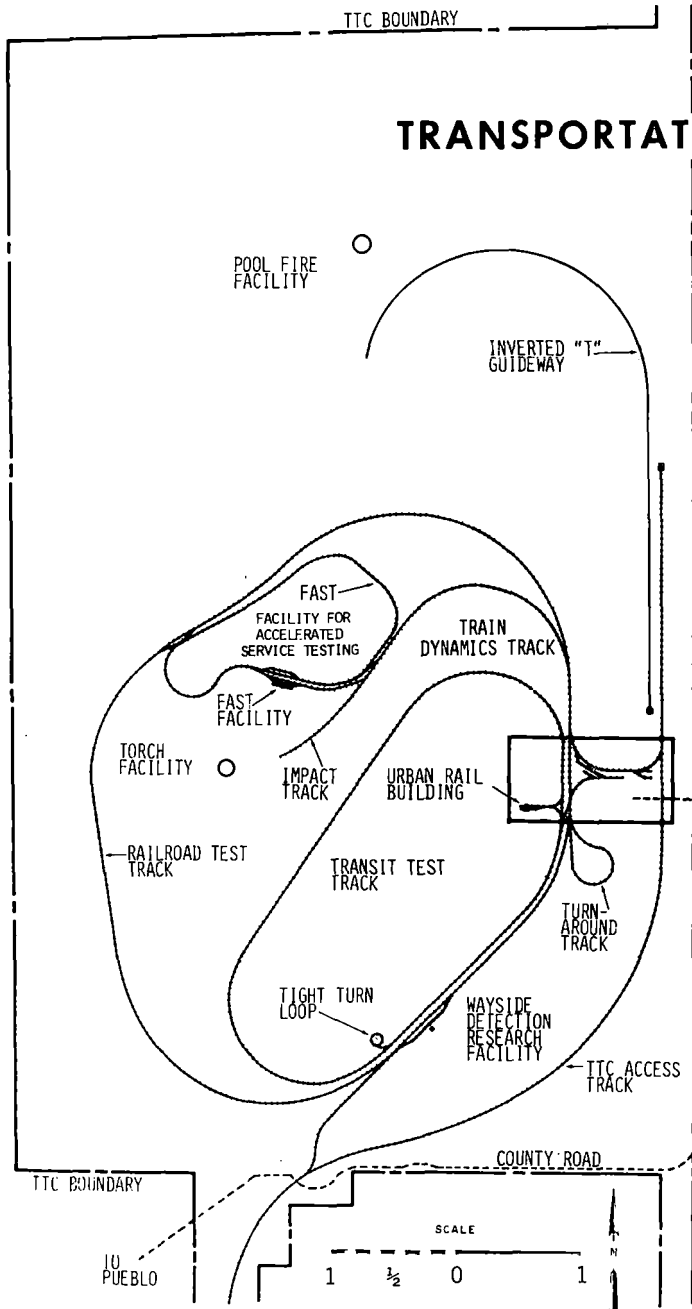
The Transit Test Track, a 9.1-mile oval, is equipped with a third rail capable of variable DC voltages between 400 volts and 1500 volts for testing electric-powered rapid transit cars like the Washington Metropolitan Area Transit Authority Cars. This track has six segments representative of different types of transit track construction in use by transit authorities today. A two-mile portion is equipped with an overhead catenary for testing pantograph-equipped designs such as the Light Rail Vehicle. Testing for the Urban Mass Transportation Administration (UMTA) occurs on the Transit Track.

ADVANCED SYSTEMS FACILITIES

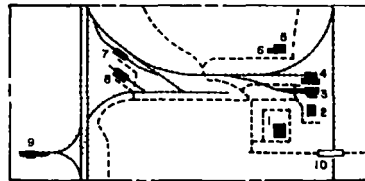
Nearly 15 miles of highly sophisticated tracks and guideways were constructed for the three advanced systems test projects which were the Center's original focus. A 6.2-mile precision rail track having an aluminum center "fin" was completed in 1971 for the Linear Induction Motor Research Vehicle. In 1974 the vehicle set a world speed record for wheel-on-rail vehicles at 255.4 mph. This precision track now serves as another access track to the Center. In 1973, three miles of special U-shaped concrete guideway were built for the Tracked Levitated Research Vehicle. Another special 5.7-mile guideway was also constructed to test the Prototype Tracked Air Cushion Vehicle -- the world's first all-electric 60-passenger tracked levitated vehicle capable of speeds to 150 mph.

TEST CENTER TOURS

The public is invited to tour the Center's facilities on Monday, Wednesday or Friday at 1:00 p.m. (federal holidays excluded.) For more information contact the Office of Public Affairs, (303) 545-5660.



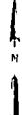
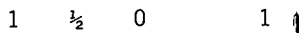
TRANSPORTATION TEST CENTER



TTC ADMINISTRATION- LABORATORY AREA

- 1 OPERATIONS BUILDING
- 2 PROJECT MANAGEMENT BUILDING
- 3 RAIL DYNAMICS LABORATORY
- 4 CENTER SERVICES BUILDING
- 5 WAREHOUSE/LABORATORY FACILITY
- 6 COMPONENTS TEST LABORATORY
- 7 TRANSIT MAINTENANCE BUILDING
- 8 STORAGE & MAINTENANCE BUILDING
- 9 URBAN RAIL BUILDING
- 10 AUTO OVERPASS

SCALE



FEDERAL RAILROAD ADMINISTRATION ATTENDEES

Richard D. Anderson
Facility Eng. & Construction Coordinator
Transportation Test Center
P.O. Box 11330
Pueblo, CO 81001

R. M. McCafferty
Chief, Systems Engineering Division
Transportation Test Center
P.O. Box 11330
Pueblo, CO 81001

Trevor R. Chapman
Program Analyst
Transportation Test Center
P.O. Box 11330
Pueblo, CO 81001

J. J. Reimers
FAST Project Test Mechanical Manager
Transportation Test Center
P.O. Box 11330
Pueblo, CO 81001

Eldon L. Ekberg
Chief, Facilities Management Division
Transportation Test Center
P.O. Box 11330
Pueblo, CO 81001

BOEING SERVICES INTERNATIONAL ATTENDEES

Thomas E. O'Brien
Site Manager

Don Miller
Supervisor, Operations & Data Production

C. E. Maddox
Deputy Site Manager

Jodi Torpey
Public Communications Coordinator

C. R. Perry
Manager, FAST Engineering Conference

Nancy Blume
Associate Engineer

Harry Mutter
Manager, Test Design & Analysis

Dick Graff
Supervisor, Test Instrumentation System

John Leary
Industrial Engineer Statistician

Ernie Smith
Engineering Test Support Planner

Jan Parlett
Cost Accountant

J. A. Gardner
Engineering Aide

Tom Cook
Manager, FAST Operations

Jim Jollay
Engineer

Randy Jackson
Senior Engineer

Glenn Sandusky
Supervisor, System Software &
Configuration Management

Gloria Ornelas
Clerk

Tom Guenther
Engineering Test Support Planner

Jeff Champine
Engineer

Tom Roderick
Carman Lead

Rich Reiff
Senior Engineer

Dave Read
Supervisor Track Management

Rich Crader Engineering Aide	Bev Wheeler Maintenance Data Evaluation Analyst
Ted Berrian Engineering Test Support Planner	Doug Taylor Supervisor, Application Software Development
Curt Urban Measurement Tech Lead	Navin Parikh Senior System Analyst
Bill Rhodes Electronic Tech Lead	Ramesh Dighe Supervisor, Test Support
Jack Seyffer Supervisor, Test Data Production & FAST Software	Tom Sanchez Programmer
Troy Bomar Manager, Test Operations Department	Leroy Kuennen Supervisor, Rail Equipment Maintenance
Leon Sapp Supervisor, Equipment Maintenance & Vehicle Operations	Rick Herndon Supervisor, Motor/Heavy Equipment & Track Equipment
Don Duranso Supervisor, Quality Assurance	Ravi Margasahayam Senior, Specialist Engineer
Tim Suazo Resource Controller	Gerry O'Keefe Supervisor, Vehicle Operations
John St. Vrain Engineering Specialist	Jeff Hahne Quality Assurance Specialist
Scott Livingston Programmer	Steve Singsass Engineering Specialist
Britto Rajkumar Senior Specialist Engineer	James Morrissey Programmer
Luis Miera Quality Assurance Specialist	Ernie Shoaf Supervisor, Computer Operations/Data Entry & I/O Control
Mike Strah Programmer	Lahnona Krumanocker Programmer
Larry Benedict Rail Safety Supervisor	Carl Acker Measurements/Video Systems Specialist

MAGAZINE ATTENDEES

D. B. Mabry
Editor
Crossties Magazine

William J. Semioli
Editor
Railway Track & Structures
29 East Madison Street
Chicago, IL 60602

F. Stewart Mitchell
Modern Railroads Magazine
5 South Wabash Avenue
Chicago, IL 60603

Carl H. Wesselmann
Editor
Progressive Railroading
20 North Wacker Drive
Chicago, IL 60606

ASSOCIATION OF AMERICAN RAILROAD ATTENDEES

John A. Angold
AAR Consultant
13527 Hyacinta
Sun City West, AZ 85375

Wayne K. Minger
Director of Administration
AAR
1920 "L" Street
Washington, D.C. 20036

Charlie Bean
AAR
Transportation Test Center
P.O. Box 11130
Pueblo, CO 81001

Jesus Prieto
AAR
Transportation Test Center
P.O. Box 11130
Pueblo, CO 81001

Ronald J. Begier
FAST Technical Support
AAR
Transportation Test Center
P.O. Box 11130
Pueblo, CO 81001

Alex Rodriquez
AAR
Transportation Test Center
P.O. Box 11130
Pueblo, CO 81001

John Choros
Research Engineer
AAR Technical Center
3140 S. Federal St.
Chicago, IL 60616

Glen Staeheli
Experiment Monitor - Mechanical
AAR
Transportation Test Center
P.O. Box 11130
Pueblo, CO 81001

Bill Cruse
Track Consultant
AAR
P.O. Box 1464
404 N. Abrego Dr.
Green Valley, AZ 85614

G. W. Walker
AAR
Transportation Test Center
P.O. Box 11130
Pueblo, CO 81001

Keith L. Hawthorne
Director TTD
R&T - AAR
American Railroads Building
Washington, D.C. 20036

Leslie Woodall
Operations & Safety Consultant
AAR
2614 W. Regency Drive
Tucker, GA 30084

Thomas B. Hutcheson
Transportation Consultant
AAR
1825 Elizabeth Place
Jacksonville, FL 32205

Can-Wen Yang
Engineer
Research & Test Association of
American Railroads Technical Center
3140 S. Federal St.
Chicago, IL 60616

William Frederick Lewis
Economics & Finance Dept.
AAR
American Railroads Building
Washington, D.C. 20036

PRESENTERS

Roy A. Allen
Association of American Railroads
AAR Technical Center
3140 S. Federal St.
Chicago, IL 60616

Bruce N. Bosserman
Project Manager
Test Design & Analysis
Federal Railroad Administration
Transportation Test Center
Pueblo, CO 81001

James W. Brent
Consultant
Association of American Railroads
6303 Mandeville Road
Louisville, KY 40228

Laurens C. Collister
Consultant
Association of American Railroads
1914 Sims Street
Topeka, KS 66604

Larry E. Daniels
Boeing Services International
Transportation Test Center
P.O. Box 11449
Pueblo, CO 81001

Timothy J. Devine
Sr. Project Engineer
Griffin Wheel Company
200 West Monroe Street
Chicago, IL 60606

J. W. Gessner
President & Chief Executive Officer
Missouri Pacific Railroad Co.
210 N. 13th St.
St. Louis, MO 63103

Donald E. Gray
Analysis & Evaluation Division
Office of Rail Safety Research
Federal Railroad Administration
400 Seventh Street, S.W.
Washington, D.C. 20590

Jack E. Heiss
Boeing Services International
Transportation Test Center
P.O. Box 11449
Pueblo, CO 81001

V. E. Kahle
Sr. Assistant Chief Chemist
Southern Pacific Transportation Co.
401 "I" Street
Sacramento, CA 95814

Thomas P. Larkin
Chief, Test Operations Division
Federal Railroad Administration
Transportation Test Center
Pueblo, CO 81001

James R. Lundgren
FAST Technical Manager
Association of American Railroads
Transportation Test Center
Pueblo, CO 81001

Gregory P. McIntosh
FAST Program Manager
Federal Railroad Administration
Transportation Test Center
Pueblo, CO 81001

Howard G. Moody
Office of Rail Safety Research
Federal Railroad Administration
400 Seventh Street, S.W.
Washington, D.C. 20590

Oscar Orringer
Department of Transportation
Transportation System Center
Kendall Square
Cambridge, MA 02142

S. K. Punwani
Senior Research Engineer
AAR Technical Center
3140 S. Federal St.
Chicago, IL 60616

Roger K. Steele
Manager, Metallurgy
Federal Railroad Administration
Transportation Test Center
Pueblo, CO 81001

John W. Weber
2727 Black Hawk Road
Wilmette, IL 60091

1981 FAST CONFERENCE ATTENDANCE ROSTER

Robert Ackert
Sr. Research Associate
Algoma Steel
Queen St. West
Sault Ste. Marie, Ontario
Canada

G. G. Albin
Director - Track Quality & Tests
Engineering Department
Burlington Northern
176 East Fifth Street
St. Paul, MN 55101

Rex Alexander
Sales Engineer
Concrete Crossties
Blakeslee Prestress, Inc.
P.O. Box 510
Branford, CT 06405

Eugene C. Allen
Supervising Engineer
Parsons, Brinkerhoff, CENTEC Inc.
8200 Greensboro Drive, Suite 100
McLean, VA 22102

Paul B. Armstrong
Engineer of Track
Union Pacific
400 West Street
Salt Lake City, UT 84101

William W. Atkinson
Chief of Equipment Engineering
South Pacific Transportation Co.
#1 Market Plaza
San Francisco, CA 94105

W. S. Autrey
Chief Engineer
The Atchison, Topeka & Santa Fe Railway Co.
80 East Jackson Blvd., Room 201
Chicago, IL 60604

E. C. Bailey
Director of Engineering
Dresser, Inc.
2 Main St.
Depew, NY 14043

Benjamin F. Baker
Sales Manager
International Track Systems, Inc.
620 West 32nd St.
Ashtabula, OH 44004

John D. Baker
Engineering Special Project
The Atchison, Topeka & Santa Fe Railway Co.
80 East Jackson Blvd.
Chicago, IL 60604

Cliff Baldwin
Public Service Co. of Colorado
P.O. Box 840
Denver, CO 80201

C. D. Barton
Chief Engineer
Missouri Pacific Railroad Co.
210 N. 13th St.
St. Louis, MO 63103

John R. Baxter
General Manager
Btrec, Inc.
1581 Stone Ridge Rd.
Stone Mountain, GA 30083

D. K. Beachy
Speciality Sales Administrator
Treated Wood Products Division
Koppers Company, Inc.
Pittsburgh, PA 15219

John Beal-Preston
Pandrol, Inc.
P.O. Box 44
Bridgeport, NJ 08014

R. F. Beck
Chief Engineer
Elgin, Joilet & Eastern Railway Co.
Joliet, IL 60434

1981 FAST CONFERENCE ATTENDANCE ROSTER

Roger E. Belau
 Manager, Product Planning
 Fairmont Railway Motors
 Fairmont, MN 56031

Bernard E. Blood
 Chief Intercity Systems Division
 U.S. DOT/TSC
 Kendall Square
 Cambridge, MA 02140

Steven R. Benton
 Research City Manager
 Research Center
 Portec, Inc., R.P.P.
 300 Windsor Drive
 Oak Brook, IL 60521

D. L. Boger
 Assistant Chief Engineer
 C&NW Transport Co.
 500 W. Madison
 Chicago, IL 60606

Harry B. Berkshire
 Assistant Vice-President
 Maintenance of Way & Engineering
 Southern Pacific Transportation Co.
 #1 Market Plaza
 San Francisco, CA 94105

George Bonner
 Assistant Chief Engineering
 Engineering & MOW Dept.
 The Family Lines Rail System
 500 Water Street
 Jacksonville, FL 32202

Mario Bertolini
 President
 Blakeslee Prestress, Inc.
 P.O. Box 510
 Branford, CT 06405

J. Eloy Yanez Bordier
 General Superintendent
 F.C. Chihuahua Al Pacifico
 Chihuahua, Chih., Mexico

Allen C. Bieber
 Manager - Mechanical Design Engineer
 Locomotive Engineering Dept.
 General Electric Co.
 2901 East Lake Road
 Erie, PA 16531

R. J. Bourque
 Chief, Rail Crossing & Construction
 Canadian Transport Commission
 Terminal Plaza Building
 1222 Main St.
 Moncton, N.B. E1C 1H6

Alan J. Bing
 Consultant & Senior Staff
 Arthur D. Little, Inc.
 Acorn Park
 Cambridge, MA 02140

K. W. Bradley
 Assistant Chief Engineer Planning
 Denver & Rio Grande Western Railroad Co.
 P.O. Box 5482
 Denver, CO 80217

Fred B. Blader
 Director, Railroad Systems
 TASC
 One Jacob Way
 Reading, MA 01867

Chuck Branstrom
 Vice President
 True Temper
 Chemetron, Div. of Allegheny Int.
 111 East Wacker Drive
 Chicago, IL 60601

R. W. Blank
 Chief Materials Engineer
 Research & Tests
 Southern Railway Co.
 409 S. Henry St.
 Alexandria, VA 22314

Alan Briggs
 Sales Manager
 Rail & Track Products
 British Steel Corp.
 Dresser Tower, 601 Jefferson
 Houston, TX 77002

1981 FAST CONFERENCE ATTENDANCE ROSTER

R. G. Brohaugh
Assistant Vice President - Engineering
Burlington Northern
176 East Fifth Street
St. Paul, MN 55101

E. B. Burwell, E.V.P.
Southern Railway
Washington, D.C. 20013

Charles M. Brown
Product Development Manager
Market Development Department
Union Carbide Corporation
4625 Royal Avenue, P.O. Box 579
Niagra Falls, NY 14302

R. F. Butter
Engineer - Maintenance of Way
Pittsburgh & Lake Erie Railroad Co.
P. & L.E. Terminal Bldg.
Pittsburgh, PA 15219

James T. Brown
Assistant Chief Engineer
Bethlehem Steel Corp.
Johnstown, PA 15907

W. Nelson Caldwell
Senior Research Engineer
C&N Rail Research
3950 Hickmore Ave.
St. Laurent, Quebec, Canada H4T1K2

R. M. Brown
Chief Engineer
Engineering Dept.
Union Pacific Railroad
1416 Dodge St.
Omaha, NE 68179

Ross G. Carle
Vice President of Engineering
Railroad Dynamics
10 East Athens
Ardmore, PA 19003

Trevor Brown
Technical Director
Pandrol, Inc.
9 Holborn
London, EC1N 2NE

Sherry L. Carpenter
Director
Kansas City Southern Railway Co.
Louisiana & Arkansas Railway Co.
114 W. Eleventh St.
Kansas City, MO 64105

Anthony T. Bruno
Manager Railgrinding Services
Fairmont Railways Motors
ATB Associates
472 South Salina St.
Syracuse, NY 13202

C. Chambers
Senior Estimator
Railco Multi Construction
Sherwood, OR 97140

R. G. Buffalow
Superintendent Air Brakes
Denver & Rio Grande Western Railroad
P.O. Box 5482
Denver, CO 80217

J. G. Chandler
Project Engineer
Engineering & MOW Dept.
The Family Lines Rail System
500 Water Street
Jacksonville, FL 32202

R. L. Bullock
Manager, Research and Development
Standard Car Truck Company
332 South Michigan Ave.
Chicago, IL 60604

Joseph Chisholm
Asst. Dir. Rail Safety & Service
Rail Transport
Canadian Transport Commission
Government of Canada

1981 FAST CONFERENCE ATTENDANCE ROSTER

H. B. Christianson
Director - Train Accident Prevention
Casualty Prevention Department
Chessie System Railroads
Baltimore, MD 21201

M. J. Crespo
Transportation Engineer
Bethel Civil & Minerals, Inc.
P.O. Box 3965
San Francisco, CA 94119

Donald E. Cleveland, P.E.
Professor - Civil Engineering
University of Michigan
Ann Arbor, MI 48103

J. O. Crook, P.E.
Chief Engineer
Pounding Mill Quarry Corp.
P.O. Box 13527
Roanoke, VA 24010

Bryan Clough
Pandrol Incorporated
P.O. Box 44
Bridgeport, NJ 08014

Marino Curati
Chief Engineer
Railway Appliances, Inc.
111 East Wacker Drive
Chicago, IL 60601

R. J. Cochenour
Pittsburgh & Lake Erie Railroad
P. & L.E. Terminal Building
Pittsburgh, PA 15219

P. J. Curley
Assistant Manager, Product Sales
Transit Products
846 South Central Ave.
Hapeville, GA 30354

George R. Collier
Project Engineer Retired
Santa Fe Railroad
1311 Chipper Lane
Wichita, KS 67212

David Current
Track Maintenance Supervisor
Navajo Project
Black Mesa Lake Powell Railroad
Box W
Page, AZ 86040

Steve Conquergood
Development Engineer
Con-Force Costain
Concrete Tie Co., Ltd.
Box 3618, Station D
Edmonton, Alberta T5L4J6

Robert H. Curtin
General Manager
Deleuw Gather Parsons
1201 Connecticut Ave., N.W.
Washington, D.C. 20036

J. C. Cosgrove
President
Unit Rail Anchor Co.
2 North Riverside Plaza, Suite 2336
Chicago, IL 60606

Calvin C. Custer
Chief Metallurgist
Bethlehem Steel Corp.
Steelton, PA 17113

Carl L. Crawley
Section Chief
Power Division, Civil Department
Burn & McDonnell
P.O. Box 173
Kansas City, MO 64141

Angelo M. D'Attoma
Manager, Omark Track-Lok
Omark Industries, Unit No. 9
2091 Springdale Road
Cherry Hill, NJ 08003

1981 FAST CONFERENCE ATTENDANCE ROSTER

C. P. Davis
Maintenance Operations Engineer
Illinois Central Gulf Railroad
Two Illinois Center
233 N. Michigan Ave.
Chicago, IL 60601

Francis Dean
Principal Research Engineer
Battelle Columbus Laboratories
505 King Ave.
Columbus, OH 43201

Doug G. DeBerg
Engineer - Maintenance of Way
Toledo, Peoria & Western Railroad Co.
2000 E. Washington St.
East Peoria, IL 61611

R. B. Dehls
V.P. & Mgr. - Trans. Sales & Planning
Treated Wood Products Division
Koopers Company, Inc.
Pittsburgh, PA 15219

C. S. DeSar
Professor
Department of Civil Eng. & Eng. Mechanics
The University of Arizona
Tucson, AZ 85721

Douglas W. Dibble
Development Officer
Transportation Development Center
1000 Sherbrooke St. W.
P.O. Box 549
Montreal, Quebec H3A 2R3

Gary G. Dill
Director, New Product Sales
Frame Division
Midland Steel Products Co.
P.O. Box 6386
Cleveland, OH 44101

S. R. Ditmeyer
Director, Research & Development
Burlington Northern Railroad
176 E. Fifth Street, Room 230
St. Paul, MN 55101

Dennis Dobson
Managing Director
Pandrol, Inc.
P.O. Box 44
Bridgeport, NJ 08014

Ronald H. Dunn
Vice President
Parsons, Brinckerhoff, Centec Inc.
8200 Greensboro Drive, Suite 100
McLean, VA 22102

J. B. Dupere
Supervisor
Quebec North Shore & Labrador Railway
Dock Office
Sept Iles, Quebec Canada

H. B. Durrant
Assistant Chief Engineer
Engineering Department
Union Pacific Railroad
1416 Dodge St.
Omaha, NE 68179

Dennis J. Dwyer
Government Affairs Representative
Railway Progress Institute
700 N. Fairfax St.
Alexandria, VA 22314

B. J. Eck
Director - Product Engineering
Griffin Wheel Company
200 West Monroe
Chicago, IL 60606

John A. Elkins
Member of Technical Staff
TASC
One Jacob Way
Reading, MA 01867

H. L. Ellis
Regional Engineer
Chessie System
Operating Headquarters Building
P.O. Box 1800
Huntington, WV 25718

1981 FAST CONFERENCE ATTENDANCE ROSTER

C. J. Engelhardt, P.E.
Senior Director
Equipment Engineering
AMTRAK
400 North Capitol St., N.W.
Washington, D.C. 20001

J. T. Evans
Acting Associate Dean
Michigan Technology University
Houghton, MI 49931

Robert A. Evans
Mechanical Consultant
3329 Flyntwood Dr.
Santa Rosa, CA 95404

John T. Ferguson
Manager, Rail Welding & Track Test
Union Pacific Railroad
Laramie, WY

William H. Ferryman
Chief Engineer Region
Engineering Division
Burlington Northern
1405 Curtis St.
Denver, CO 80202

W. L. Finn
Manager of Car Repair Engineering
Shippers Car Line Division
ACF Industries, Inc.
620 N. 2nd St.
St. Charles, MO 63301

D. Firth
Regional General Manager
Con-Force Costain
12707 - 170 Street
Edmonton, Alberta
Canada

Carl S. Fletcher
General Manager
Newton County Stone Co., Inc.
Kentland, IN 47951

Dr. Hans D. Fricke
President
U.S. Thermit, Inc.
Ridgeway Boulevard
Lakehurst, NJ 08733

Robert A. Frigstad
Manager Product Development
Technical Services
3M Co.
St. Paul, MN 55144

Ralph Frost
Technical Director
Chemetron Railway Products
111 E. Wacker Dr.
Chicago, IL 60601

Charles M. Funk
Engineer Track - ED
Union Pacific Railroad Co.
1416 Dooge St.
Omaha, NE 68179

Iwad Furuya
Manager, R&D
Nippon Steel, USA, Inc.
345 Park Ave., 41st Floor
New York City, NY 10154

D. J. Gale
Engineer of Track
Union Pacific Railroad
400 West St.
Salt Lake City, UT 84101

Erich Gehrke
Director
Btrec, Inc.
1581 Stone Ridge Rd.
Stone Mountain, GA 30083

Howard Gilbertson
Consultant
North Eastern Railroad Products, Inc.
P.O. Box 320
55 Russell St.
Woburn, MA 01801

1981 FAST CONFERENCE ATTENDANCE ROSTER

Charles Godfrey
Consultant
ABEX Corp.
P.O. Box 369
Green Valley, AZ 85614

J. G. Harris
Asst. Engineer - Mechanical
Denver & Rio Grande Western Railroad
P.O. Box 5482
Denver, CO 80217

Ben Gordon
Chief Engineering Office
Conrail
Philadelphia, PA

Dale A. Harrison
Special Products Engineer
Santa Fe Railway Co.
9th & Jackson Ave.
Topeka, KS 66605

Pedro Juarez Gracias
Asst. Chief Mech. Officer
Ferrocarriles Nacionales De Mexico
Ave. Central 140 Piso 60 Ala "A"
Mexico City, Mexico 3, D.F.

Harley H. Hartman
CF&I
Canal & Abriendo Ave.
Pueblo, CO 81004

R. L. Gray
Director Standards & Development
R.T.C. Canadian Transport Commission
Government of Canada

William G. Harvey
Executive V.P. & General Manager
Chicago & Illinois Midland Railway Co.
P.O. Box 189
Springfield, IL 62705

Bill Greenwood
Dresser, Inc.
2 Main Street
Depew, NY 14043

H. T. Hastings
Manager of Car Design & Construction
Mechanical Department
Family Lines Rail System
500 Water St.
Jacksonville, FL 32202

Harvey Haldenby
Senior Metallurgist - Shape Products
Algoma Steel
Queen St. West
Sault Ste. Marie, Ontario
Canada

E. F. Heaton
Supervisor Locomotive Equipment
Missouri Pacific Railroad Co.
210 N. 13th St.
St. Louis, MO 63103

William R. Hamilton
Director of R&D
Portec, Inc.
Railway Products Division
300 Windsor Dr.
Oak Brook, IL 60521

Robert J. Henry
Engineer
Research
Bethlehem Steep Corp.
Bethlehem, PA 18016

Edward G. Hansen
Principal Engineer
T&D Department
E.I. DuPont De Nemours & Co.
Wilmington, DE 19898

L. M. Hepler
Product Manager - Brake Shoes
Griffin Wheel Company
200 West Monroe
Chicago, IL 60606

1981 FAST CONFERENCE ATTENDANCE ROSTER

J. D. Hines
 Manager of Sales
 Unit Rail Anchor Co.
 2 North Riverside Plaza, Suite 2336
 Chicago, IL 60606

George A. Hommel
 Group Vice President - Castings
 Midland Ross
 700 S. Dock St.
 Sharon, PA 16146

Charles N. Hood
 Director Market Development
 Marketing Division
 American Steel Foundries
 3600 Prudential Plaza
 Chicago, IL 60601

Eugene Y. Huang
 Acting Associate Dean of Graduate Studies
 Michigan Technology University
 Houghton, MI 49931

Bob Hudson
 Pandrol, Inc.
 P.O. Box 44
 Bridgeport, NJ 08014

David J. Hughes
 President
 Pandrol, Inc.
 P.O. Box 44
 Bridgeport, NJ 08014

J. H. Hughes
 Vice President
 Kansas City Southern Railway Co.
 Louisiana & Arkansas Railway Co.
 114 W. Eleventh St.
 Kansas City, MO 64105

Larry R. Jacobson
 Project Manager
 Dalton, Dalton & Newport
 3605 Warrensville Center Rd.
 Cleveland, OH 44122

D. L. Jerman
 Senior Engineer
 M/W Standards & Testing
 National Railroad Passenger Corp.
 400 North Capitol St., N.W.
 Washington, D.C. 20001

Darrell L. Johnson
 Mechanical Inspector
 Mechanical Burlington Northern
 176 E. Fifth St.
 St. Paul, MN 55119

S. R. Johnson
 Assistant Vice President
 Operations Planning
 The Family Lines Rail System
 500 Water Street
 Jacksonville, FL 32202

W. A. Johnson
 Director - Maintenance Planning
 Engineering Department
 Burlington Northern Railroad
 176 E. Fifth St.
 St. Paul, MN 55101

C. R. Kaelin
 Director
 Technical Research & Development
 AT&SF Railway Co.
 Topeka, KS 66628

Joseph C. Kahr
 Manager, Cobra Shoe Engineering
 Engineering Department
 WABCO
 American Standard, Inc.
 Wilmerding, PA 15148

Kazuo (Jim) Kato
 Assistant General Manager
 Mitsui & Co.
 200 Park Ave.
 New York, NY 10017

Robert A. Kendall
 Senior Manager, Field Operations
 (DCP) Deleuw Cathert Parsons
 1201 Connecticut Ave., N.W.
 Washington, D.C. 20036

1981 FAST CONFERENCE ATTENDANCE ROSTER

Marty Kennedy
Pandrol, Inc.
P.O. Box 44
Bridgeport, NJ 08014

G. F. Lazar
Product Manager - Wheels
Griffin Wheel Company
200 West Monroe
Chicago, IL 60606

M. D. Kenyon
Assistant Chief Engineer
Denver & Rio Grande Western Railroad Co.
P.O. Box 5482
Denver, CO 80217

Geoffry Leeves
Pandrol, Inc.
P.O. Box 44
Bridgeport, NJ 08014

Glen Kester
Railroad Superintendent
Navajo Project
Black Mesa Lake Powell Railroad
Box W
Page, AZ 86040

Kenneth Lenzen
AREA Committee #24
Engineering Division of AAR
University of Kansas
Lawrence, KS

Michael J. Klima
Rail Marketing Engineer
Stedef, Inc.
Tysons Office Park, #14
7657 Leesburg Pike
Falls Church, VA 22043

Jack R. Long
Director, Eng. Research & Development
Midland Ross
700 S. Dock St.
Sharon, PA 16146

Dr. Sudhir Kumar
Professor & Director R.R. Eng. Lab.
Illinois Institute of Technology
11T Center
Chicago, IL 60616

Robert B. Love
Regional Sales Manager
Marketing Division
American Steel Foundries
3600 Prudential Plaza
Chicago, IL 60601

Robert L. Lantz
Regional Manager - Trans. Sales West
Forest Products Group
Koppers Company, Inc.
122 South Michigan Ave.
Chicago, IL 60603

J. K. Lynch
Manager, Transp., Sales & Rail Car
Vulcan Materials Co.
P.O. Box 7497
Birmingham, AL 35253

Kenneth W. Larsen
Program Manager
Dynamic Science, Inc.
Washington Operations
8326 Professional Hill Drive
Fairfax, VA 22031

Joseph F. Lynch
Superintendent, Metallurgy & Q.C.
Wheel, Pittsburgh Steel
Monessen Plant
Monessen, PA 15062

R. F. Lawson
Vice President - Chief Engineer
National Railroad Passenger Corp.
400 North Capitol St., N.W.
Washington, D.C. 20001

Robert N. Madderom
Pandrol, Inc.
P.O. Box 44
Bridgeport, NJ 08014

1981 FAST CONFERENCE ATTENDANCE ROSTER

Dan Mahoney
Salesman
Fabreeka Products Co.
7100 Broadway
P.O. Box 21346
Denver, CO 80221-0346

Gene D. Mall
Manager - Eastern Sales
Kerr-McGee Chemical Corp.
Kerr-McGee Center
Oklahoma City, OK 73125

N. C. Marsh
Assistant Manager, Reliability Engineering
Technical Research & Development
AT&SF Railway Co.
Topeka, KS 66628

John H. Martens
Senior Metallurgical Engineer
Bethlehem Steel Corp.
Bethlehem, PA 18016

J. R. Masters
Chief Engineer - Maintenance Planning
Engineering Department
Burlington Northern
176 East Fifth Street
St. Paul, MN 55101

Hiroshi Matsumoto
Manager
Engineering & Steel Products
NKK America, Inc.
450 Park Ave.
New York, NY 10022

Robert A. Matthews
Vice President
Railway Progress Institute
700 N. Fairfax St.
Alexandria, VA 22314

Ron Mayville
Consultant & Senior Staff
Arthur D. Little, Inc.
Cambridge, MA 02140

Donald H. McDonell
Engineer, Structural Division
Stone & Webster Engineering Corp.
P.O. Box 5406
Denver, CO 80217

Tom McElroy
Supervisor, Maintenance of Way
Quebec North Shore & Labrador Railway
Dock Office
Sept Iles, Quebec, Canada

Robert D. McIntire
Vice President & General Manager
Midland Ross
700 S. Dock St.
Sharon, PA 16146

C. W. McKee
Director R&D
Teleweld, Inc.
1555 Hawthorne Lane
West Chicago, IL 60185

Philip J. McQueen, P.E.
Consulting Engineer
30 Fairway Drive
Ignacio, CA 94947

Hubert V. Meek
Gen. Roadmaster
The Denver & Rio Grande Western Railroad
P.O. Box 5482
Denver, CO 80217

Kenneth D. Mels
Chief Locomotive Development Engineer
Electro-Motive Division
General Motors Corp.
LaGrange, IL 60525

Scott D. Miller
Sales Representative
Plasser American Corp.
2001 Myers Rd.
Chesapeake, VA 23324

1981 FAST CONFERENCE ATTENDANCE ROSTER

John R. Mitoraj
 Manager, Railroad Sales
 J. P. Ruklic Screw Co.
 13550 S. Chatham
 Blue Island, IA 60406

G. A. Musolf
 Manager, Engineering
 Standard Car Truck Company
 332 South Michigan Ave.
 Chicago, IL 60604

Chas. Moehling
 Manager, Track Engineering
 American Steel Foundries
 3600 Prudential Plaza
 Chicago, IL 60601

Walter Muzychenko
 Manager
 Railway Division Engineering
 American Koyo Corp.
 29570 Clemens Rd., P.O. Box 45028
 Westlake, OH 44145

P. L. Montgomery
 Manager, Engineering Systems
 Norfolk & Western Railway Co.
 8 North Jefferson St.
 Roanoke, VA 24042

Georg Nadorff
 Representative
 HRS Germany
 561 Beech Drive
 Kent, OH 44240

Jim E. Morenz
 CF&I
 Canal & Abriendo Ave.
 Pueblo, CO 81004

Brad Nelson
 Track Engineer
 AMAX - Henderson Mine
 Box 68
 Empire, CO 80438

Jeff Morrow
 Manager, HSLA Development
 Climax Molybdenum Co.
 3072 One Oliver Plaza
 Pittsburgh, PA 15222

O. T. Nephew
 Director of Engineering
 Teleweld, Inc.
 1555 Hawthorne Lane
 West Chicago, IL 60185

Jerry Munro
 Regional Manager
 True Temper
 Chemetron, Div. of Allegheny Int.
 111 East Wacker Drive
 Chicago, IL 60601

Ronald R. Newman
 Manager, Track Train Dynamics
 Operations Department
 Burlington Northern
 176 East Fifth Street
 St. Paul, MN 55101

Miguel Leal Murguia
 Chief Track Machinery Department
 F.C. Chihuahua Al Pacifico
 Chihuahua, Chih., Mexico

Harry S. Nichols
 President
 The Nichols Company
 P.O. Box 157
 Troy, MI 48099

Graham Murray
 Director
 Btrec, Inc.
 1581 Stone Ridge Rd.
 Stone Mountain, GA 30083

Yasuhide Nishimoto
 Department General Manager
 Mitsui & Co.
 200 Park Ave.
 New York, NY 10017

1981 FAST CONFERENCE ATTENDANCE ROSTER

Mrs. J. J. O'Dea
 Mechanical Engineer
 Research & Tests
 Southern Railway Co.
 409 S. Henry St.
 Alexandria, VA 22314

Warren B. Peterson
 Chief Engineer
 Soo Line Railroad, Company
 Box 530
 Minneapolis, MN 55440

Keisuke Ogawa
 Assistant Manager
 Steel Department
 Mitsui & Co.
 17117 W. Nine Mile Road, Suite 1440
 Southfield, MI 48075

Vincent Petrucelly
 Research Engineer
 Port Authority of New York & New Jersey
 1 Path Plaza, 3rd Floor
 Jersey City, NJ 07306

James L. Ozment
 Division Engineer
 Denver & Rio Grande Western Railroad Co.
 650 Davis Rd.
 Salt Lake City, UT 84119

A. E. Pew, III
 Director, Administration
 R&D Division
 Burlington Northern Railroad
 176 E. Fifth Street
 St. Paul, MN 55101

Romolo Panetti
 Pandrol, Inc.
 P.O. Box 44
 Bridgeport, NJ 08014

David A. Pittinger
 National Sales Manager
 Railroad Products
 Lone Star Industries, Inc.
 6416 Halsey Drive
 Woodridge, IL 60517

Stewart P. Park, Jr.
 Chief Mechanical Officer
 Maine Central Railroad Company
 242 St. John St.
 Portland, ME 04102

C. T. Popma
 Assistant Vice-President
 Quality Control & Mechanical Eng. Dept.
 CONRAIL
 1802, 1528 Walnut St.
 Philadelphia, PA 19102

Robert E. Parsons
 U.S. Department of Commerce
 National Bureau of Standards
 109 McLaughlin Hall
 Berkeley, CA 94720

A. K. Pottorff
 District Engineer
 AT&SF Railway Co.
 P.O. Box 1738
 Topeka, KS 66628

Lynn Patterson
 Sales Manager
 Fabreeka Products Co.
 7100 Broadway
 P.O. Box 21346
 Denver, CO 80221-0346

Don Powell, P.E.
 Construction Materials Engineer
 Vulcan Materials Co.
 P.O. Box 7497
 Birmingham, AL 35223

R. K. Pattison
 President
 Parsons, Brinkerhoff, Centec Inc.
 8301 Greensboro Dr., Suite 220
 McLean, VA 22102

Robert H. Prause
 Section Manager
 Battelle Columbus Laboratories
 505 King Ave.
 Columbus, OH 43201

1981 FAST CONFERENCE ATTENDANCE ROSTER

A. E. Price
 Technical Director
 Sales/Marketing
 General American Transportation Corp. - GATX
 120 South Riverside Plaza
 Chicago, IL 60606

Shaun Richmond
 Manager, Design Analysis
 Thrall Car Manufacturing Co.
 26th & State St.
 Chicago Heights, IL 60411

Julia Prudhoe
 Pandrol, Inc.
 P.O. Box 44
 Bridgeport, NJ 08014

Armin Richter
 Supervisor Systems Shop Programming
 Burlington Northern
 1675 Old Hudson Rd.
 St. Paul, MN 55106

C. L. Puri
 Regional Engineer
 Canadian Transport Commission
 60 Adelaide St. East, 4th Floor
 Toronto, Ontario
 Canada LAT 3P9

S. Rishovd
 LORAM Maintenance of Way, Inc.
 3900 Arrowhead Drive
 Hamel, MN 55340

Esteban Quintero
 Chief Inspector Carbozulia Project
 Railroad Department
 IECO
 180 Howard St.
 San Francisco, CA 94105

Al Rivoire
 Pandrol, Inc.
 P.O. Box 14
 Bridgeport, NJ 08014

Leonard U. Rastrelli
 Director, Department of Special Studies
 Instrumentation Research Division
 Southwest Research Institute
 P.O. Drawer 28510
 San Antonio, TX 78284

Stuart M. Robertson
 Chief Railroad Design Dept.
 IECO
 180 Howard St.
 San Francisco, CA 94105

A. J. Reinschmidt
 Asst. Prof. of Railway Engineering
 Pennsylvania State University
 Accounting Operations
 302 Shields Building
 University Park, PA 16802

H. L. Rose
 Assistant Vice President
 MW&S of Southern Railway Co.
 99 Spring St.
 Atlanta, GA

Ernest J. Rewucki
 Eng. of Track CP Rail
 Windsor Station, Room 401
 430 Montrose Dr.
 Montreal, Quebec, Canada H3C 3E4

Dean J. Rougas
 Assistant Manager, Railroad
 CF&I Steel
 P.O. Box 1830
 Pueblo, CO 81002

H. E. Richardson
 Assistant Chief Engineer
 Engineering & MOW Dept.
 The Family Lines Rail-System
 500 Water Street
 Jacksonville, FL 32202

R. Rought
 Chief Product Engineer
 Engineering Department
 Midland Steel Products Co.
 P.O. Box 6386
 Cleveland, OH 44101

1981 FAST CONFERENCE ATTENDANCE ROSTER

W. T. Rousis
 Supervisor, Material Control, MW
 Material Management Department
 NW Railway
 8 N. Jefferson St. - 60 B East
 Roanoke, VA 24042

Kenneth C. Rownd
 Project Engineer
 Proform, Inc.
 7901 Xerxes Avenue So.
 Minneapolis, MN 55431

J. E. Russell
 Manager, Transportation Equipment
 Industrial Chemical Division
 PPG Industries, Inc.
 One Gateway Center
 Pittsburgh, PA 15222

Brian T. Scales
 Railway Consultant
 Devine Mfe. Co.
 Pittsburgh, PA 15219

H. L. Schaaf
 Marketing
 EI DuPont Co.
 1414 Lark Dr.
 Evansville, IN 47715

K. R. Schaeffer
 General Car Inspector
 Denver & Rio Grand Railroad
 P.O. Box 5482
 Denver, CO 80217

Thomas G. Schultz
 1931 Rosebud Court
 San Jose, CA 95128

Jon Schumaker
 Executive Vice President
 Pandrol, Inc.
 P.O. Box 44
 Bridgeport, NJ 08014

C. N. Scott
 Director, Research & Test
 Southern Railway
 409 S. Henry St.
 Alexandria, VA 22313

Frank Scott
 Research Engineer
 Nelson Caldwell Service Research Eng.
 Canadian Nation Rail, CN Research Center
 3950 Hiekmore Ave.
 St. Laurent, Quebec H4T 1K2

David R. Seeley
 Pandrol, Inc.
 P.O. Box 44
 Bridgeport, NJ 08014

William W. Sellers
 President
 Standard Car Truck Company
 332 South Michigan Ave.
 Chicago, IL 60604

A. E. Shaw, Jr., P.E.
 Director - Engineering Department
 AMTRAK
 1617 J. F. Kennedy Blvd.
 Philadelphia, PA 19103

Nathan E. Smith
 Assistant V.P., Chief Engineer
 The Milwaukee Road
 516 West Jackson Blvd.
 Chicago, IL 60606

R. E. Snyder
 Director, MTC OPR
 C. & N.W. Transport Co.
 500 W. Madison St.
 Chicago, IL 60606

Bill Spencer
 Director of Maintenance Planning
 Union & Pacific Railroad
 1416 Dodge St.
 Omaha, NE 68179

1981 FAST CONFERENCE ATTENDANCE ROSTER

Harry C. Steelman
Assistant Division Engineer
Union Pacific Railroad
1745 Massachusetts Ct.
Green River, NY 82935

J. W. Thomas
Quality Control Manager
Sperry Rail Service Division
Automotive Industries, Inc.
Shelter Rock Road
Danbury, CT 06810

Max Stephens
Manager Sales
Vulcan Materials Co.
P.O. Box 80730
Atlanta, GA 30366

Robert Tobias
Track Foreman
AMAX - Henderson Mine
Box 68
Empire, CO 80438

Lars C. Strom
Project Manager
Stone & Webster Engineering Co.
P.O. Box 5406
Denver, CO 80217

Y. H. Tse
Assistant Manager - Analytical Support
Mechanical Engineering
CONRAIL
225 30th Street Station
Philadelphia, PA 19104

Eric J. Summers
System Supervisor, MOW
Engineering Department
CN Rail
Montreal, Quebec
Canada

William S. Tuinstra
Special Assistant Engineer
Staff Studies & Planning
Santa Fe Railroad Co.
80 E. Jackson
Chicago, IL 60604

J. E. Sunderland
Regional Engineer
Chessie System
Operating Headquarters Building
100 N. Charles St.
Baltimore, MD 21201

D. M. Tutko
Chief Mechanical Officer
Missouri Pacific Railroad Co.
210 N. 13th St.
St. Louis, MO 63103

F. W. B. Taylor
Highway Engineer
U.S. Army Forces Command
Hdqrs., U.S. Army Forces Command
Fort McPherson, GA 30330

Robert F. Tuve
Manager, Quality Control Engineering
Engineering and Research Department
Southern Railway System
99 Spring St., S.W.
Atlanta, GA 30303

Takao Terada
Manager - Plate & Shape Dept., Yawata Works
Nippon Steel Corporation
6-3, Otemachi 2-Chome
Chiyoda-Ku
Tokyo 100, Japan

Hugo Valladares
Asst. Chief Inspector Carbozulia Project
Railroad Department
IECO
180 Howard St.
San Francisco, CA 94105

Gerhard A. Thelen
Director
Mechanical Engineering
CONRAIL
225 30th Street Station
Philadelphia, PA 19104

Wayne Vanderleest
Pandrol Incorporated
P.O. Box 44
Bridgeport, NJ 08014

1981 FAST CONFERENCE ATTENDANCE ROSTER

Nick Ventri
Chief Mechanical Engineer
Servo Corp. of America
111 New South Road
Hicksville, NY 11802

Eric Wolf
Manager, Research
Trailer Train Co.
101 North Wacker Drive
Chicago, IL 60606

Hans Von Lange
President
Elastic Spike Corp. of America
115 East Joppa Road
Baltimore, MD 21204

Gary P. Wolf
Sr. Operations Research Analyst
Operations Research
Southern Railway System
125 Spring St. S.W., Room 815
Atlanta, GA 30303

R. P. Wallace
Director Quality Control
Chessie System
Operating Headquarters Building
P.O. Box 1800
Huntington, WV 25718

L. F. Woodlock
Chief Engineer - Maintenance of Way
Engineering Department
Burlington Northern
176 East Fifth Street
St. Paul, MN 55101

James W. Walsh
Director Freight Car Maintenance
Mechanical Department
Boston & Maine Corp.
High Street
North Billerica, MA 01882

Arthur W. Worth
Engineer Standards
CN Rail
935 de La Gauchetiere St. West
Montreal, Quebec Canada

R. H. Walsh
General Sales Manager
Holland Company
1020 Washington Ave.
Chicago Heights, IL 60411

Bruce E. Wylie
President
Robert J. Wylie Co.
295 E. Marie Ave.
West St. Paul, MN 55118

E. H. Waring
Chief Engineer
D&RGW Railroad
P.O. Box 5482
Denver, CO 80217

Ken Yates
Rail Tech. Manager, Track Products
British Steel Corp., Inc.
Workington, United Kingdom

John G. White
Vice President & General Manager
Con-Force Costain
1000-1520 - 4th St. SW
Calgary, Alberta
Canada T2R 1H5

William Zacharkiw
Pandrol, Inc.
P.O. Box 44
Bridgeport, NJ 08014

D. B. Whitehurst
Vice-President - Marketing
Griffin Wheel Company
200 West Monroe
Chicago, IL 60606

Alan Zarembski
Pandrol, Inc.
P.O. Box 44
Bridgeport, NJ 08014

ASSOCIATION OF

AMERICAN RAILROADS

RESEARCH AND TEST DEPARTMENT—OPERATIONS, PUEBLO
1138 BLUESTEM, P.O. BOX 11130, PUEBLO, COLORADO 81001

J. R. LUNDGREN
Director-AAR Operations, Pueblo
Ext. 317/281

C. W. BEAN
Assistant to Director, Pueblo
Ext. 292/317

R. J. BEGIER
Manager, FAST Technical
Support Ext. 289/281

G. W. WALKER
Manager, FAST Industry
Support Ext. 208/215

March 4, 1982

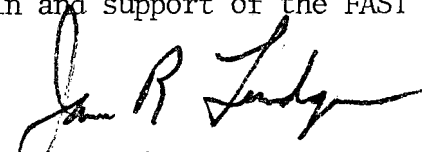
To: AREA Committee Members
AAR Mechanical Committee Members
Track-Train Dynamics Committee Members
FAST Donors

Gentlemen:

We are pleased to enclose a copy of the Proceedings of our November, 1981 FAST Engineering Conference.

These proceedings represent a selection of the more important findings from the major FAST Experiments after five years of operation.

Your continued interest in and support of the FAST Program is sincerely appreciated.



J. R. Lundgren, Director
AAR Operations, Pueblo

JRL:1bb

Attach.

cc: W. J. Harris, Jr.



1981 FAST ENGINEERING CONFERENCE PROCEEDINGS

ERRATA SHEET

- Page 48 - Figure 8 - "Wyoming Granite", is also known as "CEB".
- Page 49 - Figure 13 - Caption should read: "Change in grain size distribution, Georgia Granite Ballast - Section 17 (concrete ties)".
- Page 50, Table 2 - "Section 18" should be "Section 17".
- Page 51, Table 3 - "III-6" should be "III-8".
- Page 52, First paragraph - "90 MGT" should be "190 MGT".
- Page 53, Question No. 2 - Change "Shoule" to "Should".
- Page 53, Question No. 5, Answer No. 2 - "granite" should be "granite/granite like".
- Page 63, First paragraph - Change "1% grade" to ".1% grade".
- Page 63 - Figure 2 - Change "BALLAST: Slag, 14" deep" to "BALLAST: Slag, 15" deep".
- Page 65, Table 1 - Delete asterisk next to "Clips 99".
Add asterisk next to heading, "FAILURES*".
- Page 68 - Delete bracket in Table 3.
- Page 69 - Delete brackets in Table 4.
- Page 69 - Delete: "@RAIL BASE)" at the top of Figure 15.
Add: "at rail base" to caption of Figure 15.
- Page 71, Column 2, Paragraph 2 - Delete: "clip and".
- Page 87 - Figure 12 - Caption should read: "Auto Spectrum Concrete Tie; Heavy Corrugations".
- Page 99 - Column 2, Paragraph 2 - Change "studs" to "strips".
Delete "to strips".
- Page 115, Column 1, Paragraph 3 - Change "assending" to "ascending".
- Page 117, Column 2 - Under equation, change " $\mu_{X,Y}$ = variance. . ." to " $\sigma_{X,Y}$ = variance".
- Page 136, Column 1, Paragraph 2 - Change "affects" to "effects".
- Page 178 - Figures 6 and 7 are reversed.

Continued . . .



Errata Sheet (Continued)

Page 181 - Figure 12 - Caption should read "Flange Thickness..."

Page 182 , Column 2, Paragraph 2 - "S2" should be "S²"

Page 184, Table 9 - Model equation should be:

$$"Y = \underline{0.01303} + (0.00179 + 0.00040X1 - 0.00026X2 - 0.00080X3 - 0.00011X5) \text{ mileage}"$$

Corrections are underlined.

Page 184, Table 10 - Model equation should be:

$$"Y = \underline{0.00298} + (\underline{0.00293} + \underline{0.00035X1} + \underline{0.00028X2} - \underline{0.00149X3} - \underline{0.00008X4} - \underline{0.00013X5}) \text{ mileage}"$$

Corrections are underlined.

Page 188, Table 13 - Change caption from "Wrought" to "Cast".

Page 193, Column 2, Paragraph 6 - "Table 16" should be "Table 17".

Page 220, Column 1, Paragraph 1 - "+0.02 percent" should be "± 0.02 percent".

Page 203, Column 2 - Note change "metal behavior or carbon . . ." to "metal behavior of carbon . . ."

Page 218 - Equation 3 is " $w_f \propto \mu_f F_f \sqrt{\frac{a}{r}}^2 + (\Theta w \tan \beta)^2$ "

It should be " $w_f \propto \mu_f F_f \sqrt{\frac{a}{r}^2 + (\Theta w \tan \beta)^2}$ "

Page 218, Column 2, Paragraph 4 - "lasers ²³" should be "lasers (2 and 3)"

Page 219, Column 1, Paragraph 1 - "lasers 1 and 2" should be "lasers 1 and 3"

Page 221 - Figure 6 - Data point missing for empty - should be 13 (1b rads)

Page 232, Column 2, Paragraph 5 - "Table 2" should read "Table 1".

Page 234, Figure 17 - Photo is upside down.

Page 249, Figure 3 - Caption should read "TTC Wheel Measuring Device".

Figure 4 - Caption should read "TTC Rail Measuring Device".

Page 250, Reference 6 is the source document for the material presented in the Appendix.

Continued . . .



Errata Sheet (Continued)

Page 250, Appendix 1 - "R" in the two equations should be "RR".

From TDOP representation:

$$" B_5 b = B_6 b^2 "$$

Should be: $" B_5 b + B_6 b^2 "$

FAST Engineering Conference
FAST Engineering Conference - 1981
Proceedings, 1982
US DOT FR/TTTC-82/01

SMEAD 00 YP335A

**PROPERTY OF FRA
RESEARCH & DEVELOPMENT
LIBRARY**

NOTICE

This document is disseminated under the sponsorship of the Department of Transportation in the interest of information exchange. The United States Government assumes no liability for its contents or use.

NOTICE

The United States Government does not endorse products or manufacturers. Trade or manufacturers' names appear herein solely because they are considered essential to the object of this report.